
Random Unitary Operations

and

Quantum Darwinism

A thesis submitted for the degree of doctor of sciences (Dr. rer. nat.) by Nenad Balanesković M. Sc.
from Nis (Serbia) and approved by the department of physics
Darmstadt 2016 - The University of Technology Darmstadt - D17 - Department 5



TECHNISCHE
UNIVERSITÄT
DARMSTADT

Institut für Angewandte Physik
Hochschulstraße 4a
64289 Darmstadt, Germany

Approved PhD-thesis by Nenad Balanesković M. Sc. from Nis (Serbia)

Advisory no 1: Prof. Dr. Gernot Alber

Advisory no 2: Prof. Dr. Reinhold Walser

Date of submission: December 9th, 2015

Date of final examination: February 1st, 2016

Darmstadt - D17 - Department 5

The following articles have emerged from this PhD-thesis:

Nenad Balanesković, »*Random unitary evolution model of quantum Darwinism with pure decoherence*«, Eur. Phys. J. **D 69**, 232 (2015)

Zufällige unitäre Operationen und Quanten Darwinismus

Zur Erlangung des Grades eines Doktors der Naturwissenschaften (Dr. rer. nat.) vorgelegte und vom Fachbereich Physik genehmigte Dissertation von Nenad Balanesković M. Sc. aus Nis (Serbien)
Darmstadt 2016 - Technische Universität Darmstadt - D17 - FB 5



TECHNISCHE
UNIVERSITÄT
DARMSTADT

Institut für Angewandte Physik
Hochschulstraße 4a
64289 Darmstadt, Germany

Genehmigte Dissertation von Nenad Balanesković M. Sc. aus Nis (Serbien)

1. Gutachten: Prof. Dr. Gernot Alber
2. Gutachten: Prof. Dr. Reinhold Walser

Tag der Einreichung: 09.12.2015

Tag der Prüfung: 01.02.2016

Darmstadt - D17 - FB5

Die folgenden Artikel sind dieser Dissertation entsprungen:

Nenad Balanesković, »*Random unitary evolution model of quantum Darwinism with pure decoherence*«, Eur. Phys. J. **D 69**, 232 (2015)

Erklärung zur Dissertation

Hiermit versichere ich, die vorliegende Dissertation ohne Hilfe Dritter und nur mit den angegebenen Quellen und Hilfsmitteln angefertigt zu haben. Alle Stellen, die aus Quellen entnommen wurden, sind als solche kenntlich gemacht. Diese Arbeit hat in gleicher oder ähnlicher Form noch keiner Prüfungsbehörde vorgelegen.

Darmstadt, den

(Nenad Balanesković)
(E-Mail: balaneskovic@gmx.net)

Curriculum Vitae - Nenad Balanesković

Personal Information

Nationality: German
Date of birth: May 14, 1984
Place of birth: Nis, Serbia
Academic degrees: Master of Science in Physics (2011)
Address: Seehofstraße 12A, 60594 Frankfurt am Main
Tel.: 069/617554
E-Mail: balaneskovic@gmx.net

Education

since october 2011	PhD studies at TU Darmstadt.
2011	Master's degree from TU Darmstadt; Thesis: »Nonequilibrium and the Functional Renormalization Group«.
2008 - 2011	Graduate studies in physics (MSc.) at TU Darmstadt.
2008	Bachelor's degree from TU Darmstadt; Thesis: »Nonequilibrium Initial Conditions for Plasma Instabilities«.
2005 - 2008	Undergraduate studies in physics (BSc.) at TU Darmstadt.
2005	Abitur (university entrance qualification) acquired at Carl-Schurz-Schule in Frankfurt/M.
2000 - 2005	Secondary school at Carl-Schurz-Schule in Frankfurt/M.
1991 - 1999	Elementary school and middle school in Negotin, Serbia.

Professional and Teaching Experience

2016: March, **Hannover**: DPG-conference (contributions: poster »Attractor Spaces of Dissipatively Dephased Random Unitary Evolution and Quantum Darwinism« & presentation »Random Unitary Evolution Model of Dissipation, Dephasing and Quantum Darwinism«)

2016: January, **Bad Honnef**: 605-th DPG-seminar (contribution: poster »Qubit Model of Dissipation, Dephasing and Quantum Darwinism based on Random Unitary Evolution«)

2015-2016: **TU Darmstadt**: Organization of tutoring sessions and exams for the lecture »Theoretical Physics I: classical mechanics« by Prof. Dr. Gernot Alber

2015: October, **Bad Honnef**: 600-th DPG-seminar (contribution: poster »Dephasing, Dissipation and Quantum Darwinism - an RUO perspective«)

2015: May, **Pecs** (Hungary): 3rd Work Meeting (contribution: presentation »Random Unitary Operations and Quantum Darwinism: pure decoherence vs dissipation«)

2015: **TU Darmstadt**: Tutoring recitation sessions for the lecture »Theoretical Quantum Optics« by Prof. Dr. Gernot Alber (together with Nils Trautmann)

2015: March, **Heidelberg**: DPG-conference & May, **Bad Honnef**: 586-th DPG-seminar (contribution: poster »Decoherence, Dissipation and Quantum Darwinism - an RUO perspective«)

2014: **TU Darmstadt**: May-August, Bachelor-Thesis of Marc Mendler »Quantum Darwinism and dissipation in open quantum systems« (supervision together with Prof. Dr. Gernot Alber)

2014: March, **Berlin**: DPG-conference (contribution: presentation »Quantum Darwinism, the Appearance of Classicality and Random Unitary Operations (RUO)«)

2013: **TU Darmstadt**: May-August, Bachelor-Thesis of Felix Weber »Iterative quantum operations and group-invariant projections« (supervision together with Prof. Dr. Gernot Alber)

2013: **TU Darmstadt**: Zertifikat Hochschullehre (Higher Education Certificate) of the HDA (Hochschuldidaktische Arbeitsstelle)

2013: March, **Hannover**: DPG-conference (contribution: poster »Koenig-Digraph Interaction Model of Decoherence and Quantum Darwinism«)

2012-2013: **TU Darmstadt**: Organization of tutoring sessions and exams for the lecture »Theoretical Physics I: classical mechanics« by Prof. Dr. Gernot Alber

2012: **TU Darmstadt**: Organization of tutoring sessions and exams for the lecture »Theoretical Physics II: quantum mechanics« by Prof. Dr. Gernot Alber

2012: March, **Stuttgart**: DPG-conference & May, **Bad Honnef**: 500-th DPG-seminar (contribution: poster »Asymptotic Long-Time Properties of Decoherence and Quantum Darwinism«)

2011-2012: **TU Darmstadt**: Organization of tutoring sessions and exams for the lecture »Theoretical Physics III: electrodynamics« by Prof. Dr. Gernot Alber

2011: **TU Darmstadt**: Tutoring recitation sessions in „Introduction to Theoretical Physics“ by Prof. Dr. Jochen Wambach.

2010: **TU Darmstadt**: Teaching award of the Gerhard Herzberg Gesellschaft.

2010: **TU Darmstadt**: Tutoring recitation sessions in „Theoretical Physics II: Quantum Mechanics“ by Prof. Dr. Gernot Alber.

2009-2010: **TU Darmstadt**: Tutoring recitation sessions in „Theoretical Physics I: Classical Mechanics“ by Prof. Dr. Jürgen Berges.

2002-: Private tutoring for (highschool) students in physics and mathematics.

Scholarships

2005 - 2007: Scholarship of the Studienstiftung des deutschen Volkes (reimbursement of expenses for books etc.).

2002 - 2005: Scholarship of the Gemeinnützige Hertie-Stiftung for secondary school students (reimbursement of expenses for books).

Languages

German (bilingual), English (fluent), Russian (elementary knowledge), Serbian (native speaker).

Computer Skills

Languages: C++, D and Delphi (preferred languages), HTML, PHP and Java, Mathematica, MATLAB, Octave, Maple, Maxima, Sage, Haskell, VBA, Perl, Python, R.

Operating Systems: Windows-XP, -7, 8, Linux.

General Applications: Microsoft Office (Word, PowerPoint, Excel), Open Office, Gnuplot, Origin, Euler, L^AT_EX, E^WT_EX.

»All that we know is just a drop of water springing from an endless sea of the unknown.«

Sir Isaac Newton

»Das Universum«, denkt Raimundo Velloz, »was für ein Unsinn!« Die Einheit ist ein methaphysischer Schwindel. [...] Es gibt nicht ein Universum, es gibt deren Millionen und Millionen, eins im anderen, und in jedem fünf, zehn, vierzehn verschiedene Universen. Er mag die konzentrische Gedankenfolge, Begriffe in zunehmenden und abnehmenden Konnotationsreihen. Man geht von der Kaffeebohne aus, der Kaffeekanne, die sie enthält, der Küche, welche die Kaffeekanne enthält, dem Haus, das die Küche enthält, dem Häuserblock, der das Haus enthält... Und man kann fortfahren mit den zwei Aspekten des Bildes, mit der Kaffeebohne, die tausend Universen einschließt, und dem Universum des Menschen, ein Universum innerhalb der weiß wie vieler Universen, das vielleicht - er erinnert sich, das irgendwo gelesen zu haben - nur ein Stückchen von der Schuhsohle eines kosmischen Kindes ist, das in einem Garten spielt (dessen Blumen natürlich die Sterne sind). Dieser Garten gehört zu einem Land, das zu einem Universum gehört, das ein Stückchen Zahn einer Maus ist, gefangen in einer Mausefalle, die man auf dem Tisch eines Dachbodens in einem Haus in der Vorstadt aufgestellt hatte. Die Vorstadt gehört zum... Ein Stückchen von irgend etwas, doch immer nur ein Stückchen; Größe ist eine jämmerliche Illusion.

Julio Cortázar, »Gewisse Veränderungen« from »Die Nacht auf dem Rücken«, Suhrkamp-Verlag (1998).

Das Universum (das andere die Bibliothek nennen) setzt sich aus einer unbestimmten, vielleicht unendlichen Zahl sechseckiger Galerien zusammen, mit weiten Luftschächten in der Mitte, eingefasst von sehr niedrigen Geländern. Von jedem Sechseck kann man die unteren und oberen Stockwerke sehen: ohne Ende. Die Anordnung der Galerien ist immer gleich. Zwanzig Bücherregale, fünf breite Regale auf jeder Seite, verdecken alle Seiten außer zweien; ihre Höhe, die des Raums, übertrifft kaum die eines normalen Bibliothekars. [...] ich sage es ist nicht unlogisch zu denken, dass die Welt unendlich ist. Wer sie für begrenzt hält, postuliert, dass an entlegenen Orten die Gänge und Treppen und Sechsecke auf unfassliche Art aufhören können - was absurd ist. Wer sie für unbegrenzt hält, der vergisst, dass die mögliche Zahl der Bücher Grenzen setzt. Ich bin so kühn, die folgende Lösung des alten Problems vorzuschlagen: *Die Bibliothek ist unbegrenzt und zyklisch*. Wenn ein ewiger Wanderer sie in einer beliebigen Richtung durchmāße, so würde er nach Jahrhunderten feststellen, dass dieselben Bände in derselben Unordnung wiederkehren (die, wiederholt, eine Ordnung wäre: Die Ordnung). Meine Einsamkeit erfreut sich dieser eleganten Hoffnung.

Jorge Luis Borges, »Die Bibliothek von Babel« from »Fiktionen«, Fischer Taschenbuchverlag, 11th Ed. (2011).

»Ich hinterlasse den verschiedenen Zukünften (nicht allen) meinen Garten der Pfade, die sich verzweigen. Fast sofort hatte ich begriffen; *Der Garten der Pfade, die sich verzweigen* war der chaotische Roman. Die Wendung: *verschiedenen Zukünften (nicht allen)* brachte mich auf das Bild der Verzweigung in der Zeit, nicht im Raum. [...] In allen Fiktionen entscheidet sich ein Mensch angesichts verschiedener Möglichkeiten für eine und eliminiert die anderen; im Werk des schier unentwirrbaren Ts'ui Pen entscheidet er sich - gleichzeitig - für alle. Er *erschafft* so verschiedene Zukünfte, die ebenfalls auswuchern und sich verzweigen. Daher die Widersprüche im Roman. [...] Im Werk von Ts'ui Pen kommen sämtliche Lösungen vor; jede einzelne ist der Ausgangspunkt weiterer Verzweigungen. Manchmal streben die Pfade dieses Labyrinths zueinander hin; [...]«

Jorge Luis Borges, in »Der Garten der Pfade, die sich verzweigen« from »Fiktionen«, Fischer Taschenbuchverlag, 11th Ed. (2011).

Abstract

We study the behavior of Quantum Darwinism (Zurek, *Nature Physics* **5**, 181 - 188 (2009)) within the iterative, random unitary operations qubit-model of pure decoherence (Novotný *et al*, *New Jour. Phys.* **13**, 053052 (2011)). We conclude that Quantum Darwinism, which describes the quantum mechanical evolution of an open system from the point of view of its environment, is not a generic phenomenon, but depends on the specific form of initial states and on the type of system-environment interactions. Furthermore, we show that within the random unitary model the concept of Quantum Darwinism enables one to explicitly construct and specify artificial initial states of environment that allow to store information about an open system of interest and its pointer-basis with maximal efficiency.

Furthermore, we investigate the behavior of Quantum Darwinism after introducing dissipation into the iterative random unitary qubit model with pure decoherence in accord with V. Scarani *et al* (*Phys. Rev. Lett.* **88**, 097905 (2002)) and reconstruct the corresponding dissipative attractor space. We conclude that in Zurek's qubit model Quantum Darwinism depends on the order in which pure decoherence and dissipation act upon an initial state of the entire system. We show explicitly that introducing dissipation into the random unitary evolution model in general suppresses Quantum Darwinism (regardless of the order in which decoherence and dissipation are applied) for all positive non-zero values of the dissipation strength parameter, even for those initial state configurations which, in Zurek's qubit model and in the random unitary model with pure decoherence, would lead to Quantum Darwinism.

Finally, we discuss what happens with Quantum Darwinism after introducing into the iterative random unitary qubit model with pure decoherence (asymmetric) dissipation and dephasing, again in accord with V. Scarani *et al* (*Phys. Rev. Lett.* **88**, 097905 (2002)), and reconstruct the corresponding dissipative-dephasing attractor space. We conclude that dephasing does not influence the dynamics of quantum systems in Zurek's qubit model of Quantum Darwinism. Similarly, we see that also within the random unitary evolution dephasing does not alter or influence the (dis-)appearance of Quantum Darwinism: i.e. the random unitary evolution of a quantum state governed by the quantum operation enclosing pure decoherence, dissipation and dephasing is in the asymptotic limit of many iterations significantly determined by the interplay between pure decoherence and dissipation, whereas the dephasing part of the random unitary evolution does not contribute to the corresponding asymptotic attractor space of the random unitary iteration.

Abstract

Wir untersuchen das Verhalten von Quanten Darwinismus (Zurek, *Nature Physics* **5**, 181 - 188 (2009)) im Rahmen des iterativen Qubit-Modells der reinen Dekohärenz basierend auf zufälligen unitären Operationen (Novotný *et al*, *New Jour. Phys.* **13**, 053052 (2011)). Wir schlussfolgern, dass Quanten Darwinismus, der die quantenmechanische Evolution des offenen Systems aus der Perspektive seiner Umgebung beschreibt, kein generisches Phänomen ist, sondern von der spezifischen Form der Anfangszustände sowie der Wechselwirkungen zwischen System und Umgebung abhängt. Des Weiteren wird gezeigt, dass es innerhalb des zufälligen unitären Modells das Konzept des Quanten Darwinismus' erlaubt, explizit jene künstlichen Anfangszustände der Umgebung zu konstruieren, die Information über das beobachtete offene System und seine Zeiger-Zustandsbasis mit maximaler Effizienz speichern können.

Des Weiteren wird auch das Verhalten des Quanten Darwinismus' nach der Einführung der Dissipation in das zufällige, unitäre Qubit-Modell mit reiner Dekohärenz (gemäß V. Scarani *et al*, *Phys. Rev. Lett.* **88**, 097905 (2002)) studiert und der entsprechende dissipative Attraktorraum rekonstruiert. Wir schlussfolgern, dass im Zureks Qubit-Modell Quanten Darwinismus von der Reihenfolge abhängt, in der reine Dekohärenz und Dissipation auf den Anfangszustand des Gesamtsystems wirken. Wir zeigen explizit, dass das Einführen von Dissipation in das zufällige, unitäre Modell im Allgemeinen, und zwar für alle positiven Werte des Dissipationsstärkeparameters, den Quanten Darwinismus unterdrückt (ungeachtet der Reihenfolge, in der Dissipation und reine Dekohärenz wirken), sogar im Bezug auf jene Anfangszustände, die im Rahmen des Zurekschen sowie des zufälligen, unitären Modells mit reiner Dekohärenz das Auftreten des Quanten Darwinismus' erlauben würden.

Schlussendlich diskutieren wir, was mit dem Quanten Darwinismus passiert, nachdem man in das zufällige, unitäre Modell mit reiner Dekohärenz (asymmetrische) Dissipation und Dephasierung (wieder gemäß V. Scarani *et al*, *Phys. Rev. Lett.* **88**, 097905 (2002)) einführt, und rekonstruieren den entsprechenden dissipativ-dephasierten Attraktorraum. Wir schlussfolgern, dass Dephasierung die Dynamik von Quantensystemen in Zureks Modell des Quanten Darwinismus' nicht beeinflusst. Gleichmaßen sehen wir, dass auch im Rahmen der zufälligen, unitären Evolution die Dephasierung keinen Einfluss auf das Auftreten oder Verschwinden des Quanten Darwinismus' hat: mit anderen Worten, die zufällige, unitäre Entwicklung eines Quantenzustandes, bestimmt durch die reine Dekohärenz, Dissipation und Dephasierung einschließende Quantenoperation, hängt im asymptotischen Limes vieler Iterationen nur vom Zwischenspiel zwischen reiner Dekohärenz und Dissipation ab, wogegen der Dephasierung erzeugende Teil der zufälligen, unitären Evolution zum entsprechenden asymptotischen Attraktorraum nicht beiträgt.



Overview

The problem of the *quantum-to-classical transition* lies at the core of the fundamental interpretation of quantum mechanics. After all, it aims at investigating under which conditions effectively classical systems and properties around us emerge from the underlying quantum domain. To be more precise, this at first vague task addresses three questions which need to be answered:

1. *The existence of the preferred basis*: What singles out the preferred physical quantities (observables) in nature, or, in other words, why are physical systems usually observed to be in well-defined states (eigenstates) and not in superpositions of these states instead?
2. *The non-observability of interference*: Why is it extremely difficult (but not impossible) to observe quantum interference effects on macroscopic scales?
3. *The existence of outcomes*: Why do measurements yield outcomes at all, i.e. what selects (»picks«) a particular measurement result among the different outcome possibilities described by the corresponding quantum probability distribution?

The last of the three issues may be regarded as the (in)famous »measurement problem« of quantum mechanics which has caused a lot of discussions in the past and still remains unsolved. This »measurement problem« will also remain unsolved within the framework of this thesis, since it is almost inevitably connected with the (personally preferred) choice of a specific interpretation of quantum mechanics [6].

On the other hand, the concept of decoherence, introduced by Joos and Zeh in the 1970s and experimentally confirmed as a standard physical effect in the 1990s [2], turned out as undisputed when it comes to resolving the first two problems of the quantum-to-classical transition. This is expected, since these first two issues of the the quantum-to-classical transition and their resolution can be formulated in purely operational terms within the standard formalism of quantum mechanics, as already anticipated by the seminal work of Everett from 1957 [1] in the framework of his »*many worlds interpretation*«.

Namely, Everett's revolutionary concept of relative states abandoned the closeness of physical systems and the Copenhagen interpretation of quantum measurements by pointing out that in nature quantum systems always have to be regarded as embedded into a larger environment, whereas interferences between eigenstates of an open system interacting with its environment have to be accepted as objectively real, possible realizations of system's quantum evolution. Such an interpretation motivated Joos and Zeh to conclude that quantum measurements may be viewed as an interaction between an open system of interest and its environment, the latter monitoring the former. As a result of this measurement-like interaction a particular outcome (eigenvalue) of the observed system and its associated eigenstate are singled out from the set of all possible measurement results (realizations, »worlds«), such that interferences between states of a system's eigenbasis tend to zero in the limit of large environments containing many constituents. This suppression of interference terms between eigenstates in a system's density matrix w.r.t. large environments is termed decoherence and has resolved so far not only the problem with the non-observability of interference, but has also accounted for a valid explanation of the preferred system's basis (eigenbasis) by its surroundings.

Thus, according to the decoherence paradigm, the presence of large environments induces the loss of quantum coherences between system's eigenstates by letting the environment act as a »container« for information about the observed system of interest and its quantum coherences. In the end, after decoherence has accomplished its task, we are left with an almost completely mixed (»quasi-classical«) state of the observed system comprising only classical correlations between its corresponding eigenstates, whereas quantum correlations between systems eigenstates have leaked out into the environment.

Despite this success, the concept of decoherence has left many unanswered issues related with the quantum-to-classical transition, one of the most intriguing being the behavior of the environment after numerous interactions with the observed system. It was Zurek who in 1981 asked in this context, after taking the assumption of a tensor product decomposition of quantum systems into subsystems and the inherent necessity of such decomposition for the formulation of the decoherence program into account, whether one may ignore the environment when studying the evolution of open systems by degrading it to the role of an uncontrollable »remainder« of quantum system's under observation [3, 4]. This is an important question, especially when taking into account that environmental degrees of freedom, although uncontrollable and not directly relevant for considered observations, nevertheless contribute significantly to the evolution of the state of the system. How can we deal with the physical role of the environment during the process of decoherence?

Zurek suggests the following approach: first we need to endow quantum systems with a tensor product structure, which is a suitable mathematical formalism accounting for an appropriate description of mutually distinct subsystems (state spaces) within the entire universe a priori conceived as a closed system. For, decoherence is possible only if there is a freedom of subdividing an entire (closed) system into open subsystems that mutually interact. Second, we have to give up the idea of an “absolute” resolution of the quantum-to-classical transition by postulating and accepting the relevance of the distinct state subspaces and properties (such as decoherence itself) that emerge as a result of the correlation between these relatively (via tensor product) defined spaces.

Without any doubt, this relative view of systems and correlations leads to counterintuitive, nonclassical implications. Nevertheless, as already the issue of quantum entanglement has shown, these implications should not be taken as paradoxes that have to be further resolved. After all, as we shall also see in the course of this book, the quantum measurement process, understood as interaction between the observed open system and its environment, always creates entangled states between at least two subspaces of the entire system after decoherence has singled out the preferred system’s eigenbasis by suppressing quantum coherences in the limit of an increasing number of environmental degrees of freedom [9, 10]. In other words, as Schlosshauer points out (s. [6], page 103): *»Accepting some properties of nature as counterintuitive is indeed a satisfactory path to take in order to arrive at a description of nature that is as complete and objective as is allowed by the range of our experience (which is based on inherently local observations)«*. Interestingly, this »acceptance of counterintuitive physical results« also returns us to the original intention of Everett’s relative-states approach, when Everett himself demanded quantum coherences should be accepted as existing physical phenomena if von Neumann’s collapse postulate was to be explained from the basic principles of quantum theory instead of being postulated, as originally done by the Copenhagen interpretation.

But how can we utilize the existence of quantum coherences and their rapid suppression as a result of environment-induced decoherence of an open system interacting with its surroundings? So far we have focussed primarily on observations obtainable purely at the label of an open system of interest, regarding the environment solely as a »sink« carrying away (delocalizing) quantum coherences between system’s eigenbasis (also known as pointer basis). After all, this is a standard approach of a decoherence program which assumes that one does not have to observe the environment or interact with it, since the process of singling out system’s pointer states plays the most important role when trying to explain the emergence of system’s classical states from the quantum mechanical »substrate« and its dynamics.

However, since the system-environment interaction constantly encodes information about the observed system in the environment, the latter may be regarded as constituting a huge resource for the indirect acquisition of information about the system. Furthermore, we have to notice that in most cases observers gain information about the state of an open system by means of indirect observations. These indirect observations of the observed system amounts to intercepting fragments of environmental degrees of freedom that have interacted with the system in the past and thus contain information about system’s state. An indirect observation of an open system by its environment through the interception of environmental degrees of freedom (also known as non-demolition measurement [7]) is of crucial importance for the understanding of the quantum-to-classical transition. This fact becomes clear when taking into account the following characteristic feature of classical physics: in classical physics the state of a system can be reconstructed and agreed upon by numerous independent observers, each of which may be initially completely ignorant about the system’s state, without disturbing it in the course of a measurement. Precisely in this sense one may say that classical states preexist objectively, as the common understanding of the notion “classical reality” indeed suggests. On the other hand, measurements performed on a closed quantum system will in general tend to dramatically change the state of the observed system, which is why one cannot regard quantum states of a closed system as existing in the way classical states do.

Exactly because of the fact that any direct measurement performed on the observed system would, in general, always change (or even destroy) the system’s state, we have to figure out how classical reality emerges from the quantum dynamical evolution and what is the mechanism which leads to the »objectification« of observables. The environment-induced superselection of system’s preferred states (pointer states) [10] resolves this central problem of the quantum-to-classical transition, since it indeed explains why only a certain subset of all possible states (possible »worlds« from Everett’s point of view) in system’s Hilbert space are actually stable.

Zurek and his collaborators were the first to investigate and demonstrate that an environment, besides being a »which state monitor« for system eigenstates (pointer states), also plays an important role as a quantum memory which stores the relevant information about the observed system into its environmental fragments [3, 4, 8, 10]. Thus, Zurek has extended the role of environment from the medium selecting a system’s preferred (pointer) states and delocalizing coherences between these pointer states, to the means for transmitting and efficiently storing information about the state of the observed (monitored, measured) system. In other words, from Zurek’s perspective, the environment of an open system is not only a »sink« for information about non-classical correlations between system’s pointer states (as seen by the usual decoherence approach), but also a communication channel and a memory for transferring and storing information.

This operational role of environment has its own merits due to the fact that, since (Shannon-like) information (Shannon-entropy) about the effectively decohered system and its pointer basis, encoded in the environment and its fragments (parts), can be acquired without having to interact directly with the fragile system itself.

Apparently, if we reverse the perspective of the usual decoherence-paradigm by focussing thoroughly on the environment (assumed to comprise a huge number of storage cells, alias fragments) and its behavior in the limit of many interactions with the observed system (long-time limit) we are tempted, according to Zurek, to pose the following central questions and accept them as vital for the appropriate resolution of the quantum-to-classical transition problem: How is information about an open system *redundantly* and *robustly* stored in a large number of distinct environmental fragments (storage cells) such that multiple observers can recover this information without disturbing the system's state and without communicating (interacting) with each other, thereby achieving effective classicality of the state? And which kind of information about an open system is stored in the environment? [3, 4, 6, 8]

In order to answer these questions, Zurek has initiated a research project carried out under the name »environment as a witness program«. It studies which type of information about an open system can be stably stored and proliferated throughout the entire environment. The measure of (classical or quantum [3, 4, 5, 6, 8, 10]) mutual information has usually been used in order to explicitly quantify the degree of redundancy of information imprinted on environmental fragments as a result of many system-environment interactions.

The importance of redundancy in the framework of quantum measurement has been emphasized by Zurek already in the 1980s [10]. This notion of redundancy can be recovered from the mutual information in a following way: as already known [13, 15, 16, 17] mutual information (namely its both versions, Shannon-like and von Neumann-like) represents the amount of information about the open system under observation that can be acquired by measuring (intercepting) a fragment of the environment or even the entire environment. Although, from the practical point of view, the amount of information enclosed (stored) by each environmental fragment always turns out to be a little bit lower than the maximum information provided by the observed open system itself (as indicated by the system's von Neumann entropy) [10], this does not change the following facts:

- the classical mutual information depends on the choice of particular observables associated with the open system and its environment, quantifying how precise the outcome of a measurement of a given system's observable can be predicted after measuring this observable indirectly by intercepting a certain environmental fragment, whereas
- the quantum mutual information, as a generalization of classical mutual information, measures the amount of entropy generated after destroying all (quantum) correlations between an open system and its environment, quantifying the degree of system-environment correlations and their quantum or classical nature [5].

Since the classical mutual information expressed by means of Shannon-entropies and the quantum mutual information including von Neumann entropies have been confirmed to nearly coincide in the limit of system's effective decoherence, we will argue in the forthcoming chapters that the quantum mutual information quantifies the information gain and capacity of a quantum channel which transfers the (nearly) classical information about system's pointer basis into the environment. This operational interpretation of the quantum mutual information [13] will also enable us to investigate the practical applicability of the well-known fact that those system's observables which can be imprinted most completely in many distinguishable subsets of the environment coincide precisely with the pointer observable selected by the system-environment interaction [5, 10]. In other words, it is enough to intercept a relatively small fraction of the environment (when compared with the number of its constituents) to infer a high amount of the maximum (mutual) information about the system's pointer state, whereas all other non-pointer states of the open system under (indirect) observation could not be reconstructed because the information about their corresponding system-observables is not redundantly stored.

These environment-supersampled states of the observed system are thus states least perturbed by the interaction with the environment which can be most easily inferred, without disturbing the system, by intercepting environmental degrees of freedom: in other words, those system observables and their states most immune (invariant) with respect to the system-environment interaction are system's pointer states [5, 10]. Since the same information about the system's pointer observable is stored independently in numerous environmental cells (fragments), the number of such environmental fragments containing the full information about the system's pointer states is called the redundancy of these pointer observables of the observed system.

Thus, a high redundancy of system's observables means that multiple observers can measure these observables on different environmental fragments without interacting with each other and will automatically reach agreement on their results. In this sense, an effectively objective existence can be ascribed to the environment-supersampled states by saying that the pointer states of the system have survived numerous interactions with the environment and may be considered as »quasi-classical«, interaction-robust system's states, whose information has been efficiently transmitted and transferred into environmental fragments.

Similar to the Darwinistic concept »survival of the fittest«, the system's pointer states singled out by decoherence represent the »fittest« (»quasi-classical«) states of an open system that survive numerous interactions (measurements) with their environment long enough to deposit (imprint) multiple copies of their information into environmental storage cells [8].

This was a motivation for Zurek to coin the term »Quantum Darwinism« (QD) in order to name the phenomenon of decoherence-induced superselection of system's pointer states by their environment (comprising many constituents) and the efficient storage and redundant emergence of Classicality (classical information about the system's pointer basis) throughout the system's surroundings. The main task of this book will be primarily devoted to the investigation of the mathematical and physical conditions for the emergence of QD from the perspective of different physical models and the possibility of their practical application to the efficient information storage.

Although the research linked with the objectification of observables by redundancy, the »environment as a witness« program and the explicit dynamical evolution of the objectification is currently still an ongoing investigation, we may conclude, after taking numerous interesting studies involving more detailed and realistic system–environment models [8] into account, that Quantum Darwinism, based upon the attempt to give up the closed-system paradigm and describe observations as the interception of (system's) information redundantly and robustly stored in the environment, represents a very promising candidate for a purely quantum-mechanical account of the emergence of classicality from the quantum mechanical dynamics. One of the aims of this book will be to investigate whether it is possible to identify some universal, model-independent features of Quantum Darwinism that may be useful in resolving the problem of quantum-to-classical transition.

However, in the following we will also concentrate not only on the fundamental aspect of the quantum-to-classical transition related with physical conditions for the emergence of classical reality from quantum mechanical dynamics, but also on the operative aim of QD addressing the optimal (efficient) transfer and storage of system's »classical« Shannon-information (alias Shannon-entropy of an effectively decohered system) in the corresponding environment. Thus, both aspects of QD, the fundamental as well as its operative (practical) part, will be discussed in this thesis. In order to accomplish this, we first give a detailed exposition of mathematical criteria for the appearance of QD w.r.t. open systems and their environments consisting of qubits, before offering a detailed discussion of physical implications which can be drawn from the established mathematical QD-criteria. In sections 2-3 we therefore briefly introduce basic mathematical and physical concepts behind QD, especially the mathematical notion of partial information plots, quantum mutual information and its connection with a physical storage of information about an open system of interest into environment.

We conclude section 3 by discussing Zurek's toy qubit model of QD as a standard way of approaching the problem of efficient information storage. The main section of this first part of the book, section 4, presents the QD-condition, before offering a concise discussion about the operational interpretation of the quantum mutual information (subsection 4.1). This operational interpretation of the quantum mutual information allows us to conclude that from the physical point of view QD indicates highest efficiency for storing system's Shannon-entropy into its environment, whereas from the mathematical perspective QD includes a set of restrictions which allow one to establish a one-to-one correspondence between cardinalities of two eigenvalue sets and their corresponding entropies (subsection 4.2.3). In the end, it turns out that the so called »classically coherent qubit system-environment states« [13] comply with the specified set of QD-restrictions and thus validate the QD-conditions.

However, the largest part of section 4 (subsections 4.2.1-4.2.2, 4.2.4-4.2.5 and 4.4) deals with matrix structures of a joint system-environment density matrix in a standard computational basis that adhere to the QD-condition, which we conjecture to be the only possible QD-conformal matrix structures of system-environment states (subsection 4.3). This enables us to formulate in subsection 4.2.3 mathematical criteria for its validation, which a given matrix structure of a joint system-environment density matrix and its reduced density matrices of an open system and its environment have to fulfill (regardless of the concrete type of interaction that leads to a particular system-environment density matrix). Finally, we also focus on physical implications of the established QD-criteria, especially w.r.t. the interaction between an open system and its environment, which is also extensively used in the course of Zurek's approach towards QD [5], and conclude the discussion with a short summary (section 5).

Having introduced the concept of QD, we turn our attention to its behavior in the framework of different physical models. Accordingly, we intend to compare two qubit models of Quantum Darwinism: Zurek's evolution model [5] and the random unitary operations model [11, 29, 30] of an open k -qubit system S interacting with an n -qubit environment E . According to Zurek's model the one qubit open system acts via Controlled-NOT (CNOT)-transformations as a control unit on each of the n mutually non-interacting environmental qubits (targets) *only once*. On the other hand, the random unitary evolution generalizes Zurek's interaction procedure by iterating the directed graph (digraph) of CNOT-interactions between a $k \geq 1$ qubit open system and mutually non-interacting environmental qubits, represented by the corresponding quantum operation channel, many times until the underlying dynamics forces the initial (input) state $\hat{\rho}_{SE}^{\text{in}}$ of the system and its environment to converge to the final (output) system-environment state $\hat{\rho}_{SE}^{\text{out}}$. Such asymptotically evolved

system-environment final states can then be described by a subset of the total system-environment Hilbert-space, the so-called *attractor space*, and attractor states therein. From the practical point of view, we want to answer four questions:

1) Assuming that the pointer basis of a decohered open system exists, which initial system-environment states lead to Quantum Darwinism both in Zurek's and the random unitary model? We will see that in both models there are preferred initial state structures, particularly the initial product state $\hat{\rho}_{SE}^{in} = \hat{\rho}_S^{in} \otimes \hat{\rho}_E^{in}$, with a pure $k \geq 1$ qubit system $\hat{\rho}_S^{in}$ and a pure environmental one-registry state $\hat{\rho}_E^{in}$ of n mutually non-interacting qubits (for instance neutral atoms) in the standard computational basis, which lead to Quantum Darwinism in Zurek's and in the random unitary model. However, we will also see differences between both models: whereas in Zurek's model the above pure initial system-environment product state leads to Quantum Darwinism for all $k \geq 1$, the random unitary model will allow efficient storage of system's Shannon-information (computed with respect to system's pointer basis) into environment only for one qubit open systems, as long as the environment comprises only qubit (two-level) storage cells.

2) Does Quantum Darwinism, and thus a perfect transfer of system's Shannon-entropy into its environment, depend on a specific model being used, or is it a model-independent phenomenon? Namely, since the random unitary evolution can model open systems subject to pure decoherence by singling out the corresponding pointer states as a result of the asymptotic iterative dynamics, it also enables one to specify (in comparison with Zurek's model) which types of system-environment initial states store the "classical" Shannon-information about an open system and its pointer-basis efficiently in the surrounding environment and what happens with Quantum Darwinism if we use (in both models) non-CNOT members of the one-parameter family of unitary qubit-qubit transformations. Finally, we also want to use the random unitary model to see whether Quantum Darwinism appears if we introduce into the corresponding interaction digraph (CNOT or non-CNOT) interactions between environmental qubits. Unfortunately, it will turn out that Quantum Darwinism depends on the underlying dynamical model and appears both in Zurek's and the random unitary model only if the measurement interaction transferring system's Shannon-information into the surrounding environment is the CNOT-operation, whereas other non-CNOT unitary system-environment qubit-qubit interactions would inevitably suppress the appearance of QD. Also, we will conclude that Zurek's qubit model, contrary to the random unitary evolution, is not suitable for describing the impact of mutually interacting environmental qubits on Quantum Darwinism. However, the random unitary evolution will reveal that mutually interacting environmental qubits also tend to suppress Quantum Darwinism in the asymptotic limit of many iterations.

3) Is Quantum Darwinism, and thus a perfect transfer of system's Shannon-information into the environment, possible if we introduce into both qubit models dissipation by means of the two-qubit unitary dissipative transformation with a real-valued dissipation strength in accord with the work of Scarani et al. [26]? Since random unitary evolution can model systems subject to pure decoherence by singling out the corresponding pointer states as a result of the asymptotic iterative dynamics, it also enables one to specify (in comparison with Zurek's model) which types of system-environment initial states (if any) could store the "classical" Shannon-information about an open system of interest and its pointer-basis efficiently into environment despite of dissipation. The forthcoming discussion will reveal that Quantum Darwinism remains suppressed as soon as the real-valued dissipation strength parameter is non-zero, indicating that dissipation in general, in Zurek's as well as in the random unitary evolution model, causes partial leakage of system's Shannon-information into the fraction of a larger environment that is a priori traced out when considering the environment E of interest.

4) Are there initial density matrix structures of system and its environment that would allow to store the system's Shannon-information in the environment efficiently (and thus let QD emerge) if we introduce dissipation and dephasing into the corresponding asymptotic random unitary dynamics? In this context we conclude, by extending Zurek's dissipative model with an additional, unitary two-qubit dephasing operator, as discussed by Scarani et al. [26] (with a real-valued dephasing rate), that dephasing does not influence the results of this qubit model obtained w.r.t. the pure decoherence or the dissipative dynamics. Similarly, after introducing the dissipative-dephasing unitary two-qubit operator from [26] into the iterative random unitary dynamics, we see that also within the random unitary evolution model dephasing does not alter or influence the appearance of Quantum Darwinism: in other words, the random unitary evolution of a quantum state, governed by the unitary transformation leading to pure decoherence (CNOT transformation), dissipation and dephasing, is in the asymptotic limit of many iterations significantly determined by the interplay between pure decoherence and dissipation, whereas the dephasing part of the corresponding quantum operation does not contribute to the attractor space of the asymptotic random unitary iteration.

This thesis is organized as follows: In part I we discuss mathematical criteria for the appearance of QD. After a short introduction into historical and physical aspects of QD (sections 1 and 2), we discuss in section 3 mathematical aspects of QD (quantum mutual information, partial information plots, system's classical information and its redundancy, see subsection 3.1) and Zurek's toy qubit model of QD as a specific physical example and application of introduced mathematical concepts (subsection 3.2). This concludes the introductory part of the thesis.

In section 4 the main topic of part I is discussed: the mathematical criteria for the appearance of QD. We begin our discussion by relating the mutual information with quantum channel capacity and the efficiency of storing system's Shannon-information (»classical entropy«) in its environment (subsection 4.1). This enables us to interpret Zurek's concept of QD from the information-theoretical point of view. In subsections 4.2-4.4 we turn our attention to density matrix structures of the system-environmental output state which satisfy mathematical and physical QD-criteria regardless of the dynamics which has generated them. Such established QD-criteria allow us to generalize the CNOT-transformation used within the framework of Zurek's qubit toy model to a one-parameter family of unitary transformations and explore whether QD appears after applying Zurek's evolution algorithm w.r.t. members of this one-parameter family of transformations other than CNOT (subsection 4.2.5). Section 5 summarizes the results of part I.

Part II, the central part of the thesis, is mainly dedicated to the description of QD in the framework of the iterative, random unitary evolution model. In section 7 we discuss Zurek's qubit toy model of QD w.r.t. different input states of an open system and its environment (the latter comprising mutually interacting or non-interacting qubits). This approach will help us to specify those density matrix structures of input states which, after undergoing Zurek's CNOT-evolution, enable us to use the environment as an efficient quantum memory for system's Shannon-information.

In section 8 we introduce the formalism of random unitary evolution and investigate its predictions regarding the appearance of QD w.r.t. pure decoherence. This enables us to compare the behavior of QD in the framework of Zurek's and the random unitary model from the perspective of pure decoherence. In sections 9 and 10 we extend and complete the discussion of QD and its dynamical stability by introducing into Zurek's and the random unitary evolution model dissipation and dephasing, respectively. Finally, section 11 offers a brief summary of the most important conclusions obtained throughout the entire Part II of the book, as well as an outlook on further interesting problems.

Technical details are discussed in 12 appendices (part III): in Appendix A we discuss criteria for basis independence of mutual information, which is of use when transforming QD-compliant density matrix structures established in Part I of the book between different coordinate bases. Appendix B introduces a matrix realignment method which is extensively used in section 4 when discussing the QD-compliance of different density matrix structures. Appendix C presents some simple quantum Darwinistic density matrix structures that are used in section 4 as »building blocks« when designing more general density matrix structures for open qubit systems and their environments comprising an arbitrarily high (but finite) number of constituents (qubits). These three Appendices are connected with Part I of the thesis.

The remaining nine Appendices are associated with Part II of the book: Appendix D lists exemplary input states and von Neumann entropies of the entire system and its subsystems obtained from the corresponding output states in the course of Zurek's qubit model of QD. Appendix E explains the relation between QD and the CNOT symmetry states in Zurek's and in the random unitary qubit model. Appendices F and G briefly introduce the Gram-Schmidt-orthonormalization procedure and the QR-decomposition, respectively. In Appendix H we reconstruct minimal, maximal and intermediate attractor spaces of the random unitary model with pure decoherence. Appendix I exemplifies the application of the Gram-Schmidt-orthonormalization procedure to the states of the minimal attractor space of the random unitary model with pure decoherence. Appendix J offers a list of output states of the random unitary evolution with pure decoherence used in section 8. Appendix K derives the explicit form of a general unitary transformation comprising pure decoherence, dissipation and dephasing which is more suitable for numerical results discussed in sections 9 and 10. Finally, Appendix L presents useful diagrammatical computation schemes for obtaining output density matrices which are discussed in section 10 in the framework of Zurek's qubit model of QD.

Acknowledgements

I would like to thank my supervisor Prof. Dr. Gernot Alber for having offered me the opportunity to deal extensively with Quantum Darwinism and Random Unitary Operations in the framework of my PhD-research and thus gain new insights into its widely applicable analytical and numerical techniques. In addition, I also thank him for his support, encouragement and also for his strong interest in my topic of research, as well as for enlightening discussions which allowed me to broaden my theoretical knowledge. Furthermore, special credits go to my colleagues Zsolt Bernad, Mauricio Torres, Ullrich Seyfarth, Joe Rennes, Jaroslav Novotny, Florian Sokoli, Holger Frydrych and Nils Trautmann for enlightening discussions and constructive critical suggestions. Finally, I would also like to thank my family for constant support and love.

Contents

I	Mathematical Criteria for the Appearance of Quantum Darwinism	23
1	Introduction	24
2	Physical aspects of Quantum Darwinism	25
3	Mutual information (MI) and mathematical aspects of Quantum Darwinism	26
3.1	Partial Information Plots (PIP)	27
3.2	Zurek's toy qubit-model of Quantum Darwinism	28
4	QD-condition and its validation	30
4.1	On operational interpretation of the quantum Mutual Information	31
4.1.1	Information gain and entanglement cost	31
4.1.2	Classical discrete noisy symmetric channels	32
4.1.3	Classical channel capacity C and Shannon's coding theorem	33
4.1.4	Quantum channel noise and quantum channel capacity χ	34
4.1.5	»Quantum Darwinism is generic«	36
4.1.6	Quantum information gain of a measurement	38
4.1.7	Quantum error correction	40
4.1.8	Schumacher's quantum coding theorem	42
4.1.9	Quantum Darwinism and χ	43
4.1.10	Conclusions	47
4.2	Quantum Darwinistic many-qubit system-environment output states	48
4.2.1	Assumption 1: system's pointer states do not overlap, no environmental coherences	48
4.2.2	Assumption 2: system's pointer states do not overlap, environmental coherences allowed	52
4.2.3	Necessary and sufficient conditions for Quantum Darwinism	55
4.2.4	Assumption 3: system's pointer states overlap, no environmental coherences	59
4.2.5	Assumption 4: system's pointer states overlap, environmental coherences allowed	62
4.3	Conjecture	72
4.4	Quantum Darwinistic density matrix structures for many-qubit open systems	73
5	Summary	74
II	Random Unitary Evolution and Quantum Darwinism	76
6	Introduction	77
7	A qubit toy-model of Quantum Darwinism	79
7.1	Different system-environment input states	80
7.2	Zurek's model of Quantum Darwinism and non-CNOT interactions	83
7.3	Zurek's model of Quantum Darwinism with mutually interacting environmental qubits	84
8	Random unitary model of Quantum Darwinism	85
8.1	Minimal attractor space and its structure	86
8.1.1	State structure of the attractor space	87
8.1.2	Results of the CNOT-evolution	91
8.1.3	Non-CNOT-evolution	97
8.1.4	Concluding remarks: Quantum Darwinism in the minimal $\lambda = 1$ attractor space of the random unitary evolution model with respect to f	98
8.2	Short time limit of the random unitary evolution	99

8.3	Maximal attractor space and its structure	101
8.3.1	State structure of the attractor space	103
8.3.2	Results of the CNOT-evolution	104
8.3.3	Non-CNOT-evolution	120
8.4	Mutual Information-comparison: maximal and minimal vs intermediate attractor spaces	120
8.5	Summary and outlook	123
9	Random Unitary model of Quantum Darwinism with dissipation	124
9.1	Random unitary operations perspective on Quantum Darwinism: pure decoherence vs dissipation	125
9.2	Numerical reconstruction of the dissipative attractor space	128
9.3	Analytic reconstruction of the dissipative attractor space	130
9.4	Summary and outlook	131
10	Random Unitary model of Quantum Darwinism with dissipation and dephasing	132
10.1	Pure decoherence, dissipation and dephasing in Zurek's model of Quantum Darwinism	133
10.2	Numerical reconstruction of the dissipative-dephased attractor space	135
10.3	Analytic reconstruction of the dissipative-dephased attractor space	137
10.4	Summary and outlook	138
11	Conclusions and outlook	139
III	Appendices	141
A	On basis dependence of MI w.r.t. basis changes in Eq. (13)	141
B	Matrix realignment method for partial traces of $(\mathbb{C}^M \otimes \mathbb{C}^N)$-density matrices	142
C	QD-conformal matrix structures of $\hat{\rho}_{SE}^{out}$ for $(k = 1, n = 1)$	142
D	List of exemplary input and output states in Zurek's model of Quantum Darwinism	149
E	Quantum Darwinism and eigenstates of Eq. (9)-(10)	149
F	Gram-Schmidt orthonormalization	150
G	QR-decomposition	151
H	Analytic reconstruction of attractor spaces	151
H.1	Minimal attractor space	152
H.1.1	Dimensionality	152
H.1.2	State structure	152
H.2	Maximal attractor space	155
H.2.1	Dimensionality	155
H.2.2	State structure	156
H.3	Intermediate attractor spaces	156
H.3.1	Dimensionality	156
H.3.2	State structure	158
I	Gram-Schmidt-Orthonormalization (GSO) of the minimal $\{\lambda = 1\}$ attractor space in Eq. (365)	163
I.1	Case study: $k = 1$ qubit S, $n \geq 1$ qubit E	164
I.1.1	The $ 0\rangle \langle 0 $ -subspace of S	164
I.1.2	The $ 1\rangle \langle 0 $ - and $ 0\rangle \langle 1 $ -subspaces of S	165
I.1.3	The $ 1\rangle \langle 1 $ -subspace of S	166
I.2	Generalization to open k-qubit S	167
J	Output states $\hat{\rho}_{SE}^{out}$ of the random unitary evolution used in section 8	167
J.1	Output states $\hat{\rho}_{SE}^{out}$ of the random unitary evolution for the maximal attractor space	167
J.2	Output states $\hat{\rho}_{SE}^{out}$ of the random unitary evolution for the minimal attractor space	169
J.3	Output state $\hat{\rho}_{SE}^{out}$ of the random unitary evolution for the intermediate attractor space	172

K	Eq. (258) for specific parameter values	172
L	S-E-output states for the asymmetric dissipation in Zurek's qubit model	174
	References, List of Figures, List of Tables and Index	175

Part I

Mathematical Criteria for the Appearance of Quantum Darwinism

Abstract

We discuss mathematical criteria for the appearance of Quantum Darwinism (QD), introduced by Zurek (Nature Physics 5, 181 - 188 (2009)) as an attempt at explaining the emergence of Classicality from the quantum mechanical dynamics of open quantum systems interacting with their respective environments. The open system and its environment are modeled as physical entities consisting of qubits. We establish general necessary and sufficient mathematical criteria (»QD-criteria«) which a given matrix structure of a joint system-environment density matrix and its reduced density matrices of the corresponding qubit subsystems (apart from a given unitary invariance of their eigenvalue spectra) have to fulfill, in order for the QD-'plateau' of the quantum mutual information, plotted with respect to the environmental fraction-parameter, to appear, regardless of the concrete type of interaction that leads to the QD-compliant system-environment output states. We also investigate physical implications of the aforementioned mathematical QD-criteria that also adhere to general theorems for arbitrary (and not only for qubit) open systems discussed by F. G. S. L. Brandão, M. Piani and P. Horodecki in Nat. Com. 6, 7908 (2015). This helps us to better understand the special role played by the Controlled-NOT unitary operation among all other members of a more general one-parameter family of unitary transformations, especially with respect to Zurek's qubit model of QD and its description within the mathematical framework of the introduced QD-criteria. Finally, some conclusions concerning the structure of environment and the appearance of QD for open quantum systems containing more than one qubit are outlined.

1 Introduction

In order to overcome the system-observer duality postulated by the Copenhagen interpretation of quantum mechanics, **H. Everett III** proposed in the late 1950s the so called »relative state interpretation« of quantum mechanical systems and their dynamics governed by the Schroedinger equation [1]. Instead of exempting the »observer« from the deterministic laws of quantum dynamics, the »relative state interpretation« abandons Bohr's system-observer duality by **1)** assuming the existence of a total quantum state $|\Psi\rangle$ which should physically represent the entire universe enclosing an open system S and its environment E , **2)** upholding the universal validity of the Schroedinger evolution and **3)** postulating that after a measurement process each term within the expansion of $|\Psi\rangle$ (formulated w.r.t. the eigenbasis of the measured S -observable) has to correspond to a physical state that, as a particular »outcome« (result) of a measurement, must not be singled out *a priori*, neither formally nor physically. Since each of the physical (observable) S -states within a total quantum state $|\Psi\rangle$ may be, according to Everett, interpreted as relative to the state of other part (E) of the composite system (the universe), one remains inclined to view each addend in the S -eigenbasis expansion of $|\Psi\rangle$ as an alternative measurement outcome (or a particular evolutionary »branch«) of a »constantly splitting universe«.

However, instead of pursuing this speculative »many-worlds-interpretation« of Everett, we focus on the principle of decoherence, previously introduced in the 1970s by **E. Joos** and **H. D. Zeh** [2], which **W. H. Zurek** incorporated into the formalism of Everett's »relative state interpretation« during the 1980s in order to explain the emergence of the objective existence (reality) from quantum mechanical dynamics [3]. Since decoherence, occurring as a consequence of interaction (entanglement) between a measured open system S and its environment E , leads, in the limit of large environments containing many constituents that monitor S frequently, to the effective rapid disappearance (suppression) of purely quantum correlation (quantum interference) terms in $|\Psi\rangle$, Zurek names his decoherence-based extension of Everett's relative state concept the »existential interpretation«. By assigning a »relative objective existence« particularly to those »environment-superselcted« robust S -states (also known as *pointer states* of S) that appear most immune towards constant monitoring by their surrounding environment E , the »existential interpretation« attempts to define reality in accordance with a usual perception of classical S -states, the latter being those quantum (»quasi-classical«) S -states which can be inquired (measured) without being simultaneously perturbed or destroyed.

A thorough inspection of physical properties of the S - E -interaction would, in principle, enable the observer to determine the set of observable pointer states that can be measured on the system S without perturbing it, thus finding out the »objective« (classical) state of the system. Certainly, in $|\Psi\rangle$ different objective states of S are entangled in an unambiguous way with the corresponding parts (fractions) of E , giving rise to Everett's mutually excluding measurement outcomes (»branches«) of $|\Psi\rangle$. In this sense, one may say that different parts of E , representing individual observer identities and their objective states, label different $|\Psi\rangle$ -branches as physically distinct states, thus behaving as »memory cells« which store classical information about S and its interaction-robust pointer states.

Due to the rapid, decoherence-induced suppression of interference terms in $|\Psi\rangle$ between different environmental memory states, represented by outer-diagonal entries of the total S - E -state $\hat{\rho}_{\text{tot}} = |\Psi\rangle\langle\Psi|$, quantum (cat-like) superpositions in $\hat{\rho}_{\text{tot}}$ vanish exponentially w.r.t. the number of environmental constituents, whereas »quasi-classical« S -states, encoded in diagonal entries of $\hat{\rho}_{\text{tot}}$, leave redundant information copies (stable physical records or imprints) of themselves throughout the entire E . Following Zurek's line of argumentation [4], it may be concluded that those quantum mechanical S -states that appear robust towards constant monitoring by E would leave numerous copies of information about themselves in E over a long period of time (corresponding to many S - E -interactions). This simply implies that the more information copies of itself a certain S -state is able to store in E after many S - E -interactions, the more »quasi-classical« it becomes. In this way it may be said that the environment *superselects*, as a result of its constant interaction with the observed system S , the »pointer-state«-subset of all possible quantum S -state superpositions which, in turn, encloses those most interaction-robust, quasi-classical S -states, that have survived the aforementioned »constant monitoring over a long period of time«.

In the end, after decoherence has done its job, the observer can, by intercepting parts of E , determine the state, as well as the »pointer-basis« of the system S without perturbing it. Since, similar to the Darwinistic concept »survival of the fittest«, the S -pointer states represent the »fittest« (»quasi-classical«) states (among all possible quantum superpositions of S -states) that survive numerous S - E -interactions (measurements), Zurek has recently coined an expression **Quantum Darwinism (QD)** for the decoherence-induced environmental superselection of quasi-classical S -pointer states described so far [5].

In the following we intend to give a detailed exposition of mathematical criteria *necessary and sufficient* for the appearance of QD w.r.t. open systems S and their environments E consisting of qubits, before offering a detailed discussion of physical implications which can be drawn from the established mathematical QD-criteria.

The first part of the book is organized as follows. In sections 2-3 we introduce briefly basic mathematical and physical concepts behind QD, especially the mathematical notion of partial information plots, quantum mutual information and its connection with a physical storage of information about system S into environment E . We conclude section 3 by discussing Zurek's toy qubit model of QD as a standard way of approaching the problem of efficient information storage. The main section of this first part of the book, section 4, presents the QD-condition, before offering a concise discussion about the operational interpretation of the quantum mutual information (subsection 4.1). This operational interpretation of the quantum mutual information allows us to conclude that QD indicates from the physical point of view highest efficiency for storing system's Shannon-entropy into environment E , whereas from mathematical perspective QD encloses a set of restrictions which allow one to establish a one-to-one correspondence between cardinalities of two eigenvalue sets and their corresponding entropies (subsection 4.2.3). However, the largest part of section 4 (subsections 4.2.1-4.2.2, 4.2.4-4.2.5 and 4.4) deals with matrix structures of a joint system-environment density matrix $\hat{\rho}_{SE}$ in a standard computational basis that adhere to the QD-condition, which we conjecture to be the only possible QD-conformal matrix structures of $\hat{\rho}_{SE}$ (subsection 4.3). This enables us to formulate in subsection 4.2.3 mathematical criteria both necessary and sufficient for its validation, which a given matrix structure of a joint system-environment density matrix $\hat{\rho}_{SE}$ and its reduced density matrices $\hat{\rho}_S$ and $\hat{\rho}_E$ have to fulfill (regardless of the concrete type of interaction that leads to $\hat{\rho}_{SE}$). Finally, we also focus on physical implications of the established QD-criteria, especially w.r.t. the Controlled-NOT (CNOT) interaction between S and E , which is also extensively used in the course of Zurek's approach towards QD [5], and conclude the discussion with a short summary (section 5). All detailed calculations and theorems useful for the main text are part of three separate appendices: in appendix A we address unitary invariance of QD-conformal matrix structures established in the main text. Appendix B presents matrix realignment methods for partial tracing which are extensively used in the main text. Appendix C lists and discusses in detail QD-conformal matrix structures of $\hat{\rho}_{SE}$ containing a one qubit S and a one qubit E that are used as a reference for constructing more general matrix structures of $\hat{\rho}_{SE}$ in section 4.

2 Physical aspects of Quantum Darwinism

Usually, most decoherence-based explanations of the emergence of Classicality from quantum mechanical dynamics deal solely with observations which can be made at the level of an open system S , degrading its environment E to the role of a »sink« that carries away information about the pointer-basis of the observed system S and does not have to be further investigated after the S - E -interaction has singled out the interaction-robust S -states by decoherence [2, 6]. However, since the S - E -interaction constantly encodes information about the system in the environment by entangling S with E , one is tempted to assume that the environment indeed constitutes a large resource (»reservoir«) which could be used for the purpose of indirect acquisition of information about the system. Furthermore, if we realize that in most experimental setups observers acquire and gather information about the state of a system of interest by means of indirect observations, in other words by intercepting fragments of environment (»environmental degrees of freedom«) that have already interacted with the system in the past and thus enclose information about its preferred pointer-state, it would appear feasible to try to use a certain well-prepared environmental state as a »quantum memory card« that could store relevant information about an observed system. This point of view would modify and broaden the role of the environment, imposing it with a two-fold task of selecting preferred states for S (via decoherence, which implies the delocalization of local phase coherences between these states), as well as transmitting information about the pointer-state of the system.

From the point of view of a well-established everyday-experience classical states »pre-exist« objectively and as such constitute »classical reality« in a sense that the state of a system can be measured and agreed upon by many independent observers (which initially do not interact directly with a system under consideration and certainly do not interact with each other) *without disturbing it* (the so called **non-demolition measurement** [7]). This notion of a non-demolishing measurement of S would not be possible for completely closed systems, for these would lack their surroundings and thus the possibility of indirect measurements (performed by intercepting fragments of E), which would in turn lead to an inevitable alteration of the observed S -state. Therefore, it is impossible to regard quantum states of closed S as existing in a »classical sense«, which forces us to pose the following question [3]: *how does classical reality emerge from the quantum background, i.e., what causes »objectification« of observables in the above »classical« sense?* Or, since information about the open system is encoded in the environment and could be acquired without directly disturbing it (S), we may restate the question in a following manner: *which sort of information is **redundantly and robustly** memorized (imprinted) on numerous distinct environmental fragments, such that multiple observers may retrieve this information in a non-demolishing fashion, thereby confirming effective classicality of the state?*

Already Everett's »relative state interpretation« states clearly that in quantum theory objective existence of S has to be seen as a consequence of its relationship towards the observer or the environment, contrary to the classical case, where the existence of a measured system remains a »sole responsibility« of the »pre-existent« system itself. Consequently, the

above questions on the emergence of Classicality may also acquire the following corset: *Why could, according to Everett, relative states exist objectively if and only if observer should solely measure observables that commute with, as Zurek puts it, the »preexisting mixed state of the system«, e.g. with its decohered pointer observable [4]?* QD tries to answer this question by offering the most natural explanation based on the so called »environment as a witness«-program which interprets the environment E as a communication channel, trying simultaneously to investigate what kind of information about the system of interest can E store and proliferate in a stable, complete and redundant way.

Whereas the decoherence paradigm usually distinguishes between an open quantum system S and its environment E, without specifying the structure of the latter, QD subdivides E into *non-overlapping subenvironments* (»storage cells«) that have to be accessible to measurements and adhere to the demand that observables entangled with different subenvironments should mutually commute. According to the QD-assumption observers can find out the state of S indirectly, since its correlations with E allow the environment to absorb information about S and thus become a »witness« to the state of the observed system. In this context, objectivity of S-pointer states arises due to the fact that *the same* information about these states can be obtained independently by numerous observers from many environmental fragments, indicating that it is possible to quantify the »degree of objectivity« of S-states by simply counting the number of copies of their information record in E. This number of information copies deposited by a particular S-state into environmental fragments after many S-E-interactions reveals its **redundancy** - the higher the redundancy of a particular S-state is, the more »quasi-classical« it appears.

This is indeed the main idea of QD: only states that may be monitored (measured) without becoming perturbed (and which coincide with pointer states of S [8]) could survive numerous S-E-interactions long enough to deposit (imprint) multiple copies of their information into E, indicating that sufficiently large E-fragments that have caused the decoherence of S could usually provide enough information for multiple observers to infer the state of S. Thus, it may be concluded that high information redundancy of S-states within E implies that some information about the »fittest« S-observable that survived environmental monitoring has been successfully distributed throughout E, equipping the environment with the role of a reliable witness that stores redundant copies of information about preferred observables (alias pointer states of S), thus accounting for objective existence (»ein-selection« [3]) of preferred S-pointer states¹.

3 Mutual information (MI) and mathematical aspects of Quantum Darwinism

To explicitly quantify the degree of completeness and redundancy R of information about S imprinted on E, one usually uses the measure of **quantum mutual information (MI)** [4, 8], which quantifies the amount of information about S that can be acquired by simply probing (intercepting) E-fragments. The MI $I(S : E)$ between S and its E,

$$I(S : E) = H(S) + H(E) - H(S, E), \quad (1)$$

may be interpreted as *basis-independent* information about S shared with E, separating the joint entropy $H(S, E)$ of the composite system from the sum of the two subsystem-entropies $H(S)$ and $H(E)$. All entropies in (1) are positive-semi-definite and of **von Neumann** type, e.g. $H(X) = H(\hat{\rho}_X) = -\text{Tr}(\hat{\rho}_X \log_2 \hat{\rho}_X)$ for a density matrix $\hat{\rho}_X$ of a given (sub-)system X [4]. (1) also indicates the amount of R with which the information $H(S)$ about S is stored in E and its fragments (subsets): (1) vanishes in case of non-correlated density matrices $\hat{\rho}_S$ and $\hat{\rho}_E$ of S and E, implying $I_{\text{prod}}(S : E) = I(\hat{\rho}_{S,E}^{\text{prod}}) = 0$ for $\hat{\rho}_{S,E}^{\text{prod}} = \hat{\rho}_S \otimes \hat{\rho}_E$ and $I(\hat{\rho}_{S,E}^{\text{class}}) = H(S_{\text{class}})$ for classically correlated $\hat{\rho}_{S,E}^{\text{class}}$, with a basis-dependent Shannon entropy (»classical information«)

$$H(S_{\text{class}}) = -\sum_i p_i \log_2 p_i = H(\{|\pi_i\rangle\}), \quad p_i = \text{Tr}_E \langle \pi_i | \hat{\rho}_{S,E}^{\text{class}} | \pi_i \rangle, \quad (2)$$

where probabilities p_i emerge as partial traces of an effectively decohered (»quasi-classical«) S-state $\hat{\rho}_S^{\text{class}}$ w.r.t. the particular pointer-basis $\{|\pi_i\rangle\}$ of S (with the maximum $I(\hat{\rho}_{S,E}) = 2H(S_{\text{class}})$ of $I(S : E)$ indicating information about quantum correlations between S and E) [4, 5].

$\{|\pi_i\rangle\}$ corresponds to the set of instantaneous eigenstates of a particular observable which coincides with the set of states on the diagonal of $\hat{\rho}_S$ only in the limit of (almost) complete decoherence of S, $\hat{\rho}_S \approx \hat{\rho}_S^{\text{class}}$, since only then we may regard $\{|\pi_i\rangle\}$ as a set of »quasi-classical« pointer-states w.r.t. the particular S-observable. In general, $H(\hat{\rho}_S) \geq H(\{|\pi_i\rangle\})$, and since $H(\{|\pi_i\rangle\})$ in (2) coincides with $H(\hat{\rho}_S)$ only in the decoherence limit, (1) and its Shannon-like version

$$I_{\text{Sh}}(\{|\pi_i\rangle\} : \{|\lambda_j\rangle\}) = H(\{|\pi_i\rangle\}) + H(\{|\lambda_j\rangle\}) - H(\{|\pi_i\rangle\}, \{|\lambda_j\rangle\}) \quad (3)$$

¹The QD-concept of redundancy does not collide with the »no-cloning theorem«, for this theorem forbids cloning of arbitrary *unknown* quantum states, whereas within the course of QD decoherence »ein-selects« and imprints onto E-fragments copies of information about preferred (»fittest«) observables (pointer states) of S.

have to fulfill the relation [3, 8]

$$I(S : E) \geq I_{Sh}(\{\pi_i\} : \{A_j\}), \quad (4)$$

where $\{A_j\}$ denotes a set of eigenstates w.r.t. the observable of E . Thus, (3) and (4) imply that for realistic S and their E the amount of information about S that can be stored in each E -fragment in general has to be smaller than the maximum information provided by S itself (in other words $H(\{\pi_i\})$), since within realistic physical settings perfect proliferation of information cannot be realized.

3.1 Partial Information Plots (PIP)

We study an open k -qubit S that interacts with a composite E endowed with a structure $E \equiv \mathcal{E}_1 \otimes \mathcal{E}_2 \otimes \dots \otimes \mathcal{E}_n$ consisting of n qubits ($n, k \in \mathbb{N}$). This tensor decomposition of E into n non-overlapping parts allows us to identify each E -qubit with a particular fragment (»storage cell«) \mathcal{F} of E , indicating that all qubits within S and E are to be regarded *mutually distinguishable* and labeled by two sets of natural numbers, $\{1, \dots, k\}$ for S and $\{1, \dots, n\}$ for E . Accordingly, we intend to consider information $H(S)$ about S that can be gathered by intercepting \mathcal{F} , which may contain one or even more E -qubits that store $H(S)$. How much $H(S)$ can be obtained by intercepting \mathcal{F} containing a fraction $0 < f \leq 1$

$$f = \frac{\# \text{ subsystems (qubit-cells) in } \mathcal{F}}{\# \text{ subsystems (qubit-cells) in } E} \quad (5)$$

of E -qubits and which observable (pointer-basis) of S is recorded in E with highest R [4, 5]? Redundancy R_δ of interaction-robust information records about S denotes, due to (5), the number of disjoint fragments in the subset $\mathcal{F} \equiv E_{f_\delta}$ of E each of which can supply enough $H(S)$ (apart from a fraction $0 \leq \delta < 1$ of information that could not be proliferated throughout E due to inevitable information losses). Thus, we need to focus on the f_δ -dependence of the MI (1) if we wish to infer R_δ of stored $H(S)$ -records within \mathcal{F} . A convenient way to demonstrate the effects of QD is to consider **Partial Information Plots (PIP)** [4, 5]: these are two-dimensional plots which display the dependence of $I(S : E)$ on f_δ , i.e. $I(S : E_{f_\delta})$. If we interpret E as a set of $1 \leq m \leq n$ disjoint subsets (fragments) \mathcal{F}_i (with $\mathcal{F} = \bigcup_{i=1}^m \mathcal{F}_i$, $1 \leq m \leq n$ and $\mathcal{F}^c = E \setminus \mathcal{F}$ containing E -qubits not involved in the computation of (1)), each of them enclosing an arbitrary number of qubits N_i (with $\sum_{i=1}^m N_i = n$), then it is possible to characterize $I(S : E_{f_\delta})$ w.r.t. the fraction $f_\delta = \frac{|\mathcal{F}|}{n} = \frac{l}{n}$ of E -qubits that provide $H(S)$ by means of (1) (where $|\mathcal{F}| = l \in \mathbb{N}$ denotes the cardinality of the set \mathcal{F} , $n = |E|$ and $|\mathcal{F}^c| = n - |\mathcal{F}|$). $I(S : E_{f_\delta})$ emerges from (1) by performing partial tracing on $\hat{\rho}_S$, $\hat{\rho}_E$ and $\hat{\rho}_{SE}$, relating $H(\hat{\rho}_{SE})$ to $H(\hat{\rho}_S)$ and $H(\hat{\rho}_E)$, whose eigenvalues $\{\lambda_1, \dots, \lambda_d\}$ (where d is the dimensionality of $\hat{\rho}$ in question) have to be determined, before we can compute all $H(\hat{\rho}) = -\sum_{i=1}^d \lambda_i \log_2 \lambda_i \geq 0$, $\sum_{i=1}^d \lambda_i \stackrel{!}{=} 1$. One usually starts by tracing out all but $n(1 - f_\delta)$ E -qubits, where f_δ increases monotonously within the interval $f \in [\frac{1}{n}, \frac{2}{n}, \dots, \frac{n}{n}]$ ($n \in \mathbb{N}$), and computing the necessary eigenvalues that enter the following fractionalized version of (1)

$$I(S : E_{f_\delta}) = H(S) + H(E_{f_\delta}) - H(S, E_{f_\delta}), \quad (6)$$

while stipulating that each E -qubit should be traced out in *chronological order* (the register states $|z\rangle \equiv |q_1 \dots q_n\rangle$ of E in the standard computational basis are to be traced out from *right to left*, starting with qubit $q_n \in \{0, 1\}$ and ending with qubit $q_1 \in \{0, 1\}$) [4].

Although decoherence ein-selects $\{\pi_i\}$ of the monitored S , it alone does not for numerous E -observers to gain access to the available $H(S_{\text{class}})$ that needs to be proliferated (copied) throughout E , so that different observers could acquire it by intercepting \mathcal{F}_i of E , instead of altering the S -state by direct measurements [4]. The unitary measurement S - E -interaction $\hat{U}_{\text{int}}^{SE}$ acts in the course of QD as a copy-machine that distributes and imprints numerous copies of $H(S_{\text{class}})$ into \mathcal{F}_i of E by inducing entanglement between constituents of S and the corresponding »storage cells« of E . The simplest form of $\hat{U}_{\text{int}}^{SE}$ is an entanglement-inducing, unitary two-qubit S - E -transformation

$$\hat{U}_{\text{int}}^{SE} = \sum_j \hat{S}_j \otimes \hat{E}_j \Rightarrow \hat{S}_j |\pi_i\rangle = \lambda_i^{(j)} |\pi_i\rangle \forall (i \wedge j), \quad (7)$$

describing simultaneous monitoring of different Hermitean S -observables \hat{S}_j by E -operators \hat{E}_j , which amounts to the commutation relation $[\hat{S}_j, \hat{U}_{\text{int}}^{SE}] = 0$ (*non-demolition criterion*) and means that $\{\pi_i\}$ of S should be simultaneous (unperturbed) eigenstates of \hat{S}_j in the decoherence and measurement limit [6]. Thus, if we know the exact form of $\hat{U}_{\text{int}}^{SE}$,

which defines the evolution of S , then it will be easy to infer the pointer-basis $\{|\pi_i\rangle\}$ via (7). Without specifying the type of $\hat{U}_{\text{int}}^{\text{SE}}$ at this point, we may conclude that QD should manifest itself in the following form of PIP (s. Fig. 1 below) [4]: States of $\hat{\rho}_{S,E}$ created by decoherence (due to the constant monitoring of $\{|\pi_i\rangle\}$ by E), allow one to gain almost all of $H(S_{\text{class}})$ accessible through local measurements from a small E -fraction $f_\delta \leq k/n \ll 0.5$, forcing the corresponding PIPs to converge asymptotically to (2) (QD-'plateau' in Fig. 1). More (quantum-like) information (with $I(S : E_{f_\delta}) > H(S_{\text{class}})$) can be accessed only via global measurements on S and an E -fragment $f_\delta > 0.5$ corresponding to at least more than a half of E . In Fig. 1 the QD-'plateau' of PIPs is an indication of einselection, meaning that, each fragment \mathcal{F} of E that is large enough (i.e. $\dim \mathcal{F} \geq \dim S$) can enclose (almost) all of $H(S_{\text{class}})$, since in the limit $n \gg 1$ of effective decoherence, $H(S)$ in (6) approaches $(1 - \delta) H(S_{\text{class}})$ from (2), whereas $H(E_{f_\delta})$, which is *in general less* than $(1 - \delta) H(S_{\text{class}}) \approx H(S, \mathcal{F})$, corresponds to the maximal Shannon-entropy of the reduced $\hat{\rho}_{\mathcal{F}} = \sum_k p_k |A_k^{\mathcal{F}}\rangle \langle A_k^{\mathcal{F}}|$, s. (3)-(4), which reaches $H(S_{\text{class}})$ solely after decoherence has already effectively singled out $\{|\pi_i\rangle\}$ [8], since then the E -»pointer basis« $\{|A_j^{\mathcal{F}}\rangle\}$, correlated with $\{|\pi_i\rangle\}$ as $\hat{\rho}_{S,\mathcal{F}} = \sum_k p_k |\pi_k\rangle \langle \pi_k| |A_k^{\mathcal{F}}\rangle \langle A_k^{\mathcal{F}}| = \text{Tr}_{E \setminus \mathcal{F}} \hat{\rho}_{S,E}$, fulfills $\langle A_j^{\mathcal{F}} | A_k^{\mathcal{F}} \rangle \approx \delta_{jk}$.

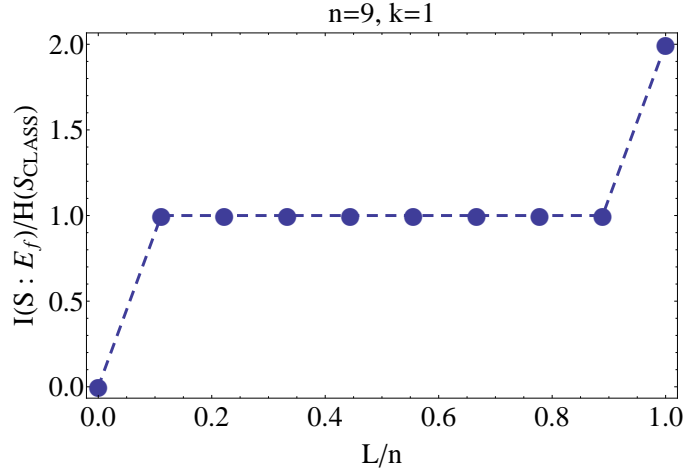


Figure 1: Partial information plot (PIP) of mutual information (MI) and the redundancy $R_{\delta=0} = R$ of system's »classical« entropy $H(\hat{\rho}_S^{\text{ut}}) \approx H(S_{\text{class}})$ stored in the n -qubit environment E w.r.t. the E -fraction parameter $0 < f = f_{\delta=0} = L/n \leq 1$ after the CNOT-evolution from (9)-(12) in accord with Zurek's qubit model: The initial S - E -state $\hat{\rho}_{SE}^{\text{in}} = \hat{\rho}_S^{\text{in}} \otimes \hat{\rho}_E^{\text{in}}$ involves a $k = 1$ qubit pure $\hat{\rho}_S^{\text{in}}$ (with $|\Psi_S^{\text{in}}\rangle = a|0\rangle + b|1\rangle$, $(a, b) \in \mathbb{C}$) and $\hat{\rho}_E^{\text{in}} = |0_n\rangle \langle 0_n|$ [4].

Thus, for $n \gg 1$ relations $H(E_{f_\delta}) \approx (1 - \delta) H(S_{\text{class}})$ and $I(S : E_{f_\delta}) \approx H(E_{f_\delta}) \approx (1 - \delta) H(S_{\text{class}})$ are valid already after considering a typical \mathcal{F} that corresponds to a small fraction f_δ of the entire E (in praxi this means $f_\delta \ll 0.5$), meaning that observers would find in E at least $1/f_\delta$ E -fragments \mathcal{F} which can independently reveal all (except δ of the missing) $H(S_{\text{class}})$. Clearly, convergence of $I(S : E_{f_\delta})$ to $(1 - \delta) H(S_{\text{class}})$ for $n \gg 1$ results in redundancy

$$R_\delta = 1/f_\delta, 0 \leq \delta < 1, I(S : E_{f_\delta}) \approx (1 - \delta) H(S_{\text{class}}) \text{ (effective decoherence)} \quad (8)$$

of $H(S_{\text{class}})$ which implies objectivity, since only if (8) applies observers can discover the same $\{|\pi_i\rangle\}$ *indirectly* and *independently* from each other and agree on their results. R_δ can be inferred from the length of the QD-'plateau' (in units of the minimal possible $|\mathcal{F}|$ -value²), from $I(S : E_{f_\delta}) = 0$ to $I(S : E_{f_\delta}) = (1 - \delta) H(S_{\text{class}})$, whereas δ relaxes the demands on completeness of $H(S_{\text{class}})$ w.r.t. more realistic physical settings [4, 5, 8]. In the following we will consider, without any loss of generality, perfect proliferation and duplication of $H(S_{\text{class}})$ throughout E and set $\delta \stackrel{!}{=} 0 \Rightarrow f_0 \stackrel{!}{=} f \Rightarrow R_0 \stackrel{!}{=} R$ in (8). Furthermore, we discuss in section 4 mathematical criteria for the appearance of QD w.r.t. $n \gg 1$, $H(S) \approx H(S_{\text{class}})$.

3.2 Zurek's toy qubit-model of Quantum Darwinism

The most common unitary, entanglement-inducing, operation used in the framework of numerous physical problems is the Controlled-NOT-gate (CNOT) [4, 8, 10], the most simple unitary two-qubit quantum-gate transforming a product state $|x, y\rangle = |x\rangle |y\rangle$ of two qubits $x, y \in \{0, 1\}$ into an entangled state by treating S -qubits as control-units and E -qubits as their targets w.r.t. the, for simplicity, standard one-qubit computational basis $\{|0\rangle, |1\rangle\}$.

Then one can incorporate the CNOT-gate $\hat{U}_{\text{CNOT}} |i\rangle_S |j\rangle_E = |i\rangle_S |i \oplus j\rangle_E$ (where \oplus denotes addition modulo 2) into

²In case of E -qubits we have $\min |\mathcal{F}| = 1$.

(7) by introducing the one-parameter family of two-qubit transformations between qubits i (control) and j (target), $\hat{I}_j = |0\rangle_j \langle 0| + |1\rangle_j \langle 1|$

$$\hat{U}_{ij}^{(\phi)} = |0\rangle_i \langle 0| \otimes \hat{I}_j + |1\rangle_i \langle 1| \otimes \hat{u}_j^{(\phi)}, \quad (9)$$

indicating that only if an S-qubit i should be in an excited state, the corresponding targeted E-qubit j has to be modified by a $(0 \leq \phi \leq \pi)$ -parameter $\hat{u}_j^{(\phi)}$ [11]

$$\hat{u}_j^{(\phi)} = \cos \phi \underbrace{\left(|0\rangle_j \langle 0| - |1\rangle_j \langle 1| \right)}_{=\hat{\sigma}_z} + \sin \phi \underbrace{\left(|0\rangle_j \langle 1| + |1\rangle_j \langle 0| \right)}_{=\hat{\sigma}_x}, \quad (10)$$

which for $\phi = \pi/2$ yields the CNOT-gate (with Pauli matrices $\hat{\sigma}_l$, $l \in \{x, y, z\}$)

$$\hat{u}_j^{(\phi=\pi/2)} = \left(|0\rangle_j \langle 1| + |1\rangle_j \langle 0| \right) = \hat{\sigma}_x \quad (11)$$

Now we turn our attention to the simplest qubit-model of QD, as suggested by Zurek [4, 5], involving an open pure $k = 1$ -qubit S (with $|\Psi_S^{\text{in}}\rangle = a|0\rangle + b|1\rangle$, $(a, b) \in \mathbb{C}$ and $|a|^2 + |b|^2 \stackrel{!}{=} 1$), which acts as a control-unit on its n -qubit target $E \equiv \mathcal{E}_1 \otimes \mathcal{E}_2 \otimes \dots \otimes \mathcal{E}_n$. Then the interaction between S and E has to occur as follows:

1. Start with a pure $k = 1$ -qubit open $\hat{\rho}_S^{\text{in}} = |\Psi_S^{\text{in}}\rangle \langle \Psi_S^{\text{in}}|$ and an arbitrary n -qubit $\hat{\rho}_E^{\text{in}}$, where $\hat{\rho}_{SE}^{\text{in}} = \hat{\rho}_S^{\text{in}} \otimes \hat{\rho}_E^{\text{in}}$.
2. Apply (9)-(11), such that the S-qubit interacts in a chronological order successively and only once with each one-qubit $\mathcal{F}_i \equiv \mathcal{E}_i$ ($\bigcup_{i=1}^n \mathcal{F}_i = E$) of E until all n mutually distinguishable E-qubits have interacted with S , resulting in an entangled (in general not necessarily a product) state $\hat{\rho}_{SE}^{\text{out}} \neq \hat{\rho}_S^{\text{out}} \otimes \hat{\rho}_E^{\text{out}}$.
3. Construct the PIP of the MI by successively tracing out in a chronological order $(n - L)$ qubits in $\hat{\rho}_{SE}^{\text{out}}$ and $\hat{\rho}_{SE}^{\text{out}}$ - this leads to the L -qubit $\hat{\rho}_{E_L}^{\text{out}}$ and $\hat{\rho}_{S E_L}^{\text{out}}$, with $0 < L \leq n$, and $0 < f = \frac{L}{n} \leq 1$. Compute the eigenvalue spectra $\{\lambda_1, \dots, \lambda_{d(f)}\}$ of $\hat{\rho}_S^{\text{out}}$, $\hat{\rho}_{E_f}^{\text{out}}$ and $\hat{\rho}_{S E_f}^{\text{out}}$ and the f -dependent $H(\hat{\rho}(f)) = -\sum_{i=1}^{d(f)} \lambda_i \log_2 \lambda_i \geq 0$, $\sum_{i=1}^{d(f)} \lambda_i \stackrel{!}{=} 1$, yielding (6), which we divide by $H(S_{\text{class}}) \approx H(\hat{\rho}_S^{\text{out}})$ to obtain the ratio $I(S : E_f) / H(S_{\text{class}})$ that quantifies the amount of the proliferated $H(S_{\text{class}})$ and R of the measured $\{\pi_i\}$.

We start with $\hat{\rho}_{SE}^{\text{in}} = \hat{\rho}_S^{\text{in}} \otimes \hat{\rho}_E^{\text{in}}$ where $\hat{\rho}_S^{\text{in}} = |\Psi_S^{\text{in}}\rangle \langle \Psi_S^{\text{in}}|$ and $|\hat{\rho}_E^{\text{in}}\rangle = |0_n\rangle \equiv |0\rangle^{\otimes n}$ (E-ground state). Let S transform each E-qubit via (11) without losses and *only once* until the entire E is affected, yielding

$$\begin{aligned} |\Psi_{SE_{L=n}}^{\text{out}}\rangle &= a|0\rangle \otimes |0_{L=n}\rangle + b|1\rangle \otimes |1_{L=n}\rangle \Rightarrow \left\{ |a|^2, |b|^2, 0 \text{ (} 2^{L+1} - 2 \text{ times)} \right\} \cdot (1 - \delta_{L,n}) + \\ &\quad \left\{ 1, 0 \text{ (} 2^{n+1} - 1 \text{ times)} \right\} \cdot \delta_{L,n} \Rightarrow H_{SE_L} (0 \leq L \leq n) = H(S_{\text{class}}) \cdot (1 - \delta_{L,n}) \\ \hat{\rho}_{E_L}^{\text{out}} &= |a|^2 |0_L\rangle \langle 0_L| + |b|^2 |1_L\rangle \langle 1_L| \Rightarrow \left\{ |a|^2, |b|^2, 0 \text{ (} 2^L - 2 \text{ times)} \right\} \Rightarrow H_{E_L} (0 < L \leq n) = H(S_{\text{class}}) \\ \hat{\rho}_S^{\text{out}} &= |a|^2 |0\rangle \langle 0| + |b|^2 |1\rangle \langle 1| \Rightarrow \left\{ |a|^2, |b|^2 \right\} \Rightarrow H_S (0 \leq L \leq n) = H(S_{\text{class}}) = -|a|^2 \log_2 |a|^2 - |b|^2 \log_2 |b|^2, \end{aligned} \quad (12)$$

which shows that $I(S : E_f)$, after the L -th E-qubit has been taken into account when computing the corresponding eigenvalues, increases from zero to $I(S : E_f) = H(S) + H(E_f) - H(S, E_f) \equiv H(S_{\text{class}}) \Rightarrow I(S : E_f) / H(S_{\text{class}}) = 1$, implying that each \mathcal{F}_i of E supplies complete information about the S-pointer observables $\{\pi_i\}$ [4]. Since the very first CNOT-operation forces S to decohere completely into its $\{\pi_i\} \equiv \{|0\rangle, |1\rangle\}$, one encounters the influence of QD on S : from all possible S -states, which started its dynamics within a pure $\hat{\rho}_S^{\text{in}}$, only diagonal elements survive constant monitoring of E , whereas off-diagonal elements of $\hat{\rho}_S^{\text{in}}$ vanish due to decoherence, i.e. monitoring of S by E selects a preferred $\{\pi_i\}$, leading to a continued increase of its R throughout E . After decoherence we obtain $I(S : E_f) = I_{\text{Sh}}(|0\rangle, |1\rangle : \{A_i^{\mathcal{F}}\}) = H(S_{\text{class}}) = H(E_f) = H(S, E_f)$, s. also (3), valid for any \mathcal{F}_i of E w.r.t. its effectively decohered »memory states« $\{A_i^{\mathcal{F}}\}$, as long $f < 1$. After inclusion of the entire E ($f = 1$) we obtain the maximum $I(S : E) = 2H(S_{\text{class}})$ of MI (»quantum peak«, accessible through global measurements of $\hat{\rho}_{SE}^{\text{out}}$ due to $H(S, \mathcal{F} = E) = 0$).

Since each E-qubit in (12) is assumed to contain a perfect information replica about $\{\pi_i\}$, its R is given by the number of \mathcal{F}_i (qubits) in E , e.g. $R = n$. $\{\pi_i\}$ is selected *per constructionem* via (9)-(11) and it remains unchanged under (11), which copies $H(S_{\text{class}})$ about $\{\pi_i\}$ into consecutive \mathcal{F}_i of E . This constrains the form of MI in its PIP (see Fig. 1), which jumps from 0 to $H(S_{\text{class}})$ of S at $f = 1/n$, continues along the 'plateau' until $f = 1 - 1/n$, before it eventually

jumps up again to $2H(S_{\text{class}})$ at $f = 1$. Thus, from $\hat{U}_{\text{int}}^{\text{SE}}$ in (9)-(11) we can infer $\{|\pi_i\rangle\}$ regardless of the order in which the n E-qubits are being successively traced out. $I(S : E_f)/H(S_{\text{class}}) \geq 1$ indicates high R (objectivity) of $H(S_{\text{class}})$ proliferated without losses (since $\delta = 0$) throughout E. Also, by intercepting already one E-qubit \mathcal{F}_i we can reconstruct $\{|\pi_i\rangle\}$. Only if we need a small \mathcal{F}_i , enclosing maximally $n \cdot f = k \ll n$ E-qubits [4], to reconstruct $\{|\pi_i\rangle\}$, QD appears: i.e., it is not only important that the PIP-'plateau' appears, more relevant is its length proportional to R of $\{|\pi_i\rangle\}$.

In the next section we will establish general mathematical criteria for the appearance of QD (regardless of a specific (7) that leads to $\hat{\rho}_{\text{SE}}^{\text{out}}(L)$), which would enable us to shed new light on Zurek's toy qubit-model and explain how the QD-'plateau' with high R could appear even if the corresponding E-pointer states should partly overlap. We will also gain a more detailed acquaintance with the CNOT-gate (9)-(11) from mathematical and physical perspective, enabling us to explain its outstanding role when it comes to copying $H(S_{\text{class}})$ into \mathcal{F}_i of E in comparison with other $\hat{u}_j^{(\phi)}$ in (9)-(10).

4 QD-condition and its validation

Given the output state

$$|\Psi_{\text{SE}}^{\text{out}}\rangle = \sum_{i,\beta} c_i |\varphi_i\rangle \otimes |\phi_i^{\beta(n)}\rangle, \quad (c_i \neq 0) \in \mathbb{C}, i \in \{1, \dots, 2^k\}, \beta(n) \in \{1, \dots, 2^n\}, \quad (13)$$

comprising an open ($k \in \mathbb{N}$)-qubit system S and its ($n \in \mathbb{N}$)-qubit environment E (states $|\varphi_i\rangle \equiv |\chi\rangle^{\otimes k}$, with $|\chi\rangle \in \{|0\rangle = (1, 0)^T, |1\rangle = (0, 1)^T\}$ (T denotes transposition), belong to the standard computational S-basis and $|\phi_i^{\beta(n)}\rangle \equiv \mathcal{N}_{\beta,i}^{-1/2} |\xi\rangle^{\otimes n}$, with $\mathcal{N}_{\beta,i} \in \mathbb{C}, |\xi\rangle \in \{|0\rangle, |1\rangle\}$, to the standard computational E-basis (eigenbasis) of $\hat{\sigma}_z$, respectively³), one can obtain the corresponding density matrices $\hat{\rho}_{\text{SE}}^{\text{out}}, \hat{\rho}_S^{\text{out}}$, and $\hat{\rho}_E^{\text{out}}$ in accordance with the following prescriptions

$$\begin{aligned} \hat{\rho}_{\text{SE}}^{\text{out}} &= \sum_{i,\beta,j,\gamma} c_i c_j^* |\varphi_i\rangle \langle \varphi_j| \otimes |\phi_i^{\beta(n)}\rangle \langle \phi_j^{\gamma(n)}|, \quad \beta(n) \equiv \beta(L=n) \\ \hat{\rho}_{\text{SE}}^{\text{out}}(L) &= \text{Tr}_{E^{1-f}}(\hat{\rho}_{\text{SE}}^{\text{out}}) = \sum_{i,\beta,j,\gamma} c_i c_j^* |\varphi_i\rangle \langle \varphi_j| \otimes |\phi_i^{\beta(L)}\rangle \langle \phi_j^{\gamma(L)}| \underbrace{\langle \phi_i^{\beta(n-L)} | \phi_j^{\gamma(n-L)} \rangle}_{\text{due to } \text{Tr}_{E^{1-f}}}, \quad (0 \leq f = \frac{(L \in \mathbb{N})}{n} \leq 1) \\ \hat{\rho}_S^{\text{out}} &= \sum_{i,\beta,j,\gamma} c_i c_j^* |\varphi_i\rangle \langle \varphi_j| \underbrace{\langle \phi_i^{\beta(n)} | \phi_j^{\gamma(n)} \rangle}_{:= [r_{\beta,\gamma}^{i,j} + \delta_{ij} \delta_{\beta\gamma} (1 - r_{\beta,\gamma}^{i,j})]} \equiv \text{Tr}_{E^0}[\hat{\rho}_{\text{SE}}^{\text{out}}] = \text{Tr}_E[\hat{\rho}_{\text{SE}}^{\text{out}}], \quad (0 < r < 1), \quad r_{\beta,\gamma}^{i,j} \equiv r_{\beta(L=n),\gamma(L=n)}^{i,j} \\ \hat{\rho}_E^{\text{out}} &= \sum_{i,\beta,\gamma} |c_i|^2 |\phi_i^{\beta(n)}\rangle \langle \phi_i^{\gamma(n)}| \equiv \text{Tr}_S[\hat{\rho}_{\text{SE}}^{\text{out}}], \quad \hat{\rho}_E^{\text{out}}(L) = \sum_{i,\beta,\gamma} |c_i|^2 |\phi_i^{\beta(L)}\rangle \langle \phi_i^{\gamma(L)}| \underbrace{\langle \phi_i^{\beta(n-L)} | \phi_j^{\gamma(n-L)} \rangle}_{\equiv \text{Tr}_S \text{Tr}_{E^{1-f}}[\hat{\rho}_{\text{SE}}^{\text{out}}]} \equiv \text{Tr}_S \text{Tr}_{E^{1-f}}[\hat{\rho}_{\text{SE}}^{\text{out}}] \end{aligned} \quad (14)$$

with a decoherence factor $r_{\beta,\gamma}^{i,j} \in \mathbb{R}$ (where $\lim_{n \rightarrow \infty} r_{\beta,\gamma}^{i,j} = 0 \forall (\beta, \gamma)$), such that $H(S)$ of S approaches its »classical value«

(Shannon entropy) $H(S_{\text{class}}) = -\sum_{i=1}^{2^k} |c_i|^2 \log_2 |c_i|^2$ ($|c_i|^2$ denote the diagonal eigenvalues of a completely decohered open system S, see also (3) above). In what follows we will assume this behaviour of the decoherence factor r to hold w.r.t. large E with $n \gg 1$, leading to an effectively decohered open system S with $\lim_{n \rightarrow \infty} H(S) = H(S_{\text{class}})$.

When looking at (13), we see that it represents the most general S-E-output state from the point of view of QD [4, 5], since each S-pointer state $|\varphi_i\rangle$ is correlated with an arbitrary linear combination of E-computational basis states $|\phi_i^{\beta(n)}\rangle$, which therefore also carry an index i in relation to the weightings $c_i \in \mathbb{C} \setminus \{0\}$, whereas index β may attain values from a subset $\mathcal{E}_{\text{sub}} \subseteq \{1, \dots, 2^n\}$. Thus, we formulate the so called »QD-condition«, whose validation will be of main concern to the forthcoming discussion:

Given the QD-condition (with $I(S : E_f)$ as in (6), $\delta = 0$ and an optimal value $1/n \leq f_{\text{opt}} \leq k/n$ of the fraction-parameter f)

$$\frac{I(S : E_f)}{H(S_{\text{class}})} = \frac{H(S) + H(E_f) - H(S, E_f)}{H(S_{\text{class}})} \equiv \frac{I_{\text{Sh}}(\{S\} : \{E_f\})}{H(S_{\text{class}})} \geq 1, \quad \text{with } (H(S) \equiv H(\{S\}) \approx H(S_{\text{class}})), \quad (15)$$

³In the following we will restrict our attention, for the sake of simplicity and without any loss of generality, to the standard CNOT-computational bases (eigenbases) of (11) for S and E, since the quantum mutual information $I(S : E_f)$ represents a basis independent von Neumann entropy whose normalized Shannon-version (3) $I(\{S\} : \{E_f\})/H(S_{\text{class}})$, that appears in the limit of effective decoherence, does not change its value w.r.t. any unitary changes (transformations) of bases in S or E (s. appendix A). The register states $|z\rangle \in \{1, \dots, 2^m\}$ of an $m \in \mathbb{N}$ qubit system are to be read in a chronological order, from left-to-right, i.e. $|z\rangle \equiv |q_1 \dots q_m\rangle = \sum_{i=1}^m q_i 2^{i-1}$, starting with qubit $q_1 \in \{0, 1\}$ and ending with qubit $q_m \in \{0, 1\}$.

which matrix-structure should $\hat{\rho}_{SE}^{\text{out}}$ display if $H(E_f) \geq H(S, E_f)$ is to remain true at least $\forall (k \leq L \leq n \gg 1)$ and regardless of the order in which the n E-qubits are being successively traced out?

In order to answer this question we need to discuss all possible assumptions that could occur w.r.t. the overlap $\sum_{\beta, \gamma} \langle \phi_i^{\beta(L)} | \phi_j^{\gamma(L)} \rangle$ in $\hat{\rho}_E^{\text{out}}$ and $\hat{\rho}_{SE}^{\text{out}}$ (equation (14) above), where $0 \leq (L \in \mathbb{N}) \leq n$ denotes the number of E-qubits which have **not** been partially traced out when discussing the dependence of $I(S : E_f)$ in (15) on the fraction $f = L/n$ of those E-qubits that constitute the matrices $\hat{\rho}_{SE}^{\text{out}}(L)$ and $\hat{\rho}_E^{\text{out}}(L)$.

4.1 On operational interpretation of the quantum Mutual Information

The previous discussion of Zurek's toy qubit-model of QD has shown that the characteristic 'plateau' of quantum MI $I(S : E_f)$ in (6), which quantifies the degree of correlations between interacting subsystems S and E , appears w.r.t. the environmental fraction f if the corresponding E-»memory cells« become mutually orthogonal in the decoherence as well as the interaction limit. Accordingly, Zurek's toy qubit-model of QD revealed to us in subsection 3.2 not only the importance of orthogonality of the environmental »memory states« $|\phi_i^{\beta(n)}\rangle$, correlated with the corresponding S -pointer states $|\varphi_i\rangle$ in (13), for the emergence of »quasi-classicality«, but it also highlighted the correlation-free structure of QD-conform output states $\hat{\rho}_{SE}^{\text{out}}(L)$ in (12), which all lack correlation terms $|\varphi_{i \neq j}\rangle \langle \varphi_j|$ between different S -pointer states (see also (14) above), as soon as one traces out a single E-qubit from $\hat{\rho}_{SE}^{\text{out}}(L)$ ($L = n - 1$), and remain correlation-free throughout the entire L -range $0 < L < n$.

This is reasonable, for effective decoherence of $\hat{\rho}_{SE}^{\text{out}}(L)$ implies a (sufficiently) rapid disappearance of pointer state correlations, as already indicated in (15). However, $\hat{\rho}_{SE}^{\text{out}}(L)$ does not have to remain correlation-free $\forall L < n$, since the contents of the present section will show us that partially overlapping environmental »memory states« can also lead to the validation of the QD-condition (15), if we enforce certain constraints on non-diagonal entries of $\hat{\rho}_{SE}^{\text{out}}(L)$, as long as these outer-diagonal entries *appear throughout* the entire L -range $0 < L < n$ (which was not the case in the course of Zurek's qubit model discussed so far). Since, as already pointed out in the previous section, the relation $H(S, \mathcal{F}) \geq H(E_f)$ allows equality only in the limit of effective decoherence, it will turn out that the QD-condition imposes a strong constraint on (physically and mathematically) allowed structures of matrix elements in $\hat{\rho}_{SE}^{\text{out}}(L)$, regardless of the concrete type of interaction $\hat{U}_{\text{int}}^{SE}$ in (7) that leads to $\hat{\rho}_{SE}^{\text{out}}(L)$.

However, before proceeding, let us make some remarks concerning the operational interpretation of the quantum MI $I(S : E_f)$ in (6), since this will also help us understand the significance of the optimal R-value $R_{\text{opt}} = f_{\text{pt}}^{-1}$ in (15).

4.1.1 Information gain and entanglement cost

The classical Shannon-version (3) of the quantum MI is usually defined by means of the conditional Shannon-entropy $H(S | |A_j\rangle)$ of S w.r.t. a given (particular) outcome $|A_j\rangle$ from the eigenbasis $\{|A_j\rangle\}$ of E [4]

$$\begin{aligned} H(S | |A_j\rangle) &= H(S, |A_j\rangle) - H(|A_j\rangle) = -\text{Tr} \left[\hat{\rho}_{S| |A_j\rangle} \log_2 \hat{\rho}_{S| |A_j\rangle} \right] \\ \hat{\rho}_{S| |A_j\rangle} &= \langle A_j | \hat{\rho}_{S,E} | A_j \rangle p_j^{-1} \\ p_j &= \text{Tr} \langle A_j | \hat{\rho}_{S,E} | A_j \rangle, \text{ (s.(2) above),} \end{aligned} \tag{16}$$

which emerges from the conditional density matrix $\hat{\rho}_{S| |A_j\rangle}$ by separating out of the joint entropy $H(S, |A_j\rangle)$ the information about E and quantifies information about S that is still missing after measuring (»finding out«) the (particular) state $|A_j\rangle$ of E . In other words, if we ask how much information about a specific observable S (characterized by its eigenbasis $\{|\pi_i\rangle\}$) will remain obscure after the observable E with eigenbasis $\{|A_j\rangle\}$ is measured, we need to average $H(S | |A_j\rangle)$ in (16) in accord with

$$H(S | \{|A_j\rangle\}) = \sum_j p_j H(S | |A_j\rangle), \tag{17}$$

thus obtaining the basis-dependent Shannon-conditional entropy $H(S | \{|A_j\rangle\})$ which, together with the joint probability distribution $p_{i,j} = \langle \pi_i, A_j | \hat{\rho}_{S,E} | \pi_i, A_j \rangle$, enters into the computation of the Shannon-MI from (2).

Therefore, taking (16) and (17) into account, we may point out that the quantum MI (6) indicates how much do S and E know about each other without referring to specific observables of the two subsystems. But what does the term »knowing« mean operationally? And what do we mean when saying that the quantum MI »quantifies the degree of correlations between interacting subsystems«? The degree of correlations simply indicates the physical (quantum or classical) nature of information shared between S and E, as already exemplified in subsection 3.2 above. On the other hand, we need to be careful with the notion of »knowing« or measuring a quantum system, since measurements in general alter quantum systems under observation, which is certainly not the case for classical systems. In this sense, we will be more specific by adopting the argumentation line of [13] which demonstrates that quantum MI defines the *optimal rate* (»information gain«) of classical communication or the *maximal entanglement-assisted capacity of a quantum measurement for transmitting classical information*.

Namely, if we look at the so called *classically coherent qubit S – E-states* (with the corresponding orthonormal bases $\{|i\rangle\}_{i=1}^{2^k}$ and $\{|\varphi_j\rangle\}_{j=1}^{2^n}$, respectively)

$$|\psi_{\text{out}}\rangle = \sum_i \sqrt{p_i} |i\rangle_S |\varphi_i\rangle_E, \quad (18)$$

which were frequently used in subsection 3.2 above within the framework of QD, we may interpret them as a result of a controlled, cptp (unital) map, alias a controlled, unital measurement procedure $\mathcal{M}(\cdot) \equiv \left\{ \sum_i p_i |i\rangle_S \langle i| \otimes \mathcal{M}_{E_i}(\cdot) \right\}$, with

POVM operators $\mathcal{M}_{E_i}(\cdot) = K_i^E(\cdot) K_i^{E\dagger}$ acting upon an n-qubit E and its input state $\hat{\rho}_E^{\text{in}}$ in $\hat{\rho}_{SE}^{\text{in}} = \hat{\rho}_S^{\text{in}} \otimes \hat{\rho}_E^{\text{in}}$ [14] (where a pure k-qubit input state $\hat{\rho}_S^{\text{in}}$ of S usually represents the control entity, as indicated by the subindex »i« in \mathcal{M}_{E_i} , and K_i^E denote Kraus operators that generate the operator sum representation of a measurement $\mathcal{M}(\cdot)$ [15, 16]), such that it is possible to decompose the measurement output $\hat{\rho}_{SE_L}^{\text{out}}$ (in which $n - L$ qubits from E have been traced out, $0 \leq L \leq n$) according to

$$\begin{aligned} \hat{\rho}_{SE_L}^{\text{out}} &= |\psi_{\text{out}}\rangle \langle \psi_{\text{out}}| = \sum_i p_i |i\rangle_S \langle i| \otimes \text{Tr}_{E_{n-L}} \{ \mathcal{M}_{E_i}(\hat{\rho}_E^{\text{in}}) \}, \\ \mathcal{M}(\cdot) &= \sum_i p_i |i\rangle_S \langle i| \otimes \mathcal{M}_{E_i}(\cdot) \Rightarrow \mathcal{M}(2^{-n} \hat{I}_n) = 2^{-n} \hat{I}_n. \end{aligned} \quad (19)$$

By doing so, [13] demonstrates that the so called **information gain** $g := q - e$, which involves the number q of S-qubits, whose classical information content is to be transmitted to E_L (q is therefore also known as the *classical communication cost*, here $q = k$), as well as the so called (maximal possible) *entanglement cost* $0 \leq e = \log_2 D_s \leq k$, calculated w.r.t. the Schmidt-rank D_s between S and E_L in $\hat{\rho}_{SE_L}^{\text{out}}$ of (19), is bounded from above

$$g := q - e \leq I(\mathcal{M}) = \max_{\{\hat{\rho}_S^{\text{out}}\}} I(S : E_L), \quad (20)$$

by the quantity $I(\mathcal{M})$ which emerges by maximizing the quantum MI $I(S : E_L)$ of (19) w.r.t. all possible system output states $\hat{\rho}_S^{\text{out}} = \text{Tr}_{E_L}(\hat{\rho}_{SE_L}^{\text{out}})$. In this sense one may say that $I(\mathcal{M})$ (and thus the maximized quantum MI) hints at an *optimal rate at which a measurement gathers (classical) information* about S. For instance, by looking at $\hat{\rho}_{SE_L}^{\text{out}}$ in (12) we see that $g = 1 - 1 = 0 \forall (0 < L < n)$, whereas $g = 1 - 0 = 1$ for $L = n$. This indicates that mainly those states $\hat{\rho}_{E_L}^{\text{out}}$ with a minimal entanglement cost e have a tendency to amplify the effects of QD. In the following subsection 4.2 we will characterize mathematically precisely those matrix structures $\hat{\rho}_{E_L}^{\text{out}}$ which allow us to achieve the maximal possible information gain $I(\mathcal{M})$ from (20) by adhering to the QD-condition (15) $\forall (0 < L < n)$.

4.1.2 Classical discrete noisy symmetric channels

Following Shannon's prominent paper [17] we may describe, without any loss of generality, symmetric discrete classical noisy channels between an extensive source X^k that generates binary sequences $x_{\text{seq}} = x_1 x_2 x_3 \dots x_k$ of length k (with mutually independent message bits (»symbols«) $x_i \in \{0, 1\}$, $i \in \{1, \dots, k\}$) and transmits them to the recipient source Y^k as a sequence $y_{\text{seq}} = y_1 y_2 y_3 \dots y_k$ (with $y_i \in \{0, 1\}$, $i \in \{1, \dots, k\}$) by means of the corresponding *probability vectors* $P(X^k) = (p(x_1), \dots, p(x_k))^T$ and $P(Y^k) = (p(y_1), \dots, p(y_k))^T$ that indicate success probabilities for transmitting a symbol x_i and receiving a message bit (a »symbol«) y_i . Additionally, in order to describe the influence of the channel on the transmitted message sequence y_{seq} one needs to specify the *symmetric conditioned probability matrix* $P_\varepsilon(X^k|Y^k) := [p_{ij}(\varepsilon)]_{k \times k}$ for transmitting x_i after having received y_j (with $i, j \in \{1, \dots, k\}$) whose entries $p_{ij}(\varepsilon) := p_\varepsilon(x_i|y_j)$ indicate the magnitude of transmission failure quantified by the noise parameter $0 \leq \varepsilon \leq 1$ (where $P(X^k) = P_\varepsilon(X^k|Y^k) P(Y^k)$).

By means of $P(X^k)$, $P(Y^k)$ and $P_\varepsilon(X^k|Y^k)$ one can easily compute the *joint probability matrix* $P(X^k, Y^k)$ and its entries $p(x_i, y_j) = p_\varepsilon(x_i|y_j) p(y_j)$ (by exploiting the theorem of Bayes), as well as the Shannon-entropies

$H(\{X^k\}) = -\sum_i p(x_i) \log_2 p(x_i)$, $H(\{Y^k\}) = -\sum_j p(y_j) \log_2 p(y_j)$ and the conditioned Shannon-entropy (equivocation [15, 16])

$$H(\{X^k\}|\{Y^k\}) = -\sum_{i,j} p(x_i, y_j) \log_2 p_\varepsilon(x_i|y_j), \quad (21)$$

in accordance with (16) and (17). (21) enables us to reexpress the Shannon-like mutual information I_{Sh} in (3) as

$$I_{Sh}(\{X^k\} : \{Y^k\}) = H(\{X^k\}) - H(\{X^k\}|\{Y^k\}), \quad (22)$$

which demonstrates that conditioning reduces the Shannon-entropy $H(\{X^k\})$ of the originator source X^k . Therefore, we may also say that the Shannon-like mutual information in (22) offers an appropriate measure of true (noisless) information about the source message X^k available to the recipient Y^k , whereas the equivocation $H(\{X^k\}|\{Y^k\})$ measures the absolute amount of informationless channel noise ε .

4.1.3 Classical channel capacity C and Shannon's coding theorem

Shannon interprets the mutual information (22) as a net channel capacity for transmitting x_{seq} w.r.t. a given probability distribution $P(X^k)$ of X^k [17], thereby defining the *channel capacity* C as a maximum achievable $I_{Sh}(\{X^k\} : \{Y^k\})$ taken over all possible probability distributions $P(X^k)$ of an input (originator source) X^k according to

$$C := \max_{P(X^k)} I_{Sh}(\{X^k\} : \{Y^k\}), \quad (23)$$

such that (23) achieves its maximum, at least w.r.t. discrete, *symmetric* classical channels, for equal probability distribution $P(X^k) = (p(x_1), \dots, p(x_k))^T = (k^{-1}, \dots, k^{-1})^T$ of input message bits x_i [15, 16]. As a second step, (23) leads us to the following definition of a *typical sequence* x_{seq}^{typ} [15, 16, 17]:

Given a 1-bit message source X with $P(X) = (p(x_1))^T$, $p(x_1 = 0) = q$, $p(x_1 = 1) = 1 - q$ ($0 < q < 1$), $\delta \ll 1$ and $H(\{X\}) = f(q) = -q \log_2 q - (1 - q) \log_2 (1 - q)$, then any sequence x_{seq}^{typ} (from the set Ω of all possible $|\Omega| = 2^k$ sequences x_{seq} of length k that can be generated by X^k), which satisfies

$$\begin{aligned} & \left| \frac{1}{k} \log_2 \frac{1}{p(x_{seq}^{typ})} - H(\{X\}) \right| < \delta \\ & \Rightarrow \left(\frac{1}{k} \log_2 \frac{1}{p(x_{seq}^{typ})} - H(\{X\}) \right)^2 < \delta^2 \\ & \Leftrightarrow 2^{-k[H(\{X\})+\delta]} < p(x_{seq}^{typ}) < 2^{-k[H(\{X\})-\delta]} \end{aligned} \quad (24)$$

is said to be typical within the error δ . Then the probability $p(x_{seq} \in M)$ that x_{seq} belongs to the typical subset $M \subset \Omega$ containing only typical sequences x_{seq}^{typ} will behave in the limit of extremely long sequences ($k \rightarrow \infty$) equiprobably, in accordance with

$$\begin{aligned} & \lim_{k \rightarrow \infty} p(x_{seq} \in M) = 2^{-kH(\{X\})} \\ & \Leftrightarrow p(x_{seq} \in M) = 2^{k[H(\{X\})-1]} = \frac{|M|}{|\Omega|}, \end{aligned} \quad (25)$$

whereas the number of typical sequences amounts to $|M| = 2^{kH(\{X\})}$.

Finally, Shannon uses (24) and (25) in order to formulate his well-known *classical coding theorem*, which utilizes the fact that in the limit $k \rightarrow \infty$ of infinite sequence lengths only typical sequences x_{seq}^{typ} are generated by the source X^k and transmitted to the recipient Y^k [15, 16, 17]:

Given a channel capacity C and a symbol source X^k (with $H(\{X^k\}) = kH(\{X\})$ due to the mutual independence of message bits x_i within $x_{seq} \equiv x_{seq}^{typ} \in M \subset \Omega$), which is used at an information rate $\bar{R} = \frac{n}{k} \leq C$ of $n < k$ distinguishable bits per time unit (i.e. $n = k\bar{R}$ bits and thus $N_{ts_{eq}}^{\bar{R}} = 2^n$ distinguishable typical sequences $(x_{seq}^{typ})^*$ are generated by X^k in duration of each typical message sequence x_{seq}^{typ} of length k), then there exists a code for which message symbols x_i of $(x_{seq}^{typ})^*$ can be transmitted through the channel with an arbitrary small error $\delta \ll 1$, according to the error probability

$$\begin{aligned} p_{err} &= \left(1 - p\left((x_{seq}^{typ})^* \in M\right) \right) \sim 2^{-k\delta} \\ &\Rightarrow \lim_{k \rightarrow \infty} p_{err} = 0, \end{aligned} \quad (26)$$

whereas the probability $p((x_{seq}^{typ})^* \in M)$ for transmitting a specific (distinguishable) typical sequence $(x_{seq}^{typ})^*$ out of a set M of $|M| = 2^{kH(\{X\})}$ possible typical sequences x_{seq}^{typ} amounts to

$$p((x_{seq}^{typ})^* \in M) = \frac{N_{tseq}^{\bar{R}}}{|M|} = \frac{2^n}{2^{kH(\{X\})}} = 2^{k[\bar{R} - H(\{X\})]}. \quad (27)$$

(26) and (27) indicate that the channel capacity $C \geq \bar{R}$ represents a maximal (ideal) rate at which (typical) input messages x_{seq}^{typ} («bit blocks of length k ») can be made uniquely distinguishable.

4.1.4 Quantum channel noise and quantum channel capacity χ

Quantum message \mathbf{M} is a «qubit block» of length n represented by the tensor state $|\mathbf{M}\rangle = |q_1 q_2 \dots q_n\rangle$, with each qubit $|q_i\rangle$ (for $i = \{1, \dots, n\}$) randomly selected from a symbol alphabet $\{|x_k\rangle\}_{k=1}^{N_s}$ of size N_s . Let the occurrence probability of each symbol $|x_k\rangle$ be p_k . Then the input state $\hat{\rho}_{\mathbf{M}}$ of a quantum message \mathbf{M} may be expressed as

$$\hat{\rho}_{\mathbf{M}} = |\mathbf{M}\rangle \langle \mathbf{M}| = \hat{\rho}_1 \otimes \dots \otimes \hat{\rho}_n = \hat{\rho}^{\otimes n}, \quad (28)$$

with a one qubit density operator $\hat{\rho}_i = \hat{\rho} = \sum_{k=1}^{N_s} p_k |x_k\rangle \langle x_k|$. Suppose the originator sends the message (28) to the recipient via a given quantum channel $\mathcal{E}(\cdot)$ such that the received «message qubit block» $\hat{\sigma}_{\mathbf{M}}$ acquires the operator sum representation

$$\hat{\sigma}_{\mathbf{M}} = \mathcal{E}(\hat{\rho}_{\mathbf{M}}) = \sum_{k=1}^{N_s} \hat{U}_k \hat{\rho}_{\mathbf{M}} \hat{U}_k^\dagger = \hat{\sigma}_1 \otimes \dots \otimes \hat{\sigma}_n \neq \hat{\rho}_{\mathbf{M}}, \quad (29)$$

with unitary transformations \hat{U}_k and $\hat{\sigma}_i = \mathcal{E}(\hat{\rho}_i)$. Then the Holevo-Schumacher-Westmoreland (HSW) capacity theorem states [15, 16]:

Given a «qubit block» source $\{\hat{\rho}_i\}$ with associated probability distribution $\{p_i = p(\hat{\rho}_i)\}$, the capacity χ of a noisy quantum channel $\mathcal{E}(\cdot)$ providing the (one qubit) operation $\hat{\sigma}_i = \mathcal{E}(\hat{\rho}_i)$ is given by

$$\begin{aligned} I_{Sh}(\{X^n\} : \{Y^n\}) &< \chi = \max_{\{p_i\}} [S(\langle \hat{\sigma}_i \rangle) - \langle S(\hat{\sigma}_i) \rangle] \\ &= \max_{\{p_i\}} [S(\mathcal{E}(\langle \hat{\rho}_i \rangle)) - \langle S(\mathcal{E}(\hat{\rho}_i)) \rangle] = \max_{\{p_i\}} \left[S\left(\sum_i p_i \hat{\sigma}_i\right) - \sum_i p_i S(\hat{\sigma}_i) \right] \\ &= \max_{\{p_i\}} \left\{ S\left[\mathcal{E}\left(\sum_i p_i \hat{\rho}_i\right)\right] - \sum_i p_i S(\mathcal{E}(\hat{\rho}_i)) \right\}, \end{aligned} \quad (30)$$

with X^n and Y^n (which generate and receive classical message codes of length n , respectively) denoting decohered (Shannon-like) versions of density matrices $\hat{\rho}_{\mathbf{M}}$ and $\hat{\sigma}_{\mathbf{M}}$ from (28) and (29), whereas $S(\cdot)$ represents in the present subsection 4.1 the von Neumann-entropy, χ' corresponds to the Holevo-bound and $\langle \cdot \rangle = \sum_i p_i (\cdot)$ stands for averaging over $\{p_i\}$.

Thus, according to the HSW-theorem (30) quantum channel capacity χ represents the maximum (ideal) code rate for which the probability of transmission error can be made arbitrarily small for sufficiently long code lengths ($n \gg 1$) of $|\mathbf{M}\rangle$. This means that if the originator chooses among $2^{n\bar{R}}$ distinguishable message possibilities with a code rate $\bar{R} > 0$, i.e. given a typical set $\Omega^{typ} \equiv \{\hat{\sigma}_{\mathbf{M}}^{typ}\}$ of received typical «qubit blocks» $\hat{\sigma}_{\mathbf{M}}^{typ}$ with cardinality $|\Omega^{typ}| = 2^{n\bar{R}}$, there is a corresponding set of POVM measurement operators $\{\hat{E}_{\mathbf{M}}\}$ (with $\hat{E}_0 = \hat{I}_n - \sum_{\mathbf{M} \neq 0} \hat{E}_{\mathbf{M}}$) such that the probability $p_{\mathbf{M}}$ of the recipient identifying $\mathbf{M} \in \Omega^{typ}$ is given by

$$p_{\mathbf{M}} = \text{Tr} [\hat{\sigma}_{\mathbf{M}} \hat{E}_{\mathbf{M}}], \quad (31)$$

whereas the corresponding averaged error probability $\langle p_{err} \rangle$ (associated with the measurement operator \hat{E}_0 for non-typical «qubit blocks» $\mathbf{M} \notin \Omega^{typ}$) amounts to

$$\langle p_{err} \rangle = \frac{\sum_{\mathbf{M} \neq 0} p_{\mathbf{M}}^{err}}{2^{n\bar{R}}}, \quad p_{\mathbf{M}}^{err} = 1 - p_{\mathbf{M}}. \quad (32)$$

In other words, if $\bar{R} < \chi$, then the HSW-theorem assures that for a given quantum channel $\mathcal{E}(\cdot)$ there exist quantum codes of large lengths ($n \gg 1$), for which $\langle p_{err} \rangle$ for recipient failing to identify a transmitted codeword $\hat{\sigma}_M = \mathcal{E}(\hat{\rho}_M)$ given an originator codeword $\hat{\rho}_M$ in (32) can be made arbitrarily small, i.e. $\lim_{n \rightarrow \infty} \langle p_{err} \rangle = 0$.

As an example that should illustrate the applicability of the HSW-theorem let us consider the depolarizing channel [15, 16]

$$\mathcal{E}(\hat{\rho}_i) = p \frac{\hat{I}_1}{2} + (1-p) \hat{\rho}_i \quad (33)$$

w.r.t. orthogonal one qubit input symbols $\hat{\rho}_1 = |0\rangle\langle 0|$ and $\hat{\rho}_1 = |1\rangle\langle 1|$ (associated with probabilities $p_2 = 1-p_1$), since this kind of input symbols would appropriately reflect the preassumption of the QD-condition (15) that characterizes an open system S (the originator source in the present context) as an effectively decohered entity interacting with its environment E (the recipient). For (33) we obtain the Holevo-bound χ' from (30)

$$\begin{aligned} \chi'(p, p_1) &= S \left[\mathcal{E} \left(\sum_{i=1}^2 p_i \hat{\rho}_i \right) \right] - \sum_{i=1}^2 p_i S[\mathcal{E}(\hat{\rho}_i)] \\ &= - \left[\frac{p}{2} + (1-p)p_1 \right] \log_2 \left[\frac{p}{2} + (1-p)p_1 \right] - \left[\frac{p}{2} + (1-p)(1-p_1) \right] \log_2 \left[\frac{p}{2} + (1-p)(1-p_1) \right] - f\left(\frac{p}{2}\right), \end{aligned} \quad (34)$$

and thus

$$\chi(p) = \max_{\{p_i\}} \chi'(p, p_1) = \chi'(p, p_1)|_{p_i=1/2} = 1 - f\left(\frac{p}{2}\right), \quad (35)$$

where $f\left(\frac{p}{2}\right)$ corresponds to the one qubit entropy function $f(q)$ introduced in (24), with $f\left(\frac{p}{2}\right) = f(q)|_{q=p/2}$. From (35) it can be readily inferred that $\chi(p)$ displays two extreme points: 1) $\chi(p) = 1$ for $p = 0$ (this corresponds to the ideal channel which leaves each input symbol $\hat{\rho}_i$ unchanged, $\mathcal{E}(\hat{\rho}_i) = \hat{\rho}_i$) and 2) $\chi(p) = 0$ for $p = 1$ (this corresponds to the useless, noisy channel which maps each input symbol $\hat{\rho}_i$ to a mixed one qubit state $\mathcal{E}(\hat{\rho}_i) = \frac{\hat{I}_1}{2}$, indicating that the input $\hat{\rho}_i$ cannot be deciphered by the recipient). However, what happens if we choose $0 < p < 1$? For example, if we assume $p = 0.1$ we are confronted with an almost ideal quantum channel (33), yielding for (35) $f\left(\frac{p}{2}\right)|_{p=0.1} \approx 0.25 \Rightarrow \chi(p=0.1) \approx 0.75$ qubits.

What does this capacity value of $\chi(p=0.1) \approx 0.75$ qubits mean? The HSW-theorem says explicitly that it is possible to transmit codewords of sufficient lengths $n \gg 1$ with vanishing averaged error probability $\langle p_{err} \rangle$ as long as the code rate $\bar{R} = l/n$ of l generated distinguishable qubits per time unit among n possible qubits adheres to the condition $\bar{R} = l/n < \chi = 0.75$, indicating that in the limit $n \gg 1$ the message M sent to the recipient has to include 25 % redundancy qubits and 75 % payload qubits (containing new information) among its n sent qubits. In other words, χ is an ideal (indirect) *measure of redundancy within a sent code-message M* , whereby the term »redundancy« hints in the present context at the number of qubits enclosing already known (identical or copied) information content, implanted into the n -qubit message M in order to correct all possible noise-induced transmission errors that might attack single qubits within M during transmission.

χ and quantum mutual information

When seeking for an appropriate quantum correlation measure between two open systems, **H. J. Groenewald** proposed in 1971 [18] that the Holevo-bound χ' ought to be regarded as an adequate quantum version of the classical (Shannon-like) mutual information, in accordance with classical capacity C (23) and (4). On the other hand, **A. Winter** argued in 2004 [19] that upholding the analogy between Shannon's and the HSW capacity theorem would necessitate usage of the quantum version $I(\hat{\rho}_M : \hat{\sigma}_M)$ of Shannon's mutual information (22), since $I(\hat{\rho}_M : \hat{\sigma}_M)$ also registers the presence of quantum correlations between two open and interacting quantum systems (as explicated in the course of $I(S : E_f)$ in (6) above). However, in despite of numerous reasonable explanations there is an important shortcoming in the scope of aforementioned argumentations if we take the analogy between χ and C too literally [19]: if we would aim to regard the quantum mutual information $I(S : E_f)$ from (6) instead of the Holevo-bound χ' as an appropriate measure for channel capacity χ that also takes into account the nature of correlations between two systems $\hat{\rho}_M$ (originator) and $\hat{\sigma}_M$ (recipient), we would have to maximize the corresponding von Neumann mutual information $I(\hat{\rho}_M : \hat{\sigma}_M)$ w.r.t. the input $\hat{\rho}_M$, as already demonstrated within the course of the classical capacity C in (23). Unfortunately, it is, strictly speaking, not allowed to set $\chi = \max_{\{\hat{\rho}_M\}} I(\hat{\rho}_M : \hat{\sigma}_M)$, since it is impossible to quantum mechanically define a composite system consisting of $\hat{\rho}_M$ and $\hat{\sigma}_M$ and its joint von Neumann-entropy $S(\hat{\rho}_M, \hat{\sigma}_M)$ due to the fragility of quantum mechanical systems and the corresponding practical fact that after a non-trivial channel operation $\mathcal{E}(\cdot)$ has acted upon an input state $\hat{\rho}_M$ this originator system, contrary to the classical case, simply does not exist any more and is transformed into an output state $\hat{\sigma}_M \neq \hat{\rho}_M$!

Nevertheless, modern research indicates [15, 16] that the quantity

$$I^{\text{coh}}(\hat{\rho}_{\mathbf{M}} : \hat{\sigma}_{\mathbf{M}}) = S(\hat{\sigma}_{\mathbf{M}}) - S_{\mathbf{E}}(\hat{\rho}_{\mathbf{M}}, \hat{\sigma}_{\mathbf{M}}), \quad (36)$$

known as *coherent information*, indeed behaves analogously to Shannon's mutual information in (3) and (23) by utilizing the notion of the so called exchange entropy $S_{\mathbf{E}}(\hat{\rho}_{\mathbf{M}}, \hat{\sigma}_{\mathbf{M}})$ between open quantum systems $\hat{\rho}_{\mathbf{M}}$ and $\hat{\sigma}_{\mathbf{M}}$: in order to compute $S_{\mathbf{E}}(\hat{\rho}_{\mathbf{M}}, \hat{\sigma}_{\mathbf{M}})$ one starts with a given mixed input state $\hat{\rho}_{\mathbf{M}}$ and purifies it by means of an arbitrary reference quantum system \hat{R} according to $\hat{\rho}_{\mathbf{MR}} = |\psi_{\mathbf{MR}}\rangle\langle\psi_{\mathbf{MR}}|$; then letting the channel $\mathcal{E}(\cdot)$ act upon $\hat{\rho}_{\mathbf{MR}}$ one is led to the output state $\hat{\rho}_{\mathbf{M}'\mathbf{R}'} = \mathcal{E}(\hat{\rho}_{\mathbf{MR}})$, from which the von-Neumann entropies $S(\hat{\sigma}_{\mathbf{M}}) = S(\text{Tr}_{\mathbf{R}'}[\hat{\rho}_{\mathbf{M}'\mathbf{R}'}])$ and $S_{\mathbf{E}}(\hat{\rho}_{\mathbf{M}}, \hat{\sigma}_{\mathbf{M}}) = S(\hat{\rho}_{\mathbf{M}'\mathbf{R}'})$ follow. Although the connection (analogy) between (36) and Shannon's mutual information (3) has not been validated in a mathematically rigorous manner so far, we will follow the methodology of [13, 15, 16] and establish this analogy for physically motivated purposes as a conjecture which has already been implemented in (19) and (20) above. Thus, bearing in mind the analogy with (23), we may set the following »conjecture« for the adequate description of the quantum channel capacity χ :

$$\chi \equiv \max_{\{\hat{\rho}_{\mathbf{M}'\mathbf{R}'}\}} I^{\text{coh}}(\hat{\rho}_{\mathbf{M}} : \hat{\sigma}_{\mathbf{M}}), \quad (37)$$

with a maximization taken w.r.t. the probability distribution of the output state $\hat{\rho}_{\mathbf{M}'\mathbf{R}'}$, whereas a more detailed physical discussion of the relationship between coherent information $I^{\text{coh}}(\hat{\rho}_{\mathbf{M}} : \hat{\sigma}_{\mathbf{M}})$ and quantum mutual information $I(\hat{\rho}_{\mathbf{M}} : \hat{\sigma}_{\mathbf{M}})$ will take place in the forthcoming paragraphs (such as 4.1.6) of the present subsection 4.1.

4.1.5 »Quantum Darwinism is generic«

Before investigating mathematical and physical relations between $I^{\text{coh}}(\hat{\rho}_{\mathbf{M}} : \hat{\sigma}_{\mathbf{M}})$ and $I(\hat{\rho}_{\mathbf{M}} : \hat{\sigma}_{\mathbf{M}})$, let us make a slight digression and take a closer look at the interaction map between an arbitrary open system S and its arbitrary environment E in the course of Zurek's qubit model of QD (subsection 3.2) from the perspective of [14]. Zurek's QD aims at explaining two fundamental physical facts by extensively using the concept of quantum channels $\mathcal{E}(\cdot)$ as an operator-sum representation of a measurement map:

1) Objectivity of observables

Fact 1: »Observers that access a quantum system by probing (measuring) parts (fragments) of E can learn only about the measurement of a preferred (pointer) observable of S and its pointer states (pointer basis). This pointer basis of S should be independent of which part is being intercepted, which is a consequence of the basic mathematical and physical rules of quantum mechanics and therefore a generic assumption of QD.«

This means, if we model the interaction $\Lambda : \mathcal{D}(S) \rightarrow \mathcal{D}(\mathcal{F}_1 \otimes \dots \otimes \mathcal{F}_n)$ between an arbitrary open system S and its arbitrary tensor product environment $E \equiv \mathcal{F}_1 \otimes \dots \otimes \mathcal{F}_n$ as a completely positive, trace-preserving (cptp) map between sets $\mathcal{D}(X)$ of density matrices over the Hilbert space X and demand that Λ has to adhere to the Fact 1, then the following theorem has to hold [14]:

Theorem 1: Define a dimond norm $\|\Lambda_1 - \Lambda_2\|_{\diamond} := \sup_X \|(\Lambda_1 - \Lambda_2) \otimes \text{id}(X)\|_1 / \|X\|_1$ (where $\|X\|_1 := \text{Tr}[(X^\dagger X)^{1/2}]$)

stands for the trace norm and $\text{id}(X) = X$) which measures the degree of similarity between two cptp maps Λ_1 and Λ_2 , and $\text{Tr}_{\setminus X}$ as the partial trace over all subsystems of E except X , such that $\Lambda_j := \text{Tr}_{\setminus \mathcal{F}_j} \circ \Lambda$ denotes the effective dynamics from $\mathcal{D}(S)$ to $\mathcal{D}(\mathcal{F}_j)$ for fixed $1 \gg \delta > 0$, then there exists a POVM $\{M_k\}_k$ (with $M_k \geq 0$ and $\sum_k M_k = I$) w.r.t. the outcome k and a set $S \subseteq \{1, \dots, n\}$ with $|S| \geq (1 - \delta)n$ such that $\forall j \in S$

$$\|\Lambda_j - \mathcal{E}_j\|_{\diamond} \leq \left(\frac{27 \ln(2) (d_S)^6 \log_2(d_S)}{n \delta^3} \right)^{1/3}, \quad (38)$$

with a fixed $d_S = \dim(S)$, $\mathcal{E}_j(X) := \sum_k \text{Tr}(M_k X) \hat{\sigma}_{j,k}$ and the outcome state $\hat{\sigma}_{j,k} \in \mathcal{D}(\mathcal{F}_j)$.

The most important conclusion which can be inferred from Theorem 1 are:

- For fixed $d_S = \dim(S)$ and $1 \gg \delta > 0$ one obtains in the limit of large E ($n \gg 1$) $\lim_{n \rightarrow \infty} \|\Lambda_j - \mathcal{E}_j\|_{\diamond} = 0$, i.e. the dynamics Λ_j from $\mathcal{D}(S)$ to $\mathcal{D}(\mathcal{F}_j)$ designed to be compliant with Fact 1 is appropriately approximated by the operator sum representation $\mathcal{E}_j(X) := \sum_k \text{Tr}(M_k X) \hat{\sigma}_{j,k}$ w.r.t. the outcome state $\hat{\sigma}_{j,k} \in \mathcal{D}(\mathcal{F}_j)$ for a given measurement outcome of a Λ -pointer observable $\{M_k\}_k$. This operator sum representation $\mathcal{E}_j(X)$ is also termed a measure and prepare map (quantum channel) [14]. In other words, the effective dynamics from $\mathcal{D}(S)$ to $\mathcal{D}(\mathcal{F}_j)$ for almost all $j \in \{1, \dots, n\}$ is close to \mathcal{E}_j w.r.t. the same measurement $\forall j$. Thus, the evolution Λ is well approximated by

a measurement $\{M_k\}_k$ of S , followed by the distribution (proliferation) of the classical result k throughout E , which finally leads to the same quantum state $\hat{\sigma}_{j,k} \forall \mathcal{F}_j$.

- Since a measurement $\{M_k\}_k$ that generates the operator-sum representation $\mathcal{E}_j(X)$ is independent on j , (38) consequently does not depend on E -fragments (subsystems) \mathcal{F}_j , enforcing the objectivity of the measured outcome state $\hat{\sigma}_{j,k}$. In this sense, [Theorem 1](#) addresses the objectivity of observables which results from general physical and mathematical («generic») properties of operator sum representations and the corresponding pointer observables $\{M_k\}_k$ of the interaction Λ [15, 16].
- If the joint output state $\hat{\rho}_{S,\mathcal{F}_j}^{\text{out}}$, resulting from the evolution Λ_j , corresponds (approximatively) to a convex combination of classically coherent states with tensor product structure⁴ $\hat{\rho}_{S,\mathcal{F}_j}^{\text{out}} \approx \sum_i p_i \hat{\rho}_{S,i}^{\text{out}} \otimes \hat{\rho}_{\mathcal{F}_j,i}^{\text{out}}$ w.r.t a given (classical) probabilistic ensemble $\{p_i, \hat{\rho}_{S,i}^{\text{out}}\}$ and $\forall j$ (see also (18) and (19) above), then there exists a POVM $\{M_k\}_k$ for most cptp maps \mathcal{E}_j . This conclusion appears as a consequence of the following *chain rule for mutual information* [14]

$$I\left(A : \prod_{j=1}^n B_j\right) = I(A : B_1) + \sum_{i=2}^n I\left(A : B_i \middle| \prod_{j=1}^{i-1} B_j\right)$$

(where $I(A : B|C) = I(A : BC) - I(A : C)$ denotes the *conditional mutual information* between A and B given C as known) and is indeed sufficient for the appearance of QD, however it is not necessary for the validity of the QD-condition (15), for, as will be demonstrated in subsection 4.2 below, the QD-plateau can appear even if matrix structures of $\hat{\rho}_{S,\mathcal{F}_j}^{\text{out}}$ for qubit subsystems S and \mathcal{F}_j should not strictly adhere to the «entanglement monogamy» of classically coherent states (18) and (19), in agreement with [Theorem 1](#).

2) Objectivity of outcomes

Fact 2: «Different observers that measure different environmental fragments should obtain (almost) full information about the preferred (pointer) observable of S and will agree on obtained results (measurement outcomes), which is a consequence of a special type of interactions in nature, such as, for instance, the CNOT-interaction (11).»

When it comes to the objectivity of outcomes Zurek's QD requires a stronger condition in order to satisfy [Fact 2](#): not only does the effective dynamics Λ_j from $\mathcal{D}(S)$ to $\mathcal{D}(\mathcal{F}_j)$ have to be close to \mathcal{E}_j for almost all $j \in \{1, \dots, n\}$ w.r.t. the same measurement $\{M_k\}_k$ (pointer observable of the interaction Λ), but also a sufficient fraction of observers gaining access to environmental fragments \mathcal{F}_j should be able to obtain almost full information about possible measurement outcomes. This requirement is accounted for in the following theorem [14]:

Theorem 2: Let $[n] := \{1, \dots, n\}$, $\Lambda : \mathcal{D}(S) \rightarrow \mathcal{D}(\mathcal{F}_1 \otimes \dots \otimes \mathcal{F}_n)$. If for any subset $S_t \subseteq [n]$ of t elements $\Lambda_{S_t} := \text{Tr}_{\bigcup_{l \in \mathcal{F}_t} \mathcal{F}_l} \circ \Lambda$ represents the effective channel dynamics from $\mathcal{D}(S)$ to $\mathcal{D}\left(\bigotimes_{l \in S_t} \mathcal{F}_l\right)$, then for every fixed $1 \gg \delta > 0$, there exists a POVM $\{M_k\}_k$ (with $M_k \geq 0$ and $\sum_k M_k = I$) w.r.t. the outcome k such that for more than a $(1 - \delta)$ -fraction of the $S_t \subseteq [n]$

$$\|\Lambda_{S_t} - \mathcal{E}_{S_t}\|_{\diamond} \leq \left(\frac{27 \ln(2) (d_S)^6 \log_2(d_S) t}{n \delta^3} \right)^{1/3}, \quad (39)$$

with a fixed $d_S = \dim(S)$, $\mathcal{E}_{S_t}(X) := \sum_k \text{Tr}(M_k X) \hat{\sigma}_{S_t,k}$ and the outcome states $\hat{\sigma}_{S_t,k} \in \mathcal{D}\left(\bigotimes_{l \in S_t} \mathcal{F}_l\right)$.

Thus, [Theorem 2](#) and (39) implies: Let Λ_{S_t} be a cptp map from S to $\bigotimes_{l \in S_t} \mathcal{F}_l$ which is approximated by $\mathcal{E}_{S_t}(X) := \sum_k \text{Tr}(M_k X) \hat{\sigma}_{S_t,k}$ for a POVM $\{M_k\}_k$ and the outcome states $\hat{\sigma}_{S_t,k} \in \mathcal{D}\left(\bigotimes_{l \in S_t} \mathcal{F}_l\right)$. Then, if t observers having access to $t/n \approx 1$ environmental fragments $\bigotimes_{l \in S_t} \mathcal{F}_l$ gain almost full information about a particular measurement outcome of $\{M_k\}_k$, the corresponding measurement outcomes will turn out to be objective.

– $\hat{\rho}_{S,\mathcal{F}_j}^{\text{out}} \approx \sum_i p_i \hat{\rho}_{S,i}^{\text{out}} \otimes \hat{\rho}_{\mathcal{F}_j,i}^{\text{out}}$ is also known as «entanglement monogamy structure» [4, 5, 14], since each classical (diagonal) matrix entry $\hat{\rho}_{S,i}^{\text{out}}$ of system's output state is unambiguously connected with mutually orthogonal output state \mathcal{F}_j -subspaces $\hat{\rho}_{\mathcal{F}_j,i}^{\text{out}}$ of E and its computational basis.

4.1.6 Quantum information gain of a measurement

Although (37) represents only a reasonable physical conjecture without a strict mathematical verification, we can utilize it when discussing the physical connection between the quantum channel capacity χ and the quantum mutual information $I(\hat{\rho}_M : \hat{\sigma}_M)$ for an input state $\hat{\rho}_M$ and an output state $\hat{\sigma}_M = \mathcal{E}(\hat{\rho}_M)$ of the quantum channel $\mathcal{E}(\cdot)$ in the following way⁵: Since we cannot use $\hat{\rho}_M$ when computing $I^{\text{coh}}(\hat{\rho}_M : \hat{\sigma}_M)$ in (36) due to the fact that $\hat{\rho}_M$ simply does not exist any more after passing through the measurement channel $\mathcal{E}(\cdot)$, contrary to the case of the classical information theory, we have to construct $I^{\text{coh}}(\hat{\rho}_M : \hat{\sigma}_M)$ and the quantum mutual information $I(S : E_f)$ from the output state $\hat{\sigma}_M$ by means of the so called **State Merging Protocol** [13]. This state merging protocol illustrates the quantum measurement as an interaction process between at least two subsystems, the (effectively decohered or classical) system of interest X_A (Alice) that needs to be monitored and its environment X_B (Bob), which results into maximal entanglement creation between X_A and X_B that leads to the transmission of the classical bit message in X_A (containing the classical Shannon-information $H(S_{\text{class}}) = H(\{X_A\})$) from X_A to X_B in accordance with Fig. 2 below.

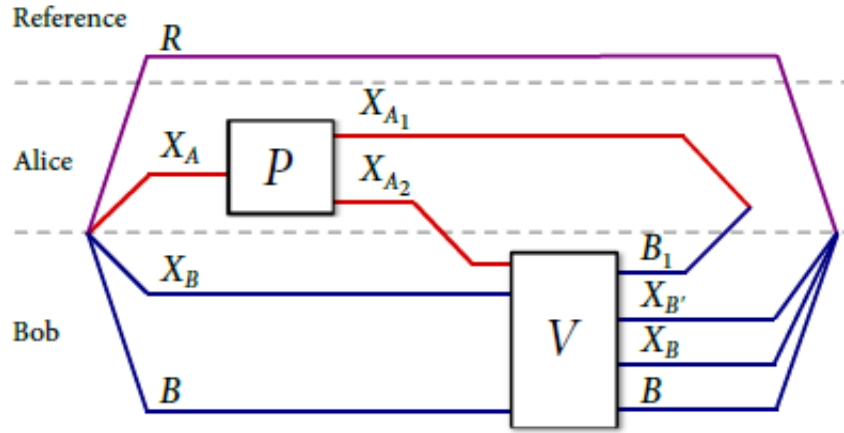


Figure 2: Sketch of the protocol for state merging of a classically coherent state on systems $\hat{R}X_AX_BB$. P denotes the permutation of states in the orthonormal basis $\{|x\rangle\}$ of X_A , which splits X_A into two subsystems. The operation V is an isometry which performs the merging task by generating entanglement between X_A and X_B , as guaranteed by Uhlmann's theorem. Source: [13], courtesy of **J. Rennes**.

In order to utilize the concept of decoherence inherent to the notion of quantum measurement we equip the mixed state system X_A with a reference system $\hat{R}(\equiv \hat{\rho}_R)$ that purifies it and start with the overall input state $\hat{\rho}_{X_AX_BB R}$, as indicated in Fig. 2, which we assume to be pure and of the classically coherent form (for a probability distribution $p_{X_AX_B}$)

$$|\psi\rangle_{X_AX_BB R}^{\text{in}} = \sum_{x_A x_B} \sqrt{p_{x_A x_B}} |x_A\rangle |x_B\rangle \otimes |\psi_{x_A x_B}\rangle_R \quad (40)$$

on X_AX_B w.r.t. their orthonormal bases $\{|x_A\rangle\}_{x_A \in X_A}$ and $\{|x_B\rangle\}_{x_B \in X_B}$, whereas $|\psi_{x_A x_B}\rangle_R$ denotes the part of the overall Hilbert space $\mathcal{H}_{X_AX_BB R}$ that purifies X_A (in paragraph 4.1.9 we will notice that the overall input state $\hat{\rho}_{X_AX_BB R}$ does not have to be of the form (40), however the output states that results from the quantum measurement process illustrated in Fig. 2 has to (at least) effectively behave as a classically coherent state in the limit of large environments with $n \gg 1$ constituents (qubits), an issue which will also be addressed thoroughly in the forthcoming subsection 4.2). One can describe the quantum measurement process by starting with (40) and proceeding in compliance with the following state merging algorithm consisting of three steps (s. Fig. 2):

1. Alice applies a local permutation $P_{X_A} \rightarrow X_{A1}X_{A2}$ in the basis $\{|x_A\rangle\}_{x_A \in X_A}$ and splits X_A into two subsystems X_{A1} and X_{A2} (permutation + state splitting).
2. Alice sends X_{A2} to Bob. The state of $X_{A1}\hat{R}$ is, after permutation, given by $\sim \hat{\mathbb{I}}_{X_{A1}} |X_{A1}|^{-1} \otimes \hat{\rho}_R$, where $|X_{A1}| = \dim(X_{A1})$.
3. Bob performs a local isometry $V_{X_{A2}X_BB} \rightarrow X_{B'}X_BB_1$ which splits X_{A2} into $X_{B'}$ and B_1 and entangles X_{A1} with B_1 (entanglement + state merging), generating an output state

⁵The author would like to thank Dr. **J. Rennes** for inspiring discussions regarding the operational interpretation of the quantum mutual information, especially from the perspective of his paper [13].

$$\omega_{X_B, X_B B R X_{A_1} B_1} \approx (\mathcal{E}_{X_A X_B B} \otimes \text{id}_R) (\hat{\rho}_{X_A X_B B R}) = (P_{X_A} \otimes V_{X_B} \otimes \text{id}_R) (\hat{\rho}_{X_A X_B B R}) = (\hat{\rho}_{X_B, X_B B R}) \otimes \Phi_{X_{A_1} B_1}^E, \quad (41)$$

where $\Phi_{X_{A_1} B_1}^E$ denotes a maximally entangled state of Schmidt-rank $D_s = |X_A| = 2^k$ (s. (19) and (20) above).

Bob holds a purification of $\hat{\mathbb{I}}_{X_{A_1}} |X_{A_1}|^{-1} \otimes \hat{\rho}_R$, namely the subsystems X_B, B_1 , since $\hat{\mathbb{I}}_{X_{A_1}} |X_{A_1}|^{-1} \otimes \hat{\rho}_R$ is the reduced state of (41). Finally, referring to Uhlmann's theorem (42)-(43), we may conclude that all purifications are equivalent up to local isometries, meaning that there must exist an isometry $V_{X_{A_2} X_B B} \rightarrow X_B, X_B B B_1$ on Bob's side that transforms $\hat{\mathbb{I}}_{X_{A_1}} |X_{A_1}|^{-1} \otimes \hat{\rho}_R$ into (41).

Uhlmann's theorem [15, 16]: Let $\hat{\rho}$ and $\hat{\sigma}$ be density matrices acting on \mathbb{C}^n . Let $\hat{\rho}^{1/2}$ be the unique positive square root of $\hat{\rho}$ and

$$|\psi_\rho\rangle = \sum_{i=1}^n \left(\rho^{1/2} |e_i\rangle \right) \otimes |e_i\rangle \in \mathbb{C}^n \otimes \mathbb{C}^n \quad (42)$$

a purification of $\hat{\rho}$ w.r.t. the orthonormal basis $\{|e_i\rangle\}$ ($\rho^{1/2} \in \mathbb{C}$). Then the fidelity

$$F(\hat{\rho}, \hat{\sigma}) = \text{Tr} \left[\sqrt{\sqrt{\hat{\rho}} \hat{\sigma} \sqrt{\hat{\rho}}} \right] = \max_{\{|\psi_\sigma\rangle\}} |\langle \psi_\rho | \psi_\sigma \rangle|, \quad (43)$$

where $|\psi_\sigma\rangle$ denotes a purification of $\hat{\sigma}$, represents the maximum overlap between purifications or their distinguishability («distance»).

In other words, the quantum measurement process illustrated in Fig. 2 merges subsystems X_{A_1} and X_{B_1} of X_A and X_B by entangling them. The degree of this entanglement (alias the corresponding Schmidt-rank D_s) determines indirectly the information gain g in (20) obtainable from a given output state $\omega_{X_B, X_B B R X_{A_1} B_1}$ that emerges from a certain quantum channel $\mathcal{E}(\cdot)$ in the following way:

Adopting the conjecture (37) one can show [13] that w.r.t. the unital cptp quantum measurement map $\mathcal{M}(\cdot) \equiv \left\{ \sum_{X_A} \mathcal{M}_{X_A} \otimes \text{id}_R \right\}(\cdot)$ with POVM operators $\mathcal{M}_{X_A}(\cdot) = K_{X_A}(\cdot) K_{X_A}^\dagger$ and unitary Kraus-operators K_{X_A} that generate the operator-sum representation of $\mathcal{M}(\cdot)$, the quantity $I(\mathcal{M})$ (maximized w.r.t. the probability distribution of $\hat{\rho}_{A R}^{\text{out}}$) in

$$g := q - e \leq I(\mathcal{M}) = \max_{\{\hat{\rho}_{A R}^{\text{out}}\}} I(\hat{R} : X_B)_{\omega_{X_B R}^{\text{out}}}, \quad (44)$$

with

$$\begin{aligned} I(\hat{R} : X_B)_{\omega_{X_B R}^{\text{out}}} &= S(X_B)_{\omega_{X_B R}^{\text{out}}} + S(\hat{R})_{\omega_{X_B R}^{\text{out}}} - S(\hat{R}, X_B)_{\omega_{X_B R}^{\text{out}}} = S(\hat{R})_{\omega_{X_B R}^{\text{out}}} - \underbrace{S(\hat{R} | X_B)_{\omega_{X_B R}^{\text{out}}}}_{:=q} - \underbrace{S(\hat{R} | X_B)_{\omega_{X_B R}^{\text{out}}}}_{:=e} \\ &= S(X_B)_{\omega_{X_B R}^{\text{out}}} + \underbrace{I^{\text{coh}}(\hat{R} : X_B)_{\omega_{X_B R}^{\text{out}}}}_{\equiv X} \end{aligned} \quad (45)$$

computed w.r.t. the output state

$$\omega_{X_B R}^{\text{out}} = \sum_{X_A X_B} |x_B\rangle \langle x_B| \otimes \text{Tr}_{X_A} \left\{ (\mathcal{M}_{X_A} \otimes \text{id}_R) (\hat{\rho}_{X_A R}^{\text{in}}) \right\}, \quad (46)$$

(with $\hat{\rho}_{X_A R}^{\text{in}} = \text{Tr}_{X_B} [\hat{\rho}_{X_A X_B R}^{\text{in}}]$ and $\hat{\rho}_{X_A X_B R}^{\text{in}}$ as in (40) above) being a reduced state of defines the optimal rate of transformed classically coherent output state (where $|\tilde{x}_A\rangle \langle \tilde{x}_A| = \mathcal{M}_{X_A}(|x_A\rangle \langle x_A|)$)

$$|\psi\rangle_{\tilde{X}_A X_B R}^{\text{out}} = \sum_{X_A X_B} \sqrt{p_{X_A X_B}} |\tilde{x}_A\rangle |x_B\rangle \otimes |\psi_{X_A X_B}\rangle_R, \quad (47)$$

defines the **optimal rate (upper bound) of classical communication (information) gain** g or the **maximal entanglement-assisted capacity of a quantum measurement** for transmitting classical information $H(S_{\text{class}})$ of X_A , represented by the communication cost $q := S(\hat{R})_{\omega_{X_B R}^{\text{out}}} = k$ of k qubits that X_A sends to X_B , under consideration of the entanglement

cost e , given by $0 \leq e := S(\hat{R}|X_B)_{\omega_{X_B R}^{\text{out}}} = \log_2 D_s \leq k$, which measures the amount of channel noise that disturbs the transmission of the k -qubit message from X_A to X_B .

Thus, in (44)-(47) we recognize that the Schmidt-rank D_s determines the amount of channel noise (entanglement cost e) in the course of a quantum measurement (after all, e corresponds according to (45) to the equivocation $S(\hat{R}|X_B)_{\omega_{X_B R}^{\text{out}}}$, which was identified in paragraph 4.1.2 as (classical) channel noise). In paragraph 4.1.9 we will deal more thoroughly with thermodynamical aspects of entanglement cost.

Now, let us adopt the interpretation from the beginning of the current subsection 4.1 according to which $I(S : E_f)$ from (6) indicates w.r.t. the given output state $\omega_{X_B/X_B B R X_{A_1} B_1}$ how much does the environment X_B know about the system of interest X_A after $\mathcal{E}(\cdot)$ has acted upon the input state $\hat{\rho}_{X_A X_B B R}$. In addition, due to the fact that if in $\omega_{X_B/X_B B R X_{A_1} B_1}$ from (41) one does not need a maximally entangled state $\phi_{X_{A_1} B_1}^E$ for acquiring the entire $H(S_{\text{class}})$ about X_A we may conclude that the environment X_B already possesses a sufficiently high amount of $H(S_{\text{class}})$. In this sense, the output state $\omega_{X_B/X_B B R X_{A_1} B_1}$ in (41) represents the state of minimal information gain g in (20) and the aim of QD is to minimize the amount of entanglement cost e needed when measuring X_A , which is the reason why in (18)-(20) we had allowed the entanglement cost e to range over the interval $0 \leq e = \log_2 D_s \leq k$.

However, the necessity for minimizing the entanglement cost e is not the only difference between $\omega_{X_B R}^{\text{out}}$ in (46) of the standard State-Merging-Protocol and its QD-version $\hat{\rho}_{S E_L}^{\text{out}}$ from (19): the main conceptual discrepancy between the standard State-Merging-Protocol and its QD-compliant implementation concerns the form of the POVM operators. Whereas the POVMs $\mathcal{M}_{X_A}(\cdot)$ from (46) act upon an open system of interest X_A , measuring it directly, the QD-compliant POVMs $\mathcal{M}_{E_i}(\cdot)$ of (19) manipulate the environment E while leaving the open system S unchanged. The latter controlled manipulation of E by S , which lies at the heart of the QD-approach to the emergence of Classicality, allows us to vary e w.r.t. the environmental fraction parameter f in (5) and thus search for the optimal matrix structure of $\hat{\rho}_{S E_L}^{\text{out}}$ that leads to QD ($\hat{\rho}_{S E_L}^{\text{out}}$ in (12), as well as the corresponding PIP in Fig. 1, are only specific examples that, as already remarked in paragraph 4.1.1, emphasize the difference between minimal and maximal e -values and their influence on the appearance of the QD-plateau. A more detailed comparison of (46) with (19) will be given in paragraph 4.1.9).

Furthermore, from the point of view of QD one could accept e as a quantitative level of useless (redundant) information $(1 - \chi)$, as indicated by (34) and (35), which a message of S has to contain if E should be able to decipher its entire $H(S_{\text{class}})$ by intercepting a minimal number of environmental »storage cells« (qubits). This issue leads us to the domain of quantum error correction and quantum coding which we will explore in paragraphs 4.1.7 and 4.1.8, before focussing again on the physical relationship between $I(S : E_f)$ and the quantum channel capacity χ in paragraph 4.1.9.

4.1.7 Quantum error correction

Classical error correction

For the sake of simplicity let us start with error correcting classical symmetric noisy channels: for this purpose we consider the following binary symmetric classical bit-flip channel defined by ($k = 2$, s. remarks prior to (21) above) [15, 16]

$$\begin{aligned} P(X^k) &= (p(x_1) = q, p(x_2) = 1 - q)^T \\ P(Y^k) &= (p(y_1) = q + \varepsilon - 2\varepsilon q, p(y_2) = 1 - q - \varepsilon + 2\varepsilon q)^T \\ P_\varepsilon(X^k | Y^k) &:= [p_{ij}(\varepsilon)]_{k \times k} = \begin{pmatrix} 1 - \varepsilon & \varepsilon \\ \varepsilon & 1 - \varepsilon \end{pmatrix}, \end{aligned}$$

where q and $1 - q$ represent the success probabilities for transmitting symbols $(x_1, x_2) \in \{0, 1\}$ and ε denotes the channel noise (bit flip probability) which flips (disturbs) bits of transmitted »bit block« messages. For such bit-flip channels we can suggest the following prescription for preserving classical messages from errors if the error rate is assumed to be for example smaller than 1 error per 3 bits:

1. Copy the bits »0« and »1« three times, i.e. $0 \rightarrow 000$ and $1 \rightarrow 111$ and send these three logical bit entities carrying redundant information through the channel.
2. Suppose that we obtain a bit sequence »001«. Then, if the bit flip probability ε is not too high, we may conclude that it is likely that the third bit of the sequence »001« was flipped (»majority voting principle«).

However, what is the quantitatively allowed domain for ε within which the majority voting may be applied? This is easily obtained by computing the probability ε_{tot} that two or more bits are flipped, rendering the majority voting useless:

$$\varepsilon_{\text{tot}} = 3\varepsilon^2(1 - \varepsilon) + \varepsilon^3 = 3\varepsilon^2 - 2\varepsilon^3. \quad (48)$$

Then the majority voting may be applied only if $\varepsilon > \varepsilon_{\text{tot}}$, leading with (48) to the constrain $\varepsilon < 0.5$.

An alternative way for dealing with the above bit-flip channel offers the *coding principle of Hamming* [15, 16] which also works only if the error rate is assumed to be smaller than 1 error per 3 bits: Suppose we want to preserve a 2-bit code (sequence) $x_{\text{seq}} = x_1 x_2$ from transmission errors (with $x_i \in \{0, 1\}$). Then one should double the input code (increase of redundancy) $x_{\text{seq}} = x_1 x_2 \rightarrow x_{\text{seq}}^D = x_1 x_2 x'_1 x'_2$ such that $x_1 = x'_1$ and $x_2 = x'_2$ (initial conditions). Furthermore, introduce a third control bit $x_3 \in \{0, 1\}$ such that, depending on the original input sequence $x_{\text{seq}} = x_1 x_2$,

$$x_1 + x_2 + x_3 = \text{even} \in \{0, 2\}$$

applies. Finally, send a sequence $x_{\text{seq}}^{\text{control}} = x_{\text{seq}}^D x_3 = x_1 x_2 x'_1 x'_2 x_3$ through the bit-flip channel. Depending on the outcome of this transmission our reasoning may be two-fold. Assume that we obtain a sequence $x_{\text{seq}}^{\text{control}}$ with $x_1 = x'_1$ and $x_2 \neq x'_2$. Then we can guess whether x_2 or x'_2 has been disturbed (flipped) by considering the following two conditions:

- if $x_1 + x_2 + x_3 = \text{even} \in \{0, 2\} \Rightarrow x'_2$ is incorrect (flipped);
- if $x_1 + x_2 + x_3 = \text{odd} \in \{1, 3\} \Rightarrow x_2$ is incorrect (flipped).

Quantum error correction

Now consider the quantum analogon of the classical bit flip channel discussed w.r.t. (48):

$$\mathcal{E}(\hat{\rho}) = p \hat{\sigma}_x \hat{\rho} \hat{\sigma}_x + (1 - p) \hat{\rho}. \quad (49)$$

The corresponding error correction algorithm for (49) involves the concept of »syndrome measurements« by means of the the following three steps [15, 16]:

1. Encode a qubit state $a|0\rangle + b|1\rangle$ as $a|000\rangle + b|111\rangle \equiv a|0_L\rangle + b|1_L\rangle$ (redundant encoding) with logical qubits $|0_L\rangle$ and $|1_L\rangle$.
2. (49) leads to errors (bit-flips). Suppose that one or no errors occurred in $a|0_L\rangle + b|1_L\rangle$ after passing through (49). Then we can use the following error-detection (syndrome) diagnosis: **I)** Assume for example that the first qubit in $a|0_L\rangle + b|1_L\rangle$ has been flipped

$$(a|000\rangle + b|111\rangle) \xrightarrow{\mathcal{E}} (a|100\rangle + b|011\rangle). \quad (50)$$

II) In order to reconstruct which qubit of $a|0_L\rangle + b|1_L\rangle$ in (50) has been disturbed compare output qubits 1 and 2 as well as qubits 2 and 3 by performing non-local »syndrome measurements« $\hat{\sigma}_z^{(1)} \otimes \hat{\sigma}_z^{(2)} \otimes \hat{I}$ and $\hat{I} \otimes \hat{\sigma}_z^{(2)} \otimes \hat{\sigma}_z^{(3)}$ on the output $a|100\rangle + b|011\rangle$. This tells us which qubit is flipped: if $\hat{\sigma}_z^{(1)} \otimes \hat{\sigma}_z^{(2)}$ leads to the eigenvalue 1 and $\hat{\sigma}_z^{(2)} \otimes \hat{\sigma}_z^{(3)}$ also to the eigenvalue 1, no error occurred; if $\hat{\sigma}_z^{(1)} \otimes \hat{\sigma}_z^{(2)}$ leads to the eigenvalue (-1) and $\hat{\sigma}_z^{(2)} \otimes \hat{\sigma}_z^{(3)}$ to the eigenvalue 1, then the first qubit flipped, which was indeed the case in (50). Syndrome measurements do not give information about the amplitudes a and b in (50), which also means that syndrome measuring the output $a|100\rangle + b|011\rangle$ does not destroy the quantum states that need to be preserved from errors of \mathcal{E} .

3. Recover the source message: based on eigenvalues of non-local syndrome measurements from the previous step we need to apply $\hat{\sigma}_x^{(1)} \otimes \hat{I} \otimes \hat{I}$ to the output state (50) in order to error-correct the first qubit. This type of recovery works if the bit-flip affect one or fewer qubits of the input $a|000\rangle + b|111\rangle$ under condition $0.5 > \varepsilon > \varepsilon_{\text{tot}}$, as in the classical case (48). This can be easily seen if arguing by means of fidelity (43) $F(|\psi\rangle, \hat{\rho}) = \sqrt{\langle\psi|\hat{\rho}|\psi\rangle}$ as a »distance measure« between a pure $|\psi\rangle$ state and a desired (mixed) state $\hat{\rho}$. The object of quantum error correction is to obtain $F \approx 1$ between an input $|\psi\rangle$ and $\hat{\rho}$ after error correction. In (50) we have without error-correction $\hat{\rho} = (1 - p)|\psi\rangle\langle\psi| + p\hat{\sigma}_x|\psi\rangle\langle\psi|\hat{\sigma}_x$ and thus a minimal fidelity $F = \sqrt{(1 - p) + \langle\psi|\hat{\sigma}_x|\psi\rangle^2} \Rightarrow F(|\psi\rangle = |0\rangle) = \sqrt{1 - p}$. After performing error-correction upon (50) we have (with ε as in (48) above and assuming that at most one qubit of $a|0_L\rangle + b|1_L\rangle$ is affected by \mathcal{E}) $\hat{\rho} = [(1 - \varepsilon)^3 + 3\varepsilon(1 - \varepsilon)^2]|\psi\rangle\langle\psi| \Rightarrow F \geq \sqrt{(1 - \varepsilon)^3 + 3\varepsilon(1 - \varepsilon)^2} = \sqrt{1 - 3\varepsilon^2 + 2\varepsilon^3}$, indicating that the value of F for the storage of the quantum state $|\psi\rangle$ can be improved if we demand $\varepsilon < 0.5$, in accordance with (48).

Error-correction bounds

The above example dealing with the quantum bit-flip channel in (49) has preassumed that the error rate of \mathcal{E} in (50) does not exceed 1 qubit per transmission of $a|0_L\rangle + b|1_L\rangle$. However, if we ask how many redundant copies n of k qubits (ergo which level of redundancy n)

does a non-degenerate input message (code) have to contain if we want to encode k originator's qubits into $n \geq k$ (recipient) qubits in such a way that errors on maximally $t \geq 0$ qubits are tolerated, then we need to consider the following *quantum* version of *Hamming's bound* [15, 16]:

$$\sum_{j=0}^t \binom{n}{j} 3^j 2^k \leq 2^n, \quad (51)$$

since there are $\binom{n}{j}$ sets (qubit-locations), each of which can be attacked by three types of errors -corresponding to 3 Pauli matrices ($\hat{\sigma}_x, \hat{\sigma}_y, \hat{\sigma}_z$) and leading to 3^j possible errors for each qubit- such that the total number of errors on t or fewer qubits amounts to $\sum_{j=0}^t \binom{n}{j} 3^j$. In order to encode k qubits in a non-degenerate way each of $\sum_{j=0}^t \binom{n}{j} 3^j$ errors has to correspond to an orthogonal subspace of dimension 2^k and needs to be imbedded into the entire 2^n -dimensional space of n qubits, validating (51).

On the other hand, if we wish to encode k qubits into n qubits in a way that we can correct errors on any t qubits of originator's code-message, we need a redundancy n corresponding to the Singleton-bound

$$n \geq 4t + k, \quad (52)$$

which, unlike the Hamming's quantum bound, specifies the level of redundancy for originator's message not only w.r.t. non-degenerate, but also w.r.t. degenerate codes, for which errors on different qubits could, contrary to the classical case, also lead to the same corrupted codeword. Nevertheless, for the case of the bit-flip channel (49) discussed above ($k = 1$, $t = 1$) both (51) and (52) yield for the level of redundancy $n \geq 5$ qubits. In other words, if we tolerate at most 1 error per transmission through the bit-flip channel (49) we would need at least 5 copies of the 1 qubit input message in order to preserve its content from channel corruption (noise) by means of syndrome measurements.

Due to the fact that within the QD qubit-model of Zurek [4, 5] (s. Figure 1 and (12) above) already an environment containing only $n = 1$ qubit suffices to obtain error-free decoding of the $k = 1$ qubit source message, we may conclude that Zurek's qubit model of QD, although compliant with the Hamming and Singleton quantum bounds (51) and (52), both of which enforcing the redundancy condition $n \geq 1$, indeed offers a too idealized perspective on the decoherence-induced emergence of Classicality by assuming that the proliferation of the k »S-qubit block« into E takes place without errors ($t = 0$).

On the other hand, recent more realistic qubit models of QD, such as the iterative Random Unitary Operations qubit model outlined in [11] (which we will discuss extensively in relation to QD in the second part of this writing), within which k qubits of S may interact randomly (according to a given initial probability distribution weighing the corresponding qubit-qubit interactions) and more than once with each of the n E -qubits, involve a more complex interaction picture by allowing the quantum channel \mathcal{E} proliferating information about S to E to exert $t \geq 1$ errors on k qubits of the originator's input code.

Nevertheless, even in the case of such more sophisticated qubit models of QD PIPs of $I(S : E_{f=1})$ w.r.t. n will adhere to the Hamming and Singleton-bounds and thus indicate the redundant size n of E necessary for efficient error-correcting transmission (encoding) of classical Shannon-information $H(S_{\text{class}})$ about S , as well as for reliable predictions of the maximum achievable value of $I(S : E_{f=1})$ in the limit $n \gg 1$ of increasing number n of environmental qubit constituents.

4.1.8 Schumacher's quantum coding theorem

Besides preserving the transmitted message of the originator from numerous channel-induced errors, it is also important, from the point of view of the recipient, to effectively store the received information with a minimum of required storage cells. Therefore, it would be optimal if one could quantitatively estimate the maximal compressibility (compression rate) of the input message. For a received message »qubit block« $\hat{\sigma}_M$ in (29) which emerges as a result of a ctp measurement map $\mathcal{E}(\cdot)$ acting on originator's input $\hat{\rho}_M$ in (28) and its n »one qubit symbols« $\hat{\rho}_i$ according to $\hat{\sigma}_i = \mathcal{E}(\hat{\rho}_i)$, Schumacher's coding theorem estimates the lower bound for the compression factor (compression rate) $\eta = m/n$ of originator's message $\hat{\rho}_M$ (the compression ratio » m/n « defining η indicates the relationship between an n qubit message of maximum length and its compressed $m < n$ qubit version). Consequently, *Schumacher's coding theorem* acquires the following general formulation⁶ [15, 16]:

For general »qubit block« messages M of asymptotically increasing length $n \gg 1$, the achievable compression factor $\eta = m/n$ for compressing an n qubit message into a qubit message of length $m < n$ is lower-bounded by the

⁶The originator's message $\hat{\rho}_M$ is w.r.t. I^{coh} from (36) often assumed to be in a mixed state, i.e. each message symbol $\hat{\rho}_i$ is usually regarded as being in an effectively mixed one qubit state with $S(\hat{\rho}_i) > 0$.

»best compression measure«, the von Neumann entropy $S(\hat{\rho}_i)$ of each \mathbf{M} -symbol $\hat{\rho}_i$, in accordance with

$$\eta \geq S(\hat{\rho}_i), \quad (53)$$

since $S(\hat{\rho}_i)$ represents the entropy carried by each message symbol $\hat{\rho}_i$ alias redundant information within $\hat{\rho}_{\mathbf{M}}$ susceptible to compression.

The following important conclusions can be drawn from Schumacher's coding theorem:

- The lower the $S(\hat{\rho}_i)$, the higher the message compression potential!
- There is no code that is capable of compressing a purely random classical n -bit sequence as generated by a classical Shannon-source $H(\{X^n\}) = n$, since in that case $S(\hat{\rho}_i) = 1$. However, as soon as randomness is no longer evenly distributed among bits »0« and »1« ($H(\{X^n\}) < n$), there is information redundancy and the possibility of reducing the n -bit sequence of the originator to a size $m < n$.
- In the course of Zurek's qubit model of QD quantum mutual information $I(S : E_f)$ is used in order to describe the optimal storage of the classical information content about the open system S of interest into the environment E , presupposing that the message of the source S , (which, as a result of subsequent CNOT-interactions, becomes effectively decohered alias quasi-classical), should not be compressed, which is the reason why one usually plots $\frac{I(S : E_f)}{H(S_{\text{class}})}$, normalized w.r.t. the Shannon-entropy $H(S_{\text{class}})$ of S , vs. the environmental fraction parameter $f = L/n$ (where $0 \leq L \leq n$ corresponds to the number of E -qubits which have not been traced out, see for example Fig. 1 and (15) above). On the contrary, the aim of the QD approach to the emergence of Classicality aims at maximally compressing the length of recipient's (environmental) n -qubit decoded version of the original k -qubit message transmitted and stored into the n -qubit E by the source S .
- Furthermore, since S and E contribute to $\frac{I(S : E_f)}{H(S_{\text{class}})}$ not until the CNOT-channel $\mathcal{E}(\cdot)$ in (9)-(11) has acted upon the entire composite system, we may characterize the information content of S as quasi-classical and seek for a minimal (non-zero) number $0 < L = L_{\min}$ of E -qubits that one needs to enclose into the computation of $\frac{I(S : E_f)}{H(S_{\text{class}})}$, in order to reconstruct the entire classical information $H(S_{\text{class}})$ about S , in accordance with $\frac{I(S : E_f)}{H(S_{\text{class}})} \Big|_{f_{\min}=L_{\min}/n} \stackrel{!}{=} 1$ (see subsection 3.2 above). This minimal number L_{\min} of E -qubits corresponds to the maximal compressibility of the E -decoded n -qubit version of stored k -qubit S -message and thus to the maximal redundancy $R_{\max}^f = f_{\min}^{-1}$ from (8). Therefore, we may conclude that $\frac{I(S : E_{f \leq 1})}{H(S_{\text{class}})}$ measures the optimal compressibility $0 < \eta_{\text{opt}}^E = \frac{L_{\min}}{n} \leq \eta^E = \frac{L}{n}$ of the E -decoded n -qubit version of the stored k -qubit S -message. According to subsection 3.2 this optimal compressibility η_{opt}^E indicates the appearance of QD only if $\eta_{\text{opt}}^E = \frac{L_{\min}}{n} \leq \frac{k}{n}$, since in this case the observer needs to intercept a minimal fraction $L_{\min} \leq k$ of n environmental qubits in order to reconstruct the S -pointer basis. Should $L > (L_{\min} \leq k)$, then, strictly speaking, no QD appears from the practical point of view.

4.1.9 Quantum Darwinism and χ

Gathering all important key features of previous subsections together we may conclude that χ corresponds to the optimal value $\max_{\{\hat{\rho}_{\mathbf{A}\mathbf{R}}^{\text{out}}\}} I^{\text{coh}}(X_B : \hat{R})$ of the coherent information alias to the maximum $\max_{\{\hat{\rho}_{\mathbf{A}\mathbf{R}}^{\text{out}}\}} I(X_B : \hat{R})$ of the quantum

mutual information between two systems X_B and \hat{R} (s. paragraph 4.1.6, (44)-(47) above) and defines a measure of redundant information within a source code, which has to be sent to the recipient in order to transmit the code with a vanishing error (paragraphs 4.1.7 and 4.1.8). QD turns this picture upside down from the perspective of the $1 \leq L \leq n$ -qubit environment $X_B \equiv E_L$ (with L counting those E -qubits which have not been traced out) interacting with the open pure input system $\hat{\rho}_{\mathbf{A}\mathbf{R}}^{\text{in}} \equiv \hat{\rho}_S^{\text{in}}$ (s. paragraph 4.1.6 above): in Zurek's model of QD (s. for example (12) in subsection 3.2 above for an open $k = 1$ system S) one implements the standard State-Merging-Protocol of [13] by usually starting with a pure input state $\hat{\rho}_{S\mathbf{E}}^{\text{in}} = \hat{\rho}_S^{\text{in}} \otimes \hat{\rho}_E^{\text{in}}$ (that does not have to necessarily be of classically coherent type from (18) above), where $\hat{\rho}_S^{\text{in}} = \hat{\rho}_{\mathbf{A}\mathbf{R}}^{\text{in}} = \hat{\rho}_{\mathbf{A}}^{\text{in}} \otimes \hat{\rho}_{\mathbf{R}}$ corresponds to the pure k -qubit open system S (which contains the mixed part $\hat{\rho}_{\mathbf{A}}^{\text{in}}$ purified by a reference system \hat{R} and its input density matrix $\hat{\rho}_{\mathbf{R}}$, in accordance with paragraph 4.1.6), whereas the environmental input state is of the form $\hat{\rho}_E^{\text{in}} = |\xi\rangle^{\otimes n} \langle \xi|$ (with $\xi \in \{0, 1\}$). Then a ctp measurement map $\mathcal{M}(\cdot) \equiv \{p_i |i\rangle_S \langle i| \otimes \mathcal{M}_{E_i}(\cdot)\}$ with POVMs $\mathcal{M}_{E_i}(|\xi\rangle^{\otimes n} \langle \xi|) = |i \oplus \xi\rangle^{\otimes n} \langle i \oplus \xi|$ (where $|\xi\rangle^{\otimes n}$ belongs to the orthonormal computational register basis $\{|\phi_j\rangle\}$ of an n -qubit E , s. (18) and paragraph 4.1.5), associated for instance with a qubit-qubit CNOT-interaction (9)-(11), is applied to $\hat{\rho}_{S\mathbf{E}}^{\text{in}}$, leading to the so called classically coherent output states (18)-(19) [14]

$$\begin{aligned}\hat{\rho}_{SE_L}^{\text{out}} &= |\psi_{\text{out}}\rangle \langle \psi_{\text{out}}| = \sum_i p_i |i\rangle_S \langle i| \otimes \text{Tr}_{E_{n-L}} \{ \mathcal{M}_{E_i} (\hat{\rho}_E^{\text{in}}) \}, \\ &= \sum_i p_i |i\rangle_S \langle i| \otimes \text{Tr}_{E_{n-L}} \left\{ \underbrace{|\mathbf{i} \oplus \xi\rangle^{\otimes n} \langle \mathbf{i} \oplus \xi|}_{:=|E_i\rangle \langle E_i|} \right\},\end{aligned}\quad (54)$$

which generate the 'QD-plateau' in the corresponding PIPs (s. Figure 1). This is apparent, since for a classically coherent state the principle of »entanglement monogamy« applies (paragraph 4.1.5), as is the case in (54), where each environmental n -qubit output state $|E_i\rangle$ is uniquely connected with a single pointer state $|i\rangle$ of S such that⁷ $\langle E_i | E_j \rangle = \delta_{i,j}$. Consequently, we argued in paragraph 4.1.6 that a measurement may be reinterpreted by means of the **State-Merging-Protocol** [13] which entangles S and E and allows us to extract the optimal information gain g (s. (20) above) of a quantum measurement (54) as an interplay between the communication cost q (corresponding to the number of qubits in $\hat{\rho}_S^{\text{out}}$ whose classical Shannon-information $H(S_{\text{class}})$, s. (15) above, is to be transmitted to E , here $q = k$) and the entanglement cost e (indicating the maximal possible Schmidt-rank between the output subsystems $\hat{\rho}_S^{\text{out}}$ and $\hat{\rho}_{E_L}^{\text{out}}$ of (54) above). Certainly, w.r.t. QD we have to change the perspective and trace out parts of E (as in (19) and (54) above), instead of tracing out the mixed part $\hat{\rho}_A^{\text{in}} = \hat{\rho}_A^{\text{out}} = \sum_i p_i |i\rangle_S \langle i|$ of the open system of interest $\hat{\rho}_S^{\text{out}} = \text{Tr}_{E_L} [\hat{\rho}_{SE_L}^{\text{out}}]$ in (54), as already done in (46).

Nevertheless, these details are only of minor significance for the appropriate application of the State-Merging-Protocol in the course of the QD-versions (19) and (54) of (46). Much more important is the following conclusion: If we accept the interpretation of $I(S : E_f)$ from (6) as the amount of information about the system of interest S that the environment E already possesses as a consequence of a given ctp measurement map $\mathcal{M}(\cdot) \equiv \mathcal{E}(\cdot) = \sum_i p_i |i\rangle_S \langle i| \otimes \mathcal{M}_{E_i}(\cdot) = \sum_i p_i |i\rangle_S \langle i| \otimes$

$K_i^E(\cdot) K_i^{E\dagger}$, then in order to see the QD-plateau in the corresponding PIPs of $I(S : E_f)$ emerge, we need to minimize the degree of entanglement (the entanglement cost e) in $\hat{\rho}_{SE_L}^{\text{out}}$ between S and E_L in (54), since the lower e -value (54) offers, the higher $I(S : E_f)$ -value would be obtained, indicating that E already knows almost everything about $H(S_{\text{class}})$ (for concrete examples of this minimization of e consult paragraph 4.1.1 again, including (12) from subsection 3.2).

Since the optimal quantum information gain g (20) of a quantum measurement \mathcal{M} arises as a maximum $\max_{\{\hat{\rho}_S^{\text{out}}\}} I^{\text{coh}}(S : E_L)$ of the coherent information between $\hat{\rho}_S^{\text{out}}$ and $\hat{\rho}_{E_L}^{\text{out}}$ of (54), we may interpret, according to paragraph 4.1.6, the corresponding quantum mutual information $S(\hat{\rho}_{SE_L}^{\text{out}}) \equiv$ joint entropy of the total output state $\hat{\rho}_{SE_L}^{\text{out}}$

$$I(S : E_L) = S(\hat{\rho}_S^{\text{out}}) + S(\hat{\rho}_{E_L}^{\text{out}}) - S(\hat{\rho}_{SE_L}^{\text{out}}) = \underbrace{S(\hat{\rho}_S^{\text{out}})}_{:=q} - \underbrace{S(\hat{\rho}_{SE_L}^{\text{out}} | \hat{\rho}_{E_L}^{\text{out}})}_{:=e} = S(\hat{\rho}_{E_L}^{\text{out}}) + I^{\text{coh}}(S : E_L) \quad (55)$$

and its maximum value w.r.t. the (in general non-pure) output state $\hat{\rho}_{AR}^{\text{out}} \equiv \hat{\rho}_S^{\text{out}}$ of S , $\max_{\{\hat{\rho}_S^{\text{out}}\}} I(S : E_L)$, as a maximization

of the quantum channel capacity w.r.t. the coherent information $I^{\text{coh}}(S : E_L) = S(\hat{\rho}_S^{\text{out}}) - S(\hat{\rho}_{SE_L}^{\text{out}}) \equiv -S(\hat{\rho}_{E_L}^{\text{out}} | \hat{\rho}_S^{\text{out}})$ which is already contained in (55) [14, 15, 16]. This is reasonable, since $I^{\text{coh}}(S : E_L)$ is only »conjectured« in (37) as playing the same role as Shannon's mutual information $I_{\text{Sh}}(\{X^k\} : \{Y^k\})$ from (23), without being regarded as completely equivalent. However, if, for a given output state $\hat{\rho}_{SE_L}^{\text{out}}$, the value of $I^{\text{coh}}(S : E_L)$ remains positive semi-definite, $I^{\text{coh}}(S : E_L) \geq 0 \forall (1 \leq L \leq n)$, then this automatically leads to the appearance of the QD-plateau in the corresponding PIP, and vice versa. Apparently, by maximizing $I^{\text{coh}}(S : E_L)$ one, from the perspective of Zurek's qubit model of QD (subsection 3.2), automatically optimizes $I(S : E_L)$ in (55) and with it the information storage capacity (redundancy) $R^f = f^{-1}$ of E , as well as the transmission capacity χ' (30) of the corresponding quantum channel⁸ $\mathcal{E}(\cdot)$, in other words $\max_{\{\hat{\rho}_S^{\text{out}}\}} I(S : E_L) \equiv \chi$.

Therefore, we may conclude that from the operational point of view $I(S : E_L)$ in (55) answers the two following questions (problems):

⁷Nevertheless, in subsection 4.2 we will, as indicated in paragraph 4.1.5, demonstrate that an output state does not have to be necessarily and strictly classically coherent in order for QD to appear; this would mean that the argumentation of [14] remains valid even if the output state $\hat{\rho}_{SE_L}^{\text{out}}$ does not strictly display the classically coherent form of (54).

⁸Namely, the condition $I^{\text{coh}}(S : E_L) \geq 0 \forall (1 \leq L \leq n)$ holds in the limit of effective decoherence outlined in (8), w.r.t. which the relation $S(E_f) \approx H(S_{\text{class}})$, due to the approximatively fulfilled »entanglement monogamy« of $\hat{\rho}_{SE_L}^{\text{out}}$, remains valid in general (as is the case for example within Zurek's qubit model of QD in (12) of subsection 3.2). Classically coherent output states (18) are precisely those which structurally adhere to the principle of »entanglement monogamy« of $\hat{\rho}_{SE_L}^{\text{out}}$ discussed in paragraph 4.1.5, therefore fulfilling the condition $I^{\text{coh}}(S : E_L) \geq 0 \forall (1 \leq L \leq n)$ that leads to QD.

1. How many qubits ($1 \leq m \leq n$) among n possible does E need to decode a k -qubit message of S with minimal transmission error?
2. What is an optimal compression rate of a decoded n -qubit version of the k -qubit S -message stored in E such that the stored S -message can be reconstructed completely from a minimal number of E -qubits?

A consequence of these questions is the interpretation of (55) as a measure of optimal quantum channel capacity χ , maximal redundancy R (number of E -qubits, each of which containing the entire $H(S_{\text{class}})$, subsection 3.2) and the highest compressibility η_{opt}^E of resources that the n -qubit E needs to decode the uncompressed k -qubit message of S with minimal transmission error [14], or, in other words:

1. $I(S : E_{f=1})$ measures the optimal quantum channel capacity χ and the minimal redundant size R^f of E (number of environmental qubits, each of which containing the entire $H(S_{\text{class}})$) necessary for efficient error-correcting transmission (encoding) of the classical Shannon-information $H(S_{\text{class}})$ about S .
2. $I(S : E_{f<1})$ measures, from the point of view of E , the optimal decoding compressibility (compression rate) f_{opt} (8) for an n -qubit version of a (not compressed) k -qubit classical (effectively decohered) S -message transmitted to E . This optimal compression rate corresponds to $f_{\text{opt}} = \frac{L_{\text{min}}}{n} = \eta_{\text{opt}}^E \leq \frac{k}{n} \ll 1$, with optimal redundancy (8) $R_{\text{opt}}^f = \frac{1}{f_{\text{opt}}} = \frac{n}{L_{\text{min}}} \leq \frac{n}{k} \gg 1$. QD aims at obtaining R_{opt}^f from the corresponding PIPs of $I(S : E_f)/H(S_{\text{class}})$ by minimizing the entanglement cost e between S and E in (55). The task of finding appropriate general matrix structures of $\hat{\rho}_{\text{SEL}}^{\text{out}}$ from (54) that lead to this minimization of e will be pursued in the forthcoming subsections.

These two answers indicate that the entanglement cost e tends to diminish the value of $I(S : E_L)$ in (55) thus reducing the optimal QD-redundancy R_{opt}^f , which is the reason why we could term e »redundancy loss« or »channel noise«, for the higher the R^f -value one obtains from (55), the lower the e -value that would emerge, leading to an increase of $I(S : E_L)$, and vice versa. Indeed, higher R^f -values indicate higher transmission capacity χ' (30) of $H(S_{\text{class}})$ for a given quantum channel $\mathcal{E}(\cdot)$ with minimal transmission error. This is also the case for Zurek's qubit model of QD: for example, from (12) we compute R^f to be $R^f = n = R_{\text{opt}}^f$, which is precisely the optimal redundancy for a 1-qubit open system ($k = 1$). Thus, $R_{\text{opt}}^f = n$ shows that w.r.t. (12) the QD-plateau in Fig. 1 appears already after intercepting one of n possible E -qubits, indicating that in this case already one environmental qubit suffices in order to guarantee efficient error-correcting decoding of transmitted Shannon-information $H(S_{\text{class}})$ about S by the recipient E . In this sense we also may view QD as an indication for the highest transmission rate R_{opt}^f of classical information about S to E (i.e. the highest number of redundant $H(S_{\text{class}})$ -copies in E) with a minimal number $n \cdot f_{\text{opt}}$ of environmental memory cells needed for the complete reconstruction of $H(S_{\text{class}})$ by E (in (12) already one E -qubit suffices to reconstruct $H(S_{\text{class}})$ completely).

Maxwell's demon and g

In (55) we used a conjecture (37) to interpret the maximization of the quantum mutual information $I(S : E_L)$ as representing operationally the optimal quantum channel capacity χ in (30) alias an optimal rate at which a quantum measurement, according to paragraph 4.1.6, gathers information about the open system of interest. However, since we concentrate in (15) on the physical aspect of optimal storage capacity (redundancy) R_{opt} for a given (prepared) environment E , we will abandon the concept of coherent information $I^{\text{coh}}(S : E_L)$, which served as an operational argument for an alternative interpretation of $I(S : E_L)$ from the practical point of view of information theory, and concentrate in the forthcoming subsections on the notion of entanglement cost e in (55) which (15) aims to minimize in order to ensure the highest storage capacity R_{opt} of E manifested as the QD-plateau in the corresponding PIP-plots of $I(S : E_L)$, as already emphasized w.r.t. (20). Therefore, we conclude the current subsection by discussing a broader physical interpretation of entanglement cost e from the perspective of the Second Law of thermodynamics and quantum information theory⁹.

In the course of thermodynamics and his theory of heat J. C. Maxwell was the first who in 1871 outlined a thought experiment in which he was able to demonstrate that one could design a machine that would, if ever realized (constructed), in principle violate the Second Law of thermodynamics [15, 16]! Such a »hell machine« Maxwell was keene to propose consists of an isolated ideal gas container (»vessel«), which is separated by a wall into two chambers. The absolute temperature T_{ideal} of the gas is uniform and given by the average kinetic energy $E_{\text{ideal}} = 3k_B T/2$ (k_B is the Boltzmann constant) of its molecules. Certainly, since E_{ideal} and T_{ideal} are macroscopic measures, individual gas molecules have different velocities, however they do not have a »temperature«. Now, Maxwell lets an imaginary creature (a »demon«) guard the trapdoor between two chambers that allows individual molecules to pass from one chamber to another without friction. This »Maxwell's demon« inspects the velocities of all molecules, allowing only the faster ones (i.e. those

⁹The author would like to thank Prof. Dr. R. Renner for his interesting review-talk »A quantum perspective on Maxwell's demon« given at the Johann Wolfgang Goethe-University of Frankfurt/M on April 30th, 2014.

molecules with average kinetic energies $E' > E$) to pass for instance from the left to the right chamber of the vessel. As a result of this »demonic influence«, after a long period of time, most of the fast gas molecules are found in the right chamber of the container, increasing its temperature w.r.t. the temperature of the left chamber containing mainly slow gas molecules.

Clearly, this simultaneous heating of the right and cooling of the left chamber of the vessel, carried out by the demon without investment of energy or work, contradicts the Second Law of thermodynamics, which asserts that heat, as a measure of the average kinetic energy of the gas, cannot flow spontaneously from a cold to a hot body, or, equivalently, that in an isolated system entropy as a measure of disorder (randomness) can only increase. Even worse: the artificially created temperature difference between the two chambers of the vessel could even be employed to extract usable work, apparently leading to the *perpetuum mobile of the second kind*! Maxwell tried to solve this paradox by arguing that the Second Law of thermodynamics, as a statistical law, applies only to large number particles (macroscopic level), whereas at a microscopic level aberrations in the behaviour of entropy may occur [20]. On the other hand, L. Szilárd observed in 1929 that in order to measure molecular velocities the »demon« would have to irreversibly spend some kind of energy to spot the slow and the fast molecules and decide whether or not to open the trapdoor [15, 16]. This forced him to introduce the concept of *information entropy* by simplifying Maxwell's demon paradox to the scenario in which the demon represents an engine observing a single gas molecule in the vessel. If this »demonic engine« could be realized, then the demon would, should he know where the gas molecule was located, move a frictionless piston to confine it, without investing effort (work expenditure). On the other hand the pressure effect of the molecule on the piston confining it could be applied to, for instance, lift a weight (corresponding to the *perpetuum mobile* generation of useful work).

In order to save the Second Law of thermodynamics Szilárd came to the conclusion that the balance of entropy contributions during the process (cycle) of demon's observations has to consider the positive entropy associated with the information concerning the demon's memory regarding the observed gas molecule and its velocity. In this context there are only two possibilities: either the demon keeps a record of all of its binary decisions (i. e. of opening or closing the trapdoor), in which case the demon's memory space and its positive entropy (the number of accessible memory states in demon's mind) increases, or it (the demon) deletes the entire gathered information one bit per unit of time due to its exhausted memory space. The latter erasure of demon's information content represents an irreversible process that, from the point of view of thermodynamics [20], »must increase the entropy of the surrounding environment of the demon«, as R. Landauer used to put it in 1961 [15, 16], formulating the lower bound for the energy dissipation and the corresponding environmental entropy increase associated with information erasure, nowadays known as the *Landauer's principle*:

The energy dissipated into the environment by the erasure of a single bit of information is at least $k_B T \log 2$, leading to an increase of environmental entropy by at least $k_B \log 2$.

After all, for a given bit memory cell the corresponding binary value, which may be »0« or »1«, is after erasure reset, for example, to »0«, making it impossible to deduce (reconstruct) the original state of the bit memory cell prior to its erasure. It is easy to understand the origin of this lower bound estimate emphasized by Landauer for erasure-induced increase of environment entropy from the perspective of Shannon's classical information theory: let us interpret the demon's memory which should be cleared as a binary source $X = \{0, 1\}$ with a uniform probability distribution $p(1) = p(0) = 1/2$ for the memory bit being either in state »1« or »0«. Then, as seen in paragraph 4.1.2, the self information associated with any of the two events $x \in X$ corresponds to $I_{\text{self}}(x) = -\ln p(x) = -\ln [1/2] = \ln 2$ in physical k_B -units of the natural logarithm, leading to the average Shannon-like entropy

$$H(\{X\}) = k_B \langle I_{\text{self}}(x) \rangle = k_B [-p(0) \ln p(0) - p(1) \ln p(1)] = k_B \ln 2 \quad (56)$$

of the source X . Thus, according to the Landauer's principle, when cleaning the memory one converts information content of each information bit into energy of memory's average information. In 1980s C. Bennett [21] has shown that this energy of memory's average information may be, by means of (56), identified with the heat $Q = k_B T \langle I_{\text{self}}(x) \rangle = k_B T \ln 2$, which also corresponds to the equivocation $H(\{X\}|\{Y\})$ of the classical communication channel in (21) between X and its environment Y (the vessel and gas molecules). Since the cleared memory of the demon may be described as a single-event source $X' = \{0\}$, with probability $p(0) = 1$, zero event information $I_{\text{self}}(0) = -\ln p(0) = -\ln 1 = 0$ and zero Shannon-entropy $H(\{X'\}) = k_B \langle I_{\text{self}}(0) \rangle = 0$, we notice readily that the difference ΔH in memory entropy before and after erasure is $\Delta H = H(\{X'\}) - H(\{X\}) = -k_B \ln 2$, corresponding to the amount of entropy communicated to demon's environment in accordance with Landauer's principle. For Szilárd the only important issue was that the entropy increase ΔH occurs during the resetting (erasure) process in order to validate the Second Law of thermodynamics, since each erasure process must generate some form of heat that cannot be transformed into useful work without having to endure the effects of »noise« (equivocation) $H(\{X\}|\{Y\})$ when sending information through classical channels (thermodynamic and information-theoretic irreversibility). Therefore, ΔH does not only indicate Landauer's lower bound of the erasure-induced environmental entropy increase, but it also points out the most important aspect of quantum information theory

that contrasts Shannon's classical information theory, according to which *information is physical* (this kind of reasoning is not apparent from the perspective of Shannon's information theory). This simply means that processing of information (including its creation, manipulation, proliferation and erasure) involves physical laws that necessitate information obliteration due to the finite size of demon's memory (there are no Turing machines with infinite memory in reality) and lead to irreversible computations from whose outputs one is not capable to reconstruct the corresponding inputs. In other words, Bennett identifies: $\Delta H = Q$ [21].

Since Bennett was able to identify in his 1980s paper the classical channel noise with the amount of heat Q transfered to the entire environment of the demon after erasing the information content from demon's memory, we also may say, referring to the identification of the classical channel noise with the corresponding equivocation (21) in paragraph 4.1.2, that thermodynamic irreversibility of information processing quantified by Q induces noise within the classical quantum channel [21]. Following Bennetts more recent arguments from 2003 [21] one may also offer the following quantum information theoretic interpretation of ΔH from Landauer's principle: if we look at Maxwell's demon as a quantum gate (such as, for example, the CNOT-gate that represents idealized measurements), then by applying the conjecture (37) to Landauer's principle we may state that ΔH corresponds to the entanglement cost e in (44), generating entanglement-induced noise («heat») of the quantum channel $\mathcal{E}(\cdot)$ in (55) which diminishes the amount of the optimal quantum channel capacity $\max_{\{\hat{\rho}_S^{\text{out}}\}} I(S : E_L) \equiv \chi$. Therefore, by minimizing e in (55) we indeed maximize $I(S : E_L)$ and with it

the quantum information gain g of a measurement, since a minimal amount of entanglement needed to reconstruct the classical information $H(S_{\text{class}}) = S(\hat{\rho}_S^{\text{out}}) := q = k$ of an open, effectively decohered system S (i.e. entanglement cost e) indicates the amount of demon's memory (here corresponding to the memory of the observer that intercepts fragments of system's environment E) that needs to be occupied by the knew relevant information about S . In other words, e quantifies the amount of measurement interactions that the demon needs to perform in order to reconstruct $H(S_{\text{class}})$: the more measurements the observer (the demon) needs to perform, the smaller will be the value of the quantum mutual information $I(S : E_L)$ in (55) which measures the amount of $H(S_{\text{class}})$ that one can already infer from a given output state $\hat{\rho}_{E_L}^{\text{out}}$ of the system's environment E and its fragments and the less storage cells of its memory the demon will have to clear. Therefore, minimizing e implies minimization of the entropy amount transfered from demon's memory to its (total) environment $\hat{\rho}_{SE_L}^{\text{out}}$ which needs to be considered when keeping track of different entropy contributions in (55) if one wants the Second Law of thermodynamics to hold even for microscopic (quantum) systems (Caution: from the perspective of the quantum demon the environment is not only E , but the total system $\hat{\rho}_{SE_L}^{\text{out}}$ consisting of S and E !). Contrary to the quantum case (where the quantum nature of correlation necessitates the incorporation of the entropy associated demon's memory into (55) above), in the course of macroscopic (classical) systems the amount of demon's memory entropy transfered to $\hat{\rho}_{SE_L}^{\text{out}}$ is of no significance and may be ignored when computing different entropy contributions from interacting physical (sub)systems [20]. Accordingly, we may conclude that (55) asserts that a quantum Maxwell's demon could indeed transform heat into usable work, however it would need to «consume» entanglement (perform measurements), as indicated by e , in order to perform such tasks [21]. This is the main reason why we need to minimize the joint von Neumann entropy $S(\hat{\rho}_{SE_L}^{\text{out}})$ in (55), as will be done in the next subsection 4.2, since only the minimal $S(\hat{\rho}_{SE_L}^{\text{out}})$ leads to the minimal entanglement cost $e \equiv \Delta H$, associated with the quantum equivocation $S(\hat{\rho}_S^{\text{out}} | \hat{\rho}_{E_L}^{\text{out}})$.

Summarizing, we may conclude that the Landauer's principle may be transferred to the quantum domain by utilizing (37) and conjecturing the quantum entanglement cost e as addressing quantitatively the entropy amount of demon's memory that needs to be transferred into its environment $\hat{\rho}_{SE_L}^{\text{out}}$ (after all, each measurement device or demon has to possess a finite memory unit from which one has to clear away useless (qu-)bits and their information content from time to time). Minimal e -values lead to the maximal quantum information gain g , indicating that in order to obtain a maximal g according to (20) one needs to minimize the influence of demon's memory entropy on $\hat{\rho}_{SE_L}^{\text{out}}$, in other words: $\min_{\{\hat{\rho}_S^{\text{out}}\}} S(\hat{\rho}_{SE_L}^{\text{out}}) \Rightarrow \min_{\{\hat{\rho}_S^{\text{out}}\}} e$. Thus, also in the quantum domain we may regard Landauer's principle as enclosing an informal

belief that there is an intrinsic cost $e \equiv \Delta H$ for every elementary act of information processing. Nevertheless, information processing and acquisition have, as pointed out in [21], no intrinsic, irreducible thermodynamic cost, whereas the act of information destruction (erasure) does indeed have an irreducible thermodynamic cost, a cost e exactly sufficient to 'preserve' the Second Law of thermodynamics from the demon's influence. This means that, citing Bennett again [21], «measurement and copying could be intrinsically irreversible, however we have to ensure that all manipulations of information processing are performed in such a way as to overwrite previous (old) information» in demon's finite memory, corresponding to $e > 0$.

4.1.10 Conclusions

Quantum mutual information $I(S : E_f)$ from (6) answers the following two operational questions (tasks):

1. How many qubits ($1 \leq m \leq n$) among n possible does E need to decode a k -qubit message of S with minimal transmission error?
2. What is an optimal compression rate of a decoded n -qubit version of the k -qubit S -message stored in E such that the stored S -message can be reconstructed completely from a minimal number of E -qubits?

Related to these two questions are the following answers (solutions):

1. $I(S : E_{f=1})$ measures optimal quantum channel capacity χ and the minimal redundant size of E (number of environmental qubits) necessary for efficient error-correcting transmission (encoding) of classical Shannon-information $H(S_{\text{class}})$ about S .
2. $I(S : E_{f<1})$ measures, from the point of view of E , the optimal decoding compressibility (compression rate) for an n -qubit version of a (not compressed) k -qubit effectively classical (decohered) S -message transmitted to E . This optimal compression rate corresponds to $0 < f_{\text{opt}} = \frac{L_{\text{min}}}{n} = \eta_{\text{opt}}^E \leq \frac{k}{n} \ll 1$, with an optimal redundancy $R_{\text{opt}}^f = \frac{1}{f_{\text{opt}}} = \frac{n}{L_{\text{min}}} \leq \frac{n}{k} \gg 1$. QD aims at obtaining R_{opt}^f from the corresponding PIPs of $I(S : E_f) / H(S_{\text{class}})$ by minimizing the entanglement cost e between S and E in (55).

4.2 Quantum Darwinistic many-qubit system-environment output states

Now we again turn our attention to the mathematical criteria necessary and sufficient for the appearance of QD. Zurek's toy qubit-model of QD has shown that the characteristic 'plateau' of quantum MI $I(S : E_f)$ in (6) appears w.r.t. f if the corresponding E -»memory cells« become mutually orthogonal for $n \gg 1$. However, $\hat{\rho}_{SE}^{\text{out}}(L)$ does not have to remain correlation-free $\forall L < n$, since the present section will show us that partially overlapping E -»memory states« can also validate (15) if we enforce certain constraints on non-diagonal entries of $\hat{\rho}_{SE}^{\text{out}}(L)$. Since the relation $H(S, \mathcal{F}) \geq H(E_f)$ allows equality only in the limit $n \gg 1$, it will turn out that (15) imposes a strong constraint on physically allowed $\hat{\rho}_{SE}^{\text{out}}(L)$, regardless of the concrete type of interaction $\hat{U}_{\text{int}}^{SE}$ in (7) that leads to $\hat{\rho}_{SE}^{\text{out}}(L)$. We summarize in Table 1 the most important ($k = 1, n = 1$) $\hat{\rho}_{SE}^{\text{out}}$ of appendix C that lead to QD and generalize them to the case of QD-compliant ($k = 1, n > 1$) $\hat{\rho}_{SE}^{\text{out}}$ by introducing in (13)-(15) general output states $|\Psi_{SE}^{\text{out}}\rangle$ that entangle subspaces of a k -qubit S , associated with states $\{|\varphi_i\rangle\}_{i=1}^{i=2^k}$, with subspaces of n -qubit E -registry states $\left\{|\phi_i^{\beta(n)}\rangle\right\}_{\beta(n)=1}^{\beta(n)=2^n}$. The overlap $\sum_{\beta, \gamma} \langle \phi_i^{\beta(n)} | \phi_j^{\gamma(n)} \rangle := \left[r_{\beta, \gamma}^{i,j} + \delta_{ij} \delta_{\beta, \gamma} (1 - r_{\beta, \gamma}^{i,j}) \right]$ between different $|\phi_i^{\beta(n)}\rangle$ in (14) is associated with a decoherence factor $r_{\beta, \gamma}^{i,j}$ which gives the strength of decoherence that turns an initially pure input $\hat{\rho}_S^{\text{in}}$ into an almost (classical) diagonal output $\hat{\rho}_S^{\text{out}} \approx \text{diag}(|c_1|^2, \dots, |c_{2^k}|^2)$ with $H(S) \approx H(S_{\text{class}})$. The present subsection will also give a dependence of $r_{\beta, \gamma}$ on n and k , in accord with [14]. Moreover, constraints we intend to impose on $\sum_{\beta, \gamma} \langle \phi_i^{\beta(L)} | \phi_j^{\gamma(L)} \rangle$ between $(0 < L \leq n)$ w.r.t. indices $i \in \{1, \dots, 2^k\}$ and $\beta(L) \in \{1, \dots, 2^L\}$ will help us classify the QD-compliant ($k \geq 1, n > 1$)- $\hat{\rho}_{SE}^{\text{out}}(L)$. We intend to start with the most restrictive constraints one could impose on $\sum_{\beta, \gamma} \langle \phi_i^{\beta(L)} | \phi_j^{\gamma(L)} \rangle$, before gradually relaxing them, since this will lead to the most general ($k \geq 1, n > 1$)-versions of QD-compliant $\hat{\rho}_{SE}^{\text{out}}$ in Table 1.

4.2.1 Assumption 1: system's pointer states do not overlap, no environmental coherences

This assumption corresponds to the constraint

$$\sum_{\beta, \gamma} \langle \phi_i^{\beta(L-k)} | \phi_j^{\gamma(L-k)} \rangle \stackrel{!}{\sim} \sum_{\beta, \gamma} \delta_{ij} \delta_{\beta(L-k) \gamma(L-k)}, \beta(L-k), \gamma(L-k) \in \{1 + (i-1)2^{L-k}, \dots, i \cdot 2^{L-k}\}$$

and implies that each pointer-state projector $|\varphi_i\rangle \langle \varphi_i|$ of S , as a diagonal ($2^L \times 2^L$)-block of $\hat{\rho}_{SE}^{\text{out}}(L)$, has itself a diagonal structure (without overlapping diagonal elements in $\hat{\rho}_{SE}^{\text{out}}(L)$, indicating that different S -projector subspaces of $\hat{\rho}_{SE}^{\text{out}}(L)$ are to be regarded as *mutually disjoint* or *mutually orthogonal* from the perspective of E and its n -qubit registry states $|\phi_i^{\beta(L)}\rangle$), whereas transition elements $|\varphi_i\rangle \langle \varphi_j|$ of S (i.e. off-diagonal ($2^L \times 2^L$)-blocks of $\hat{\rho}_{SE}^{\text{out}}(L)$), vanish.

Thus, assumption 1 insists that **1)** 2^k subdivisions of a total of 2^L E -registry states $|\phi_i^{\beta(L)}\rangle$ in $\hat{\rho}_{SE}^{\text{out}}(L)$

QD-compliant ($k = 1, n = 1$)-matrix structures of $\hat{\rho}_{SE}^{out}$ in (289), appendix C

- (297): $(e, h) \neq 0 \wedge (f \neq 0 \vee f = 0)$
- (299): $(a, j) \neq 0 \wedge (d \neq 0 \vee d = 0)$
- (300) $(a, e, h, j) \neq 0 \wedge b \neq 0$, including (301)-(302), as well as (303) and (304) as their generalized version
- (306): $(a, e, h, j, b) \neq 0 \wedge (c = -g, f, d) \neq 0$, enclosing (307)-(309) and (310) as their generalized version
- (311): $(a, e, h, j) \neq 0 \wedge (c = -g) \neq 0$ and (329) with $(a = e, h) \neq 0, j = 0 \wedge (c, f) \neq (-g = 0), |c|^2 = |f|^2 = e \cdot h/2$
- (315): $(a, e, h, j) \neq 0 \wedge (d, f) \neq 0$ and (321)-(322): $(a = e \wedge h = j \wedge (c = -g) = d = f)$, with $|c|^2 = a \cdot h/2$

Approximately QD-compliant ($k = 1, n = 1$)-matrix structures of $\hat{\rho}_{SE}^{out}$ in (289), appendix C

- (330): $(a, h, j) \neq 0 \wedge c \neq (-g = 0)$ with (331)
- (332): $(a, h, j) \neq 0 \wedge d \neq 0$ with (333)
- (334): $(a, h, j) \neq 0 \wedge (c, d) \neq 0 \wedge (c \neq -g = 0)$ with (338) and $h = j$
- (342): $(a, h, j) \neq 0 \wedge (c, i) \neq 0 \wedge (c \neq -g = 0) \wedge (-i \neq b = 0)$ with (344) and $|i| \approx 0$
- (345): $(a, h, j) \neq 0 \wedge (d, i) \neq 0 \wedge (i \neq -b = 0)$ with (347) and $|i| \approx 0$
- (348): $(a, h, j) \neq 0 \wedge (c, d, i) \neq 0 \wedge (c \neq -g = 0) \wedge (-i \neq b = 0)$ with (347) and $|i| \approx 0, \text{Re}\{i\} \ll 1$

Table 1: QD-compliant ($k = 1, n = 1$)-matrix structures of $\hat{\rho}_{SE}^{out}$ in (289)

(each of which associated with 2^k S-projectors $|\varphi_i\rangle\langle\varphi_i|$ remain mutually orthogonal and **2**) (maximally) 2^{L-k} E-registry states belonging to the same diagonal S-subspace also remain mutually orthogonal. This leads to the matrix structures of $\hat{\rho}_{SE}^{out}$ and $\hat{\rho}_E^{out}$ (with $L \geq k$ and $L < k$) in (59) below, which correspond exactly to the structure of classically coherent states that adhere to the principle of »entanglement monogamy« [4, 5, 14] and generalize (297) (with $f = 0$) and

(299) (with $d = 0$), satisfying (15) with $H(S, E_f) = H(E_f) = H_{\max}(E_f) = -\sum_{g=1}^{2^L} |c_g^E|^2 \log_2 |c_g^E|^2 = H(S_{\text{class}}) \forall L \leq n$ as long as $L \geq k$ (compare with (12) for $n > L \geq k$).

Otherwise, if $L < k$, different S-projector subspaces of $\hat{\rho}_{SE}^{out}(L)$ in (59) would not be mutually disjoint any more, leading in general to an increment of diagonal $\hat{\rho}_E^{out}(L)$ -eigenvalues, implying $H(E_{\text{dec}}) < H(S, E_{\text{dec}})$, since in this case $H(E_{\text{dec}}) < H_{\max}(E_f)$, whereas the entropy of $\hat{\rho}_{SE}^{out}(L)$ still satisfies $H(S, E_{\text{dec}}) = H_{\max}(E_f)$. It is easy to illustrate this issue by means of the following ($k = 2, n = L = 3$)-matrix structure of $\hat{\rho}_{SE}^{out}$, for which (59) asserts: **1**)

there are due to $k = 2$ and $L = n = 3$ four diagonal (2×2) -matrices $D_l = \text{diag} \left[|c_{l,2+1}^E|^2, |c_{(l+1),2}^E|^2 \right]$ in $\hat{\rho}_{SE}^{out}(L \geq k)$

for $l \in \{0, \dots, 2^k - 1 = 3\}$ whose entries $|c_{l,2+1}^E|^2$ and $|c_{(l+1),2}^E|^2$ should sum up to one of the four probabilities $|c_i|^2$ w.r.t. one of the four diagonal subspaces $|\varphi_i\rangle\langle\varphi_i|$ of S. Therefore, $\hat{\rho}_{SE}^{out}(L \geq k)$ displays the $(2^5 \times 2^5)$ -structure

$$\hat{\rho}_{SE}^{out}(L \geq k) = \text{diag} \left[\underbrace{D_0, 0, 0, 0, 0, 0, 0, 0}_{|00\rangle\langle 00| \text{ of } S}, \underbrace{0, 0, D_1, 0, 0, 0, 0, 0}_{|01\rangle\langle 01| \text{ of } S}, \underbrace{0, 0, 0, 0, D_2, 0, 0, 0}_{|10\rangle\langle 10| \text{ of } S}, \underbrace{0, 0, 0, 0, 0, 0, D_3, 0}_{|11\rangle\langle 11| \text{ of } S} \right]. \quad (57)$$

(57) will, due to the mutual disjointness of the D_l , definitely validate (15), irrespectively of how we distribute the four S-probabilities $|c_i|^2$ among the total of 8 diagonal entries $|c_g^E|^2$ of the D_l -submatrices; **2**) However, due to the fact that we also aim at adhering to (15) for $k = L = 2$, we have to take a closer look at (57): here we may associate the 8 diagonal entries $|c_g^E|^2$ with the following projectors of the $n = L = 3$ qubit E

$$\begin{aligned} |c_1^E|^2 &\sim |000\rangle\langle 000|, |c_2^E|^2 \sim |100\rangle\langle 100|, |c_3^E|^2 \sim |010\rangle\langle 010|, |c_4^E|^2 \sim |110\rangle\langle 110|, |c_5^E|^2 \sim |001\rangle\langle 001| \\ |c_6^E|^2 &\sim |001\rangle\langle 001|, |c_7^E|^2 \sim |101\rangle\langle 101|, |c_8^E|^2 \sim |011\rangle\langle 011|, |c_9^E|^2 \sim |111\rangle\langle 111| \end{aligned} \quad (58)$$

$$\begin{aligned}
\hat{\rho}_{\text{E}}^{\text{out}}(L \geq k) &= \sum_{i, \beta(L)} |c_i|^2 |\phi_i^{\beta(L)}\rangle \langle \phi_i^{\beta(L)}| = \begin{pmatrix} |c_1^{\text{E}}|^2 & \cdots & 0 \\ \vdots & \ddots & \vdots \\ 0 & \cdots & |c_{2^L}^{\text{E}}|^2 \end{pmatrix}_{2^L \times 2^L}; \\
\hat{\rho}_{\text{E}_{\text{dec}}}^{\text{out}}(L) &= \hat{\rho}_{\text{E}}^{\text{out}}(L < k) = \sum_{l=0}^{2^k-1} D_l^{\text{dec}}; \\
\hat{\rho}_{\text{SE}}^{\text{out}}(L \geq k) &= \sum_{i, \beta(L)} |c_i|^2 |\varphi_i\rangle \langle \varphi_i| \otimes |\phi_i^{\beta(L)}\rangle \langle \phi_i^{\beta(L)}| = \\
&\begin{pmatrix} \mathbf{A}_0 & \mathbf{0}_{2^L \times 2^L (2^k-1)} & & \\ \mathbf{0}_{2^L (2^k-1) \times 2^L} & \ddots & & \\ & & \mathbf{A}_l & \mathbf{0}_{2^L \times 2^L (2^k-1-l)} \\ & & \mathbf{0}_{2^L (2^k-1-l) \times 2^L} & \ddots \\ & & & \mathbf{A}_{2^k-1} \end{pmatrix}_{2^{L+k} \times 2^{L+k}}; \\
\hat{\rho}_{\text{SE}_{\text{dec}}}^{\text{out}}(L) &= \hat{\rho}_{\text{SE}}^{\text{out}}(L < k) = \sum_{l=0}^{2^k-1} D_l^{\text{dec}} = \begin{pmatrix} D_1^{\text{dec}} & \cdots & \mathbf{0}_{2^L \times 2^L} \\ \vdots & \ddots & \vdots \\ \mathbf{0}_{2^L \times 2^L} & & D_{2^k-1}^{\text{dec}} \end{pmatrix}_{2^{L+k} \times 2^{L+k}},
\end{aligned} \tag{59}$$

where $X = \mathbf{0}_{2^{L-k} \times 2^{L-k}}$ (R_l blocks for $l = \text{fixed}$), $l \in \{0, \dots, 2^k - 1\}$, $s_l = (2^k - 1 - l) 2^{L-k}$, with

$$\begin{aligned}
D_l^{\text{dec}} &= \begin{pmatrix} |c_{l \cdot 2^L + 1}^{\text{SE}}|^2 & \cdots & 0 \\ \vdots & \ddots & \vdots \\ 0 & \cdots & |c_{(l+1) \cdot 2^L}^{\text{SE}}|^2 \end{pmatrix}_{2^L \times 2^L} \\
\mathbf{A}_0 &= \begin{bmatrix} D_0 & \cdots & \mathbf{0}_{2^{L-k} \times s_0} \\ \vdots & \ddots & \vdots \\ \mathbf{0}_{s_0 \times 2^{L-k}} & \cdots & \mathbf{0}_{s_0 \times s_0} \end{bmatrix}_{2^L \times 2^L} \quad D_0 = \begin{pmatrix} |c_1^{\text{E}}|^2 & \cdots & 0 \\ \vdots & \ddots & \vdots \\ 0 & \cdots & |c_{2^{L-k}}^{\text{E}}|^2 \end{pmatrix}_{2^{L-k} \times 2^{L-k}} \\
\mathbf{A}_l &= \begin{bmatrix} X & \cdots & X \\ \vdots & \ddots & \vdots \\ & & D_l & \mathbf{0}_{2^{L-k} \times s_l} \\ X & \cdots & \mathbf{0}_{s_l \times 2^{L-k}} & \ddots & \mathbf{0}_{s_l \times s_l} \end{bmatrix}_{2^L \times 2^L} \quad D_l = \begin{pmatrix} |c_{l \cdot 2^{L-k} + 1}^{\text{E}}|^2 & \cdots & 0 \\ \vdots & \ddots & \vdots \\ 0 & \cdots & |c_{(l+1) \cdot 2^{L-k}}^{\text{E}}|^2 \end{pmatrix}_{2^{L-k} \times 2^{L-k}} \\
\mathbf{A}_{2^k-1} &= \begin{bmatrix} \mathbf{0}_{s_0 \times s_0} & \cdots & \mathbf{0}_{2^{L-k} \times s_0} \\ \vdots & \ddots & \vdots \\ \mathbf{0}_{s_0 \times 2^{L-k}} & \cdots & D_{2^k-1} \end{bmatrix}_{2^L \times 2^L} \quad D_{2^k-1} = \begin{pmatrix} |c_{(2^k-1) \cdot 2^{L-k} + 1}^{\text{E}}|^2 & \cdots & 0 \\ \vdots & \ddots & \vdots \\ 0 & \cdots & |c_{2^L}^{\text{E}}|^2 \end{pmatrix}_{2^{L-k} \times 2^{L-k}}
\end{aligned}$$

\mathbf{A}_l contains, for fixed l , $R_l = \sum_{i=0}^l \alpha_i (2^{L-k} \times 2^{L-k})$ zero-blocks X , with recursively defined α_i , ($\alpha_0 = 0$ and $\alpha_l = \alpha_{l-1} + 2 \cdot (2^l - l) + 1$). There are maximally $2^L |c_g^{\text{E}}|^2 \neq 0$ in (59), with $g \equiv (i \cdot \beta(L) \cdot 2^{-k}) \in \{1, \dots, 2^{L-k}, 2^{L-k} + 1, \dots, 2^L\}$. Also, there are maximally 2^k of 2^{L+k} values $|c_m^{\text{SE}}|^2 \neq 0$ in (59) (i.e. only one diagonal value per each diagonal S-subspace), with $m \equiv (i \cdot \beta(L)) \in \{1, \dots, 2^L, 2^L + 1, \dots, 2^{L+k}\}$.

The first row of D_l -entries in (58) is associated with the $|0\rangle \langle 0|$ -subspace of the third E-qubit, whereas the second row displays $|c_g^{\text{E}}|^2$ -entries associated with the $|1\rangle \langle 1|$ -subspace of the third E-qubit.

Thus, by tracing out this third E-qubit we arrive at the $L = k = 2$ structure of $\hat{\rho}_{\text{SE}}^{\text{out}}(L \geq k)$ from (57) given by

$$\hat{\rho}_{SE}^{\text{out}} (L = k) = \text{diag} \left[\underbrace{D_0, 0, 0}_{|00\rangle\langle 00| \text{ of } S}, \underbrace{0, 0, D_1}_{|01\rangle\langle 01| \text{ of } S}, \underbrace{D_2, 0, 0}_{|10\rangle\langle 10| \text{ of } S}, \underbrace{0, 0, D_3}_{|11\rangle\langle 11| \text{ of } S} \right]. \quad (60)$$

But inserting $k = L = 2$ into (59) leads (in accord with appendix B) to the $\hat{\rho}_{SE}^{\text{out}} (L \geq k)$ -structure

$$\hat{\rho}_{SE}^{\text{out}} (L = k) = \text{diag} \left[\underbrace{|c_1|^2, 0, 0, 0}_{|00\rangle\langle 00| \text{ of } S}, \underbrace{0, |c_2|^2, 0, 0}_{|01\rangle\langle 01| \text{ of } S}, \underbrace{0, 0, |c_3|^2, 0}_{|10\rangle\langle 10| \text{ of } S}, \underbrace{0, 0, 0, |c_4|^2}_{|11\rangle\langle 11| \text{ of } S} \right], \quad (61)$$

which emerges from (60) after exchanging subspaces $|01\rangle\langle 01|$ and $|10\rangle\langle 10|$ of S and identifying for instance $|c_1^E|^2 = |c_1|^2$, $|c_6^E|^2 = |c_2|^2$, $|c_3^E|^2 = |c_3|^2$ and $|c_8^E|^2 = |c_4|^2$, whereas $|c_2^E|^2 = |c_4^E|^2 = |c_5^E|^2 = |c_7^E|^2 = 0$. Apparently, (61) enables us to fix the 8 $|c_9^E|^2$ -entries in (58) appropriately by ensuring the validity of (15) for $k = L = 2$, since (59) always guarantees $\hat{\rho}_{SE}^{\text{out}} = \text{diag} [|c_1|^2, |c_2|^2, |c_3|^2, |c_4|^2]$ with $H(S, E_f) = H(E_f) = H(S) \approx H(S_{\text{class}}) \forall (L \leq n)$; **3**) Unfortunately, even if we find a QD-compliant $\hat{\rho}_{SE}^{\text{out}} (L = k)$, such as (61), (59) would yield $\hat{\rho}_{SE_{\text{dec}}}^{\text{out}} (L)$ that violates (15) for $L < k$, since tracing out one more E-qubit in (61) would generate

$$\begin{aligned} \hat{\rho}_{SE_{\text{dec}}}^{\text{out}} (L) &= \hat{\rho}_{SE}^{\text{out}} (L < k) = \text{diag} \left[\underbrace{|c_1^{SE}|^2 = |c_1|^2, 0, 0}_{|00\rangle\langle 00| \text{ of } S}, \underbrace{|c_4^{SE}|^2 = |c_2|^2}_{|01\rangle\langle 01| \text{ of } S}, \underbrace{|c_5^{SE}|^2 = |c_3|^2, 0, 0}_{|10\rangle\langle 10| \text{ of } S}, \underbrace{|c_8^{SE}|^2 = |c_4|^2}_{|11\rangle\langle 11| \text{ of } S} \right] \\ \hat{\rho}_{E_{\text{dec}}}^{\text{out}} (L) &= \hat{\rho}_E^{\text{out}} (L < k) = \sum_{l=0}^{2^k-1} D_l^{\text{dec}}, \text{ with } D_0^{\text{dec}} = \text{diag} [|c_1^{SE}|^2 = |c_1|^2, 0], D_3^{\text{dec}} = \text{diag} [|c_5^{SE}|^2 = |c_3|^2, 0] \\ &\text{and } D_2^{\text{dec}} = \text{diag} [0, |c_4^{SE}|^2 = |c_2|^2], D_4^{\text{dec}} = \text{diag} [0, |c_8^{SE}|^2 = |c_4|^2], \end{aligned} \quad (62)$$

that leads to overlapping diagonal entries of different diagonal S -subspaces after tracing S out of $\hat{\rho}_{SE_{\text{dec}}}^{\text{out}} (L)$: indeed, the S -projectors $|00\rangle\langle 00|$ and $|10\rangle\langle 10|$ in $\hat{\rho}_{SE_{\text{dec}}}^{\text{out}} (L)$ from (62) are correlated with the same registry state $|0\rangle\langle 0|$ of a $L = 1$ -qubit E . The same holds for the S -projectors $|01\rangle\langle 01|$ and $|11\rangle\langle 11|$ in $\hat{\rho}_{SE_{\text{dec}}}^{\text{out}} (L)$ from (62) and the registry state $|1\rangle\langle 1|$ of a $L = 1$ -qubit E . Thus, $\hat{\rho}_{E_{\text{dec}}}^{\text{out}} = \text{diag} [|c_1|^2 + |c_3|^2, |c_2|^2 + |c_4|^2]$ in (62) contains only two diagonal entries due to the mutual dependence of the S -subspaces $|00\rangle\langle 00|$ and $|10\rangle\langle 10|$, as well as $|01\rangle\langle 01|$ and $|11\rangle\langle 11|$, meaning that (59) validates (15) only if $L \geq k$, whereas for $L < k$ E simply does not offer enough storage cells that could store the entire $H(S_{\text{class}})$ with an optimal rate $f_{\text{opt}} = k/n$. (57)-(62) and

$$H(E_{\text{dec}}) = -(|c_1|^2 + |c_3|^2) \log_2 (|c_1|^2 + |c_3|^2) - (|c_2|^2 + |c_4|^2) \log_2 (|c_2|^2 + |c_4|^2) < H(S, E_{\text{dec}}) = H(S) \equiv H(S_{\text{class}}) \quad (63)$$

demonstrate that (59) validates (15) only if we associate in $\hat{\rho}_{SE}^{\text{out}} (n \geq L \geq k)$ (maximally) 2^{L-k} $\hat{\rho}_{SE}^{\text{out}}$ -registry 2^{L+k} -qubit states (projectors) within the corresponding D_l with one of the 2^k S -probabilities $|c_{l+1}|^2$ for each of the 2^k diagonal S -subspaces according to

$$|c_{l+1}|^2 \sim |l_S\rangle\langle l_S| \otimes |j_E\rangle\langle j_E| \text{ with, } j \in [l \cdot 2^{L-k}, \dots, (l+1) \cdot 2^{L-k} - 1], |l_S\rangle\langle l_S| \otimes |j_E\rangle\langle j_E| \equiv |q_1 \dots q_{L+k}\rangle = \sum_{i=1}^{L+k} q_i 2^{i-1}, q_i \in \{0, 1\}, \quad (64)$$

such that $\text{Tr}_{E_{L-k}} [D_l] = \sum_{i=1}^{2^{L-k}} |c_{l \cdot 2^{L-k} + i}^E|^2 \stackrel{!}{=} |c_{l+1}|^2$ holds $\forall l \in \{0, \dots, 2^k - 1\}$ and one may shift (exchange) all D_l among each other without violating (15), which then leads to $f_{\text{opt}} = k/n$ for $n \geq L \geq k \geq 1$, after tracing out individual E-qubits as in appendix B. Thus, by applying (64) one can associate in (57) $|c_{l+1}|^2$ with S - E -projectors according to

$$\begin{aligned} |c_1|^2 \sim |0\rangle_{SE} \langle 0| &= \left| \begin{array}{c} \underbrace{00}_{:=0} \\ \underbrace{00}_{:=0} \end{array} \right\rangle_S \left\langle \begin{array}{c} \underbrace{00}_{:=0} \\ \underbrace{00}_{:=0} \end{array} \right| \otimes \left| \begin{array}{c} \underbrace{000}_{:=0} \\ \underbrace{000}_{:=0} \end{array} \right\rangle_E \left\langle \begin{array}{c} \underbrace{000}_{:=0} \\ \underbrace{000}_{:=0} \end{array} \right| \quad (l=0), \quad |c_2|^2 \sim |9\rangle_{SE} \langle 9| = \left| \begin{array}{c} \underbrace{10}_{:=1} \\ \underbrace{10}_{:=1} \end{array} \right\rangle_S \left\langle \begin{array}{c} \underbrace{10}_{:=1} \\ \underbrace{10}_{:=1} \end{array} \right| \otimes \left| \begin{array}{c} \underbrace{010}_{:=2} \\ \underbrace{010}_{:=2} \end{array} \right\rangle_E \left\langle \begin{array}{c} \underbrace{010}_{:=2} \\ \underbrace{010}_{:=2} \end{array} \right| \quad (l=1) \\ |c_3|^2 \sim |16\rangle_{SE} \langle 16| &= \left| \begin{array}{c} \underbrace{01}_{:=2} \\ \underbrace{01}_{:=2} \end{array} \right\rangle_S \left\langle \begin{array}{c} \underbrace{01}_{:=2} \\ \underbrace{01}_{:=2} \end{array} \right| \otimes \left| \begin{array}{c} \underbrace{001}_{:=4} \\ \underbrace{001}_{:=4} \end{array} \right\rangle_E \left\langle \begin{array}{c} \underbrace{001}_{:=4} \\ \underbrace{001}_{:=4} \end{array} \right| \quad (l=2), \quad |c_4|^2 \sim |27\rangle_{SE} \langle 27| = \left| \begin{array}{c} \underbrace{11}_{:=3} \\ \underbrace{11}_{:=3} \end{array} \right\rangle_S \left\langle \begin{array}{c} \underbrace{11}_{:=3} \\ \underbrace{11}_{:=3} \end{array} \right| \otimes \left| \begin{array}{c} \underbrace{011}_{:=6} \\ \underbrace{011}_{:=6} \end{array} \right\rangle_E \left\langle \begin{array}{c} \underbrace{011}_{:=6} \\ \underbrace{011}_{:=6} \end{array} \right| \quad (l=3) \end{aligned} \quad (65)$$

4.2.2 Assumption 2: system's pointer states do not overlap, environmental coherences allowed

This assumption corresponds to the constraint

$$\sum_{\beta, \gamma} \left\langle \phi_i^{\beta(L-k)} | \phi_j^{\gamma(L-k)} \right\rangle \stackrel{!}{\sim} \delta_{ij}, \beta(L-k), \gamma(L-k) \in \{1 + (i-1)2^{L-k}, \dots, i \cdot 2^{L-k}\}$$

and implies that each pointer-state projector (subspace) $|\varphi_i\rangle\langle\varphi_i|$ of S , may also contain outer-diagonal matrix entries, whereas diagonal elements in $\hat{\rho}_E^{\text{out}}(L)$ that belong to different S -projector subspaces of $\hat{\rho}_{SE}^{\text{out}}(L)$ are not allowed to overlap and are still to be regarded as *mutually disjoint* in the sense of assumption 1 above, although within the same diagonal S -subspace E -registry states are allowed to overlap. On the other hand, transition elements $|\varphi_i\rangle\langle\varphi_j|$ of S , (off-diagonal $(2^L \times 2^L)$ -blocks of $\hat{\rho}_{SE}^{\text{out}}(L)$), are forced to contain only zero entries. This leads to $\hat{\rho}_{SE}^{\text{out}}$ and $\hat{\rho}_E^{\text{out}}$ (with $L \geq k$ and $L < k$) in (70) below.

Matrix structures in (70) satisfy (15) only if we insist that

$$\text{Tr}_{E_{L-k}}(D_l) \stackrel{!}{=} |c_{l+1}|^2 \forall l = (i-1) \in \{0, \dots, 2^k - 1\}, \quad (66)$$

since only then one could obtain in general $H(S, E_f) = H(E_f) \geq H(S_{\text{class}}) \forall (k \leq L \leq n)$ as long as (70) persists for a fixed $L \geq k$ and thus the condition

$$\text{Tr}_{E_L} \left\{ \left(|\phi_i^\beta\rangle^{\otimes(L \geq k)} \langle \phi_i^\gamma| \right) \left(|\phi_j^\beta\rangle^{\otimes(L \geq k)} \langle \phi_j^\gamma| \right) \right\} \stackrel{!}{=} \delta_{i,j} \left[\delta_{\beta,\gamma} + (1 - \delta_{\beta,\gamma}) \cdot \blacksquare_{\beta(L-k), \gamma(L-k)}^{(l)} \right] \wedge \forall \beta(L-k), \gamma(L-k) \quad (67)$$

remains valid. (66) is necessary to ensure a decohered S , $H(S) \approx H(S_{\text{class}})$. Both $H(S, E_f)$ and $H(E_f)$ attain in general higher values than $H(S_{\text{class}})$ for $L > k$, although the outer-diagonal entries $\blacksquare \equiv \blacksquare_{\beta(L-k), \gamma(L-k)}^{(l)}$ within diagonal S -subspaces $\{|\varphi_i\rangle\langle\varphi_i|\}_{i=1}^{2^k}$ in (70) tend to decrease the maximal values of $H(S, E_{L>k})$ and $H(E_{L>k})$ (s. also (291) below). Only for $L = k$ or for certain \blacksquare -values w.r.t. $L > k$ one obtains $H(S, E_f) = H(E_f) = H(S_{\text{class}})$, as in (59). Otherwise, in (70) w.r.t. a fixed $1 < L < k$ different S -projector subspaces of $\hat{\rho}_{SE_{\text{dec}}}^{\text{out}}(L)$ would not be mutually disjoint any more (i.e. (67) does not necessarily apply), leading $\forall (1 < L < k)$ in general to the increment of diagonal $\hat{\rho}_E^{\text{out}}(L)$ -eigenvalues (consider $\hat{\rho}_{E_{\text{dec}}}^{\text{out}}(L)$ in (70) above), implying $H(E_{\text{dec}}) < H(S, E_{\text{dec}})$, since in this case $H(E_{\text{dec}}) < H(S_{\text{class}})$, whereas $H(S, E_{\text{dec}}) = H(S_{\text{class}})$ would in general still remain higher than $H(E_{\text{dec}})$ due to existent S -diagonal subspaces. As in (300) of Appendix C, only specific restrictions on outer-diagonal entries \blacksquare help us maintain (15), otherwise no QD appears. (59) may be viewed as a special case of (70), whose matrix structures also appear w.r.t. $\hat{\rho}_{SE}^{\text{out}}(L)$, $\hat{\rho}_E^{\text{out}}(L)$ and $\hat{\rho}_S^{\text{out}}$ in (12) for $n > L \geq (k = 1)$, leading to QD. Let us illustrate the above conclusions by means of $\hat{\rho}_{SE}^{\text{out}}(L = n = 3 > k = 2)$ from (57): if we modify this matrix structure in accord with (70), we would obtain four (2×2) -matrices D_l

$$D_l = \begin{pmatrix} |c_{l,2+1}^E|^2 & \blacksquare_l \\ \blacksquare_l^* & |c_{(l+1),2}^E|^2 \end{pmatrix}_{2 \times 2}, \quad l \in \{0, \dots, 2^k - 1 = 3\} \quad \blacksquare_{\beta(L-k), \gamma(L-k)}^{(l)} \equiv \blacksquare_l, \quad (68)$$

whose diagonal entries satisfy (69), in accord with (66). Tracing E out from $\hat{\rho}_{SE}^{\text{out}}(L > k)$ in (70) leads with

$$|c_{l,2+1}^E|^2 + |c_{(l+1),2}^E|^2 \stackrel{!}{=} |c_{l+1}|^2, \quad \left(|c_{l,2+1}^E|^2 \neq 0 \wedge |c_{(l+1),2}^E|^2 \geq 0 \right) \forall l \quad (69)$$

to a decohered S . All other configurations of diagonal D_l -entries with $|c_{l,2+1}^E|^2 = |c_{(l+1),2}^E|^2 = 0$ for all or some l -values violate (70), (68) and (15) by slowing down the decoherence of S (s. section 9).

However, as soon as $L < k$ in (70) and (68) it is, because of the violated condition (67), impossible to efficiently store $H(S_{\text{class}})$ into E , even if (69) could be fulfilled: QD (almost) always fails to appear due to the lack of disjointness between diagonal entries of $\hat{\rho}_{SE}^{\text{out}}(L < k = 2)$ belonging to different $\{|\varphi_i\rangle\langle\varphi_i|\}_{i=1}^{2^k}$, which interfere inappropriately when extracting $\hat{\rho}_E^{\text{out}}(L < k = 2)$. Looking again at $\hat{\rho}_{SE}^{\text{out}}(L = n = 3 > k = 2)$ in (68), with (69) valid $\forall l$, we see that (15) always remains satisfied, regardless of the \blacksquare_l -values in (68). Since (67) indicates that $\blacksquare_l \neq 0$ in (68) in general tend to decrease $H(S, E_f)$ and $H(E_f)$ below their maximal values until $H(S_{\text{class}})$ has been reached, we can specify the »critical magnitude« of \blacksquare_l -entries below which $H(S, E_f)$ and $H(E_f)$ would even exceed $H(S_{\text{class}})$.

$$\begin{aligned}
\hat{\rho}_E^{\text{out}}(L \geq k) &= \sum_{i, \beta(L), \gamma(L)} |c_i|^2 |\phi_i^{\beta(L)}\rangle \langle \phi_i^{\gamma(L)}| = \begin{pmatrix} D_0^E & \cdots & 0 \\ \vdots & \ddots & \vdots \\ 0 & \cdots & D_{2^k-1}^E \end{pmatrix}_{2^L \times 2^L}; \\
\hat{\rho}_{E_{\text{dec}}}^{\text{out}}(L) &= \hat{\rho}_E^{\text{out}}(L < k) = \sum_{l=0}^{2^k-1} D_l^{\text{dec}}; \\
\hat{\rho}_{SE}^{\text{out}}(L \geq k) &= \sum_{i, \beta(L), \gamma(L)} |c_i|^2 |\varphi_i\rangle \langle \varphi_i| \otimes |\phi_i^{\beta(L)}\rangle \langle \phi_i^{\gamma(L)}| = \\
&\begin{pmatrix} \mathbf{A}_0 & \mathbf{0}_{2^L \times 2^L(2^k-1)} \\ \mathbf{0}_{2^L(2^k-1) \times 2^L} & \ddots \\ & & \mathbf{A}_l & \mathbf{0}_{2^L \times 2^L(2^k-1-l)} \\ & & & \ddots \\ & & \mathbf{0}_{2^L(2^k-1-l) \times 2^L} & \mathbf{A}_{2^k-1} \end{pmatrix}_{2^{L+k} \times 2^{L+k}}; \\
\hat{\rho}_{SE_{\text{dec}}}^{\text{out}}(L) &= \hat{\rho}_{SE}^{\text{out}}(L < k) = \bigoplus_{l=0}^{2^k-1} D_l^{\text{dec}} = \begin{pmatrix} D_l^{\text{dec}} & \cdots & \mathbf{0}_{2^L \times 2^L} \\ \vdots & \ddots & \\ \mathbf{0}_{2^L \times 2^L} & & D_l^{\text{dec}} \end{pmatrix}_{2^{L+k} \times 2^{L+k}},
\end{aligned} \tag{70}$$

with $X = \mathbf{0}_{2^{L-k} \times 2^{L-k}}$ (R_l blocks for $l = \text{fixed}$), $l \in \{0, \dots, 2^k - 1\}$, $s_l = (2^k - 1 - l) 2^{L-k}$, $\blacksquare \equiv \blacksquare_{\beta(L-k), \gamma(L-k)}^{(l)} \neq 0$ with $\beta(L-k), \gamma(L-k) \in \{l \cdot 2^{L-k} + 1, \dots, (l+1) \cdot 2^{L-k}\}$

$$\begin{aligned}
D_l^{\text{dec}} &= \begin{pmatrix} |c_{l \cdot 2^L + 1}^{SE}|^2 & 0 & \cdots & 0 \\ 0 & & & \vdots \\ \vdots & & \ddots & 0 \\ 0 & \cdots & 0 & |c_{(l+1) \cdot 2^L}^{SE}|^2 \end{pmatrix}_{2^L \times 2^L} & D_l^E &= \begin{bmatrix} |c_{l \cdot 2^{L-k} + 1}^E|^2 & \blacksquare & \cdots & \blacksquare \\ \blacksquare & & \ddots & \vdots \\ \vdots & & & \blacksquare \\ \blacksquare & \cdots & \blacksquare & |c_{(l+1) \cdot 2^{L-k}}^E|^2 \end{bmatrix}_{2^{L-k} \times 2^{L-k}} \\
\mathbf{A}_0 &= \begin{bmatrix} D_0 & \cdots & \mathbf{0}_{2^{L-k} \times s_0} \\ \vdots & \ddots & \vdots \\ \mathbf{0}_{s_0 \times 2^{L-k}} & \cdots & \mathbf{0}_{s_0 \times s_0} \end{bmatrix}_{2^L \times 2^L} & D_0 &= \begin{pmatrix} |c_1^E|^2 & \blacksquare & \cdots & \blacksquare \\ \blacksquare & & & \vdots \\ \vdots & & \ddots & \blacksquare \\ \blacksquare & \cdots & \blacksquare & |c_{2^{L-k}}^E|^2 \end{pmatrix}_{2^{L-k} \times 2^{L-k}} \\
\mathbf{A}_l &= \begin{bmatrix} X & \cdots & X \\ \vdots & \ddots & \vdots \\ & D_l & \mathbf{0}_{2^{L-k} \times s_l} \\ X & \cdots & \mathbf{0}_{s_l \times 2^{L-k}} & \ddots & \mathbf{0}_{s_l \times s_l} \end{bmatrix}_{2^L \times 2^L} & D_l &= \begin{pmatrix} |c_{l \cdot 2^{L-k} + 1}^E|^2 & \blacksquare & \cdots & \blacksquare \\ \blacksquare & & & \vdots \\ \vdots & & \ddots & \blacksquare \\ \blacksquare & \cdots & \blacksquare & |c_{(l+1) \cdot 2^{L-k}}^E|^2 \end{pmatrix}_{2^{L-k} \times 2^{L-k}} \\
\mathbf{A}_{2^k-1} &= \begin{bmatrix} \mathbf{0}_{s_0 \times s_0} & \cdots & \mathbf{0}_{2^{L-k} \times s_0} \\ \vdots & \ddots & \vdots \\ \mathbf{0}_{s_0 \times 2^{L-k}} & \cdots & D_{2^k-1} \end{bmatrix}_{2^L \times 2^L} & D_{2^k-1} &= \begin{pmatrix} |c_{(2^k-1)2^{L-k}+1}^E|^2 & \blacksquare & \cdots & \blacksquare \\ \blacksquare & & & \vdots \\ \vdots & & \ddots & \blacksquare \\ \blacksquare & \cdots & \blacksquare & |c_{2^L}^E|^2 \end{pmatrix}_{2^{L-k} \times 2^{L-k}}
\end{aligned}$$

Submatrices \mathbf{A}_l in (70) contain, for fixed l , $R_l = \sum_{i=0}^l a_i (2^{L-k} \times 2^{L-k})$ zero-blocks X , with recursively defined a_i , ($a_0 = 0$ and $a_l = a_{l-1} + 2 \cdot (2^L - l) + 1$). There are at least 2^k of 2^L values $|c_g^E|^2 \neq 0$ and maximally 2^k of 2^{L+k} values $|c_m^{SE}|^2 \neq 0$ in (70), (m, g) as in (59) above.

Indeed, when looking at (68) we may assume, without loss of generality, that

$$|c_{l+1}^E|^2 \stackrel{!}{=} |c_{(l+1) \cdot 2}^E|^2 \stackrel{!}{=} |c_{l+1}|^2 \cdot 2^{-(L-k)} = |c_{l+1}|^2 / 2 \forall l \wedge n \geq L > k \quad (71)$$

yields the characteristic polynomial

$$\begin{aligned} \lambda^2 - |c_{l+1}|^2 \lambda + \frac{|c_{l+1}|^4}{4} - |\blacksquare_l|^2 &\Rightarrow \lambda_{1/2} = \frac{|c_{l+1}|^2}{2} \pm \sqrt{\frac{|c_{l+1}|^4}{4} + |\blacksquare_l|^2 - \frac{|c_{l+1}|^4}{4}} = \frac{|c_{l+1}|^2}{2} \pm \sqrt{|\blacksquare_l|^2} \\ &\Rightarrow |\blacksquare_l^{\text{crit}}| \stackrel{!}{=} \frac{|c_{l+1}|^2}{2} \equiv \sqrt{|c_{l+1}^E|^2 |c_{(l+1) \cdot 2}^E|^2} \Rightarrow H(S, E_f) = H(E_f) = H(S_{\text{class}}), \end{aligned} \quad (72)$$

whose eigenvalues suggest that the minimal amount $H(S, E_f)$ and $H(E_f)$ would attain, for a specific critical value $|\blacksquare_l^{\text{crit}}| \stackrel{!}{=} |c_{l+1}^E| |c_{(l+1) \cdot 2}^E| \forall l$ in (68) (with (71)), is $H(S, E_f) = H(E_f) = H(S_{\text{class}})$. Higher values than $|\blacksquare_l^{\text{crit}}|$ are not allowed due to the appearance of negative eigenvalues in (72). Within $0 \leq |\blacksquare_l|^2 \leq |\blacksquare_l^{\text{crit}}|^2$ in (72) $H(S, E_f) = H(E_f)$ in general decrease monotonously [25] from their maximal value (with $\lambda_{\text{diff}} := |c_{l+1}|^2 - |c_{(l+1) \cdot 2}^E|^2$) $H(S, E_f) = H(E_f) =$

$-\sum_{l=0}^{2^k-1} \left\{ |c_{l+1}^E|^2 \log_2 |c_{l+1}^E|^2 + \lambda_{\text{diff}} \log_2 \lambda_{\text{diff}} \right\} = H(S_{\text{class}}) + L - k > H(S_{\text{class}})$ at $|\blacksquare_l|^2 = 0$ (corresponding to (59)) to the minimal value $H(S, E_f) = H(E_f) = H(S_{\text{class}})$ at $|\blacksquare_l|^2 = |\blacksquare_l^{\text{crit}}|^2$ for (71) and $n \geq L > k \geq 1$. The same holds for other non-trivial D_L -probability distributions than (71). The \blacksquare_l in $\hat{\rho}_{SE}^{\text{out}}(L)$ for $L > k$ »merge« and therefore their number decreases when approaching $L \rightarrow k$ (s. appendix B)¹⁰. Nevertheless, (15) remains valid $\forall L > k$ due to (67) and the *mutual disjointness* between E-registry states of (70) associated with different diagonal S-subspaces, regardless of how the \blacksquare -entries in $\hat{\rho}_{SE}^{\text{out}}(L)$ change when »merging«. Thus, (70)-(66) imply $H(S, E_f) = H(E_f) \forall L > k$. For $L = k$ all \blacksquare_l in (70)-(67) and (68) are traced out, yielding, due to (66), (61) with $H(S, E_f) = H(E_f) = H(S_{\text{class}})$. Thus, we may conclude:

(70), (66) and (67) would always lead to $H(S) = H(S_{\text{class}}) \forall (0 < L \leq n)$ and $H(S, E_f) = H(E_f) \forall L \geq k$. As long as $n \geq L > k$ $H(S, E_f)$ and $H(E_f)$ will fluctuate between their minimal value (with $(m \neq m') \in \{l \cdot 2^{L-k} + 1, \dots, (l+1) \cdot 2^{L-k}\}$)

$$H(S, E_f) = H(E_f) = H(S_{\text{class}}) \text{ at } |\blacksquare_{m,m'}|^2 = |\blacksquare_{m,m'}^{\text{crit}}|^2 \stackrel{!}{=} |c_m^E|^2 |c_{m'}^E|^2 \forall l \in \{0, \dots, 2^k - 1\} \quad (73)$$

and maximal value (valid $\forall |\blacksquare_{m,m'}|^2 = 0$)

$$H(S, E_f) = H(E_f) = -\sum_{l=0}^{2^k-1} \left\{ |c_{l+1}^E|^2 \log_2 |c_{l+1}^E|^2 + \left(|c_{l+1}|^2 - |c_{(l+1) \cdot 2}^E|^2 \right) \log_2 \left(|c_{l+1}|^2 - |c_{(l+1) \cdot 2}^E|^2 \right) \right\} > H(S_{\text{class}}), \quad (74)$$

whereas the diagonal entries $|c_m^E|^2$ »merge« according to (with $r \in \{1, \dots, 2^{L-k-s}\}$)

$$|c_{r+l \cdot 2^{L-k-s}}^E|^2 = \sum_{m=2^s(r+l \cdot 2^{L-k-s}-1)+1}^{2^s(r+l \cdot 2^{L-k-s})} |c_m^E|^2 \forall l \in \{0, \dots, 2^k - 1\}, s \in \{0, \dots, L-k\}, m \in \{2^{L-k} \cdot l + 1, \dots, 2^{L-k} (l+1)\} \quad (75)$$

after the s -th E-qubit has been traced out in order to yield new 2^{L-k-s} diagonal entries $|c_r^E|^2$ of the reduced matrices $\hat{\rho}_{SE}^{\text{out}}(L-s)$ and $\hat{\rho}_E^{\text{out}}(L-s)$. For $L = k$ (70), (66) and (67) still hold, with $H(S, E_f) = H(E_f) = H(S_{\text{class}})$, as in (15), (61) and (75). For $L < k$ (70) behaves as in (59) and (62), violating (15).

There is only one type of $\hat{\rho}_{SE}^{\text{out}}(L)$ that violates (67) and nevertheless leads to $H(E) = H(S, E) \forall (1 \leq L \leq n)$ if and only if $k = 1$, namely (w.r.t. an arbitrary S-probability distribution $|c_i|^2 > 0, i \in \{1, \dots, 2^k\}$)

$$\hat{\rho}_{SE}^{\text{out}}(L) = \left(\sum_{i=1}^{2^{k-1}} |c_i|^2 |i\rangle \langle i| \right) \otimes |s_1^L\rangle \langle s_1^L| + \left(\sum_{j=2^{k-1}+1}^{2^k} |c_j|^2 |j\rangle \langle j| \right) \otimes |s_2^L\rangle \langle s_2^L|, 1 > |c_i|^2 > 0, \quad (76)$$

as an $1 \leq L \leq n$ qubit version of (300), (301)-(302), (303) and (304), with $\{|s_1^L\rangle, |s_2^L\rangle\}$ as in (302). Eigenvalues of (76),

¹⁰By »merging« of matrix entries we denote the effect which occurs after tracing out parts (qubits) of E by decreasing L by an amount of $0 < \tilde{s} \leq L-1$ E-qubits (s. appendix B), when the affected non-vanishing (overlapping) diagonal or outer-diagonal matrix-entries of $\hat{\rho}_{SE}^{\text{out}}(L)$ or $\hat{\rho}_E^{\text{out}}(L)$ are being added within $\hat{\rho}_{SE}^{\text{out}}(L-\tilde{s})$ or $\hat{\rho}_E^{\text{out}}(L-\tilde{s})$.

$$\begin{aligned} \hat{\rho}_{SE}^{\text{out}}(L) : \left\{ \lambda_i^{\text{SE}} = |c_i|^2 \right\}_{i=1}^{2^k} &\Rightarrow H(S, E_f) = H(S_{\text{class}}^{k \geq 1}), [0 + (1 - \delta_{k,1}) \cdot H(E_f)] \leq H(S_{\text{class}}^{k \geq 1}) \forall L \\ \hat{\rho}_E^{\text{out}}(L) : \lambda_1^E &= \sum_{i=1}^{2^{k-1}} |c_i|^2, \lambda_2^E = \sum_{j=2^{k-1}+1}^{2^k} |c_j|^2 \Rightarrow H(E_f) = - \sum_{i=1}^2 \lambda_i^E \cdot \log_2 \lambda_i^E \leq 1 \forall L, \end{aligned} \quad (77)$$

indicate that QD appears for (76) if and only if $k = 1$, yielding $I(S : E_f) / H(S_{\text{class}}^{k \geq 1}) = H(E_f) / H(S_{\text{class}}^{k \geq 1}) = 1$, for if one applies any $|c_i|^2 > 0$, $i \in \{1, \dots, 2^k\}$ to (77), such as $\{|c_1|^2 = 1 - (2^k - 1)\varepsilon, |c_2|^2 = \dots = |c_{2^k}|^2 = \varepsilon\}$ that induces $\{\lambda_1^E = 1 - 2^{k-1}\varepsilon, \lambda_2^E = 2^{k-1}\varepsilon\}$ (with $\varepsilon \ll 1$ for $k \geq 1$), one could use (294) and expand w.r.t. ε $H(E_f) = - \sum_{i=1}^2 \lambda_i^E \cdot \log_2 \lambda_i^E$ and $H(S_{\text{class}}^{k \geq 1})$ to obtain the relation

$$\begin{aligned} H(S_{\text{class}}^{k \geq 1}) &\approx \frac{(2^k - 1)\varepsilon}{\ln 2} - (2^k - 1)\varepsilon \log_2 \varepsilon + \mathcal{O}(\varepsilon^2) \\ H(E_f) &\approx \frac{(2^{k-1})\varepsilon}{\ln 2} - (2^{k-1})\varepsilon \log_2 \varepsilon - \underbrace{(2^{k-1})\varepsilon(k-1)}_{\geq 0} \Rightarrow H(S_{\text{class}}^{k \geq 1}) \geq H(E_f) \Rightarrow H(S_{\text{class}}^{k \geq 1}) = H(E_f) \Leftrightarrow k = 1, \end{aligned} \quad (78)$$

demonstrating that $I(S : E_f) / H(S_{\text{class}}^{k \geq 1}) = H(E_f) / H(S_{\text{class}}^{k \geq 1}) < 1$ for $k > 1$ and all non-trivial $\{|c_i|^2 > 0\}_{i=1}^{2^k}$. In (78) we use $\varepsilon = \varepsilon(k) \ll 2^{[1-k+\frac{1}{\ln 2}]} \ll 1$ in order to ensure the positivity of $H(E_{\text{dec}})$ for $k \gg 1$, corresponding in praxi to $k \geq 4$ (however, the calculation in (78) also works in the limit $k \rightarrow 1$ as long as $\varepsilon \ll 1$, without having to refer to a specific k -dependent upper-bound). Thus, (76) enables us to efficiently store maximally $H(S_{\text{class}}^{k=1}) = H(E_f)$ about a $k = 1$ S. Also, $H(E_f) / H(S_{\text{class}}^{k \geq 1})$ from (78) converges for $k \rightarrow \infty$ (with $\varepsilon = 2^{-k}$) to zero $\sim k^{-1}$:

$$\lim_{k \rightarrow \infty} [H(E_f) / H(S_{\text{class}}^{k \geq 1})] \approx \frac{2^k \varepsilon - (2^k) \varepsilon \log_2 [(2^k) \varepsilon] - (2^k) \varepsilon k}{2^k \varepsilon - (2^k) \varepsilon \log_2 [(2^k) \varepsilon]} = \left(1 - \frac{k}{1 - \log_2 \varepsilon}\right) = 1 - k \cdot \underbrace{\frac{1}{1+k}}_{\approx 1/k} \approx 1 - k \cdot \left(\frac{1}{k}\right) = 0. \quad (79)$$

Therefore: **1)** one cannot find $\hat{\rho}_{SE}^{\text{out}}(L)$ -matrix structures which simultaneously fulfil the condition in (67) for $L \geq k$ and display the form (76) for $L < k$, since $\hat{\rho}_{SE}^{\text{out}}(L \geq k)$ from (70) and $\hat{\rho}_{SE}^{\text{out}}(L \geq k)$ from (76) exclude each other - (76) emerges for $L < k$ by partial tracing only from those $\hat{\rho}_{SE}^{\text{out}}(L \geq k)$ which are as in (76), whereas (70) does not include (76), since the latter type of $\hat{\rho}_{SE}^{\text{out}}(L)$ does not validate (67); **2)** QD does not appear in (76) if $1 \leq L < (k > 1)$; **3)** the special structure of $\{|s_1^L\rangle, |s_2^L\rangle\}$ (as eigenstates of (11)) leads in (76) necessarily to $k = 1$, since $k > 1$ would suppress MI $\sim k^{-1}$ for $k \gg 1$, s. (77).

4.2.3 Necessary and sufficient conditions for Quantum Darwinism

Zurek's qubit toy model has shown us so far that QD as a physical phenomenon requires w.r.t. $|\Psi_{SE}^{\text{out}}\rangle$ in (13) the following conditions to hold:

1. $H(S) \approx H(S_{\text{class}})$, i.e. the k -qubit system S may be regarded as effectively decohered with a pointer basis $\{|\pi_i\rangle\}$.
2. Registry states of the environment E in (13) are assumed to have a tensor product structure (mutually non-overlapping »storage cells«).
3. $H(E_L) \geq H(S, E_L) \forall (k \leq L \leq n)$, regardless of the order in which single E -qubits are consecutively traced out.

Since the assumption 1 from subsection 4.2.1 transforms $|\Psi_{SE}^{\text{out}}\rangle$ from (13) into the standard Schmidt-decomposition

$$\begin{aligned} \hat{\rho}_{SE}^{\text{out}} &= \text{Tr}_A [|\tilde{\Psi}_{SEA}^{\text{out}}\rangle \langle \tilde{\Psi}_{SEA}^{\text{out}}|] \\ |\tilde{\Psi}_{SEA}^{\text{out}}\rangle &= \sum_i c_i |\varphi_i\rangle_S \otimes |\Phi_i\rangle_E \otimes |i\rangle_A \end{aligned} \quad (80)$$

(with ${}_A \langle i|i'\rangle_A = \delta_{i,i'}$, s. also (59) above), in which each state $|\varphi_i\rangle$ of system's pointer basis remains entangled with only

one environmental n -qubit registry state $|\phi_i\rangle$ (orthogonal w.r.t. other $2^n - 1$ E-registry basis states $|\phi_{i' \neq i}\rangle$), we expect it to adhere to (15) (in (80) the ancilla-state $|i\rangle_A$ serves only for purification purposes and is traced out $\forall L \leq n$). On the other hand,

$$\hat{\rho}_{SE}^{\text{out}} = \text{Tr}_A [|\chi_{SEA}^{\text{out}}\rangle \langle \chi_{SEA}^{\text{out}}|] \\ |\chi_{SEA}^{\text{out}}\rangle = \sum_{m=1}^{N_S} a_m |m\rangle_S \otimes \sum_{\substack{m \cdot N_E / N_S \\ i_m = 1 + \\ (m-1) N_E / N_S}} \beta_{i_m} |i_m\rangle_E \otimes |i_m\rangle_A, \quad (81)$$

with $a_m > 0$, $\beta_{i_m} \geq 0$, $\sum_m |a_m|^2 \stackrel{!}{=} 1$, $N_S = \dim(S) = 2^{l \cdot k}$, $N_E = \dim(E) = 2^{l \cdot n}$ (where $l \geq 1$ denotes the number of levels in each constituent-cell of S and E , i.e. $l = 1$ corresponds to qubits), ${}_S \langle m | m' \rangle_S = \delta_{m,m'}$, ${}_E \langle i_m | i_{m'} \rangle_E = \delta_{m,m'} \delta_{i_m, i_{m'}}$, and ${}_A \langle i_m | i_{m'} \rangle_A = \delta_{m,m'} \delta_{i_m, i_{m'}}$, yields a generalized version of (80). Namely, (80) emerges from (81) by setting in (81) $\forall m \in \{1, \dots, N_S\}$ $\beta_{i_m} = \delta_{i_m, i_{m'}}$ for a fixed $i_{m'} \in \{1 + (m-1) N_E / N_S, \dots, m \cdot N_E / N_S\}$. Furthermore, subsection 4.2.2 (s. (70) above) has shown us that we even may allow coherence terms between E-registry states within mutually disjoint subsets E_i of 2^n E-registry states (with $\bigcup_i |E_i| = 2^{l \cdot n}$) and still validate (15), as long as each subset E_i and its registry basis states $|i_m\rangle_E$ remain associated with only one diagonal subspace $|m\rangle \langle m|$ of S according to (81) (however, this time with ${}_A \langle i_m | i_{m'} \rangle_A = \delta_{m,m'}$).

Therefore, we want to show in the present subsection that the following double implication holds:

- If one can show that a given output state $\hat{\rho}_{SE}^{\text{out}}$ is similar to (81) or (80) w.r.t. a certain separable basis (s. also Appendix A), then QD (including the above three conditions) appears and one has

$$\text{QD} \Leftrightarrow |\chi_{SEA}^{\text{out}}\rangle. \quad (82)$$

In other words, (82) means that the above three QD-conditions are necessary and sufficient to establish the output state structure $|\chi_{SEA}^{\text{out}}\rangle$. This is what we want to show.

1) We first concentrate on the equality $H(E_L) = H(S, E_L) \forall (k \leq L \leq n)$. The implication \Leftarrow in (82) is self-evident.

2) We still concentrate on the equality $H(E_L) = H(S, E_L) \forall (k \leq L \leq n)$. In order to show the implication \Rightarrow in (82) we use the fact that QD treats environmental registry states as n -fold tensor products of one-qudit states (separable basis registry-states of E , s. also (13) above), which allows us to express the eigenvalues from the eigenspectra $\sigma(\hat{\rho}_{SE}^{\text{out}}) = \{\lambda_1^{SE}, \dots, \lambda_{N_S N_E}^{SE}\}$ and $\sigma(\hat{\rho}_E^{\text{out}}) = \{\lambda_1^E, \dots, \lambda_{N_E}^E\}$ of $\hat{\rho}_{SE}^{\text{out}}$ and $\hat{\rho}_E^{\text{out}}$, respectively (with $\sum_{i=1}^{N_S N_E} \lambda_i^{SE} = \sum_{i=1}^{N_E} \lambda_i^E \stackrel{!}{=} 1$), by means of matrix realignment methods (Appendix B) as

$$\lambda_r^{E(L)} = \sum_{i=1+(r-1)N_E}^{r \cdot N_E} \sum_{j=1}^{N_S} \lambda_{i+(j-1)N_E}^{SE(L=n)} = \sum_{j=1}^{N_S} \lambda_{r+(j-1)2^{l \cdot L}}^{SE(L)}; \lambda_{r+(j-1)2^{l \cdot L}}^{SE(L)} = \sum_{i=1+(r-1)N_E}^{r \cdot N_E} \lambda_{i+(j-1)N_E}^{SE(L=n)}, \quad (83)$$

with $l \geq 1$, $L \in \{1, \dots, n\}$, $r \in \{1, \dots, 2^{l \cdot L}\}$, $i \in \{1, \dots, 2^{l \cdot n}\}$ and $j \in \{1, \dots, 2^{l \cdot k}\}$.

Now, demanding $H(E_L) \stackrel{!}{=} H(S, E_L)$ yields with (83) $-\sum_r \lambda_r^{E(L)} \log_2 \lambda_r^{E(L)} \stackrel{!}{=} -\sum_{r,j} \lambda_{r+(j-1)2^{l \cdot L}}^{SE(L)} \log_2 \lambda_{r+(j-1)2^{l \cdot L}}^{SE(L)}$, alias

$$A_{r,j}(L) := \prod_r \left\{ \frac{\left(\sum_j \lambda_{r+(j-1)2^{l \cdot L}}^{SE(L)} \right)^{\left(\sum_j \lambda_{r+(j-1)2^{l \cdot L}}^{SE(L)} \right)}}{\prod_j \left(\lambda_{r+(j-1)2^{l \cdot L}}^{SE(L)} \right)^{\lambda_{r+(j-1)2^{l \cdot L}}^{SE(L)}}} \right\} \left\{ \begin{array}{l} \stackrel{!}{=} 1 \Leftrightarrow H(E_L) \stackrel{!}{=} H(S, E_L) \\ < 1 \Leftrightarrow H(E_L) > H(S, E_L) \\ > 1 \Leftrightarrow H(E_L) < H(S, E_L). \end{array} \right. \quad (84)$$

$A_{r,j}(L=n) = 1$ in (84) only if for each r -value there exists only one j -value in the numerator of $A_{r,j}(L=n)$, i.e. only if each environmental registry state is connected only with a unique pointer state of system S . Otherwise, if we have a map $f_r : r \xrightarrow{f_r} j$ that associates more than one diagonal pointer-subspace of S (more than one j -value) with a single environmental r -registry state, we would always obtain $A_{r,j}(L=n) > 1$ (i.e. no QD). This can be easily inferred by looking at the expression (with $x, y \in [0, 1]$)

$$(x+y)^{x+y} x^{-x} y^{-y} \geq 1, \quad (85)$$

which equals 1 only for $x = 0$ or $y = 0$ or $x = y = 0$. A generalized version of (85) is (with $0 < x_i < 1$)

$$I_n := \frac{\left(\sum_{i=1}^n x_i\right)^{\left(\sum_{i=1}^n x_i\right)}}{\prod_{i=1}^n x_i^{x_i}}. \quad (86)$$

Let us assume that $I_n > 1$. Then, applying induction $n \rightarrow n+1$ to (86) yields

$$I_{n+1} = \frac{\left(x_{n+1} + \sum_{i=1}^n x_i\right)^{\left(x_{n+1} + \sum_{i=1}^n x_i\right)}}{x_{n+1}^{x_{n+1}} \prod_{i=1}^n x_i^{x_i}} = \underbrace{\frac{\left(x_{n+1} + \sum_{i=1}^n x_i\right)^{x_{n+1}}}{x_{n+1}^{x_{n+1}}}}_{>1} \cdot \underbrace{\frac{\left(x_{n+1} + \sum_{i=1}^n x_i\right)^{\left(\sum_{i=1}^n x_i\right)}}{\prod_{i=1}^n x_i^{x_i}}}_{>1} > 1, \quad (87)$$

demonstrating that adding terms to the numerator in (86) leads to the violation of the QD-condition (15). Thus, for $H(E_{L=n}) \stackrel{!}{=} H(S, E_{L=n})$ to hold the positive eigenvalues of $\hat{\rho}_{SE}^{\text{out}}$ and $\hat{\rho}_E^{\text{out}}$ have to be the same (apart from permutations) and the corresponding ranks $\text{rank}(\hat{\rho}_{SE}^{\text{out}})$ and $\text{rank}(\hat{\rho}_E^{\text{out}})$ (i.e. the number $|\sigma(\hat{\rho}_{SE}^{\text{out}})|$ and $|\sigma(\hat{\rho}_E^{\text{out}})|$ of positive eigenvalues within the eigenspectra $\sigma(\hat{\rho}_{SE}^{\text{out}})$ and $\sigma(\hat{\rho}_E^{\text{out}})$, respectively) have to equal each other, $|\sigma(\hat{\rho}_{SE}^{\text{out}})| = |\sigma(\hat{\rho}_E^{\text{out}})|$.

However, since we want the equality $H(E_L) = H(S, E_L)$ to hold $\forall (k \leq L \leq n)$ (and not only for $L = n$), regardless of the order in which single E-qubits are consecutively traced out, we have to demand that the map $f_r : r \xrightarrow{f} j$ in (84) should be surjective, i.e. each diagonal pointer state subspace $|m\rangle_S \langle m|$ of S in (81) should be correlated with a subset E_m of 2^{L-L} E-registry states of cardinality $|E_m| > 0$ (where $\sum_m |E_m| \leq 2^{L-L}$), such that none of the E_m mutually overlap (i.e. none of the subsets E_m contain the same E-registry state $\forall (k \leq L \leq n)$). Furthermore, when looking back at Zurek's QD-model, especially at (12), we see that the corresponding map $f_r : r \xrightarrow{f} j$ is even bijective, since in (12) each diagonal pointer-state subspace of S is correlated with one unique E-registry basis state.

In order to realize that the above three QD-conditions enforce (81) we look at Venn-diagrams in Fig. 3.

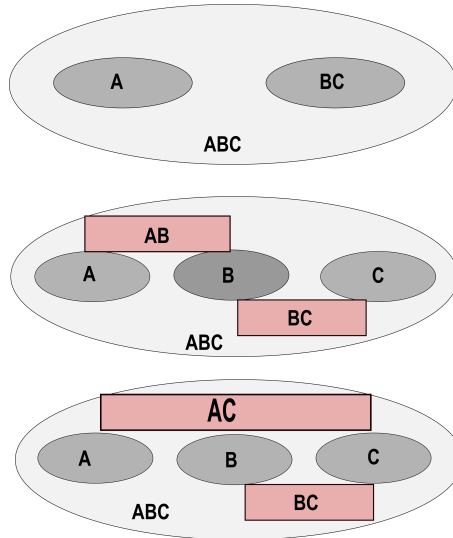


Figure 3: Venn-diagrams used w.r.t. (88).

Let us assume that we have an output state $\hat{\rho}_{ABC}^{\text{out}} \in \mathcal{H}_A \otimes \mathcal{H}_B \otimes \mathcal{H}_C$ composed of three subsystems: subsystem A is associated with an open, $k = 1$ qudit system S , whereas subsystems B and C are part of the environment E ($n = 2$). If we insist that the following entropy equalities

$$H(\hat{\rho}_{ABC}^{\text{out}}) = H(\hat{\rho}_{BC}^{\text{out}}), H(\hat{\rho}_{AB}^{\text{out}}) = H(\hat{\rho}_B^{\text{out}}), H(\hat{\rho}_{AC}^{\text{out}}) = H(\hat{\rho}_C^{\text{out}}) \quad (88)$$

should hold then the first equality in (88) corresponds exactly to the case studied in (84) above (with $L = n$) (the upper diagramm in Fig. 3) which forces us to subdivide the registry states of $\hat{\rho}_{ABC}^{\text{out}}$ into two parts (subsets), one associated with subsystem $S \equiv A$ (enclosing 2^{L-k} pointer registry states) and the other associated with $E \equiv BC$ (containing maximally 2^{L-n} registry states). However, as soon as we trace out one subsystem from $\hat{\rho}_{ABC}^{\text{out}}$ (B or C) and demand the validity of the second as well as the third equality in (88) (the middle and lower diagramm in Fig. 3, respectively), we see that it is necessary to subdivide the subsystem $E \equiv BC$ itself into two disjoint subsets of E-registry states, $E = B \cup C$, each of which containing maximally $2^{L-(L-k)}$ L-qudit E-registry states¹¹ $\forall (k \leq L \leq n)$. In turn, this also means that we have to associate each of the 2^{L-k} pointer states of S with only one of the two disjoint subsets of E in Fig. 3 if we want the equality in (84) to hold $\forall (k \leq L \leq n)$, otherwise in case of mutually overlapping state-subsets of E (84) would exceed 1.

Generalizing the setting of Fig. 3 to an n -qudit E and a $k > 1$ qudit S also means that we have to apply entropy-constraints analogous to those in (88) $\forall (k \leq L \leq n)$, which is precisely what (81) does by subdividing 2^{L-L} E-registry states into 2^{L-k} mutually disjoint subsets E_m of cardinality $0 < |E_m| \leq 2^{L-(L-k)}$, such that $\sum_{m=1}^{2^{L-k}} |E_m| \leq 2^{L-L}$. Translated to the corresponding eigenspectrum $|\sigma(\hat{\rho}_{SE_L}^{\text{out}})|$ of $\hat{\rho}_{SE_L}^{\text{out}}$ this procedure also implies that one has to subdivide all $0 < |\sigma(\hat{\rho}_{SE_L}^{\text{out}})| \leq 2^{L-L}$ non-zero eigenvalues of $\hat{\rho}_{SE_L}^{\text{out}}$ into 2^{L-k} disjoint subsets σ_m of cardinality $0 < |\sigma_m| \leq 2^{L-(L-k)}$ (with $\sum_{m=1}^{2^{L-k}} \sigma_m = |\sigma(\hat{\rho}_{SE_L}^{\text{out}})|$), which should remain disjoint $\forall (k \leq L \leq n)$. This is only possible to achieve by means of (81), since overlapping eigenvalue subsets σ_m inevitably lead to the disbalance $H(E_L) < H(S, E_L)$ that violates (15), as demonstrated in subsections 4.2.1 and 4.2.2 (s. also Appendix B and subsections 4.2.4 and 4.2.5 below). Therefore, we may conclude:

Taking all three above QD-conditions ($H(S) \approx H(S_{\text{class}})$, $H(E_L) = H(S, E_L) \forall (k \leq L \leq n)$ irrespective of the order in which single E-qudits are traced out, and E-registry states having a tensor product structure) into account one inevitably arrives at the state structure $|\chi_{SEA}^{\text{out}}\rangle$ from (81), with $H(E_L) = H(S, E_L) \forall (k \leq L \leq n) \Leftrightarrow |\sigma(\hat{\rho}_{SE_L}^{\text{out}})| = |\sigma(\hat{\rho}_{E_L}^{\text{out}})|$ due to the separability of the corresponding registry state bases in $\hat{\rho}_{SE_L}^{\text{out}}$ and $\hat{\rho}_{E_L}^{\text{out}}$.

3) Finally, exactly this separability of registry state bases in $\hat{\rho}_{SE_L}^{\text{out}}$ and $\hat{\rho}_{E_L}^{\text{out}}$, induced by the three QD-conditions listed above, enables us to treat the entropy inequality $H(E_L) > H(S, E_L)$: in this context we again start with $-\sum_{r_E} \lambda_r^{E(L)} \log_2 \lambda_r^{E(L)} > -\sum_{r_{SE}} \lambda_{r_{SE}}^{SE(L)} \log_2 \lambda_{r_{SE}}^{SE(L)}$ and obtain

$$\left[\prod_{r_E=1}^{|\sigma(\hat{\rho}_{E_L}^{\text{out}})|} \left(\lambda_{r_E}^{E(L)} \right)^{\lambda_{r_E}^{E(L)}} \right] \left[\prod_{r_{SE}=1}^{|\sigma(\hat{\rho}_{SE_L}^{\text{out}})|} \left(\lambda_{r_{SE}}^{SE(L)} \right)^{\lambda_{r_{SE}}^{SE(L)}} \right]^{-1} < 1, \quad (89)$$

where we took into account the fact now there are more $\lambda_{r_E}^{E(L)}$ than $\lambda_{r_{SE}}^{SE(L)}$ positive eigenvalues, i.e. $|\sigma(\hat{\rho}_{SE_L}^{\text{out}})| < |\sigma(\hat{\rho}_{E_L}^{\text{out}})|$. This makes sense, since now we cannot use the relations (83) which used to connect the eigenvalue spectra $\sigma(\hat{\rho}_{SE_L}^{\text{out}})$ and $\sigma(\hat{\rho}_{E_L}^{\text{out}})$ in case of $H(E_L) = H(S, E_L)$. Nevertheless, we are able to establish a relation between $|\sigma(\hat{\rho}_{SE_L}^{\text{out}})|$ and $|\sigma(\hat{\rho}_{E_L}^{\text{out}})|$ that has to remain valid if $H(E_L) > H(S, E_L)$ is to hold for a specific L -value $k < L \leq n$. Without loss of generality we may choose $\lambda_{r_{SE}}^{SE(L)} = |\sigma(\hat{\rho}_{SE_L}^{\text{out}})|^{-1}$ and $\lambda_{r_E}^{E(L)} = |\sigma(\hat{\rho}_{E_L}^{\text{out}})|^{-1}$, which, inserted into (89), yield

$$|\sigma(\hat{\rho}_{E_L}^{\text{out}})|^{-1} < |\sigma(\hat{\rho}_{SE_L}^{\text{out}})|^{-1} \Rightarrow |\sigma(\hat{\rho}_{E_L}^{\text{out}})| > |\sigma(\hat{\rho}_{SE_L}^{\text{out}})|. \quad (90)$$

This demonstrates that QD, with its three conditions listed above, allows us to establish a one to-one correspondence between cardinalities of two eigenvalue sets and their corresponding entropies, i.e.¹²

$$|\sigma(\hat{\rho}_{E_L}^{\text{out}})| \left\{ \begin{array}{l} = \\ > \\ < \end{array} \right\} |\sigma(\hat{\rho}_{SE_L}^{\text{out}})| \Leftrightarrow H(E_L) \left\{ \begin{array}{l} = \\ > \\ < \end{array} \right\} H(S, E_L). \quad (91)$$

¹¹Should one of the subsets B or C of E (or both) contain less than $2^{L-(L-k)}$ L-qudit E-registry states, then this means that not all of the 2^{L-n} E-registry states participate in $\hat{\rho}_{ABC}^{\text{out}}$. For instance, in (12) and Fig. 1 with $n > k = 1$ only two n -qubit E-registry states ($|0_n\rangle$ and $|1_n\rangle$) participate within $\hat{\rho}_{SE}^{\text{out}}$ such that each of them is uniquely correlated with only one of the S -pointer states ($|0\rangle$ and $|1\rangle$, respectively).

¹²Indeed, for instance in (12) we have seen that for $L = n$ the eigenspectrum of $\hat{\rho}_{SE_L}^{\text{out}}$ contains only one non-zero eigenvalue ($|\sigma(\hat{\rho}_{SE_L=n}^{\text{out}})| = 1$), whereas $|\sigma(\hat{\rho}_{E_L=n}^{\text{out}})| = 2$.

This proves the double implication (82). **q.e.d.** Accordingly, we may summarize our findings in a following way:

From the physical and operational point of view, QD indicates highest storage efficiency (minimal f_{opt}) of $H(S) \approx H(S_{\text{class}})$ into environment E (s. also discussion in subsection 4.1 above). However, from mathematical perspective QD is a set of conditions which allow one to establish a one-to-one correspondence between cardinalities of two eigenvalue sets and their corresponding entropies in accord with (81), (82) and (91).

However, $H(E_L) > H(S, E_L)$ emerges from (81) w.r.t. the standard (separable) computational basis only after introducing coherences between E-registry states within different diagonal pointer-state subspaces of S. Therefore, we will study in the forthcoming subsections 4.2.4 and 4.2.5 matrix structures of $\hat{\rho}_{SE}^{\text{out}}$ in the standard computational basis which allow one to reduce $H(S, E_L)$ (and thus validate (15)) by introducing into $\hat{\rho}_{SE}^{\text{out}}$ of (81) correlations between different S-pointer states which have not been considered so far. Furthermore, such matrix structures of $\hat{\rho}_{SE}^{\text{out}}$ involving correlations between different diagonal pointer state subspaces of system S will be of particular use when discussing the appearance of QD in the course of more advanced qubit network models in the second part of this book.

4.2.4 Assumption 3: system's pointer states overlap, no environmental coherences

This assumption corresponds to the constraint

$$\sum_{\beta(L), \gamma(L)} \langle \phi_i^{\beta(L)} | \phi_j^{\gamma(L)} \rangle \stackrel{!}{\sim} \sum_{\beta(L), \gamma(L)} \left[r_{\beta, \gamma}^{i, j} + \delta_{ij} \left(1 - r_{\beta, \gamma}^{i, j} \right) \right] \cdot \delta_{\beta(L), \gamma(L)}, \lim_{n \gg 1} \left[r_{\beta, \gamma}^{i, j} = r_{\beta(L=n), \gamma(L=n)}^{i, j} \right] \equiv 0,$$

which implies that all, diagonal as well as outer-diagonal, S-blocks of $\hat{\rho}_{SE}^{\text{out}}(L)$ may contain only diagonal non-zero matrix entries, leading to (92) below.

$$\hat{\rho}_{SE}^{\text{out}}(L) = \sum_{i, j, \beta} c_i c_j^* |\varphi_i\rangle \langle \varphi_j| \otimes |\phi_i^\beta\rangle \langle \phi_j^\beta| =$$

$$\begin{pmatrix} \mathbf{A}_0 & \mathbf{B}_0 & \mathbf{B}_1 & \cdots & \mathbf{B}_{2^k-3} & \mathbf{B}_{2^k-2} \\ \mathbf{B}_0^\dagger & \mathbf{A}_1 & \mathbf{B}_{2^k-1} & \mathbf{B}_{2^k} & \cdots & \mathbf{B}_{2^k-2+(2^k-2)} \\ \mathbf{B}_1^\dagger & \mathbf{B}_{2^k-1}^\dagger & \ddots & \ddots & \vdots & \vdots \\ \vdots & \mathbf{B}_{2^k}^\dagger & \cdots & \mathbf{A}_l & \mathbf{B}_j \cdots & \vdots \\ \mathbf{B}_{2^k-3}^\dagger & \vdots & \cdots & \mathbf{B}_j^\dagger \cdots & \ddots & \mathbf{A}_{2^k-2} \\ \mathbf{B}_{2^k-2}^\dagger & \mathbf{B}_{2^k-2+(2^k-2)}^\dagger & \cdots & \cdots & \mathbf{B}_{\left[\sum_{i=1}^{2^k-1} (2^k-i)\right]-1}^\dagger & \mathbf{A}_{2^k-1} \end{pmatrix}_{2^{L+k} \times 2^{L+k}}, \quad (92)$$

$$\hat{\rho}_E^{\text{out}}(L) = \sum_{i, \beta} |c_i|^2 |\phi_i^\beta\rangle \langle \phi_i^\beta| = \sum_{i=0}^{2^k-1} \mathbf{A}_i$$

with^a $\mathbf{A}_l = \text{diag} \left[|a_{l \cdot 2^L + 1}|^2, \dots, |a_{(l+1) \cdot 2^L}|^2 \right]_{2^L \times 2^L}$, $l \in \{0, \dots, 2^k - 1\}$, $\mathbf{B}_j = \text{diag} \left[b_{j \cdot 2^L + 1}, \dots, b_{(j+1) \cdot 2^L} \right]_{2^L \times 2^L}$, $j = l' - l - 1 + \sum_{i=0}^{l-1} (2^k - i) \in \left\{ 0, \dots, \left[\sum_{i=1}^{2^k-1} (2^k - i) \right] - 1 = \frac{(2^k-1)2^k}{2} - 1 \right\}$ and $0 \leq l < l' \leq 2^k - 1$.

^a j depends on a pair (l, l') of $l \neq l'$ -values, such that l marks the row and l' denotes the column of $\hat{\rho}_{SE}^{\text{out}}$ that contain a $(2^L \times 2^L)$ -block matrix \mathbf{B}_j which in turn »connects« \mathbf{A}_l with $\mathbf{A}_{l'}$.

Contrary to assumptions 1 and 2 above there are no disjoint S-pointer state subspaces of $\hat{\rho}_{SE}^{\text{out}}(L)$ (diagonal elements from different S-pointer state subspaces of $\hat{\rho}_{SE}^{\text{out}}(L)$ overlap within $\hat{\rho}_E^{\text{out}}(L)$), i.e. (92) yields in general $H(S, E_L) > H(E_L)$. However, if we do not explicitly insist that all $(2^k - 1) 2^{k-1}$ \mathbf{B}_j -submatrices in (92) should contain non-zero diagonal entries, QD-conformal $\hat{\rho}_{SE}^{\text{out}}(L)$ can be found.

Specializing (92) for open $k = 1$ S embedded into an $n \gg 1$ E, we obtain density matrices $\hat{\rho}_{SE}^{\text{out}}(L)$ and $\hat{\rho}_E^{\text{out}}(L)$ in (93) below, with $(2^L \times 2^L)$ -block matrices $\mathbf{A}_0 = \text{diag} \left[|a_1|^2, \dots, |a_{2^L}|^2 \right]$, $\mathbf{A}_1 = \text{diag} \left[|a_{2^L+1}|^2, \dots, |a_{2^{L+1}}|^2 \right]$ and $\mathbf{B}_0 = \text{diag} [b_1, \dots, b_{2^L}]$, which generalizes (312) for $n > 1$.

$$\hat{\rho}_{SE}^{\text{out}}(0 < L \leq n) = \begin{pmatrix} \mathbf{A}_0 & \mathbf{B}_0 \\ (\mathbf{B}_0)^\dagger & \mathbf{A}_1 \end{pmatrix}_{2^{L+1} \times 2^{L+1}}$$

$$\hat{\rho}_E^{\text{out}}(0 < L \leq n) = \text{diag} \left[\underbrace{|a_1|^2 + |a_{2^L+1}|^2}_{:=|\tilde{a}_1|^2}, \dots, \underbrace{|a_{2^L}|^2 + |a_{2^{L+1}}|^2}_{:=|\tilde{a}_{2^L}|^2} \right]_{2^L \times 2^L}, \quad (93)$$

The eigenvalues of $\hat{\rho}_{SE}^{\text{out}}(L)$ and $\hat{\rho}_E^{\text{out}}(L)$ in (93) coincide only if the b_i -entries on the main diagonal of the B_j are organized as in

$$\begin{aligned} |b_{i,i'}|^2 &\equiv |b_i|^2 \stackrel{!}{=} |a_i|^2 |a_{2^L+i}|^2 \Rightarrow b_i \stackrel{!}{=} a_i^* a_{2^L+i} \in \mathbb{C}, i \in \{1, \dots, 2^L\}, (0 < L \leq n) \\ \underbrace{\sum_{j=1}^{2^{L-1}} b_j}_{\neq 0} + \underbrace{\sum_{j=2^{L-1}+1}^{2^L} b_j}_{\neq 0} &= \text{Tr}_{E_L}(\mathbf{B}_0) = \sum_{i=1}^{2^L} b_i \stackrel{!}{=} 0, \forall (0 < L \leq n) \\ \text{Tr}_{E_L}(\mathbf{A}_{r-1}) &= \sum_{s=1+(r-1) \cdot 2^L}^{2^{L-r}} |a_s|^2 \stackrel{!}{=} |c_r|^2, r \equiv (l+1) \in \{1, 2^{k=1}=2\} \\ |a_{l'}|^2 &= \sum_{l''=(l'-1)2^{(n-L')}-1}^{l' \cdot 2^{(n-L')}} |a_{l''}|^2 \Rightarrow |a_{l'+2^{L'}}|^2 = \sum_{l''=(l'+2^{L'}-1)2^{(n-L')}-1}^{(l'+2^{L'}) \cdot 2^{(n-L')}} |a_{l''}|^2 \\ b_{l'} &= \sum_{\tilde{l}=(l'-1)2^{(n-L')}-1}^{l' \cdot 2^{(n-L')}} b_{\tilde{l}} \end{aligned} \quad \left. \begin{array}{l} l' \in \{1, \dots, 2^{L'}\} \\ l'' \in \{1, \dots, 2^{n+1}\} \\ \tilde{l} \in \{1, \dots, 2^n\} \\ (0 < L' < L \leq n) \end{array} \right\} \quad (94)$$

$$\Rightarrow |a_i|^2 = |a|^2 \cdot 2^{-L}, |a_{2^L+i}|^2 = |b|^2 \cdot 2^{-L}, |a|^2 + |b|^2 \stackrel{!}{=} 1$$

and contain 2^L non-vanishing elements $|\tilde{a}_i|^2 = |a_i|^2 + |a_{2^L+i}|^2$, yielding $H(S, E_L) = H(E_L)$ for $L = n \gg 1$.

The first row of (94) may be necessary but definitely not sufficient for (15). Whereas in (59)-(70) we could have been sure that $H(S)$ attains $H(S_{\text{class}})$, within (92) and (93) the outer-diagonal entries of $\hat{\rho}_{SE}^{\text{out}}$ appear in principle after tracing out E from $\hat{\rho}_{SE}^{\text{out}}(L = n)$, disabling us from storing the entire $H(S_{\text{class}})$ into E (no effective decoherence of S for $n \gg 1$). The second row of (94) mimicks the »traceless demand« $c = -g$ from (312) and guarantees $H(S) = H(S_{\text{class}})$ after tracing out E from $\hat{\rho}_{SE}^{\text{out}}(L)$ in (93), whereas the third row of (94) eliminates dissipative effects (losses of $H(S_{\text{class}}^{k \geq 1})$) from

(93), s. (66) and (69), by preventing the S -probabilities $|c_i|^2$ to »merge«. Finally, the fourth row in (94) shows how the diagonal and outer-diagonal entries of $\hat{\rho}_{SE}^{\text{out}}(L)$ in (93) change (»merge«) when tracing out $(L - L')$ E -qubits by decreasing L . $\forall 0 < L' < L \leq n \gg 1$ $B_{j=0}$ and \mathbf{A}_l in (93) would adhere to the constraints from the first three rows in (94), leading to $H(S, E_L) = H(E_L) \forall (0 < L \leq n)$. This follows by setting in (93), without loss of generality, $|a_1|^2 = \dots = |a_{2^L}|^2 = |a|^2 \cdot 2^{-L}$ and $|a_{2^L+1}|^2 = \dots = |a_{2^{L+1}}|^2 = |b|^2 \cdot 2^{-L}$ and computing $H(S, E_L)$ and $H(E_L) \forall (0 < L \leq n)$. Indeed, by looking

for example at $\hat{\rho}_{SE}^{\text{out}}(L = 1 < n = 2) = \begin{pmatrix} \tilde{\mathbf{A}}_0 & \tilde{\mathbf{B}}_0 \\ \tilde{\mathbf{B}}_0^\dagger & \tilde{\mathbf{A}}_1 \end{pmatrix}$ (with $\tilde{\mathbf{A}}_0 = \text{diag}[a + b, c + d]$, $\tilde{\mathbf{A}}_1 = \text{diag}[e + f, g + h]$, $\tilde{\mathbf{B}}_0 = \text{diag}[c_1 + c_2, c_3 + c_4]$) emerging from $\hat{\rho}_{SE}^{\text{out}}(L = n = 2) = \begin{pmatrix} \mathbf{A}_0 & \mathbf{B}_0 \\ \mathbf{B}_0^\dagger & \mathbf{A}_1 \end{pmatrix}$ (with $\mathbf{A}_0 = \text{diag}[a, b, c, d]$, $\mathbf{A}_1 = \text{diag}[e, f, g, h]$, $\mathbf{B}_0 = \text{diag}[c_1, c_2, c_3, c_4]$, $c_1 = \sqrt{a \cdot e} = -c_3 = -\sqrt{c \cdot g} \Rightarrow a = c \wedge e = g$, $c_2 = \sqrt{b \cdot f} = -c_4 = -\sqrt{d \cdot h} \Rightarrow b = d \wedge h = f$), we see that it satisfies (15) and validates the fifth row of (94) only if $a \cdot e \cdot b \cdot f \stackrel{!}{=} 4^{-1} (a \cdot f + b \cdot e)^2 \Rightarrow a \stackrel{!}{=} b \wedge e \stackrel{!}{=} f$.

Having imposed (94) upon (93) one arrives at the following ($n \gg 1$)-behavior for the B_j -entries (with $i, j \in \{1, \dots, 2^k\}$)

$$\lim_{L=n \gg 1} |b_{i'}| = \sqrt{|a_{i'}|^2 |a_{2^L+i'}|^2} \sim 2^{-n}, b_{i'} \in \mathbb{C}, i' \in \{1, \dots, 2^{L=n}\} \Rightarrow r_{\beta, \gamma}^{i \neq j} \equiv \lim_{L=n \gg 1} |b_{i'}| \sim 2^{-n} \cdot \delta_{\beta, \gamma} \forall (\beta = \beta(L = n \gg 1) \equiv i'). \quad (95)$$

$|a_{i'}|^2$ and $|a_{2^L+i'}|^2$ in (94) (with $i' \in \{1, \dots, 2^{L=n}\}$) would also have to behave according to $\lim_{n \gg 1} |a_{i'}|^2 \sim 2^{-n}$ and $\lim_{n \gg 1} |a_{2^L+i'}|^2 \sim 2^{-n}$ for $L = n \gg 1$ in (93), which in turn leads to (95). Thus, with (94) and (95) (93) will certainly

adhere to (15), at least w.r.t. $k = 1$ S and $\forall (0 < L \leq n \gg 1)$. In light of (95) we may relax the traceless condition for B_0 by allowing $\text{Tr}_E(B_0) \approx 0$ in (94), resulting in an effectively decohered S for $n \gg 1$, as long as the number $N^{(+)}$ of positive signatures approximately equals the number $N^{(-)}$ of negative signatures within B_0 , i.e. $N^{(+)} \approx N^{(-)} \Leftrightarrow \text{Tr}_E(B_0) \approx 0$.

Thus, (95) provides a quantitative characterization of the overall decoherence factor $r_S := \langle \varphi_j | \varphi_{i \neq j} \rangle \sim \sum_{\gamma, \beta} r_{\beta, \gamma}^{i \neq j} \approx 0$

associated with the overlap between two different S-pointer states. Since we prefer $H(S) \approx H(S_{\text{class}})$, we would expect that $r_{\beta,\gamma}^{i,j}$ decays exponentially for $n \gg 1$, as suggested by (95).

The $k > 1$ version of (93)

If we aim at obtaining QD for $k > 1$ S, we have to find an appropriate non-vanishing subset of those B_j in (92) which would allow us to see the QD-plateau and organize (92) for $L = n \gg 1$ as follows: **1)** Each one-qubit subspace of $\hat{\rho}_{SE}^{\text{out}}$ contains two diagonal $(2^L \times 2^L)$ -blocks A_l and A_{l+1} as well as two nearest (adjacent) outer-diagonal $(2^L \times 2^L)$ -blocks B_j (in total 4 $(2^L \times 2^L)$ -blocks). For instance, in (92) to a pair of diagonal $(2^L \times 2^L)$ -blocks $\{A_{2m}, A_{2m+1}\}$ belong an outer-diagonal matrix B_j and its B_j^\dagger (with $j = 0 + \sum_{i=1}^{2m} (2^k - i)$) within the $(m+1)$ -th »one qubit subspace« of $\hat{\rho}_{SE}^{\text{out}}$ ($L = n \gg 1$), where $m \in \{0, \dots, 2^{k-1} - 1\}$. All other B_j in (92) that do not belong to these »one-qubit subspaces« of $\hat{\rho}_{SE}^{\text{out}}$ ($L = n$) have to be zero-submatrices; **2)** All nonzero $(2^L \times 2^L)$ -blocks B_j , i.e. all »one-qubit subspaces« in $\hat{\rho}_{SE}^{\text{out}}$ ($L = n$), have to be organized as in (93) for $k = 1$, however in a **connection independent** manner: two different A_l and $A_{l' \neq l}$ of (92) connected by a certain outer-diagonal B_j must not simultaneously be connected with other $A_{l''}$ (with $l'' \neq [l \neq l']$) by means of another $B_{j'}$ (where $j' \neq j$).

We now show that for a $k > 1$ qubit S we cannot validate (15) even if we organize (92) in a »connection independent« manner: look at a $k \geq 2$ S in (92) that interacts with an $L = n \gg 1$ E, where $A_l = |A|^2 \cdot 2^{-L} \text{diag}[1, \dots, 1] = 2^{-(k+L)} \text{diag}[1, \dots, 1] \forall l \in \{0, \dots, 2^k - 1\}$, traceless $B_{j \in \{j_C\}} = 2^{-(k+L)} \text{diag}[1, \dots, -1]$ (where $\{j_C\}$ represents a subset of those B_j in (92) enabling us to maintain »connection independence« among A_l), whose eigenvalues

$$\hat{\rho}_{SE}^{\text{out}} : \lambda_1 = 2^{-(n+k-1)}, \lambda = 0 \text{ (each } 2^{n+k-1} \text{ times)}; \hat{\rho}_E^{\text{out}} : \lambda_1 = 2^{-n} \text{ (} 2^n \text{ times)}, \hat{\rho}_S^{\text{out}} : \lambda_1 = 2^{-k} \text{ (} 2^k \text{ times)}, \quad (96)$$

yield $H(S, E_L) = n + k - 1 > H(E_L) = n$ and $H(S_{\text{class}}) = k$, ergo $I(S : E_L) / H(S_{\text{class}}) = 1/k \forall (0 < L \leq n)$, i.e. QD appears only if $k = 1$. For an arbitrary probability distribution $|a_i^{(l)}|^2 = |a_l|^2 \cdot 2^{-L}$ (with $i \in \{1, \dots, 2^L\}$, $l \in \{0, \dots, 2^k - 1\}$) w.r.t. A_l , (96) yields $\forall (0 < L \leq n)$ eigenvalues

$$\hat{\rho}_{SE}^{\text{out}} : \lambda_i^j \equiv \lambda_i^{(l, l')} = |a_i^{(l)}|^2 + |a_i^{(l')}|^2; \hat{\rho}_E^{\text{out}} : \lambda_i = \sum_{l=0}^{2^k-1} |a_i^{(l)}|^2 \quad i \in \{1, \dots, 2^L\}, j \in \{1, \dots, |\mathcal{P}| = 2^{k-1}\}, \quad (97)$$

where j runs over the set \mathcal{P} of all »independently connected« $(A_l, A_{l'})$ -pairs with $(l \neq l') \in \{0, \dots, 2^k - 1\}$, showing that $\forall (L \leq n \gg 1) H(S) = H(S_{\text{class}})$ and $H(S, E_L) = - \sum_{j=1}^{2^{k-1}} \sum_{i=1}^{2^L} \lambda_i^j \log_2 \lambda_i^j \geq H(E_L) = - \sum_{j=1}^{2^{k-1}} \sum_{i=1}^{2^L} \lambda_i \log_2 \lambda_i$, with equality only for $k = 1$, since then (97) reduces to (93)-(94). As long as $k > 1$ we would always obtain (97) (no QD), since $|\mathcal{P}| = 2^{k-1}$ does not depend on how one »independently connects« the A_l .

We can easily illustrate that missing »connection independence« violates (15) and leads to non-physical $\hat{\rho}_{SE}^{\text{out}}$ by looking again at (96), but with traceless $B_j = \text{diag}[2^{-(k+L)}, \dots, -2^{-(k+L)}] \forall j$, yielding $\forall (0 < L \leq n \gg 1) \hat{\rho}_{SE}^{\text{out}}$ -eigenvalues

$$\lambda_1 = 2^{1-n-k}, \lambda_2 = 0 \text{ [both } (2^k - 1) 2^{n-1} \text{ times]}; \lambda_3 = 2^{-n}, \lambda_4 = -(2^{k-1} - 1) \cdot 2^{1-n-k} \text{ [both } 2^{n-1} \text{ times]} \quad (98)$$

and is non-physical due to negative eigenvalues λ_4 . For $(n \rightarrow \infty) \geq L \gg k$ and k fixed, λ_4 in (98) would converge to 0 as $\sim -2^{-L}$. Similar result occurs if we choose within (96) only one additional traceless $B_{j=j_B \notin \{j_C\}}$ that breaks »connection independence« of A_l -block matrices. Comparing (98) with (95) gives: For $k \geq 1$ and »connection independent« A_l and $A_{l'}$ (with $l \neq l' \in \{0, \dots, 2^k - 1\}$) we can validate (15) $\forall (0 < L \leq n \gg 1)$ if and only if $k = 1$ as in (92) due to (97). For $k \geq 1$ the decoherence rate $r_{\beta(L), \gamma(L)} \cdot \delta_{\beta(L), \gamma(L)}$ will force the $b_i^{(l, l')}$ -entries within those B_j that »independently connect« A_l and $A_{l'}$ to converge to zero as in (95) [14].

Finally, we generalize (330) (with (331) from Table 1): This type of (289) is a special case of (92), with $(2^L \times 2^L)$ -blocks $A_0 = \text{diag}[a, 0, \dots, 0]$, $A_1 = \text{diag}[j_1, \dots, j_{2^L}]$, $B_{j=0} = \text{diag}[c, 0, \dots, 0]$, ($k = 1 \leq L \leq n \gg 1$) and

$$\hat{\rho}_{SE}^{\text{out}} = \begin{pmatrix} A_0 & B_0 \\ B_0^\dagger & A_1 \end{pmatrix} a + \sum_{i=1}^{2^L} j_i = 2^L (j \cdot 2^{-L}) \stackrel{!}{=} 1 \Rightarrow \{j_2, \dots, j_{2^L}\}, \lambda_{1/2} = (a + j_1) / 2 \pm \sqrt{(a + j_1)^2 / 4 + |c|^2 - a \cdot j_1}, \quad (99)$$

whose non-zero eigenvalues equal to $\hat{\rho}_E^{\text{out}}$ (L)-eigenvalues $\{a + j_1, j_2, \dots, j_{2^L}\}$ with $H(S) \approx H(S_{\text{class}}) \forall (0 < L \leq n)$ if

$$|c|^2 \stackrel{!}{=} a \cdot j_1 \sim 2^{-L} \forall (0 < L \leq n \gg 1) \Rightarrow j_i = j \cdot 2^{-L} \forall i \in \{1, \dots, 2^L\}. \quad (100)$$

Unfortunately, for $k > 1$, $n \gg 1$ (99)-(100) would break »mutual disjointness« of different »independently connected« »one qubit S-subspaces« ($\mathbf{A}_l, \mathbf{A}_{l' \neq l}, \mathbf{B}_j$) in $\hat{\rho}_{SE}^{\text{out}}(L)$ (no QD): looking at $\hat{\rho}_{SE}^{\text{out}}(k=2, 0 < L \leq n \gg 1)$ in (92), with $\forall i$

$$\mathbf{A}_0 = \text{diag}[a, 0, \dots, 0] \equiv \mathbf{A}_2 (a \leftrightarrow d), \mathbf{A}_1 = \text{diag}[j_1^{(1)}, \dots, j_{2^L}^{(1)}] \equiv \mathbf{A}_3 (j_i^{(1)} \leftrightarrow j_i^{(3)}), \mathbf{B}_0 = \text{diag}[c_1, 0, \dots, 0] \equiv \mathbf{B}_5 (c_1 \leftrightarrow c_6). \quad (101)$$

Indeed, (101) remains the same $\forall 0 < L \leq n \gg 1$ and guarantees »connection independence« between »one qubit subspaces« ($\mathbf{A}_0, \mathbf{A}_1, \mathbf{B}_0$) and ($\mathbf{A}_2, \mathbf{A}_3, \mathbf{B}_5$). However, \mathbf{A}_1 and \mathbf{A}_3 would overlap when extracting $\hat{\rho}_E^{\text{out}}$ from $\hat{\rho}_{SE}^{\text{out}}$, causing $H(S, E_L) > H(E_L) \forall (0 < L \leq n \gg 1)$, since \mathbf{B}_0 and \mathbf{B}_5 do not contain enough significant outer-diagonal entries that could adequately diminish $H(S, E_L)$ and even (96) adheres to (15) only for $k=1, n \gg 1$. Breaking »connection independence« in (101) by allowing each of the $[\mathbf{B}_1, \dots, \mathbf{B}_4]$ to contain only one non-vanishing diagonal entry, i.e. $\mathbf{B}_r = \text{diag}[c_{r+1}, 0, \dots, 0] \forall r \in \{1, \dots, 4\}$, we would always obtain $H(S, E_L) > H(E_L)$: i.e. by setting in (101) without loss of generality $a = d = \sum_{i=1}^{2^L} j_i^{(3)} = \sum_{i=1}^{2^L} c \cdot 2^{-L} = \sum_{i=1}^{2^L} j_i^{(1)} = \sum_{i=1}^{2^L} b \cdot 2^{-L} = 1/4 = 2^{-k}$, leads w.r.t. $L < n \gg 1$, together with $\mathbf{B}_0, \mathbf{B}_5$ and the four \mathbf{B}_r (with $c_1 = c_3 = c_4 = c_6 = (4 \cdot 2^{L/2})^{-1}$, $c_2 = 1/4$, $c_5 = (4 \cdot 2^L)^{-1}$), to eigenvalues $\{(2^k - 1) \cdot 2^{-k}, (2^{k+L})^{-1} (2^L \text{ times}), 0 (2^{k+L} - 2^L - 1 \text{ times})\}$ (for $\hat{\rho}_{SE}^{\text{out}}$), whereas for $\hat{\rho}_E^{\text{out}}$ we obtain eigenvalues $\{(2^k - 2[1 - 2^{-L}]) \cdot 2^{-k}, 2^{1-k-L} (2^L - 1 \text{ times})\}$, with $H(S, E_{L < n \gg 1}) > H(E_{L < n \gg 1})$. But after inserting more than one non-zero diagonal entry into all \mathbf{B}_j of (101) (as in (311)), we obtain a non-physical $\hat{\rho}_{SE}^{\text{out}} \forall (0 < L \leq n \gg 1)$ (s.(98)): e.g. in (101) for $L = n = 2$, we obtain in the limit $n \gg 1$ one eigenvalue $\sim -n^{-1/2}$ from $\mathbf{B}_j = \text{diag}[c_{j+1}, c_{j+1}, -c_{j+1}, 0] \forall j \in \{0, \dots, 5\}$, $a = b = c = d = 1/4$, $c_1 = c_3 = c_4 = c_6 = 1/(8 \cdot \sqrt{3})$, $c_2 = 1/12$, $c_5 = 1/16$ and

$$\mathbf{A}_0 = (a/3) \text{diag}[1, 1, 1, 0], \mathbf{A}_1 = (b/4) \text{diag}[1, 1, 1, 1], \mathbf{A}_2 = (c/3) \text{diag}[1, 1, 1, 0], \mathbf{A}_3 = (d/4) \text{diag}[1, 1, 1, 1]. \quad (102)$$

(99) adheres to (15) only for $k=1$ and $n \gg 1$. For $k > 1$ and $n \gg 1$ one always obtains $H(S, E_L) > H(E_L) \forall (0 < L \leq n \gg 1)$, regardless of whether the \mathbf{B}_j in (92) (structured as in (99) $\forall j$) respect »connection independence« of \mathbf{A}_l or not, we will always obtain physical $\hat{\rho}_{SE}^{\text{out}} \forall (0 < L \leq n \gg 1)$ only if the number of diagonal entries within each of the \mathbf{B}_j does not exceed one. However, even for such physical $\hat{\rho}_{SE}^{\text{out}}$ (15) cannot be validated if $k > 1$.

4.2.5 Assumption 4: system's pointer states overlap, environmental coherences allowed

This time all matrix-entries of $\hat{\rho}_{SE}^{\text{out}}$ in (92) are in principle allowed to be non-zero, with

$$\mathbf{A}_l = \begin{pmatrix} |a_{l \cdot 2^L + 1}|^2 & \blacksquare & \dots & \blacksquare \\ \blacksquare & & & \\ \vdots & \ddots & & \vdots \\ \blacksquare & \dots & \blacksquare & |a_{(l+1) \cdot 2^L}|^2 \end{pmatrix}_{2^L \times 2^L}, \mathbf{B}_j = \begin{pmatrix} b_{j \cdot 2^L + 1} & \blacksquare & \dots & \blacksquare \\ \blacksquare & & & \\ \vdots & \ddots & & \vdots \\ \blacksquare & \dots & \blacksquare & b_{(j+1) \cdot 2^L} \end{pmatrix}_{2^L \times 2^L}, \quad (103)$$

where $j = l' - l - 1 + \sum_{i=0}^{l-1} (2^k - i) \in \left\{0, \dots, \left[\sum_{i=1}^{2^k-1} (2^k - i)\right] - 1 = \frac{(2^k-1)2^k}{2} - 1\right\}$, $l \in \{0, \dots, 2^k - 1\}$, $0 \leq l < l' \leq$

$2^k - 1$, $\blacksquare \equiv \blacksquare_{\beta(L-k), \gamma(L-k)}^{(l)} \neq 0$ (for \mathbf{A}_l) and $\blacksquare \equiv \blacksquare_{\beta(L-k), \gamma(L-k)}^{(j)} \neq 0$ (for \mathbf{B}_j). In general, (103) would collide with (15) (no mutual disjointness and connection independence of different \mathbf{A}_l), even if $b_i = \blacksquare = 0$ as in (95). Since it is known from (342) that solely $i=0$ and $\blacksquare \equiv 0$ could lead to QD, whereas $|i| = \varepsilon \ll 1$, $|\blacksquare| = \varepsilon \ll 1$ in general yields $H(E_f) < H(S, E_f) \forall 0 < L \leq n \gg 1$, as in (291), we now generalize those $\hat{\rho}_{SE}^{\text{out}}$ from Table1 not discussed so far.

Generalization of (306), (307)-(309) and (310)

This is an extreme case of (289), with $\hat{\rho}_{SE}^{\text{out}}(L)$ without vanishing entries. Turning back to (76) we notice that for $k \geq 1, n \geq 1$ its only QD-conformal extension (with $|s_1^L\rangle$ and $|s_2^L\rangle$ as in (76), $1 \leq L \leq n$) is

$$|\Psi_{SE}^{\text{out}}(L)\rangle = \sum_{i=1}^{2^{k-1}} a_i |i\rangle |s_1^L\rangle + \sum_{j=2^{k-1}+1}^{2^k} a_j |j\rangle |s_2^L\rangle, \hat{\rho}_{SE}^{\text{out}}(L) = |\Psi_{SE}^{\text{out}}(L)\rangle \langle \Psi_{SE}^{\text{out}}(L)|, \sum_{i=1}^{2^k} |a_i|^2 \stackrel{!}{=} 1, \quad (104)$$

where $H(E_f) = -\sum_{i=1}^2 \lambda_i^E \log_2 \lambda_i^E \leq 1 \forall L$ from (77), $H(S) = H(S_{\text{class}})$ and $H(S, E_f)$ behaves in a two-fold way: **1)** if $L = n \geq 1$, (104) is pure $H(S, E_f) = 0 < H(E_f)$, yielding according to (15) $I(S : E_f) = 2H(S_{\text{class}})$ («quantum peak»); **2)** For $1 \leq L < n$ (104) contains 2^{k-1} »diagonal S-subspaces« (with their A_l - and B_j -blocks structured as a combination of (93) and (103)), half of which are organized according to $|s_1^L\rangle \langle s_1^L|$, whereas the remaining 2^{k-1} »diagonal S-subspaces« of (104) remain ordered according to $|s_2^L\rangle \langle s_2^L|$. This implies $I(S : E_f) = H(S_{\text{class}})$, since $H(S, E_f) = H(E_f) = H(S_{\text{class}}^{k=1}) \forall (1 \leq L < n)$, as in (77). For (104) QD does not appear for $k \geq 1$ and $1 \leq L \leq n$, since $\hat{\rho}_{SE}^{\text{out}}$ of (104) has for $k \geq 1$ only two eigenvalues $\lambda_1 = \sum_{i=1}^{2^{k-1}} |a_i|^2$ and $\lambda_2 = \sum_{j=2^{k-1}+1}^{2^k} |a_j|^2$ (with $\lambda_1 + \lambda_2 \stackrel{!}{=} 1$), corresponding to eigenvalues of $k = 1$ S. Thus: if we organize $\hat{\rho}_{SE}^{\text{out}}(L)$ according to (104), we could maximally store $1 \geq H(S_{\text{class}}) = -\lambda_1 \log_2 \lambda_1 - \lambda_2 \log_2 \lambda_2 > 0$ of a $k = 1$ S, even if one should insist on $k > 1$ (the PIP for (104) is given by Fig. 1), i.e. in (104) (15) holds only for $k = 1$.

Generalization of (315)

(76) and (104) are the only matrix structures of $\hat{\rho}_{SE}^{\text{out}}(L)$ from (289) whose $(k = n = 1)$ -versions involve non-vanishing b and i entries and nevertheless satisfy (15). This is why we now concentrate mainly on those $\hat{\rho}_{SE}^{\text{out}}(L)$ in Table 1 with $b = i = 0$ and $\blacksquare \equiv 0 \forall A_l$ in (103). One such $\hat{\rho}_{SE}^{\text{out}}(L)$ is (315), which for $n \geq 1$ corresponds to (92), however with

$$B_j = \begin{pmatrix} 0 & \cdots & b_{j, 2^L+1} \\ \vdots & \ddots & \vdots \\ b_{(j+1) \cdot 2^L} & \cdots & 0 \end{pmatrix}_{2^L \times 2^L}, \quad j = l' - l - 1 + \sum_{i=0}^{l-1} (2^k - i) \in \left\{ 0, \dots, \left[\sum_{i=1}^{2^k-1} (2^k - i) \right] - 1 = \frac{(2^k - 1) 2^k}{2} - 1 \right\}, \quad (105)$$

(where $0 \leq l < l' \leq 2^k - 1$) which means that each B_j -submatrix contains only outer-diagonal entries aligned on its secondary diagonal and leads to the same types of characteristic polynomials as in (93) and (97).

Namely, (92) with (103) would only persist for $L = n$, since the overlap (with $r_S = 0$, $r_{\beta, \gamma}^{i,j} = 0 \neq c_{\beta, \gamma}^{i,j}$)

$$\begin{aligned} \sum_{\beta, \gamma} \left\langle \phi_i^{\beta(L=n)} | \phi_j^{\gamma(L=n)} \right\rangle &\stackrel{!}{\sim} \delta_{\beta, \gamma} + c_{\beta, \gamma}^{i,j} \cdot (1 - \delta_{i,j}) (\delta_{[\beta+\gamma], (2^L=n+1)} - \delta_{\beta, \gamma}) \equiv (\hat{\rho}_{SE}^{\text{out}}(L=n))_{i,j}^{\beta, \gamma} \\ \lim_{n \gg 1} \left[c_{\beta, \gamma}^{i,j} = c_{\beta(L=n), \gamma(L=n)}^{i,j} \right] &\equiv 0 \end{aligned} \quad (106)$$

is non-zero solely as long as one does not trace out any E-qubits! As soon as we trace out at least one E-qubit ($L < n$) from $\hat{\rho}_{SE}^{\text{out}}$, the entries $b_{i, i' \neq i}^{(l, l')}$ (with i, i' as in (94)) of the B_j in (105) »connecting« ($A_l, A_{l' \neq l}$) tend to immediately vanish according to matrix realignment methods of appendix B, since they couple different, mutually (qubit-wise) orthogonal $|\phi_i^{\beta(L)}\rangle$, which in turn destroys the matrix structure in (92) and (105). Thus, for $L < n$ we obtain $H(E_L) < H(S, E_L)$.

This was not the case when dealing with B_j of (92), since therein the b_i -entries couple each $|\phi_i^{\beta(L)}\rangle$ with itself.

(92) and (103), with (94) modified in accord with (106), represents a $k \geq 1, n \geq 1$ version of (315) that does not validate (15) for a $k > 1$ S, even if we respect »connection independence« of »one qubit S-subspaces« ($A_l, A_{l' \neq l}, B_j$) in $\hat{\rho}_{SE}^{\text{out}}$ and simultaneously have $L = n$. Only for $k = 1 \wedge L = n$ one would satisfy (15). But, since (106) violates (15) $\forall (0 < L < n, \wedge k \geq 1)$, (106) does not lead to QD in general.

Nevertheless, there are special cases of (105)-(106) that could lead to QD, which we want to discuss now.

Generalization of (297) for $f \neq 0$ and of (299) for $d \neq 0$

Both structures (297) (for $f \neq 0$) and (299) (for $d \neq 0$) can be generalized to $L = n > k = 1$ E with $(2^L \times 2^L)$ -blocks $A_0 = \text{diag}[a, 0, \dots, 0]$, $A_1 = \text{diag}[0, \dots, 0, j]$, $\tilde{A}_0 = \text{diag}[0, \dots, 0, e]$, $\tilde{A}_1 = \text{diag}[h, 0, \dots, 0]$ and

$$\hat{\rho}_{SE}^{\text{out}} = \begin{pmatrix} A_0 & B_0 \\ B_0^\dagger & A_1 \end{pmatrix}_{2^{L+1} \times 2^{L+1}}, \quad \hat{\rho}_{SE}^{\text{out}} = \begin{pmatrix} \tilde{A}_0 & \tilde{B}_0 \\ \tilde{B}_0^\dagger & \tilde{A}_1 \end{pmatrix}_{2^{L+1} \times 2^{L+1}}, \quad B_0 = \begin{bmatrix} 0 & \cdots & d \\ \vdots & \ddots & \vdots \\ 0 & \cdots & 0 \end{bmatrix}_{2^L \times 2^L}, \quad \tilde{B}_0 = \begin{bmatrix} 0 & \cdots & 0 \\ \vdots & \ddots & \vdots \\ f & \cdots & 0 \end{bmatrix}_{2^L \times 2^L}, \quad (107)$$

as special cases of (105)-(106). In this sense we may regard in (107) the $\hat{\rho}_{SE}^{\text{out}}(L)$ with $(a, j, d) \neq 0$ as another version of the $\hat{\rho}_{SE}^{\text{out}}(L)$ with $(e, h, f) \neq 0$,

since the latter yields $\lambda^{1+n-2} \left[(h - \lambda)(e - \lambda) - |f|^2 \right] \stackrel{!}{=} 0$, corresponding to the characteristic polynomial of the former matrix-structure with $e \leftrightarrow a$, $h \leftrightarrow j$, $f \leftrightarrow d$ and leading to the same relevant (non-zero) eigenvalues as in (298). As in (105)-(106), (107) persists only as long as $L = n \gg 1$. However, here we will always see QD $\forall 1 \leq L \leq n$, since $L < n$ causes those matrix-structures from (59) with maximal $H(E_L)$ -values to emerge. We illustrate how one can generalize (107) to $(k > 1, n > 1)$ by looking at

$$|\hat{\rho}_{SE}^{\text{out}}(k=2, L=n=4)\rangle = a|00\rangle \otimes |0000\rangle + b|10\rangle \otimes |0010\rangle + c|01\rangle \otimes |0001\rangle + d|11\rangle \otimes |0011\rangle. \quad (108)$$

(108) will definitely lead to Zurek's »quantum peak«, since $H(S, E_L) = 0 < H(E_L) = H(S) = H(S_{\text{class}})$ as long as $L = n$, as in (92) with (103), $A_0 = |a|^2 |0000\rangle \langle 0000|$, $A_1 = |b|^2 |0010\rangle \langle 0010|$, $A_2 = |c|^2 |0001\rangle \langle 0001|$, $A_3 = |d|^2 |0011\rangle \langle 0011|$ and

$$\begin{aligned} B_0 &= a \cdot b^* |0000\rangle \langle 0010|, B_1 = a \cdot c^* |0000\rangle \langle 0001|, B_2 = a \cdot d^* |0000\rangle \langle 0011| \\ B_3 &= b \cdot c^* |0010\rangle \langle 0001|, B_4 = b \cdot d^* |0010\rangle \langle 0011|, B_5 = c \cdot d^* |0001\rangle \langle 0011|. \end{aligned} \quad (109)$$

After tracing out the fourth E-qubit ($L = 3$) the first B_j in (109) that disappear according to appendix B are B_1, B_2, B_3 and B_4 . The most »immune« S-subspaces in (109) that remain after tracing out the fourth E-qubit are precisely the »one qubit subspaces« (A_0, A_1, B_0) and (A_2, A_3, B_5), yielding $0 < H(S, E_L) < H(E_L) = H(S) = H(S_{\text{class}})$. After tracing out the second E-qubit ($L = k = 2$) only (A_0, A_1, A_2, A_3) »survive«, similar to (59), leading to $0 < H(S, E_L) = H(E_L) = H(S) = H(S_{\text{class}})$. Accordingly, due to (59), (15) fails to hold for $L = 1 < k$, since then $0 < H(E_L) < H(S, E_L) = H(S) = H(S_{\text{class}})$. We generalize (107) for $k > 1, n > 1$ by assuming:

1) Each $(2^L \times 2^L)$ -block A_l may contain only one diagonal $(2^{L-k} \times 2^{L-k})$ -block D_l with non-zero diagonal entries (whereas $\forall \blacksquare \equiv 0$) such that D_l and $D_{l' \neq l}$ remain mutually disjoint $\forall l$ as in (70); 2) $\hat{\rho}_{SE}^{\text{out}}$ for a $k > 1$ S and an $n \geq 1$ E possesses $2^k (2^n \times 2^n)$ -blocks A_l and $2^{2k} - 2^k (2^n \times 2^n)$ -blocks B_j (as in (92)). Each of the relevant $2^{2k-1} - 2^{k-1}$ B_j above the main diagonal of $\hat{\rho}_{SE}^{\text{out}}$ may contain only one non-zero outer-diagonal entry $b_{i, i' \neq i}^{(l, l')} \in \mathbb{C}$ »connecting« A_l and $A_{l' \neq l}$ within a »one qubit subspace« ($A_l, A_{l' \neq l}, B_j$) $\forall (l \neq l') \in \{0, \dots, 2^k - 1\}$ (with $0 \leq l < l' \leq 2^k - 1$); 3) We may choose only one diagonal entry in D_l and only one diagonal entry in $D_{l' \neq l}$ and »connect« them within ($A_l, A_{l' \neq l}, B_j$) by the corresponding non-zero outer-diagonal entry $b_{i, i' \neq i}^{(l, l')} \in \mathbb{C}$ of B_j as in (315), i.e. all B_j may contain only one $b_{i, i' \neq i}^{(l, l')} \in \mathbb{C}$ to avoid non-physical $\hat{\rho}_{SE}^{\text{out}}$.

In general, $\hat{\rho}_{SE}^{\text{out}} (n \geq L > 0, n > k + 1)$ (since QD preassumes $n \gg 1$), organized according to 1)-3), always leads to $H(E_L) > H(S, E_L) > 0$ for $L = n$, s. (107). Only if each D_l contains only one diagonal value, $H(E_L) = H(S) = H(S_{\text{class}}) > H(S, E_L) = 0$. If we »connect« more than one diagonal entry between different D_l as in (315), it would yield non-physical $\hat{\rho}_{SE}^{\text{out}}$ similar to (99). Indeed, $\hat{\rho}_{SE}^{\text{out}} (k=2, L=n=3)$ with $\blacksquare \equiv 0 \forall D_l = |c_l|^2 \cdot 2^{L-k} \text{diag}[1, \dots, 1]_{2^{L-k} \times 2^{L-k}} \wedge l \in \{0, \dots, 2^k - 1\}$ and all $B_j = B_{(l, l')}, 0 \leq l < l' \leq 2^{k-1} - 1$ containing two $b_{i, i' \neq i}^{(l, l')} \in \mathbb{C}$, with $i \in [1, \dots, 2^{L-k} = 2]$ and $|b_{i, i' \neq i}^{(l, l')}| = |a_i^{(l)}| |a_{2^{L-k} + (l'-1)2^{L-k} + 1 - i}^{(l')}| = |c_l| |c_{l'}| \cdot 2^{L-k}$, yields negative eigenvalue(s) as in (102).

In general, tracing out $k > n - L \geq 1$ E-qubits allows us to decompose $\hat{\rho}_{SE}^{\text{out}}$ organized according to 1)-3) into 2^{n-L} diagonal quasi »one qubit subspaces« $\left(\tilde{A}_r = \bigoplus_{i=(r-1)2^{k-n+L}}^{r \cdot 2^{k-n+L}-1} A_i, \tilde{B}_r \right)$ (with $r \in \{1, \dots, 2^{n-L}\}$), each corresponding to a » $(k - n - L)$ -qubit subspace« composed of 2^{k-n-L} A_l arranged in order of increasing l -values, as well as of all $B_j \in \tilde{B}_r \equiv \{B_j | B_j = B_{(l, l')}, (r-1)2^{k-n+L} \leq l < l' \leq r \cdot 2^{k-n+L} - 1\}$ that mutually »connect« the A_l , however with \tilde{B}_r not involving those B_j that »connect« the A_l from two different $(\tilde{A}_r, \tilde{B}_r)$ and $(\tilde{A}_{r' \neq r}, \tilde{B}_{r' \neq r})$. As long as $n > k + 1$ and $k > n - L \geq 1$, we obtain $H(E_L) > H(S, E_L) > H(S) = H(S_{\text{class}})$, i.e. from $\hat{\rho}_{SE}^{\text{out}} (k=2, L=n=4 > k+1)$ in (108)-(109) we see that after tracing out one E-qubit in $\hat{\rho}_{SE}^{\text{out}}$, ($L = n - 1 = 3$), $\{B_1, B_2, B_3, B_4\}$ do not contribute to $H(S, E_L)$. Nevertheless, B_0 and B_5 in (108)-(109) for $L = n - 1 = 3$ ensure that (15) holds due to $H(E_L) = H(S) = H(S_{\text{class}}) > H(S, E_L) > 0$.

If each of the A_l in (108)-(109) contains more than one non-zero diagonal entry, we obtain, due to (72), $H(E_L) > H(S, E_L) > H(S) = H(S_{\text{class}})$. For $n - L = k$ $\hat{\rho}_{SE}^{\text{out}}$ organized according to 1)-3) acquires the form (70) (all B_j become zero-matrices), with $H(E_L) = H(S, E_L) > H(S) = H(S_{\text{class}}) \forall (k < L \leq n - k)$, as predicted by (72). After tracing out $n - k$ E-qubits L will eventually reach $L = k$ and the D_l turn into plain numbers, yielding $H(E_{L=k}) = H(S, E_{L=k}) = H(S) = H(S_{\text{class}})$, as in (59). This is precisely what happens in (108)-(109) after tracing out $n - L = 2$ E-qubits, since then $L = k$. As in (59), no QD appears for $0 < L < k$.

$\hat{\rho}_{SE}^{\text{out}}$ organized according to 1)-3) yields $H(S) = H(S_{\text{class}})$, validating (15) only if $n \geq L \geq k, \wedge n > k + 1$, since then $H(E_L) > H(S, E_L) \forall (n - k < L \leq n)$, $H(E_L) = H(S, E_L) \forall (k \leq L \leq n - k)$ and $H(E_L) < H(S, E_L) \forall (0 < L < k)$.

Finally, we generalize (332) from Table 1, which is a generalized version of (107) with solely one B_j containing only one outer-diagonal entry. For $k = 1$ and $(0 < L \leq n \gg 1)$ we obtain $\hat{\rho}_{SE}^{\text{out}}$ as in (107) with the $(2^L \times 2^L)$ -block

$$\mathbf{A}_1 = \text{diag}[j_1, \dots, j_{2^L}], j_1 = h \cdot 2^{-L} = j_2 = \dots = j_{2^L} = j \cdot 2^{-L} \neq 0 \text{ and } a + \sum_{i=1}^{2^L} j_i = a + j \stackrel{!}{=} 1. \quad (110)$$

All arguments which used to prevent (99) from validating (15) for $k > 1$, $n \geq 1$ also apply for (110). However, since d in (110) will immediately vanish after tracing out one E-qubit by means of appendix B, (15) is violated for $0 < L < n$. Thus, although (110) satisfies (15) for $L = n$ if one fixes $|d|^2 = a \cdot j_{2^L} = a \cdot j \cdot 2^{-L}$, in accord with (333), it does not lead to QD. Also, (345) shows that inserting outer diagonal $\blacksquare \neq 0$ into the S-subspace $|1\rangle\langle 1|$ into (110) violates (15), even if $L = n$.

Combining (312), (315), (76) and (104)

Organizing $\hat{\rho}_{SE}^{\text{out}}$ ($k > 1$, $n > k$) according to

$$\begin{aligned} |\hat{\rho}_{SE}^{\text{out}}(k > 1, 0 < m \leq n)\rangle &= \sum_{l=0}^{2^{k-2}-1} [c_l |l\rangle \otimes |s_1^m\rangle \otimes |0_{n-m}\rangle + c_{2^{k-1}-l} |2^k - 1 - l\rangle \otimes |s_2^m\rangle \otimes |0_{n-m}\rangle] \\ &+ \sum_{l=2^{k-2}}^{2^{k-1}-1} [c_l |l\rangle \otimes |s_1^m\rangle \otimes |1_{n-m}\rangle + c_{2^{k-1}-l} |2^k - 1 - l\rangle \otimes |s_2^m\rangle \otimes |1_{n-m}\rangle], \end{aligned} \quad (111)$$

(with $|s_r^m\rangle = |s_r\rangle^{\otimes m}$, $r \in \{1, 2\}$ and $|s_r\rangle$ as in (76) above) we see that $H(S) \approx H(S_{\text{class}}) \equiv H(S_{\text{class}}^{k>1})$ as long as $n-m > 0$. As soon as $n = m$, $H(S_{\text{class}})$ in (111) coincides with $H(S_{\text{class}}^{k=1})$ in (104), leading to the violation of (15). For $m = 1$, $n - m > 0$ and $L = n$ (111) remains pure with $H(S_{\text{class}}) \geq H(E_L) > H(S, E_L) = 0$ («quantum peak» only for $k = 2$), but already after tracing out a single E-qubit $H(S_{\text{class}}) \geq H(E_L) > H(S, E_L) > 0 \forall (m < L < n)$ as long as at least one of the one qubit E-registry states $\{|0\rangle, |1\rangle\}$ remains within (111), s. (302)-(303), such as after setting $n = 3$, $k = 2$ and $m = 1$ into (111) and tracing out one E-qubit ($L = 2$). For $0 < L = m$ (111) yields $H(E_L) = H(S, E_L) < H(S_{\text{class}}^{k>1})$ (compare with (104) above), which still adheres to (15). Finally, in case of $0 < L < m$ (111) turns into (76), which does not lead to QD and forces us to fix $m \leq k$ if we want to validate (15) $\forall (m \leq L \leq n)$ with $H(S) \approx H(S_{\text{class}})$ and $m/n \leq f_{\text{opt}} \leq k/n$. With $m > 1$ and $n - m > 0$, (111) leads to $H(S) \approx H(S_{\text{class}}) \equiv H(S_{\text{class}}^{k>1})$. For $n = L > m > 1$ $H(S_{\text{class}}) \geq H(E_L) > H(S, E_L) = 0$, as follows by setting $m = k = 2$ and $n = L = 3$ into (111).

One can inductively generalize the inputs $[n = 3, k = 2, m = 1]$ and $[n = 3, k = 2, m = 2]$ studied so far by concluding that as long as $n - m > 0$, the E-registry states $\{|0_{n-m}\rangle, |1_{n-m}\rangle\}$ in (111) will guarantee $H(S_{\text{class}}) \geq H(E_L) > H(S, E_L) = 0 \forall L = n \geq k > 1$ (with equality only for $k = 2$) by preventing the appearance of $\hat{\rho}_E^{\text{out}}$ in (76). Namely, when looking at the $\hat{\rho}_E^{\text{out}}$ -eigenvalues from (111) in

$$\begin{aligned} \hat{\rho}_E^{\text{out}}(m < L \leq [n \geq k > 1], m > 1, n - m > 0) : \lambda_{1/2}^E &= 2^{m-1} (\Lambda_1 \pm \Lambda_2), \lambda_{3/4}^E = 2^{m-1} (\Lambda_3 \pm \Lambda_4) \\ \Lambda_{1/2} &= 2^{-m} \sum_{l=0}^{2^{k-2}-1} [|c_l|^2 \pm |c_{2^{k-1}-l}|^2], \Lambda_{3/4} = 2^{-m} \sum_{l=2^{k-2}}^{2^{k-1}-1} [|c_l|^2 \pm |c_{2^{k-1}-l}|^2], \end{aligned} \quad (112)$$

we see that $H(S_{\text{class}}) = H(E_L)$ only for $k = 2$ and $H(S_{\text{class}}) \geq H(E_L) > H(S, E_L) = 0 \forall m < L \leq [n \geq k > 1] \wedge m > 1$, $n - m > 0$, as in (307)-(309), (310), (104) and

$$\begin{aligned} \hat{\rho}_{SE}^{\text{out}}(m < L < [n \geq k > 1], m > 1, n - m > 0) : \lambda_1^{SE} &= \lambda_1^E + \lambda_2^E = 2^m \Lambda_1, \lambda_{3/4}^{SE} = 2^{m-1} (\Lambda_3 \pm \Lambda_4) = \lambda_{3/4}^E \\ \Rightarrow \lambda_2^{SE} &= 1 - (\lambda_1^{SE} + \lambda_3^{SE} + \lambda_4^{SE}) = 0; \Lambda_{1/2} = 2^{-m} \sum_{l=0}^{2^{k-2}-1} [|c_l|^2 \pm |c_{2^{k-1}-l}|^2], \Lambda_{3/4} = 2^{-m} \sum_{l=2^{k-2}}^{2^{k-1}-1} [|c_l|^2 \pm |c_{2^{k-1}-l}|^2]. \end{aligned} \quad (113)$$

Also for $0 < L = m > 1$ (111) yields $H(E_L) = H(S, E_L) < H(S_{\text{class}}^{k>1})$, s. (104), validating (15). Finally, for $0 < L < [m > 1]$ (111) turns into (76), which does not lead to QD and forces us to bound m as $m \leq k$ if we want to validate (15) $\forall (1 < m \leq L \leq n)$ with $m/n \leq f_{\text{opt}} \leq k/n$.

Thus, (111) validates (15) $\forall (1 \leq m \leq L \leq n)$, due to (112), (113), (307)-(309), (310) and (104), with $m/n \leq f_{\text{opt}} \leq k/n$, $m \leq k$ and $n - m > 0$. Accordingly,

$$|\hat{\rho}_{SE}^{\text{out}}(k = 1, 0 < m < n)\rangle = c_0 |0\rangle \otimes |s_1^m\rangle \otimes |0_{n-m}\rangle + c_1 |1\rangle \otimes |s_2^m\rangle \otimes |1_{n-m}\rangle, \quad (114)$$

and

$$\hat{\rho}_{SE}^{\text{out}}(k = 1, 0 < m < n) = |c_0|^2 |0\rangle\langle 0| \otimes |s_1^m\rangle\langle s_1^m| \otimes |0_{n-m}\rangle\langle 0_{n-m}| + |c_1|^2 |1\rangle\langle 1| \otimes |s_2^m\rangle\langle s_2^m| \otimes |1_{n-m}\rangle\langle 1_{n-m}| \quad (115)$$

validate (15) $\forall (0 < L \leq n)$, $f_{\text{opt}} = 1/n$, whereas

$$\begin{aligned}\hat{\rho}_{SE}^{\text{out}} = & \sum_{l=0}^{2^{k-2}-1} \left[|c_l|^2 |l\rangle \langle l| \otimes |s_1^m\rangle \langle s_1^m| \otimes |0_{n-m}\rangle \langle 0_{n-m}| + |c_{2^k-1-l}|^2 |2^k-1-l\rangle \langle 2^k-1-l| \otimes |s_2^m\rangle \langle s_2^m| \otimes |0_{n-m}\rangle \langle 0_{n-m}| \right] \\ & + \sum_{l=2^{k-2}}^{2^k-1} \left[|c_l|^2 |l\rangle \langle l| \otimes |s_1^m\rangle \langle s_1^m| \otimes |1_{n-m}\rangle \langle 1_{n-m}| + |c_{2^k-1-l}|^2 |2^k-1-l\rangle \langle 2^k-1-l| \otimes |s_2^m\rangle \langle s_2^m| \otimes |1_{n-m}\rangle \langle 1_{n-m}| \right],\end{aligned}\quad (116)$$

with $k > 1$, $0 < m < n$, validates (15) $\forall (1 \leq m < L \leq n)$, due to (112), (113), (307)-(309), (310) and (104), for $m/n < f_{\text{opt}} \leq k/n$, $m < k$ and $n - m > 0$.

Generalization of (334) to $k = 1$ and $n \gg 1$

We look at $\hat{\rho}_{SE}^{\text{out}} (k = 1, L = n > 1)$ with $\mathbf{A}_0 = \text{diag} [|a_S|^2, 0, \dots, 0]_{2^L \times 2^L}$, $\mathbf{A}_1 = |j|^2 2^{-L} \cdot \text{diag} [1, \dots, 1]_{2^L \times 2^L}$ and

$$B_0 = c |0_L\rangle \langle 0_L| + d |0_L\rangle \langle 1_L|, \quad c = d, \quad \text{with } j_1 = h \cdot 2^{-L} = j_2 = \dots = j_{2^L} = j \cdot 2^{-L} \neq 0 \text{ and } a + \sum_{i=1}^{2^L} j_i = a + j \stackrel{!}{=} 1, \quad (117)$$

leading to the same type of characteristic polynomial as in (334). (117) yields $\lim_{n \gg 1} H(S) = H(S_{\text{class}})$, validating (15) $\forall (0 < L \leq n)$. Since the structure of outer-diagonal entries in (117) will persist $\forall (0 < L \leq n)$ (s. appendix B), we see that the $(n > 2)$ -version of (117) with

$$B_0 = \sum_{j=1}^{2^L} c_j |0_L\rangle \langle z_j^L|, \quad c_1 = \dots = c_{2^L}, \quad (118)$$

where $|z_j^L\rangle \in I_L \equiv \{|z_j^L\rangle\}$ are the $(0 < L \leq n)$ -qubit E_L -registry states in (13), validates (15) for $L = n$ if

$$|c|^2 \stackrel{!}{=} 2^{-2n} |a_S|^2 |j|^2 \quad (2^L \text{ times}) \quad \forall (1 \leq L \leq [n > 1]), \quad (119)$$

which collides with constraints on outer-diagonal $\hat{\rho}_{SE}^{\text{out}}$ -matrix entries in (312) and (315). From (118) we see that the $(n > 2)$ -version of (117) w.r.t. $\{|s_1^L\rangle, |s_2^L\rangle\}$ from (302) is ($\hat{I}_L \equiv L$ -qubit identity matrix)

$$\begin{aligned}\hat{\rho}_{SE}^{\text{out}} (L \leq n) = & |a|^2 |0\rangle \langle 0| \otimes |z_j^L\rangle \langle z_j^L| + a b^* |0\rangle \langle 1| \otimes 2^{-n/2} 2^{-(n-L)/2} |z_j^L\rangle \langle s_1^L| \\ & + a^* b |1\rangle \langle 0| \otimes 2^{-n/2} 2^{-(n-L)/2} |s_1^L\rangle \langle z_j^L| + |b|^2 |1\rangle \langle 1| \otimes \hat{I}_L 2^{-L}\end{aligned}\quad (120)$$

violates (15) after tracing out E -qubits, as follows $\forall (0 < L < n)$ in (120) with, for instance, $n = 2$ and $L = 1 < n = 2$ w.r.t. $|z_j^L\rangle = |0_L\rangle$, whose eigenvalues

$$\begin{aligned}\hat{\rho}_{SE}^{\text{out}} : \lambda_{1/2}^{SE} = & \Lambda \pm \sqrt{\Lambda^2 + 2^{-(2n-L)} |a|^2 \cdot |b|^2}, \quad \lambda_3^{SE} = \frac{|b|^2}{2^L} \quad (2^L - 1 \text{ times}) \\ \hat{\rho}_E^{\text{out}} : \lambda_1^E = & |a|^2 + \frac{|b|^2}{2^L}, \quad \lambda_2^E = \frac{|b|^2}{2^L} \quad (2^L - 1 \text{ times}); \quad \Lambda := 2^{-1} |a|^2 - 2^{-(L+1)} |b|^2,\end{aligned}\quad (121)$$

yield, after expanding w.r.t. $\epsilon := 2^{-(2n-L)} \cdot \Lambda^{-2} |a|^2 \cdot |b|^2 < 1$ to $\mathcal{O}(\epsilon^2)$ with (294) and $(1 \pm x)^{a \in \mathbb{R}} \approx 1 \pm ax + \mathcal{O}(x^2)$ ($|x| \ll 1$), $H(S, E_{L=1 < n=2}) \approx H(E_{L=1 < n=2}) + \epsilon \Lambda (1 + [2 \ln 2]^{-1}) > H(E_{L=1 < n=2})$. (15) is also violated by replacing in (120)

$$|s_1^L\rangle \leftrightarrow (-1)^{M+M_{n-L}+l_{\text{alt}}} |s_2^L\rangle \quad (122)$$

for $L = n$ (where M and M_{n-L} denote the number of $|1\rangle$ -one qubit states in $|z_j^n\rangle$ and within the $(n-L)$ -qubit part $|z_j^{(n-L)}\rangle$ that has been traced out from $|z_j^n\rangle$, respectively, whereas $l_{\text{alt}} \in \{0, 1\}$)¹³.

Without loss of generality, let us assume in (122) $L = n = 2$, $l_{\text{alt}} = 0$ and $|z_j^{L=n=2}\rangle = |0_{L=n=2}\rangle$, $M = M_{n-L=0} = 0$.

¹³Since we also assume $\hat{\rho}_{SE}^{\text{out}}$ in (122) to be spanned by E -basis states $\{|z_j^L\rangle \langle z_j^L|, |z_j^L\rangle \langle s_2^L|, |s_2^L\rangle \langle z_j^L|, \hat{I}_L\}$, whose participation within the Liouville-decomposition of $\hat{\rho}_{SE}^{\text{out}}$ could initiate the appearance of M (depending on $\hat{\rho}_E^{\text{out}}$), whereas M_{n-L} would simply appear as a result of tracing out E -qubits in (122). Finally, l_{alt} reflects the freedom of changing (altering) the signature within $|s_2^L\rangle$ without changing the eigenvalue spectrum of (122).

Then the first row of B_0 from (118) displays a structure $[c_1, -c_2, -c_3, c_4]$ (with $c_i = a \cdot b^* 2^{-2} \forall i \in \{1, \dots, 4\}$ and A_0 and A_1 remaining the same), from which we obtain the same eigenvalues as in (120) and the same generalization (119) w.r.t. $n > 1$. Unfortunately, if we trace out in (122) one E-qubit (with, for instance, $L = 1 < n = 2$, $l_{alt} = 0$ and $|z_j^{L=1 < n=2}\rangle = |0_{L=1 < n=2}\rangle$, $M = M_{n-L=1} = 0$), results in (121) will not change either, i.e. (122) validates (15) only for $L = n$ (no QD).

Finally, we join (120) with (122) as in

$$\hat{\rho}_{SE}^{out}(L \leq n) = |a|^2 |0\rangle \langle 0| \otimes |z_j^L\rangle \langle z_j^L| + ab^* |0\rangle \langle 1| \otimes 2^{-n/2} 2^{-(n-L)/2} |z_j^L\rangle \left(\langle s_1^L| + (-1)^{M+M_{n-L}+l_{alt}} \langle s_2^L| \right) \\ + a^* b |1\rangle \langle 0| \otimes 2^{-n/2} 2^{-(n-L)/2} \left(|s_1^L\rangle + (-1)^{M+M_{n-L}+l_{alt}} |s_2^L\rangle \right) \langle z_j^L| + |b|^2 |1\rangle \langle 1| \otimes \hat{I}_L 2^{-L} \quad (123)$$

and assume again $L = n = 2$, $l_{alt} = 0$ and $|z_j^{L=n=2}\rangle = |0_{L=n=2}\rangle$, $M = M_{n-L=0} = 0$. Interestingly, (123) with

$$B_0 = c_1 |0_L\rangle \langle 0_L| + c_4 |0_L\rangle \langle 1_L|, \quad c_1 = c_4 = a \cdot b^* 2^{-1} \quad (2^{L-1} \text{ times}). \quad (124)$$

leads to $H(S, E_L) = H(E_L) \forall (0 < L \leq n)$, satisfying (15) since both $\hat{\rho}_{SE}^{out}$ and $\hat{\rho}_E^{out}$ yield eigenvalues $\lambda_1 = |a|^2 + |b|^2 \cdot 2^{-(n-L)}$ and $\lambda_2 = |b|^2 \cdot 2^{-(n-L)} (2^{n-L} - 1 \text{ times})$. Thus, (123) generalizes (117) to $\hat{\rho}_{SE}^{out}(k = 1, n > 2)$, such that within the row of B_0 associated with an $|a|^2$ -entry and its E-registry state $|z_j^L\rangle$ there are 2^{L-1} non-zero entries c_i ($i \in \{1, \dots, 2^{L-1}\}$).

Now, assuming $c_i = c \in \mathbb{C} \forall i \in \{1, \dots, 2^{L-1}\}$, we see that (123) leads to QD, since its characteristic polynomial contains, apart from non-zero eigenvalues $(\lambda - |b|^2 \cdot 2^{-n})$, the substructure of degree 2 as a generalization of (337) to $L \leq (n > 1)$

$$(\lambda - \lambda_1)(\lambda - \lambda_2) \stackrel{!}{=} 0 \Rightarrow \lambda_{1/2} = p \pm \sqrt{p^2 + 2^{n-1} |c|^2 - 2^{1-n} |a|^2 |b|^2}, \quad (125)$$

(with $p := |a|^2/2 + |b|^2/4$) which yields the corresponding ($n > 1$)-version of (337)

$$|c|^2 \stackrel{!}{=} 2^{2-2n} |a|^2 |b|^2 \Rightarrow c = 2^{1-n} a \cdot b^* \in \mathbb{C}, \quad (2^{L-1} \text{ times}) \quad \forall (1 \leq L \leq [n > 1]), \quad (126)$$

that also collides with (119) and with constraints on outer-diagonal $\hat{\rho}_{SE}^{out}$ -entries in (312) and (315). (123) displays (for $0 < L \leq (n > 1)$) within the row of B_0 associated with an $|a|^2$ -entry and its E-registry state $|z_j^L\rangle$ 2^{L-1} identical outer diagonal non-zero entries $c_i = c \in \mathbb{C} \forall i \in \{1, \dots, 2^{L-1}\}$, each vanishing for $n \gg 1 \sim 2^{-n+1} \forall (1 < L \leq n)$, with $H(S) = H(S_{class})$. For $L = 1$ (123) reduces to (99), however with a different condition on the remaining outer-diagonal entry c , as in (126). (337), (338), (125) and (126) demonstrate that QD appears for $k = 1$, $n \geq 1$ only if all $c_i \neq 0$ of B_0 in (123) have the same form $\forall (0 < L \leq n)$. Since we can set those $|b|^2 \cdot 2^{-L}$ for $L = n = 2$ within A_1 of (124) that are not connected with $|a|^2$ in A_0 by means of B_0 to 0 (as long as $L = n$), validating (15) $\forall (0 < L \leq n = 2)$, we introduce into (123) $|b|^2 |1\rangle \langle 1| \otimes (-1)^{\tilde{M}+l_{alt}} 2^{-n/2} \bigotimes_{i=1}^n \hat{O}_i \cdot \delta_{L,n}$, appearing only for $L = n$, with a traceless one-qubit E-operator $\hat{O}_i = (\sqrt{2})^{-1} [|1\rangle \langle 1| - |0\rangle \langle 0|]$ and \tilde{M} counting the number of $|0\rangle \langle 0|$ -states in $|z_j^n\rangle \langle z_j^n|$ (within $\hat{\rho}_E^{in}$). Thus, the final version of (117) and (123) leading to QD is

$$\hat{\rho}_{SE}^{out}(L \leq n) = |a|^2 |0\rangle \langle 0| \otimes |z_j^L\rangle \langle z_j^L| + ab^* |0\rangle \langle 1| \otimes 2^{-n/2} 2^{-(n-L)/2} |z_j^L\rangle \left(\langle s_1^L| + (-1)^{M+M_{n-L}+l_{alt}} \langle s_2^L| \right) \\ + a^* b |1\rangle \langle 0| \otimes 2^{-n/2} 2^{-(n-L)/2} \left(|s_1^L\rangle + (-1)^{M+M_{n-L}+l_{alt}} |s_2^L\rangle \right) \langle z_j^L| \\ + |b|^2 |1\rangle \langle 1| \otimes \left(\hat{I}_L 2^{-L} + (-1)^{\tilde{M}+l_{alt}} 2^{-n/2} \bigotimes_{i=1}^n \hat{O}_i \cdot \delta_{L,n} \right). \quad (127)$$

(127) with (124)-(126) is the only valid, QD-conformal generalization of (117) that validates (15) $\forall ([k = 1] \leq L \leq n)$. (329) in Table 1 can be generalized as (334) without violating (15) by **1**) transposing B_0 and $(B_0)^\dagger$ in (120), (122) and (127) (i.e. $B_0 \leftrightarrow (B_0)^T$ and $(B_0)^\dagger \leftrightarrow [(B_0)^\dagger]^T$), **2**) exchanging diagonal S-subspaces $|0\rangle \langle 0| \leftrightarrow |1\rangle \langle 1|$ and **3**) using the same constraints (119) and (126). (323)-(327) and (339)-(341) imply: (329) with (334) leads to non-physical $\hat{\rho}_{SE}^{out}$.

Outer-diagonal entries $\blacksquare \neq 0$ within A_L and Zurek's toy model of QD Introducing into the S-subspace $|1\rangle \langle 1|$ of (120) non-vanishing outer-diagonal entries $\blacksquare \neq 0$, similar to the i-entries in (348), no QD-plateau appears as long as one does not validate (119) in (118): We illustrate this by starting again with Zurek's input state configuration $\hat{\rho}_{SE}^{\text{in}} = \hat{\rho}_S^{\text{in}} \otimes \hat{\rho}_E^{\text{in}}$, where $|\Psi_S^{\text{in}}\rangle = a|0\rangle + b|1\rangle$ ($a, b \in \mathbb{C}$) and $\hat{\rho}_E^{\text{in}} = |0_n\rangle \langle 0_n|$. This time, however, we apply $\hat{u}_j^{(\phi=\pi/3)}$ instead of (11), obtaining

$$\hat{\rho}_{SE}^{\text{out}}(L=n) = |a|^2 |0\rangle \langle 0| \otimes |0_n\rangle \langle 0_n| + a \cdot b^* |0\rangle \langle 1| \otimes |0_n\rangle \langle 0_n| (\langle 0| 2^{-1} + \langle 1| 2^{-1} \sqrt{3})^{\otimes n} + a^* \cdot b |1\rangle \langle 0| \otimes (2^{-1} |0\rangle + 2^{-1} \sqrt{3} |1\rangle)^{\otimes n} |0_n\rangle \langle 0_n| + |b|^2 |1\rangle \langle 1| \otimes (2^{-1} |0\rangle + 2^{-1} \sqrt{3} |1\rangle)^{\otimes n} (\langle 0| 2^{-1} + \langle 1| 2^{-1} \sqrt{3})^{\otimes n}, \quad (128)$$

with each targeted E-qubit (index j) changed as $\hat{u}_j^{(\phi=\pi/3)} |0_j\rangle = 2^{-1} |0_j\rangle + 2^{-1} \sqrt{3} |1_j\rangle$ and $\hat{u}_j^{(\phi=\pi/3)} |1_j\rangle = -2^{-1} |1_j\rangle + 2^{-1} \sqrt{3} |0_j\rangle$. Apparently, (128) does not adhere to (119), but it still ensures $H(S) \approx H(S_{\text{class}})$ for $n \gg 1$, since all outer-diagonal entries in B_0 of (128) tend to zero $\sim 2^{-n}$ and one has already for $n = 3$ and $a = b = 1/\sqrt{2}$: $H(S) = 0,989 \approx H(S_{\text{class}}) = 1$. On the other hand, for $L = n$ the eigenvalues of $\hat{\rho}_{SE}^{\text{out}}$ and $\hat{\rho}_E^{\text{out}}$ in (128) are given in (129), yielding

$$\begin{aligned} \hat{\rho}_{SE}^{\text{out}} : \lambda_{1/2}^{SE(L=n)} &= 2^{-1} (|a|^2 + |b|^2) \pm \sqrt{4^{-1} (|a|^2 + |b|^2)^2 - \underbrace{2^{-2L+(n-L)} \cdot |b|^4}_{:=\epsilon}} \approx 2^{-1} [(|a|^2 + |b|^2) \pm (|a|^2 + |b|^2)] \\ \hat{\rho}_E^{\text{out}} : \lambda_{1/2}^{E(L=n)} &= 2^{-1} (|a|^2 + |b|^2) \pm \sqrt{4^{-1} (|a|^2 - |b|^2)^2 + \underbrace{2^{-2L+2(n-L)} \cdot |a|^2 |b|^2}_{:=\epsilon_0}} \approx 2^{-1} [(|a|^2 + |b|^2) \pm (|a|^2 - |b|^2)], \end{aligned} \quad (129)$$

$H(E_{L=n}) \approx H(S) = 0,989 \approx H(S_{\text{class}}) = 1 > H(S, E_{L=n}) = 0,089 \approx 0$ and thus $I(S : E_{L=n=3})/H(S_{\text{class}}) \approx 1,9$ (»quantum peak«) already for $n = 3$ ($\equiv n \gg 1$, since the ϵ -terms in (129) can be neglected). However, after tracing out $n - 1$ E-qubits in (128) (s. appendix B) one obtains for $n = 3$ and $L = 1$ (with $a = b = 1/\sqrt{2}$): $H(S, E_{L=1}) \approx H(E_{L=1}) + 0.14$ and thus $I(S : E_{L=1 < n=3})/H(S_{\text{class}}) \approx 0.86 < 1$ (no QD, since ϵ approaches zero faster than ϵ_0). Since $I(S : E_L)$ changes monotonously with increasing $0 < L \leq n$ [25], we expect from (129) that $I(S : E_L)$ would increase from $I(S : E_{L=1 < n})$ to $I(S : E_{L=n})$, which can be confirmed when looking at (128) for $L = 2 < n = 3$ and $a = b = 1/\sqrt{2}$, in which case $I(S : E_{L=2 < n=3})/H(S_{\text{class}}) \approx 0.95 < 1$, s. PIP in Fig. 4 below. $I(S : E_L)/H(S_{\text{class}})$ in Fig. 4 indicates that $\hat{u}_j^{(\phi=\pi/3)}$ represents an inappropriate »copy machine« from the point of view of the S-pointer basis, which is still an eigenbasis of (11). To see QD in (128) we need an operation (11) that maximally entangles one-qubit E-states $|0_j\rangle$ and $|1_j\rangle$ with each other, whereas $\hat{u}_j^{(\phi=\pi/3)}$ entangles $|0_j\rangle$ with $|1_j\rangle$ and vice versa only partially, since there is a non-zero probability $p(|0_j\rangle \rightarrow |0_j\rangle) = p(|1_j\rangle \rightarrow |1_j\rangle) = 1/4$ for an E-qubit target state to remain unaltered by $\hat{u}_j^{(\phi=\pi/3)}$ (accordingly, $p(|0_j\rangle \rightarrow |0_j\rangle) = p(|1_j\rangle \rightarrow |1_j\rangle) = 0$ for (11) indicates maximal entanglement between $|0_j\rangle$ and $|1_j\rangle$).

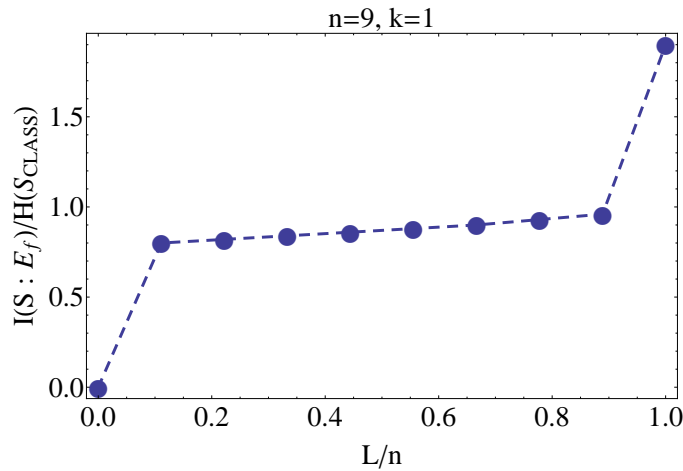


Figure 4: PIP for (128), with $k = 1$, $0 < L \leq n = 9$, $f = L/n$, $\hat{\rho}_S^{\text{in}} = |\Psi_S^{\text{in}}\rangle \langle \Psi_S^{\text{in}}|$ (where $|\Psi_S^{\text{in}}\rangle = a|0\rangle + b|1\rangle$), $\hat{\rho}_E^{\text{in}} = |0_n\rangle \langle 0_n|$ and $\hat{\rho}_{SE}^{\text{in}} = \hat{\rho}_S^{\text{in}} \otimes \hat{\rho}_E^{\text{in}}$. After acting upon $\hat{\rho}_{SE}^{\text{in}}$ by $\hat{u}_j^{(\phi=\pi/3)}$ from (9)-(10) in accord with Zurek's algorithm, no QD appears.

Between S (described by $\{|\pi_i\rangle\}$) and its E the simplest two-qubit transformation that enables us to copy $H(S_{\text{class}})$ into E with $f_{\text{opt}} = k/n$ is (9)-(11), (maximal S - E -entanglement). All other (9)-(10) with $\phi \neq \pi/2$ do not lead to QD («imperfect copy machines»). If S should be described by another $\{|\pi'_i\rangle\} \neq \{|\pi_i\rangle\}$, we could always transform all QD-conformal $\hat{\rho}_{SE}^{\text{out}}$ w.r.t. $\{|\pi'_i\rangle\}$, s. appendix A, i.e. w.r.t. $\{|\pi'_i\rangle\}$ (9)-(10) with $\phi \neq \pi/2$ would be a »perfect copy machine«.

Combining (120) and (122) What happens if we introduce into A_0 in (118) more than one diagonal entry and connect each of them with A_1 -diagonal entries as in (120)? From $\hat{\rho}_{SE}^{\text{out}}$ ($L = n \geq 2$) with $A_0 = 2^{-1} |a|^2 \text{diag}[1, 0, \dots, 0, 1]$, $A_1 = |b|^2 2^{-L} \cdot \text{diag}[1, \dots, 1]$ and B_0 in

$$B_0 = \sum_{j=1}^{2^L} \left\{ c_j^{(1)} |0_L\rangle \langle z_j^L| + c_j^{(2^L)} |1_L\rangle \langle z_j^L| \right\}, \quad c_1^{(i)} = \dots = c_{2^L}^{(i)} = c \in \mathbb{C} \forall i \in \{1, 2^L\}, \quad (130)$$

we obtain eigenvalues

$$|c|^2 = \begin{cases} |a|^2 |b|^2 \cdot 2^{-2(n+1)} \forall i \in \{1, 2^L\} \text{ if } (n > 1) \text{ even} \\ |a|^2 |b|^2 \cdot 2^{-(n+1/2)} \forall i \in \{1, 2^L\} \text{ if } (n > 1) \text{ odd} \end{cases}, \text{ colliding with (119)}$$

$$\hat{\rho}_{SE}^{\text{out}} : 2^{-1} |a|^2, 2^{-L} |b|^2 \text{ (} 2^L - 1 \text{ times)}, 2^{-1} |a|^2 + 2^{-L} |b|^2; \hat{\rho}_E^{\text{out}} : 2^{-L} |b|^2 \text{ (} 2^L - 2 \text{ times)}, 2^{-1} |a|^2 + 2^{-L} |b|^2 \text{ (2 times)}, \quad (131)$$

yielding $H(S, E_{L=n}) > H(E_{L=n})$ (no QD). However, after organizing the signature of the entries $c_i^{(2^L=n)} \forall i \in \{1, \dots, 2^L=n\}$ of B_0 in (130) in accord with the $\hat{\rho}_{SE}^{\text{out}}$ -subspace $|0\rangle \langle 1| \otimes |z_{j=2^L=n}^{L=n}\rangle \langle s_2^{L=n}| (-1)^{M+M_{n-L}+l_{\text{alt}}}$ from (122) (with, for instance, $|z_{j=2^L=n}^{L=n=2}\rangle = |11\rangle$, $M_{n-L} = 0$, $M = 2$ and $l_{\text{alt}} = 0$) and still insisting that (119) holds, we see $H(S, E_{L=n \geq 2}) = H(E_{L=n \geq 2})$: namely, in (130) we have to insist on A_0 -entries being equally distributed, since when introducing additional diagonal entries into A_0 we generate matrix structures of type (329), that necessitate us to impose this equal probability distribution upon all non-zero A_0 -diagonal entries. Thus, for $L = n \geq 2$ one can validate (15) by organizing the signature of the c-entries of the first row of B_0 from (130) in accord with $|s_1^{L=n}\rangle$, as in (120), and the signature of the c-entries of the $2^L=n$ -th row of B_0 by means of $|s_2^{L=n}\rangle$ in (122). But trying to organize the c-signatures of both, the first as well as the $2^L=n$ -th row of B_0 , according to $|s_2^{L=n}\rangle$ in (122) violates (15) as in (131).

Contradictions when extending (130) Choosing, for instance, $c_{i=2^L=n=2}^{(2^L=n=2)} = \pm c_i^{(1)} = c \in \mathbb{C} \forall i \in \{1, \dots, 2^L=n=2\}$ in (130), we will reproduce a contradiction $|c|^2 \stackrel{!}{=} z_1^{-1} |a|^2 |b|^2 \stackrel{!}{=} z_2^{-1} |a|^2 |b|^2$ for $(z_1 \neq z_2) \in \mathbb{R}^+ \forall n \geq 2$, which also occurs in (130) $\forall n \geq 2$ if we fix in B_0 the $2^L=n$ entries $c_i^{(1)} = c \in \mathbb{C}$ and maximally $(2^L=n-1)$ entries $c_i^{(2^L)} = \pm c \in \mathbb{C} \forall i \in \{1, \dots, 2^L=n\}$, since (323)-(327) and (339)-(341) show that regardless of how we fix the entries f or g , namely as in (94), (119) or (126), we get non-physical $\hat{\rho}_{SE}^{\text{out}}$. $\hat{\rho}_{SE}^{\text{out}}$ ($L = n \geq 2$) from (130), however this time with $A_0 = |a|^2 2^{-L} \cdot \text{diag}[1, \dots, 1]$, A_1 unchanged and B_0 given by

$$c_1^{(1)} = \dots = c_{2^L}^{(1)} = c_1^{(1)} = \dots = c_1^{(2^L)} = c \in \mathbb{C}, \quad (132)$$

yields the same type of contradiction $\forall n \geq 2$, regardless of whether one organizes the signatures of c -entries in the first row and the first column of B_0 in accord with $|s_1^{L=n}\rangle$ or with $|s_2^{L=n}\rangle$: **1)** by fixing in B_0 all c according to (94); **2)** by introducing into B_0 of (132) additional diagonal entries $c_i^{(i)} \forall i \in \{1, \dots, 2^L\}$ organized as in (94). In general, (132) leads to non-physical $\hat{\rho}_{SE}^{\text{out}}$, as already predicted in (323)-(327) and (329).

In (130) one could obtain for $L = (n \equiv \text{even})$ $H(S, E_{L=n}) = H(E_{L=n})$ if one sets in B_0 only the entries $c_1^{(1)}, c_{2^L}^{(1)}, c_2^{(2^L)}$ and $c_j^{(2^L)}$ ($\forall (j \equiv \text{odd}) \in \{3, \dots, 2^L=n-1\}$) to equal $\pm(c \in \mathbb{C}) \neq 0$ (regardless of the signature), with $|c|^2 \stackrel{!}{=} |a|^2 |b|^2 \cdot 2^{-2n-1}$. After tracing out one E -qubit ($L < [n \equiv \text{even}]$) (s. appendix B), we would, as in (335)-(338) and (329), have to demand for instance $|c|^2 \stackrel{!}{=} |a|^2 |b|^2 \cdot 2^{-3}$ for $L = 1 < n = 2$, which is in conflict with the actual preferred value $|c|^2 \stackrel{!}{=} |a|^2 |b|^2 \cdot 2^{-2n-1}$ that remains unchanged $\forall L < [n \equiv \text{even}]$, with $H(S, E_{L < n}) > H(E_{L < n}) \forall L < [n \equiv \text{even}]$. However, fixing in B_0 of (130) $\forall L = [n \equiv \text{odd}] > 2$ only $c_1^{(1)}, c_{2^L}^{(1)}, c_2^{(2^L)}$ and $c_j^{(2^L)}$ ($\forall (j \equiv \text{odd}) \in \{3, \dots, 2^L=n-1\}$ or $\forall j \in \{3, \dots, 2^L=n-1\}$) to equal $\pm(c \in \mathbb{C}) \neq 0$ (regardless of the signature), always yields contradictions as in (132).

Each outer-diagonal entry added to B_0 (previously organized as in (93)) forces us to implement constraints (119) or (126) to all c that collide with those in (94), leading in general to non-physical $\hat{\rho}_{SE}^{\text{out}}$, as in (323)-(327), (329) and (339)-(341).

QD-conformal extensions of (130) Inserting into B_0 of (130) for $L = n = 2$ the second row with c -signatures as in $|0\rangle \langle 1| \otimes |z_{j=2}^{L=n=2}\rangle \langle s_1^{L=n=2}| \equiv |0\rangle \langle 1| \otimes |10\rangle \langle s_1^{L=n=2}|$ yields, with $A_0 = \text{diag} [|a|^2/3, |a|^2/3, 0, \dots, 0, |a|^2/3]$, A_1 unchanged and B_0 given by (133) (with an optimal $|c|^2 \stackrel{!}{=} |a|^2 |b|^2 \cdot (9 \cdot 2^{2n})^{-1} \neq (119)$), $H(S, E_{L=n \geq 2}) > H(E_{L=n \geq 2})$ from $\{3^{-1} |a|^2 \text{ (2 times)}, 2^{-L} |b|^2 \text{ (2}^L - 1 \text{ times)}, 3^{-1} |a|^2 + 2^{-L} |b|^2\}$, $\{2^{-L} |b|^2 \text{ (2}^L - 3 \text{ times)}, 3^{-1} |a|^2 + 2^{-L} |b|^2 \text{ (3 times)}\}$ (for $\hat{\rho}_{SE}^{\text{out}}$ and $\hat{\rho}_E^{\text{out}}$, respectively).

$$c_1^{(i)} = \dots = c_{2^L}^{(i)} = c \in \mathbb{C} \forall i \in \{1, 2, 2^L\}, \quad (133)$$

The same occurs when fixing c -signatures in all three rows of B_0 from (133) as in $|0\rangle \langle 1| \otimes |z_j^{L=n=2}\rangle \langle s_2^{L=n=2}| (-1)^{M+M_{n-L}+l_{alt}}$ (where $M = 1$, $M_{n-L} = 0$, $l_{alt} = 0$ for $|z_{j=2}^{L=n=2}\rangle = |10\rangle$). However, if we organize the c -signatures in two of the B_0 -rows in (133) in accord with $|s_1^{L=n=2}\rangle$ and the c -signatures in the remaining B_0 -row by means of $|s_2^{L=n=2}\rangle$ (and vice versa), we would always obtain for $|c|^2$ the well-known type of contradiction from (132): i.e. extending (130) by adding one more row of outer-diagonal matrix entries into B_0 (organized according to $|s_1^{L=n=2}\rangle$ or $|s_1^{L=n=2}\rangle$) yields non-physical $\hat{\rho}_{SE}^{\text{out}}$ as in (323)-(327) and (339)-(341).

To omit contradictions we organize within all rows in B_0 (for $L = n = 2$) of (130) the c -signatures either according to $|s_1^{L=n=2}\rangle$ or according to $|s_2^{L=n=2}\rangle$ and obtain for $|c|^2 \stackrel{!}{=} 2^{-4n} |a|^2 |b|^2 \neq (119)$ $H(S, E_{L=n \geq 2}) > H(E_{L=n \geq 2})$ from

$$\hat{\rho}_{SE}^{\text{out}} : 2^{-L} |a|^2 \text{ (2}^L - 1 \text{ times)}, 2^{-L} |b|^2 \text{ (2}^L - 1 \text{ times)}; 2^{-L}; \hat{\rho}_E^{\text{out}} : 2^{-L} \text{ (2}^L \text{ times)}, \quad (134)$$

since organizing the c -signatures of all rows of B_0 in (130) either according to $|s_2^{L=n=2}\rangle$ or $|s_1^{L=n=2}\rangle$ completely mixes diagonal S -subspaces of $\hat{\rho}_{SE}^{\text{out}}$, violating (15). On the other hand, by organizing 2^{L-1} of the B_0 -rows and their c -signatures according to $|s_1^{L=n=2}\rangle$ and the remaining half of the B_0 -rows and their c -signatures in accord with $|s_2^{L=n=2}\rangle$, we obtain (also for $|c|^2 \stackrel{!}{=} 2^{-4n} |a|^2 |b|^2 \neq (119)$) from $\{2^{-L} |a|^2 \text{ (2}^L - 2 \text{ times)}, 2^{-L} |b|^2 \text{ (2}^L - 2 \text{ times)}, 2^{-L} \text{ (2 times)}\}$ and $\{2^{-L} \text{ (2}^L \text{ times)}\}$ for $\hat{\rho}_{SE}^{\text{out}}$ and $\hat{\rho}_E^{\text{out}}$, respectively, $H(S, E_{L=n}) > H(E_{L=n})$. Thus: for $L = n$ only (127) with (126) and

$$\begin{aligned} \hat{\rho}_{SE}^{\text{out}} = & |b|^2 |1\rangle \langle 1| \otimes \hat{I}_L 2^{-L} + 2^{-1} |a|^2 |0\rangle \langle 0| \otimes \left(|z_j^L\rangle \langle z_j^L| + |z_{j' \neq j}^L\rangle \langle z_{j' \neq j}^L| \right) + a \cdot b^* 2^{-n/2} 2^{-(n-L)/2} |0\rangle \langle 1| \otimes \left[|z_j^L\rangle \langle s_1^L| \right. \\ & \left. + |z_{j' \neq j}^L\rangle \langle s_2^L| (-1)^{M+M_{n-L}+l_{alt}} \right] + a^* b \cdot 2^{-n/2} 2^{-(n-L)/2} |1\rangle \langle 0| \otimes \left(|s_1^L\rangle \langle z_j^L| + (-1)^{M+M_{n-L}+l_{alt}} |s_2^L\rangle \langle z_{j' \neq j}^L| \right) \end{aligned} \quad (135)$$

(with c as in (119)) satisfy (15) (s. (321)-(322) and (329)). Adding further rows or columns into B_0 of (135) yields either contradictions, or violates (15), as in (323)-(327) and (329). However, while we know that (127) adheres to (15) $\forall (0 < L \leq n)$, we see that (135) after tracing out one E -qubit violates (15): this is clear if we look at (135), with, for instance, $0 < L = 1 < n = 2$, $|z_j^L\rangle = |0_{L=1 < n=2}\rangle$, $|z_{j' \neq j}^L\rangle = |1_{L=1 < n=2}\rangle$, $M = 2$, $l_{alt} = 0$ and $M_{n-L} = 1$, since then $H(S, E_{L=1 < n=2}) = H(E_{L=1 < n=2})$, however only if we apply the condition $|c|^2 \stackrel{!}{=} 2^{(n-L)-2n} |a|^2 |b|^2 = 2^{-3} |a|^2 |b|^2$ on c -entries, which collides with the actual structure $|c|^2 \stackrel{!}{=} 2^{-2n} |a|^2 |b|^2 = 2^{-4} |a|^2 |b|^2$ for B_0 -entries in (135) w.r.t. $L = 1 < n = 2$ as in (119). Thus, (135) validates (15) only for $L = n$ (no QD).

Only (127) leads to QD and validates (15) $\forall [k = 1] \leq L \leq n \gg 1$, ensuring $H(S) = H(S_{\text{class}}^{k=1})$.

It is impossible to extend (127) in a QD-conformal manner by adding to B_0 rows of the same signature-structure as in

$$\begin{aligned} \hat{\rho}_{SE}^{\text{out}} = & |b|^2 |1\rangle \langle 1| \otimes \hat{I}_L 2^{-L} + 2^{-1} |a|^2 |0\rangle \langle 0| \otimes \left(|z_j^L\rangle \langle z_j^L| + |z_{j' \neq j}^L\rangle \langle z_{j' \neq j}^L| \right) + a \cdot b^* 2^{-n/2} 2^{-(n-L)/2} |0\rangle \langle 1| \otimes \left[|z_j^L\rangle \langle z_{j' \neq j}^L| \right. \\ & \left. + \left(\langle s_1^L| + \langle s_2^L| (-1)^{M+M_{n-L}+l_{alt}} \right) + a^* b \cdot 2^{-n/2} 2^{-(n-L)/2} |1\rangle \langle 0| \otimes \left(|s_1^L\rangle + (-1)^{M+M_{n-L}+l_{alt}} |s_2^L\rangle \right) \left[|z_j^L\rangle + \langle z_{j' \neq j}^L| \right] \right], \end{aligned} \quad (136)$$

which leads only with (119) (that collides with (126) and the form of c -entries in (136)) to $H(S, E_{L=n \geq 2}) > H(E_{L=n \geq 2})$ from $\{2^{-1} |a|^2, 2^{-L} |b|^2 \text{ (2}^L - 1 \text{ times)}, 2^{-1} |a|^2 + 2^{-L} |b|^2\}$ and $\{2^{-1} |a|^2 + 2^{-L} |b|^2 \text{ (2 times)}, 2^{-L} |b|^2 \text{ (2}^L - 2 \text{ times)}\}$ (for $\hat{\rho}_{SE}^{\text{out}}$ and $\hat{\rho}_E^{\text{out}}$, respectively). Introducing into (136) the \hat{O}_i -term from (127) yields (for $|c|^2 \stackrel{!}{=} 2^{-2n} |a|^2 |b|^2 \neq (126)$) from $\{2^{-1} |a|^2, 2^{1-L} |b|^2 \text{ (2}^{L-1} - 1 \text{ times)}, 2^{-1} |a|^2 + 2^{1-L} |b|^2\} \wedge \{2^{-1} |a|^2 + 2^{1-L} |b|^2 \text{ (2 times)}, 2^{1-L} |b|^2 \text{ (2}^{L-1} - 2 \text{ times)}\}$

(for $\hat{\rho}_{SE}^{\text{out}}$ and $\hat{\rho}_E^{\text{out}}$, respectively) $H(S, E_{L=n \geq 2}) > H(E_{L=n \geq 2})$. Continuing this trend to the case of 2^{L-n} non-zero diagonal entries $2^{-L} |a|^2$ within A_0 of (136) we see that

$$\begin{aligned} \hat{\rho}_{SE}^{\text{out}}(L \leq n) = & \left(|a|^2 |0\rangle \langle 0| + |b|^2 |1\rangle \langle 1| \right) \otimes \hat{I}_L 2^{-L} + a \cdot b^* 2^{-n/2} 2^{-(n-L)/2} |0\rangle \langle 1| \otimes \left[\sum_{j=1}^{2^L} |z_j^L\rangle \right] \left(\langle s_1^L| + \langle s_2^L| (-1)^{M+M_{n-L}+l_{\text{att}}} \right) \\ & + a^* b \cdot 2^{-n/2} 2^{-(n-L)/2} |1\rangle \langle 0| \otimes \left(|s_1^L\rangle + (-1)^{M+M_{n-L}+l_{\text{att}}} |s_2^L\rangle \right) \left[\sum_{j=1}^{2^L} \langle z_j^L| \right] \end{aligned} \quad (137)$$

leads (only for $|c|^2 \stackrel{!}{=} 2^{-2n} |a|^2 |b|^2$ that collides with (126) and the form of c-entries in (137)) to

$$\begin{aligned} \hat{\rho}_{SE}^{\text{out}} : & 2^{-L} |a|^2, 2^{-L} |b|^2 \text{ (both } 2^L - 2 \text{ times)}, 2^{-L} |b|^2 \text{ (2 times)}; \hat{\rho}_E^{\text{out}} : 2^{-L} \text{ (} 2^L \text{ times)} \\ \Rightarrow & H(S, E_{L=n \gg 1}) = H(S_{\text{class}}^{k=1}) + H(E_{L=n \gg 1}) = H(S_{\text{class}}^{k=1}) + L. \end{aligned} \quad (138)$$

Increasing the number of diagonal entries within A_0 of (127), (137) yields $\lim_{n \gg 1} I(S, E_{L=n}) / H(S_{\text{class}}^{k=1}) = 0$. (125) may contain only one pair of overlapping diagonal entries but not more, otherwise QD disappears. In (99) we can choose for c not only (99) but also (126) or (119) (despite of violated (99)-condition) and still be sure that (15) is (approximately) validated $\forall [k=1] \leq L \leq n \gg 1$. This is why (127) satisfies (15) even for $n \gg L \rightarrow 1$.

($k > 1, n \geq 1$) **generalization of (334)**

We investigate whether (127) and its signature-distribution of the c-entries can be extended to $k > 1$ open S and $n > 1$ E and concentrate on ($k = L = n = 2$)- $\hat{\rho}_{SE}^{\text{out}}$, with »connection independent« ($2^L \times 2^L$)-blocks $A_0 = \text{diag}[|a|^2, 0, \dots, 0]$, $A_1 = 2^{-L} \cdot \text{diag}[|b|^2, \dots, |b|^2]$, $A_2 = \text{diag}[0, |c|^2, 0, \dots, 0]$, $A_1 \leftrightarrow A_3 \Leftrightarrow |b|^2 \leftrightarrow |d|^2$ and

$$B_0 = \begin{bmatrix} c_1 & 0 & 0 & c_1 \\ 0 & 0 & 0 & 0 \\ 0 & 0 & 0 & 0 \\ 0 & 0 & 0 & 0 \end{bmatrix}, B_5 = \begin{bmatrix} 0 & 0 & 0 & 0 \\ 0 & c_2 & c_2 & 0 \\ 0 & 0 & 0 & 0 \\ 0 & 0 & 0 & 0 \end{bmatrix}, \quad (139)$$

leading for $|c_1|^2 \stackrel{!}{=} |a|^2 \cdot |b|^2 \cdot 2^{-2n+1}$ and $|c_2|^2 \stackrel{!}{=} |c|^2 \cdot |d|^2 \cdot 2^{-2n+1}$ (best choices) to the eigenvalues

$$\hat{\rho}_{SE}^{\text{out}} : \frac{|d|^2}{2^L}, \frac{|b|^2}{2^L} \text{ (each } 2^L - 1 \text{ times)}, |a|^2 + \frac{|b|^2}{2^L}, |c|^2 + \frac{|d|^2}{2^L}; \hat{\rho}_E^{\text{out}} : |a|^2 + \frac{|b|^2 + |d|^2}{2^L}, |c|^2 + \frac{|b|^2 + |d|^2}{2^L}, \frac{|b|^2 + |d|^2}{2^L} \text{ (} 2^L - 2 \text{ times)}, \quad (140)$$

with $H(S^{k=2}) \approx H(S_{\text{class}}^{k=2})$, or, for $i' \in \{0, \dots, 2^{k-1} - 1\}$, $k > 2, \wedge L = n \geq k$ and $\{ |a_i|^2 \}_{i=1}^{i=2^k}$, the eigenvalues

$$\hat{\rho}_{SE}^{\text{out}} : \frac{|a_{2i'+1}|^2}{2^L} \text{ (} 2^L - 1 \text{ times)}, |a_{2i'}|^2 + \frac{|a_{2i'+1}|^2}{2^L}; \hat{\rho}_E^{\text{out}} : |a_{2i'}|^2 + 2^{-L} \cdot \sum_{j=0}^{2^{k-1}-1} |a_{2j+1}|^2, 2^{-L} \cdot \sum_{j=0}^{2^{k-1}-1} |a_{2j+1}|^2 \text{ (} 2^L - 2^{k-1} \text{ times)}, \quad (141)$$

with $H(S^{k>1}, E_{L=n}) > H(E_{L=n})$. (139)-(141) also demonstrate that organizing in (101) the B_j -submatrices in accord with (119) or (126) leads to physical, not QD-compliant states $\hat{\rho}_{SE}^{\text{out}}$ even when one adheres to the »connection independence« of the corresponding A_l (with $l \in \{0, \dots, 2^k - 1\}$). For instance, in (101) with $a = d = \sum_{i=1}^{2^L} j_i^{(3)} = \sum_{i=1}^{2^L} c \cdot 2^{-L} =$

$\sum_{i=1}^{2^L} j_i^{(1)} = \sum_{i=1}^{2^L} b \cdot 2^{-L} = 1/4 = 2^{-k}$ and $c_2 = c_3 = c_4 = c_5 = 0$, whereas c_1 and c_6 remain arbitrary, the eigenvalue spectra $\{3/4, 1/4\}$ (for $\hat{\rho}_E^{\text{out}}$) and $\{1/8 \text{ (2 times)}, 0 \text{ (2 times)}, 3/16 \pm \sqrt{D_1}, 3/16 \pm \sqrt{D_2}\}$ (for $\hat{\rho}_{SE}^{\text{out}}$) remain physical with $H(S, E_{L=1 < n}) > H(E_{L=1 < n})$ (for $n \gg 1$) w.r.t. all values of $D_1 := 2^{-8} + 2^8 |c_1|^2$ and $D_2 := 2^{-8} + 2^8 |c_6|^2$ within $0 \leq D_1, D_2 \leq 9 \cdot 2^{-8}$. If we violate this »connection independence« between the A_l by choosing in (139), without any loss of generality $|a|^2 = |b|^2 = |c|^2 = |d|^2 = 2^{-k} = 1/4$, and (with $c_1 = 2^{-k} \cdot 2^{-n+1}$ and $c_2 = 2^{-k} \cdot 2^{-n}$)

$$B_2 = \begin{bmatrix} c_1 & 0 & 0 & c_1 \\ 0 & 0 & 0 & 0 \\ 0 & 0 & 0 & 0 \\ 0 & 0 & 0 & 0 \end{bmatrix}, B_3 = \begin{bmatrix} 0 & 0 & 0 & 0 \\ 0 & c_1 & 0 & 0 \\ 0 & c_1 & 0 & 0 \\ 0 & 0 & 0 & 0 \end{bmatrix}, B_4 = \begin{bmatrix} c_2 & 0 & 0 & c_2 \\ 0 & c_2 & c_2 & 0 \\ 0 & c_2 & c_2 & 0 \\ c_2 & 0 & 0 & c_2 \end{bmatrix}, \quad (142)$$

which imply different types of organizing (127) and (137) matrix structures within the B_j submatrices of $\hat{\rho}_{SE}^{out}$. Since criteria imposed on c -entries within (127) and (137) collide with each other, we are led by (139) and (142) in general to non-physical $\hat{\rho}_{SE}^{out}$ with contradicting conditions on c -entries, similar to (132). E.g. (142) yields $\forall (0 < L \leq n \gg 1)$ $\hat{\rho}_{SE}^{out}$ -eigenvalues $\lambda_1 = (7 + \sqrt{65}) \cdot 2^{-n-k-1}$, $\lambda_2 = (7 - \sqrt{65}) \cdot 2^{-n-k-1}$, $\lambda_3 = -2^{-n-k}$ [each 2^{n-1} times], $\lambda_4 = 2^{-n-k}$ (2^n times). Thus, for $k > 1$ we cannot obtain QD by organizing the B_j as in (127). (142) shows that organizing in (101) the B_j as in (119) or (126) leads to physical, however still not QD-compliant $\hat{\rho}_{SE}^{out}$ when violating »connection independence« of the A_l (with $l \in \{0, \dots, 2^k - 1\}$), similar to (101) after setting $c_1 = c_3 = c_4 = c_6 = (4 \cdot \sqrt{2}\sqrt{2})^{-1} = 1/8$, $c_2 = (4 \cdot \sqrt{2})^{-1}$ and $c_5 = (8 \cdot \sqrt{2})^{-1}$ (as in (338)). Setting in (101), without loss of generality, $a = d = \sum_{i=1}^{2^L} j_i^{(3)} = \sum_{i=1}^{2^L} c \cdot 2^{-L} = \sum_{i=1}^{2^L} j_i^{(1)} = \sum_{i=1}^{2^L} b \cdot 2^{-L} = 1/4 = 2^{-k}$, with arbitrary entries $[c_1, \dots, c_6]$ of the B_r for $r \in \{0, \dots, 5\}$, in general yields non-physical $\hat{\rho}_{SE}^{out}$, i.e. there is no general physical and QD-compliant solution to the eigenvalue equation of (101) with arbitrary $[c_1, \dots, c_6]$.

4.3 Conjecture

Taking into account all results obtained in subsections 4.2.1-4.2.5 we want to discuss here the plausibility of the following conjecture:

$f_{opt} = k/n$ for storing $H(S) = H(S_{class})$ into E can be achieved if we organize $\hat{\rho}_{SE}^{out}$ according to the following conjecture:

$\hat{\rho}_{SE}^{out}$ -structures in Table 2 below are the only QD-conformal matrices w.r.t. the open k -qubit S and its n -qubit E (apart from its equivalent versions $\hat{\rho}_{S'E'}^{out}$, emerging after unitarily transforming $\hat{\rho}_{SE}^{out}$ by (284) as in appendix A)

(59) and (70)
(93)-(94), (99)
(117), (126)-(127)
(107), (108)-(109) w.r.t. the case $n \geq L > 0$, $n > k + 1$
(76), (104), (111) and (115)-(116)

Table 2: QD-conformal $\hat{\rho}_{SE}^{out}$ -matrix structures for a k -qubit open S and its n -qubit E with $(k \geq 1, n \geq 1)$.

that cannot be extended by adding arbitrary non-zero outer-diagonal entries to $\hat{\rho}_{SE}^{out}$ such that the extended $\hat{\rho}_{SE}^{out}$ still validates (15) $\forall (k \leq L \leq n)$.

Plausibility argument: (59) and (70) are basic matrix structures of $\hat{\rho}_{SE}^{out}$ closely related to Zurek's concept of »entanglement monogamy« [14] which can be combined with, for instance, (93)-(94) or (107), and thus validate (15) at least for $L = n$, ensuring $H(S) = H(S_{class}^{k=1})$ in the limit $n \gg 1$. However, w.r.t. QD $\hat{\rho}_{SE}^{out}$ has to adhere to (15) not only for $L = n$, but also $\forall [k \geq 1] \leq L \leq n$. The only way to extend (59) and (70) to other QD-conformal $\hat{\rho}_{SE}^{out}$ -matrices are:

1) (93)-(94) guarantees QD only for $k = 1$ S . If we add an arbitrary outer-diagonal entry within B_0 of (93), we would, as in (94), and (119) and (126), have to apply conditions on outer-diagonal $\hat{\rho}_{SE}^{out}$ -matrix entries that are mutually incompatible, as shown in (323)-(327), (329), (339)-(341) and (132), indicating that it is impossible to extend (93)-(94) in a QD-conformal manner by simply adding arbitrary outer-diagonal entries to B_0 of (93), since this would force us to apply to all B_0 -entries conditions (119) or (126), that, combined with (94), always lead to non-physical $\hat{\rho}_{SE}^{out}$. The only way for extending (93) in a way that would preserve the physical nature of $\hat{\rho}_{SE}^{out}$ would be to organize the c -entries and their signatures within B_0 in accord with $\{|s_1^L\rangle, |s_2^L\rangle\}$, however, as (130) and (134)-(138) show, although yielding physical $\hat{\rho}_{SE}^{out}$, this way of extending (93) does not satisfy (15). It is not allowed to introduce in (93) outer-diagonal entries within A_0 and A_1 , since 1) we do not intend to decrease $H(E_L)$ but $H(S, E_L)$, instead, and 2) (93) with non-zero outer-diagonal entries in A_0 and A_1 potentially leads to non-physical $\hat{\rho}_{SE}^{out}$, as indicated by (320). As a special case of (93)-(94), (99) also leads to QD only for $k = 1$ and can, for identical reasons, be extended in a QD-conformal manner only by introducing structures (117) and (126)-(127), however, since conditions that have to be imposed upon B_0 -entries within the latter collide with (94), (93)-(94) and (99) cannot be extended by adding arbitrary non-zero outer-diagonal entries to B_0 .

2) (117), (126)-(127) lead to QD only for $k = 1$. It is possible to extend them in a way that one obtains physical $\hat{\rho}_{SE}^{out}$ that even satisfy (15), but only for $L = n$ (s. (135), (136), (137)): (117), (126)-(127) cannot be extended by adding arbitrary non-zero outer-diagonal entries to B_0 .

3) (107), (108)-(109) w.r.t. $n \geq L > 0$, $n > k + 1$ lead to QD even if $k > 1$, using (70). Their advantage when

compared with (93)-(94) and (99) is based on the instability of their outer-diagonal entries, when tracing out E-qubits from $\hat{\rho}_{SE}^{\text{out}}$ (s. appendix B). Thus, we could also combine (59) and (70) with (105) by allowing in (107) within the $|0\rangle\langle 1|$ -S-subspace more than one entry on the secondary diagonal to be non-zero as long as we simultaneously ensure that the one qubit S-subspaces (for $k = 1$ containing $|0\rangle\langle 0|$, $|1\rangle\langle 1|$, B_0) remain mutually disjoint and connection independent when extending (107) to the ($k > 1$, $n > 1$)-case, which would adhere to (15) $\forall [k \geq 1] \leq L \leq n$. However, it is not possible to extend (107) and (108)-(109) by increasing the number of outer-diagonal entries aligned along the secondary diagonal of B_0 , since that would violate (15) for $k = 1$ S or even induce non-physical $\hat{\rho}_{SE}^{\text{out}}$ for $k > 1$ S. (107) also cannot be extended by means of (93)-(94) or (99), since combining all these matrix-structures would force us to implement conditions on outer-diagonal entries in B_0 appearing w.r.t. (117) and (126)-(127) that mutually collide with conditions in (94) (non-physical $\hat{\rho}_{SE}^{\text{out}}$), as in (132), (323)-(327), (329) and (339)-(341): (107), (108)-(109) ($n \geq L > 0$, $n > k + 1$) cannot be extended by adding arbitrary outer-diagonal entries to B_0 .

4) (76), (104), (111) and (116)-(115): We know from appendix C w.r.t. the case $k = n = L = 1$ that these structures are, apart from (70), the only allowed possibilities to combine outer-diagonal entries within A_0 , A_1 and B_0 of $\hat{\rho}_{SE}^{\text{out}}$ ($k = n = L = 1$) that adhere to (94) and still lead to physical $\hat{\rho}_{SE}^{\text{out}}$ which satisfy (15) $\forall (k \leq L \leq n)$ by involving $\{|s_1^L\rangle, |s_2^L\rangle\}$, with $k = 1$ for (76), (104) and (114)-(115) and $k > 1$ for (111) and (116). Since introducing arbitrary outer-diagonal entries into (76), (104), (111) and (116)-(115) disturbs the symmetry of $\{|s_1^L\rangle, |s_2^L\rangle\}$, as in (132), it follows: (76), (104), (111) and (116)-(115) cannot be extended by adding arbitrary non-zero outer-diagonal entries to B_0 . This strongly supports the conjecture in Table 2, regardless of a specific (7) that leads to $\hat{\rho}_{SE}^{\text{out}}(L)$.

4.4 Quantum Darwinistic density matrix structures for many-qubit open systems

Taking all results from subsections 4.2.1-4.3 into account, we see that it is possible to generalize QD-conformal matrix structures of $\hat{\rho}_{SE}^{\text{out}}$ from Tab. 2 to $k > 1$ qubit S only by embedding them into mutually disjoint one-qubit subspaces of S. This is done by means of a third ancilla subsystem A (s. also subsection 4.2.3) according to the following prescriptions:

- Generalization of (93)-(94), which, purified by system A, has the form

$$|\chi_1^{\text{out}}\rangle_{SEA} = \sum_{m=1}^2 \frac{a_m}{\sqrt{N_E}} |m\rangle_S \otimes \left(\sum_{i=1}^{N_E/2} |i\rangle_E \otimes |i\rangle_A + (-1)^{m+1} \sum_{j=N_E/2+1}^{N_E} |j\rangle_E \otimes |j\rangle_A \right), \quad (143)$$

with $N_E = \dim(E) = 2^n$, ${}_A \langle i|i'\rangle_A = \delta_{i,i'}$ and ${}_A \langle j|j'\rangle_A = \delta_{j,j'}$. Its generalization to $k > 1$ qubit S can be expressed as

$$\begin{aligned} |\chi_2^{\text{out}}\rangle_{SEA} &= \sum_{m=1}^{N_S} (1 - \delta_{m \bmod 2, 0}) \cdot (N_E/N_S)^{-1/2} \cdot \\ &\left\{ a_m |m\rangle_S \otimes \left(\sum_{i_m=1+}^{(m-1/2)N_E/N_S} |i_m\rangle_E \otimes |i_m\rangle_A + \sum_{j_m=(m-1/2)N_E/N_S+1}^{m \cdot N_E/N_S} |j_m\rangle_E \otimes |j_m\rangle_A \right) \right. \\ &\left. + a_{m+1} |m+1\rangle_S \otimes \left(\sum_{i_m=1+}^{(m-1/2)N_E/N_S} |i_m\rangle_E \otimes |i_m\rangle_A - \sum_{j_m=(m-1/2)N_E/N_S+1}^{m \cdot N_E/N_S} |j_m\rangle_E \otimes |j_m\rangle_A \right) \right\}, \quad (144) \end{aligned}$$

with $N_S = \dim(S) = 2^k$, ${}_A \langle i|i'\rangle_A = \delta_{i,i'}$ and ${}_A \langle j|j'\rangle_A = \delta_{j,j'}$. (144) leads to $H(S) = H(S_{\text{class}})$ and $H(S, E_L) = H(E_L) \forall (k \leq L \leq n)$.

- Generalization of (107) and (108)-(109), purified by system A, has the form

$$|\chi_3^{\text{out}}\rangle_{SEA} \langle \chi_3^{\text{out}}| = |\chi'\rangle \langle \chi'| + |\chi''\rangle \langle \chi''|, \quad (145)$$

where

$$|\chi'\rangle = \sum_{\hat{m}=1}^{N_S} a_{\hat{m}} |\hat{m}\rangle_S \otimes \sum_{i_{\hat{m}}=1+(\hat{m}-1)N_E/N_S}^{\hat{m} \cdot N_E/N_S} \beta_{i_{\hat{m}}} |i_{\hat{m}}\rangle_E \otimes |i_{\hat{m}}\rangle_A, \quad (146)$$

with ${}_A \langle i_{\hat{m}} | i'_{\hat{m}'} \rangle_A = \delta_{\hat{m}, \hat{m}'} \delta_{i_{\hat{m}}, i'_{\hat{m}'}}$, $\hat{m}' = N_S - \hat{m} + 1$, $i'_{\hat{m}'} = N_E - i_{\hat{m}} + 1$, and

$$\begin{aligned} |\chi''\rangle &= \sum_{m=1}^{N_S/2} a_m |m\rangle_S \otimes \beta_{i_m} |i_m\rangle_E \otimes |i_m\rangle_A \\ &+ \sum_{\tilde{m}=N_S/2+1}^{N_S} a_{\tilde{m}} |\tilde{m}\rangle_S \otimes \beta_{i_{\tilde{m}}} |i_{\tilde{m}}\rangle_E \otimes |i_{\tilde{m}}\rangle_A, \end{aligned} \quad (147)$$

with

$$\begin{aligned} {}_A \langle i_m | i'_{m'} \rangle_A &= (1 - \delta_{m, m'}) \cdot \delta_{i_m, 1+(m-1)N_E/N_S} \delta_{i'_{m'}, 1+(m'-1)N_E/N_S} \\ {}_A \langle i_{\tilde{m}} | i'_{\tilde{m}'} \rangle_A &= (1 - \delta_{\tilde{m}, \tilde{m}'} \cdot \delta_{i_{\tilde{m}}, \tilde{m} \cdot N_E/N_S} \delta_{i'_{\tilde{m}'}, \tilde{m}' \cdot N_E/N_S} \\ {}_A \langle i_m | i_{\tilde{m}} \rangle_A &= (1 - \delta_{\tilde{m}, N_S+1-m}) \cdot \delta_{i_m, 1+(m-1)N_E/N_S} \delta_{i_{\tilde{m}}, \tilde{m} \cdot N_E/N_S}. \end{aligned}$$

- Generalization of (127) has the form

$$\begin{aligned} |\chi_4^{\text{out}}\rangle_{SE} \langle \chi_4^{\text{out}}| &= \sum_{m=1}^{N_S} (1 - \delta_{m \bmod 2, 0}) \cdot \left\{ |\Psi_m\rangle_{SE} \langle \Psi_m| - |a_{m+1}|^2 |m+1\rangle_S \langle m+1| \otimes |\Gamma_m\rangle_E \langle \Gamma_m| \right. \\ &\quad \left. + 2^{-(n-k)} |a_{m+1}|^2 |m+1\rangle_S \langle m+1| \otimes \hat{I}_{n-k} \otimes |m\rangle_{\varepsilon_2} \langle m| \right\}. \end{aligned} \quad (148)$$

where $|s_1^L\rangle = \left(\frac{1}{\sqrt{2}}\right)^L (|0\rangle + |1\rangle)^{\otimes L}$, $|s_2^L\rangle = \left(\frac{1}{\sqrt{2}}\right)^L (|0\rangle - |1\rangle)^{\otimes L}$ and $\langle s_1^L | s_2^L \rangle = 0$ as in (302) above, $E = \varepsilon_1 \otimes \varepsilon_2$,

$$\begin{aligned} |\Psi_m\rangle_{SE} &= a_m |m\rangle_S \otimes |1 + (m-1)2^{n-k}\rangle_E + a_{m+1} |m+1\rangle_S \otimes |\Gamma_m\rangle_E \\ |\Gamma_m\rangle_E &= 2^{-(n-k)/2} \left(|s_1\rangle_{\varepsilon_1}^{\otimes n-k} + (-1)^{M+l_{\text{alt}}} |s_2\rangle_{\varepsilon_1}^{\otimes n-k} \right) \otimes |m\rangle_{\varepsilon_2}, \end{aligned}$$

$M \equiv$ number of $|1\rangle$ -one qubit states of the ε_1 -part in $|1 + (m-1)2^{n-k}\rangle_E$ and $l_{\text{alt}} \in \{0, 1\}$ denotes the signature of $|s_2\rangle_{\varepsilon_1}^{\otimes n-k}$.

5 Summary

Taking the discussion of the previous sections into account, we see that QD appears only if the following conditions apply (regardless of the concrete type of the S-E-interaction $\hat{U}_{\text{int}}^{SE}$ in (7) that leads to $\hat{\rho}_{SE}^{\text{out}}(L)$):

Condition 1: $H(S) \approx H(S_{\text{class}})$, i.e. the k -qubit system S may be regarded as effectively decohered with a pointer basis $\{|\pi_i\rangle\}$.

Condition 2: Registry states of the environment E in (13) are assumed to have a tensor product structure (mutually non-overlapping »storage cells«).

Condition 3: $H(E_L) \geq H(S, E_L) \forall (k \leq L \leq n)$, regardless of the order in which single E -qubits are consecutively traced out.

These three conditions are necessary and sufficient to ensure the validity of the double implication

$$\text{QD} \Leftrightarrow |\chi^{\text{out}}\rangle_{SEA} \quad (149)$$

with the state structure $|\chi_{SEA}^{\text{out}}\rangle$ given by

$$|\chi^{\text{out}}\rangle_{SEA} = \sum_{m=1}^{N_S} a_m |m\rangle_S \otimes \sum_{\substack{i_m = 1+ \\ (m-1)N_E/N_S}}^{m \cdot N_E/N_S} \beta_{i_m} |i_m\rangle_E \otimes |i_m\rangle_A, \quad (150)$$

with $a_m > 0$, $\beta_{i_m} \geq 0$, $\sum_m |a_m|^2 \stackrel{!}{=} 1$, $N_S = \dim(S) = 2^{l \cdot k}$, $N_E = \dim(E) = 2^{l \cdot n}$ (where $l \geq 1$ denotes the number of levels in each constituent-cell of S and E , i.e. $l = 1$ corresponds to qubits), ${}_S \langle m | m' \rangle_S = \delta_{m, m'}$, ${}_E \langle i_m | i'_{m'} \rangle_E = \delta_{m, m'} \delta_{i_m, i'_{m'}}$, and ${}_A \langle i_m | i'_{m'} \rangle_A = \delta_{m, m'} \delta_{i_m, i'_{m'}}$ (ancilla states). If one can show that a given output state $\hat{\rho}_{SE}^{\text{out}}$ is similar to (150) w.r.t. a certain separable basis (s. also Appendix A), then QD (including the above three conditions) appears.

Furthermore, we have come to the following conclusions:

- From the physical and operational point of view, QD indicates highest storage efficiency (minimal f_{opt}) of $H(S) \approx H(S_{\text{class}})$ into environment E (s. also discussion in subsection 4.1 above). However, from mathematical perspective QD is a set of conditions which allow one to establish a one-to-one correspondence between cardinalities of two eigenvalue sets and their corresponding entropies in accord with (149), (150) and

$$|\sigma(\hat{\rho}_{E_L}^{\text{out}})| \left\{ \begin{array}{l} = \\ > \\ < \end{array} \right\} |\sigma(\hat{\rho}_{S E_L}^{\text{out}})| \Leftrightarrow H(E_L) \left\{ \begin{array}{l} = \\ > \\ < \end{array} \right\} H(S, E_L). \quad (151)$$

- $H(E_L) > H(S, E_L)$ emerges from (150) w.r.t. the standard (separable) computational basis only after introducing coherences between E-registry states within different diagonal pointer-state subspaces of S. We conjectured that the only matrix structures of $\hat{\rho}_{S E}^{\text{out}}$ in the standard computational basis which allow one to reduce $H(S, E_L)$ (and thus validate (15)) by introducing into $\hat{\rho}_{S E}^{\text{out}}$ of (150) correlations between different $k \geq 1$ qubit S-pointer states are listed in Table 2 (subsection 4.3) and (143)-(148) of subsection 4.4.
- Between a qubit-system S (described by the standard computational pointer basis $\{|\pi_i\rangle\}$) and its qubit E the simplest entanglement-inducing two-qubit transformation which allows QD to appear, thus enabling us to copy the classical amount of S-information into E-fragments optimally, is the well-known CNOT-transformation (9)-(11), as a special member of a one-parameter ϕ -valued family of transformations (with $\phi = \pi/2$). All other members of this one-parameter family of transformations $\hat{U}_{ij}^{(\phi)}$ with $\phi \neq \pi/2$ do not lead to QD in this context («imperfect copy machines»), since the density matrices of S and E are described by eigenstates of $\hat{U}_{ij}^{(\phi=\pi/2)}$. However, if S should be described by another pointer basis $\{|\pi'_i\rangle\} \neq \{|\pi_i\rangle\}$, then we could always transform the QD-conform matrix structures obtained from assumptions 1-4 above w.r.t. $\{|\pi'_i\rangle\}$ as indicated in appendix A, thus concluding that this time w.r.t. $\{|\pi'_i\rangle\}$ $\hat{U}_{ij}^{(\phi)}$ from (9)-(10), with another parameter value $0 < (\phi \neq \pi/2) < \pi$, would represent a «perfect copy machine» in the sense of QD.
- Entanglement monogamy structure (separable, classically coherent states) $\hat{\rho}_{S, \mathcal{F}_j}^{\text{out}} = \sum_i p_i \hat{\rho}_{S,i}^{\text{out}} \otimes \hat{\rho}_{\mathcal{F}_j,i}^{\text{out}}$ [14] of the overall qubit S-E-output system $\hat{\rho}_{S, \mathcal{F}_j}^{\text{out}}$ (with \mathcal{F}_j denoting fragments of E, s. for instance (5) above) leads to QD and is sufficient for its appearance. However, it is not necessary for the appearance of QD, since also the qubit S-E-output states $\hat{\rho}_{S, \mathcal{F}_j}^{\text{out}} \approx \sum_i p_i \hat{\rho}_{S,i}^{\text{out}} \otimes \hat{\rho}_{\mathcal{F}_j,i}^{\text{out}}$ whose matrix structure converges towards the one corresponding to classically coherent (separated) states (19) in the limit of large environments E with many $n \gg 1$ constituents (qubits), as explicated in subsection 4.2. Thus, $\lim_{n \gg 1} (\hat{\rho}_{S, \mathcal{F}_j}^{\text{out}}) = \sum_i p_i \hat{\rho}_{S,i}^{\text{out}} \otimes \hat{\rho}_{\mathcal{F}_j,i}^{\text{out}}$ also generates the QD-plateau in the corresponding PIPs, in agreement with general theorems of [14] valid for arbitrary (and not only for qubit) open systems.
- Advanced qubit models of QD can lead to the appearance of QD only under a weaker condition in the limit of effective decoherence, for which $\lim_{n \gg 1} (\hat{\rho}_{S, \mathcal{F}_j}^{\text{out}}) = \sum_i p_i \hat{\rho}_{S,i}^{\text{out}} \otimes \hat{\rho}_{\mathcal{F}_j,i}^{\text{out}}$, whereas matrix structures $\hat{\rho}_{S, \mathcal{F}_j}^{\text{out}}$ corresponding exactly to classically coherent states (19) emerge only in the course of idealized qubit models of QD, such as Zurek's qubit model of QD discussed in subsection 3.2.

Part II

Random Unitary Evolution and Quantum Darwinism

Abstract

We study the behavior of Quantum Darwinism (Zurek, [5]) within the iterative, random unitary operations qubit-model of pure decoherence (Novotný *et al*, [29]). We conclude that Quantum Darwinism, which describes the quantum mechanical evolution of an open system from the point of view of its environment, is not a generic phenomenon, but depends on the specific form of input states and on the type of system-environment interactions. Furthermore, we show that within the random unitary model the concept of Quantum Darwinism enables one to explicitly construct and specify artificial input states of environment that allow to store information about an open system of interest and its pointer-basis with maximal efficiency.

Furthermore, we investigate the behavior of Quantum Darwinism after introducing dissipation into the iterative random unitary qubit model with pure decoherence in accord with V. Scarani *et al* [26] and reconstruct the corresponding dissipative attractor space. We conclude that in Zurek's qubit model Quantum Darwinism depends on the order in which pure decoherence and dissipation act upon an input state of the entire system. We show explicitly that introducing dissipation into the random unitary evolution model in general suppresses Quantum Darwinism (regardless of the order in which decoherence and dissipation are applied) for all positive non-zero values of the dissipation strength parameter, even for those input state configurations which, in Zurek's qubit model and in the random unitary model with pure decoherence, would lead to Quantum Darwinism.

Finally, we discuss what happens with Quantum Darwinism after introducing into the iterative random unitary qubit model with pure decoherence (asymmetric) dissipation and dephasing, again in accord with [26], and reconstruct the corresponding dissipative-dephased attractor space. We conclude that dephasing does not influence the dynamics of quantum systems in Zurek's qubit model of Quantum Darwinism. Similarly, we see that also within the random unitary evolution dephasing does not alter or influence the (dis-)appearance of Quantum Darwinism: i.e. the random unitary evolution of a quantum state governed by the unitary transformation enclosing pure decoherence (CNOT transformation), dissipation and dephasing is in the asymptotic limit of many iterations solely determined by the interplay between pure decoherence and dissipation, whereas the dephasing part of the random unitary evolution does not contribute to the corresponding attractor space of the asymptotic random unitary iteration.

6 Introduction

From everyday-experience, classical states »pre-exist« objectively and as such constitute »classical reality« in a sense that the state of an open system S can be measured and agreed upon by many independent, mutually non-interacting observers, without being disturbed. This is done by intercepting fragments (\equiv observers) of the environment E (indirect or non-demolition measurement [2, 7]). Thus, one may ask: which sort of information about system S is redundantly and robustly memorized by numerous distinct E -fragments, such that multiple observers may retrieve this same information in a non-demolishing fashion, thereby confirming the effective classicality of the S -state?

Zurek's concept of Quantum Darwinism tries to answer the above question by investigating what kind of information about system S the environment E can store and proliferate in a stable, complete and redundant way. It turns out that this redundantly stored information proliferated throughout environment E is the Shannon-entropy of the decohered system S , that contains information about S -pointer states [14, 5].

These pointer-states, also known as interaction-robust S -states, are those S -states most immune (invariant) towards numerous interactions with the environment E . They are singled out by a characteristic dynamical phenomenon, an interaction-induced decoherence, which explains the process of destruction of quantum superpositions between states of an open quantum system S as a consequence of its interaction with an environment E . Most decoherence-based explanations of the emergence of classical S -states from quantum mechanical dynamics deal solely with observations which can be made at the level of system S , degrading its environment E to the role of a »sink« that carries away unimportant information about the preferred pointer-basis of the observed system S [2].

However, whereas the decoherence paradigm usually distinguishes between an open system S and its environment E , without specifying the structure of the latter, Quantum Darwinism subdivides the environment E into *non-overlapping subenvironments* (fragments or »storage cells«) accessible to measurements, that have already interacted with system S in the past and thus enclose Shannon-information (entropy) about its preferred (pointer) states (i.e. E -registry states are assumed to have a *tensor product* structure). In other words, Quantum Darwinism changes the perspective and regards the environment E as a large resource (»quantum memory«) which could be used for indirect acquisition and storage of relevant information about system S and its pointer-basis (i.e. E becomes a »witness« to the observed S -state) [5].

Accordingly, one can quantify the »degree of objectivity« of S -states by simply counting the number of copies of their information record in environment E . This number of copies of the information deposited by a particular S -state into environmental fragments after many S - E -interactions reveals its redundancy R . The higher the R of a particular S -state, the more »classical« it appears.

Similar to the Darwinistic concept »survival of the fittest«, the S -pointer states represent the »fittest« (»quasi-classical«) states of an open system S that survive numerous S - E -interactions (measurements) long enough to deposit (imprint) multiple copies of their information into environment E [8]. Ergo: high information redundancy of S -states within environment E implies that information about the »fittest« observable (pointer state) of system S that survived constant monitoring by the environment E has been successfully distributed throughout all E -fragments, enabling the environment to store redundant copies of information about preferred S -observables and thus account for their objective existence (»ein-selection« [3, 10]).

In the following we intend to compare two qubit models of Quantum Darwinism: Zurek's C(ontrolled-)NOT-evolution model [5] and the random unitary operations model [11, 29, 30] of an open k -qubit system S interacting with an n -qubit environment E . According to Zurek's model the one qubit ($k = 1$) open system S acts via two-qubit CNOT-transformations as a control unit upon each of the n mutually non-interacting E -qubits (targets) *only once*. On the other hand, the random unitary evolution generalizes Zurek's interaction procedure by iterating the directed graph (digraph) of CNOT-interactions between a $k \geq 1$ qubit system S and mutually non-interacting E -qubits, represented by the corresponding quantum operation channel, $N \gg 1$ times until the underlying dynamics forces the input state $\hat{\rho}_{SE}^{\text{in}}$ of the entire system to converge to the output state $\hat{\rho}_{SE}^{\text{out}}$. Such asymptotically evolved $\hat{\rho}_{SE}^{\text{out}}$ can then be described by a subset of the total Hilbert-space $\mathcal{H}_{SE} = \mathcal{H}_S \otimes \mathcal{H}_E$, the so-called *attractor space*, and attractor states therein.

From the practical point of view, we want to answer four questions. 1) Which $\hat{\rho}_{SE}^{\text{in}}$ lead to Quantum Darwinism? 2) Does Quantum Darwinism, and thus a perfect transfer of Shannon-entropy into environment E , depend on a specific model being used, or is it a model-independent phenomenon? Namely, since the random unitary evolution can model systems S subject to pure decoherence by singling out the corresponding pointer states as a result of the asymptotic iterative dynamics, it also enables one to specify (in comparison with Zurek's model) which types of input states $\hat{\rho}_{SE}^{\text{in}}$ store the »classical« Shannon-information about system S and its pointer-basis efficiently into environment E and what happens with Quantum Darwinism if we use (in both models) non-CNOT members $\hat{u}^{(\phi \neq \pi/2)}$ of the one-parameter (ϕ -parameter) family $\hat{u}^{(\phi)}$ of unitary qubit-qubit transformations, with $\hat{u}^{(\phi = \pi/2)}$ corresponding to the CNOT-transformation. Finally,

we also want to use the random unitary model to see whether Quantum Darwinism appears if we introduce into the corresponding interaction digraph $\hat{u}^{(\phi)}$ -interactions between E-qubits. 3) Is Quantum Darwinism, and thus a perfect transfer of system's Shannon-information into environment E, possible if we introduce into both qubit models dissipation by means of the two-qubit unitary dissipative transformation $\hat{u}(\alpha)$ with a real-valued dissipation strength α in accord with [26]? Since the random unitary evolution can model systems S subject to pure decoherence by singling out the corresponding pointer states as a result of the asymptotic iterative dynamics, it also enables one to specify (in comparison with Zurek's model) which types of input states $\hat{\rho}_{SE}^{\text{in}}$ (if any) could store the "classical" Shannon-information about an open system S and its pointer-basis efficiently into environment E despite of dissipation. Unfortunately, the results of the forthcoming discussion will reveal that Quantum Darwinism remains suppressed as soon as the real-valued dissipation strength parameter α is non-zero, indicating that dissipation in general, in Zurek's as well as in the random unitary evolution model, causes partial leakage of system's Shannon-information into the fraction of a larger environment E' (with $E \subset E'$) that is a priori traced out when considering the environment E of interest. 4) Are there input density matrix structures $\hat{\rho}_{SE}^{\text{in}}$ that would allow to store $H(S_{\text{class}})$ into E efficiently (and thus let QD emerge) if we introduce dissipation and dephasing into the corresponding asymptotic random unitary dynamics of $\hat{\rho}_{SE}^{\text{out}}$? In this context we easily conclude, by extending Zurek's dissipative model with an additional, unitary two-qubit dephasing operator $\hat{u}(\gamma)$ from [26] (with a real-valued dephasing rate γ), that dephasing does not influence the results of this qubit model obtained w.r.t. the pure decoherence or the dissipative dynamics. Similarly, after introducing the dissipative-dephasing unitary two-qubit operator from [26] into the iterative random unitary dynamics of $\hat{\rho}_{SE}^{\text{out}}$, we see that also within the random unitary evolution model dephasing does not alter or influence the (dis-)appearance of Quantum Darwinism: in other words, the random unitary evolution of a quantum state governed by the unitary Kraus-transformation $\hat{U}(\phi = \pi/2, \alpha_1, \alpha_2, \gamma)$, enclosing pure decoherence (CNOT transformation, parameter $\phi = \pi/2$), dissipation (parameter α_1 and α_2) and dephasing (parameter γ), is in the asymptotic limit of many iterations solely determined by the interplay between pure decoherence and dissipation, whereas the dephasing part of the unitary Kraus-transformation $\hat{U}(\phi = \pi/2, \alpha_1, \alpha_2, \gamma)$ does not contribute to the corresponding attractor space of the asymptotic random unitary iteration.

This second part of the book is organized as follows: Section 7 deals with basic physical and mathematical concepts of Quantum Darwinism (mutual information, CNOT-transformation, partial information plots, S-pointer states) and discusses this phenomenon within the framework of Zurek's qubit CNOT-evolution toy model [5]. We thereby see that for an open pure k-qubit S-input state $\hat{\rho}_S^{\text{in}}$ the CNOT-transformation leads to Quantum Darwinism only if one starts with $\hat{\rho}_{SE}^{\text{in}} = \hat{\rho}_S^{\text{in}} \otimes \hat{\rho}_E^{\text{in}}$ and $\hat{\rho}_E^{\text{in}}$ prepared as a pure n-qubit E-registry state of rank one. In section 8 we first introduce the mathematical formalism of iterated random unitary evolution [11, 29, 30]. In subsections 8.1 and 8.4 we show that introducing CNOT-interactions between E-qubits suppresses the appearance of Quantum Darwinism. In subsection 8.2 we present numerical results of the iterated random unitary evolution, concluding that Zurek's qubit model of Quantum Darwinism cannot be interpreted as a short-time limit (\equiv small number N of iterations) of the random unitary evolution model.

Then we turn our attention in subsection 8.3 to the asymptotic ($N \gg 1$) behavior of mutual information within the random unitary qubit model. This asymptotic behavior of mutual information of iterated, random unitarily evolved output states $\hat{\rho}_{SE}^{\text{out}}$ allows us to conclude that Quantum Darwinism and its appearance depends in general on an underlying model used to describe interactions between S- and E-qubits. Finally, we summarize the most important results of our discussion before giving a brief outlook on interesting future research problems connected with Quantum Darwinism (subsection 8.5).

In section 9 we introduce the dissipative unitary two-qubit operator $\hat{u}(\alpha)$ from [26] into the iterative random unitary dynamics of $\hat{\rho}_{SE}^{\text{out}}$. Then, in subsection 9.1 we first compare results regarding Quantum Darwinism obtainable from Zurek's qubit model (with and without dissipation) with predictions of the dissipative random unitary model for $\alpha = 0$ and $\alpha > 0$ in the asymptotic limit of $N \gg 1$ iterations. Finally, in the main part of section 9 (subsections 9.2-9.3) we reconstruct the dissipative attractor space of the random unitary model of Quantum Darwinism both numerically and analytically, before summarizing the most important conclusions and giving a short outlook on interesting future research problems in subsection 9.4.

In section 10 we introduce the dissipative-dephasing unitary two-qubit operator from [26] into the iterative random unitary dynamics of $\hat{\rho}_{SE}^{\text{out}}$. In subsection 10.1 we compare Zurek's qubit model of QD involving pure decoherence as discussed in section 7 with predictions of the dissipative-dephased random unitary model for dissipation strength $\alpha_1 = \alpha_2 = \alpha = 0$, dephasing rate $\gamma = 0$ and $N \gg 1$ iterations. Finally, in the main part of the section (subsections 10.2 and 10.3) we reconstruct the dissipative and dephased attractor space of our the random unitary model of QD both numerically and analytically, before summarizing the most important conclusions in subsection 10.4.

Section 11 closes this book by offering a brief summary of most important result obtained throughout the entire discussion of QD and its mathematical as well as physical properties, before giving some hints on possible future research topics. All detailed analytic calculations are given in 9 appendices: Appendix D displays output states $\hat{\rho}_{SE}^{\text{out}}$ of Zurek's

CNOT-evolution used and discussed in section 7. Appendix E explains why only the CNOT-transformation leads to Quantum Darwinism, both in Zurek's and the random unitary evolution model. In Appendix F and Appendix G we briefly introduce the Gram-Schmidt orthogonalization and the QR-decomposition, respectively, both methods being of extensive use in Appendix H when determining the structure of relevant attractor subspaces. In Appendix H we derive (dimensionally) maximal, minimal and intermediate attractor subspaces that are used in the course of interpretation of random unitarily evolved $\hat{\rho}_{SE}^{\text{out}}$ in section 8. As a consequence of Appendix H we demonstrate in Appendix I how the Gram-Schmidt orthogonalization algorithm can be applied to linear independent states of the minimal attractor space. Appendix J contains a list of $\hat{\rho}_{SE}^{\text{out}}$ obtained by means of (dimensionally) maximal and minimal attractor spaces that are necessary for the discussion of the random unitary evolution in section 8. Appendix K derives the general unitary transformation involving pure decoherence (CNOT-transformation), dissipation and dephasing that is necessary for the discussion of the random unitary evolution in section 10. Finally, Appendix L presents some analytic calculations of S-E-output states $\hat{\rho}_{SE}^{\text{out}}$ necessary for discussing QD within the framework of Zurek's dephased-dissipative qubit model.

7 A qubit toy-model of Quantum Darwinism

In this section we again briefly describe the simplest qubit model of Quantum Darwinism, as suggested by Zurek [5], involving an open pure $k = 1$ -qubit S (with $|\Psi_S^{\text{in}}\rangle = a|0\rangle + b|1\rangle$, $(a, b) \in \mathbb{C}$ and $|a|^2 + |b|^2 \stackrel{!}{=} 1$), which acts as a control-unit on its ($n \in \mathbb{N}$)-qubit target (environment) $E \equiv \mathcal{E}_1 \otimes \mathcal{E}_2 \otimes \dots \otimes \mathcal{E}_n$. Subsequently, we apply Zurek's qubit evolution model to different input states $\hat{\rho}_{SE}^{\text{in}}$ of the total system and investigate whether Quantum Darwinism appears within this model with respect to different members of a one-parameter family of unitary transformations that also encloses, as a special case, the unitary Controlled-NOT (CNOT) operation.

According to Zurek's qubit model the interaction between system S and environment E has to occur as follows (s. also subsection 2):

1. Start with a pure $k = 1$ -qubit open $\hat{\rho}_S^{\text{in}} = |\Psi_S^{\text{in}}\rangle \langle \Psi_S^{\text{in}}|$ and an arbitrary n -qubit $\hat{\rho}_E^{\text{in}}$, where $\hat{\rho}_{SE}^{\text{in}} = \hat{\rho}_S^{\text{in}} \otimes \hat{\rho}_E^{\text{in}}$.
2. Apply the CNOT-gate $\hat{U}_{\text{CNOT}} |i\rangle_S |j\rangle_E = |i\rangle_S |i \oplus j\rangle_E$ (where \oplus denotes addition modulo 2), such that the S -qubit i interacts successively and only once with each qubit j of E until all n E -qubits have interacted with S , resulting in an entangled state $\hat{\rho}_{SE}^{\text{out}}$.
3. Trace out successively (for example from *right to left*) $(n - L)$ qubits in $\hat{\rho}_E^{\text{out}}$ and $\hat{\rho}_{SE}^{\text{out}}$ - this yields the L -qubit $\hat{\rho}_{EL}^{\text{out}}$ and $\hat{\rho}_{SE_L}^{\text{out}}$, with $0 < L \leq n$, and $0 < f = \frac{L}{n} \leq 1$.
4. Compute the eigenvalue spectra $\{\lambda_1, \dots, \lambda_{d(f)}\}$ of $\hat{\rho}_S^{\text{out}}$, $\hat{\rho}_{E_f}^{\text{out}}$ and $\hat{\rho}_{SE_f}^{\text{out}}$ and the f -dependent von Neumann entropies $H(\hat{\rho}(f)) = -\sum_{i=1}^{d(f)} \lambda_i \log_2 \lambda_i \geq 0$, $\sum_{i=1}^{d(f)} \lambda_i \stackrel{!}{=} 1$ (where $d(f)$ is the dimensionality of $\hat{\rho}(f)$ in question).
5. Divide all entropies by $H(S_{\text{class}})$ to obtain the ratio $I(S : E_f) / H(S_{\text{class}})$, with **mutual information** (MI)

$$I(S : E_f) = H(S) + H(E_f) - H(S, E_f), \quad (152)$$

that quantifies the amount of the proliferated Shannon entropy («classical information») [8, 13]

$$H(S_{\text{class}}) = -\sum_i p_i \log_2 p_i = H(\{|\pi_i\rangle\}), \quad (153)$$

where probabilities $p_i = \text{Tr}_E \langle \pi_i | \hat{\rho}_{SE}^{\text{class}} | \pi_i \rangle$ emerge as partial traces of an effectively decohered («quasi-classical») S -state $\hat{\rho}_S^{\text{class}}$ w.r.t. the particular S -pointer-basis $\{|\pi_i\rangle\}$, and the redundancy

$$R = 1/f^* \quad (0 < f^* \leq 1) \text{ with } I(S : E_{f=f^*}) \approx H(S_{\text{class}}) \quad (n \gg 1) \quad (154)$$

of the measured $\{|\pi_i\rangle\}$ in the limit $n \gg 1$ of effective decoherence.

6. Finally, plot $I(S : E_f) / H(S_{\text{class}})$ vs $0 < f \leq 1$ (**Partial Information Plot (PIP)** of MI).

Now, we know from subsection 2 that the input state $\hat{\rho}_{SE}^{\text{in}} = |\Psi_S^{\text{in}}\rangle \langle \Psi_S^{\text{in}}| \otimes |0_n\rangle \langle 0_n|$ (with $|0_n\rangle \equiv |0\rangle^{\otimes n}$) leads to the PIP-plateau' in Fig. 1, indicating that only if we need a small fraction of the environment E enclosing maximally $n \cdot f^* = k \ll n$ E -qubits [5], to reconstruct the S -pointer basis $\{|\pi_i\rangle\}$, Quantum Darwinism appears: i.e., it is not only important that the

PIP-'plateau' appears, more relevant is its length $1/f^* \equiv R$ of $\{|\pi_i\rangle\}$. Therefore, we restate the main question we aim to address w.r.t. Zurek's and the random unitary operations model:

Which types of input states $\hat{\rho}_{SE}^{in}$ validate the relation

$$\frac{I(S : E_f)}{H(S_{class})} = \frac{H(S) + H(E_f) - H(S, E_f)}{H(S_{class})} \geq 1, \quad (155)$$

with $H(S) \approx H(S_{class})$ and $H(E_f) \geq H(S, E_f)$ at least $\forall (k \leq L \leq n \gg 1)$, regardless of the order in which the n E -qubits are being successively traced out from the output state $\hat{\rho}_{SE}^{out}$?

7.1 Different system-environment input states

In order to answer this question we discuss in the following the f -dependence of MI for different $\hat{\rho}_{SE}^{in}$ from the point of view of Zurek's qubit model. Fig. 5 below displays the behavior of the MI vs f for different $\hat{\rho}_E^{in}$ from Tab. 8 in D which justifies the following conclusions:

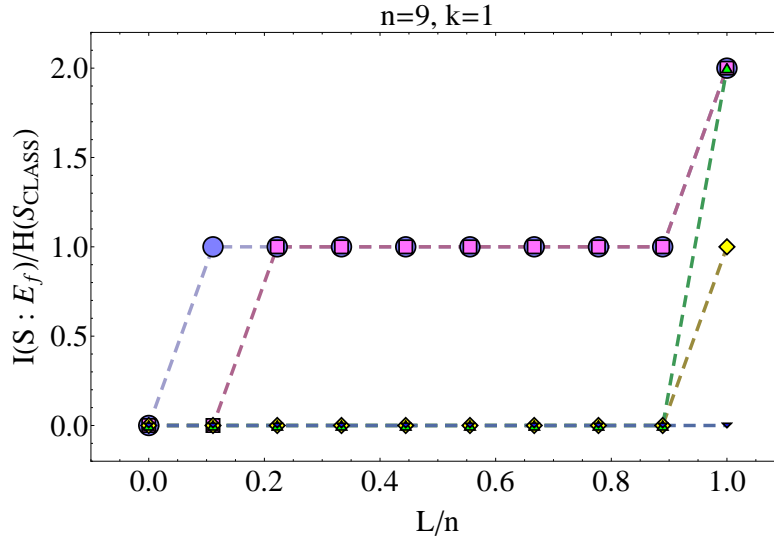


Figure 5: PIP for $\hat{\rho}_{SE}^{out}$ from $\hat{\rho}_{SE}^{in} = |\Psi_S^{in}\rangle \langle \Psi_S^{in}| \otimes \hat{\rho}_E^{in}$ (where $k = 1$, $n = 9$, $|\Psi_S^{in}\rangle = a|0\rangle + b|1\rangle$) and different $\hat{\rho}_E^{in}$ (s. also Tab. 8 in Appendix D) in Zurek's qubit model.

It is in general important in which order one traces out E -qubits from the output-state $\hat{\rho}_{SE}^{out}$, as indicated by the \bullet -dotted curve (Quantum Darwinism appears) and the \blacksquare -dotted curve (no Quantum Darwinism, since $H(E_L) = H(S, E_L)$ holds only $\forall (k < L \leq n)$, but not for $L = k$): when tracing out E -qubits as in (12) from right to left Quantum Darwinism appears only if, for each fixed value of $(k \leq L < n)$, $\hat{\rho}_{SE_L}^{out}$ acquires the structure displayed in (12), that emerges when starting the CNOT-evolution with a pure, n -qubit registry state $\hat{\rho}_E^{in} = |0_n\rangle \langle 0_n|$. Introducing classical correlations into $\hat{\rho}_{SE}^{in} = \hat{\rho}_S^{in} \otimes \hat{\rho}_E^{in}$ (with a one-qubit pure $\hat{\rho}_S^{in}$) by writing $\hat{\rho}_E^{in}$ as a convex sum of pure n -qubit registry states $\{|y\rangle \langle y|, y \in \{0, \dots, 2^n - 1\}\}$ in the standard computational basis tends in general to suppress the appearance of the MI-plateau: in case of a totally mixed $\hat{\rho}_E^{in}$ the MI is even zero $\forall (0 < L < n)$, as indicated by the \blacklozenge -dotted and \blacktriangle -dotted curves in Fig. 5. Quantum correlations within $\hat{\rho}_E^{in}$ do not improve the situation, but lead in general to $H(S) = H(\hat{\rho}_{SE}^{out}) < H(S_{class})$ instead, as shown by the \blacktriangledown -dotted curve in Fig. 5.

This is also clear when looking at the input state $\hat{\rho}_{SE}^{in} = \hat{\rho}_S^{in} \otimes \hat{\rho}_E^{in}$, with a $k = 1$ qubit pure $\hat{\rho}_S^{in}$ and an $n = 8$ qubit $\hat{\rho}_E^{in} = 3^{-1} \cdot (|0_n\rangle \langle 0_n| + |1_n\rangle \langle 1_n| + |10_{n-1}\rangle \langle 10_{n-1}|)$, which leads to the output state

$$\begin{aligned} \hat{\rho}_{SE}^{out} &= |a|^2 |0_k\rangle \langle 0_k| \otimes \hat{\rho}_E^{in} + |b|^2 |1_k\rangle \langle 1_k| \otimes \hat{\rho}_E^{(1)} \\ &\quad + a \cdot b^* |0_k\rangle \langle 1_k| \otimes \hat{A}_E^{(2)} + a^* \cdot b |1_k\rangle \langle 0_k| \otimes [\hat{A}_E^{(2)}]^\dagger \\ \hat{\rho}_E^{(1)} &= 3^{-1} \cdot (|0_n\rangle \langle 0_n| + |1_n\rangle \langle 1_n| + |01_{n-1}\rangle \langle 01_{n-1}|) \\ \hat{A}_E^{(2)} &= 3^{-1} \cdot (|0_n\rangle \langle 1_n| + |1_n\rangle \langle 0_n| + |10_{n-1}\rangle \langle 01_{n-1}|). \end{aligned} \quad (156)$$

(156) yields MI-values $0 \leq I(S : E_{L=1}) \leq 0.0817042$ (with $I(S : E_{L=1}) = 0$ for $(|a|^2 = 1, |b|^2 = 0)$ or $(|b|^2 = 1, |a|^2 = 0)$)

and $I(S : E_{L=1}) = 0.0817042$ for $|a|^2 = |b|^2 = 1/2$, $I(S : E_L) = 3^{-1} \cdot H(S_{\text{class}}) \forall (2 \leq L < n)$ and $I(S : E_{L=n}) = 4 \cdot 3^{-1} \cdot H(S_{\text{class}})$, as depicted in Fig. 6 below (\bullet -dotted curve) w.r.t. $|a|^2 = |b|^2 = 1/2$. Clearly, there is no QD, since the MI-'plateau' of the \bullet -dotted curve in Fig. 6 appears for $L = 2 > k = 1$, however w.r.t. the MI-value $I(S : E_L) = 3^{-1} \cdot H(S_{\text{class}}) = 3^{-1} < 1$.

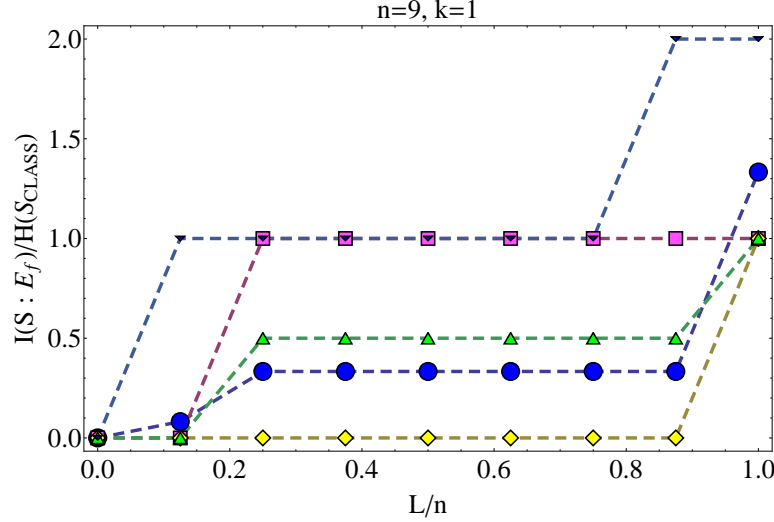


Figure 6: PIP for different $\hat{\rho}_{SE}^{\text{out}}$; for details s. main text.

We can extend Zurek's interaction algorithm to systems S with more than one qubit ($k > 1$) by assuming E to contain $n' = k \cdot n \gg k$ qubit-cells (i.e. one subdivides n' E -qubits into k disjoint subsets $E = \bigcup_{i=1}^k E_i$ with $|E_i| = n \forall i$) and allowing each S -qubit to interact with only one E_i -subset of environment E and only once with each of the $n \gg k$ E -qubits within the particular E_i . Then, with $\hat{\rho}_{SE}^{\text{in}} = \hat{\rho}_S^{\text{in}} \otimes \hat{\rho}_E^{\text{in}}$, $\hat{\rho}_E^{\text{in}} = |0_{n'}\rangle \langle 0_{n'}|$ and a pure two-qubit ($k = 2$) state $\hat{\rho}_S^{\text{in}}$, the corresponding PIP is given $\forall (k = 2 \leq L \leq n' - k)$ by the \bullet -dotted plateau in Fig. 5, whereas $H(S, E_L) < H(E_L)$ holds $\forall (n' - k + 1 \leq L \leq n')$ and for $0 < L = 1 < k = 2$ one has¹⁴ $0 \leq I(S : E_{L=1}) / H(S_{\text{class}}) \leq 0.5$ (s. also Fig. 7 below, as well as subsections 4.2.3-4.2.5 and (107)-(109) above). Thus, in Zurek's pure decoherence qubit-model of Quantum Darwinism the specified CNOT-evolution yields the MI-plateau also for pure $\hat{\rho}_S^{\text{in}}$ with $k > 1$ qubits if we start its evolution within $\hat{\rho}_{SE}^{\text{in}} = \hat{\rho}_S^{\text{in}} \otimes \hat{\rho}_E^{\text{in}}$ and with a pure one registry n' -qubit state $\hat{\rho}_E^{\text{in}} = |y\rangle \langle y|$ ($y \in \{0, \dots, 2^{n'} - 1\}$) in the standard computational basis. Unfortunately, introducing entanglement into $\hat{\rho}_{SE}^{\text{in}}$ does not improve the situation from the perspective of QD: for instance, if we look at the input state $\hat{\rho}_{SE}^{\text{in}} = \hat{\rho}_S^{\text{in}} \otimes \hat{\rho}_E^{\text{in}}$, with a $k = 2$ qubit pure Bell-state $\hat{\rho}_S^{\text{in}} = |\tilde{\Psi}_S^{\text{in}}\rangle \langle \tilde{\Psi}_S^{\text{in}}|$ (where $|\tilde{\Psi}_S^{\text{in}}\rangle = 2^{-1/2}(|00\rangle + |11\rangle)$) and an $n' = 2 \cdot n$ qubit $\hat{\rho}_E^{\text{in}} = |0_{n'}\rangle \langle 0_{n'}|$, which leads to the output state $\hat{\rho}_{SE}^{\text{out}}$ that emerges from (12) by simply replacing $n \leftrightarrow n'$, $|0\rangle \leftrightarrow |00\rangle$, $|1\rangle \leftrightarrow |11\rangle$ and setting $a = b = 2^{-1/2}$. Therefore, entangling the S -qubits reduces the Shannon-value of $H(S) = H(S_{\text{class}}^{k=1}) = 1$ w.r.t. the Shannon-entropy $H(S_{\text{class}}^{k=2})$ of an unentangled, decohered and maximally mixed system S which stands in the denominator of (155). This is the reason why the corresponding PIP looks almost the same as the one in Fig. 1, however, with the essential difference that the MI-'plateau' ranging from $L = 1$ to $L = n' - 1$ for the Bell-like $\hat{\rho}_S^{\text{in}}$ attains a constant MI-value c with $0.5 \leq c < 1$, violating (155) (again, the lower c -value is achieved for $\{|a_i|^2 = 2^{-k}\}_{i=0}^{2^{k-1}-1} \forall i$ in $\hat{\rho}_S^{\text{in}}$, whereas the upper c -bound remains out of range).

On the other hand, even if we try to entangle a $k = 1$ qubit S with an $n > 1$ qubit E in $\hat{\rho}_{SE}^{\text{in}}$ and start with $\hat{\rho}_{SE}^{\text{in}} \neq \hat{\rho}_S^{\text{in}} \otimes \hat{\rho}_E^{\text{in}}$ QD would, in general, not appear. E.g., by starting with entangled input states $|\Psi_{SE}^{\text{in}}\rangle = 2^{-1/2}(|0\rangle_S |0_n\rangle_E + |1\rangle_S |x\rangle_E)$ we obtain within Zurek's qubit model the output states $|\Psi_{SE}^{\text{out}}\rangle = 2^{-1/2}(|0\rangle_S |0_n\rangle_E + |1\rangle_S |y\rangle_E)$, with

$$\begin{aligned} \text{I) } x = 10_{n-1} &\Rightarrow y = 01_{n-1} \Rightarrow I(S : E_{L=1}) = 0, I(S : E_{1 < L \leq n}) = \underbrace{H(S_{\text{class}})}_{:=1} \\ \text{II) } x = 0_{n-1}1 &\Rightarrow y = 1_{n-1}0 \Rightarrow I(S : E_{1 \leq L \leq n-2}) = H(S_{\text{class}}), I(S : E_{n-1 \leq L \leq n}) = 2 \cdot H(S_{\text{class}}) \\ \text{III) } x = 1_n &\Rightarrow y = 0_n \Rightarrow I(S : E_L) = 0 \forall (1 \leq L \leq n) \end{aligned} \quad (157)$$

¹⁴the lower bound follows from the trivial initial probability distribution $\{|a_i|^2 = 1, |a_{i'}|^2 = 0 \forall i' \neq i\}$ in $\hat{\rho}_S^{\text{in}}$, whereas the upper bound emerges from $|a_i|^2 = 2^{-k} \forall i \in \{0, \dots, 2^k - 1\}$.

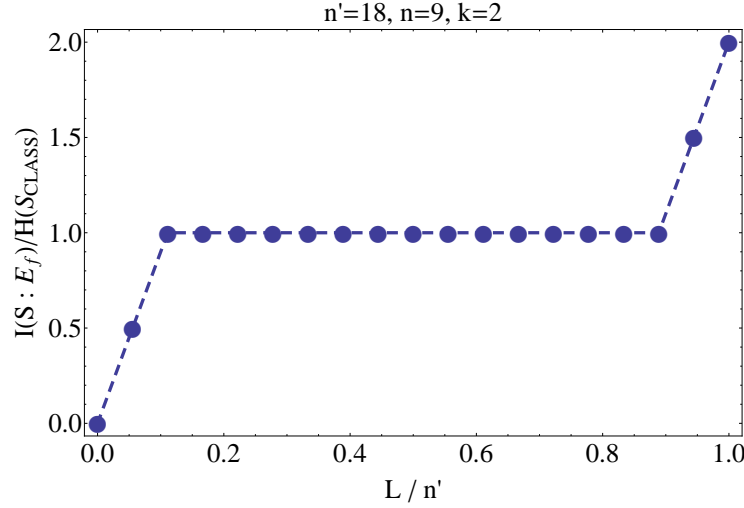


Figure 7: PIP for $\hat{\rho}_{SE}^{\text{out}}$ from $\hat{\rho}_S^{\text{in}} = |\Psi_S^{\text{in}}\rangle \langle \Psi_S^{\text{in}}| \otimes \hat{\rho}_E^{\text{in}}$ (where $k = 2$, $n' = 8 = 2 \cdot n$, $|\Psi_S^{\text{in}}\rangle = a|0\rangle + b|1\rangle$) and $\hat{\rho}_E^{\text{in}} = |0_n\rangle \langle 0_n|$.

and the corresponding PIPs, namely the \blacksquare -dotted curve in Fig. 6 (case I) in (157) above), the \blacktriangledown -dotted curve in Fig. 6 (case II) in (157) above) and the \blacktriangledown -dotted curve in Fig. 5 (case III) in (157) above). Among all three cases in (157) only $\hat{\rho}_{SE}^{\text{out}}$ corresponding to case II) adheres to (155). Unfortunately, whether QD appears in case II) of (157) or not, depends on the order in which one traces out single E-qubits: for if we trace out in case II) of (157) within $|1_{n-1}0\rangle$ the first $n - 1$ qubits $|1\rangle^{\otimes n-1}$ (from left to right, i.e. contrary to the third step of Zurek's algorithm listed above), we would obtain $H(S) = H(S, E_{L=1}) = H(S_{\text{CLASS}}) = 1$, $H(E_{L=1}) = 0$ and thus $I(S : E_{L=k=1}) = 0$, which would violate (155). In other words, in order to validate (155) one needs to entangle each of the S-pointer states with appropriate E-states. How can one perform this »appropriate entanglement« between S and E in $\hat{\rho}_{SE}^{\text{in}}$?

Certainly, if we deliberately design $\hat{\rho}_{SE}^{\text{in}}$ such that it remains unaltered under the CNOT-evolution by entangling the pointer-basis $\{|\pi_i\rangle\} \equiv \{|0\rangle, |1\rangle\}$ of a $k = 1$ qubit system S with one-qubit E-eigenstates $|s_1\rangle = 2^{-1/2}(|0\rangle + |1\rangle)$ and $|s_2\rangle = 2^{-1/2}(|0\rangle - |1\rangle)$ of the CNOT-transformation (Pauli matrix) $\hat{\sigma}_x$ according to

$$\begin{aligned} |\Psi_{SE}^{\text{in}}(L=n)\rangle &= a|0\rangle \otimes |s_1^{L=n}\rangle + b|1\rangle \otimes |s_2^{L=n}\rangle \\ |s_m^L\rangle &= |s_m\rangle^{\otimes L}, \quad \hat{\sigma}_x |s_m\rangle = \underbrace{(-1)^{m+1}}_{:=\lambda} |s_m\rangle \end{aligned} \quad (158)$$

(with $m \in \{1, 2\}$, $\langle s_1 | s_2 \rangle = 0$), (158) would lead to the PIP displayed in Fig. 1: i.e. Quantum Darwinism would appear. One can even show that (158) leads to Quantum Darwinism only for $k = 1$ qubit system S (s. Appendix E).

Are there also other QD-compliant entanglement possibilities between $\{|\pi_i\rangle\}$ and $\{|s_1\rangle, |s_2\rangle\}$ that adhere to (155)? No. Clearly, choosing simply $\hat{\rho}_{SE}^{\text{in}(1)} = |\Psi_S^{\text{in}}\rangle \langle \Psi_S^{\text{in}}| \otimes \hat{\rho}_E^{\text{in}}$ with $|\Psi_S^{\text{in}}\rangle = a|0\rangle + b|1\rangle$ and $\hat{\rho}_E^{\text{in}} = |s_1^{L=n}\rangle \langle s_1^{L=n}|$ or $\hat{\rho}_E^{\text{in}} = |s_2^{L=n}\rangle \langle s_2^{L=n}|$ would not change the purity of such $\hat{\rho}_{SE}^{\text{in}}$ and its reduced density matrices $\hat{\rho}_S^{\text{in}}$ and $\hat{\rho}_E^{\text{in}}$ in the framework of Zurek's QD-model, yielding $\hat{\rho}_{SE}^{\text{in}(1)} = \hat{\rho}_{SE}^{\text{out}(1)}$ and thus $I(S : E_L) = 0 \forall (1 \leq L \leq n)$. Otherwise, the input state $\hat{\rho}_{SE}^{\text{in}(2)} = |\Psi_S^{\text{in}}\rangle \langle \Psi_S^{\text{in}}| \otimes \hat{\rho}_E^{\text{in}}$ with $\hat{\rho}_E^{\text{in}} = 2^{-1} \cdot (|s_1^{L=n}\rangle \langle s_1^{L=n}| + |s_2^{L=n}\rangle \langle s_2^{L=n}|)$ would even be more inappropriate, since its output state

$$\begin{aligned} \hat{\rho}_{SE}^{\text{out}(2)} &= (|a|^2 |0\rangle \langle 0| + |b|^2 |1\rangle \langle 1|) \otimes \hat{\rho}_E^{\text{in}} + \\ &+ (a \cdot b^* |0\rangle \langle 1| + a^* \cdot b |1\rangle \langle 0|) \otimes 2^{-1} \cdot (|s_1^{L=n}\rangle \langle s_1^{L=n}| + (-1)^n |s_2^{L=n}\rangle \langle s_2^{L=n}|) \end{aligned} \quad (159)$$

suggests that the decoherence of S can be maintained only for E containing an odd number $n \gg 1$ of qubits, whereas for even n -values the corresponding $\hat{\rho}_S^{\text{out}(2)}$ would remain pure. This is apparently a behavior of $\hat{\rho}_{SE}^{\text{out}(2)}$ which is not allowed from the perspective of Zurek's QD-model, which preassumes that in the decoherence limit of large E the system's output density matrix approaches a completely mixed (»classical«) state exponentially fast, regardless of n being odd or even. Nevertheless, even if we set $n \in \mathbb{N}^+$ to attain an odd value and thus obtain from (159) $H(S) = H(S_{\text{CLASS}})$, we would still get from (159) for all odd n the eigenspectra $\sigma(\hat{\rho}_{SE}^{\text{out}(2)}) \equiv \{2^{-1}|a|^2 (2\times), 2^{-1}|b|^2 (2\times)\}$ and $\sigma(\hat{\rho}_E^{\text{out}(2)}) \equiv \{2^{-1}|a|^2 (2\times), 2^{-1}|b|^2 (2\times)\}$, yielding $H(S, E_L) = H(S_{\text{CLASS}}) + H(E_L)$, $H(E_L) = 1$ and $I(S : E_L) = 0 \forall (1 \leq L \leq n)$.

However, (159) also indicates another problematic issue of Zurek's QD-model: in (159) as well as in (12) we do not need to enforce $n \gg 1$ in order to obtain a decohered system S . On the contrary, both in (159) and (12) already an $n = 1$ qubit E suffices to ensure $H(S) = H(S_{\text{class}})$. This indicates that in order to simulate and utilize decoherence process in a more realistic fashion we need to take into account more advanced dynamical models of QD, within which $H(S)$ smoothly approaches $H(S_{\text{class}})$ in the limit $n \gg 1$. This will precisely be the main task of section 8 below.

Finally, before concluding this subsection we turn our attention to the entangled input state

$$|\Psi_{SE}^{\text{in}}\rangle = 2^{-1/2} (|0\rangle_S |\gamma_n\rangle_E + |1\rangle_S |\mu_n\rangle_E), \quad (160)$$

with $|\gamma_n\rangle_E = 2^{-1/2} (|0_n\rangle_E + |1_n\rangle_E)$, $|\mu_n\rangle_E = 2^{-1/2} (|0_n\rangle_E - |1_n\rangle_E)$ and ${}_E\langle\mu_n|\gamma_n\rangle_E = 0$. (160) is interesting, since it entangles, similar to (158), the two pointer basis states of a $k = 1$ qubit system S with two mutually orthogonal n -qubit E -states $|\gamma_n\rangle_E$ and $|\mu_n\rangle_E$, each of which containing a convex sum of two E -registry states. Although $|\gamma_n\rangle_E$ and $|\mu_n\rangle_E$ are not CNOT-symmetry states, would (160) still adhere to (155) in the course of Zurek's QD-model? No. After applying Zurek's evolution algorithm to (160) one obtains the output state

$$|\Psi_{SE}^{\text{out}}\rangle = 2^{-1/2} (|0\rangle_S |\gamma_n\rangle_E + |1\rangle_S |\mu'_n\rangle_E), \quad (161)$$

with $|\mu'_n\rangle_E = -|\mu_n\rangle_E$, yielding $H(S, E_L) = H(S) + H(E_L) = H(S_{\text{class}}) + 1 = 1 + 1 = 2 \forall (1 \leq L < n)$ and $H(S, E_{L=n}) = H(S) = H(S_{\text{class}}) = H(E_{L=n}) = 1$. Thus, (161) leads to the PIP depicted by the \blacklozenge -dotted curve in Fig. 6, i.e. there is no MI-'plateau'. This result points out once more that (158) is the only way of entangling S and its pointer basis with E that adheres to (155) only for $k = 1$.

Indeed, replacing in (160) $|0\rangle_S \leftrightarrow |0_k\rangle_S$ and $|1\rangle_S \leftrightarrow |1_k\rangle_S$ for $k > 1$ and performing Zurek's algorithm as done w.r.t. Fig. 7, we would still obtain from the corresponding $|\bar{\Psi}_{SE}^{\text{out}}\rangle$, which emerges from (161) by the same replacements $|0\rangle_S \leftrightarrow |0_k\rangle_S$ and $|1\rangle_S \leftrightarrow |1_k\rangle_S$, the identity $H(S) = H(S_{\text{class}}^{k=1}) = 1 < H(S_{\text{class}}^{k>1})$. This is the reason why (161) would never lead to QD, since, as shown w.r.t. the Bell-like, $k = 2$ qubit input S -state $\hat{\rho}_S^{\text{in}}$ (with $\hat{\rho}_{SE}^{\text{in}} = \hat{\rho}_S^{\text{in}} \otimes \hat{\rho}_E^{\text{in}}$ and $\hat{\rho}_E^{\text{in}} = |0_{n'=2n}\rangle\langle 0_{n'=2n}|$) described by Fig. 7, $H(S_{\text{class}}^{k>1})$ in the denominator of the corresponding expression (155) would always exceed $H(S) = H(S_{\text{class}}^{k=1}) = 1$ in the numerator of (155) which the $k > 1$ version of (161) still yields.

The only way to ensure that $H(S)$ in the numerator of (155) yields the Shannon-entropy of a $k > 1$ qubit S would be, for instance, to entangle the $2^{k=2}$ pointer states of a $k = 2$ qubit S with $|\gamma_{n'=2n}\rangle_E$ and $|\mu_{n'=2n}\rangle_E$ according to

$$\hat{\rho}_{SE}^{\text{in}} = \frac{1}{4} \{ [|0_2\rangle_S \langle 0_2| + |1_2\rangle_S \langle 1_2|] \otimes |\gamma_{n'}\rangle_E \langle \gamma_{n'}| + [|1_0\rangle_S \langle 1_0| + |01\rangle_S \langle 01|] \otimes |\mu_{n'}\rangle_E \langle \mu_{n'}| \}, \quad (162)$$

which in the framework of Zurek's QD-model leads to the output state

$$\hat{\rho}_{SE}^{\text{out}} = \frac{1}{8} \left\{ [|0_2\rangle_S \langle 0_2| + |1_2\rangle_S \langle 1_2|] \otimes |\bar{\Psi}_{E(1)}^{\text{out}}\rangle_E \langle \bar{\Psi}_{E(1)}^{\text{out}}| + [|1_0\rangle_S \langle 1_0| + |01\rangle_S \langle 01|] \otimes |\bar{\Psi}_{E(2)}^{\text{out}}\rangle_E \langle \bar{\Psi}_{E(2)}^{\text{out}}| \right\}, \quad (163)$$

with $|\bar{\Psi}_{E(1)}^{\text{out}}\rangle_E = |0_{n'=2n}\rangle_E + |1_{n'=2n}\rangle_E$, $|\bar{\Psi}_{E(2)}^{\text{out}}\rangle_E = |x\rangle_E^{\otimes n'/2} - |y\rangle_E^{\otimes n'/2}$, $x \equiv 01$, $y \equiv 10$. From (163) we obtain $H(S) = H(S_{\text{class}}^{k=2}) = 2$, $H(S, E_{L=n}) = H(E_{L=n}) = 0$, $H(S, E_L) = 3 = H(S_{\text{class}}^{k=2}) + H(E_L)$ for $(1 \leq L < k)$, $H(S, E_L) = 3 > H(S_{\text{class}}^{k=2}) = H(E_L)$ for $(k \leq L < n')$ and a PIP given by the \blacktriangle -dotted curve in Fig. 6 (no QD).

7.2 Zurek's model of Quantum Darwinism and non-CNOT interactions

In subsection 4.2.5, as well as from (128)-(129) and Fig. 4, we have seen that in Zurek's qubit model of Quantum Darwinism among all $\hat{u}_i^{(\phi)}$ of (9)-(10) only the CNOT-evolution $\hat{u}_i^{(\phi=\pi/2)}$ leads to the appearance of the PIP-plateau w.r.t. the S -pointer basis $\{|\pi_i\rangle\} \equiv \{|0\rangle, |1\rangle\}$ and (155) if one starts the CNOT-evolution with the artificial, "symmetry-adjusted" and entangled input state (158), in which case Quantum Darwinism appears only for $k = 1$ qubit system S , or if one starts the CNOT-evolution with $\hat{\rho}_{SE}^{\text{in}} = \hat{\rho}_S^{\text{in}} \otimes \hat{\rho}_E^{\text{in}}$ (where $\hat{\rho}_S^{\text{in}}$ denotes a pure open $k \geq 1$ qubit system S and $\hat{\rho}_E^{\text{in}} = |y\rangle\langle y|$ with $y \in \{0, \dots, 2^n - 1\}$), in which case $H(S, E_L) \leq H(E_L) \forall (k \leq L \leq n)$. However, before concluding this section we want to investigate (if possible) in the course of the forthcoming subsection the impact of mutually interacting E -qubits on the appearance of QD.

7.3 Zurek's model of Quantum Darwinism with mutually interacting environmental qubits

We conclude the present section by investigating what happens with MI in Zurek's QD model if we introduce interactions between E-qubits. For the sake of simplicity, and without loss of generality, we again concentrate mainly on the CNOT-evolution, since subsection 7.2 has indicated that within Zurek's original QD-model only the CNOT-transformation allows one to see the MI-'plateau' for specific input states $\hat{\rho}_{SE}^{in}$, in accord with (155).

The main problem with Zurek's QD-model when it comes to discussing mutually interacting E-qubits is connected with the fact that its algorithm describing the CNOT-evolution of quantum states does not specify how to incorporate and treat CNOT-interactions between environmental qubits. For example, let us assume that we have to deal with the well-known input state $\hat{\rho}_{SE}^{in} = |\Psi_S^{in}\rangle \langle \Psi_S^{in}| \otimes \hat{\rho}_E^{in}$, with a $k = 1$ qubit pure S-state $|\Psi_S^{in}\rangle$ and an n -qubit ground state $\hat{\rho}_E^{in} = |0_n\rangle \langle 0_n|$ in the standard computational basis. However, as a difference to the original Zurek's QD-model from subsection 7.1 we allow within E qubits 1 and 2 to interact via CNOT such that qubit 1 defines the control unit, whereas qubit 2 represents a target. This can be easily described by means of the directed graph (digraph) of interactions between n E-qubits as shown in Fig. 8 (graph a) therein).

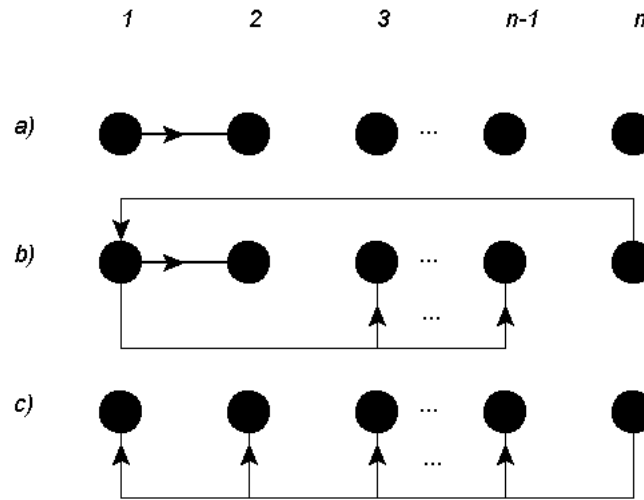


Figure 8: Some directed graphs of interactions (interaction digraphs, IDs) between n environmental qubits. Arrows indicate the direction of interactions, pointing from a control qubit to the corresponding target qubit.

In the interaction digraph (ID) a) of Fig. 8 the arrow direction indicates the direction in which the CNOT-transformation acts upon its target, i.e. the arrow points from the control qubit to the target qubit. Now, we could, for instance, stipulate that one should first apply the CNOT interactions between the one S-qubit in $\hat{\rho}_{SE}^{in}$ and each of the n environmental qubits in accord with the well-known evolution algorithm, before letting the E-qubits interact with each other as in the ID a) of Fig. 8. After all interactions have been successively applied in this manner, one may trace out single E-qubits as explained in subsection 7.1 w.r.t. Fig. 1 and compute the corresponding PIPs. Unfortunately, even if we decide to treat mutually interacting E-qubits in this way, we would obtain unexpected results. Let us look at three examples.

Example 1: Starting with $\hat{\rho}_{SE}^{in} = |\Psi_S^{in}\rangle \langle \Psi_S^{in}| \otimes \hat{\rho}_E^{in}$, with a $k = 1$ qubit pure S-state $|\Psi_S^{in}\rangle$ and an n -qubit ground state $\hat{\rho}_E^{in} = |0_n\rangle \langle 0_n|$, we obtain, after applying n CNOT-interactions between the one S-qubit and n E-qubits as suggested by the original Zurek's QD-model, followed by the CNOT-interaction between the first and the second E-qubit in accord with an ID a) of Fig. 8, the output S-E-state $\hat{\rho}_{SE}^{out}$ which emerges from (12) by replacing $|1_n\rangle_E \leftrightarrow |101_{n-2}\rangle_E$. In other words, introducing a single CNOT-interaction between two E-qubits does not alter the QD-compliant density matrix structure (12) dramatically, which is the reason why $\hat{\rho}_{SE}^{out}$ leads to the same PIP as the one in Fig. 1. The same type of QD-compliant density matrix structures, similar to $\hat{\rho}_{SE}^{out}$ and (12), would also appear when starting with an arbitrary, pure, one E-registry input state $\hat{\rho}_E^{in} = |y\rangle \langle y|$ with $y \in \{0, \dots, 2^n - 1\}$ and two arbitrary mutually interacting E-qubits.

Example 2: As a second example let us look at $\hat{\rho}_{SE}^{in} = |\Psi_S^{in}\rangle \langle \Psi_S^{in}| \otimes \hat{\rho}_E^{in}$, with $|\Psi_S^{in}\rangle$ denoting a pure, $k = 1$ qubit S-state, $\hat{\rho}_E^{in} = 2^{-1} \cdot (|0_n\rangle \langle 0_n| + |1_n\rangle \langle 1_n|)$ and an ID as in Zurek's original QD-model, however this time supplemented by the CNOT interaction structure in b) of Fig. 8: according to the ID b) of Fig. 8 we apply, after implementing CNOT interactions between the one S-qubit and all n E-qubits, among the E-qubits CNOT operations successively between qubits 1 and 2, 1 and 3, ..., 1 and $n - 1$ (with the first E-qubit representing always the control), before we finally let the n -th

E-qubit interact with the first E-qubit via CNOT, now with the n -th E-qubit being the control instance. This procedure would generate the output state

$$\hat{\rho}_{SE}^{\text{out}} = \left(|a|^2 |0\rangle_S \langle 0| + |b|^2 |1\rangle_S \langle 1| \right) \otimes \hat{A}_1 + (a \cdot b^* |0\rangle_S \langle 1| + b \cdot a^* |1\rangle_S \langle 0|) \otimes \hat{A}_2, \quad (164)$$

with $\hat{A}_1 = 2^{-1} \cdot (|0_n\rangle \langle 0_n| + |0_{n-1}1\rangle \langle 0_{n-1}1|)$ and $\hat{A}_2 = 2^{-1} \cdot (|0_n\rangle \langle 0_{n-1}1| + |0_{n-1}1\rangle \langle 0_n|)$. (164) yields entropy relations $H(S) = H(S_{\text{class}})$, $H(S, E_L) = H(E_L) = H(S_{\text{class}}) \forall (1 \leq L < n)$, $H(S, E_{L=n}) = H(E_{L=n}) = 1$ and a PIP as in Fig. 1, however, this time without a »quantum peak« $2 \cdot H(S_{\text{class}})$ due to $I(S : E_{L=n}) = H(S_{\text{class}})$. The ID structure leading to (164) is interesting, since it suggests that one could restore QD in the scope of Zurek's qubit model by introducing interactions among E-qubits: after all, from subsection 7.1 we know that treating $\hat{\rho}_{SE}^{\text{in}} = |\Psi_S^{\text{in}}\rangle \langle \Psi_S^{\text{in}}| \otimes \hat{\rho}_E^{\text{in}}$, with $|\Psi_S^{\text{in}}\rangle$ denoting a pure, $k = 1$ qubit S-state and $\hat{\rho}_E^{\text{in}} = 2^{-1} \cdot (|0_n\rangle \langle 0_n| + |1_n\rangle \langle 1_n|)$ containing mutually non-interacting E-qubits, by Zurek's standard evolution algorithm leads to a PIP given by \blacklozenge -dotted curves in Fig. 5 and Fig. 6 (complete suppression of QD), whereas mutually interacting E-qubits, organized in accord with a specific ID b) of Fig. 8, were able to allow an efficient storage of $H(S_{\text{class}})$ into E.

Example 3: Finally, we look at $\hat{\rho}_{SE}^{\text{in}} = |\Psi_S^{\text{in}}\rangle \langle \Psi_S^{\text{in}}| \otimes \hat{\rho}_E^{\text{in}}$, with $|\Psi_S^{\text{in}}\rangle$ denoting a pure, $k = 1$ qubit S-state, $\hat{\rho}_E^{\text{in}} = 2^{-1} \cdot (|0_n\rangle \langle 0_n| + |0_{n-1}1\rangle \langle 0_{n-1}1|)$ and an ID as in Zurek's original QD-model, however this time supplemented by the CNOT interaction structure in c) of Fig. 8: according to the ID c) of Fig. 8 we apply, after implementing CNOT interactions between the one S-qubit and all n E-qubits, among the E-qubits CNOT operations successivly between qubits n and 1, n and 2, ..., n and $n-1$ (with the n -th E-qubit representing always the control). This procedure would generate the output state

$$\hat{\rho}_{SE}^{\text{out}} = |a|^2 |0\rangle_S \langle 0| \otimes \hat{A}_3 + |b|^2 |1\rangle_S \langle 1| \otimes \hat{A}_4 + a \cdot b^* |0\rangle_S \langle 1| \otimes \hat{A}_5 + b \cdot a^* |1\rangle_S \langle 0| \otimes \left[\hat{A}_5 \right]^\dagger, \quad (165)$$

with $\hat{A}_3 = 2^{-1} \cdot (|0_n\rangle \langle 0_n| + |1_n\rangle \langle 1_n|)$, $\hat{A}_4 = 2^{-1} \cdot (|0_{n-1}1\rangle \langle 0_{n-1}1| + |1_{n-1}0\rangle \langle 1_{n-1}0|)$ and $\hat{A}_5 = 2^{-1} \cdot (|0_n\rangle \langle 0_{n-1}1| + |1_n\rangle \langle 1_{n-1}0|)$. (165) yields entropy relations $H(S) = H(S_{\text{class}})$, $H(E_{L=n}) = H(S_{\text{class}}) + H(S, E_{L=n}) = H(S_{\text{class}}) + 1$, $H(S, E_L) = H(S_{\text{class}}) + H(E_L) = H(S_{\text{class}}) + 1 \forall (1 \leq L < n)$ and a PIP given by \blacklozenge -dotted curves in Fig. 5 and Fig. 6. Since we know from Fig. 5 (\bullet -dotted curve) that treating $\hat{\rho}_{SE}^{\text{in}} = |\Psi_S^{\text{in}}\rangle \langle \Psi_S^{\text{in}}| \otimes \hat{\rho}_E^{\text{in}}$, with $|\Psi_S^{\text{in}}\rangle$ denoting a pure, $k = 1$ qubit S-state and $\hat{\rho}_E^{\text{in}} = 2^{-1} \cdot (|0_n\rangle \langle 0_n| + |0_{n-1}1\rangle \langle 0_{n-1}1|)$ containing mutually non-interacting E-qubits, by Zurek's standard evolution algorithm leads to the appearance of the MI-'plateau', we are tempted to conclude that equipping Zurek's QD-model with mutually interacting E-qubits, organized in accord with a specific ID c) of Fig. 8, destroys QD.

Taking the above three examples into account, it is impossible to point out a clear trend when it comes to describing the influence of interactions among E-qubits on QD in the course of Zurek's qubit model. In other words, we see that, depending on stipulations regarding the way one treats and applies interactions between E-qubits in accord with the corresponding IDs, QD may appear or could even be suppressed. This is a further inconsistency of Zurek's toy model which we aim to circumvent in the forthcoming section and thus obtain a more clear picture of interactions between E-constituents and their influence on the efficient information storage by introducing more advanced qubit evolution models of pure decoherence and QD.

8 Random unitary model of Quantum Darwinism

In the present section we summarize the iterative evolution formalism of the random unitary model before discussing its most important results regarding Quantum Darwinism in subsections 8.1-8.4.

Random unitary operations can model the pure decoherence of open system S with k qubits (control, index i) interacting with n E-qubits (targets j) (as indicated in the directed interaction graph (digraph) in Fig. 9) by the one-parameter family of two-qubit 'controlled-U' unitary transformations (in the standard one-qubit computational basis $\{|0\rangle, |1\rangle\}$)

$$\hat{U}_{ij}^{(\phi)} = |0\rangle_i \langle 0| \otimes \hat{I}_1^{(j)} + |1\rangle_i \langle 1| \otimes \hat{u}_j^{(\phi)} \quad (166)$$

(where $\hat{I}_1^{(j)} = |0\rangle_j \langle 0| + |1\rangle_j \langle 1|$). (166) indicates that only if an S-qubit i should be in an excited state, the corresponding targeted E-qubit j has to be modified by a $(0 \leq \phi \leq \pi)$ -parameter $\hat{u}_j^{(\phi)}$ [11] (with Pauli matrices $\hat{\sigma}_l$, $l \in \{x, y, z\}$)

$$\hat{u}_j^{(\phi)} = \hat{\sigma}_z^{(j)} \cos \phi + \hat{\sigma}_x^{(j)} \sin \phi \Rightarrow \hat{u}_j^{(\phi=\pi/2)} = \hat{\sigma}_x^{(j)}, \quad (167)$$

which for $\phi = \pi/2$ yields the CNOT-gate [11, 29, 30, 38]. Arrows of the interaction digraph (ID) in Fig. 9 from S- to E-qubits represent two-qubit interactions $\hat{u}_{ij}^{(\phi)}$ between randomly chosen qubits i and j with probability distribution p_e

used to weight the edges $e = (ij) \in M$ of the digraph (E-qubits are in general allowed to interact among themselves). All interactions are well separated in time. The S-qubits do not interact among themselves. In order to model the decoherence-induced measurement process of system S by environment E we let an input state $\hat{\rho}_{SE}^{\text{in}}$ evolve by virtue of the following iteratively applied random unitary quantum operation (completely positive unital map) $\mathcal{P}(\cdot) \equiv \sum_{e \in M} K_e(\cdot) K_e^\dagger$ (with Kraus-operators $K_e := \sqrt{p_e} \hat{U}_e^{(\phi)}$) [11, 29, 30]:

1. The quantum state $\hat{\rho}(N)$ after N iterations is changed by the (N + 1)-th iteration to the quantum state (quantum Markov chain)

$$\hat{\rho}(N+1) = \sum_{e \in M} p_e \hat{U}_e^{(\phi)} \hat{\rho}(N) \hat{U}_e^{(\phi)\dagger} \equiv \mathcal{P}(\hat{\rho}(N)). \quad (168)$$

2. In the asymptotic limit $N \gg 1$ $\hat{\rho}(N)$ is independent of $(p_e, e \in M)$ and determined by linear attractor spaces $\mathcal{A}_\lambda \subset \mathcal{B}(\mathcal{H}_{SE})$, as subspaces of the Hilbert-space $\mathcal{B}(\mathcal{H}_{SE})$ of linear operators w.r.t. the total S-E-Hilbert space $\mathcal{H}_{SE} = \mathcal{H}_S \otimes \mathcal{H}_E$ for the eigenvalues λ (with $|\lambda| = 1$), that contain mutually orthonormal solutions (attractor »states«) $\hat{X}_{\lambda,i}$ of the eigenvalue equation [29, 30]

$$\hat{U}_e^{(\phi)} \hat{X}_{\lambda,i} \hat{U}_e^{(\phi)\dagger} = \lambda \hat{X}_{\lambda,i}, \quad \forall e \in M. \quad (169)$$

3. For known attractor spaces \mathcal{A}_λ we get from an initial state $\hat{\rho}_{SE}^{\text{in}}$ the resulting S-E-state $\hat{\rho}_{SE}^{\text{out}} = \hat{\rho}_{SE}$ ($N \gg 1$) spanned by $\hat{X}_{\lambda,i}$

$$\hat{\rho}_{SE}^{\text{out}} = \mathcal{P}^N(\hat{\rho}_{SE}^{\text{in}}) = \sum_{|\lambda|=1, i=1}^{d^\lambda} \lambda^N \text{Tr}\{\hat{\rho}_{SE}^{\text{in}} \hat{X}_{\lambda,i}^\dagger\} \hat{X}_{\lambda,i}, \quad (170)$$

where d^λ denotes the dimensionality of the attractor space \mathcal{A}_λ w.r.t. the eigenvalue λ .

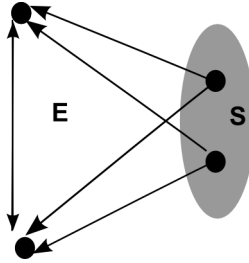


Figure 9: Interaction digraph (ID) between system S and environment E with pure decoherence within the random unitary model [11].

In other words, (166)-(170) indicate that the cptp-map $\mathcal{P}(\cdot) : \mathcal{B}(\mathcal{H}_{SE}) \rightarrow \mathcal{B}(\mathcal{H}_{SE})$ acts upon the Hilbert-space $\mathcal{B}(\mathcal{H}_{SE})$ of linear operators w.r.t. \mathcal{H}_{SE} , such that the corresponding total attractor space \mathcal{A} for all eigenvalues λ (with $|\lambda| = 1$),

$$\mathcal{A} := \bigoplus_{\lambda} \mathcal{A}_\lambda \quad (171)$$

may be expressed as a direct sum over mutually orthogonal attractor λ -subspaces \mathcal{A}_λ defined as the kernel

$$\begin{aligned} \mathcal{A}_\lambda &:= \text{Ker}(\mathcal{P} - \lambda I) = \{X \in \mathcal{B}(\mathcal{H}_{SE}) | \mathcal{P}(X) = \lambda X\} \\ \mathcal{A}_\lambda \cap \mathcal{A}_{\lambda'} &= \{\emptyset\} \quad \forall (\lambda \neq \lambda') \text{ with } |\lambda| = |\lambda'| = 1 \end{aligned} \quad (172)$$

of \mathcal{P} w.r.t. its eigenvalue λ (I is the identity map). Thus, (172) from (171) is another way for expressing (169) [30].

8.1 Minimal attractor space and its structure

What happens with Quantum Darwinism in the framework of the random unitary evolution model if we let the E-qubits interact with each other? From [29] we know that an ID with all mutually interacting E-qubits leads to the minimal attractor space structure (365) (Appendix H) associated with an eigenvalue $\lambda = 1$ of (170). However, for this minimal $\lambda = 1$ attractor subspace of (170) to emerge one does not need to insist that *all* n E-qubits should interact with each other. It suffices to have a strongly connected ID that contains a closed arrow path between n E-qubits [11, 29, 30]. However, as indicated in Appendix H, $2n - 3$ is the critical (and maximal) number of $\hat{U}_j^{(\phi)}$ -bindings that one may insert

between E-qubits into the ID of Fig. 9 and still avoid the minimal $d^{\lambda=1}$ from (363) in Appendix H. Thus, for $\geq 2(n-1)$ $\hat{u}_j^{(\phi)}$ -bindings between E-qubits the corresponding ID remains strongly connected, leading always to the minimal $\lambda = 1$ attractor space (365) of Appendix H, whereas the $\lambda = -1$ attractor space of (170) vanishes already after inserting a single interaction arrow into environment E (s. Appendices H.1 and H.3). Here we first turn to the physical interpretation of (365) from Appendix H.

8.1.1 State structure of the attractor space

The main differences between the maximal and the minimal $\lambda = 1$ attractor subspace (s. (380) and (365) in Appendix H) that mainly determine the process of decoherence and transfer of $H(S_{\text{class}})$ to E are two-fold: 1) within the minimal $\lambda = 1$ attractor subspace (365) only the ground E-registry state $|0_n\rangle$ appears, whereas in (380) of the maximal $\lambda = 1$ attractor subspace all 2^n E-registry states contribute; 2) On the other hand, in (380) the E-registry states $|y\rangle$ are correlated within the diagonal S-subspace $|0_k\rangle\langle 0_k|$ only with each other, whereas (365) also allows the remaining E-registry state $|0_n\rangle$ to be correlated with the $\hat{u}_j^{(\phi)}$ -symmetry state $|s_{c_1}^n\rangle$. This means that effectively the contribution of the S-subspace $|0_k\rangle\langle 0_k|$ in (365) to $I(S : E_L)$, contrary to (380), becomes exponentially suppressed due to $|s_{c_1}^n\rangle$. The implications of this exponential, decoherence induced suppression of S-subspace $|0_k\rangle\langle 0_k|$ in (365) regarding Quantum Darwinism will be discussed in the forthcoming subsection.

However, before continuing our discussion of QD in the course of the random unitary evolution model let us pause and assume that by means of appropriately designed quantum operations (that for the sake of simplicity we omit to specify at a present point) the following global S – E-state

$$|\phi_{SE}^{\text{out}}\rangle = \sum_{i=0}^{2^k-1} a_i |i\rangle \otimes |\varphi_i\rangle^{\otimes n}, \quad a_i \in \mathbb{C} \quad (173)$$

(with $\sum_{i=0}^{2^k-1} |a_i|^2 = 1$) has been generated. $|\phi_{SE}^{\text{out}}\rangle$ involves a standard computational basis $\{|i\rangle, i \in 2^k\}$ of a k-qubit subsystem S (with $\langle i|j\rangle = 0$ for $i \neq j$), as well as a not necessarily orthogonal set of environmental relative n-qubit states $|\varphi_i\rangle^{\otimes n}$ (with $\langle \varphi_i|\varphi_j\rangle \neq 0$ for $i \neq j$). Thus, $|\phi_{SE}\rangle$ corresponds to a sum of strongly correlated states of S and E. This correlation structure will enable us to gain a detailed insight into

When dealing with these mutually non-orthogonal environmental states $|\varphi_i\rangle^{\otimes n}$ we will encounter the opportunity of conveniently changing the values of the decoherence factor $r = |\langle \varphi_i|\varphi_j\rangle|^n$ by varying the extent of the overlap $\underbrace{\langle \varphi_i|\varphi_j\rangle}_{:=\xi}$,

which enters into the global S – E-state

$$\hat{\rho}_{SE}^{\text{out}} = |\phi_{SE}^{\text{out}}\rangle \langle \phi_{SE}^{\text{out}}| = \sum_{i,j=0}^{2^k-1} a_i a_j^* |i\rangle \langle j| \otimes |\varphi_i\rangle^{\otimes n} \langle \varphi_j|. \quad (174)$$

after tracing out irrelevant environmental degrees of freedom. Since we concentrate on the resulting state $\hat{\rho}_{SE}^{\text{out}}$, ignoring the behavior of the environmental fraction parameter f during the evolution of the initial S – E state configuration, it appears reasonable to assume an environment consisting of n sectors (fractions). The fraction parameter f would then count the number of E-sectors that have not been traced out from (174) as irrelevant, displaying the monotonically increasing behavior as in Zurek's qubit model. Thus, if only $0 \leq (L \in \mathbb{R}) \leq n$ of n environmental sectors would be considered as relevant to the computation of MI, one would reduce $E = E_{f=1}$ to an E_f -environment (with $f = L/n$) by tracing out the irrelevant $(n-L)$ states $|\varphi_i\rangle^{\otimes (n-L)}$ in (174), which would lead us to the following density matrices of S, E_f and the global S – E_f -state¹⁵:

$$\begin{aligned} \hat{\rho}_{SE_f}^{\text{out}} &= \sum_{i,j=0}^{2^k-1} a_i a_j^* |i\rangle \langle j| \otimes |\varphi_i\rangle^{\otimes L} \langle \varphi_j| \cdot |\xi^{(n-L)}| \\ \hat{\rho}_{E_f}^{\text{out}} &= \sum_{i=0}^{2^k-1} |a_i|^2 |\varphi_i\rangle^{\otimes L} \langle \varphi_i|, \quad \sum_{i=0}^{2^k-1} |a_i|^2 = 1 \\ \hat{\rho}_S^{\text{out}} &= \sum_{i,j=0}^{2^k-1} a_i a_j^* |i\rangle \langle j| \cdot |\xi^{(n)}|. \end{aligned} \quad (175)$$

As a further step we investigate the behavior of (175) and the corresponding MIs for $k = 1$ and $k = 2$ open qubit systems S according to the following procedure:

¹⁵with mutually orthogonal global S-E states $\langle i; \varphi_i|j; \varphi_j\rangle = 0$ due to the orthogonality of the computational basis S -states

- Compute MI from (175) for a fixed k-qubit S and a fixed number n of E-qubits.
- Plot MI w.r.t. $0 \leq (f = L/n) \leq 1$ for a particular value of $r = |\xi^{(n-L)}|$.

MI for k = 1 and k = 2 qubit systems S For a k = 1 qubit S the density matrices (175) acquire (with $|a_i|^2 = 2^{-k} \forall i$) the following forms:

$$\begin{aligned}\hat{\rho}_{S E_f}^{\text{out}} &= \frac{1}{2} \left(|0, \varphi_0\rangle^{\otimes(L+1)} \langle 0, \varphi_0| + |1, \varphi_1\rangle^{\otimes(L+1)} \langle 1, \varphi_1| \right. \\ &\quad \left. + |0, \varphi_0\rangle^{\otimes(L+1)} \langle 1, \varphi_1| \cdot |\xi^{(n-L)}| + |1, \varphi_1\rangle^{\otimes(L+1)} \langle 0, \varphi_0| \cdot |\xi^{(n-L)}| \right) \\ \hat{\rho}_{E_f}^{\text{out}} &= \frac{1}{2} |\varphi_0\rangle^{\otimes L} \langle \varphi_0| + \frac{1}{2} |\varphi_1\rangle^{\otimes L} \langle \varphi_1| \\ \hat{\rho}_S^{\text{out}} &= \frac{1}{2} |0\rangle \langle 0| + \frac{1}{2} |1\rangle \langle 1| + \frac{1}{2} |0\rangle \langle 1| \cdot |\xi^{(n)}| + \frac{1}{2} |1\rangle \langle 0| \cdot |\xi^{(n)}|.\end{aligned}\tag{176}$$

Density matrices $\hat{\rho}_{S E_f}^{\text{out}}$ and $\hat{\rho}_S^{\text{out}}$ do not pose any computational problems since their dyadics consist of mutually orthogonal vectors which can be easily formulated in a 2-dim and $(L+1)$ -dim computational basis, respectively. However, regarding the environmental density matrix $\hat{\rho}_{E_f}^{\text{out}}$ additional considerations are in order, since the states $|\varphi_0\rangle$ and $|\varphi_1\rangle$ are *per definitionem* not *a priori* orthogonal.

In order to gain computational access to in general non-orthogonal environmental states one first notes that the decoherence factor r indicates how strong particular E-states »violate« the orthonormality requirement necessary for an appropriate practical computability of $\hat{\rho}_{E_f}^{\text{out}}$ and its eigenvalue spectrum. In other words, by changing the value of ξ (and thus of r) one automatically manipulates the mutual orthogonality of E-states. Accordingly, we may stipulate that

$$|\varphi_1\rangle^{\otimes L} = c |\varphi_0\rangle^{\otimes L} + d |\varphi_0^\perp\rangle^{\otimes L}, \quad (\text{with } c, d \in \mathbb{C} \text{ and } \langle \varphi_0 | \varphi_0^\perp \rangle \stackrel{!}{=} 0)\tag{177}$$

violates the orthonormality requirement towards $|\varphi_0\rangle$ because of the contribution parallel to the $|\varphi_0\rangle$ -state, whereas $|\varphi_0^\perp\rangle$ represents its orthogonal counterpart. Using (177) $\hat{\rho}_{E_f}^{\text{out}}$ from (176) may be rewritten as

$$\begin{aligned}\hat{\rho}_{E_f}^{\text{out}} &= \frac{1}{2} |\varphi_0\rangle^{\otimes L} \langle \varphi_0| + \frac{1}{2} \left(c |\varphi_0\rangle^{\otimes L} + d |\varphi_0^\perp\rangle^{\otimes L} \right) \left({}^{\otimes L} \langle \varphi_0| c^* + {}^{\otimes L} \langle \varphi_0^\perp| d^* \right) \\ &= \frac{1}{2} |\varphi_0\rangle^{\otimes L} \langle \varphi_0| + \frac{1}{2} \left(|c|^2 |\varphi_0\rangle^{\otimes L} \langle \varphi_0| + c d^* |\varphi_0\rangle^{\otimes L} \langle \varphi_0^\perp| \right. \\ &\quad \left. + c^* d |\varphi_0^\perp\rangle^{\otimes L} \langle \varphi_0| + |d|^2 |\varphi_0^\perp\rangle^{\otimes L} \langle \varphi_0^\perp| \right),\end{aligned}\tag{178}$$

where $|c|^2 + |d|^2 = 1$ imposes a restriction on the overlaps within the decoherence factor r , since varying the probabilities $|c|^2$ and $|d|^2$ leads to different decoherence factors in $\hat{\rho}_{S E_f}^{\text{out}}$ and $\hat{\rho}_S^{\text{out}}$.

There are three types of decoherence behavior that one may expect from MI plots generated by means of (176) and (178):

1. Limit $\{|c|^2 = 0, |d|^2 = 1\}$: This leads to $\xi = 0$ and thus to $r = 0$ (perfect decoherence), since $\langle \varphi_0 | \varphi_1 \rangle = 0$ (vanishing overlaps between environmental states). We expect the MI plot w.r.t. f to display perfectly the darwinistic plateau from Zurek's qubit model (including the $2 \cdot H(S_{\text{class}})$ -peak) due to an ideal orthogonality of both environmental states. This kind of environment permits perfect storage of the entire classical information concerning S.
2. Limit $\{|c|^2 = 1, |d|^2 = 0\}$: This enforces $\xi = 1$ and $r = 1$ (absence of decoherence), implying that the entire E inhabits only one type of possible states (»one state E«), since $\langle \varphi_0 | \varphi_1 \rangle = 1$. In this case MI w.r.t. f should be a continuous zero-function $\text{MI}(f) = 0 \forall f$, indicating the incapability of E to store any classical information about S.
3. Limit $\{|c|^2 = 0.5, |d|^2 = 0.5\}$: The symmetrization of the overlap probabilities $|c|^2$ and $|d|^2$ generates a mixed environment with $\xi = 0.5$ and $r = (0.5)^{(n-L)}$. This time the MI plot w.r.t. f should exhibit a less distinct form of the »classicality plateau« corresponding to the value $\text{MI}(0 < f < 1) \leq H(S_{\text{class}})$, as well as a diminished »boundary peak« at $f = 1$ with $\text{MI}(f = 1) < 2 \cdot H(S_{\text{class}})$.

Indeed, Fig. 10 below confirms these expectations. MI $H(S : E_f)$ displays a typical darwinistic plateau saturated at $H(S : E_f) = H(S_{\text{class}}) = 1$ in case of perfect decoherence ($r = 0$), including the $2 \cdot H(S_{\text{class}})$ -peak at $f = 1$. This »boundary peak« of MI appears only if the evolved global S – E-state $\hat{\rho}_{S E_f}^{\text{out}}$ remains pure, which is precisely the case for (174) above. As the efficiency of decoherence decreases environmental states become mutually similar (undistinguishable), disabling E to store classical information $H(S_{\text{class}})$ attributed to S.

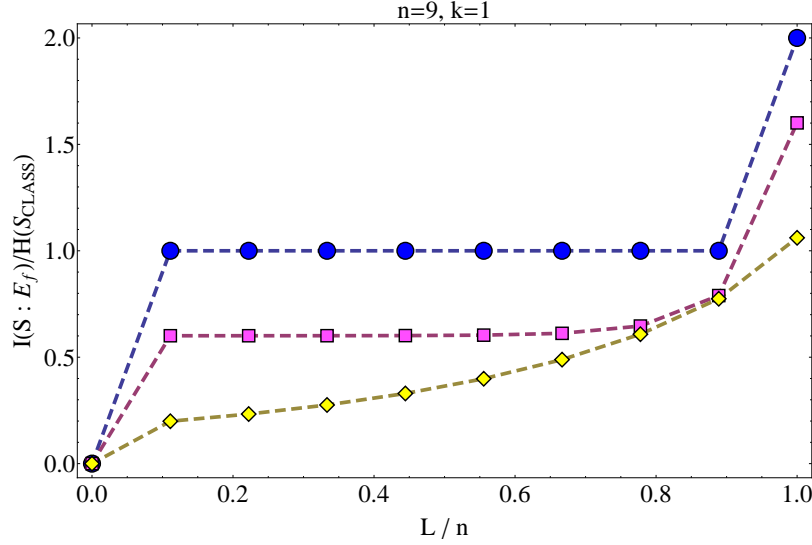


Figure 10: MI for an output state (174) of a $k = 1$ qubit S w.r.t. $f = L/n$ (with $0 \leq (L \in \mathbb{R}^+) \leq n$) of an $n = 9$ qubit E due to different decoherence factors r ($r = 0$, \bullet -dotted curve; $r = 0.5$, \blacksquare -dotted curve; $r = 0.9$, \blacklozenge -dotted curve).

Analogous conclusions can be drawn also for a $k = 2$ qubit system S , with main difference concerning the value classical information $H(S_{\text{CLASS}}) = 2$ and the density matrices $\hat{\rho}_{S E_f}^{\text{out}}$, $\hat{\rho}_S^{\text{out}}$ and $\hat{\rho}_{E_f}^{\text{out}}$ in (175):

$$\begin{aligned} \hat{\rho}_{S E_f}^{\text{out}} &= \sum_{i,j=0}^3 a_i a_j^* |i\rangle \langle j| \otimes |\varphi_i\rangle^{\otimes L} \langle \varphi_j| \cdot |\xi^{(n-L)}| \\ \hat{\rho}_{E_f}^{\text{out}} &= \sum_{i=0}^3 |a_i|^2 |\varphi_i\rangle^{\otimes L} \langle \varphi_i|, |a_i|^2 = 2^{-k} \\ \hat{\rho}_S^{\text{out}} &= \sum_{i,j=0}^3 a_i a_j^* |i\rangle \langle j| \cdot |\xi^{(n)}|, \end{aligned} \quad (179)$$

with a computational basis $\{|i\rangle, i \in (0, 1, 2, 3)\}$ of S and *a priori* non-orthogonal E-states $\{|\varphi_i\rangle, i \in (0, 1, 2, 3)\}$ that can be decomposed in parallel and orthogonal parts in accordance with (177): $|\varphi_i\rangle = \sum_{m \neq i=0}^{2^k-1} (A_m |\varphi_m\rangle + B_m |\varphi_m^\perp\rangle)$ ($A_m, B_m \in \mathbb{C}$).

Quantum Darwinism of $|\varphi_{S E_f}^{\text{out}}\rangle$ in the large n limit

All results of the previous subsection can be generalized w.r.t. the large n limit involving infinite number of E-qubits. The present subsection aims at showing that even in case of an imperfect decoherence of S ideal storage of its classical information can be achieved by allowing the number n of environmental qubits to grow unboundedly, since in this limit $n \rightarrow \infty$ *a priori* non-orthogonal states $\{|\varphi_i\rangle\}$ of E (see (177) above) tend to become mutually orthogonal.

In order to clarify this statement let us start again with a state $|\varphi_{S E_f}^{\text{out}}\rangle$ in (173). Each of the E-states $|\varphi_i\rangle^{\otimes n}$ correlated with a computational basis of S may be regarded as possessing an individual structure

$$|\varphi_i\rangle = A |e_i\rangle + B \sum_{l \neq i=0}^{2^k-1} |e_l\rangle \cdot (2^k - 1)^{-1/2}, \quad (A, B \in \mathbb{C}), \quad (180)$$

with 2^k basis vectors $\{|e_i\rangle\}$ satisfying $\langle e_i | e_j \rangle = \delta_{ij}$. (180) generalizes (177) by decomposing the particular E-state into an orthogonality preserving part weighted by A and a decoherence inducing contribution weighted by B , which generates deviations from the orthogonality requirement since it contains a sum of orthogonal vectors of the remaining $(2^k - 1)$ basis vectors $\{|e_l\rangle, l \neq i\}$. From the requirement $\langle \varphi_i | \varphi_i \rangle \stackrel{!}{=} 1$ we furthermore gain a constraint

$$\langle \varphi_i | \varphi_i \rangle \stackrel{!}{=} 1 \Rightarrow |A|^2 + |B|^2 \stackrel{!}{=} 1 \quad (181)$$

for the weighing prefactors in (180).

On the other hand, the overlap

$$\begin{aligned} \xi := \langle \varphi_m | \varphi_i \rangle &\stackrel{m \neq i}{=} \left(A^* \langle e_m | + B^* \sum_{l' \neq m=0}^{2^k-1} \langle e_{l'} | \cdot (2^k - 1)^{-1/2} \right) \left(A |e_i\rangle + B \sum_{l \neq i=0}^{2^k-1} |e_l\rangle \cdot (2^k - 1)^{-1/2} \right) \\ &= (2^k - 1)^{-1/2} \cdot (A^* B + A B^*) + |B|^2 \\ &= 2\Re(A^* B) \cdot (2^k - 1)^{-1/2} + |B|^2 \end{aligned} \quad (182)$$

allows one to express the decoherence factor of an n-qubit E as

$$r = |\langle \varphi_m | \varphi_i \rangle^n| \stackrel{m \neq i}{=} \left(2\Re(A^*B) \cdot (2^k - 1)^{-1/2} + |B|^2 \right)^n. \quad (183)$$

The limits $|B|^2 = 0 \Rightarrow r = 0$ and $|B|^2 = 1 \Rightarrow r = 1$ confirm that (183) indeed encapsulates an appropriate physical behavior of the decoherence factor $0 \leq r \leq 1$.

Now that we have seen that (180) describes decoherence adequately, we can readily reformulate the environmental part of $|\phi_{SE}^{\text{out}}\rangle$ from (173) as

$$\begin{aligned} |\varphi_i\rangle^{\otimes n} &= \left(A |e_i\rangle + B \cdot (2^k - 1)^{-1/2} \underbrace{\sum_{l \neq i=0}^{2^k-1} |e_l\rangle}_{:=|e_L\rangle} \right)^{\otimes n} \Rightarrow \\ |\varphi_i\rangle^{\otimes n} &= A^n |e_i\rangle^{\otimes n} + B^n \cdot (2^k - 1)^{-n/2} |e_L\rangle^{\otimes n} + \\ &\sum_{h=0}^n \left\{ A^h B^{(n-h)} \cdot (2^k - 1)^{-(n-h)/2} |e_i\rangle^{\otimes h} |e_L\rangle^{\otimes (n-h)} \right\}, \end{aligned} \quad (184)$$

allowing us to conclude (assuming the deviating weight to be comparably small $|B| \ll 1$ in relation to $|A|$) its convergence towards an orthogonality preserving part in the large n-limit:

$$\lim_{n \rightarrow \infty} |\varphi_i\rangle^{\otimes n} = A^n |e_i\rangle^{\otimes n}. \quad (185)$$

(185) reflects precisely the above statement from the beginning of this subsection we intended to prove. Thus, the environmental states $|\varphi_i\rangle^{\otimes n}$ converge towards mutual orthogonality even if we do not presuppose perfect decoherence to have previously »eliminated« the coherence overlaps ξ in (182), as long as one has the freedom of choosing the number of E-qubits arbitrarily high. \square

Finally, as pertaining to the results (184) and (185) we may consider the large n limits of $\hat{\rho}_{SEf=1}^{\text{out}}$ and $\hat{\rho}_{E_{f=1}}^{\text{out}}$ from (175)

$$\begin{aligned} \lim_{n \rightarrow \infty} \left\{ \hat{\rho}_{E_{f=1}}^{\text{out}} = \sum_{i=0}^{2^k-1} |a_i|^2 |\varphi_i\rangle^{\otimes n} \langle \varphi_i| \right\} \\ = \sum_{i=0}^{2^k-1} |a_i|^2 |e_i\rangle^{\otimes n} \langle e_i| \cdot |A|^{2n} \\ \lim_{n \rightarrow \infty} \left\{ \hat{\rho}_{SEf=1}^{\text{out}} \right\} = \sum_{i,i'=0}^{2^k-1} |A|^{2n} a_i a_{i'}^* |i\rangle \langle i'| \otimes |e_i\rangle^{\otimes n} \langle e_{i'}|, \end{aligned} \quad (186)$$

as well as the normalization condition $\text{Tr}_{SEf} \left(\lim_{n \rightarrow \infty} \left\{ \hat{\rho}_{SEf=1}^{\text{out}} \right\} \right) \stackrel{!}{=} 1$, which imposes a constraint on $|A|$:

$$\begin{aligned} \text{Tr}_{SEf} \left(\lim_{n \rightarrow \infty} \left\{ \hat{\rho}_{SEf=1}^{\text{out}} \right\} \right) \stackrel{!}{=} 1 &\Rightarrow \sum_{i=0}^{2^k-1} |A|^{2n} |a_i|^2 = 1 \\ &\Rightarrow |A| = \left(\underbrace{\sum_{i=0}^{2^k-1} |a_i|^2}_{:=1} \right)^{-1/(2n)} = 1. \end{aligned} \quad (187)$$

From (187) we definitely notice that in the large n limit $\lim_{n \rightarrow \infty} |A| = 1$, indicating the mutual orthogonality of environmental states. Thus, even if $1 \gg r \neq 0$, the »classicality plateau« of MI in Fig. 10 would increase with increasing number of E-qubits until it saturates at the maximum (»classical«) entropy value $H(S_{\text{class}})$ of S in the limiting case of infinite environments.

Environments consisting of perfectly distinguishable states represent an optimal measuring apparatus, capable of recognizing and storing information about all preferred states of S (\equiv its computational basis). Such »ideal« environments are therefore suitable for a demonstration of the concept of Quantum Darwinism and its effects. The redundancy R of an »ideal« n-qubit E is simply $R = 1/f_{cl} = n$, since already an environmental fraction of $f_{cl} = 1/n$ suffices to store the entire classical information about S. This is precisely the message of the »classicality plateau«: f_{cl} is to be regarded as a *minimal* fraction of E-qubits that has to be taken into account in order for the MI to reach the »saturation value« $H(S_{\text{class}})$. For »ideal« environments we thus encounter the most efficient storage of »S-classicality«.

8.1.2 Results of the CNOT-evolution

Decomposing $\hat{\rho}_{SE}^{\text{in}}$ for $n \gg k$ S-qubits by means of (170) and (only) linear independent $\hat{X}_{\lambda,i}$ from (365), after first orthonormalizing all $\hat{X}_{\lambda,i}$ in accord with the Gram-Schmidt algorithm (s. Appendix F and Appendix I), we obtain the CNOT-asymptotically evolved $\hat{\rho}_{SE}^{\text{out}}$ displayed in (404)-(408) of Appendix J.2. We consider in the following different inputs $\hat{\rho}_{SE}^{\text{in}}$ of the random unitary evolution and their PIPs obtained from the corresponding outputs $\hat{\rho}_{SE}^{\text{out}}$.

D) $\hat{\rho}_{SE}^{\text{in}} = \hat{\rho}_S^{\text{in}} \otimes \hat{\rho}_E^{\text{in}}$, **k-qubit pure** $\hat{\rho}_S^{\text{in}}, \hat{\rho}_E^{\text{in}} = |1_n\rangle \langle 1_n|$ (**Fig. 11, ■-dotted curve**), $\hat{\rho}_E^{\text{in}} = |0_n\rangle \langle 0_n|$ (**Fig. 17, ◆, ○, □-dotted curves**)

Numerous interesting conclusions can be obtained by looking at the behavior of MI with respect to the number n of E-qubits. For instance, within the maximal attractor space we need at least $n \geq 5$ E-qubits in order to see stable convergence of $I(S : E_{L=n})/H(S_{\text{class}})$, as indicated by the blue, ●-dotted curve associated with $\hat{\rho}_{SE}^{\text{in}} = |\Psi_S^{\text{in}}\rangle \langle \Psi_S^{\text{in}}| \otimes \hat{\rho}_E^{\text{in}}$, with $|\Psi_S^{\text{in}}\rangle = \sum_{m=0}^1 a_m |m\rangle$ ($|a_m|^2 = 2^{-1} \forall m$), $n > k = 1$ and $\hat{\rho}_E^{\text{in}} = |0_n\rangle \langle 0_n|$ in Fig. 11. However, for the minimal $\lambda = 1$ attractor subspace the same input state $\hat{\rho}_{SE}^{\text{in}}$ leads for $k = 1$ to the output state in (404) of Appendix J.2 with non-zero eigenvalues in (188) (valid $\forall 1 \leq L \leq n$, with $\epsilon_L := 2^{-2n+L} (2^{2(n-L)-1} - 1) |a_0|^2 |a_1|^2$ and a decoherence factor $0 \leq r := \langle s_1^{L=n} | \hat{\rho}_E^{\text{in}} | s_1^{L=n} \rangle = 2^{-n} \leq 1$)

$$\begin{aligned} \hat{\rho}_{SE}^{\text{out}} : \lambda_1^{SE} &= |a_1|^2 \cdot 2^{-L} \quad (2^L - 1 \text{ times}) \\ \lambda_{2/3}^{SE} &= \left(2^{-1} |a_0|^2 + |a_1|^2 \cdot 2^{-L+1} \right) \pm \sqrt{2^{-2} |a_0|^4 + |a_1|^4 \cdot 2^{-2(L+1)} - \epsilon_L} \\ \hat{\rho}_E^{\text{out}} : \lambda_1^E &= |a_0|^2 + |a_1|^2 \cdot 2^{-L}, \quad \lambda_2^E = |a_1|^2 \cdot 2^{-L} \quad (2^L - 1 \text{ times}) \\ \hat{\rho}_S^{\text{out}} : \lambda_{1/2}^S &= \frac{1}{2} \pm \sqrt{\frac{1}{4} - |a_0|^2 |a_1|^2 (1 - 2^{-2n})}, \end{aligned} \quad (188)$$

whose PIP is given by the yellow, ◆-dotted curve in Fig. 17. Apparently, the absence of the $\lambda = -1$ attractor subspace is crucial for the appearance of Quantum Darwinism in case of $\hat{\rho}_E^{\text{in}} = |0_n\rangle \langle 0_n|$.

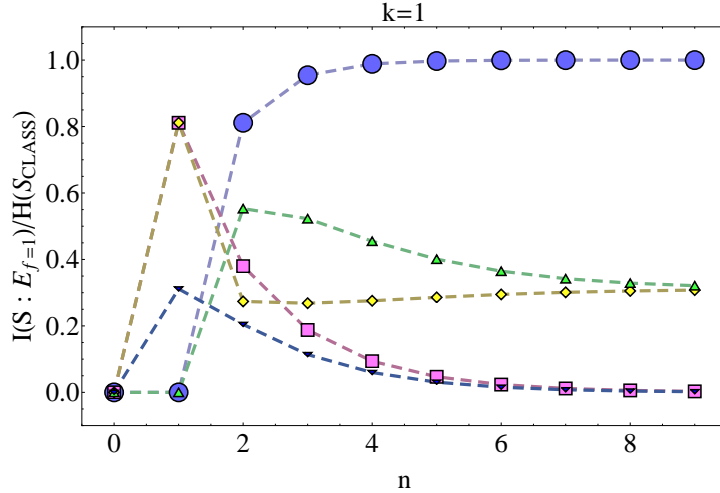


Figure 11: $I(S : E_{L=n})/H(S_{\text{class}})$ vs n after random iterative $\hat{u}_j^{(\phi=\pi/2)}$ -evolution of $\hat{\rho}_{SE}^{\text{in}} = |\Psi_S^{\text{in}}\rangle \langle \Psi_S^{\text{in}}| \otimes \hat{\rho}_E^{\text{in}}$ ($N \gg 1$), with a $k = 1$ qubit $|\Psi_S^{\text{in}}\rangle = \sum_{m=0}^1 a_m |m\rangle$ ($|a_m|^2 = 2^{-1} \forall m$) and different $\hat{\rho}_E^{\text{in}}$ (with $\geq 2(n-1)$ E-bindings). $I(S : E_{L=n})/H(S_{\text{class}})$ vs n for $\hat{\rho}_E^{\text{in}} = |0_n\rangle \langle 0_n|$ (blue, ●-dotted curve, 0 E-bindings) is also displayed.

On the other hand, the ○-dotted and the □-dotted curve in Fig. 17 also demonstrate what happens within the minimal $\lambda = 1$ attractor subspace for the output state in (404) of Appendix J.2 with $k \geq 2$ S-qubits: since in the limit $n \gg k > 1$ (404) of Appendix J.2 leads to the same form (204) as (395) of J.1, we see that with increasing number k of S-qubits (i.e. in the limit $n \sim k \gg 1$) $I(S : E_{L=n})/H(S_{\text{class}})$ from (404) of Appendix J.2 will also behave

(with $|a_i|^2 = 2^{-k} \forall i \in \{0, \dots, 2^k - 1\}$) as

$$I(S : E_{L=n \sim k \gg 1}) / H(S_{\text{class}}) \sim 2^{-k}.$$

Accordingly, one also has (again with $|a_i|^2 = 2^{-k} \forall i \in \{0, \dots, 2^k - 1\}$)

$$I(S : E_{L=n \gg k \gg 1}) / H(S_{\text{class}}) = 0.$$

In Fig. 11 we also see what happens with MI if $\hat{\rho}_E^{\text{in}}$, such as $\hat{\rho}_E^{\text{in}} = |1_n\rangle \langle 1_n|$, contains only E-registry states that do not participate within a given, in this case minimal $\lambda = 1$ attractor subspace: $I(S : E_{L=n}) / H(S_{\text{class}})$ (red, ■-dotted curve) tends to zero in the limit $n \gg k$. This can be easily explain by taking into account the fact that $\hat{\rho}_{SE_{L=n}}^{\text{out}}$ from (405) in Appendix J.2 yields the (non-zero) eigenvalues

$$\begin{aligned} \lambda_1^{SE} &= |a_0|^2 (2^n - 1)^{-1} \text{ (1 times)}; \lambda_2^{SE} = |a_1|^2 2^{-n} (2^n - 1 \text{ times}); \lambda_3^{SE} = |a_0|^2 (2^n - 1)^{-1} 2^{3-n} + |a_1|^2 2^{-n} \text{ (1 times)} \\ \lambda_1^E &= |a_1|^2 2^{-n} \text{ (1 times)}; \lambda_2^E = 2^{-n} + |a_0|^2 (2^n - 1)^{-1} 2^{-n} (2^n - 1 \text{ times}) \\ \lambda_{1/2}^S &= 2^{-1} \pm \sqrt{2^{-2} - |a_0|^2 |a_1|^2 (1 - 2^{-2n})} \end{aligned}$$

and acquires for a $k = 1$ qubit S the form

$$\lim_{n \gg k=1} \hat{\rho}_{SE_{L=n}}^{\text{out}} = 2^{-n} \cdot \sum_{m=0}^1 |a_m|^2 |m\rangle \langle m| \otimes \hat{I}_n, \quad (189)$$

in the limit $n \gg k = 1$, one therefore obtains $H(S : E_{L=n \gg k=1}) = H(E_{L=n \gg k=1}) + H(S_{\text{class}})$. Thus, we obtain $\lim_{n \gg k=1} I(S : E_{L=n}) / H(S_{\text{class}}) = 0$ and conclude that $\hat{\rho}_E^{\text{in}}$ which are not contained in ("recognized" by) the minimal $\lambda = 1$ attractor subspace do not contribute to $I(S : E_L) / H(S_{\text{class}})$ in the limit $n \gg k = 1$. Also, since for $k > 1$ $\hat{\rho}_{SE_{L=n}}^{\text{out}}$ from (405) in Appendix J.2 leads in the limit $n \gg k \geq 1$ to (189) with $m \in \{0, \dots, 2^k - 1\}$, one may conclude that $\hat{\rho}_{SE_{L=n}}^{\text{out}}$ from (405) in Appendix J.2 leads to $\lim_{n \gg k \geq 1} I(S : E_{L=n}) / H(S_{\text{class}}) = 0 \forall k$.

II) $\hat{\rho}_{SE}^{\text{in}} = \hat{\rho}_S^{\text{in}} \otimes \hat{\rho}_E^{\text{in}}$, $k = 1$ -qubit pure $\hat{\rho}_S^{\text{in}}$, $\hat{\rho}_E^{\text{in}} = 2^{-1}(|0_n\rangle \langle 0_n| + |1_n\rangle \langle 1_n|)$ (Fig. 11, ◆-dotted curve)

From Fig. 11 (yellow, ◆-dotted curve) we also conclude that this type of $\hat{\rho}_{SE}^{\text{in}}$ never leads within the minimal $\lambda = 1$ attractor subspace to $I(S : E_{L=n}) / H(S_{\text{class}}) = 1$ in the limit $n \gg k$, since in this case the corresponding $\hat{\rho}_{SE}^{\text{out}}$ from (406) in Appendix J.2 acquires the form

$$\lim_{n \gg k} \hat{\rho}_{SE_{L=n}}^{\text{out}} = |a_0|^2 |0\rangle \langle 0| \otimes \left\{ \hat{I}_n 2^{-n-1} + \frac{1}{2} |0_n\rangle \langle 0_n| \right\} + |a_1|^2 |1\rangle \langle 1| \otimes 2^{-n} \cdot \hat{I}_n, \quad (190)$$

which always yields

$$\begin{aligned} \lim_{n \gg k} H(S, E_{L=n}) &= -\frac{|a_0|^2}{2} (1 + 2^{-n}) \log_2 \left(\frac{|a_0|^2}{2} (1 + 2^{-n}) \right) - (2^n - 1) \frac{|a_0|^2}{2^{1+n}} \log_2 \frac{|a_0|^2}{2^{1+n}} - |a_1|^2 \log_2 \frac{|a_1|^2}{2^n} \\ &\approx_{n \gg 1} -\frac{|a_0|^2}{2} \log_2 \frac{|a_0|^2}{2} + |a_1|^2 n - |a_1|^2 \log_2 |a_1|^2 - \frac{|a_0|^2}{2} \log_2 \frac{|a_0|^2}{2^{1+n}} \\ &> \lim_{n \gg k} H(E_{L=n}) = - (2^n - 1) \left(\frac{|a_0|^2}{2^{1+n}} + \frac{|a_1|^2}{2^n} \right) \log_2 \left(\frac{|a_0|^2}{2^{1+n}} + \frac{|a_1|^2}{2^n} \right) \\ &\quad - \left\{ \frac{|a_0|^2}{2} (1 + 2^{-n}) + \frac{|a_1|^2}{2^n} \right\} \log_2 \left\{ \frac{|a_0|^2}{2} (1 + 2^{-n}) + \frac{|a_1|^2}{2^n} \right\} \\ &\approx_{n \gg 1} -\frac{|a_0|^2}{2} \log_2 \frac{|a_0|^2}{2} + |a_1|^2 n - |a_1|^2 \log_2 \left(\frac{|a_0|^2}{2} + |a_1|^2 \right) - \frac{|a_0|^2}{2} \log_2 \left(\frac{|a_0|^2}{2^{1+n}} + \frac{|a_1|^2}{2^n} \right) \\ &\quad \underbrace{\quad \quad \quad}_{:=c_1 < -|a_1|^2 \log_2 |a_1|^2} \quad \underbrace{\quad \quad \quad}_{:=c_2 < -\frac{|a_0|^2}{2} \log_2 \frac{|a_0|^2}{2^{1+n}}} \end{aligned}$$

(as can be easily confirmed from the corresponding eigenspectra of $\lim_{n \gg k} \hat{\rho}_{SE_{L=n}}^{\text{out}}$ and $\lim_{n \gg k} \hat{\rho}_{SE}^{\text{out}}$, s. also (226) below). This means that correlation terms in (406) from Appendix J.2, that we deliberately ignored in (190), force $I(S : E_{L=n}) / H(S_{\text{class}})$ to converge to the MI-value $I(S : E_{L=n}) / H(S_{\text{class}}) = 0.3$ in the limit $n \gg k$. The same occurs if we choose $|\Psi_E^{\text{in}}\rangle = 2^{-1/2} \cdot (|0_n\rangle + |1_n\rangle)$ as an environmental input state (green, ▲-dotted curve in Fig. 11), since its $\hat{\rho}_{SE}^{\text{out}}$ (s. again (406) in Appendix J.2) acquires in the limit $n \gg k$ the same form (190). Thus, no Quantum Darwinism appears for these types of $\hat{\rho}_E^{\text{in}}$.

III) $\hat{\rho}_{SE}^{\text{in}} = \hat{\rho}_S^{\text{in}} \otimes \hat{\rho}_E^{\text{in}}$, $k = 1$ -qubit pure $\hat{\rho}_S^{\text{in}}$, $\hat{\rho}_E^{\text{in}} = 2^{-n} \hat{I}_n$ (Fig. 11, ▼-dotted curve)

As in (227) below, $\hat{\rho}_{SE}^{\text{out}}$ from (407) of Appendix J.2 leads in the limit $n \gg k$ to

$$\lim_{n \gg k} \hat{\rho}_{SE}^{\text{out}} = (|a_0|^2 |0\rangle \langle 0| + |a_1|^2 |1\rangle \langle 1|) \otimes 2^{-n} \hat{I}_n, \quad (191)$$

yielding $H(S, E_{L=n \gg k}) = H(S_{\text{class}}) + H(E_{L=n \gg k}) = H(S_{\text{class}}) + n$, i.e. completely mixed $\hat{\rho}_E^{\text{in}}$ leads also within the minimal $\{\lambda = 1\}$ attractor subspace to $I(S : E_{L=n \gg k}) / H(S_{\text{class}}) = 0$ (s. Fig. 11, blue, ▼-dotted curve).

IV) $|\psi_{SE}^{\text{in}}\rangle = a|0_{k=1}\rangle \otimes |s_1^{L=n}\rangle + b|1_{k=1}\rangle \otimes |s_2^{L=n}\rangle$ (Fig. 17, ◆-dotted curve)

The output state $\hat{\rho}_{SE}^{\text{out}}$ from (408) of Appendix J.2 (emerging from the random unitary evolution of this entangled $\hat{\rho}_{SE}^{\text{in}}$) and its eigenspectrum indicate that $\forall 0 < L < n$ $H(S, E_L) - H(E_L) = -\frac{1}{2} \log_2 \frac{1}{2} + (1 - x_L) \log_2 (1 - x_L) > 0$ (where $x_L := 2^{n-L-1} \cdot (2^n - 1)^{-1}$). In other words, the corresponding PIP has the same behavior as displayed by the blue, ▼-dotted curve in Fig. 15. Therefore, without the $\lambda = -1$ attractor subspace the minimal $\lambda = 1$ attractor subspace does not suffice to ensure that Quantum Darwinism appears, as is the case with the maximal attractor space discussed in subsection 8.3 below.

On the other hand, if we choose $\hat{\rho}_{SE}^{\text{in}} = \hat{\rho}_S^{\text{in}} \otimes \hat{\rho}_E^{\text{in}}$ as an input in (170), with $\hat{\rho}_E^{\text{in}} = |s_1^{L=n}\rangle \langle s_1^{L=n}|$, $\hat{\rho}_S^{\text{in}} = |a|^2 |0\rangle \langle 0| + a \cdot b * |1\rangle \langle 0| + a * b |0\rangle \langle 1| + |b|^2 |1\rangle \langle 1|$ (and $r = 1$, i.e. no decoherence), we obtain the output states and their respective eigenvalues as displayed in Tab. 3 below.

State	Matrix Form	Eigenvalues
$\hat{\rho}_S^{\text{out}}$	$ a ^2 0\rangle \langle 0 + b ^2 1\rangle \langle 1 $ $+ a \cdot b * 0\rangle \langle 1 + a * b 1\rangle \langle 0 $	$\lambda_{1/2} = \frac{1}{2} \pm \frac{1}{2}$
$\hat{\rho}_E^{\text{out}}$	$ s_1^{L=n}\rangle \langle s_1^{L=n} $	$\begin{cases} \lambda_i = 0 \text{ for } i = 1, \dots, 2^n - 1 \\ \lambda_i = 1 \text{ for } i = 2^n \end{cases}$
$\hat{\rho}_{S,E}^{\text{out}}$	$\begin{cases} a ^2 0\rangle \langle 0 + b ^2 1\rangle \langle 1 \\ + a * b 0\rangle \langle 1 \\ + a \cdot b * 1\rangle \langle 0 \end{cases} \otimes s_1^{L=n}\rangle \langle s_1^{L=n} $	$\begin{cases} \lambda_i = 0 \text{ for } i = 1, \dots, 2^{n+1} - 1 \\ \lambda_{2^{n+1}} = 1 \end{cases}$

Table 3: Output states $\hat{\rho}_S^{\text{out}}$, $\hat{\rho}_E^{\text{out}}$ and $\hat{\rho}_{S,E}^{\text{out}}$ for input configuration $\hat{\rho}_{SE}^{\text{in}} = \hat{\rho}_S^{\text{in}} \otimes \hat{\rho}_E^{\text{in}}$ with $\hat{\rho}_E^{\text{in}} = |s_1^{L=n}\rangle \langle s_1^{L=n}|$.

Since $|s_1^{L=n}\rangle$ is invariant under CNOT-transformations and $r = 1$ one would expect that $I(S : E) = 0 \forall n$. Indeed, calculating the corresponding entropies we arrive at:

$$\left. \begin{aligned} H(E^{\text{out}}) &= 0 \\ H(S^{\text{out}}) &= 0 \\ H(S^{\text{out}}, E^{\text{out}}) &= 0 \end{aligned} \right\} I(S^{\text{out}} : E^{\text{out}}) = 0 - 0 + 0 = 0. \quad (192)$$

This result holds for all $k \geq 1$ qubits of S . It is apparent that the $|s_1^{L=n}\rangle \langle s_1^{L=n}|$ -state of E does not change the input product state due to its invariance under CNOT-transformations. This was also the case for Zurek's qubit model of QD.

An interesting choice for an environment is $\hat{\rho}_{SE}^{\text{in}} = \hat{\rho}_S^{\text{in}} \otimes \hat{\rho}_E^{\text{in}}$ as an input in (170), with $\hat{\rho}_E^{\text{in}} = |s_2^{L=n}\rangle \langle s_2^{L=n}|$, $\hat{\rho}_S^{\text{in}} = |a|^2 |0\rangle \langle 0| + a \cdot b * |1\rangle \langle 0| + a * b |0\rangle \langle 1| + |b|^2 |1\rangle \langle 1|$ and $r = 0$, leading us to output states and eigenvalues outlined in Tab. 4 below.

Thus, calculating the corresponding entropies one obtains:

$$\left. \begin{aligned} H(E^{\text{out}}) &= \log_2 (2^n - 1) \\ H(S^{\text{out}}) &= -|a|^2 \log_2 |a|^2 - |b|^2 \log_2 |b|^2 = H(S_{\text{class}}) \\ H(S^{\text{out}}, E^{\text{out}}) &= H(E^{\text{out}}) + H(S_{\text{class}}) \end{aligned} \right\} I(S : E) = H(S_{\text{class}}) + H(E^{\text{out}}) - H(S_{\text{class}}) - H(E^{\text{out}}) = 0. \quad (193)$$

(192) indicates that even if we find an input $\hat{\rho}_E^{\text{in}}$ that constrains the decoherence factor r to a certain constant value $\forall n$, we are, similar to Zurek's initial approach, not able to extract any information about an open system S that has undergone iterative random unitary evolution from $I(S : E)$ if we assign to $\hat{\rho}_E^{\text{in}}$ a CNOT-invariant state $|s_1^{L=n}\rangle \langle s_1^{L=n}|$. Also, (193) is precisely the conclusion which remains valid in the course of Zurek's idealized qubit-model: in case of perfect (effective) decoherence one would expect the MI to vanish, indicating that the entire uncertainty about S cannot

State	Matrix Form	Eigenvalues
$\hat{\rho}_S^{\text{out}}$	$ a ^2 0\rangle \langle 0 + b ^2 1\rangle \langle 1 $	$\lambda_1 = a ^2, \lambda_2 = b ^2$
$\hat{\rho}_E^{\text{out}}$	$\hat{I}_n \left[a ^2 2^{-n} + 2^{-2n} a ^2 (1 - 2^{-n})^{-1} + b ^2 (2^n - 1)^{-1} \right] +$ $- s_1^{L=n}\rangle \langle s_1^{L=n} \left[2^{-n} a ^2 (1 - 2^{-n})^{-1} + b ^2 (2^n - 1)^{-1} \right]$	$\lambda_i = (2^n - 1)^{-1}$ for $i = 1, \dots, 2^n - 1$ $\lambda_{2^n} = 0$
$\hat{\rho}_{S,E}^{\text{out}}$	$\left(a ^2 2^{-n} + 2^{-2n} a ^2 (1 - 2^{-n})^{-1} \right) 0\rangle \langle 0 \otimes \hat{I}_n$ $+ 1\rangle \langle 1 \otimes \hat{I}_n b ^2 (2^n - 1)^{-1}$ $- 2^{-n} a ^2 (1 - 2^{-n})^{-1} 0\rangle \langle 0 \otimes s_1^{L=n}\rangle \langle s_1^{L=n} $ $- b ^2 (2^n - 1)^{-1} 1\rangle \langle 1 \otimes s_1^{L=n}\rangle \langle s_1^{L=n} $	$\lambda_i = (2^n - 1)^{-1} a ^2$ for $i = 1, \dots, 2^n - 1$ $\lambda_i = (2^n - 1)^{-1} b ^2$ for $i = 2^n, \dots, 2^{1+n} - 2$ $\lambda_i = 0$ for $i = (2^{n+1} - 1), 2^{1+n}$

Table 4: Output states $\hat{\rho}_S^{\text{out}}$, $\hat{\rho}_E^{\text{out}}$ and $\hat{\rho}_{S,E}^{\text{out}}$ for input configuration $\hat{\rho}_{S,E}^{\text{in}} = \hat{\rho}_S^{\text{in}} \otimes \hat{\rho}_E^{\text{in}}$ with a one-qubit pure $\hat{\rho}_S^{\text{in}}$ and $\hat{\rho}_E = 2^{-n} (|0\rangle - |1\rangle)^{\otimes n} (|0\rangle - |1\rangle)^{\otimes n}$.

be encoded within E if we choose an environmental input-state $\hat{\rho}_E^{\text{in}} = |s_2^{L=n}\rangle \langle s_2^{L=n}|$ orthogonal to the CNOT-invariant input-state $\hat{\rho}_E^{\text{in}} = |s_1^{L=n}\rangle \langle s_1^{L=n}|$. (193) holds $\forall k \geq 1$ qubits of S. Since both $\{|s_1^{L=n}\rangle, |s_2^{L=n}\rangle\}$ are CNOT-symmetry states, we will obtain within the random unitary model of QD for $\hat{\rho}_{S,E}^{\text{in}}$ leading to (192) and (193) vanishing MI-values $\forall L \leq n$ and $\forall N$.

The decoherence factor r may be used as a criterion when we have to decide whether a proposed input state $\hat{\rho}_{S,E}^{\text{in}} = \hat{\rho}_S^{\text{in}} \otimes \hat{\rho}_E^{\text{in}}$ is to be regarded as QD-conformal or not, since r has to converge to zero in the large n limit in order to represent physical decoherence processes. This fact allows us to rule out numerous input states of the environment $\hat{\rho}_E^{\text{in}}$ in advance as QD-suppressing without being forced to examine their eigenvalue spectra in great detail. As an illustration let us consider the state $\hat{\rho}_E^{\text{in}} = |\tilde{\phi}_n\rangle \langle \tilde{\phi}_n| \cdot (1 - 2^{-n})^{-1}$ as a possible environmental input state (with $|\tilde{\phi}_n\rangle = |s_1^{L=n}\rangle - 2^{-n/2} |0_n\rangle$). Is this state QD-conformal? Instead of dealing with the eigenvalue spectrum, we may also discuss the decoherence factor r of $\hat{\rho}_E^{\text{in}}$, which in this case takes the form $r = (1 - 2^{-n})$. In the large n limit we get $\lim_{n \rightarrow \infty} r = 1$, corresponding to a rather inappropriate behavior from the point of view of QD, according to which an open system S should tend to become more coherent when enlarging its environment, which is actually the opposite to the common understanding of the decoherence process [2]. Therefore we may ignore the state $\hat{\rho}_E^{\text{in}} = |\tilde{\phi}_n\rangle \langle \tilde{\phi}_n| \cdot (1 - 2^{-n})^{-1}$ as QD-suppressing and unphysical, which would also be confirmed by its eigenvalue spectrum, containing a subset of negative eigenvalues. Other potential, non-physical »input choices« for the state $\hat{\rho}_E$ that can be rejected using the introduced »decoherence« argument, are summarized in Tab. 5 below.

$\hat{\rho}_E^{\text{in}}$	Remark
$\hat{\rho}_E^{\text{in}} = (s_1^{L=n}\rangle \langle s_1^{L=n} - \tilde{\phi}_n\rangle \langle \tilde{\phi}_n) \cdot 2^{-n}$	$r = 2 - 2^{-n} \Rightarrow$ $\lim_{n \rightarrow \infty} r = 2$
$\hat{\rho}_E^{\text{in}} = -(\tilde{\phi}_n\rangle \langle \tilde{\phi}_n - s_2^{L=n}\rangle \langle s_2^{L=n}) \cdot 2^{-n}$	$r = -2^{-n} (1 - 2^{-n})^2 \Rightarrow$ $r(n=0) = r(n \gg 1) = 0$ $r < 0$ for $n \in]0, \infty[$
$\hat{\rho}_E^{\text{in}} = (\tilde{\phi}_n\rangle \langle s_1^{L=n} + s_1^{L=n}\rangle \langle \tilde{\phi}_n) \cdot (2 - 2^{-n})^{-1}$	$r = 1 - \frac{2^{-n}}{2 - 2^{-n}} \Rightarrow$ $\lim_{n \rightarrow \infty} r = 1$

Table 5: Non-physical $\hat{\rho}_E^{\text{in}}$ -states

Nevertheless, there certainly are unphysical states $\hat{\rho}_E^{\text{in}}$ that can be rejected only after a detailed exploration of their eigenspectrum, such as

$$\begin{aligned}
\hat{\rho}_E^{\text{in}} &= (|s_1^{L=n}\rangle \langle s_1^{L=n}| + |\tilde{\phi}_n\rangle \langle \tilde{\phi}_n|) \cdot (2 - 2^{-n})^{-1}, r = 2 \cdot (2 - 2^{-n})^{-1} - 2^{-n} \\
\hat{\rho}_E^{\text{in}} &= (|\tilde{\phi}_n\rangle \langle \tilde{\phi}_n| + |s_2^{L=n}\rangle \langle s_2^{L=n}|) \cdot (2 - 2^{-n})^{-1}, r = (2 - 2^{-n})^{-1} - 2^{-n} \\
\hat{\rho}_E^{\text{in}} &= -(|\tilde{\phi}_n\rangle \langle s_2^{L=n}| + |s_2^{L=n}\rangle \langle \tilde{\phi}_n|) \cdot 2^{n-1}, r = 0,
\end{aligned} \tag{194}$$

which are characterized by a non-physical eigenspectrum, containing negative eigenvalues.

The only physically suitable combination of the CNOT-invariant state $|s_1^{L=n}\rangle$ and its orthogonal counterpart $|s_2^{L=n}\rangle$ (with $\langle s_2^{L=n} | s_1^{L=n} \rangle = 0$) appears to be

$$\hat{\rho}_E^{\text{in}} = \frac{1}{2} (|s_1^{L=n}\rangle \langle s_1^{L=n}| + |s_2^{L=n}\rangle \langle s_2^{L=n}|) \Rightarrow r = \frac{1}{2}. \quad (195)$$

(s. also (410) in Appendix J.2 for further details. A slightly different superposition $|s_1^{L=n}\rangle \langle s_1^{L=n}| - |s_2^{L=n}\rangle \langle s_2^{L=n}|$ could not qualify for a physical E input state because $\text{Tr}_E (|s_1^{L=n}\rangle \langle s_1^{L=n}| - |s_2^{L=n}\rangle \langle s_2^{L=n}|) = 0$). (195) and (410) from Appendix J.2 indicate that MI should tend to zero in the large n limit if we let the corresponding $\hat{\rho}_E^{\text{in}}$ state interact with a pure k qubit system $\hat{\rho}_S^{\text{in}}$ via iterative CNOT applications. Since $r = 0.5$ leads solely to partial decoherence of $\hat{\rho}_S^{\text{in}} \forall n$, we may conclude that $I(S_{\text{out}} : E_{\text{out}})$ emerging from an input environment (195) should remain constant $\forall n \geq 1$ after attaining a certain value < 1 for an $n = 1$ qubit environment. Indeed, when looking at (410) from Appendix J.2 with $n \geq k = 1$ and $|a_0|^2 = |a_1|^2 = 1/2$ we obtain (non-zero subsets of) eigenspectra

$$\begin{aligned} \hat{\rho}_{SE}^{\text{out}} : \lambda_1^{SE} &= 2^{-1} \text{ (1 times)}, \lambda_2^{SE} = (2^{k+n+1} - 4)^{-1} \text{ (2}^{k+n} - 2 \text{ times)} \\ \hat{\rho}_E^{\text{out}} : \lambda_1^E &= 2^{-1} \text{ (1 times)}, \lambda_2^E = (2^{n+1} - 2)^{-1} \text{ (2}^n - 1 \text{ times)} \\ \hat{\rho}_S^{\text{out}} : \lambda_1^S &= 3/4, \lambda_2^S = 1/4, \end{aligned} \quad (196)$$

from which it immediately follows that $\forall L = n \gg k = 1$

$$\begin{aligned} H(S, E_{L=n}) &= H(E_{L=n}) + 2^{-1} = 1 + 2^{-1} \cdot \log_2(2^n - 1) + 2^{-1} \\ H(S) &= 4^{-1} \cdot \log_2 4^{-1} - 3 \cdot 4^{-1} \cdot \log_2(3 \cdot 4^{-1}) = 0.811 < H(S_{\text{class}}) = 1 \Rightarrow \\ I(S : E_{L=n}) &= 0.311 < H(S_{\text{class}}), I(S : E_{L=0}) = H(S) = 0.811, \end{aligned} \quad (197)$$

which is illustrated in Fig. 12 below.

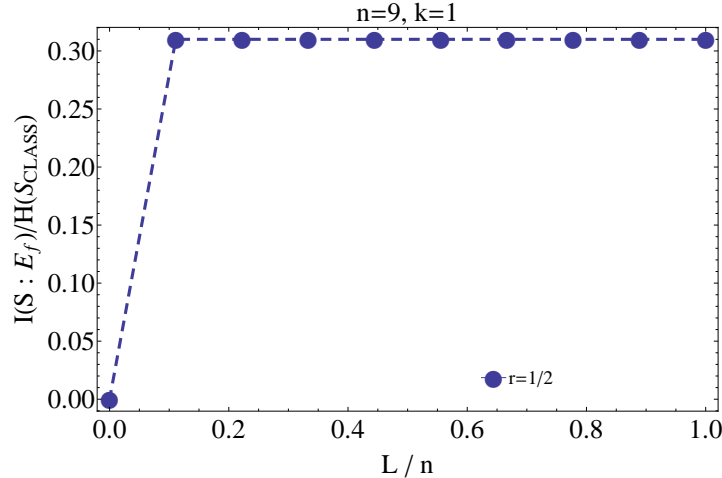


Figure 12: PIP for the random unitary CNOT-evolution of $\hat{\rho}_{SE}^{\text{in}} = \hat{\rho}_S^{\text{in}} \otimes \hat{\rho}_E^{\text{in}}$ ($N \gg 1$), with a pure $k = 1$ qubit system $\hat{\rho}_S^{\text{in}}$, $n = 9$ qubit $\hat{\rho}_E^{\text{in}} = \frac{1}{2} (|s_1^{L=n}\rangle \langle s_1^{L=n}| + |s_2^{L=n}\rangle \langle s_2^{L=n}|)$, $H(S) = 0.811 < H(S_{\text{class}})$ and a symmetric probability distribution $|a_0|^2 = |a_1|^2 = 1/2$ for each diagonal element of $\hat{\rho}_S^{\text{in}}$, $r = \frac{1}{2}$.

The constant MI-plateau at $I(S : E_{L=n}) = 0.311 < 1$ in Fig. 12 arises due to cancellations of numerous non-diagonal, partly excited matrix elements of $\hat{\rho}_E^{\text{in}}$ in (195), leaving the ground state and the completely excited dyadics (projectors) $|0_n\rangle \langle 0_n|$ and $|1_n\rangle \langle 1_n|$ of E as main contributions to the final asymptotic state of the entire S-E-system. This interplay between the projectors to the ground and totally excited E-state forces the MI to reside at the $0.31 \cdot H(S_{\text{class}})$ -value for pure $k = 1$ qubit systems S , i.e. no QD.

V) $\hat{\rho}_{SE}^{\text{in}} = \hat{\rho}_S^{\text{in}} \otimes \hat{\rho}_E^{\text{in}}$, $k = 2$ -qubit pure Bell-state $|\Psi_S^{\text{in}}\rangle = 2^{-1/2} (|0\rangle + |2^{k=2} - 1\rangle)$, $\hat{\rho}_E^{\text{in}} = |0_n\rangle \langle 0_n|$ (Fig. 13, •-dotted curve)

Introducing entanglement into $\hat{\rho}_S^{\text{in}}$ by starting, for instance, with a Bell-like $k = 2$ qubit S-input state and a ground state $\hat{\rho}_E^{\text{in}}$ we obtain the output state $\hat{\rho}_{SE}^{\text{out}}$ from (411) in Appendix J.2, which is, in the limit $n \gg k$ dominated by the approximated expression

$$\lim_{n \gg k} \hat{\rho}_{SE}^{\text{out}} = \frac{1}{2} |0\rangle \langle 0| \otimes |0_n\rangle \langle 0_n| + |3\rangle \langle 3| \otimes 2^{-n-1} \cdot \hat{I}_n. \quad (198)$$

Comparing (189) with (198), we expect the MI of the latter to exceed $I(S : E_L)$ obtained from (189) $\forall L \leq n$, since in (198), similar to (190), not all diagonal S-subspaces are correlated with \hat{I}_n . Indeed, the PIP in Fig. 13 confirms this expectation when compared with the ■-dotted curve in Fig. 11.

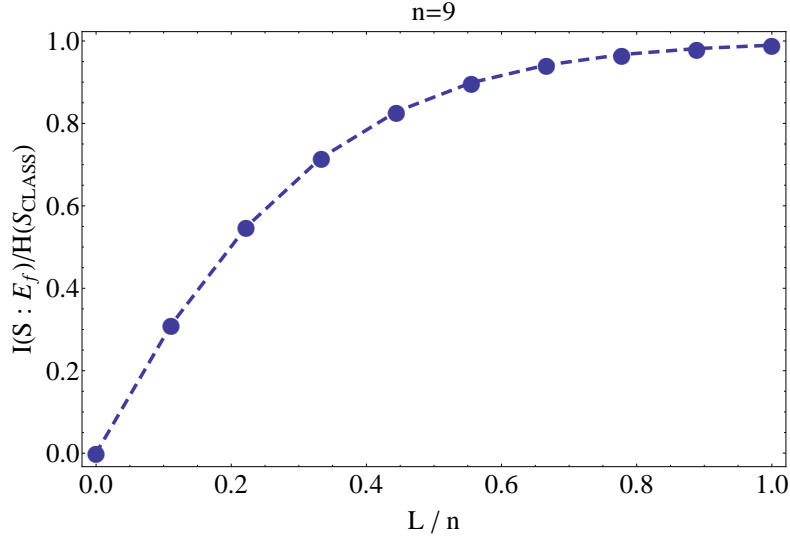


Figure 13: PIP for the random unitary CNOT-evolution of $\hat{\rho}_{SE}^{\text{in}} = \hat{\rho}_S^{\text{in}} \otimes \hat{\rho}_E^{\text{in}}$ ($N \gg 1$), with a pure $k = 2$ qubit Bell-system $|\Psi_S^{\text{in}}\rangle = 2^{-1/2} (|0\rangle + |2^{k=2}-1\rangle)$, $n = 9$ qubit $\hat{\rho}_E^{\text{in}} = |0_n\rangle \langle 0_n|$, $H(S) = 1 = H(S_{\text{class}}^{k=2})$ and a probability distribution $\{|a_0|^2 = |a_3|^2 = 1/2, |a_1|^2 = |a_2|^2 = 0\}$ for diagonal elements of $\hat{\rho}_S^{\text{in}}$, $r = 2^{-n}$. The same PIP occurs also for the random unitary CNOT-evolution of $|\Psi_{SE}^{\text{in}}\rangle = 2^{-1/2} (|0_{k=1}0_n\rangle + |1_{k=1}1_n\rangle)$, s. main text.

Unfortunately, the Shannon-entropy $H(S_{\text{class}}^{k=1})$ by which we divide the MI in Fig. 13 corresponds to the amount of the »classical« information about a $k = 1$ qubit S and not to the Shannon-entropy $H(S_{\text{class}}^{k=2})$ of an unentangled, decohered and maximally mixed $k = 2$ qubit system S, i.e. $H(S_{\text{class}}) = H(S_{\text{class}}^{k=1}) \neq H(S_{\text{class}}^{k=2})$. Thus, as in the course of Zurek's QD-model from section 7, entanglement within $\hat{\rho}_S^{\text{in}}$ tends to a priori decrease the amount of the »classical« information about S that can be transferred to E, which collides with the QD-condition (155). Accordingly, random unitary evolution involving IDs with mutually interacting E-qubits also does not lead to the MI-'plateau' of the corresponding PIPs w.r.t. the above $\hat{\rho}_{SE}^{\text{in}} = \hat{\rho}_S^{\text{in}} \otimes \hat{\rho}_E^{\text{in}}$ involving a maximally entangled, Bell-like $\hat{\rho}_S^{\text{in}}$.

VI) $|\Psi_{SE}^{\text{in}}\rangle = 2^{-1/2} (|0_{k=1}0_n\rangle + |1_{k=1}1_n\rangle)$ (Fig. 13, •-dotted curve)

In the asymptotic limit ($N \gg 1$) we obtain from the entangled S-E-input state $|\Psi_{SE}^{\text{in}}\rangle = 2^{-1/2} (|0_{k=1}0_n\rangle + |1_{k=1}1_n\rangle)$ the output state $\hat{\rho}_{SE}^{\text{out}}$ from (412) in Appendix J.2, which is, for $n \gg k = 1$, dominated by the approximated expression analogous to the one in (198) after replacing $|3\rangle \leftrightarrow |1_{k=1}\rangle$. This is the reason why $\hat{\rho}_{SE}^{\text{out}}$ emerging from the random unitary evolution of $|\Psi_{SE}^{\text{in}}\rangle = 2^{-1/2} (|0_{k=1}0_n\rangle + |1_{k=1}1_n\rangle)$ leads to the same PIP as the one in Fig. 13 in the decoherence limit $n \gg k = 1$ and the asymptotic limit $N \gg 1$. Again, no QD appears.

VII) $|\Psi_{SE}^{\text{in}}\rangle = 2^{-1/2} (|0_{k=1}\gamma_n\rangle + |1_{k=1}\mu_n\rangle)$

In the asymptotic limit ($N \gg 1$) we obtain from the entangled S-E-input state $|\Psi_{SE}^{\text{in}}\rangle = 2^{-1/2} (|0_{k=1}\gamma_n\rangle + |1_{k=1}\mu_n\rangle)$, with $|\gamma_n\rangle = 2^{-1/2} (|0_n\rangle + |1_n\rangle)$ and $|\mu_n\rangle = 2^{-1/2} (|0_n\rangle - |1_n\rangle)$, the output state $\hat{\rho}_{SE}^{\text{out}}$ from (413) in Appendix J.2, which is, for $n \gg k = 1$, dominated by the approximated expression

$$\lim_{n \gg k} \hat{\rho}_{SE}^{\text{out}} = \frac{1}{4} |0\rangle \langle 0| \otimes (|0_n\rangle \langle 0_n| + 2^{-n} \cdot \hat{I}_n) + |1_{k=1}\rangle \langle 1_{k=1}| \otimes 2^{-n-1} \cdot \hat{I}_n, \quad (199)$$

which yields the eigenspectra

$$\begin{aligned}\hat{\rho}_{SE}^{\text{out}} : \lambda_1^{SE} &= \frac{1}{4} \text{ (1 times)}, \lambda_2^{SE} = 2^{-n-2} \text{ (2}^n - 1 \text{ times)}, \lambda_3^{SE} = 2^{-n-1} \text{ (2}^n \text{ times)} \\ \hat{\rho}_E^{\text{out}} : \lambda_1^E &= \frac{1}{4} + 3 \cdot 2^{-n-2}, \lambda_2^E = 3 \cdot 2^{-n-2} \text{ (2}^n - 1 \text{ times)} \\ \hat{\rho}_S^{\text{out}} : \lambda_1^S &= 1/2 \text{ (2 times)}\end{aligned}$$

and thus

$$\begin{aligned}H(E_{L=n \gg 1}) &= -3 \cdot 2^{-n-2} (2^n - 1) \log_2 3 \cdot 2^{-n-2} - \left(\frac{1}{4} + 3 \cdot 2^{-n-2} \right) \log_2 \left(\frac{1}{4} + 3 \cdot 2^{-n-2} \right) \\ &\stackrel{n \gg 1}{\sim} \frac{3n}{4} + 2 - \frac{3}{4} \log_2 3 = H(S, E_{L=n \gg 1}) + \underbrace{\frac{4}{8} - \frac{3}{4} \log_2 3}_{<0} < H(S, E_{L=n \gg 1}) \\ H(S, E_{L=n \gg 1}) &= -2^{-n-2} (2^n - 1) \log_2 2^{-n-2} - \frac{1}{4} \log_2 \frac{1}{4} - 2^n 2^{-n-1} \log_2 2^{-n-1} \\ &\approx \frac{3}{2} \left(1 + \frac{n}{2} \right) > H(E_{L=n \gg 1}) \\ &H(S) = H(S_{\text{class}}) = 1 \\ &\Rightarrow I(S : E_{L=n \gg 1}) \approx 0.375 \cdot H(S_{\text{class}}),\end{aligned} \tag{200}$$

i.e. QD and the corresponding MI-'plateau' at $I(S : E_{L=n \gg 1}) = H(S_{\text{class}})$ cannot appear. Due to the monotonicity of the MI [15, 16, 25], the PIP of (199) will, as was the case for (198), tend to zero for $L \rightarrow 0$ similarly to the PIP in Fig. 13. Thus, $|\Psi_{SE}^{\text{in}}\rangle = 2^{-1/2} (|0_{k=1}\gamma_n\rangle + |1_{k=1}\mu_n\rangle)$ does not lead to QD, both in Zurek's (s. (160) in section 7 above) as well as in the random unitary model with mutually interacting E-qubits.

8.1.3 Non-CNOT-evolution

Since the minimal $\lambda = 1$ attractor subspace contains $|0_n\rangle$ as the only allowed E-registry state, we may expect according to Appendix E that no MI-'plateau' should appear in PIPs corresponding to the random unitary evolution of $\hat{\rho}_{SE}^{\text{in}} = |\Psi_S^{\text{in}}\rangle \langle \Psi_S^{\text{in}}| \otimes \hat{\rho}_E^{\text{in}}$, with $|\Psi_S^{\text{in}}\rangle = \sum_{m=0}^{2^k-1} a_m |m\rangle$ and $\hat{\rho}_E^{\text{in}} = |0_n\rangle \langle 0_n|$ if we apply in (168) $\hat{u}_j^{(\phi \neq \pi/3)}$ instead of the CNOT-transformation $\hat{u}_j^{(\phi=\pi/2)}$. (409) of Appendix J.2 (obtained by means of the corresponding orthonormalized attractor space in Tab. 13 of Appendix I with $c_1 \neq 2^{-1/2}$) displays $\hat{\rho}_{SE}^{\text{out}}$ of $\hat{\rho}_{SE}^{\text{in}}$ from Fig. 17 for $k = 1$ qubit system S , random unitarily evolved by means of $\hat{u}_j^{(\phi=\pi/3)}$. The corresponding numerical PIP is presented in Fig. 14 (◆-dotted curve): again, the decoherence factor is $r = 0.75$, but for $n = 9$ E-qubits in Fig. 14 we are able to obtain $H(S) \approx H(S_{\text{class}}) = 1$. However, since (409) of Appendix J.2 acquires in the limit $n \gg k$ the form

$$\begin{aligned}\lim_{n \gg k} \hat{\rho}_{SE_{L=n}}^{\text{out}} &= |a_0|^2 |0_k\rangle \langle 0_k| \otimes |0_n\rangle \langle 0_n| + |a_1|^2 |1\rangle \langle 1| \otimes 2^{-n} \hat{I}_n \\ \Rightarrow H(S, E_{L=n \gg k}) &= H(S_{\text{class}}) + n > H(E_{L=n \gg k}) = -\lambda_1^E \log_2 \lambda_1^E - (2^n - 1) \lambda_2^E \log_2 \lambda_2^E,\end{aligned} \tag{201}$$

with

$$\lambda_1^E = \left(|a_0|^2 + 2^{-n} |a_1|^2 \right), \lambda_2^E = 2^{-n} |a_1|^2,$$

$I(S : E_{L=n}) / H(S_{\text{class}})$ will only approach the value 1 after taking into account the entire environment E . Thus, with respect to the minimal $\lambda = 1$ attractor subspace (365) from Appendix H non-CNOT $\hat{u}_j^{(\phi)}$ also suppress the appearance of the MI-'plateau' for $\hat{\rho}_{SE}^{\text{in}}$ considered so far.

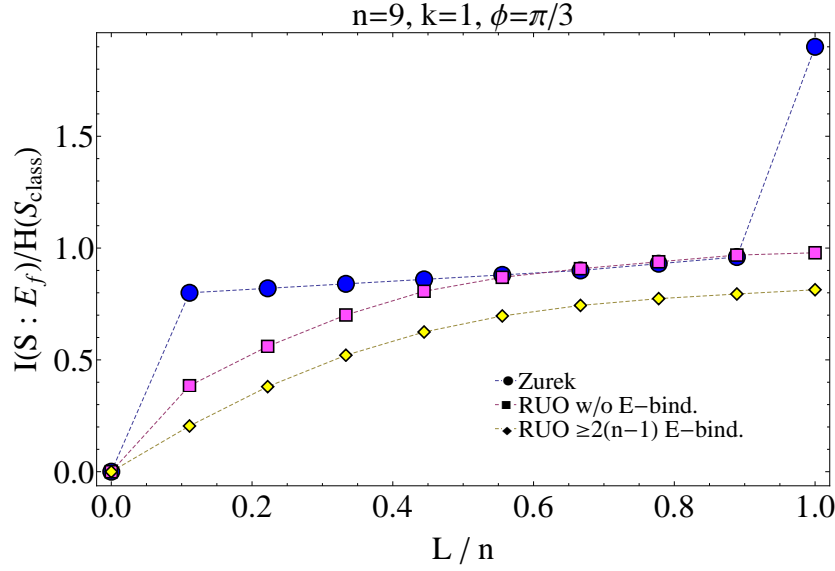


Figure 14: PIP for $\hat{\rho}_{SE}^{out}$ from $\hat{\rho}_{SE}^{in}$ in Fig. 1, ($a = b = 1/\sqrt{2}$) after acting upon $\hat{\rho}_E^{in}$ by $\hat{u}_j^{(\phi=\pi/3)}$ from (166)-(167) in Zurek's (•-dotted curve) and the random unitary (RUO) model (with $N \gg 1$, s. sections 4 and 7).

8.1.4 Concluding remarks: Quantum Darwinism in the minimal $\lambda = 1$ attractor space of the random unitary evolution model with respect to f

After a short digression of the preceding two subsections we return to the random unitary model from the point of view of an environmental fraction parameter f . The MI plots from Fig. 1, Fig. 17 and Fig. 11 to Fig. 14 w.r.t. n indicate for which initial $S - E$ -configurations one may expect Quantum Darwinism to develop when resolving the MI w.r.t. f (for a fixed n qubit E) after infinitely many CNOT-applications. Already at this point it appears obvious that Quantum Darwinism does not manifest itself in case of excited initial environments or for open $k > 1$ qubit S . On the other hand, what may be said about Quantum Darwinism from the point of view of potentially »promising« $S - E$ -initial states such as a one qubit S (or a strongly entangled k qubit S) embedded into an unexcited E ?

For a MI of an initial $S - E$ configuration from (12), i.e.

$$\hat{\rho}_{SE}^{in} = \hat{\rho}_S^{in} \otimes \hat{\rho}_E^{in}$$

$$\hat{\rho}_S^{in} = |a|^2 |0\rangle \langle 0| + a \cdot b^* |1\rangle \langle 0| + a^* \cdot b |0\rangle \langle 1| + |b|^2 |1\rangle \langle 1|; \hat{\rho}_E^{in} = |0_n\rangle \langle 0_n|,$$

with $|a|^2 = |b|^2 = 1/2$, Fig. 1 indicates that in the large n limit $H(S_{class})$ tends to completely manifest itself in E (corresponding to a perfect storage of »S-classicality« by E). Furthermore, we may even notice that the »classicality plateau« in Fig. 1 explicitly refers to the computational basis $\{|0\rangle, |1\rangle\}$ of an open $k = 1$ qubit S as the set of preferred states being darwinistically einselected after a long time period (\equiv infinitely many CNOT-applications) has elapsed, as a consequence of a constant monitoring of S by its environment. This is easily seen by expressing the asymptotic state of S , $\hat{\rho}_S^{out}$, from (12), in form of a Bloch-vector decomposition:

$$\hat{\rho}_S^{out} = \frac{1}{2} (\mathbf{1}_{2 \times 2} + \vec{p} \cdot \vec{\sigma}) = \frac{1}{2} \begin{pmatrix} 1 + p_z & p_x - ip_y \\ p_x + ip_y & 1 - p_z \end{pmatrix}, \quad (202)$$

with a probabilistic Bloch-vector $\vec{p} = (p_x, p_y, p_z)$ and $\vec{\sigma} = (\sigma_x, \sigma_y, \sigma_z)$, involving standard Pauli matrices $\sigma_x = \begin{pmatrix} 0 & 1 \\ 1 & 0 \end{pmatrix}$, $\sigma_y = \begin{pmatrix} 0 & -i \\ i & 0 \end{pmatrix}$ and $\sigma_z = \begin{pmatrix} 1 & 0 \\ 0 & -1 \end{pmatrix}$ in the σ_z -eigenbasis. Comparing (202) with $\hat{\rho}_S^{out}$ from (12) one obtains four restrictions

$$\left. \begin{aligned} 1 + p_z &= 2|a|^2 \\ 1 - p_z &= 2|b|^2 \end{aligned} \right\} p_z = 1 - 2|b|^2$$

$$\frac{1}{2}(p_x - ip_y) = rba^*, \quad \frac{1}{2}(p_x + ip_y) = rab^*, \quad (203)$$

which enforce $p_x = p_y = 0$, indicating that the preferred »classical« basis of $\hat{\rho}_S^{out}$ in the long-time limit (after iteratively

many CNOT-applications) is given by the eigenbasis of σ_z , ergo $\{|0\rangle, |1\rangle\}$.

Focussing on the MI and its $\hat{\rho}_{SE}^{\text{out}}$ in Fig. 1 w.r.t. a parameter $f = L/n$ of an $n = 9$ qubit ground state E, one obtains the PIPs for different k -values of S-qubits as depicted by the \blacklozenge , \circ and \square -dotted curves in Fig. 17 below. From Fig. 17 (\blacklozenge -dotted curve) we may deduce that the redundancy R of the asymptotic S and its preferred states in E is maximally 1, meaning that one has to enclose the entire E ($f = 1$) into the measurement procedure in order to store the whole amount of $H(S_{\text{class}})$. Thus, in the scope of the random unitary model with mutually interacting E-qubits Quantum Darwinism, contrary to our previous assumptions and to Zurek's qubit model, does not appear for an initial S – E-product state consisting of a pure one qubit S and its n qubit ground state E.

Similar results also hold if one resolves the asymptotic MI of an initial Bell-like pure 2-qubit S embedded into a ground state n qubit E or of an entangled initial state $|\Psi_{SE}^{\text{in}}\rangle = 2^{-1/2}(|0_{k=1}0_n\rangle + |1_{k=1}1_n\rangle)$, whose PIPs are visualized in Fig. 13, w.r.t. the fraction parameter f : no Quantum Darwinism appears! The similar dependence of MI on f as in Fig. 17 below is obtained for the S – E-input configuration $|\Psi_{SE}^{\text{in}}\rangle = 2^{-1/2}(|0_{k=1}\gamma_n\rangle + |1_{k=1}\mu_n\rangle)$: for all these entangled S – E-input configurations the Quantum Darwinistic MI-'plateau' does not appear when MI is resolved w.r.t. the fraction parameter f of an n -qubit E (with n fixed).

What are the reasons for the absence of Quantum Darwinism from the present random unitary model involving IDs with mutually interacting E-qubits? (The author would like to thank **W. H. Zurek** for interesting discussions regarding this question during the 500th DPG seminar »Highlights of Quantum Optics« in Bad Honnef, 6 - 11 May 2012) It has already been pointed out that mutually interacting E-qubits pose strong limitations to the storage capacity of the environment they constitute due to a relatively restricted structure of the attractor space corresponding to the proposed random unitary evolution model. However, interactions among E qubits are not the only reason for the absence of Quantum Darwinism. As far more important appears in this context the random application of iterated CNOT transformations, leading to an unavoidable and irreversible »spreading« of information about S throughout the entire E and loss of information about the state of $\hat{\rho}_{SE}^{\text{out}}$ corresponding to iteration steps 1, ..., $N - 1$ (earlier evolution times). This randomly induced leakage of information about the state of $\hat{\rho}_{SE}^{\text{out}}$ for iteration steps 1, ..., $N - 1$ is indeed a consequence of the fact that the random unitary evolution (166)-(170) is described by a quantum Markov-chain (168) and, as such, a non-unitary effect that prohibits the appearance of the »boundary« $2 \cdot H(S_{\text{class}})$ -peak occurring in Zurek's PIP of Fig. 1, since randomly iterated asymptotic S – E-states possess in general a non-pure character. Namely, as we have seen in the previous subsection concerning an ideal Quantum Darwinistic output state $|\phi_{SE}^{\text{out}}\rangle$ in (173), the purity of the resulting asymptotic overall S – E-state remains a vital requirement for the appearance of a $2 \cdot H(S_{\text{class}})$ -peak in PIPs w.r.t. f . This requirement is apparently not accounted for in the course of the random unitary model with mutually interacting E-qubits, which generates asymptotic S – E-states that are in general not pure because of the mentioned randomly induced »leakage« of information.

In this sense it may be stated that we should not expect the »boundary« $2 \cdot H(S_{\text{class}})$ -peak to reappear in the random unitary PIPs after the proposed dimensional enlargement of the corresponding minimal attractor space (365) from Appendix H by assuming completely non-interacting E qubits (see subsection 8.3). The general S – E-output states of the random unitary model would thus remain non-pure even after their attractor space has been enlarged. On the other hand, the existence of the $2 \cdot H(S_{\text{class}})$ -peak is not a crucial aspect when it comes to deciding whether the random unitary evolution model (with mutually interacting or non-interacting E-qubits) incorporates the most basic feature of Quantum Darwinism - the »classicality plateau«. For these results do not contradict the PIPs obtained from Zurek's qubit model, since in reference to the random unitary model we may only conclude with certainty that, in general, Quantum Darwinism presupposes conceptually the validity of the decoherence approach (first introduced in [2]), whereas, on the other hand, decoherence does not necessitate the conceptual framework of Quantum Darwinism in order to function properly.

Still there is hope that by enlarging the dimension of the minimal attractor space (365) from Appendix H within the random unitary model one could obtain higher redundancies $n \geq R > 1$ that would indicate the (partial) effect of Quantum Darwinism. If this should be the case, then one could also argue that assuming completely non-interacting E qubits should introduce and guarantee higher physical objectivity into the random unitary model. This objective aspect would then, consequently, lead to the appearance of Quantum Darwinism. In this sense one could even regard Quantum Darwinism and its presence or absence in a certain qubit model as a »quantitative measure« of the objectivity and efficiency of information transfer and storage implemented within its conceptual framework. Therefore, before dealing with mathematical details of an enlarged random unitary attractor space, we have to elaborate the notion of »objectivity« in physics. This task will be pursued in the forthcoming subsection 8.3.

8.2 Short time limit of the random unitary evolution

Before looking at the analytic structure of the corresponding maximal attractor space we discuss whether one may interpret Zurek's qubit model of Quantum Darwinism as the short time limit (corresponding to the small number N of

iterations) of the random unitary evolution involving pure decoherence. Within the random unitary operation-formalism we obtain another type of PIP-behavior: inserting $\hat{\rho}_{SE}^{\text{in}}$ from Fig. 1 into (168) we obtain for pure decoherence (with $\phi = \pi/2$, $|a|^2 = |b|^2 = 1/2$ and $p_e = 1/|M| \forall e$) after $N \gg 1$ iterations the PIP in Fig. 15, which suggests that Zurek's Quantum Darwinistic-'plateau' [5] appears only in the limit $N \rightarrow \infty$ (we will obtain this asymptotic limit $N \rightarrow \infty$ of the random unitary evolution analytically in subsection 8.3). Thus, Zurek's qubit model of Quantum Darwinism does not appear as the short-time limit (small N -values, e.g. $N \leq 10$) of the random unitary evolution model with pure decoherence.

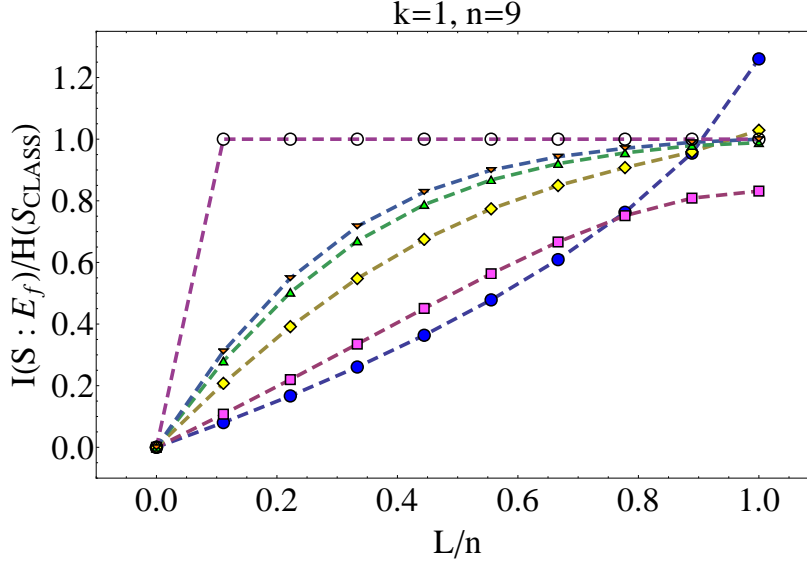


Figure 15: PIP of simulated, random unitarily CNOT-evolved MI vs $0 < f \leq 1$ for $\hat{\rho}_{SE}^{\text{in}} = \hat{\rho}_S^{\text{in}} \otimes \hat{\rho}_E^{\text{in}}$ in (12) and $\hat{\rho}_{SE}^{\text{out}}$ from (166)-(168) w.r.t. N (\bullet , $N = 1$; \blacksquare , $N = 2$; \blacklozenge , $N = 5$; \blacktriangle , $N = 10$; \blacktriangledown , $N = 10^3$; \circ , $N = \infty$). For $N = \infty$ s. subsection 8.3.2.

Furthermore, we also notice in Fig. 15 a transient process of the random unitary iteration which occurs for relatively small $N \in \{1, \dots, 10\}$: for instance, in Fig. 15 we see that for $N = 1$ the MI reaches at $L = n$ a value $> H(S_{\text{class}})$, whereas already $N = 2$ leads to $I(S : E_{L=n}) < H(S_{\text{class}})$. On the other hand, for $N = 5$ we obtain $I(S : E_{L=n}) = H(S_{\text{class}}) + \epsilon$, whereas $N = 10$ yields $I(S : E_{L=n}) = H(S_{\text{class}}) - \epsilon$, with $\epsilon \ll 1$. Only for $N > 10$ we are able to see a definitive trend for the MI in the PIP of Fig. 15, which approaches the smooth asymptotic MI-profile of the minimal attractor space from Fig. 17 (\blacklozenge -dotted curve) at $N = 10^4$. The asymptotic $N = \infty$ case of the maximal attractor space (the MI-'plateau') corresponding to the PIP of (395) in Appendix J.1 (the \blacksquare -dotted curve in Fig. 17) is also displayed in Fig. 15. For $N > 10^4$ the \blacktriangledown -dotted curve will approach the MI-'plateau' only slowly.

A similar transient process of the random unitary iteration appears if we simulate (168) for pure decoherence (with $\phi = \pi/2$, $|a|^2 = |b|^2 = 1/2$ and $p_e = 1/|M| \forall e$) and w.r.t. $\hat{\rho}_{SE}^{\text{in}} = \hat{\rho}_S^{\text{in}} \otimes \hat{\rho}_E^{\text{in}}$, with a $k = 1$ -qubit pure $\hat{\rho}_S^{\text{in}}$ and $\hat{\rho}_E^{\text{in}} = 2^{-1}(|0_{n=9}\rangle\langle 0_{n=9}| + |1_{n=9}\rangle\langle 1_{n=9}|)$ mutually non-interacting E-qubits. After $N \gg 1$ (i.e. $N = 10^4$) we see from the upper left PIP (\blacktriangledown -dotted curve) of Fig. 16 that the MI and its f -dependence perfectly approach the asymptotic \circ -dotted curve ($N = \infty$) of the maximal attractor space, corresponding to the \blacksquare -dotted curve of the PIP in Fig. 23, after having passed through the transient random unitary iteration process for $N \in \{1, \dots, 5\}$. Only for $N > 5$ we see the unambiguous convergence of the PIP towards the \circ -dotted curve in the upper left plot of Fig. 16.

However, the transient unitary iteration process is not particularly important. Of much higher significance is the iteration limit $N \gg 1$ (represented by the \blacktriangledown -dotted curves) in Fig. 16, which approaches the asymptotic \circ -dotted curves of the minimal attractor $\lambda = 1$ subspace from the upper right, lower left and lower right PIPs in Fig. 16 as soon as one introduces between E-qubits CNOT-interactions, regardless of how one organizes the CNOT-bindings between E-qubits within the ID of Fig. 9: for instance, one could decide to organize the CNOT-bindings between E-qubits from the upper right and the two lower PIPs in Fig. 16, without any loss of generality, in accord with Fig. 41 of Appendix H.3.2 or choose a completely different initial structure of CNOT-interactions between E-qubits when simulating the iterative Markov-chain evolution (168) and still obtain the same PIPs from Fig. 16 above.

This means that already a single interaction between E-qubits leads in the limit $N \gg 1$ to the PIPs of the minimal $\lambda = 1$ attractor space for $\hat{\rho}_{SE}^{\text{in}}$ in Fig. 16. An increasing number of CNOT-bindings between E-qubits only implies that the corresponding PIP will approach the \circ -dotted curve(s) in Fig. 16 faster in the limit $N \gg 1$, without altering the fact that

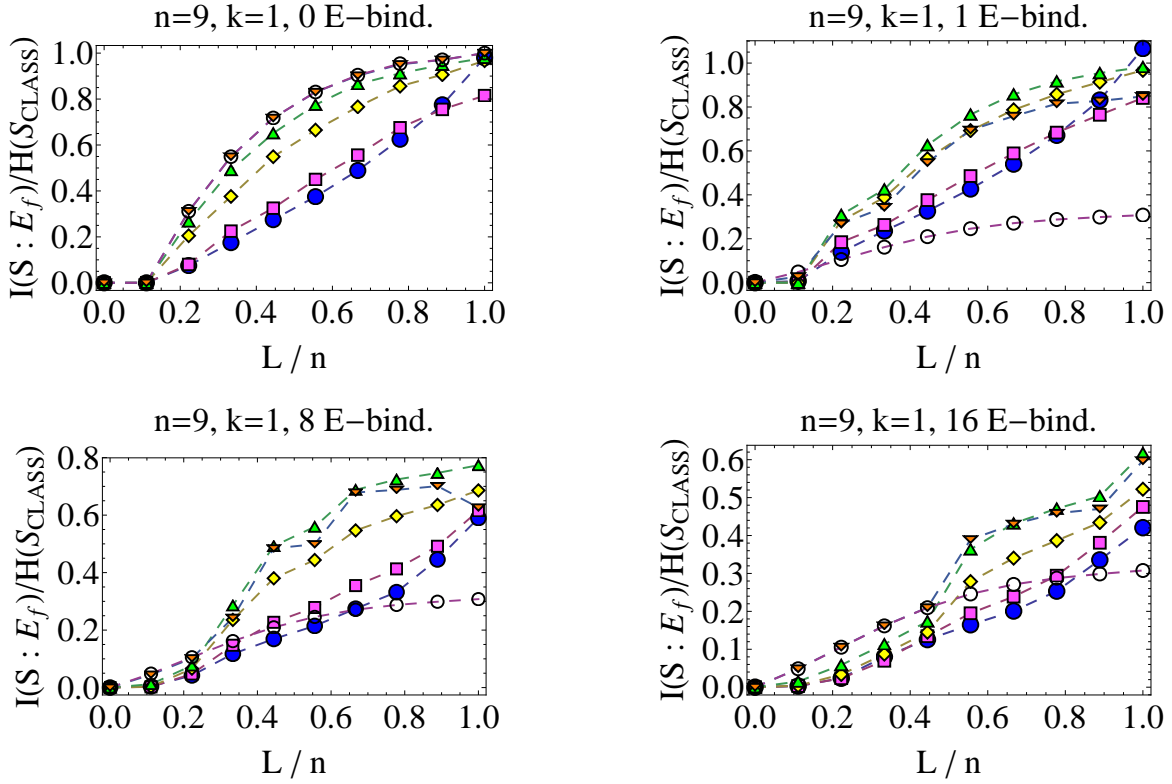


Figure 16: PIP of simulated random unitary-MI vs $0 < f \leq 1$ for $\hat{\rho}_{SE}^{\text{in}} = \hat{\rho}_S^{\text{in}} \otimes \hat{\rho}_E^{\text{in}}$, with a $k = 1$ -qubit pure $\hat{\rho}_S^{\text{in}}$, $\hat{\rho}_E^{\text{in}} = 2^{-1}(|0_{n=9}\rangle\langle 0_{n=9}| + |1_{n=9}\rangle\langle 1_{n=9}|)$ and $\hat{\rho}_{SE}^{\text{out}}$ from (166)-(168) with $\phi = \pi/2$, for different N -values and an increasing number of CNOT-bindings between E-qubits: $N = 1$ (\bullet -dotted curves), $N = 2$ (\blacksquare -dotted curves), $N = 5$ (\blacklozenge -dotted curves), $N = 10$ (\blacktriangle -dotted curves), $N = 10^4$ (\blacktriangledown -dotted curves) and $N = \infty$ (\circ -dotted curves). For $N = \infty$ and 0 E-bindings s. subsection 8.3.2.

for $N \gg 1$ and $\hat{\rho}_{SE}^{\text{in}}$ from Fig. 16 the single CNOT-binding between E-qubits leads to the same \circ -dotted curve of the minimal $\lambda = 1$ attractor subspace, as does an ID with the critical number of $2(n-1) = 16$ CNOT-bindings between E-qubits that yields precisely the minimal $\lambda = 1$ attractor subspace structure (365) from Appendix H.1.2.

A detailed physical interpretation of the above findings (simulation results) displayed in Fig. 15 and Fig. 16 will be given in the forthcoming subsections 8.3 and 8.4.

8.3 Maximal attractor space and its structure

When dealing with Koenig-IDs [31] we always obtain attractor (sub-)spaces with maximal dimension d^λ (determined by (378)-(379) in Appendix H), since in such IDs E-qubits are not allowed to interact with each other. Therefore, we turn our attention in the following subsections to the description of analytical attractor space structures associated with Koenig-IDs and determined in Appendix H. However, before we proceed let us motivate our decision for choosing mutually non-interacting E-qubits as an appropriate model for QD within the iterated random unitary evolution mechanism.

The previous version of the random unitary model of QD from subsection 8.1 involved the CNOT-like interaction as a member of the ϕ -parameter family (166)-(167) of transformations $\hat{u}_j^{(\phi)}$ between the qubits of S (indexed by the letter i) and E (index j). In the course of such a decoherence model, applied to realize a description of an open k -qubit quantum system S being measured by an n -qubit E , the corresponding environmental qubits have been targeted by the S -qubits iteratively many times, whereby the application of CNOT-transformations (166)-(167) to each E-qubit j was assumed to occur randomly (according to the a priori fixed probability distribution). The random CNOT-application, along with the strongly restricted storage capacity of the corresponding attractor space of the model, were found responsible for the breakdown of QD w.r.t. the environmental fraction parameter f in the limit of large environments ($n \rightarrow \infty$). In order to enlarge the storage capacity of the random unitary model we have to enlarge its attractor space, an attempt which, as will be shown below, amounts at changing the interaction behaviour of environmental qubits towards each other.

As an illustration of the changes necessary to ensure objectivity within the random unitary model consider the modified interaction structure between S and E displayed involving Fig. 9, however without interaction arrows between E-qubits. As usual, arrows denote CNOT-interactions initiated from S-qubits according to the prescription (166)-(167). Contrary to the previous version of the random unitary model, we may notice one crucial difference when looking at mutually non-interacting E-qubits in Fig. 9: this time, we stipulate that the environmental qubits may not interact among each other. However, this appears to be the only significant modification of the previous random unitary model! Is it important? The answer is affirmative.

To understand the significance of this single modification in Fig. 9 (i.e. mutually non-interacting E-qubits), it is instructive to consider the following five requirements w.r.t. the modified random unitary evolution model which an ideal measurement process has to satisfy [33, 34]:

- **Requirement 1:** *interactions between S and E have to act as one-parameter families of automorphisms.* This requirement was already satisfied within the framework of the previous random unitary model with mutually interacting E-qubits. CNOT-transformation (166)-(167) represents a ϕ -parameter family of unitary transformations which is, in this case, directed towards environmental qubits in order to simulate the measurement process: after all, when measuring an open system S environment E becomes imprinted with information about the preferred basis states of S. This fact raises the CNOT-transformation to the status of the most frequently applied, entanglement generating mathematical constructs, that captures the essence of the quantum mechanical measurement process: namely the back action of the measured system on its environment. Certainly, it goes without saying that entanglement of S with E also induces changes of the monitored system, which especially manifests itself in the limit of infinitely many CNOT-applications. In the context of these iterative, randomly activated CNOT-transformations the random unitary model also manages to describe the indirect influence of the measuring device on the measured object (system S).
- **Requirement 2:** *any physical model of decoherence should utilize the tensor product structure of the Hilbert space \mathcal{H} .* This requirement is also fulfilled already within the »old« random unitary model. Decoherence is a pure quantum mechanical effect; therefore it comes as no surprise that the random unitary model should likewise utilize the mathematical Hilbert space formalism, especially its tensor product structure. For only tensor products enable us to partition the Hilbert space into subspaces, which is an unavoidable requirement when discussing quantum measurements: without subspaces in \mathcal{H} the probabilistic character of quantum measurements could not manifest itself and the measurement problem would thus not appear any more, indicating that the only in this case existent global indivisible state $|\psi\rangle$ of the Universe evolves completely deterministically as demanded by the Schrödinger equation.
- **Requirement 3:** *mutual dynamical independence of observers and measuring devices.* This is exactly the theoretical aspect that has not yet been accomplished by our previous random unitary model. Fig. 9 above suggests a way out of this problem by demanding a qubit environment composed of independent constituents that do not interact mutually. This standpoint ensures that there is no flow of relevant information about S between single environmental qubits, which also means that E-qubits are allowed to acquire and enlarge their knowledge of the observed system only by means of individually performed direct or indirect measurements on S. On the other hand, in our previous random unitary model we faced a problem that all n qubits of E effectively behaved as one single qubit, thereby causing an even stronger restriction of the available attractor space and diminishing its capacity to store the classical amount of information about S. In light of these facts we may state that mutually non-interacting environmental qubits may be understood as individual observers who perform their measurements independently, whereas the »old« random unitary model had to deal with observers exchanging gathered facts, which in the end reduces to a single observer who just distributes his measurement results to his »colleagues«. This picture undoubtedly disagrees with a standard image of objective (mutually independent) acquisition of knowledge. Accordingly, we consider from now on only mutually independent qubits as environmental constituents.
- **Requirement 4:** *unitary transformations entering decoherence models should act in an entanglement-inducing manner.* This requirement is automatically satisfied by the bare mathematical structure of CNOT-transformations, which entangle two qubits from different subsystems of the global S—E-state, as it should be the case during measurement processes. This entangling effect adheres perfectly to the main concept of QD, which uses mutually independent environmental degrees of freedom as »witnesses« that can be intercepted in order to gain in an indirect way the desired knowledge of S. However, without entanglement between S and E no information flow from the observed system to its »witnesses« would take place, which would accordingly annulate the most basic preassumption of decoherence models - the »openness« of measured systems towards its environments, leading consequently to the disappearance of the measurement problem.

- **Requirement 5:** *unitary transformations entering into decoherence models may disturb the measured system only minimally.* QD may be regarded as a direct and the most illustrative conceptual implementation of the indirect measurement tactics explained in the last section. After all, the main idea of QD consists in intercepting information about S that has been accumulated (stored) in different environmental fractions after a longer period of time (ergo after infinitely many CNOT-applications), during which the system has had a chance of imprinting the part of its information most robust towards decoherence (i. e. the »classical« information about S) into the pointer basis of E. By intercepting environmental fragments external observers measure S in an indirect, almost non-demolishing way. If we should stick to Belavkin's and Braginsky's ideas [7, 33], then the intercepted environmental fragments would represent the aforementioned »quantum probe« that carries away (»witnesses«) the relevant information about S by means of entanglement to external conscious observers (the first step of an indirect measurement). Finally, the conscious observer perceives the transferred information that has survived the monitoring process and interprets it (the second step of an indirect measurement), thereby consistently closing the »measurement circle«.

Summa summarum, the decoherence model illustrated in Fig. 9 involving only mutually non-interacting E-qubits may be regarded as an appropriate, physical objectivity guaranteeing generalization of the previous random unitary model, offering a possibility of enlarging the corresponding attractor space whose determination will be the next important and challenging task of our investigation regarding QD and its physical limitations. Still, there is hope (if not even an expectation) that the assumption of a mutually non-interacting qubit environment could lead to the reappearance of QD due to the larger attractor space one should obtain from such a generalized random unitary model. If this should be the case, then we could indeed confirm that only entanglement, together with a tensor structure of the underlying Hilbert space, allows an appropriate, physical invariants preserving implementation of different symmetries, designed to explain the basic features of the measurement process, at least as long as one provides a monitoring environment of »mutually independent witnesses«, since only such an environment involving mutually independent (conscious) observers would enforce the consolidation of truly objective scientific knowledge. Invoking the terminology of automorphisms it may be stated that the CNOT-transformation as a one-parameter family of automorphisms (166)-(167) distinguishes per construction those states of an open system S (»measuring invariants«), which are most robust w.r.t. decoherence (the pointer states) and therefore become imprinted into the environment E (the »quantum probe«). Consequently, the computation of the mutual information for the global S-E-state and its subsystems, usually pursued within the framework of QD, corresponds to an indirect interception of information about S that has been stored in E, as demanded by the second step of the aforementioned indirect measurement technique from **Requirement 5**.

Finally, we also have to accept that initially one has to assume $\hat{\rho}_{SE}^{in} = \hat{\rho}_S^{in} \otimes \hat{\rho}_E^{in}$, since this assumption is necessary in order for the quantum channel $\mathcal{E}(\cdot) \equiv \sum_{e \in M} K_e(\cdot) K_e^\dagger$ from (168) to act as a universal dynamical cptp-map: as already known, a universal dynamical cptp-map is a map which does not explicitly depend on the state it acts upon (i.e. the Kraus operators K_e in $\mathcal{E}(\cdot)$ do not depend on $\hat{\rho}_{SE}^{in}$ which is inserted into the quantum channel). This is necessary, since universal dynamical cptp-maps describe a plausible physical evolution for every input state $\hat{\rho}_{SE}^{in}$. In other words, a dynamical map is a universal dynamical cptp-map if and only if it is induced from an extended S-E-system with the initial condition $\hat{\rho}_{SE}^{in} = \hat{\rho}_S^{in} \otimes \hat{\rho}_E^{in}$, where $\hat{\rho}_S^{in}$ is fixed for any $\hat{\rho}_E^{in}$ [35]. Certainly, one may at first argue that if the system E, initially described by $\hat{\rho}_E^{in}$, is out of our control, this product state assumption for $\hat{\rho}_{SE}^{in}$ is not necessarily fulfilled. Nevertheless, the control on the system S and its state $\hat{\rho}_S^{in}$ is enough to assure that $\hat{\rho}_{SE}^{in} = \hat{\rho}_S^{in} \otimes \hat{\rho}_E^{in}$ holds, for we know that it suffices to prepare a pure state in S, for instance by making a projective measurement as explained in [36], to assure that at the initial time the global system $\hat{\rho}_{SE}^{in}$ is in a product state with no correlations between S and E (vanishing MI)¹⁶.

8.3.1 State structure of the attractor space

From H we know that for the random unitary evolution the attractor space consists of two subspaces (380) and (381) from Appendix H associated with eigenvalues $\lambda = 1$ and $\lambda = -1$ of (169), respectively.

The main (largest) part of the attractor states $\tilde{X}_{\lambda=1,i}$ can be attributed to the $|0_k\rangle\langle 0_k|$ -subspace of system S, since the $\lambda = 1$ -attractor subspace describes the impact of pure decoherence on system S during the iterative evolution (168) of $\hat{\rho}_{SE}^{in}$. However, in order to realize the physical significance of the $\lambda = -1$ -attractor subspace we will discuss in the following subsection the random unitary evolution of some of the $\hat{\rho}_{SE}^{in}$ from Tab. 8 that have already been studied in the course of Zurek's evolution in sections 3 and 7.

¹⁶As indicated in [35], it is a well-known fact that if one of the bipartite parts of $\hat{\rho}_{SE}^{in}$, let us assume S, is pure, then the MI of $\hat{\rho}_{SE}^{in}$ also has to be zero, regardless of the specific structure contained in $\hat{\rho}_E^{in}$.

8.3.2 Results of the CNOT-evolution

Now we look at the random unitary CNOT-evolution from the analytical point of view by utilizing the attractor space structure from subsection 8.3.1 and concentrating on the following input states $\hat{\rho}_{SE}^{in}$ (with $n \gg k \geq 1$) :

I) $\hat{\rho}_{SE}^{in} = \hat{\rho}_S^{in} \otimes \hat{\rho}_E^{in}$, **k-qubit pure** $\hat{\rho}_S^{in}$, $\hat{\rho}_E^{in} = |0_n\rangle \langle 0_n|$

Decomposing $\hat{\rho}_{SE}^{in}$ for $n \gg k \in \{1, 2, 3\}$ S-qubits by means of (170) and $\hat{X}_{\lambda,i}$ from (380)-(381) in Appendix H that are already Gram-Schmidt orthonormalized, we obtain the CNOT-asymptotically evolved $\hat{\rho}_{SE}^{out}$ displayed in (395) of Appendix J.1. The corresponding PIP obtained from $\hat{\rho}_{SE}^{out}$ in (395) of Appendix J.1 for $k \in \{1, 2, 3\}$ S-qubits is displayed in Fig. 17 below.

Fig. 17 demonstrates that within the random unitary operations model Quantum Darwinism appears only for $k = 1$ pure $\hat{\rho}_S^{in}$ even if we set $\hat{\rho}_E^{in} = |y\rangle \langle y| \forall y \in \{0, \dots, 2^n - 1\}$ for mutually non-interacting E-qubits, whereas for $n \sim k \gg 1$ the maximal $I(S : E_{L=n})$ -value that can be achieved after enclosing the entire environment E behaves as

$$\lim_{n \sim k \gg 1} I(S : E_{L=n}) / H(S_{class}) \sim 2^{-k}.$$

This follows from (395) of Appendix J.1 which, with (without loss of generality) $|a_i|^2 = 2^{-k} \forall i \in \{0, \dots, 2^k - 1\}$ and for $k > 1$, acquires in the limit $n \gg 1$ the form

$$\lim_{n \gg 1} \hat{\rho}_{SE_{L=n}}^{out} = |a_0|^2 |0_k\rangle \langle 0_k| \otimes |0_n\rangle \langle 0_n| + \sum_{m=1}^{2^k-1} |a_m|^2 |m\rangle \langle m| \otimes 2^{-n} \hat{I}_n. \quad (204)$$

(204) leads to $H(S) \approx H(S_{class}) = k$ (with a decoherence factor $0 \leq r = \langle s_1^n | \hat{\rho}_E^{in} | s_1^n \rangle = 2^{-n} \leq 1$), and non-zero eigenvalues

$$\lambda_1^{SE} = |a_0|^2 = 2^{-k} \text{ (1 times)}, \lambda_2^{SE} = |a_m|^2 2^{-n} = 2^{-(k+n)} (2^n [2^k - 1] \text{ times}),$$

yielding (for fixed n and increasing k)

$$\lim_{n \sim k \gg 1} H(S, E_{L=n}) = 2k + k \cdot 2^{-k}.$$

Accordingly, the eigenvalues of $\lim_{n \gg 1} \hat{\rho}_{SE_{L=n}}^{out}$ from (204),

$$\lambda_1^E = |a_0|^2 + 2^{-n} (1 - |a_0|^2) \text{ (1 times)}, \lambda_2^E = 2^{-n} (1 - |a_0|^2) ([2^n - 1] \text{ times}),$$

lead (as in Fig. 17) to

$$\lim_{n \sim k \gg 1} H(E_{L=n}) = k + k \cdot 2^{1-k} \\ \lim_{n \sim k \gg 1} I(S : E_{L=n}) / H(S_{class}) = 2^{-k}.$$

This trend can also be confirmed by plotting the MI of a random unitarily CNOT-evolved $\hat{\rho}_{SE}^{in} = |\Psi_S^{in}\rangle \langle \Psi_S^{in}| \otimes |0_{n=9}\rangle \langle 0_{n=9}|$, with a $k = 2$ qubit $|\Psi_S^{in}\rangle = \sum_{m=0}^{2^k-1} a_m |m\rangle$ ($|a_m|^2 = 2^{-k} \forall m$) and without interaction bindings between E-qubits, w.r.t. the number n of E-qubits, as done in Fig. 18 below. Fig. 18 demonstrates that, contrary to the •-dotted curve in Fig. 11, for a $k = 2$ qubit pure $\hat{\rho}_S^{in}$ the corresponding PIP displays an N-dependent behavior: i.e. depending on whether the number N of iterations in (168) is even or odd, the maximum of the $I(S : E_{L=n}) / H(S_{class})$ approaches in the limit $n \gg 1$ the (same) value 2^{-1} from below or above, respectively. This »oscillation« of MI w.r.t. N arises due to the terms associated with the $(-1)^N$ -prefactor in (395) of Appendix J.1, whose contributions tend to zero for $n \gg 1$. This is precisely what one would expect from an output state $\hat{\rho}_{SE}^{out}$ of a random unitary evolution, namely a well defined, N-independent convergence value of $I(S : E_{L=n}) / H(S_{class})$ w.r.t. increasing n -values. Also the •-dotted curve in Fig. 11 displays this well-defined, N-independent convergence of MI in the limit $n \gg 1$, since the corresponding $I(S : E_{L=n}) / H(S_{class})$ tends to one for $n \gg 1$, regardless of N being odd or even. Thus, in the limit $n \gg 1$ both Fig. 18 and Fig. 11 display N-independent, convergent behavior of the MI, despite the fact that w.r.t. relatively small n -values the N-dependence of the MI does arise. After all, when talking about QD with pure decoherence we are mainly interested in utilizing the decoherence process in order to store and transfer $H(S_{class})$ into E, bearing in mind that effective decoherence of S appears only for large environments, i.e. $n \gg 1$.

$\forall k \geq 1$. Apparently, the random unitary evolution model suggests that in order to store $H(S_{\text{class}})$ into environment E efficiently one needs environments consisting of qudit-cells (2^k -level systems). This conjecture is also supported by (354) from Appendix E, which indicates that for Quantum Darwinism to appear w.r.t. $k > 1$ one needs 2^k symmetry states. Unfortunately, the qubit-qubit $\hat{u}_j^{(\phi)}$ -transformation in (166)-(167) (and thus also the CNOT) offers only two symmetry states $\{|s_{c1}\rangle, |s_{c2}\rangle\}$. Therefore, one would require a qubit-qudit version of (166)-(167) in order to see Quantum Darwinism.

On the other hand, for $k = 1$ $\hat{\rho}_{SE_L}^{\text{out}}$ and $\hat{\rho}_{E_L}^{\text{out}}$ from (395) in Appendix J have $\forall (1 \leq L \leq n)$ identical non-zero eigenvalues

$$\begin{aligned}\lambda_1^{(S)E} &= |a_1|^2 2^{-L} ([2^L - 1] \text{ times}) \\ \lambda_2^{(S)E} &= 2^{-1} |a_0|^2 + 2^{-(L+1)} |a_1|^2 + \\ &\sqrt{\left(2^{-1} |a_0|^2 + |a_1|^2 2^{-(L+1)}\right)^2 - g_N} \\ &= |a_0|^2 + 2^{-L} |a_1|^2 (1 \text{ times}),\end{aligned}$$

with $g_N := |a_0|^2 |a_1|^2 2^{-2n+L} \left[\underbrace{1 - (-1)^{2N}}_{:=0} \right]$, due to the $\lambda = -1$ attractor subspace and its contributions in $\lambda_2^{(S)E}$ proportional to $(-1)^{2N}$ and characterized by the iteration number N from (170). Again, $H(S) \approx H(S_{\text{class}})$ for $n \gg k$ due to eigenvalues

$$\lambda_{1/2}^S = 1/2 \pm \sqrt{1/4 - \left(1 - 2^{-2n} [1 + (-1)^N]^2\right) |a_0|^2 |a_1|^2}$$

of $\hat{\rho}_S^{\text{out}}$ from (395) in Appendix J.

Other choices for $\hat{\rho}_S^{\text{in}}$

When looking at $\hat{\rho}_{SE}^{\text{out}}$ in (12) from Zurek's qubit model of QD we notice that by starting the CNOT-evolution with $\hat{\rho}_{SE}^{\text{in}} = \hat{\rho}_S^{\text{in}} \otimes \hat{\rho}_E^{\text{in}}$ enclosing a completely mixed $\hat{\rho}_S^{\text{in}} = \sum_{i=0}^{2^k-1} |a_i|^2 |i\rangle \langle i|$ and a ground state $\hat{\rho}_E^{\text{in}} = |0_n\rangle \langle 0_n|$ QD remains essentially untouched: i.e. the only detail that changes in the corresponding PIP emerging from $\hat{\rho}_{SE}^{\text{out}}$, evolved from a product state input of a completely mixed $k = 1$ qubit $\hat{\rho}_S^{\text{in}}$ and a ground state $\hat{\rho}_E^{\text{in}}$ according to Zurek's algorithm, is the disappearance of the $2 \cdot H(S_{\text{class}})$ -peak at $f = 1$. In other words, the PIP of $\hat{\rho}_{SE}^{\text{out}}$ looks almost like the one in Fig. 1, however this time with $I(S : E_{L=n}) = H(S_{\text{class}})$ (s. also the ■-dotted curve in Fig. 17), which still adheres to (155). This is obvious when bearing in mind that $\hat{\rho}_{SE}^{\text{out}}$, in accord with Zurek's evolution algorithm, corresponds to $\hat{\rho}_{SE}^{\text{out}}$ in (12), however without contributions (addends) correlated with outer-diagonal S-subspaces $|0\rangle_S \langle 1|$ and $|1\rangle_S \langle 0|$, i.e.

$$\begin{aligned}\hat{\rho}_{SE}^{\text{out}} &= \hat{\rho}_{SE}^{\text{out}} - a \cdot b^* |0\rangle \langle 1| \otimes |0_{L=n}\rangle \langle 1_{L=n}| - a^* \cdot b |1\rangle \langle 0| \otimes |1_{L=n}\rangle \langle 0_{L=n}| \\ &\hat{\rho}_{SE}^{\text{out}} \text{ as in (12)}.\end{aligned}\tag{205}$$

Since $\hat{\rho}_{SE}^{\text{out}}$ remains non-pure even for $L = n$, the MI-'quantum peak' does not appear.

This invariance of QD for completely mixed $\hat{\rho}_S^{\text{in}}$ in Zurek's qubit model is a subtle and important difference when compared with the random unitary evolution model: namely if we let $\hat{\rho}_{SE}^{\text{in}}$, that has led to (205) in Zurek's qubit model, evolve according to the random unitary model (166)-(168) by iteratively applying $\hat{u}_j^{(\phi=\pi/2)}$ (CNOT-transformations) between a single S-qubit ($k = 1$) and n E-qubits, we obtain in the asymptotic limit $N \gg 1$

$$\hat{\mu}_{SE}^{\text{out}} = |a_0|^2 |0\rangle \langle 0| \otimes |z^n\rangle \langle z^n| + |a_1|^2 |1\rangle \langle 1| 2^{-n/2} \sum_{i=1}^n \left\{ 2^{-1/2} \hat{I}_1 + (-1)^{N/n+1} \cdot \hat{B}_1^{\pi/2} \right\}\tag{206}$$

(where $z^{L=n} \in \{0, \dots, 2^n - 1\}$), which corresponds to $\hat{\rho}_{SE}^{\text{out}}$ this time given by (395) of Appendix J.1 (with $k = 1$), however without addends associated with outer-diagonal S-subspaces $|0\rangle_S \langle 1|$ and $|1\rangle_S \langle 0|$.

We know from the discussion w.r.t. (127) in subsection 4.2.5 that $\hat{B}_1^{\pi/2}$ is a traceless operator which contributes to (206) only for $L = n$ and does not influence the corresponding MI of $\hat{\mu}_{SE}^{\text{out}}$, since it approaches zero $\sim 2^{-n}$ for $n \gg 1$, which is why we may, without loss of generality, ignore it when trying to anticipate the PIP of (206). Without the $\hat{B}_1^{\pi/2}$ -addend (206) resembles (198), leading to the PIP from Fig. 13. Again, we conclude that the absence of the $\{\lambda = -1\}$ attractor subspace in (395) of Appendix J.1 is crucial for the appearance of QD, since it enables one to use quantum correlations between outer-diagonal S-subspaces $|0\rangle_S \langle 1|$ and $|1\rangle_S \langle 0|$ with E-registry states as »tools« for performing a perfect transfer of $H(S_{\text{class}})$ into E by means of decoherence. However, starting with a mixed (i.e. already decohered)

$\hat{\rho}_S^{\text{in}} = \sum_{i=0}^{2^k-1} |a_i|^2 |i\rangle \langle i|$ within $\hat{\sigma}_{SE}^{\text{in}} = \hat{\rho}_S^{\text{in}} \otimes \hat{\rho}_E^{\text{in}}$ within the framework of the random unitary CNOT-model (where $\hat{\rho}_E^{\text{in}} = |0_n\rangle \langle 0_n|$) does not allow to utilize the mechanism of decoherence as a means for transferring $H(S_{\text{class}})$ into E in the first place due to the absence of outer-diagonal S-subspaces $|0\rangle_S \langle 1|$ and $|1\rangle_S \langle 0|$ in $\hat{\sigma}_{SE}^{\text{in}}$, as well as in $\hat{\mu}_{SE}^{\text{out}}$ from (206).

Thus, the random unitary model, contrary to Zurek's qubit model, points out the importance of decoherence and thereby singles out the product input state $\hat{\rho}_{SE}^{\text{in}} = \hat{\rho}_S^{\text{in}} \otimes \hat{\rho}_E^{\text{in}}$ as an appropriate structure of an S-E-input state necessary for efficiently storing $H(S_{\text{class}})$ into E. This becomes even more apparent if we generalize $\hat{\sigma}_{SE}^{\text{in}} = \hat{\rho}_S^{\text{in}} \otimes \hat{\rho}_E^{\text{in}}$ with $\hat{\rho}_S^{\text{in}} = \sum_{i=0}^{2^k-1} |a_i|^2 |i\rangle \langle i|$ and $\hat{\rho}_E^{\text{in}} = |0_n\rangle \langle 0_n|$ to system S comprising $k \geq 1$ qubits. Letting $\hat{\sigma}_{SE}^{\text{in}} = \hat{\rho}_S^{\text{in}} \otimes \hat{\rho}_E^{\text{in}}$ undergo random unitary evolution we obtain in the asymptotic limit $N \gg 1$ (after ignoring the traceless $\hat{B}_1^{\pi/2}$ -term and addends $(-1)^N 2^{-n} \sum_{m=1}^{2^k-2} |a_m|^2 |m\rangle \langle m| \otimes |s_2^n\rangle \langle s_2^n|$ in (395) of Appendix J.1 associated with the $\{\lambda = -1\}$ attractor subspace, since the latter approach zero $\sim 2^{-2n}$ for $n \gg 1$)

$$\hat{\sigma}_{SE}^{\text{out}} = |a_0|^2 |0\rangle \langle 0| \otimes |0_L\rangle \langle 0_L| + \sum_{i=1}^{2^k-1} |a_i|^2 |i\rangle \langle i| \otimes 2^{-L} \hat{I}_L, \quad (207)$$

with non-zero eigenvalues

$$\begin{aligned} \hat{\sigma}_{SE}^{\text{out}} : \lambda_1^{SE} &= |a_0|^2 \text{ (1 times)}, \lambda_2^{SE} = |a_i|^2 2^{-L} \text{ (} 2^L \text{ times } \forall i \in \{1, \dots, 2^k-1\}) \\ \hat{\sigma}_E^{\text{out}} : \lambda_1^E &= |a_0|^2 + 2^{-L} (1 - |a_0|^2) \text{ (1 times)}, \lambda_2^E = 2^{-L} (1 - |a_0|^2) \text{ (} 2^L - 1 \text{ times)} \\ \hat{\sigma}_S^{\text{out}} : \lambda_1^S &= |a_i|^2 \text{ (} 2^k \text{ times)}, \end{aligned}$$

yielding

$$\begin{aligned} H(S) &= H(S_{\text{class}}) = \sum_{i=0}^{2^k-1} |a_i|^2 \log_2 |a_i|^2, \quad H(S, E_L) = H(S_{\text{class}}) + (1 - |a_0|^2) L \\ H(E_L) &= - \left(\frac{[2^L-1]|a_0|^2+1}{2^L} \right) \log_2 \left[|a_0|^2 + 2^{-L} (1 - |a_0|^2) \right] + (1 - |a_0|^2) L (1 - 2^{-L}) \\ &\quad - [1 - 2^{-L}] (1 - |a_0|^2) \log_2 (1 - |a_0|^2) \end{aligned} \quad (208)$$

and thus

$$\begin{aligned} H_E(L = n \gg k) &\approx \underbrace{-|a_0|^2 \log_2 |a_0|^2 - (1 - |a_0|^2) \log_2 (1 - |a_0|^2)}_{:= H(S_{\text{class}}^{k=1})} + (1 - |a_0|^2) n \\ H_{SE}(L = n \gg k) &\approx H(S_{\text{class}}^k) + (1 - |a_0|^2) n. \end{aligned} \quad (209)$$

(209) demonstrates that $H(S, E_{L=n \gg k}) = H(E_{L=n \gg k})$ holds in the limit $n \gg k$ of effective decoherence only for $k = 1$, otherwise for $k > 1$ $H(S_{\text{class}}^k)$ in $H_{SE}(L = n \gg k)$ always exceeds $H(S_{\text{class}}^{k=1})$ from $H_E(L = n \gg k)$ for an arbitrary, non-trivial probability S-distribution $\left\{ |a_i|^2 > 0 \right\}_{i=0}^{2^k-1}$, leading to $H(S, E_{L=n \gg k > 1}) > H(E_{L=n \gg k > 1})$. But even if we look at (208) for $L < n$ we may express the MI as

$$I(S : E_L) = - \left(\frac{[2^L-1]|a_0|^2+1}{2^L} \right) \log_2 \left[|a_0|^2 + 2^{-L} (1 - |a_0|^2) \right] - (1 - |a_0|^2) L \cdot 2^{-L} - (1 - |a_0|^2) \log_2 (1 - |a_0|^2) [1 - 2^{-L}], \quad (210)$$

from which the limits

$$\begin{aligned} \lim_{|a_0|^2 \rightarrow 0} I(S : E_L) &= \lim_{|a_0|^2 \rightarrow 1} I(S : E_L) = 0 \\ B &:= \left\{ \lim_{|a_0|^2 \rightarrow 2^{-k}} I(S : E_L) \right\} \Big|_{L=k} = - (2^{1-k} - 2^{-2k}) \log_2 (2^{1-k} - 2^{-2k}) - (1 - 2^{-k})^2 \log_2 (1 - 2^{-k}) - 2^{-k} (1 - 2^{-k}) k \end{aligned} \quad (211)$$

follow. The quantity B in (211) is particularly interesting, since it allows us to test in an easy manner whether QD appears or not: should (155) be violated at $L = k$, then QD does not appear. Now, since for $L = n \gg k > 1$ (209) has indicated

that QD fails to appear, whereas at least for $L = n \gg k = 1$ (155) remains violated. Therefore, (211) could enable us to test whether QD appears at least for a $k = 1$ qubit S . Namely,

$$B|_{k=1} = \underbrace{\frac{3}{2} \left(1 - \frac{\log_2 3}{2} \right)}_{:=c < 1} < 1 \equiv H(S_{\text{class}}^{k=1}) \quad (212)$$

clearly shows that even for $L = k = 1 < n$ the MI $I(S : E_{L=k=1 < n})$ -value lies below the Shannon-entropy value $H(S_{\text{class}}^{k=1})$. In other words, even for a $k = 1$ qubit S $I(S : E_{L=k=1 < n})$ from (211) falls monotonously from $H(S_{\text{class}}^{k=1})$ (at $L = n \gg k = 1$) to $I(S : E_L) = 0$ (at $L = 0$). Thus, for $k = 1$ we also do not see QD. Also, performing the limit $k \gg 1$ in B of (211) we obtain $\lim_{k \gg 1} B = 0$ (all addends tend to zero), which once more confirms the absence of QD for $k > 1$.

Clearly, we may state that for input states $\widehat{\sigma}_{kSE}^{\text{in}} = \widehat{\rho}_S^{\text{in}} \otimes \widehat{\rho}_E^{\text{in}}$ with $\widehat{\rho}_S^{\text{in}} = \sum_{i=0}^{2^k-1} |a_i|^2 |i\rangle \langle i|$ the contribution of the $\{\lambda = -1\}$ attractor subspace may be neglected within the corresponding output $\widehat{\sigma}_{kSE}^{\text{in}}$ of the random unitary evolution model with IDs containing mutually non-interacting E -qubits. In other words, even if we assume that the E -qubits within $\widehat{\sigma}_{kSE}^{\text{in}} = \widehat{\rho}_S^{\text{in}} \otimes \widehat{\rho}_E^{\text{in}}$ do not interact with each other, only the $\{\lambda = 1\}$ subspace of the maximal attractor space determines the asymptotic dynamics of the entire system and its subsystems if $\widehat{\rho}_S^{\text{in}}$ should be in an already decohered (maximally mixed) state.

We arrive at analogous conclusions by random unitarily evolving an entangled input state $\widehat{\mu}_{kSE}^{\text{in}} = 2^{-k} \sum_{i=0}^{2^k-1} |i\rangle \langle i| \otimes |z_n^{(i)}\rangle \langle z_n^{(i)}|$, where $z_n^{(i)} \in \mathcal{M} \equiv \{0, \dots, 2^k - 1\} \subset \{0, \dots, 2^n - 1\}$ runs over a subset of the first 2^k among 2^n possible E -registry states (i.e. $|\mathcal{M}| = 2^k$): the asymptotic state emerging from (170) and (380) of Appendix H.2.2 (for the same reasons outlined above we in advance ignore, without any loss of generality, the contribution (381) of the $\{\lambda = -1\}$ attractor subspace in Appendix H.2.2)

$$\widehat{\mu}_{kSE}^{\text{out}} = 2^{-k} \left\{ |0\rangle \langle 0| \otimes |0_L\rangle \langle 0_L| + \sum_{i=1}^{2^k-1} |i\rangle \langle i| \otimes 2^{-L} \widehat{I}_L \right\}, \quad (213)$$

which corresponds to (207) with $\left\{ |a_i|^2 = 2^{-k} \right\}_{i=0}^{2^k-1}$. Accordingly, (213) leads to non-zero eigenvalues

$$\begin{aligned} \widehat{\mu}_{kSE}^{\text{out}} : \lambda_1^{SE} &= 2^{-k} \text{ (1 times)}, \lambda_2^{SE} = 2^{-(k+L)} \text{ (2^L times } \forall i \in \{1, \dots, 2^k - 1\})} \\ \widehat{\mu}_{kE}^{\text{out}} : \lambda_1^E &= 2^{-k} + 2^{-L} (1 - 2^{-k}) \text{ (1 times)}, \lambda_2^E = 2^{-L} (1 - 2^{-k}) \text{ (2^L - 1 times)} \\ \widehat{\mu}_{kS}^{\text{out}} : \lambda_1^S &= |a_i|^2 \text{ (2^k times)} \end{aligned}$$

and thus to

$$\begin{aligned} H(S) &= H(S_{\text{class}}) = \sum_{i=0}^{2^k-1} |a_i|^2 \log_2 |a_i|^2 \\ H(E_L) &= -2^{-k} \left(1 + \frac{[2^k-1]}{2^L} \right) \log_2 \left[2^{-k} \left(1 + \frac{[2^k-1]}{2^L} \right) \right] \\ &\quad - \frac{(2^L-1)(2^k-1)}{2^{k+L}} \log_2 \left(\frac{2^k-1}{2^{k+L}} \right) \\ H(S, E_L) &= -2^{-k} \log_2 2^{-k} - \frac{2^L(2^k-1)}{2^{k+L}} \log_2 \frac{1}{2^{k+L}} = \underbrace{H(S_{\text{class}})}_{:=k} + (1 - 2^{-k}) L. \end{aligned} \quad (214)$$

For a fixed $k \geq 1$ and $n \gg L \gg k$ (214) yields

$$H(E_L) = H(S, E_L) - \underbrace{(1 - 2^{-k}) \log_2 [2^k - 1]}_{>0} < H(S, E_L), \quad (215)$$

from which we immediately conclude that $H(E_L) = H(S, E_L)$ holds only for $k = 1$ in the limit $n \gg 1$ of effective decoherence. Otherwise, $\forall k > 1$ one has $\lim_{k \gg 1} (1 - 2^{-k}) \log_2 [2^k - 1] \approx k = H(S_{\text{class}})$, as can be inferred from Tab. 6 below.

k	$(1 - 2^{-k}) \log_2 [2^k - 1]$
1	0
2	1.19
3	2.46
4	3.66
5	4.78

Table 6: Convergence of (215) towards $H(E_L) = H(S, E_L) - H(S_{\text{class}})$ for increasing k-values.

Indeed, we see that, taking (215) into account, $\lim_{L=n \gg k \gg 1} \frac{I(S:E_L)}{H(S_{\text{class}})} = 1 - \frac{k}{H(S_{\text{class}})} = 0$, i.e. for $L = n \gg k \gg 1$ the quantity $\frac{I(S:E_L)}{H(S_{\text{class}})}$ tends to zero. However, if we look at (214) for $L = k$ we obtain

$$H(E_{L=k}) = \underbrace{\frac{k}{2} + H(S_{\text{class}})}_{:=H(S, E_{L=k})} - \frac{k}{2^{k+1}} - \frac{1}{2} [1 + 2^{-k}] \log_2 [1 + 2^{-k}] < H(S, E_{L=k}), \quad (216)$$

which suppresses the appearance of QD for $k = 1$, such that $H(S, E_{L=k})$ exceeds $H(E_{L=k})$ even for $k \gg 1$.

Furthermore, setting in (214) $L = n \gg k$ for a fixed k, we obtain

$$H(S) = k, H(S, E_{L=n \gg k}) = k + (1 - 2^{-k})n, H(E_{L=n \gg k}) = -2^{-k} \log_2 2^{-k} - \log_2 2^{-n}, \quad (217)$$

and thus

$$\lim_{L=n \gg k} \frac{I(S:E_L)}{H(S_{\text{class}})} = \frac{n}{2^k \cdot k}. \quad (218)$$

(218) would attain or exceed $H(S_{\text{class}})$ only if $\frac{n}{2^k \cdot k} \geq 1$, implying $n \geq 2^k \cdot k$. This means that $I(S:E_L)$ obtained from $\widehat{\mu}_{kSE}^{\text{out}}$ in (213) can attain $H(S_{\text{class}})$ at $L = n$ in case of a k-qubit S only if its E is composed of many qudit-cells (2^k -level systems). This is another indication for correctness of the qudit-cell conjecture formulated above.

Finally, the qudit-cell conjecture manifested in (204) in the form $\lim_{n \sim k \gg 1} I(S:E_{L=n})/H(S_{\text{class}}) = 2^{-k}$ can also be recovered from (214) by setting $L = n \approx k$, which yields

$$H(S) = H(S_{\text{class}}) = k, H(S, E_{L=n \approx k}) = 2k, H(E_{L=n \approx k}) = 2^{1-k} \log_2 2^{1-k} - \log_2 2^{-k} \quad (219)$$

and thus

$$\lim_{n \sim k \gg 1} I(S:E_{L=n})/H(S_{\text{class}}) = 2^{1-k} \Rightarrow \lim_{n \sim k \gg 1} I(S:E_{L=n}) = 2^{1-k} \cdot H(S_{\text{class}}). \quad (220)$$

The prefactor 2 in (220) is of no significance, much more important is the fact that (220) suggests the following conclusion: a $k > 1$ qubit S starting within $\hat{\rho}_{SE}^{\text{in}} = \hat{\rho}_S^{\text{in}} \otimes \hat{\rho}_E^{\text{in}}$, with a pure k-qubit $\hat{\rho}_S^{\text{in}}$ and $\hat{\rho}_E^{\text{in}} = |0_n\rangle\langle 0_n|$ comprising mutually non-interacting E-qubits, behaves in the asymptotic limit $N \gg 1$ of the random unitary model w.r.t. the corresponding PIPs as the attractor space of a mixed S-E-state $\widehat{\mu}_{kSE}^{\text{out}}$ from (213), since, as also shown in Fig. 17, with increasing number k of S-qubits the contribution of the maximal $\{\lambda = -1\}$ attractor subspace (381) of Appendix H.2.2 decreases due to the overall normalization factor 2^{-k} in $\widehat{\mu}_{kSE}^{\text{out}}$ from (213) and $\hat{\rho}_{SE}^{\text{out}}$ from (395) of Appendix J.1 with $\left\{ |a_i|^2 = 2^{-k} \right\}_{i=0}^{2^k-1}$. We will illustrate this conclusion by the following two examples.

Examples for $\widehat{\mu}_{kSE}^{\text{out}}$ from (213)

Let us first start with an input state

$$\widehat{\mu}_{kSE}^{\text{in}} = 2^{-(k-1)} \{ |0\rangle\langle 0| \otimes |0_{L=n}\rangle\langle 0_{L=n}| + |1\rangle\langle 1| \otimes |1_{L=n}\rangle\langle 1_{L=n}| \}, \quad (221)$$

which after undergoing a random unitary evolution yields for $N \gg 1$ the output state

$$\widehat{\mu}_{kSE}^{\text{out}} = 2^{-1} \left\{ |0\rangle\langle 0| \otimes |0_L\rangle\langle 0_L| + |1\rangle\langle 1| \otimes 2^{-L} \widehat{I}_L \right\} + (-1)^N 2^{-1} |1\rangle\langle 1| 2^{-n/2} \bigotimes_{i=1}^n \hat{B}_1^{\pi/2} \cdot \delta_{L,n}, \quad (222)$$

where we also take into account the contribution of the $\{\lambda = -1\}$ attractor subspace (381) (Appendix H.2.2) proportional

to the (traceless) $(-1)^N$ -term. (222) leads to the non-zero eigenvalues

$$\begin{aligned}
& \widehat{\mu}_{kSE}^{\text{out}} (L = n) : \lambda_1^{SE} = 2^{-1} (1 \times), \lambda_{2/3}^{SE} = 2^{-(n+1)} (1 \pm (-1)^N) \text{ (each } 2^{n-1} \times) \\
& \widehat{\mu}_{kE}^{\text{out}} (L = n) : \lambda_1^E = 2^{-(n+1)} (2^n + 1 - (-1)^N) ([1 - \delta_{n \bmod 2, 0}] \times), \lambda_2^E = 2^{-(n+1)} (1 - (-1)^N) ([2^{n-1} \delta_{n \bmod 2, 0}] \times) \\
& \lambda_3^E = 2^{-(n+1)} (1 - (-1)^N) ([2^{n-1} - 1] \delta_{n \bmod 2, 0} \times), \lambda_4^E = 2^{-(n+1)} (2^n + 1 + (-1)^N) (\delta_{n \bmod 2, 0} \times) \\
& \lambda_5^E = 2^{-(n+1)} (1 + (-1)^N) ([1 - \delta_{n \bmod 2, 0}] 2^{n-1} \times), \lambda_6^E = 2^{-(n+1)} (1 - (-1)^N) ([1 - \delta_{n \bmod 2, 0}] [2^{n-1} - 1] \times) \\
& \widehat{\mu}_{kSE}^{\text{out}} (L < n) : \lambda_1^{SE} = 2^{-1} (1 \times), \lambda_2^{SE} = 2^{-(L+1)} (2^L \times) \\
& \widehat{\mu}_{kE}^{\text{out}} (L < n) : \lambda_1^E = 1 (\delta_{L, n} \times), \lambda_2^E = 2^{-(L+1)} (2^L - 1 \times), \lambda_3^E = 2^{-(L+1)} (2^L + 1) (1 - \delta_{L, n} \times) \\
& \widehat{\mu}_{kS}^{\text{out}} : \lambda_1^S = 2^{-1} (2 \times),
\end{aligned}$$

which in turn generate the n -dependence of MI in Fig. 19 below and lead to the PIP in Fig. 17 (\blacklozenge -dotted curve).

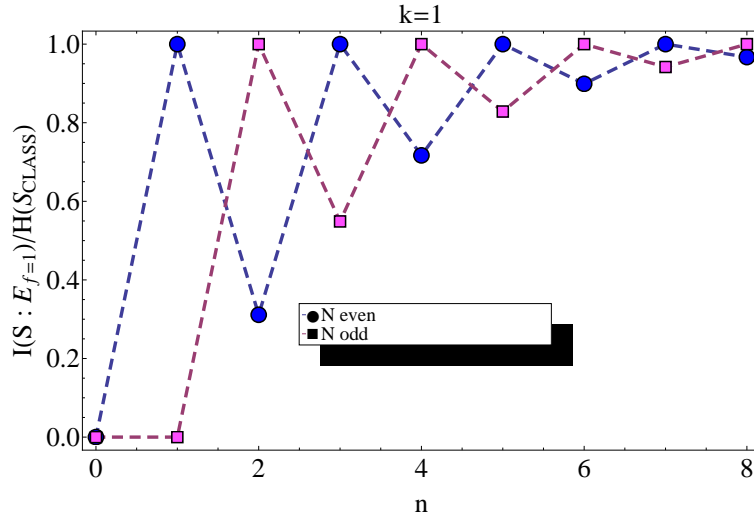


Figure 19: PIP after random iterative $\widehat{u}_j^{(\phi=\pi/2)}$ -evolution of $\widehat{\mu}_{kSE}^{\text{in}} = 2^{-(k=1)} \{|0\rangle \langle 0| \otimes |0_{L=n}\rangle \langle 0_{L=n}| + |1\rangle \langle 1| \otimes |1_{L=n}\rangle \langle 1_{L=n}|\}$ ($N \gg 1$), without interaction bindings between E-qubits, plotted w.r.t. the number n of E-qubits.

Again, we see in Fig. 19 a well-defined, N -independent convergence of $I(S : E_{L=n}) / H(S_{\text{class}})$ to one for $n \gg 1$. Thus, (222) does not lead to QD, since its eigenvalues lead to the entropy relation

$$\begin{aligned}
H(E_L) &= -(1 - \delta_{L, n}) 2^{-1} [1 + 2^{-L}] \log_2 (2^{-1} [1 + 2^{-L}]) + 2^{-1} (L + 1) [1 + 2^{-L}] \\
&< H(S, E_L) = 2^{-1} [L + 2]
\end{aligned} \tag{223}$$

valid $\forall L \leq n$. Apparently, when looking at the eigenvalue spectra of (222) we recover $H(S) = H(S_{\text{class}}) = k = 1$ and conclude that the normalization prefactor 2^{-1} in (222) causes $H(S, E_L)$ to exceed $H(E_L) \forall L < n$.

Finally, our second example deals with an input state

$$\begin{aligned}
\widehat{\mu}_{kSE}^{\text{in}} &= 2^{-(k=2)} \{|0\rangle \langle 0| \otimes |0_n\rangle \langle 0_n| + |3\rangle \langle 3| \otimes |1_n\rangle \langle 1_n| \\
&|1\rangle \langle 1| \otimes |0_{n-1}\rangle \langle 0_{n-1}| + |2\rangle \langle 2| \otimes |1_{n-1}\rangle \langle 1_{n-1}|\},
\end{aligned} \tag{224}$$

with n mutually non-interacting E-qubits. (224) leads, in the asymptotic limit of the random unitary evolution, to the output state

$$\begin{aligned}
\widehat{\mu}_{kSE}^{\text{out}} &= 2^{-2} \left\{ |0\rangle \langle 0| \otimes |0_n\rangle \langle 0_n| + \sum_{i=1}^3 |i\rangle \langle i| \otimes 2^{-n} \widehat{I}_n \right\} + (-1)^N 2^{-2} \left\{ |3\rangle \langle 3| 2^{-n/2} \bigotimes_{i=1}^n \widehat{B}_1^{\pi/2} \right. \\
&\quad \left. 2^{-n} (|1\rangle \langle 1| + |2\rangle \langle 2|) \otimes |s_2^n\rangle \langle s_2^n| \right\},
\end{aligned} \tag{225}$$

whose n -dependence of the MI is given in Fig. 20 below, whereas the corresponding PIP is represented by the \blacktriangle -dotted curve in Fig. 17.

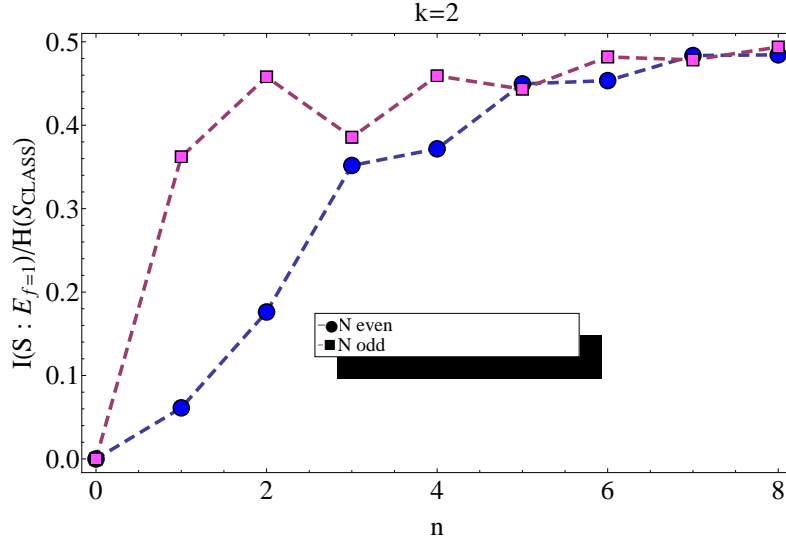


Figure 20: PIP after random iterative $\hat{u}_j^{(\phi=\pi/2)}$ -evolution of $\hat{\mu}_{kSE}^{\text{in}}$ in (224) ($N \gg 1$), without interaction bindings between E-qubits, plotted w.r.t. the number n of E-qubits.

From Fig. 20 we see that the maximal value of $I(S : E_{L=n}) / H(S_{\text{class}})$ approaches the N -independent value 0.5 in the limit $n \gg 1$, as one would expect from a well-defined asymptotic (fixed) state to behave. Also, (225) indicates that for $n \gg 1$ contributions from the maximal $\{\lambda = -1\}$ attractor subspace (381) (Appendix H.2.2) associated with the prefactor $(-1)^N$ may be neglected. Thus, the n -dependence of the MI in Fig. 20 also supports the qudit-cell conjecture represented by the \blacktriangle -dotted curve in Fig. 17.

II) $\hat{\rho}_{SE}^{\text{in}} = \hat{\rho}_S^{\text{in}} \otimes \hat{\rho}_E^{\text{in}}$, $k = 1$ -qubit pure $\hat{\rho}_S^{\text{in}}, \hat{\rho}_E^{\text{in}} = 2^{-1}(|0_n\rangle\langle 0_n| + |1_n\rangle\langle 1_n|)$ (Fig. 23, \blacksquare -dotted curve)

The PIP obtained from a random unitarily $\hat{u}_j^{(\phi=\pi/2)}$ -evolved $\hat{\rho}_{SE}^{\text{out}}$ in (396) of Appendix J.1 for $k = 1$ S-qubit is displayed in Fig. 23 below (red, \blacksquare -dotted curve). We see that if $\hat{\rho}_E^{\text{in}}$ contains correlations between E-registry states one is even not able to extract $H(S_{\text{class}})$ after taking the entire E into account when computing $I(S : E_L)$, since according to Fig. 23 $I(S : E_{L=n}) / H(S_{\text{class}}) < 1$. This can be easily explained by looking at the $n \gg k$ limit of (396) in Appendix J.1

$$\lim_{n \gg k} \hat{\rho}_{SE_{L=n}}^{\text{out}} = |a_0|^2 |0_k\rangle\langle 0_k| \otimes \hat{\rho}_E^{\text{in}} + |a_1|^2 |1\rangle\langle 1| \otimes 2^{-n} \hat{I}_n \Rightarrow H(S) = H(S_{\text{class}}) \Rightarrow \lim_{n \gg k} \hat{\rho}_{E_{L=n}}^{\text{out}} = |a_0|^2 \hat{\rho}_E^{\text{in}} + |a_1|^2 2^{-n} \hat{I}_n. \quad (226)$$

The (non-zero) eigenvalues

$$\lambda_1^{SE} = |a_0|^2 2^{-1} \text{ (2 times)}, \lambda_2^{SE} = |a_1|^2 2^{-n} \text{ (2}^n \text{ times)}$$

(for $\lim_{n \gg k} \hat{\rho}_{SE_{L=n}}^{\text{out}}$), as well as eigenvalues

$$\lambda_1^E = |a_0|^2 2^{-1} + |a_1|^2 2^{-n} \text{ (2 times)}, \lambda_2^E = |a_1|^2 2^{-n} \text{ ([2}^n - 2] \text{ times)}$$

(for $\lim_{n \gg k} \hat{\rho}_{E_{L=n}}^{\text{out}}$), yield (for $0 < |a_0|^2 < 1$)

$$\lim_{n \gg k} H(S, E_{L=n}) = H(S_{\text{class}}) + |a_0|^2 + |a_1|^2 n > \lim_{n \gg k} H(E_{L=n}),$$

since $\lim_{n \gg k} H(E_{L=n})$ contains two addends,

$$A_1 := -|a_1|^2 \log_2 \frac{|a_1|^2}{2^n} + 2^{1-n} |a_1|^2 \log_2 \frac{|a_1|^2}{2^n}, A_2 := -(|a_0|^2 + 2^{1-n} |a_1|^2) \cdot \log_2 (2^{-1} |a_0|^2 + 2^{-n} |a_1|^2),$$

with $A_1 < -|a_1|^2 \log_2 \frac{|a_1|^2}{2^n}$ and $A_2 < -|a_0|^2 \log_2 \frac{|a_0|^2}{2}$. In other words, if correlations between E-registry states persist throughout the process of tracing out E-qubits from (226), (155) will be violated and the MI-'plateau' disappears,

confirming the corresponding results obtained by means of Zurek's model of Quantum Darwinism (s. also discussion from subsection 8.4 below). Effectively the same PIP emerges if one starts the above random unitary evolution with $|\Psi_E^{\text{in}}\rangle = 2^{-1/2}(|0_n\rangle + |1_n\rangle)$ since contributions within the corresponding $\hat{\rho}_{SE}^{\text{out}}$ associated with non-classical correlation terms $|0_n\rangle\langle 1_n|$ and $|1_n\rangle\langle 0_n|$ also vanish in the limit ($k \leq L < n \gg k$) (s. (396) in Appendix J.1).

Finally, plotting $I(S : E_{f=1})/H(S_{\text{class}})$ w.r.t. n for $\hat{\rho}_{SE}^{\text{out}}$ in (396) of Appendix J.1 and the $k = 1$ S-qubit leads to a well-defined, N -independent convergence of the MI to the value 1, as shown in Fig. 21 below.

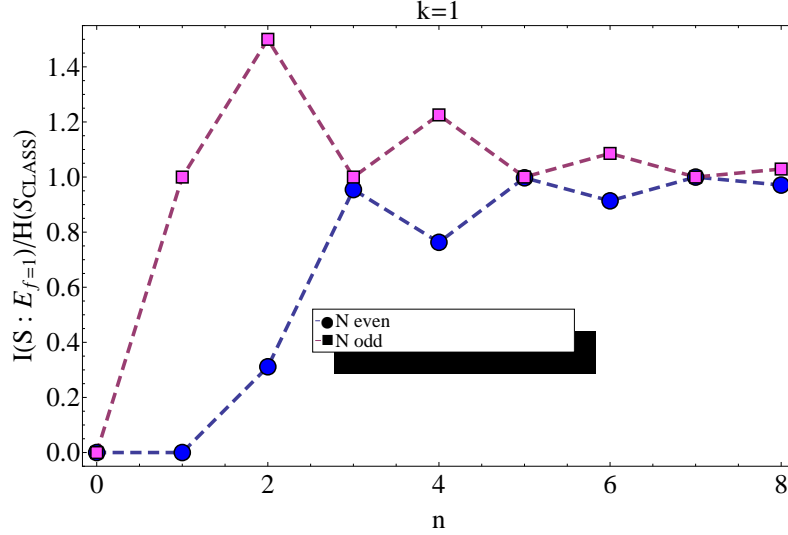


Figure 21: PIP after random iterative $\hat{u}_j^{(\phi=\pi/2)}$ -evolution of $\hat{\rho}_{SE}^{\text{in}} = |\Psi_S^{\text{in}}\rangle\langle\Psi_S^{\text{in}}| \otimes \hat{\rho}_E^{\text{in}}$ ($N \gg 1$), with a pure $k = 1$ qubit $|\Psi_S^{\text{in}}\rangle = \sum_{m=0}^1 a_m |m\rangle$ ($|a_m|^2 = 2^{-1} \forall m$), and $\hat{\rho}_E^{\text{in}} = 2^{-1}(|0_n\rangle\langle 0_n| + |1_n\rangle\langle 1_n|)$ (0 E-bindings) w.r.t. n , s. main text.

Unfortunately, this convergence of $I(S : E_L)/H(S_{\text{class}})$ to 1 breaks down as soon as $L < n$, as indicated by Fig. 23 (■-dotted curve). Finally, we can also visualize the influence of the maximal $\{\lambda = -1\}$ attractor subspace (381) (Appendix H.2.2) associated with the prefactor $(-1)^N$ in (396) from Appendix J.1 to the entire PIP of $I_{\text{tot}}(S : E_L)/H(S_{\text{class}})$ w.r.t. $f = L/n$ from Fig. 23 (■-dotted curve) by simply subtracting from this PIP of the entire maximal attractor space all $I_{\text{part}}(S : E_L)/H(S_{\text{class}})$ -values between $0 \leq f \leq 1$ calculated from (396) in Appendix J.1 by deliberately ignoring all addends associated with the prefactor $(-1)^N$. In Fig. 22 below this difference $|I_{\text{tot}} - I_{\text{part}}|$ is normalized by I_{part} and plotted w.r.t. $f = L/n$ in order to show the percentage that the maximal $\{\lambda = -1\}$ attractor subspace (381) (Appendix H.2.2) contributes to $I_{\text{tot}}(S : E_L)/H(S_{\text{class}})$ (■-dotted curve in Fig. 23, obtained for example and without loss of generality w.r.t. an odd N -value from (166)-(170) above) w.r.t. f .

From Fig. 22 we see that the maximal $\{\lambda = -1\}$ attractor subspace (381) (Appendix H.2.2) has the highest contribution to the PIP of (396) from Appendix J.1 for $L = 0, 1$ (100 % and 75%, respectively), which is of no significance, since the value of I_{tot} is already very low ($< 0.01 \ll 1$) at $L = 1$. $\forall (2 \leq L \leq n)$ does not exceed 0.01 attained for $L = n$ due to the existing traceless $\hat{B}_1^{\pi/2}$ -addend in (396) from Appendix J.1. Summa summarum, we may conclude that already environmental input states $\hat{\rho}_E^{\text{in}}$ containing more than one E-registry state (i.e. $\hat{\rho}_E^{\text{in}}$ which are not of rank one w.r.t. E-registry states of the standard computational basis) lead in the course of the random unitary evolution with IDs containing mutually non-interacting E-qubits to asymptotic output states $\hat{\rho}_{SE}^{\text{out}}$ in which the contribution of the maximal $\{\lambda = -1\}$ attractor subspace (381) (Appendix H.2.2) to the corresponding PIP may be neglected in the limit $n \gg 1$ of effective decoherence.

III) $\hat{\rho}_{SE}^{\text{in}} = \hat{\rho}_S^{\text{in}} \otimes \hat{\rho}_E^{\text{in}}$, $k = 1$ -qubit pure $\hat{\rho}_S^{\text{in}}$, $\hat{\rho}_E^{\text{in}} = 2^{-n}\hat{I}_n$ (Fig. 23, •-dotted curve)

An extreme case for $\hat{\rho}_E^{\text{in}}$ containing classical correlations between E-registry states is the totally mixed environmental n -qubit input state which leads according to Fig. 23 (blue, •-dotted curve) to $\lim_{n \gg k} I(S : E_{L=n})/H(S_{\text{class}}) \approx 0$. This follows from the $n \gg k$ limit

$$\lim_{n \gg k} \hat{\rho}_{SE_{L=n}}^{\text{out}} = (|a_0|^2 |0\rangle\langle 0| + |a_1|^2 |1\rangle\langle 1|) \otimes 2^{-n}\hat{I}_n \Rightarrow H(S, E_{L=n \gg k}) = H(S_{\text{class}}) + H(E_{L=n \gg k}) \quad (227)$$

of (397) in Appendix J.1.

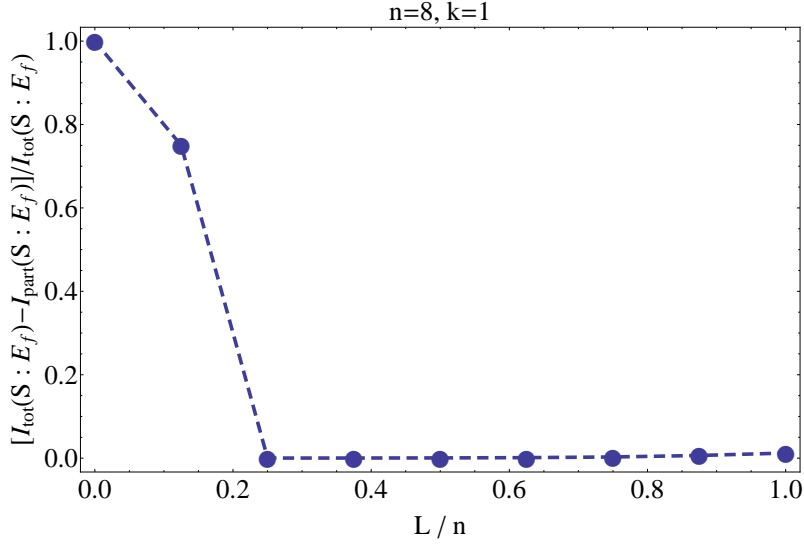


Figure 22: PIP of $|I_{\text{tot}} - I_{\text{part}}|/I_{\text{tot}}$ after random iterative $\hat{u}_j^{(\phi=\pi/2)}$ -evolution of $\hat{\rho}_{SE}^{\text{in}} = |\Psi_S^{\text{in}}\rangle\langle\Psi_S^{\text{in}}| \otimes \hat{\rho}_E^{\text{in}}$ ($N \gg 1$), with a pure $k = 1$ qubit $|\Psi_S^{\text{in}}\rangle = \sum_{m=0}^1 a_m |m\rangle$ ($|a_m|^2 = 2^{-1} \forall m$), $n = 8$ and $\hat{\rho}_E^{\text{in}} = 2^{-1}(|0_n\rangle\langle 0_n| + |1_n\rangle\langle 1_n|)$ (0 E-bindings) w.r.t. $f = L/n$, s. main text.

In other words, completely mixed $\hat{\rho}_E^{\text{in}}$ are not suitable for efficiently storing $H(S_{\text{class}})$ into E with $f \leq k/n$.

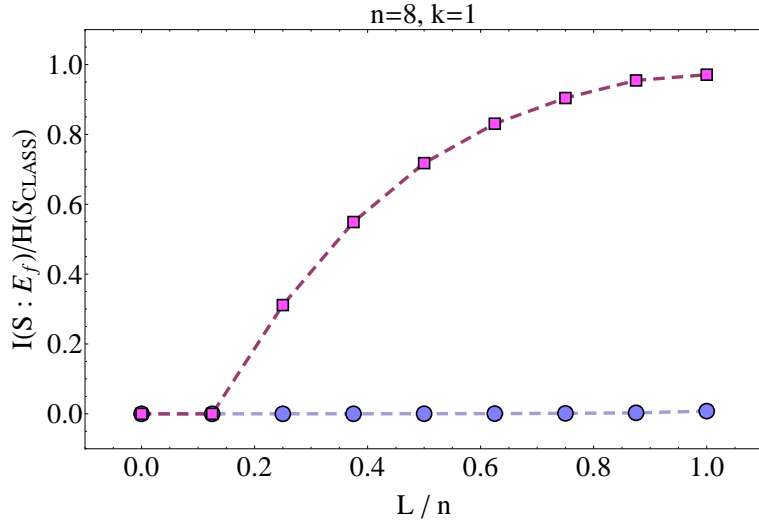


Figure 23: PIP after random iterative $\hat{u}_j^{(\phi=\pi/2)}$ -evolution of $\hat{\rho}_{SE}^{\text{in}} = |\Psi_S^{\text{in}}\rangle\langle\Psi_S^{\text{in}}| \otimes \hat{\rho}_E^{\text{in}}$ ($N \gg 1$), with a pure $k = 1$ qubit $|\Psi_S^{\text{in}}\rangle = \sum_{m=0}^1 a_m |m\rangle$ ($|a_m|^2 = 2^{-1} \forall m$), $n = 8$ and different $\hat{\rho}_E^{\text{in}}$ (0 E-bindings), s. main text.

But also performing the limit $n \gg 1$ within the non-zero eigenvalues of (397) from Appendix J.1

$$\begin{aligned}
 \hat{\rho}_{SE}^{\text{out}} : \lambda_1^{SE} &= |a_0|^2 \cdot 2^{-L} \text{ (} 2^L - 2 \text{ times)}, \lambda_2^{SE} = |a_1|^2 \cdot 2^{-L} \text{ (} 2^L - 2 \text{ times)}, \lambda_3^{SE} = 2^{-L} \text{ (} 2 \text{ times)} \\
 \hat{\rho}_E^{\text{out}} : \lambda_1^E &= 2^{-L} \text{ (} 2^L \text{ times)} \\
 \hat{\rho}_S^{\text{out}} : \lambda_{1/2}^S &= 2^{-1} \pm \sqrt{\underbrace{\left(\frac{2^{n-1}|a_0|^2}{2^n}\right)^2 + \left(\frac{2^{n-1}|a_1|^2}{2^n}\right)^2 + \frac{|a_0|^2|a_1|^2}{2^{2n}} \cdot \left\{(-1)^N \left(2 + (-1)^N\right) - (2^{2n-1} - 1)\right\}}_{:=D}} \quad (228)
 \end{aligned}$$

indicates that $H(S, E_{L=n}) = H(S_{\text{class}}) + n - 2^{1-n}H(S_{\text{class}})$, $H(E_{L=n}) = n$ and $\lim_{n \rightarrow \infty} H(S) = H(S_{\text{class}})$, since for $n \gg 1$ the term D under the square-root of $\lambda_{1/2}^S$ in (228) converges to $\lim_{n \gg 1} D = (|a_0|^2 - |a_1|^2)^2 \cdot 2^{-2}$. Accordingly, one obtains $\lim_{n \gg 1} H(S, E_{L=n}) = H(S_{\text{class}}) + n = H(S_{\text{class}}) + H(E_{L=n})$, which explains why the maximal value $I(S : E_{L=n})$ of the MI tends to zero in the limit $n \gg 1$ of effective decoherence, as indicated by the •-dotted curve in Fig. 23 and the n -dependence of $I(S : E_{L=n})/H(S_{\text{class}})$ in Fig. 24 below.

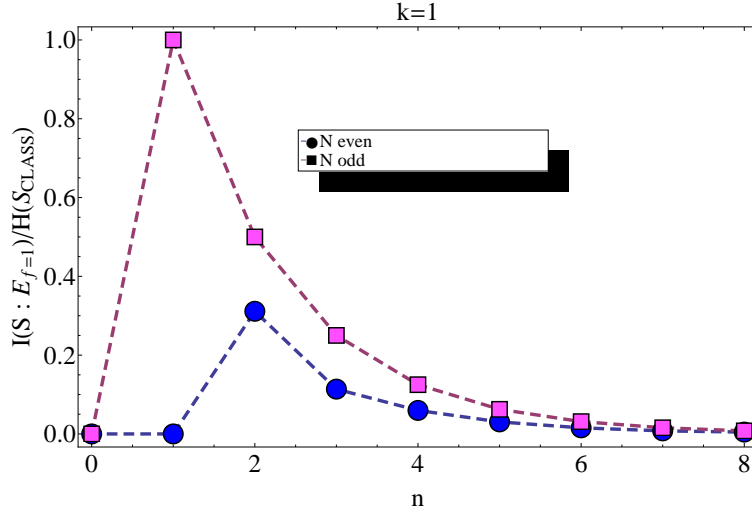


Figure 24: PIP after random iterative $\hat{u}_j^{(\phi=\pi/2)}$ -evolution of $\hat{\rho}_{SE}^{\text{in}} = |\Psi_S^{\text{in}}\rangle \langle \Psi_S^{\text{in}}| \otimes \hat{\rho}_E^{\text{in}}$ ($N \gg 1$), with a pure $k = 1$ qubit $|\Psi_S^{\text{in}}\rangle = \sum_{m=0}^1 a_m |m\rangle$ ($|a_m|^2 = 2^{-1} \forall m$), and $\hat{\rho}_E^{\text{in}} = 2^{-n} \hat{I}_n$ (0 E-bindings) w.r.t. n , s. main text.

Finally, we also want to confirm our intuitive understanding of the maximally mixed environmental input state and its influence on QD within the maximal attractor space of the random unitary model by discussing the input state

$$\hat{\rho}_{SE}^{\text{in}} = |\Psi_S^{\text{in}}\rangle \langle \Psi_S^{\text{in}}| \otimes \underbrace{(\hat{I}_n - |1_n\rangle \langle 1_n|)}_{:= \hat{\rho}_E^{\text{in}}} (2^n - 1)^{-1}, \quad (229)$$

with a pure $k = 1$ qubit $|\Psi_S^{\text{in}}\rangle = \sum_{m=0}^1 a_m |m\rangle$ and an almost completely mixed $\hat{\rho}_E^{\text{in}}$. We expect the maximum of $I(S : E_{L=n})$ emerging from the random unitary evolution of (229) to be higher than the one computed from (397) in Appendix J.1. Now, (229) leads in the asymptotic limit $N \gg 1$ to the output state

$$\begin{aligned} \hat{\rho}_{SE}^{\text{out}} = & |a_0|^2 |0_k\rangle \langle 0_k| \otimes \hat{\rho}_E^{\text{in}} + a_0 a_1^* |0_k\rangle \langle 1_k| \otimes (2^n - 1)^{-1} (|s_1^n\rangle \langle s_1^n| - 2^{-n/2} |1_n\rangle \langle s_1^n|) \\ & + a_0^* a_1 |1_k\rangle \langle 0_k| \otimes (2^n - 1)^{-1} (|s_1^n\rangle \langle s_1^n| - 2^{-n/2} |s_1^n\rangle \langle 1_n|) + |a_1|^2 |1_k\rangle \langle 1_k| \otimes (2^n - 1)^{-1} (1 - 2^{-n}) \hat{I}_n \\ & + (-1)^N (2^n - 1)^{-1} [a_0 a_1^* |0_k\rangle \langle 1_k| \otimes (|s_2^n\rangle \langle s_2^n| - (-1)^n 2^{-n/2} |1_n\rangle \langle s_2^n|) \\ & + a_0^* a_1 |1_k\rangle \langle 0_k| \otimes (|s_2^n\rangle \langle s_2^n| - (-1)^n 2^{-n/2} |s_2^n\rangle \langle 1_n|) \\ & - 2^{-n/2} |a_1|^2 |1_k\rangle \langle 1_k| \otimes \hat{B}_L^{\pi/2} \cdot \delta_{L,n}], \end{aligned} \quad (230)$$

whose PIP w.r.t. n is given in Fig. 25 below.

Fig. 25 indeed indicates that the maximum value $I(S : E_{L=n})$ for $n \gg 1$ is probably higher than the corresponding value in Fig. 24, since both maxima at $n = 2$ (even N) and $n = 1$ (odd N) in Fig. 25 exceed those in Fig. 24. Resolving $I(S : E_{L=n=8})$ from Fig. 25 and Fig. 24 w.r.t. $f = L/n$ we obtain Fig. 26 below, from which we see that (230) really leads to the highest $I(S : E_{L=n=8})$ -value, followed by the corresponding $I(S : E_{L=n=8})$ -values w.r.t. (397) from Appendix J.1 and (407) from Appendix J.2, the latter being associated with the minimal $\{\lambda = 1\}$ attractor subspace.

Also, the contribution of the maximal $\{\lambda = -1\}$ attractor subspace (381) (Appendix H.2.2) associated with the prefactor $(-1)^N$ in (397) from Appendix J.1 may be neglected for $n \gg 1$, since the maximum MI-value even when taking all subspaces of the maximal attractor space into account lies in Fig. 26 below 0.01 (already) for $n = 8$.

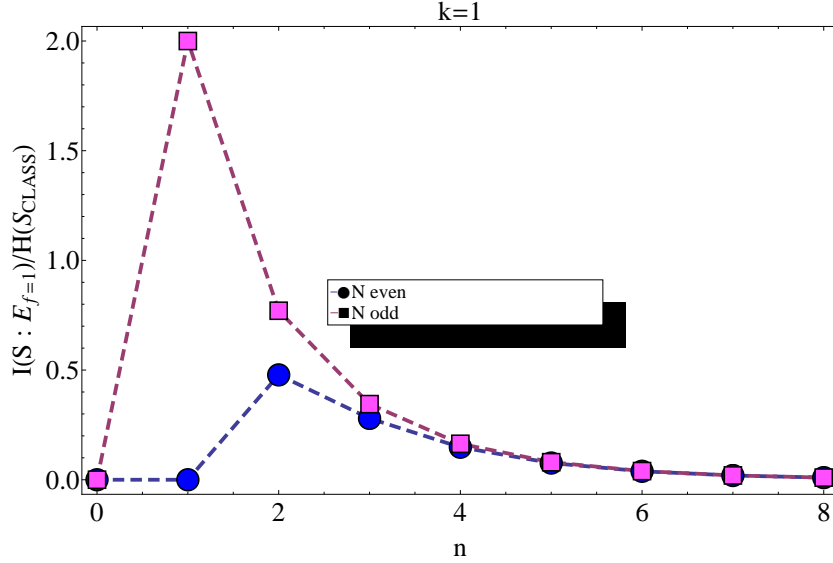


Figure 25: PIP after random iterative $\hat{u}_j^{(\phi=\pi/2)}$ -evolution of $\hat{\rho}_{SE}^{in} = |\Psi_S^{in}\rangle \langle \Psi_S^{in}| \otimes \hat{\rho}_E^{in}$ ($N \gg 1$), with a pure $k = 1$ qubit $|\Psi_S^{in}\rangle = \sum_{m=0}^1 a_m |m\rangle$ ($|a_m|^2 = 2^{-1} \forall m$), and $\hat{\rho}_E^{in} = (\hat{I}_n - |1_n\rangle \langle 1_n|) (2^n - 1)^{-1}$ (0 E-bindings) w.r.t. n , s. main text.

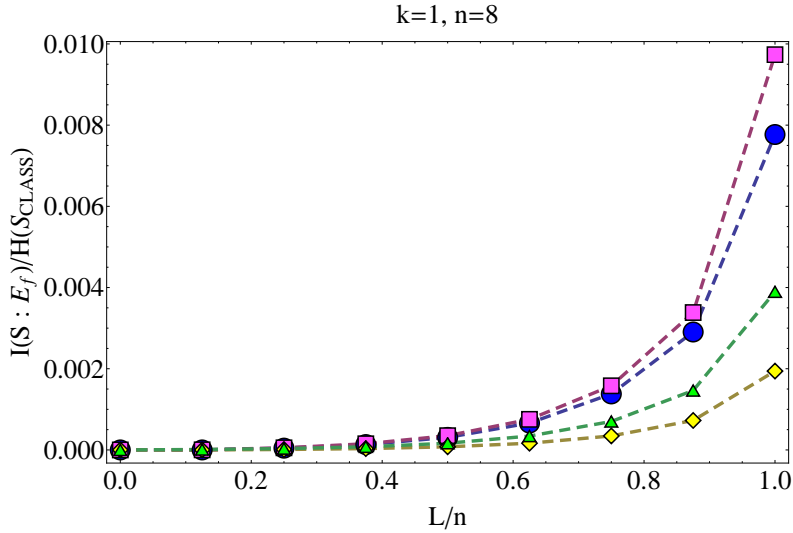


Figure 26: PIPs of (397) in Appendix J.1 after $N \gg 1$ iterations and w.r.t. $f = L/(n = 8)$ (\bullet -dotted curve for $\{\lambda = \pm 1\}$ attractor subspaces, \blacktriangle -dotted curve only for $\{\lambda = 1\}$ attractor subspace), (230) (\blacksquare -dotted curve) and (407) in Appendix J.2 (\blacklozenge -dotted curve), s. main text.

All these results clearly show that sums of E-registry states within $\hat{\rho}_E^{in}$ tend to suppress the corresponding MI when resolved w.r.t. $f = L/n$ and $n \gg 1$. In other words, as soon as $\hat{\rho}_E^{in} \neq |y\rangle \langle y|$ (with $y \in \{0, \dots, 2^n - 1\}$) in $\hat{\rho}_{SE}^{in} = |\Psi_S^{in}\rangle \langle \Psi_S^{in}| \otimes \hat{\rho}_E^{in}$, the corresponding PIP after the asymptotic random unitary evolution will tend to zero $\forall L \leq (n \gg 1)$, implying that within Zurek's and the random unitary model we may say that the more addends (E-registry states and their mutual correlations) $\hat{\rho}_E^{in}$ comprises, the lower values will be attained by $I(S : E_{L=n \gg 1})$ in the course of its PIP.

IV) $\hat{\rho}_{SE}^{in} = \hat{\rho}_S^{in} \otimes \hat{\rho}_E^{in}$, $k = 1$ -qubit pure $\hat{\rho}_S^{in}$, $\hat{\rho}_E^{in} = 2^{-1} (|0_n\rangle \langle 0_n| + |10_{n-1}\rangle \langle 10_{n-1}|)$

This type of $\hat{\rho}_E^{in}$ leads within the random unitary model to $\hat{\rho}_{SE}^{out}$ in (398) of Appendix J.1, demonstrating that within the random unitary model it is, as was the case with Zurek's model, in principle important in which order one traces out single E-qubits: if we trace out the first left E-qubit in $|10_{n-1}\rangle \langle 10_{n-1}|$ for a fixed L-value $L = L^*$ with $k \leq L^* < n$, $\hat{\rho}_{SE^{L^*}}^{out}$ in (398) of Appendix J.1 would reduce to $\hat{\rho}_{SE^{L^*}}^{out}$ from (395), validating (155) at least $\forall (k \leq L \leq L^*)$. However, in general this is not what we demand from $\hat{\rho}_{SE}^{out}$ whose E should allow complete reconstruction of $H(S_{class})$ regardless of the order in which one decides to intercept environmental fragments (qubits). This implies that among all possible combinations (sums) of E-registry states only the pure (one) E-registry state $\hat{\rho}_E^{in} = |y\rangle \langle y| \forall y \in \{0, \dots, 2^n - 1\}$ leads to Quantum Darwinism, both in Zurek's and the random unitary model.

V) $|\Psi_{SE}^{in}\rangle = a|0_{k=1}\rangle \otimes |s_1^{L=n}\rangle + b|1_{k=1}\rangle \otimes |s_2^{L=n}\rangle$ (Fig. 1)

This artificial $\hat{\rho}_{SE}^{in}$ entangles each S-pointer state with one of the $\hat{U}_j^{(\phi)}$ -symmetry states $\{|s_{c_1}^L\rangle, |s_{c_2}^L\rangle\}$, validating (155), according to Appendix E, only for $c_1 = c_2 = 1/2$, which is why we obtain for the corresponding $\hat{\rho}_{SE}^{out}$ in (399) of Appendix J.1 exactly the same PIP as the one displayed in Fig. 1: $\hat{\rho}_{SE}^{in}$ simply does not change $\forall N \gg 1$ due to invariance of E towards $\hat{U}_j^{(\phi=\pi/2)}$ and the fact that the $\lambda = -1$ attractor subspace in (381) of Appendix H.2.2 contributes to the random unitary evolution of $\hat{\rho}_{SE}^{in}$ for a $k = 1$ qubit system S only a phase $(-1)^N$ -factor within the $|0\rangle \langle 1|$ - and $|1\rangle \langle 0|$ -subspace of system S. For $k > 1$ one could obtain Quantum Darwinism according to (380)-(381) from Appendix H.2.2 only if one entangles two S-pointer states $\{|0_{k>1}\rangle, |1_{k>1}\rangle\}$ with available CNOT-symmetry states $\{|s_1^L\rangle, |s_2^L\rangle\}$. However, this would enable us to store only $0 < H(S) = H(S_{class}) \leq 1$ corresponding to a $k = 1$ qubit system S. In order to store $H(S_{class})$ of a $k > 1$ qubit S one needs 2^k symmetry states of $\hat{U}_{ij}^{(\phi)}$ (s. (166) above) with which one could entangle the 2^k S-pointer states $\{|\pi_i\rangle\} \equiv \{|i\rangle\}_{i=0}^{2^k-1}$, otherwise if the number of S-pointer states exceeds the number of available $\hat{U}_{ij}^{(\phi)}$ -symmetry states, Quantum Darwinism disappears (s. (352)-(354) in Appendix E).

Now we turn our attention to the input state $\hat{\rho}_{SE}^{in} = \hat{\rho}_S^{in} \otimes \hat{\rho}_E^{in}$ with a $k = 1$ qubit pure $\hat{\rho}_S^{in}$ given by $|\Psi_S^{in}\rangle = \sum_{m=0}^1 a_m |m\rangle$ and $\hat{\rho}_E^{in} = \frac{1}{2} (|s_1^{L=n}\rangle \langle s_1^{L=n}| + |s_2^{L=n}\rangle \langle s_2^{L=n}|)$ which we encountered in (195), in the course of the minimal attractor space. Will this state allow us to see QD? The random unitarily CNOT-evolved output state

$$\hat{\rho}_{SE}^{out} = (|a_0|^2 |0\rangle \langle 0| + |a_1|^2 |1\rangle \langle 1|) \otimes \hat{\rho}_E^{in} + \left(\frac{a \cdot b^*}{2} |0\rangle \langle 1| + \frac{a^* \cdot b}{2} |1\rangle \langle 0| \right) \otimes (|s_1^{L=n}\rangle \langle s_1^{L=n}| + (-1)^N |s_2^{L=n}\rangle \langle s_2^{L=n}|) \quad (231)$$

leads to the same, N-dependent PIP-curves when plotted w.r.t. n or w.r.t. $f = L/n$, namely the one in Fig. 27 below.

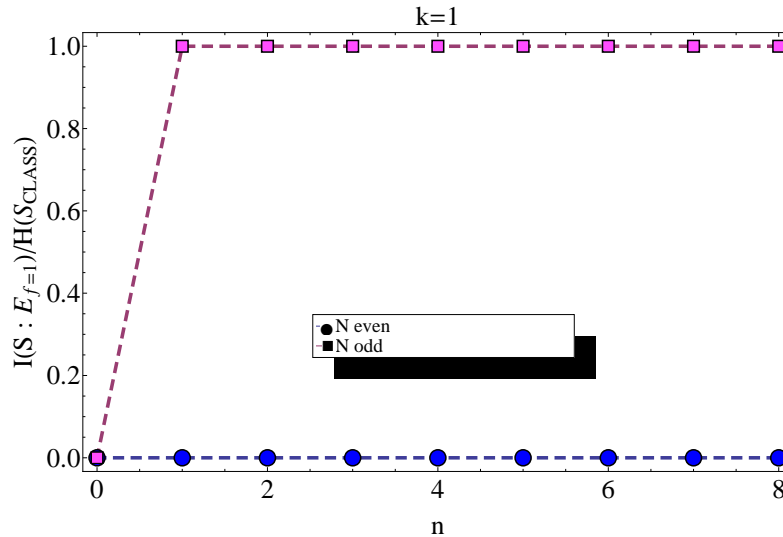


Figure 27: PIP of a random unitarily CNOT-evolved $\hat{\rho}_{SE}^{in} = \hat{\rho}_S^{in} \otimes \hat{\rho}_E^{in}$ ($N \gg 1$) with a $k = 1$ qubit pure $\hat{\rho}_S^{in}$ given by $|\Psi_S^{in}\rangle = \sum_{m=0}^1 a_m |m\rangle$ and $\hat{\rho}_E^{in} = \frac{1}{2} (|s_1^{L=n}\rangle \langle s_1^{L=n}| + |s_2^{L=n}\rangle \langle s_2^{L=n}|)$ w.r.t. n . The corresponding PIP w.r.t. $f = L/n$ and its curves for even and odd N-values are exactly the same.

Fig. 27 demonstrates why (195) does not lead to QD within the maximal attractor space of the random unitary qubit model: the behavior of the MI depends on N , implying that for an odd number of CNOT-iterations the MI-'plateau' appears, whereas for each even N -value QD is completely suppressed. This »oscillatory«, N -dependent behavior of $I(S : E_L)/H(S_{\text{class}})$ w.r.t. $L = n$ (and $f = L/n$) is unacceptable from the point of view of a clear, N -independent convergence of the MI towards a well-defined value we were able to establish when discussing different $\hat{\rho}_{SE}^{\text{in}}$ in previous subsections. Even worse: the value of $H(S)$ also »oscillates« with N : one has either $H(S) = H(S_{\text{class}})$ (N odd) or $H(S) = 0$ (N even). This does not offer a stable »trend« of $I(S : E_L)/H(S_{\text{class}})$ w.r.t. N , which is why we cannot use (195) as a reliable »quantum memory« for storing $H(S_{\text{class}})$.

Finally, letting the input state $\hat{\rho}_{SE}^{\text{in}} = \sum_{i=0}^{2^k-1} |a_i|^2 |i\rangle \langle i| \otimes \frac{1}{2^{1-n/2}} (|0_n\rangle \langle s_1^{L=n}| + |s_1^{L=n}\rangle \langle 0_n|)$ evolve random unitarily via CNOT we obtain for $N, n \gg 1$ the output states

$$\begin{aligned}\hat{\rho}_{SE}^{\text{out}} &= |a_0|^2 |0\rangle \langle 0| \otimes \hat{\rho}_{SE}^{\text{in}} + \sum_{i=1}^{2^k-1} |a_i|^2 |i\rangle \langle i| \otimes |s_1^{L=n}\rangle \langle s_1^{L=n}| \\ \hat{\rho}_E^{\text{out}} &= |a_0|^2 \hat{\rho}_{SE}^{\text{in}} + (1 - |a_0|^2) |s_1^{L=n}\rangle \langle s_1^{L=n}| \\ \hat{\rho}_S^{\text{out}} &= \sum_{i=0}^{2^k-1} |a_i|^2 |i\rangle \langle i|,\end{aligned}\tag{232}$$

where we deliberately neglected, without loss of generality, traceless contributions $\sim (-1)^N |2^k - 1\rangle \langle 2^k - 1| 2^{-n/2} \bigotimes_{i=1}^n \hat{B}_i^{\pi/2} \cdot \delta_{L,n}$ ($L \in \{0, 1\}$) of the minimal $\{\lambda = -1\}$ attractor space (381) (Appendix H.2.2), which tend to zero $\sim 2^{-n}$. (232)

also coincides with the output state one would obtain after random unitarily CNOT-evolving $\hat{\rho}_{SE}^{\text{in}} = \sum_{i=0}^{2^k-1} |a_i|^2 |i\rangle \langle i| \otimes \frac{1}{2^{1-n/2}} (|0_n\rangle \langle s_1^{L=n}| + |s_1^{L=n}\rangle \langle 0_n|)$ within the minimal $\{\lambda = 1\}$ attractor subspace (365) (Appendix H.2.2). Without explicitly computing the eigenspectra of the output states (232) we can easily anticipate that $\hat{\rho}_{SE}^{\text{out}}$ in (232) does not represent a proper physical state since already for $k = L = n = 1$ the matrix structure of $\hat{\rho}_{SE}^{\text{out}}$ connects the outer-diagonal entries within the $|0\rangle_S \langle 0|$ -subspace of S with a zero environmental entry $|1\rangle_E \langle 1|$, which is according to (315)-(319) of Appendix C forbidden and inevitably leads to eigenspectra comprising negativ real-valued or even complex-valued eigenvalues.

VI) $\hat{\rho}_{SE}^{\text{in}} = \hat{\rho}_S^{\text{in}} \otimes \hat{\rho}_E^{\text{in}}$, $k = 2$ -qubit pure Bell-state $|\Psi_S^{\text{in}}\rangle = 2^{-1/2} (|0\rangle + |2^{k=2} - 1\rangle)$, $\hat{\rho}_E^{\text{in}} = |0_n\rangle \langle 0_n|$ (Fig. 28, lower graph, •-dotted curve)

The output state for this $\hat{\rho}_{SE}^{\text{in}}$ is given in (401) of Appendix J.1. The corresponding PIPs w.r.t. n and $f = L/n$ are given in Fig. 28 below. By inspecting the eigenspectra of both subsystems $\hat{\rho}_S^{\text{out}}$ and $\hat{\rho}_E^{\text{out}}$

$$\begin{aligned}\hat{\rho}_S^{\text{out}} : \lambda_{1/2}^S &= 2^{-1} \left(1 - 2^{-n} \left[1 \pm (-1)^N \right] \right) \\ \hat{\rho}_E^{\text{out}} : \lambda_1^E &= 2^{-n-k} \left[1 + (-1)^{N+n} \right] \quad (2^{n-1} \text{ times}), \quad \lambda_2^E = 2^{-n-k} \left[1 - (-1)^{N+n} \right] \quad (2^{n-1} - 1 \text{ times}), \\ \lambda_3^E &= 2^{-n-k} \left[(2^n + 1) - (-1)^{N+n} \right] \quad (1 \text{ times}),\end{aligned}\tag{233}$$

we see that $H(S) = H(S_{\text{class}}) = 1$ with which we used to normalize $I(S : E_L)$ in Fig. 28 corresponds to the Shannon-entropy w.r.t. the $k = 1$ qubit S instead of a $k = 2$ qubit S . In other words, in a decohered S is contained only the Shannon-entropy $H(S_{\text{class}}^{k=1}) = 1 < H(S_{\text{class}}^{k=2})$ of a completely mixed $k = 1$ qubit S . Indeed, according to the upper graph of Fig. 28 we see that $I(S : E_{L=n})$ converges for $n \gg 1$ to the N -independent value 1 of $H(S_{\text{class}}) = k = 1$, whereas $\lim_{n \rightarrow \infty} H(S) = H(S_{\text{class}}) = 1$ and $\lim_{n \rightarrow \infty} H(E_{L=n}) = \lim_{n \rightarrow \infty} H(S, E_{L=n}) = 2^{-1}$. However, as soon as we resolve $I(S : E_L)$ w.r.t. $f = L/n$ we do not see the MI-'plateau' of QD.

VII) $|\Psi_{SE}^{\text{in}}\rangle = 2^{-1/2} (|0_{k=1}0_n\rangle + |1_{k=1}1_n\rangle)$ (Fig. 29)

The output state for this $\hat{\rho}_{SE}^{\text{in}}$ is given in (402) of Appendix J.1. The corresponding PIP w.r.t. n is given in Fig. 29 below. The eigenspectra of both subsystems $\hat{\rho}_S^{\text{out}}$ and $\hat{\rho}_E^{\text{out}}$ are exactly the same as those in (233). Indeed, the PIP in Fig. 29 confirms that $I(S : E_{L=n})$ converges for $n \gg 1$ to the N -independent value 1 of $H(S_{\text{class}}) = k = 1$, whereas the corresponding PIP w.r.t. $f = L/n$ is given by the lower graph of Fig. 28 above. As was the case w.r.t. (221), no QD appears. Even for $k > 1$ (402) of Appendix J.1 would lead to the same PIP w.r.t. $f = L/n$ as the one in the lower graph of Fig. 28, however this time with $I(S : E_L)$ normalized by the Shannon-entropy $H(S_{\text{class}}^{k=1}) = 1 < H(S_{\text{class}}^{k=2})$ still corresponding to information content of a $k = 1$ qubit completely mixed S . Therefore, evolving $|\Psi_{SE}^{\text{in}}\rangle = 2^{-1/2} (|0_{k=1}0_n\rangle + |1_{k=1}1_n\rangle)$ random unitarily does not lead to QD $\forall k \geq 1$.

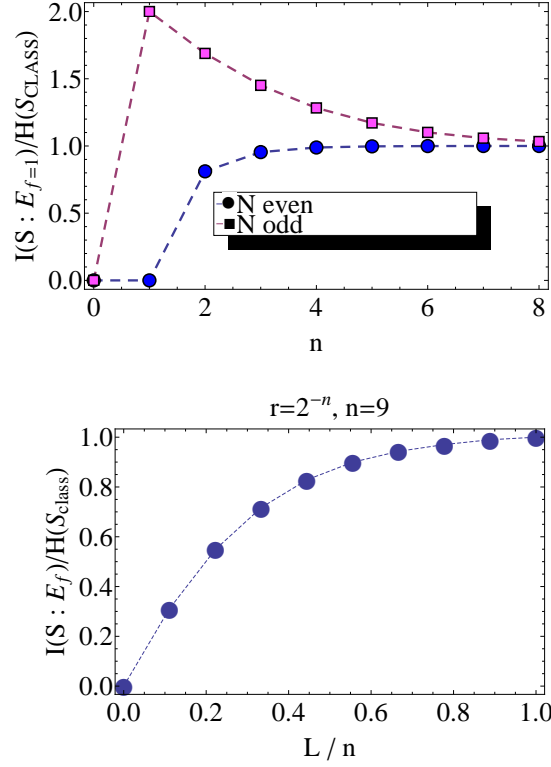


Figure 28: PIPs w.r.t. n and $f = L/n$ of a random unitarily evolved $\hat{\rho}_{SE}^{in} = \hat{\rho}_S^{in} \otimes \hat{\rho}_E^{in}$ ($N \gg 1$), with a $k = 2$ -qubit pure Bell-state $|\Psi_S^{in}\rangle = 2^{-1/2}(|0\rangle + |2^{k=2} - 1\rangle)$ and $\hat{\rho}_E^{in} = |0_n\rangle\langle 0_n|$. $H(S) = H(S_{class}^{k=1}) < H(S_{class}^{k=2})$.

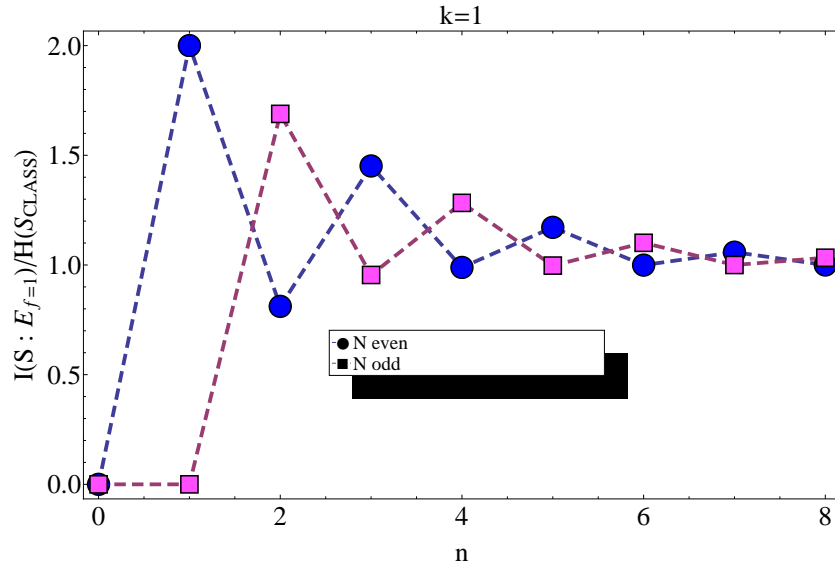


Figure 29: PIPs w.r.t. n of a random unitarily evolved $|\Psi_{SE}^{in}\rangle = 2^{-1/2}(|0_{k=1}0_n\rangle + |1_{k=1}1_n\rangle)$ ($N \gg 1$), $H(S) = H(S_{class}^{k=1}) = 1$. The corresponding PIP w.r.t. $f = L/n$ is given by the lower graph of Fig. 28 above.

VIII) $|\Psi_{SE}^{in}\rangle = 2^{-1/2}(|0_{k=1}\gamma_n\rangle + |1_{k=1}\mu_n\rangle)$

The output state emerging from the random unitary CNOT-evolution of this input state (with $|\gamma_n\rangle = 2^{-1/2}(|0_n\rangle + |1_n\rangle)$ and $|\mu_n\rangle = 2^{-1/2}(|0_n\rangle - |1_n\rangle)$) is given in (403) of Appendix J.1. The corresponding PIP w.r.t. n is displayed Fig. 30 below.

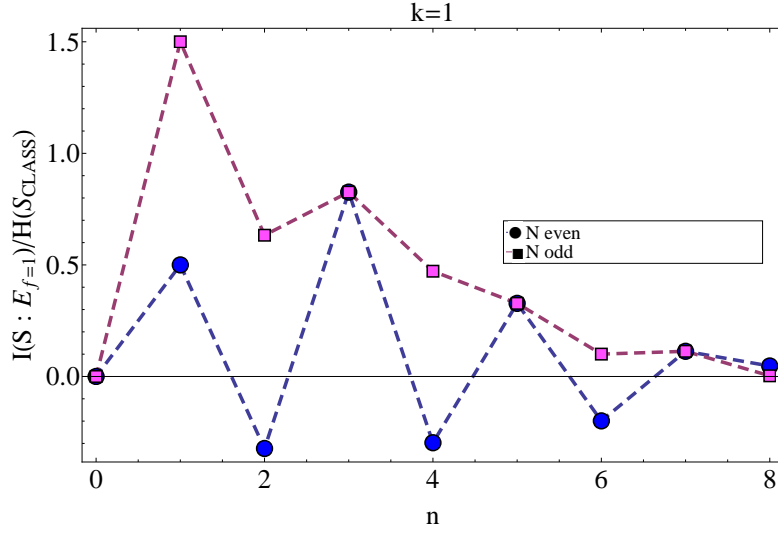


Figure 30: PIPs w.r.t. n of a random unitarily CNOT-evolved $|\Psi_{SE}^{in}\rangle = 2^{-1/2}(|0_{k=1}\gamma_n\rangle + |1_{k=1}\mu_n\rangle)$ ($N \gg 1$), $\lim_{n \gg 1} H(S) = 0 < H(S_{class}^{k=1}) = 1$.

In order to obtain (403) of Appendix J.1 we need to use the following relations

$$\begin{aligned}
\langle \gamma_n | \mu_n \rangle &= \langle s_1^n | \mu_n \rangle = 0, \langle s_2^n | \gamma_n \rangle = 2^{-(n+1)/2} (1 + (-1)^n), \langle s_2^n | \mu_n \rangle = 2^{-(n+1)/2} (1 + (-1)^{n+1}), \langle s_1^n | \gamma_n \rangle = 2^{-(n-1)/2} \\
\langle \mu_n | \bigotimes_{i=1}^n \hat{B}_0^{\pi/2} | \mu_n \rangle &= -2^{-n/2-1} (1 + (-1)^n), \langle \mu_n | \bigotimes_{i=1}^n \hat{B}_1^{\pi/2} | \mu_n \rangle = -\langle \mu_n | \bigotimes_{i=1}^n \hat{B}_0^{\pi/2} | \mu_n \rangle, (\hat{B}_0^{\pi/2})^\dagger = -\hat{B}_0^{\pi/2} \\
\text{Tr}_{E_{n-L}} \{ |\gamma_n\rangle \langle s_2^n| \} &= 2^{-(n-L+1)/2} \{ |0_L\rangle + (-1)^{n-L} |1_L\rangle \} \langle s_2^L|, \text{Tr}_{E_{n-L}} \{ |\mu_n\rangle \langle s_2^n| \} = 2^{-(n-L+1)/2} \{ |0_L\rangle - (-1)^{n-L} |1_L\rangle \} \langle s_2^L| \\
\text{Tr}_{E_{n-L}} \{ |\gamma_n\rangle \langle s_1^n| \} &= 2^{-(n-L+1)/2} \{ |0_L\rangle + |1_L\rangle \} \langle s_1^L|, \text{Tr}_{E_{n-L}} \{ |\mu_n\rangle \langle s_1^n| \} = 2^{-(n-L+1)/2} \{ |0_L\rangle - |1_L\rangle \} \langle s_1^L| \\
&= \sum_{l=1}^n \text{Tr}_{SE} \left\{ \left(|1_k\rangle \langle 1_k| \bigotimes_{i=1}^l |s_2^l\rangle \langle s_2^l| \bigotimes_{i=1}^{n-l} |s_1^l\rangle \langle s_1^l| \right) \left(\frac{|1_k\rangle \langle 1_k|}{2} \otimes |\mu_n\rangle \langle \mu_n| \right) \right\} = \\
&= \sum_{l=1}^n \frac{1}{2} |\langle s_2^l | \mu_l \rangle|^2 |\langle s_1^{n-l} | \mu_{n-l} \rangle|^2 = \frac{1}{2} \sum_{l=1}^n 2^{-(l+1)} (1 - (-1)^l)^2 \cdot (0)^{n-l} = \begin{cases} 2 - 2^{-n} & \text{for } l = n = 2m, m \in \mathbb{N}^+ \\ 0, & \text{else} \end{cases},
\end{aligned} \tag{234}$$

which, together with the PIP in Fig. 30, demonstrate, that in the limit $n \gg 1$ of effective decoherence (403) of Appendix J.1 turns into a pure state $\hat{\rho}_{SE}^{out} = |0_{k=1}\rangle \langle 0_{k=1}| \otimes |\gamma_n\rangle \langle \gamma_n|$. In other words, only in the limit $n \gg 1$ (403) of Appendix J.1 represents a physical state, which unfortunately suppresses completely the appearance of QD. Indeed, from (403) of Appendix J.1 and Fig. 30 one obtains $\lim_{n \gg 1} H(S) = \lim_{n \gg 1} H(S, E_{L=n}) = \lim_{n \gg 1} H(E_{L=n}) = 0$ and $\lim_{n \gg 1} I(S : E_L) / H(S_{class}) = 0 \cdot 0 = 0 \forall L \leq n$. Thus, as was the case for Zurek's qubit model and the minimal attractor space of the random unitary model, $|\Psi_{SE}^{in}\rangle = 2^{-1/2}(|0_{k=1}\gamma_n\rangle + |1_{k=1}\mu_n\rangle)$ does not lead to QD even if we let it CNOT-evolve in accord with the iterative random unitary approach.

Finally, taking all results obtained so far into account, we come to the following conclusion: the only entangled input S-E-state which allows QD to appear after the CNOT-evolution, both within the framework of Zurek's and the random unitary model with maximal attractor space, is the input state $|\Psi_{SE}^{in}\rangle = a|0_{k=1}\rangle \otimes |s_1^{L=n}\rangle + b|1_{k=1}\rangle \otimes |s_2^{L=n}\rangle$ entangling the two pointer states $\{|0_{k=1}\rangle, |1_{k=1}\rangle\}$ of a $k = 1$ qubit S in the standard computational basis with the two CNOT-symmetry states $\{|s_1^{L=n}\rangle, |s_2^{L=n}\rangle\}$. Interestingly, this »symmetrized« entangled $|\Psi_{SE}^{in}\rangle$ is the only input state which remains invariant (unchanged) under CNOT-transformations, both within the framework of Zurek's and the random unitary model with maximal attractor space $\forall N$. In other words, the PIP w.r.t. n and $f = L/n$ of a random unitarily CNOT-evolved $|\Psi_{SE}^{in}\rangle = 2^{-1/2}(|0_{k=1}\gamma_n\rangle + |1_{k=1}\mu_n\rangle) = |\Psi_{SE}^{out}\rangle$ is the same as the PIP from Fig. 1 emerging from the CNOT-evolution in accord with Zurek's model $\forall N$. Thus, $|\Psi_{SE}^{in}\rangle = a|0_{k=1}\rangle \otimes |s_1^{L=n}\rangle + b|1_{k=1}\rangle \otimes |s_2^{L=n}\rangle$ is the only input state whose output state (being itself equal to the input state) yields, both within the framework of Zurek's and the random unitary model with maximal attractor space $\forall N$, the MI-'plateau' w.r.t. $f = L/n$ as well as w.r.t. n . This »self-similarity« of the PIP w.r.t. $f = L/n$ and n emerging from $|\Psi_{SE}^{in}\rangle = a|0_{k=1}\rangle \otimes |s_1^{L=n}\rangle + b|1_{k=1}\rangle \otimes |s_2^{L=n}\rangle$ in Zurek's

and the random unitary model also means that such an entangled, CNOT-symmetrized input state may be regarded as an »information hologram« whose parts contain completely the same amount of system's Shannon-information as does the entire state $|\Psi_{SE}^{in}\rangle$ with $L = n$ and $\forall n > 1$.

8.3.3 Non-CNOT-evolution

According to Appendix E we should not expect to see the MI-'plateau' in PIPs that correspond to the random unitary evolution of the input state $\hat{\rho}_{SE}^{in} = |\Psi_S^{in}\rangle \langle \Psi_S^{in}| \otimes \hat{\rho}_E^{in}$, with $|\Psi_S^{in}\rangle = \sum_{m=0}^{2^k-1} a_m |m\rangle$ and $\hat{\rho}_E^{in} = |0_n\rangle \langle 0_n|$ if we apply in (168) $\hat{u}_j^{(\phi \neq \pi/3)}$ instead of the CNOT-transformation $\hat{u}_j^{(\phi = \pi/2)}$. (400) of Appendix J.1 displays $\hat{\rho}_{SE}^{out}$ of $\hat{\rho}_{SE}^{in}$ from Fig. 6 for $k = 1$ qubit system S, random unitarily evolved by means of $\hat{u}_j^{(\phi = \pi/3)}$. The corresponding numerical PIP is presented in Fig. 14 (■-dotted curve): this time the decoherence factor is $r = 0.75$ (i.e. the decoherence process is weaker than in the CNOT-induced case of Fig. 15), but nevertheless, for $n = 9$ E-qubits in Fig. 14 we are able to obtain $H(S) \approx H(S_{class}) = 1$. Unfortunately, we notice, similar to (226) and the red, ■-dotted curve in Fig. 23, that, by letting the above $\hat{\rho}_{SE}^{in}$ from Fig. 15 evolve iteratively in accord with (168) and under influence of $\hat{u}_j^{(\phi = \pi/3)}$, $I(S : E_{L=n})/H(S_{class})$ in Fig. 14 approaches the value 1 in the limit $n \gg k$. In other words, for a non-CNOT $\hat{u}_j^{(\phi)}$ one always obtains asymptotically, when starting the evolution (168) with $\hat{\rho}_{SE}^{in}$ and a $k = 1$ qubit $\hat{\rho}_S^{in}$ from Fig. 15, $H(S, E_L) > H(E_L) \forall (1 \leq L \leq n \gg k)$ (s. (400) of Appendix J.1). Thus, for Zurek's input configuration $\hat{\rho}_{SE}^{in}$ from Fig. 1 the random unitary model also states that non-CNOT $\hat{u}_j^{(\phi)}$ will suppress the appearance of the MI-'plateau' in corresponding PIPs.

Taking into account conclusions from subsection 7.2 and subsection 8.1.3, we may point out: Between S (described by $\{|\pi_i\rangle\} \equiv \{|0\rangle, |1\rangle\}$) and its E the simplest two-qubit transformation that enables us to copy $H(S_{class})$ into E with $f = k/n$ is $\hat{u}_j^{(\phi = \pi/2)}$ (maximal S-E-entanglement). All other (166)-(167) with $\phi \neq \pi/2$ do not lead to Quantum Darwinism (»imperfect copy machines«).

8.4 Mutual Information-comparison: maximal and minimal vs intermediate attractor spaces

Here we inquire which conclusions about the MI-behavior regarding an increasing number of environmental qubit-qubit $\hat{u}_j^{(\phi = \pi/2)}$ -interactions can be drawn simply by comparing the PIPs associated with both extrema - the minimal and maximal attractor subspaces associated with an eigenvalue $\lambda = 1$ of (170).

Since the E-registry state $|0_n\rangle$ has to appear in all relevant S-subspaces of an attractor space, (380) and (365) from Appendix H.1.2 indicate that in case of E containing mutually interacting qubits the maximal $\lambda = 1$ attractor subspace structure gains additional S-subspace structures $\{|0_k\rangle \langle 0_k| \otimes |y\rangle \langle y|, |0_k\rangle \langle 0_k| \otimes |s_{c_1}^n\rangle \langle y|\}$ (structure **D**) of Appendix H with $y \in \{0, \dots, 2^n - 1\}$ that are responsible for reaching an appropriate dimensionality $d_{n \gg k}^{\lambda=1, h. bind.}$ (with $h \geq 1$) of non-Koenig-like IDs containing $\hat{u}_j^{(\phi)}$ -arrows between E-qubits. Indeed, results from Appendix H confirm this assumption. However, before we discuss PIPs related to such intermediate $\lambda = 1$ attractor subspaces, we inquire which conclusions about the MI-behavior regarding an increasing number of environmental qubit-qubit $\hat{u}_j^{(\phi)}$ -interactions can be drawn simply by comparing the PIPs associated with both extrema - the minimal and maximal attractor subspaces associated with an eigenvalue $\lambda = 1$ of (170).

Indeed, many important conclusions about the behavior of the MI with increasing number of E-qubit interactions in Fig. 9 can be drawn from a simple comparison between predictions obtained by the random unitary evolution of $\hat{\rho}_{SE}^{in}$ in Fig. 1 from the point of view of the minimal and the maximal $\lambda = 1$ attractor subspaces (380) and (365) from Appendix H.1.2, respectively. For instance, looking at the PIP associated with the maximal $\lambda = 1$ attractor subspace (380) from Appendix H.1.2 alone (for a $k \geq 1$ qubit system S), which we obtain by ignoring all addends in $\hat{\rho}_{SE}^{out}$ of (395) of Appendix J.1 proportional to $(-1)^N$, we see that the MI behaves as in the PIP emerging from $\hat{\rho}_{SE}^{out}$ in (404) of Appendix J.2 evolved with respect to the minimal $\lambda = 1$ attractor subspace. In other words, the PIP for $\hat{\rho}_{SE}^{out}$ (and a $k \geq 1$ qubit system S) in (395) of Appendix J.1 without contributions associated with the $\lambda = -1$ attractor subspace and the PIP obtained from $\hat{\rho}_{SE}^{out}$ in (404) from Appendix J.2 of the minimal $\lambda = 1$ attractor subspace are exactly the same and are given by the ♦-, ○- and □-dotted curves in Fig. 17 (this can also be confirmed numerically by iterating (168) $N \gg 1$ times, as already done in subsection 8.2). This means: $\hat{\rho}_{SE}^{out}$ from the $\lambda = 1$ -part of (395) in Appendix J.1 and $\hat{\rho}_{SE}^{out}$ in (404) from Appendix J.2, as can be readily confirmed, share the same non-zero eigenvalues (188). The presence of the $\lambda = -1$ attractor subspace (381) of Appendix H.2.2 in (395) of Appendix J.1 is essential for the appearance of Quantum Darwinism (for a $k = 1$ qubit system S) within the random unitary model. Since the $\lambda = -1$ attractor subspace disappears from the attractor space structure of a Koenig-like ID already after introducing a single interaction arrow between two E-qubits (s. Appendix

H), the PIP of a random unitarily evolved $\hat{\rho}_{SE}^{\text{in}}$ from Fig. 1 for environments E containing one or more $\hat{u}_j^{(\phi=\pi/2)}$ -bindings should be the same as the PIP of obtained from (404) in Appendix J.2 for the minimal $\lambda = 1$ attractor space, i.e. already a single interaction between E-qubits in ID of Fig. 9 destroys Quantum Darwinism in the random unitary model.

In order to confirm this last conclusion we look at an ID from Fig. 9 whose interaction structure resembles the one in **e**) of Fig. 41 in Appendix H: i.e. we assume there are (for a $k = 1$ S-qubit) $2n - 3$ bindings between n E-qubits such that qubits $\{q_1, \dots, q_{n-1}\}$ are all mutually connected by $\hat{u}_j^{(\phi=\pi/2)}$ -binding pairs, whereas between the $(n - 1)$ -th E-qubit q_{n-1} and the n -th E-qubit q_n there is only one (single) $\hat{u}_j^{(\phi=\pi/2)}$ -binding from q_{n-1} to q_n . According to Appendix H the intermediate $\lambda = 1$ attractor subspace (384) with $(2n - 3)$ $\hat{u}_j^{(\phi=\pi/2)}$ -bindings between E-qubits encloses (as the last non-strongly connected ID-structure before the critical binding number of $2(n - 1)$, with $d_{n \gg k}^{\lambda=1, (2n-3)\text{bind}} = 20$) E-registry states $S_p \equiv \{|0_n\rangle, |0_{n-2}10\rangle, |0_{n-1}1\rangle\}$ (primary) and $S_s \equiv \{|10_{n-1}\rangle\}$ (secondary). We already know from $\hat{\rho}_{SE}^{\text{out}}$ in (404) from Appendix J.2 with $\hat{\rho}_E^{\text{in}} = |1_n\rangle\langle 1_n|$ that environmental input states which do not participate within a given attractor subspace structure lead to vanishing MI-values in the limit $n \gg k$, i.e. contributions to $I(S : E_L)$ originating from E-registry states outside the underlying attractor subspace in the corresponding PIPs are practically zero (s. subsection related to the minimal $\lambda = 1$ attractor subspace (365) from Appendix H).

However, what happens within the intermediate attractor subspace (384) of Appendix H.3.2 with $(2n - 3)$ $\hat{u}_j^{(\phi=\pi/2)}$ -bindings, aligned as in **e**) of Fig. 41 in Appendix H.3.2, if we start the random unitary evolution of $\hat{\rho}_{SE}^{\text{in}} = |\Psi_S^{\text{in}}\rangle\langle \Psi_S^{\text{in}}| \otimes \hat{\rho}_E^{\text{in}}$, with a pure $k = 1$ qubit $|\Psi_S^{\text{in}}\rangle = \sum_{m=0}^1 a_m |m\rangle$ and $\hat{\rho}_E^{\text{in}} = 0.5 \cdot (|0_n\rangle\langle 0_n| + |0_{n-2}10\rangle\langle 0_{n-2}10|)$ containing primary E-registry states $|y\rangle$ with lowest logical values $y \in \{0, \dots, 2^n - 1\}$ that, according to Appendix H, participate in all relevant S-subspaces of (384) from Appendix H.3.2? $\hat{\rho}_{SE}^{\text{out}}$, obtained from this $\hat{\rho}_{SE}^{\text{in}}$ after Gram-Schmidt orthonormalizing all attractor states $\hat{X}_{\lambda,i}$ in (384) from Appendix H.3.2 and applying (170), is displayed in (414) of Appendix J.3 and leads (at $L = n$) to non-zero eigenvalues

$$\begin{aligned} \hat{\rho}_{SE}^{\text{out}} : \lambda_1^{SE} &= 2^{-1-n} (2^n - 1 \text{ times}), \lambda_2^{SE} = 2^{-1-n} (1 \times), \lambda_3^{SE} = 2^{-1} (1 \text{ times}) \\ \hat{\rho}_E^{\text{out}} : \lambda_1^{SE} &= 2^{-1-n} (2^n - 2 \text{ times}), 2^{-1-n} (2 \text{ times}) \\ \hat{\rho}_{SE}^{\text{out}} : \lambda_{1/2}^S &= 2^{-1} \pm \sqrt{2^{-2} - |a_0|^2 |a_1|^2 (1 - 2^{-2n})} \end{aligned} \quad (235)$$

and thus to exactly the same PIP as the one in Fig. 23 (red, ■-dotted curve; this can also be confirmed numerically by iterating (5) $N \gg 1$ times, as already done in subsection 8.2) as long as one does not trace out the one excited qubit from $|0_{n-2}10\rangle\langle 0_{n-2}10| \forall (1 \leq L \leq n)$ (s. also discussion related to (226) above). This confirms our previous conjecture according to which already a single interaction arrow between E-qubits in ID of Fig. 9 disturbs Quantum Darwinism. Furthermore, (235) also shows that in the limit $n \gg 1$ $I(S : E_{L=n})/H(S_{\text{class}})$ approaches 1 in accord with Fig. 31 below. In addition, we also conclude: Even if $\hat{\rho}_E^{\text{in}}$ contains E-registry states participating in all relevant S-subspaces of (384) from Appendix H.3.2, the highest amount of asymptotic MI-values one could achieve $\forall (k \leq L \leq n)$ is bounded from above by $I(S : E_L)$ obtained from the maximal attractor space (380)-(381) in Appendix H.2.2.

For $\hat{\rho}_E^{\text{in}} \neq |y\rangle\langle y| \forall y \in \{0, \dots, 2^n - 1\}$ the contribution of the $\lambda = -1$ attractor subspace (381) within the maximal attractor space (380)-(381) of Appendix H.2.2 to the random unitary evolution of $\hat{\rho}_{SE}^{\text{in}} = \hat{\rho}_S^{\text{in}} \otimes \hat{\rho}_E^{\text{in}}$ and its MI-values is negligibly small in the limit $L = n \gg k$, whereas the attractor subspace (380) in Appendix H.2.2 and its minimal version (365) from Appendix H.1.2 dominate the asymptotic dynamics of $\hat{\rho}_{SE}^{\text{in}}$. Nevertheless, contributions from the $\lambda = -1$ attractor subspace do affect outer-diagonal S-subspaces. For instance, (396) in J.1 contains the most important part of the $\lambda = -1$ attractor subspace, namely $\{|0_L\rangle\langle s_2^L|, |1_L\rangle\langle s_2^L|\}$ (and their hermitean counterparts), within S-subspaces $|0\rangle\langle 1|$ and $|1\rangle\langle 0|$. When looking at (396) in Appendix J.1 we see that these outer-diagonal S-subspaces are associated with $|0_L\rangle + |1_L\rangle \langle \Psi_E^{\text{combi}}|$ (and its hermitean counterpart, respectively), where

$$|\Psi_E^{\text{combi}}\rangle = |s_1^L\rangle + (-1)^{2n-L+N} |s_2^L\rangle$$

distributes within the $|0_L\rangle$ -th and $|1_L\rangle$ -th row (column) of (396) in Appendix J.1 2^{L-1} complex-valued, identical entries $c = 2^{1-n} a_0 \cdot a_1^*$ (alias its conjugate counterparts). If we ask ourselves what is the ideal value c_{ideal} of these 2^{L-1} identical entries in (396) of Appendix J.1, distributed within the $|0_L\rangle$ -th and $|1_L\rangle$ -th row (column) in accord with $|\Psi_E^{\text{combi}}\rangle$, for which the entropy-difference $H(S, E_{L=n}) - H(E_{L=n})$ (with $n \gg k$) is minimal, we easily obtain $c_{\text{ideal}} = 2^{-n} a_0 \cdot a_1^* \neq 2^{1-n} a_0 \cdot a_1^*$, leading us for $\hat{\rho}_{SE}^{\text{out}}$ in (396) from Appendix J.1 to eigenvalues

$$\left. \begin{aligned} \lambda_1^{SE} &= 2^{-1} |a_0|^2 \\ \lambda_2^{SE} &= 2^{1-L} |a_1|^2 (2^{L-1} - 1 \text{ times}) \end{aligned} \right\} \text{ (for } \hat{\rho}_{SE}^{\text{out}} \text{)}, \quad \left. \begin{aligned} \lambda_1^E &= 2^{-1} |a_0|^2 + 2^{1-L} |a_1|^2 (2 \text{ times}) \\ \lambda_2^E &= 2^{1-L} |a_1|^2 (2^{L-1} - 2 \text{ times}) \end{aligned} \right\} \text{ (for } \hat{\rho}_E^{\text{out}} \text{)}, \quad (236)$$

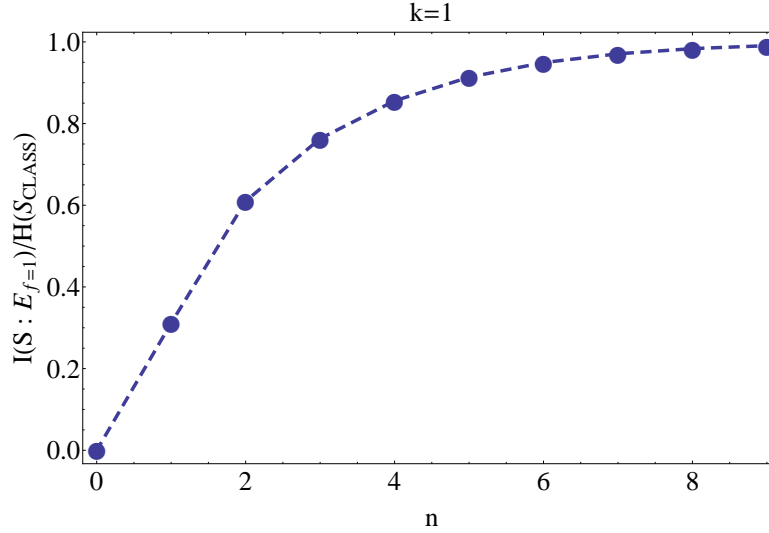


Figure 31: PIP after random iterative $\hat{u}_j^{(\phi=\pi/2)}$ -evolution of $\hat{\rho}_{SE}^{in} = |\Psi_S^{in}\rangle\langle\Psi_S^{in}| \otimes \hat{\rho}_E^{in}$ ($N \gg 1$), with a pure $k = 1$ qubit $|\Psi_S^{in}\rangle = \sum_{m=0}^1 a_m |m\rangle$ ($|a_m|^2 = 2^{-1} \forall m$) and $\hat{\rho}_E^{in} = 0.5 \cdot (|0_n\rangle\langle 0_n| + |0_{n-2}10\rangle\langle 0_{n-2}10|)$ ($2n - 3$ E-bindings) w.r.t. n , s. main text.

that, in turn, yield $H(S, E_{L=n}) > H(E_{L=n})$. In other words, even in case of outer-diagonal c-entries in (396) from Appendix J.1 fixed as $c = c_{ideal}$ $H(S, E_{L=n})$ would still always exceed $H(E_{L=n})$ (s. also subsection 4.2.5 above and the discussion of (136) therein).

The reason for this is connected with the following fact: for (395) in Appendix J.1, emerging from the random unitary CNOT-evolution of $\hat{\rho}_E^{in} = |0_n\rangle\langle 0_n|$, the diagonal value $|a_0|^2$ from the diagonal S-subspace $|0\rangle\langle 0|$ in (395) in Appendix J.1 merges with one of the diagonal values $2^{-L} |a_1|^2$ from the diagonal S-subspace $|1\rangle\langle 1|$ after extracting $\hat{\rho}_E^{out}$ from $\hat{\rho}_{SE}^{out}$ and thus decreases $H(E_L)$ with respect to $H(S, E_L)$. Fortunately, for this case $|\Psi_E^{comb1}\rangle$ is the only combination that can be made from two available CNOT-symmetry states $\{|s_1^L\rangle, |s_2^L\rangle\}$ capable of reducing $H(S, E_L)$ such that $H(S, E_L) = H(E_L) \forall (1 \leq L \leq n)$. Unfortunately, in order to correct a higher number of overlapping diagonal values between S-subspaces $|0\rangle\langle 0|$ and $|1\rangle\langle 1|$ within $\hat{\rho}_E^{out}$ (in (396) of Appendix J.1 there are two merging diagonal values between S-subspaces $|0\rangle\langle 0|$ and $|1\rangle\langle 1|$) one would also need more than two symmetry states which is impossible for the CNOT-transformation and, in general, for the ϕ -parameter family $\hat{u}_j^{(\phi)}$ of transformations in (166)-(167) (however, a higher number of symmetry states is possible for a generalized, qudit-qudit version of the CNOT-transformation). Therefore, $\hat{\rho}_{SE}^{in} = \hat{\rho}_S^{in} \otimes \hat{\rho}_E^{in}$ (with $\hat{\rho}_S^{in}$ being a pure $k = 1$ qubit system S), when being subject to CNOT-random unitary evolution leads in the asymptotic limit $N \gg 1$ of many iterations to Quantum Darwinism only if $\hat{\rho}_E^{in} = |y\rangle\langle y| \forall y \in \{0, \dots, 2^n - 1\}$, otherwise, for $\hat{\rho}_E^{in} \neq |y\rangle\langle y| \forall y \in \{0, \dots, 2^n - 1\}$ the $\lambda = -1$ attractor subspace (381) of Appendix H.2.2 does not suffice to compensate all losses of $H(E_L)$ induced in $\hat{\rho}_E^{out}$ by overlapping diagonal entries within different diagonal S-subspaces.

(414) from Appendix J.3 also depends on the order in which one traces out single E-qubits: if we trace out the one excited qubit from $|0_{n-2}10\rangle\langle 0_{n-2}10|$ for a fixed $1 \leq L = L_* < n$ in (414), (414) would reduce to (404) from Appendix J.2 and still violate (155) $\forall (1 \leq L \leq L_*)$, now in accord with the yellow, \blacklozenge -dotted curve in Fig. 17. Unfortunately, this is, according to the definition (155) of Quantum Darwinism, not the appropriate behavior one expects from $\hat{\rho}_E^{in}$ representing a suitable “quantum memory” for $H(S_{class})$.

Furthermore, by comparing the \blacksquare -dotted curve in Fig. 23 with the \blacklozenge -dotted curve in Fig. 11 we may conclude that the highest amount of asymptotic MI-values one could achieve $\forall (k \leq L \leq n)$ is bounded from above by $I(S : E_L)$ obtained from the maximal attractor space (380)-(381) of Appendix H.2.2.

Finally, one also notices once again (similar to the minimal $\lambda = 1$ attractor subspace) that $\hat{\rho}_E^{in}$ which are not contained in (“recognized” by) the corresponding intermediate $\lambda = 1$ attractor subspace do not contribute to $I(S : E_L) / H(S_{class})$ in the limit $n \gg k$. For instance, when inspecting w.r.t. $\hat{\rho}_{SE}^{in} = \hat{\rho}_S^{in} \otimes \hat{\rho}_E^{in}$ and an open pure $k = 1$ qubit $\hat{\rho}_S^{in}$, the input state $\hat{\rho}_E^{in} = |0_{n-1}1\rangle\langle 0_{n-1}1|$ for E containing n qubits with $2n - 3$ CNOT-bindings between them (s. Example 1-5 in Appendix H): in this case the outer diagonal S-subspaces $|0\rangle\langle 1|$ and $|1\rangle\langle 0|$ do not contribute to $\hat{\rho}_{SE_{L=n}}^{out}$, since their addends $|0\rangle\langle 1| \otimes |0_{n-1}1\rangle\langle s_1^{L=n}| a b^* 2^{-n/2}$ and $|1\rangle\langle 0| \otimes |s_1^{L=n}\rangle\langle 0_{n-1}1| 2^{-n/2} a^* b$ in (170) tend to zero $\sim 2^{-n}$ in the limit $n \gg k$ when compared with contributions (addends) in (170) correlated with diagonal S-subspaces $|0\rangle\langle 0|$ and $|1\rangle\langle 1|$.

This is the reason why $\hat{\rho}_{SE}^{\text{in}} = \hat{\rho}_S^{\text{in}} \otimes \hat{\rho}_E^{\text{in}}$ with an open pure $k = 1$ qubit $\hat{\rho}_S^{\text{in}}$ and $\hat{\rho}_E^{\text{in}} = |0_{n-1}1\rangle \langle 0_{n-1}1|$ for E containing n qubits with $2n - 3$ CNOT-bindings between them leads in the limit $n \gg k$ to the same output state as in (189) which clearly suppresses QD (s. also subsection 8.1.2 above). Also, by choosing $\hat{\rho}_{SE}^{\text{in}} = \hat{\rho}_S^{\text{in}} \otimes \hat{\rho}_E^{\text{in}}$ as an input in (170), with a pure, $k = 1$ qubit $\hat{\rho}_S^{\text{in}}$ and $\hat{\rho}_E^{\text{in}} = |s_1^{L=n}\rangle \langle s_1^{L=n}|$ containing, for instance, $2n - 3$ CNOT-bindings between E -qubits in accord with Fig. 41 in Appendix H.3.2, we again obtain, as in the case of the minimal and maximal attractor spaces, $I(S : E_L) = 0 \forall L \leq n$, which confirms the physical correctness of attractor space structures in (384) from Appendix H.3.2, since a vanishing MI for E that remains unaltered w.r.t. the CNOT-transformation is indeed an expected result, regardless of the number of CNOT-bindings between E -qubits in an ID of Fig. 9.

8.5 Summary and outlook

In this section we studied the appearance of Quantum Darwinism in the framework of the random unitary qubit model and compared the corresponding results (Partial Information Plots of mutual information between an open $k \geq 1$ qubit system S and its $n \gg k$ qubit environment E) with respective predictions obtainable from Zurek's qubit toy model.

We found that the only S - E -input states $\hat{\rho}_{SE}^{\text{in}}$ which lead to Quantum Darwinism within the random unitary operations model with maximal efficiency $f = f^* = k/n$, regardless of the order in which one traces out single E -qubits, are the entangled input state from equation (158) and the product state $\hat{\rho}_{SE}^{\text{in}} = \hat{\rho}_S^{\text{in}} \otimes \hat{\rho}_E^{\text{in}}$, with a pure $k = 1$ qubit $\hat{\rho}_S^{\text{in}}$ and a pure one-registry state $\hat{\rho}_E^{\text{in}} = |y\rangle \langle y| \forall y \in \{0, \dots, 2^n - 1\}$ of n mutually non-interacting qubits in the standard computational basis (Koenig-IDs).

According to the random unitary operations model one is motivated to conjecture that $\hat{\rho}_{SE}^{\text{in}} = \hat{\rho}_S^{\text{in}} \otimes \hat{\rho}_E^{\text{in}}$ with a pure $k > 1$ qubit $\hat{\rho}_S^{\text{in}}$ allows efficient storage of system's Shannon-entropy $H(S_{\text{class}})$ into environment E only if $\hat{\rho}_E^{\text{in}}$ is given by a pure one registry state $\hat{\rho}_E^{\text{in}} = |y'\rangle \langle y'|$ of mutually non-interacting n qudits (n 2^k -level systems) in the standard computational basis, with $y' \in \{0, \dots, 2^{k \cdot n} - 1\}$. This does not correspond to expectations arising from Zurek's qubit model of Quantum Darwinism, which predicts the appearance of the mutual information-'plateau' even for a $k > 1$ qubit pure $\hat{\rho}_S^{\text{in}}$ and an n qubit $\hat{\rho}_E^{\text{in}}$ within the aforementioned $\hat{\rho}_{SE}^{\text{in}} = \hat{\rho}_S^{\text{in}} \otimes \hat{\rho}_E^{\text{in}}$, indicating that Quantum Darwinism depends on the specific model on which one bases his interpretations. Furthermore, the random unitary model and Zurek's model of Quantum Darwinism must not be confused with each other, since the latter does not correspond to the short time limit (small iteration values N) of the former.

Zurek's qubit model of Quantum Darwinism does not include interactions between E -qubits, which is however the case within the random unitary operation model. Unfortunately, already after introducing a single $\hat{u}_j^{(\phi)}$ -interaction between two E -qubits into the random unitary evolution of $\hat{\rho}_{SE}^{\text{in}}$ leads to the disappearance of the mutual information-'plateau' due to the absence of the attractor subspace associated with the eigenvalue $\lambda = -1$ of (169) in case of mutually interacting E -qubits. If $\hat{\rho}_{SE}^{\text{in}} = \hat{\rho}_S^{\text{in}} \otimes \hat{\rho}_E^{\text{in}}$ contains E -registry states that do participate in the structure of intermediate attractor subspaces the behavior of the mutual information in the corresponding Partial Information Plots coincides with the Partial Information Plot obtainable by means of the maximal $\lambda = 1$ attractor subspace alone, whereas the contribution of the $\lambda = -1$ attractor subspace remains negligible for $\hat{\rho}_{SE}^{\text{in}} = \hat{\rho}_S^{\text{in}} \otimes \hat{\rho}_E^{\text{in}}$, with a pure $k \geq 1$ qubit $\hat{\rho}_S^{\text{in}}$ and $\hat{\rho}_E^{\text{in}} \neq |y\rangle \langle y|$ ($y \in \{0, \dots, 2^n - 1\}$). Thus, the random unitary model indicates that already a single interaction between E -qubits suppresses Quantum Darwinism.

On the other hand, both in Zurek's and the random unitary model we are able to confirm that correlations between qubit E -registry states (corresponding to $\hat{\rho}_E^{\text{in}} \neq |y\rangle \langle y|$), even if interactions between E -qubits are absent, tend to suppress the appearance of the mutual information-'plateau', until with respect to the completely mixed environmental input state $\hat{\rho}_E^{\text{in}} = 2^{-n} \hat{I}_n$ one obtains for the mutual information $I(S, E_L)/H(S_{\text{class}}) = 0 \forall (1 \leq L < n)$ (Zurek's model) and $\lim_{n \gg 1} I(S, E_{L=n})/H(S_{\text{class}}) = 0$ (random unitary model).

Between the system S (described by the pointer basis $\{|\pi_i\rangle\} \equiv \{|0\rangle, |1\rangle\}$) and its environment E the simplest two-qubit transformation that leads to Quantum Darwinism (both in Zurek's and the random unitary model) with maximal efficiency $f = f^* = k/n$ is the CNOT-transformation $\hat{u}_j^{(\phi=\pi/2)}$, whereas one-parameter transformations (166)-(167) with $\phi \neq \pi/2$ do not adhere to (155).

If the Quantum Darwinistic description of the emergence of classical S -states were correct, then Zurek's and the random unitary model suggest that an open (observed) system S of interest and its environment E must have started their evolution as a product state $\hat{\rho}_{SE}^{\text{in}} = \hat{\rho}_S^{\text{in}} \otimes \hat{\rho}_E^{\text{in}}$ with $\hat{\rho}_S^{\text{in}}$ denoting a pure $k \geq 1$ qubit state and $\hat{\rho}_E^{\text{in}}$ (denoting for instance the state of the rest of the universe) given by a pure one-registry state of mutually non-interacting n qudits.

The above "qudit-cell" conjecture regarding environment E of the random unitary model could be tested by explicitly determining the maximal attractor space between a $k > 1$ qubit system S and its environment E of mutually non-interacting n qudits under the impact of the generalized qubit-qudit version of the CNOT-transformation and focussing on the behavior of the mutual information within the corresponding Partial Information Plot for such maximal attractor space (Koenig-IDs).

Furthermore, one could also ask what happens with the efficiency of storing $H(S_{\text{class}})$ into environment E if one introduces into the above random unitary evolution with pure decoherence dissipative effects that would in general treat the system S in the interaction digraph of Fig. 9 not only as a control but also as a target, allowing E -qubits to react on “impulses” sent by S -qubits.

9 Random Unitary model of Quantum Darwinism with dissipation

In this section we will summarize the iterative evolution formalism of the random unitary model involving pure decoherence and dissipation before discussing its most important results regarding Quantum Darwinism in subsections 9.2-9.3.

Random unitary operations can be used to model the pure decoherence of an open system S with k qubits (control, index i) interacting with n E -qubits (targets j) (as indicated in the directed interaction graph (digraph) in Fig. 32) by the one-parameter family of two-qubit ‘controlled- U ’ unitary transformations (166)-(167). Arrows of the interaction digraph (ID) in Fig. 32 from S - to E -qubits represent two qubit interactions $\hat{u}_j^{(\phi)}$ between randomly chosen qubits i and j with probability distribution p_e used to weight the edges $e = (ij) \in M$ of the digraph.

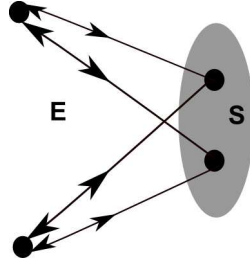


Figure 32: Interaction digraph (ID) between system S and environment E including dissipation within the random unitary evolution formalism [2].

Arrows of the interaction digraph (ID) in Fig. 32 from S - to E -qubits represent two qubit interactions $\hat{u}_j^{(\phi)}$ between randomly chosen qubits i and j with probability distribution p_e used to weight the edges $e = (ij) \in M$ of the digraph. All interactions are well separated in time. The S -qubits do not interact among themselves (furthermore, in this paper we also assume that the E -qubits, as in Zurek’s toy model, are not allowed to interact among themselves). Arrows of the interaction digraph (ID) in Fig. 32 from E - to S -qubits denote, on the other hand, a dissipative feedback of the environment E with respect to the system S represented by two qubit interactions [26, 38]

$$\begin{aligned} \hat{U}_{ij}^{\text{Diss}}(\alpha) = \exp \left[\frac{i\alpha}{2} \left(\hat{\sigma}_x^{(i)} \otimes \hat{\sigma}_x^{(j)} + \hat{\sigma}_y^{(i)} \otimes \hat{\sigma}_y^{(j)} \right) \right] = \\ \hat{I}_1^{(i)} \otimes \hat{I}_1^{(j)} + \frac{\cos \alpha - 1}{2} \left(\hat{I}_1^{(i)} \otimes \hat{I}_1^{(j)} - \hat{\sigma}_z^{(i)} \otimes \hat{\sigma}_z^{(j)} \right) \\ + \frac{i \sin \alpha}{2} \left(\hat{\sigma}_x^{(i)} \otimes \hat{\sigma}_x^{(j)} + \hat{\sigma}_y^{(i)} \otimes \hat{\sigma}_y^{(j)} \right), \end{aligned} \quad (237)$$

with a real-valued dissipation strength $0 \leq \alpha \leq \pi/2$. The total unitary two-qubit operation, accounting also for the dissipative effects in the course of the random unitary evolution, is then given by

$$\hat{U}_{ij}^{\text{Tot}}(\alpha) = \hat{U}_{ij}^{(\phi=\pi/2)} \hat{U}_{ij}^{\text{Diss}}(\alpha). \quad (238)$$

Thus, (238) models the interplay between decoherence and dissipation with respect to an open k -qubit system S and its n -qubit environment E . Replacing within the random unitary formalism with pure decoherence in (166)-(170) of section 8 $\hat{U}_{ij}^{(\phi=\pi/2)}$ by $\hat{U}_{ij}^{\text{Tot}}(\alpha)$ in (238) we are thus capable of modeling dissipative effects and their influence on QD.

In other words, in order to model the realistic measurement process of system S by its environment E we let an input state $\hat{\rho}_{SE}^{in}$ evolve by virtue of the following iteratively applied random unitary-quantum operation (completely positive unital map) $\mathcal{P}_\alpha(\cdot) \equiv \sum_{e \in M} K_e^\alpha(\cdot) K_e^{\alpha\dagger}$ (with Kraus-operators $K_e^\alpha := \sqrt{p_e} \hat{U}_e^{\text{Tot}}(\alpha)$) [11, 29, 30]:

1. The quantum state $\hat{\rho}(N)$ after N iterations is changed by the $(N+1)$ -th iteration to the quantum state (quantum Markov chain)

$$\hat{\rho}(N+1) = \sum_{e \in M} p_e \hat{U}_e^{\text{Tot}}(\alpha) \hat{\rho}(N) \hat{U}_e^{\text{Tot}\dagger}(\alpha) \equiv \mathcal{P}_\alpha(\hat{\rho}(N)). \quad (239)$$

2. In the asymptotic limit $N \gg 1$ $\hat{\rho}(N)$ is independent of $(p_e, e \in M)$ and determined by linear attractor spaces with mutually orthonormal solutions (index i) $\hat{X}_{\lambda,i}$ of the eigenvalue equation

$$\hat{U}_e^{\text{Tot}}(\alpha) \hat{X}_{\lambda,i} \hat{U}_e^{\text{Tot}\dagger}(\alpha) = \lambda \hat{X}_{\lambda,i}, \forall e \in M, \quad (240)$$

as subspaces $\mathcal{A}_\lambda \subset \mathcal{B}(\mathcal{H}_{SE})$ of the Hilbert-space $\mathcal{B}(\mathcal{H}_{SE})$ of linear operators w.r.t. the total S-E-Hilbert space $\mathcal{H}_{SE} = \mathcal{H}_S \otimes \mathcal{H}_E$ for the eigenvalues λ (with $|\lambda| = 1$) [11, 30].

3. For known attractor spaces \mathcal{A}_λ we get from an initial state $\hat{\rho}_{SE}^{\text{in}}$ the resulting S-E-state $\hat{\rho}_{SE}^{\text{out}} = \hat{\rho}_{SE}$ ($N \gg 1$) spanned by $\hat{X}_{\lambda,i}$

$$\hat{\rho}_{SE}^{\text{out}} = \mathcal{P}^N(\hat{\rho}_{SE}^{\text{in}}) = \sum_{|\lambda|=1, i=1}^{d^\lambda} \lambda^N \text{Tr}\left\{\hat{\rho}_{SE}^{\text{in}} \hat{X}_{\lambda,i}^\dagger\right\} \hat{X}_{\lambda,i}, \quad (241)$$

where d^λ denotes the dimensionality of the attractor space \mathcal{A}_λ with respect to the eigenvalue λ .

9.1 Random unitary operations perspective on Quantum Darwinism: pure decoherence vs dissipation

In this section we discuss the impact of dissipation on the f -dependence of MI in the framework of the random unitary evolution model in the asymptotic limit of many (239)-iterations ($N \gg 1$) and compare it with conclusions that can be drawn from Zurek's qubit-model of Quantum Darwinism. To be more specific, the main question we aim to address with respect to Zurek's and the random unitary operations model is: are there input states $\hat{\rho}_{SE}^{\text{in}}$ that, despite of dissipation, validate the Quantum Darwinistic relation (155)?

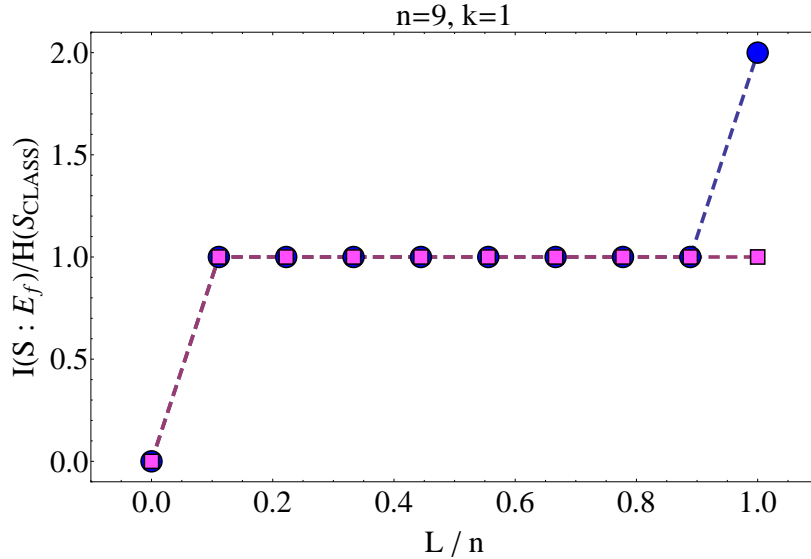


Figure 33: PIP of MI and R of $H(\hat{\rho}_S^{\text{out}}) \approx H(S_{\text{class}})$ stored in the environment E with respect to $0 < f = L/n \leq 1$, $k = 1$ qubit pure $\hat{\rho}_S^{\text{in}}, \hat{\rho}_E^{\text{in}} = |0_n\rangle \langle 0_n|$, $\hat{\rho}_{SE}^{\text{in}} = \hat{\rho}_S^{\text{in}} \otimes \hat{\rho}_E^{\text{in}}$ in (12), after the \hat{U}_{CNOT} -evolution in accord with Zurek's (•-dotted curve) and the random unitary model (with $N \gg 1$, ■-dotted curve, s. main text) [5].

Let us first start with pure decoherence ($\alpha = 0$). Within the random unitary formalism we are led to another type of PIP-behavior: inserting $\hat{\rho}_{SE}^{\text{in}}$ from Fig. 1 into (239) we obtain for $\alpha = 0$ (with, for instance, $|a|^2 = |b|^2 = 1/2$ and $p_e = 1/|M| \forall e$) after $N \gg 1$ iterations the PIP in Fig. 33 (■-dotted curve), which suggests that Zurek's MI-'plateau' [5] appears only in the limit $N \rightarrow \infty$.

For $\alpha > 0$, $|a|^2 = |b|^2 = 1/2$ and $p_e = 1/|M| \forall e$ we obtain, applying to $\hat{\rho}_{SE}^{\text{in}}$ from Fig. 1 iteratively (239) $N \gg 1$ times, the PIP in Fig. 34 (•-dotted curve) [32], which suggests that for $N \gg 1$, $\alpha > 0$, $L = n \geq 5$ one has

$$\lim_{N \gg 1} I(S : E_{L=n})/H(S_{\text{class}}) = 0.3, \quad \lim_{\alpha \rightarrow \pi/2} H(S)/H(S_{\text{class}}) = 0.8, \quad \lim_{N, n \gg 1} H(S) < H(S_{\text{class}}) = 1.$$

Thus, for $\pi/2 \geq \alpha > 0$ there is, even for Zurek's Quantum Darwinism-compliant input state $\hat{\rho}_{SE}^{\text{in}}$ from (12),

which leads to the MI-plateau in Fig. 33 (■-dotted curve) in the limit $N \rightarrow \infty$ (s. section 8), no Quantum Darwinism within the random unitary evolution model.

This also follows from the α -behavior of $I(S : E_{L=n})$ for a fixed $L = n = 6$ and $N = 100 \gg 1$ in Fig. 35 (●-dotted curve): as long as $\alpha > 0$, $I(S : E_{L=n})$ will fall below $H(S_{\text{class}}) = 1$ [32] (i.e. (238) with $\alpha > 0$ is an 'imperfect' copy-machine). Furthermore, the corresponding $H(S)$ in Fig. 35 (■-dotted curve) falls for $\alpha > 0$ below $H(S_{\text{class}}) = 1$, indicating dissipation of information about $\{\pi_i\}$ of system S . Also, exchanging in (238) the order of (166)-(167) and (237) does not affect the behavior of $I(S : E_L)/H(S_{\text{class}})$ with respect to f for $N \gg 1$: namely, in the limit $N \gg 1$ the PIP of Fig. 36, which displays the difference between a PIP of $I(S : E_L)$ from Fig. 34 and a PIP of $I_R(S : E_L)$ (emerging from the random unitary evolution (239) of $\hat{\rho}_{SE}^{\text{in}}$ for (12) with respect to the, compared with (238), reversed operator order $\hat{U}_{ij}^{\text{Tot}}(\alpha) = \hat{U}_{ij}^{\text{Diss}}(\alpha) \hat{U}_{ij}^{(\phi=\pi/2)}$) tends to zero.

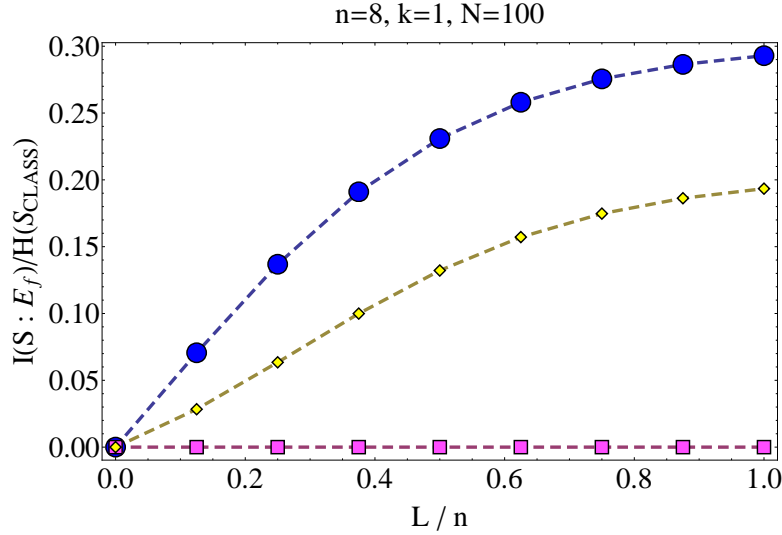


Figure 34: Random unitary evolution model: PIP of MI vs $0 < f \leq 1$ for $\alpha = \pi/2$, $\hat{\rho}_{SE}^{\text{in}} = \hat{\rho}_S^{\text{in}} \otimes \hat{\rho}_E^{\text{in}}$ ($N \gg 1$), with a $k = 1$ pure $\hat{\rho}_S^{\text{in}}$ and $\hat{\rho}_E^{\text{in}} = |0_n\rangle\langle 0_n|$ (●-dotted curve), $\hat{\rho}_E^{\text{in}} = 0.5 \cdot (|0_n\rangle\langle 0_n| + |1_n\rangle\langle 1_n|)$ (◆-dotted curve), $\hat{\rho}_E^{\text{in}} = 2^{-n} \cdot \hat{I}_n$ (■-dotted curve) [32].

However, applying (238) and $\hat{U}_{ij}^{\text{Diss}}(\alpha = \pi/2) \hat{U}_{ij}^{(\phi=\pi/2)}$ to $\hat{\rho}_{SE}^{\text{in}}$ in (12) in accord with Zurek's qubit model of Quantum Darwinism we obtain

$$\begin{aligned} |\Psi_{SE_{L=n}}^{\text{out}(1)}\rangle &= \hat{U}_{ij}^{(\phi=\pi/2)} \hat{U}_{ij}^{\text{Diss}}(\alpha = \pi/2) (|\Psi_S^{\text{in}}\rangle \otimes |0_n\rangle) = a|0\rangle|0_n\rangle + i \cdot b|0\rangle|10_{n-1}\rangle \Rightarrow \\ &H(S, E_L) = H(E_L) = H(S) = 0 \quad \forall (0 < L \leq n) \\ |\Psi_{SE_{L=n}}^{\text{out}(2)}\rangle &= \hat{U}_{ij}^{\text{Diss}}(\alpha = \pi/2) \hat{U}_{ij}^{(\phi=\pi/2)} (|\Psi_S^{\text{in}}\rangle \otimes |0_n\rangle) = a|0\rangle \otimes |0_{L=n}\rangle + b|1\rangle \otimes |1_{L=n}\rangle, \end{aligned} \quad (242)$$

showing that the order of the dissipative and the CNOT-operator in (238) does matter within Zurek's model of Quantum Darwinism.

Now we turn to other $\hat{\rho}_{SE}^{\text{in}}$ and their PIPs in Fig. 34 that we let evolve as in (166)-(167) and (239)-(241) for $\alpha > 0$, $|a|^2 = |b|^2 = 1/2$ and $p_e = 1/|M| \forall e$: the ◆-dotted curve in Fig.34 demonstrates that introducing correlations into $\hat{\rho}_E^{\text{in}}$ suppresses Quantum Darwinism within the random unitary model, as for $\alpha = 0$ in section 8: since

$$\lim_{N \gg 1} I(S : E_{L=n})/H(S_{\text{class}}) = 0.2$$

for a fixed $\alpha > 0$ and $L = n \geq 5$, no Quantum Darwinism appears.

This becomes apparent if we look at the MI $I(S : E_L)/H(S_{\text{class}})$ from the ■-dotted curve in Fig.34 (with $\hat{\rho}_E^{\text{in}} = 2^{-n} \cdot \hat{I}_n = 2^{-n} \hat{I}_1^{\otimes n}$): one has in this case

$$\lim_{N \gg 1} I(S : E_{L=n})/H(S_{\text{class}}) = 0$$

for a fixed $\alpha > 0$ and $L = n \geq 5$, i.e. completely mixed $\hat{\rho}_E^{\text{in}}$ suppress Quantum Darwinism (no MI-'plateau'),

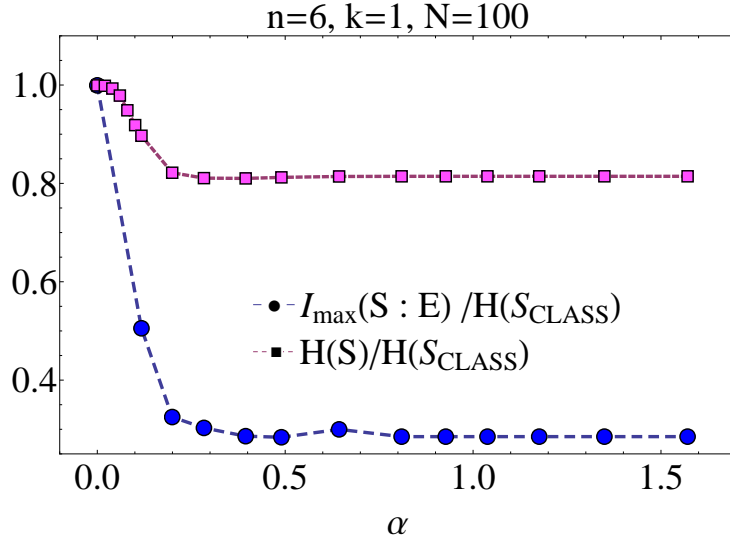


Figure 35: Random unitary evolution model: maximal value $I(S : E_{L=n}) = I_{\max}(S : E)$ of MI and $H(S)$ from Fig. 34 (•-dotted curve, $N \gg 1$) vs $0 < \alpha \leq \pi/2$ for $L = n = 6$, [32].

as in section 8.

Interestingly, for an entangled input state (with an S -probability distribution $|a|^2 = |b|^2 = 1/2$ of a $k = 1$ qubit system S)

$$|\Psi_{SE}^{\text{in}}\rangle = a |0_{k=1}\rangle |s_1^{L=n}\rangle + b |1_{k=1}\rangle |s_2^{L=n}\rangle \quad (243)$$

involving CNOT-invariant E -states

$$|s_m^n\rangle = |s_m\rangle^{\otimes n} = \left(\sqrt{2}\right)^{-n} (|0\rangle + (-1)^{m+1} |1\rangle)^{\otimes n},$$

with $\hat{\sigma}_x |s_m\rangle = (-1)^{m+1} |s_m\rangle$, $m \in \{1, 2\}$ and $\langle s_1 | s_2 \rangle = 0$, we obtain $I(S : E_L) / H(S_{\text{class}})$ that leads to Quantum Darwinism if $\alpha = 0$, as in Fig. 1 and in Fig. 33 (■-dotted curve, s. also section 8), but behaves in the limit $N \gg 1$ for $n \geq 5$ and a fixed $\alpha = \pi/2$ with respect to $f = L/n$ as the ■-dotted curve in Fig.34.

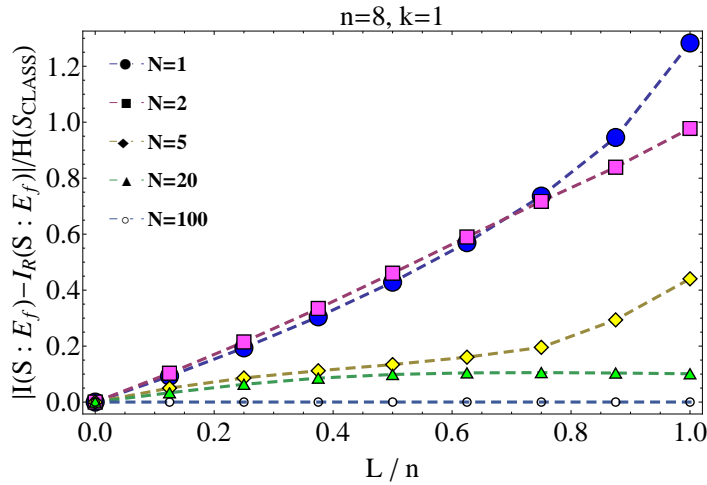


Figure 36: PIP (for $\alpha = \pi/2$) of the MI-difference $[I(S : E_L) - I_R(S : E_L)] / H(S_{\text{class}})$ w.r.t. N and the random unitary evolution of $\hat{\rho}_{SE}^{\text{in}}$ from Fig. 33, leading (with (238)) to $I(S : E_L)$ and (with $\hat{U}_{ij}^{\text{Tot}}(\alpha) = \hat{U}_{ij}^{\text{Diss}}(\alpha) \hat{U}_{ij}^{(\phi=\pi/2)}$) to $I_R(S : E_L)$ [32].

Finally, for $\hat{\rho}_{SE}^{in}$ from Fig. 1 with $N = 100$, $k = 2, 3$, $p_i = 2^{-k} \forall i \in \{0, \dots, 2^k - 1\}$ and $H(S_{class}) = k$ we obtain from the random unitary evolution the PIP as in Fig. 37, showing that for $L = n \geq 5$, $k > 1$ and $N \gg 1$ the maximal value $I(S : E_{L=n}) / H(S_{class})$ of MI tends to zero according to

$$\lim_{(k \sim n) \gg 1} I(S : E_{L=n}) / H(S_{class}) = 2^{1-k} \cdot I(S^{k=1} : E_{L=n}) / H(S_{class}^{k=1})$$

w.r.t. the maximal value $I(S^{k=1} : E_{L=n}) / H(S_{class}^{k=1})$ of MI obtained in a PIP of Fig. 34 for a $k = 1$ qubit system S . In other words, by means of Fig. 37 we may anticipate that for $L = n \geq 5$ and $N \gg 1$

$$\lim_{(k \sim n) \gg 1} I(S : E_{L=n}) / H(S_{class}) = 2^{-k},$$

i.e. no Quantum Darwinism $\forall k > 1$ (as in section 8 with $\alpha = 0$).

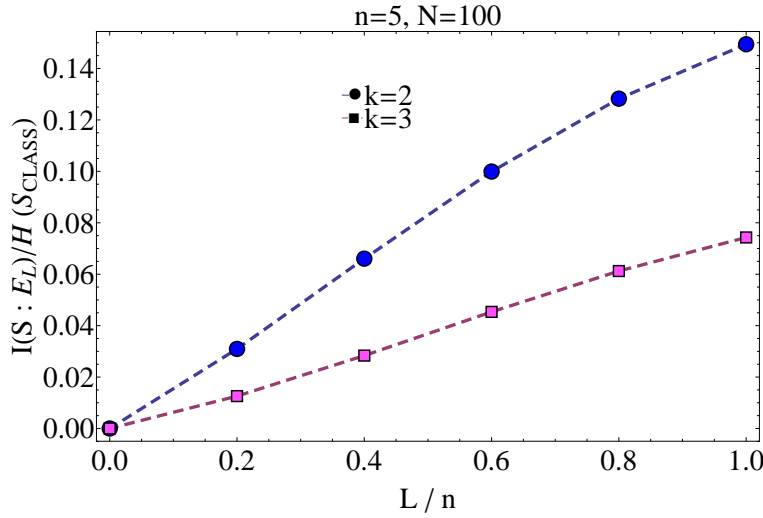


Figure 37: Random unitary evolution model: MI $I(S : E_L) / H(S_{class})$ vs $0 < f \leq 1$ for $\alpha = \pi/2$ with respect to $\hat{\rho}_{SE}^{in}$ from Fig. 33 with $N = 100$ ($N \gg 1$), $k = 2, 3$, $p_i = 2^{-k} \forall i \in \{0, \dots, 2^k - 1\}$ and $H(S_{class}) = k$, evolving iteratively by (166)-(167) and (239)-(241) [32].

9.2 Numerical reconstruction of the dissipative attractor space

Now we reconstruct the dissipative attractor space of the random unitary model by means of numerical simulations. Therefore, we start with (238) that has four eigenvalues

$\lambda \in \left\{ 1, -1, 0.5 \cdot \left(1 + \cos \alpha \pm i\sqrt{4 - (1 + \cos \alpha)^2} \right) \right\}$ [32]. When looking at the matrix structure of $\hat{\rho}_{SE}^{in}$ from Fig. 33 after $N \gg 1$ random unitary iterations (239) we notice that the outer-diagonal entries of $\hat{\rho}_{SE}^{out}$ from Fig. 34 (•-dotted curve) tend to zero $\sim n^{-N} \forall \alpha > 0$, such that we obtain

$$\hat{\rho}_{SE}^{out}(N \gg 1) = \frac{|b|^2}{2^{n+1} - 1} \cdot \hat{I}_{1+n} + \left(|a|^2 - \frac{|b|^2}{2^{n+1} - 1} \right) |0_{1+n}\rangle \langle 0_{1+n}|, \quad (244)$$

leading us to the Gram-Schmidt-orthonormalized attractor (sub-)space with respect to the eigenvalue $\lambda = 1$ [32]

$$|0_{1+n}\rangle \langle 0_{1+n}|, \left(\hat{I}_{1+n} - |0_{1+n}\rangle \langle 0_{1+n}| \right) \cdot (2^{n+1} - 1)^{-1/2}, \quad (245)$$

containing the $\{\lambda = 1\}$ -eigenstate $|0_{1+n}\rangle$ and \hat{I}_{1+n} as the trivial fixed point state of the random unitary evolution. (245) will appear $\forall \alpha > 0$, even if $\alpha \ll 1$, in which case we would need a higher number N of iterations compared with the ($\alpha = \pi/2$)-choice. Furthermore, (245) also indicates that non-vanishing dissipation also tends to create almost completely mixed output states $\hat{\rho}_{SE}^{out}$ in the limit $N \gg 1$, which violates the requirement (66) from subsection 4.2.2 and thus leads to the Shannon-entropy $H(S) = H(\{S\}) < H(S_{class}^{k=1})$ of a decohered system S .

Without a doubt, tracing E out from $\hat{\rho}_{SE}^{\text{out}} (L > k)$ in (70) leads with (69) to a decohered S . However, the non-zero outer-diagonal entries \blacksquare_l in (68) introduce an important subtlety into our argumentation, since they force us to choose the most adequate combination of eight diagonal entries $|c_{l,2+1}^E|^2$ and $|c_{(l+1),2}^E|^2 \forall l$ in (70) associated with different diagonal subspaces $\{|\varphi_i\rangle\langle\varphi_i|\}_{i=1}^{i=2^k}$ of S that would be identified with four S -probabilities $\{|c_i|^2\}_{i=1}^{i=2^k}$. Additionally, we notice that the only reasonable configuration of these eight diagonal entries turns out to be exactly (69). All other configurations $|c_{l,2+1}^E|^2 = |c_{(l+1),2}^E|^2 = 0$ for all or some l -values in (70) would violate (15) by slowing down (reducing) the decoherence of S . For example, as an extreme case one could imagine that the $(k=2, L=n=3)$ -matrix structure of $\hat{\rho}_{SE}^{\text{out}} (L \geq k)$ from (70) contains only four instead of eight diagonal entries $|c_{l,2+1}^E|^2$ and $|c_{(l+1),2}^E|^2 \forall l$. Then, at least two of the four D_l -submatrices in (68) have to be characterized by a vanishing trace and are thus, due to the missing diagonal entries that should be »connected« in the sense of (for instance) (311) with each other by means of outer diagonal entries \blacksquare_l , automatically (2×2) zero-matrices which do not contribute to the von Neumann entropies of $\hat{\rho}_{SE}^{\text{out}} (L=n=3 > k=2)$ and its reduced states of S and E . On the contrary, the vanishing of a subset of the originally available D_l -submatrices allows us to use only a half of a total of four S -probabilities $\{|c_i|^2\}_{i=1}^{i=2^k}$, forcing us to extract from the resulting density matrix $\hat{\rho}_{SE}^{\text{out}} (L=n=3 > k=2)$ the reduced state of S whose diagonal entries would be composed of convex sums of the remaining non-zero S -probabilities $\{|c_i|^2\}_{i=1}^{i=2^k}$. For instance, let us assume that solely D_0 and D_2 of $\hat{\rho}_{SE}^{\text{out}} (L=n=3 > k=2)$ from (70) and (68) are non-zero. Then one obtains for $\hat{\rho}_S^{\text{out}} (L=n=3 > k=2)$ with (69) the expression

$$\begin{aligned} \hat{\rho}_S^{\text{out}} (L=n=3 > k=2) &= \text{diag} [\text{Tr}_{E_{L-k}} (D_0), 0, 0, \text{Tr}_{E_{L-k}} (D_3)] \\ &= \text{diag} [|c_1^E|^2 + |c_2^E|^2 \stackrel{!}{=} |c_1|^2, 0, 0, |c_7^E|^2 + |c_8^E|^2 \stackrel{!}{=} |c_4|^2], \end{aligned} \quad (246)$$

whose von Neumann entropy corresponds to classical information $H(S_{\text{class}}^{k=1})$ about a $k=1$ qubit subsystem of an originally $k=2$ qubit S . Therefore, (246) collides with (15), in which we normalize $I(S : E_f)$ w.r.t. the Shannon-entropy $H(S_{\text{class}}^k)$ of an effectively decohered k -qubit S . However, since $\hat{\rho}_S^{\text{out}}$ in (246) offers only a fraction $H(S) = H(S_{\text{class}}^{k=1}) < H(S_{\text{class}}^{k=2})$ of $H(S_{\text{class}}^{k=2})$, the remaining amount $H(S_{\text{class}}^{k=2}) - H(S_{\text{class}}^{k=1})$ is simply lost irreversibly (dissipated), preventing us from seeing QD even if one could achieve $H(S, E_f) = H(E_f)$, as is still the case for $\hat{\rho}_{SE}^{\text{out}} (L=n=3 > k=2)$ of (70) constrained by (246). In order to achieve these dissipation effects w.r.t. $H(S)$ and its amount of classical information $H(S_{\text{class}}^{k \geq 1})$ we do not necessarily need vanishing D_l -submatrices in (70). On the contrary, already the violation of (69) would suffice to dissipate fractions of $H(S_{\text{class}}^{k \geq 1})$, even if none of the diagonal entries in D_l -submatrices from (70) should be zero, which appears to be the most frequent dissipation structure of $\hat{\rho}_{SE}^{\text{out}} (L)$ in the course of numerous realistic qubit interaction models of thermalization processes [26].

In other words, dissipation apparently has an opposite impact on the decoherence process of S , or, to be more precise, the decoherence of S appears to be slowed down by dissipation (dissipation of system's Shannon-entropy into the fraction of a larger environment E' (with $E \subset E'$)) which is traced out $\forall L \leq n$ when computing the corresponding PIPs).

We can confirm (245) by decomposing $\hat{\rho}_{SE}^{\text{in}}$ from Fig. 33 with $\hat{\rho}_E^{\text{in}} = |1_n\rangle\langle 1_n|$ in accord with (241), that by means of (245) yields the asymptotic state

$$\hat{\rho}_{SE}^{\text{out}} (N \gg 1) = \sum_{\lambda=1, i=1}^2 \lambda^N \text{Tr} \left\{ \hat{\rho}_{SE}^{\text{in}} \hat{X}_{\lambda,i}^\dagger \right\} \hat{X}_{\lambda,i} = \left(|1_{1+n}\rangle - |0_{1+n}\rangle \langle 0_{1+n}| \right) \cdot (2^{n+1} - 1)^{-1}, \quad (247)$$

whose asymptotic PIP coincides exactly with the numerical PIP-plot in Fig. 34 (the \blacksquare -dotted curve), giving again

$$\lim_{N \gg 1} H(S : E_{L=n}) / H(S_{\text{class}}) = 0$$

Furthermore, for $L=n \gg 1$ (244) leads (for instance with $|b|^2 = |a|^2 = 1/2 \Rightarrow H(S_{\text{class}}) = 1$) to

$$\begin{aligned} \hat{\rho}_S^{\text{out}} &\approx \text{diag} [|a|^2 + |b|^2/2, |b|^2/2] \Rightarrow H(S) \approx 0.811 \\ \hat{\rho}_E^{\text{out}} &\approx \text{diag} [|a|^2 + |b|^2 \cdot 2^{-n}, |b|^2 \cdot 2^{-n}, \dots, |b|^2 \cdot 2^{-n}]_{2^n \times 2^n} \\ \Rightarrow H(E_{L=n}) &\approx H(S_{\text{class}}) + n|b|^2, H(S, E_{L=n}) \approx H(S_{\text{class}}) + (n+1)|b|^2 \\ I(S : E_{L=n}) &\approx H(S) - |b|^2 = 0.311, \end{aligned} \quad (248)$$

as in Fig. 34 (•-dotted curve). Computing $I(S : E_{L=n})$ for different n -values yields results in Table 7, which numerically confirms that we need at least $n \geq 5$ E-qubits to approximately obtain the correct $I(S : E_{L=n})$ -maximum in Fig. 34 (•-dotted curve) for $N \gg 1$, as in section 8.

Finally, decomposing the inputs $\hat{\rho}_{SE}^{\text{in}}$ from the ♦-dotted and the ■-dotted curve in Fig. 34 in accord with (241) we obtain the asymptotic output states $\hat{\rho}_{SE}^{\text{out}(1)}$ and $\hat{\rho}_{SE}^{\text{out}(2)}$, respectively, displayed in (249), whose PIPs coincide for $N \gg 1$ exactly with those in Fig. 34 (♦- and ■-dotted curves).

$I(S : E_{L=n}) / H(S_{\text{class}})$	n
0.124	2
0.190	3
0.236	4
0.266	5
0.285	6
0.296	7
0.303	8
0.306	9
0.308	10

Table 7: $I(S : E_{L=n}) / H(S_{\text{class}})$ vs n for $\hat{\rho}_{SE}^{\text{out}} (N \gg 1)$ in Fig. 34 (•-dotted curve) [32].

$$\begin{aligned}
\hat{\rho}_{SE}^{\text{out}(1)} (N \gg 1) &= \frac{|a|^2}{2} |0_{1+n}\rangle \langle 0_{1+n}| \\
&+ \frac{|b|^2}{2} \left(\hat{I}_{1+n} - |0_{1+n}\rangle \langle 0_{1+n}| \right) \cdot (2^{n+1} - 1)^{-1} \\
\hat{\rho}_{SE}^{\text{out}(2)} (N \gg 1) &= 2^{-n} |a|^2 |0_{1+n}\rangle \langle 0_{1+n}| + \\
&\left(1 - 2^{-n} |a|^2 \right) \left(\hat{I}_{1+n} - |0_{1+n}\rangle \langle 0_{1+n}| \right) \cdot (2^{n+1} - 1)^{-1}
\end{aligned} \tag{249}$$

Thus, the analytical expression $\hat{\rho}_{SE}^{\text{out}(2)}$ for the ■-dotted curve of Fig. 34 in (249) exactly coincides with the analytical expression for the random unitarily evolved (243) with respect to $N \gg 1$, as already confirmed numerically. This validates the anticipated dissipative attractor (sub-)space (245) with respect to $\lambda = 1$ and the $k = 1$ qubit system S .

It remains to anticipate the $\{\lambda = 1\}$ -attractor (sub-)space for the $k > 1$ qubit system S and its $n \geq k$ qubit environment E : from Fig. 37 we see that the asymptotic output states $\hat{\rho}_{SE}^{\text{out}} (N \gg 1)$ for $k = 2, 3$ may be decomposed as

$$\begin{aligned}
\hat{\rho}_{SE}^{\text{out}} (N \gg 1) &= \sum_{\lambda=1, i=1}^2 \lambda^N \text{Tr} \left\{ \hat{\rho}_{SE}^{\text{in}} \hat{X}_{\lambda,i}^\dagger \right\} \hat{X}_{\lambda,i} \\
&= \langle 0_k | \hat{\rho}_S^{\text{in}} | 0_k \rangle | 0_{k+n} \rangle \langle 0_{k+n} | + \\
&\left(1 - \langle 0_k | \hat{\rho}_S^{\text{in}} | 0_k \rangle \right) \left(\hat{I}_{k+n} - | 0_{k+n} \rangle \langle 0_{k+n} | \right) \cdot (2^{n+k} - 1)^{-1},
\end{aligned} \tag{250}$$

with $\langle 0_k | \hat{\rho}_S^{\text{in}} | 0_k \rangle := p_0 = |a_0|^2 = 2^{-k}$, forcing us to fix

$$| 0_{k+n} \rangle \langle 0_{k+n} |, \left(\hat{I}_{k+n} - | 0_{k+n} \rangle \langle 0_{k+n} | \right) \cdot (2^{n+k} - 1)^{-1/2} \tag{251}$$

as the appropriate $k \geq 1$ generalization of the attractor (sub-)space (245) [32]. We can confirm (251) by approximating $H(S : E_{L=n})$ of (250) (with $H(S_{\text{class}}) = k$) with respect to $n \sim k \gg 1$, yielding with $\ln(1 \pm x) \approx \pm x + \mathcal{O}(x^2)$ [12, 32]

$$\begin{aligned}
I(S : E_{L=n}) &\approx k \cdot 2^{-k} \\
\Rightarrow I(S : E_{L=n}) / H(S_{\text{class}}) &\approx k \cdot 2^{-k} / k = 2^{-k},
\end{aligned} \tag{252}$$

in accord with Fig. 37 and section 8. Thus, (252) validates (251), which we want to reproduce in the following subsection in an analytical fashion by recurring to the eigenvalue equation (240).

9.3 Analytic reconstruction of the dissipative attractor space

Finally, we want to analytically confirm the numerically reconstructed dissipative attractor space of the random unitary model. Therefore, we start with (240) that contains $g := |M| \cdot 2^{2(k+n)}$ equations for $2^{2(k+n)}$ unknown $\hat{X}_{\lambda,i}$ -matrix entries with respect to the fixed λ -eigenvalue. We first reformulate (240) as a linear system of equations

$$A\mathbf{x} = \mathbf{0}, \tag{253}$$

with a $(g \times g)$ -matrix A and a $(1 \times g)$ -column vector \mathbf{x} containing the first $2^{2(k+n)}$ unknown $\hat{X}_{\lambda,i}$ -matrix entries and the remaining $g^2 - 2^{2(k+n)}$ zero entries. Then we can apply the QR-decomposition (s. for instance [23] and Appendix G) to A in (253) and determine from the rank r of the corresponding R -matrix the dimensionality

$$d_{n \geq k}^\lambda = 2^{2(k+n)} - r \quad (254)$$

of the attractor (sub-)space in (241) for a fixed λ -value, whereas the Q -matrix leads to all allowed $d_{n \geq k}^\lambda$ configurations of $\hat{X}_{\lambda,i}$ -matrix entries in (241). It can be explicitly shown that the QR-decomposition of (253) leads for $\lambda = 1$ of $\hat{U}_{ij}^{\text{Tot}}(\alpha)$ to $d_{n \geq k}^{\lambda=1} = 2$ and $\hat{X}_{\lambda=1,i}$ -matrix configurations (pre-configuration matrices) with respect to a $k \geq 1$ qubit S ,

$$\hat{X}_{\lambda=1,i} = \text{diag}[\blacksquare, \boxtimes, \dots, \boxtimes]_{2^{k+n} \times 2^{k+n}}, \quad \forall (0 < \alpha \leq \pi/2), \quad (255)$$

with an arbitrary \blacksquare and $(2^{k+n} - 1)$ identical entries $\boxtimes = \text{const.}$ Since we know that $|0_{k+n}\rangle \langle 0_{k+n}|$ is an eigenstate for $\lambda = 1$ of $\hat{U}_{ij}^{\text{Tot}}(\alpha)$, we may set $(\blacksquare \neq 0, \boxtimes = 0)$ as one allowed configuration in (255). The second linearly independent configuration is certainly the unity matrix \hat{I}_{k+n} as the standard fixed point state of the random unitary dynamics, given by $(\blacksquare = \boxtimes \neq 0)$. This confirms the attractor (sub-)space for $\lambda = 1$ of $\hat{U}_{ij}^{\text{Tot}}(\alpha)$ in (251) above. On the other hand, for all three remaining eigenvalues $\lambda \neq 1$ of $\hat{U}_{ij}^{\text{Tot}}(\alpha)$ we obtain by means of the QR-decomposition $d_{n \geq k}^{\lambda \neq 1} = 0 \forall (0 < \alpha \leq \pi/2)$, in accord with numerical results from subsection 9.2.

9.4 Summary and outlook

Results obtained in this section lead us to the following conclusions: the Quantum Darwinistic 'MI- plateau' appears within the dissipative random unitary model for $n \gg k = 1$ and $\hat{\rho}_{SE}^{\text{in}}$ as in Fig. 33 (\blacksquare -dotted curve) only if $\alpha = 0$ (no dissipation) and $N \rightarrow \infty$ (s. section 8).

For fixed $\alpha > 0$ the random unitary model leads to (almost completely) mixed $\hat{\rho}_{SE}^{\text{out}}(N \gg 1)$, enforcing $H(S) < H(S_{\text{class}})$ (loss of classical information about system S stored into environment E) and $H(E_L) < H(S, E_L)$ ($\hat{U}_{ij}^{\text{Tot}}(\alpha)$ as an 'imperfect copy-machine'). The attractor (sub-)space exists only with respect to $\lambda = 1$ of $\hat{U}_{ij}^{\text{Tot}}(\alpha)$ and is $d_{n \geq k}^{\lambda=1} = 2$ dimensional $\forall (0 < \alpha \leq \pi/2)$, with attractor states $\hat{X}_{\lambda=1,i}$, $i \in \{1, 2\}$ given by

$$|0_k\rangle \langle 0_k| \otimes |0_n\rangle \langle 0_n|, \quad \frac{\hat{I}_k \otimes \hat{I}_n - |0_k\rangle \langle 0_k| \otimes |0_n\rangle \langle 0_n|}{(2^{k+n} - 1)^{1/2}}.$$

Attractor (sub-)spaces with respect to the three remaining eigenvalues λ of $\hat{U}_{ij}^{\text{Tot}}(\alpha)$ are all zero-dimensional, i.e. $d_{n \geq k}^\lambda = 0 \forall \lambda \neq 1$.

Since Quantum Darwinism appears for N , $n \gg k \geq 1$ only if

$$\begin{aligned} H(S) &\approx H(S_{\text{class}}) \wedge H(E_L) \geq H(S, E_L) \\ &\Leftrightarrow I(S : E_L) / H(S_{\text{class}}) \geq 1 \end{aligned}$$

holds $\forall k \leq L \leq n$, regardless of the order in which the n E -qubits are being successively traced out from the output state $\hat{\rho}_{SE}^{\text{out}}$ [5, 31] (s. also (155) above), we see that for $\alpha > 0$ there is no $\hat{\rho}_{SE}^{\text{in}}$ within the dissipative random unitary model that leads to Quantum Darwinism [30, 32]. In Zurek's qubit-model, however, the (dis-)appearance of Quantum Darwinism depends on the order of application of $\hat{U}_{ij}^{(\phi=\pi/2)}$ and $\hat{U}_{ij}^{\text{Diss}}(\alpha)$ in (238).

As an advanced research problem it is interesting to study the impact of dephasing in the framework of Zurek's and the random unitary model on Quantum Darwinism by introducing into $\hat{U}_{ij}^{\text{Tot}}$ of (238)-(239) the unitary two-qubit dephasing-operator $\hat{U}_{ij}^{\text{Deph}}(\gamma) = \exp\left[-\frac{i}{2}\gamma\hat{\sigma}_z^{(i)} \otimes \hat{\sigma}_z^{(j)}\right]$ with a real-valued parameter (dephasing rate) $0 \leq \gamma \leq \pi$, in accord with [30]. Furthermore, one could also investigate what happens with the f -dependence of MI if one weights the two addends in (237) according to $\hat{U}_{ij}^{\text{Diss}}(\alpha_1, \alpha_2) = \exp\left[\frac{i}{2}\left(\alpha_1\hat{\sigma}_x^{(i)} \otimes \hat{\sigma}_x^{(j)} + \alpha_2\hat{\sigma}_y^{(i)} \otimes \hat{\sigma}_y^{(j)}\right)\right]$, i.e. by means of two (different) positive, real-valued parameters $\alpha_1 \neq \alpha_2$, such that $0 \leq \alpha_1 + \alpha_2 \leq \pi$.

Finally, taking the above discussion of dissipation and its impact on QD into account, we have come to the conclusion that in order to overcome the dissipative leakage of $H(S_{\text{class}})$ into a larger environment E' than the n -qubit E ($E \subset E'$) which was usually of main interest in the present section, we need to ensure that E encloses the entire (remaining part of the) universe as an appropriate environment of system S , i.e. $E \equiv E'$ (if E' should denote the universe without S). Clearly, if we think in this way, we could weight (substitute) the dissipative operator in (237) according to

$$\hat{I}_S \otimes \hat{I}_E (1 - \delta_{n,|E'|}) \hat{U}_{ij}^{\text{Diss}}(\alpha) \leftrightarrow \hat{U}_{ij}^{\text{Diss}}(\alpha), \quad (256)$$

which annuls the impact of the dissipative part in $\hat{U}_{ij}^{\text{Tot}}(\alpha)$ of (238) as soon as the number of E-qubits reaches the number $|E'|$ of constituents in E' . However, this is not the behavior we encounter in nature: from everyday experience we see that a perfect transfer of $H(S_{\text{class}})$ into E apparently works even if we enclose by E only our direct environment, which is usually much smaller than E' . How can we explain this observation if we still want to accept the omnipresence of dissipative effects that may disturb the decoherence-induced information transfer between an open, k -qubit system S and its n -qubit environment E ?

First, let us notice that even our direct environment may be thought of as an entity consisting of $n \gg k$ qubits. Second, we may also look at transferring $H(S_{\text{class}})$ into E as a process described by a certain success probability: in other words, the more qubits («storage cells») E contains, the higher the probability for efficiently storing $H(S_{\text{class}})$ into a fraction \mathcal{F} (qubit subsets) of E . In the limit $n \gg k$ of effective decoherence we thus may expect that, despite of dissipation, $H(S_{\text{class}})$ will be efficiently transferred almost into all constituents of E , which can be accounted for by weighting (substituting) $\hat{U}_{ij}^{\text{Diss}}(\alpha)$ from the dissipative part in $\hat{U}_{ij}^{\text{Tot}}(\alpha)$ of (238) with an exponentially decreasing prefactor

$$\hat{I}_S \otimes \hat{I}_E \exp[-n/k] \hat{U}_{ij}^{\text{Diss}}(\alpha) \leftrightarrow \hat{U}_{ij}^{\text{Diss}}(\alpha), \quad (257)$$

which converges to zero in the limit $n \gg k$. In other words, modifying (237)-(241) by means of (257) would suggest that in the limit of effective decoherence the dissipative random unitary model could, in principle, lead to the random unitary model of pure decoherence from (166)-(170) of section 8, which could in turn help us understand the appearance of effective information storage from system S into its environment E even when dissipative effects and information losses cannot be omitted.

10 Random Unitary model of Quantum Darwinism with dissipation and dephasing

In this section we will summarize the iterative evolution formalism of the random unitary model involving pure decoherence and dissipation before discussing its most important results regarding Quantum Darwinism in subsections 10.1-10.3. We introduce dephasing into the random unitary evolution in accord with [26], by letting the arrows of the ID in Fig. 32 from E - to S -qubits denote a dissipative-dephasing feedback of E w.r.t. S represented by two qubit interactions

$$\begin{aligned} \hat{U}_{ij}^{(\alpha_1, \alpha_2, \gamma)} &= \exp \left[\frac{i}{2} \left(\hat{H}_Y^{\alpha_1, \alpha_2} \right) \right] = \\ &= \sum_{\chi \in G} \left[\cos \left(\frac{\sqrt{V_\chi}}{2} \right) \hat{I}_1^{(i)} \otimes \hat{I}_1^{(j)} + \frac{i \hat{H}_Y^{\alpha_1, \alpha_2} \sin \left(\frac{\sqrt{V_\chi}}{2} \right)}{\sqrt{V_\chi}} \right] |\chi\rangle \langle \chi|, \\ G &\equiv \{(0_i 0_j), (1_i 0_j), (0_i 1_j), (1_i 1_j)\}, \\ V_\chi &= \begin{cases} (\alpha_1 - \alpha_2)^2 + \gamma^2 - (\alpha_2 - \alpha_1) \gamma & \text{if } \chi = (0_i 0_j) \\ (\alpha_1 + \alpha_2)^2 + \gamma^2 + (\alpha_2 + \alpha_1) \gamma & \text{if } \chi = (1_i 0_j) \\ (\alpha_1 + \alpha_2)^2 + \gamma^2 - (\alpha_2 + \alpha_1) \gamma & \text{if } \chi = (0_i 1_j) \\ (\alpha_1 - \alpha_2)^2 + \gamma^2 + (\alpha_2 - \alpha_1) \gamma & \text{if } \chi = (1_i 1_j), \end{cases} \end{aligned} \quad (258)$$

with a real-valued dissipation strength $0 \leq \alpha_1 + \alpha_2 \leq \pi$, dephasing rate $0 \leq \gamma \leq \pi$ and $\hat{H}_Y^{\alpha_1, \alpha_2} = \alpha_1 \hat{\sigma}_x^{(i)} \otimes \hat{\sigma}_x^{(j)} + \alpha_2 \hat{\sigma}_y^{(i)} \otimes \hat{\sigma}_y^{(j)} - \gamma \hat{\sigma}_z^{(i)} \otimes \hat{\sigma}_z^{(j)}$.

For the sake of numerical convenience we can express (258) according to

$$\begin{aligned} \hat{U}_{ij}^{(\alpha_1, \alpha_2, \gamma)} &= \begin{pmatrix} [1] & 0 & 0 & [2] \\ 0 & [3] & [4] & 0 \\ 0 & [5] & [6] & 0 \\ [7] & 0 & 0 & [8] \end{pmatrix} = \hat{U}_{ij}^{(\alpha_1, \alpha_2, \gamma=0)} \hat{U}_{ij}^{(\alpha_1=\alpha_2=0, \gamma)} \\ &= [1] |0\rangle_S \langle 0| \otimes |0\rangle_E \langle 0| + [2] |0\rangle_S \langle 1| \otimes |0\rangle_E \langle 1| + [3] |0\rangle_S \langle 0| \otimes |1\rangle_E \langle 1| + [4] |0\rangle_S \langle 1| \otimes |1\rangle_E \langle 0| \\ &\quad + [5] |1\rangle_S \langle 0| \otimes |0\rangle_E \langle 1| + [6] |1\rangle_S \langle 1| \otimes |0\rangle_E \langle 0| + [7] |1\rangle_S \langle 0| \otimes |1\rangle_E \langle 0| + [8] |1\rangle_S \langle 1| \otimes |1\rangle_E \langle 1| \end{aligned} \quad (259)$$

w.r.t. the standard computational basis $\{|0\rangle, |1\rangle\}$ (see Appendix K), with

$$\begin{aligned} [1] &:= \cos \left(\frac{\alpha_1 - \alpha_2}{2} \right) \exp \left[-\frac{i\gamma}{2} \right] & [2] &:= i \sin \left(\frac{\alpha_1 - \alpha_2}{2} \right) \exp \left[-\frac{i\gamma}{2} \right] & [3] &:= \cos \left(\frac{\alpha_1 + \alpha_2}{2} \right) \exp \left[\frac{i\gamma}{2} \right] \\ [4] &:= i \sin \left(\frac{\alpha_1 + \alpha_2}{2} \right) \exp \left[\frac{i\gamma}{2} \right] & [5] &:= i \sin \left(\frac{\alpha_1 + \alpha_2}{2} \right) \exp \left[\frac{i\gamma}{2} \right] & [6] &:= \cos \left(\frac{\alpha_1 + \alpha_2}{2} \right) \exp \left[\frac{i\gamma}{2} \right] \\ [7] &:= i \sin \left(\frac{\alpha_1 - \alpha_2}{2} \right) \exp \left[-\frac{i\gamma}{2} \right] & [8] &:= \cos \left(\frac{\alpha_1 - \alpha_2}{2} \right) \exp \left[-\frac{i\gamma}{2} \right]. \end{aligned}$$

The total unitary two-qubit operation is then given by

$$\hat{U}_{ij}^{\text{Tot}}(\alpha_1, \alpha_2, \gamma) = \hat{U}_{ij}^{(\phi=\pi/2)} \hat{U}_{ij}^{(\alpha_1, \alpha_2, \gamma)} = \hat{U}_{ij}^{(\phi=\pi/2)} \hat{U}_{ij}^{(\alpha_1, \alpha_2, \gamma=0)} \hat{U}_{ij}^{(\alpha_1=\alpha_2=0, \gamma)}, \quad (260)$$

which by means of (166)-(167) and (259) acquires the form

$$\begin{aligned} \hat{U}_{ij}^{\text{Tot}}(\alpha_1, \alpha_2, \gamma) = & [1] |0\rangle_S \langle 0| \otimes |0\rangle_E \langle 0| + [2] |0\rangle_S \langle 1| \otimes |0\rangle_E \langle 1| \\ & + [3] |0\rangle_S \langle 0| \otimes |1\rangle_E \langle 1| + [4] |0\rangle_S \langle 1| \otimes |1\rangle_E \langle 0| \\ & + [5] |1\rangle_S \langle 0| \otimes |1\rangle_E \langle 1| + [6] |1\rangle_S \langle 1| \otimes |1\rangle_E \langle 0| \\ & + [7] |1\rangle_S \langle 0| \otimes |0\rangle_E \langle 0| + [8] |1\rangle_S \langle 1| \otimes |0\rangle_E \langle 1|. \end{aligned} \quad (261)$$

Accordingly, the inverse two-qubit operation

$$\hat{U}_{ij}^{\text{Tot(R)}}(\alpha_1, \alpha_2, \gamma) = \hat{U}_{ij}^{(\alpha_1, \alpha_2, \gamma)} \hat{U}_{ij}^{(\phi=\pi/2)} \quad (262)$$

leads by means of (166)-(167) and (259) to the form

$$\begin{aligned} \hat{U}_{ij}^{\text{Tot(R)}}(\alpha_1, \alpha_2, \gamma) = & [1] |0\rangle_S \langle 0| \otimes |0\rangle_E \langle 0| + [2] |0\rangle_S \langle 1| \otimes |0\rangle_E \langle 0| \\ & + [3] |0\rangle_S \langle 0| \otimes |1\rangle_E \langle 1| + [4] |0\rangle_S \langle 1| \otimes |1\rangle_E \langle 1| \\ & + [5] |1\rangle_S \langle 0| \otimes |0\rangle_E \langle 1| + [6] |1\rangle_S \langle 1| \otimes |0\rangle_E \langle 1| \\ & + [7] |1\rangle_S \langle 0| \otimes |1\rangle_E \langle 0| + [8] |1\rangle_S \langle 1| \otimes |1\rangle_E \langle 0|. \end{aligned} \quad (263)$$

Thus, (260) and (263) model the interplay between decoherence, dissipation and dephasing w.r.t. an open k-qubit S and its n-qubit E. Replacing within the random unitary formalism with pure decoherence in (166)-(170) of section 8 $\hat{U}_{ij}^{(\phi=\pi/2)}$ by $\hat{U}_{ij}^{\text{Tot}}(\alpha_1, \alpha_2, \gamma)$ in (260) or $\hat{U}_{ij}^{\text{Tot(R)}}(\alpha_1, \alpha_2, \gamma)$ in (263) we are thus capable of modeling dissipative effects and their influence on QD.

In other words, in order to model the realistic measurement process of S and E we let an input state $\hat{\rho}_{SE}^{\text{in}}$ evolve by virtue of the following iteratively applied random unitary quantum operation (completely positive unital map) $\mathcal{P}_{\text{Tot}}(\cdot) \equiv \sum_{e \in M} K_e^{\text{Tot}}(\cdot) K_e^{\text{Tot}\dagger}$ (with Kraus-operators $K_e^{\text{Tot}} := \sqrt{p_e} \hat{U}_e^{\text{Tot}}(\alpha_1, \alpha_2, \gamma)$) [11, 29, 30]:

- The quantum state $\hat{\rho}(N)$ after N iterations is changed by the (N + 1)-th iteration to the quantum state

$$\hat{\rho}(N+1) = \sum_{e \in M} p_e \hat{U}_e^{\text{Tot}} \hat{\rho}(N) \hat{U}_e^{\text{Tot}} \equiv \mathcal{P}_{\text{Tot}}(\hat{\rho}(N)). \quad (264)$$

- In the asymptotic limit $N \gg 1$ $\hat{\rho}(N)$ is independent of $(p_e, e \in M)$ and determined by linear attractor spaces with mutually orthonormal solutions (index i) $\hat{X}_{\lambda, i}$ of the eigenvalue equation

$$\hat{U}_e^{\text{Tot}}(\alpha_1, \alpha_2, \gamma) \hat{X}_{\lambda, i} \hat{U}_e^{\text{Tot}}(\alpha_1, \alpha_2, \gamma) = \lambda \hat{X}_{\lambda, i}, \quad \forall e \in M, \quad (265)$$

as subspaces $\mathcal{A}_\lambda \subset \mathcal{B}(\mathcal{H}_{SE})$ of the Hilbert-space $\mathcal{B}(\mathcal{H}_{SE})$ of linear operators w.r.t. the total S-E-Hilbert space $\mathcal{H}_{SE} = \mathcal{H}_S \otimes \mathcal{H}_E$ for the eigenvalues λ (with $|\lambda| = 1$) [11, 30].

- For a known attractor space we get from an initial state $\hat{\rho}_{SE}^{\text{in}}$ the resulting S-E-state spanned by $\hat{X}_{\lambda, i}$

$$\hat{\rho}_{SE}(N \gg 1) = \mathcal{P}_{\text{Tot}}^N(\hat{\rho}_{SE}^{\text{in}}) = \sum_{|\lambda|=1, i=1}^{d_{n \geq k}^\lambda} \lambda^N \text{Tr} \left\{ \hat{\rho}_{SE}^{\text{in}} \hat{X}_{\lambda, i}^\dagger \right\} \hat{X}_{\lambda, i}, \quad (266)$$

where $d_{n \geq k}^\lambda$ denotes the dimensionality of the attractor space w.r.t. the eigenvalue λ .

10.1 Pure decoherence, dissipation and dephasing in Zurek's model of Quantum Darwinism

Let us first consider the following cases for Zurek's QD-model (s. section 7):

I) Zurek's QD-model, case $\alpha_1 \neq \alpha_2 > 0, \gamma = 0$ (asymmetric dissipation): This parameter choice generalizes the analysis of the dissipative QD-model in section 9 and [32]. Setting without loss of generality $\alpha_1 = 2\pi/3$ and $\alpha_2 = \pi/3$

in (166)-(167) and (258)-(266) we obtain from Zurek's evolution, for $L = n = 2$ and $\hat{\rho}_{SE}^{in}$ in (12), in the standard computational basis

$$\begin{aligned} |\Psi_{SE, L=n=2}^{out}\rangle &= (A + B + C)^n (|\Psi_S^{in}\rangle \otimes |0_n\rangle) = -\frac{a}{2} |0\rangle |01\rangle \\ &+ a \left[\frac{3}{4} |0\rangle + i \frac{\sqrt{3}}{4} |1\rangle \right] |00\rangle + b \left[i \frac{\sqrt{3}}{2} |0\rangle - \frac{1}{2} |1\rangle \right] |10\rangle \\ |\Psi_{SE, L=n=2}^{out(R)}\rangle &= \hat{U}_{ij}^{(\alpha_1, \alpha_2, \gamma)} \hat{U}_{ij}^{(\phi=\pi/2)} (|\Psi_S^{in}\rangle \otimes |0_n\rangle) \\ &= (A_R + B_R + C_R + D_R)^n (|\Psi_S^{in}\rangle \otimes |0_n\rangle) \\ &= \left[\frac{3}{4} a + i \frac{\sqrt{3}}{4} b \right] |0\rangle |00\rangle + \left[-\frac{1}{4} a + i \frac{\sqrt{3}}{4} b \right] |0\rangle |10\rangle \\ &+ \left[-\frac{1}{4} b + i \frac{\sqrt{3}}{4} a \right] |1\rangle |01\rangle + \left[\frac{3}{4} b + i \frac{\sqrt{3}}{4} a \right] |1\rangle |11\rangle, \end{aligned} \quad (267)$$

where $A = (\sqrt{3}/2) |0\rangle_i \langle 0| \otimes |0\rangle_j \langle 0| = A_R$, $B = i |0\rangle_i \langle 1| \otimes |1\rangle_j \langle 0|$, $C = 0.5i |1\rangle_i \langle 0| \otimes |1\rangle_j \langle 0| = C_R$, $B_R = 0.5i |0\rangle_i \langle 1| \otimes |0\rangle_j \langle 0|$ and $D_R = (\sqrt{3}/2) |1\rangle_i \langle 1| \otimes |1\rangle_j \langle 1|$ for $i \in \{1\}$ and $j \in \{1, \dots, n\}$ (the same also holds $\forall n \geq 2$, s. Appendix L). Both $|\Psi_{SE, L=n=2}^{out}\rangle$ and $|\Psi_{SE, L=n=2}^{out(R)}\rangle$ in (267) lead to $H(S) = -\sum_{i=1}^2 \lambda_i \log_2 \lambda_i < H(S_{class})$ (for $0 < \lambda_i < 1$) with eigenvalue pairs

$$\lambda_{1/2} = \frac{1}{2} \pm \frac{1}{8} \sqrt{\frac{(3|a|^2 + 4|b|^2)^2 + 4|a|^2}{\neq 16(|a|^2 - |b|^2)^2}}$$

and

$$\lambda_1^R = \frac{10}{16} |a|^2 + \frac{6}{16} |b|^2 + \frac{2i\sqrt{3}}{16} (a^*b - ab^*), \quad \lambda_2^R = \frac{10}{16} |b|^2 + \frac{6}{16} |a|^2 - \frac{2i\sqrt{3}}{16} (a^*b - ab^*),$$

respectively, violating the QD-criteria from section 4. Nevertheless, the order of $\hat{U}_{ij}^{(\alpha_1, \alpha_2)} = \hat{U}_{ij}^{(\alpha_1, \alpha_2, \gamma=0)}$ and $\hat{U}_{ij}^{(\phi=\pi/2)}$ does matter within Zurek's qubit model (s. also section 9), since the value of $H(S)$ changes when exchanging the order of the dissipative and the CNOT-part in (260). However, from the point of view of QD, it is irrelevant within Zurek's qubit model in which order one applies $\hat{U}_{ij}^{(\alpha_1, \alpha_2, \gamma=0)}$ and $\hat{U}_{ij}^{(\phi=\pi/2)}$ in (260) if $\alpha_1 \neq \alpha_2 > 0$ (QD always disappears in this case).

II) Zurek's QD-model, case $\alpha_1 = \alpha_2 = 0$, $\gamma \neq 0$ (pure dephasing): Without loss of generality we set $\gamma = \pi$ (maximal dephasing rate). Then, applying (260) to $\hat{\rho}_{SE}^{in}$ in (12) in accord with Zurek's qubit model of QD, we obtain $\forall (0 < L \leq n)$

$$\begin{aligned} |\Psi_{SE, L=n}^{out}\rangle &= \hat{U}_{ij}^{Tot}(\gamma = \pi) (|\Psi_S^{in}\rangle \otimes |0_n\rangle) = (-i)^n (a |0\rangle |0_n\rangle + (-1)^n b |1\rangle |1_n\rangle) \\ |\Psi_{SE, L=n}^{out(R)}\rangle &= \hat{U}_{ij}(\gamma = \pi) \hat{U}_{ij}^{(\phi=\pi/2)} (|\Psi_S^{in}\rangle \otimes |0_n\rangle) = (-i)^n (a |0\rangle |0_n\rangle + b |1\rangle |1_n\rangle), \end{aligned} \quad (268)$$

showing that the order of the dephasing and the CNOT-operator in (260) does not matter within Zurek's QD-model, since $\hat{U}_{ij}^{(\gamma=\pi)}$ only changes the phase of $\hat{\rho}_{SE}^{out}$: both $|\Psi_{SE, L=n}^{out}\rangle$ and $|\Psi_{SE, L=n}^{out(R)}\rangle$ in (268) lead to QD with a PIP and $I(S : E_L) / H(S_{class})$ as in (12) and Fig. 1.

III) Zurek's QD-model, case $\alpha_1 = \alpha_2 = \pi/2$, $\gamma = \pi$ (maximal dissipation and dephasing): For this parameter choice (260), applied to $\hat{\rho}_{SE}^{in}$ in (12) in accord with Zurek's qubit model of QD, yields

$$|\Psi_{SE, L=n}^{out}\rangle = (-i)^n (a |0\rangle |0_n\rangle - ib |0\rangle |10_{n-1}\rangle), \quad (269)$$

i.e. QD disappears, regardless of how one exchanges the dissipative and dephasing operators in \hat{U}_{ij}^{Tot} , whereas exchanging the order of the dissipative-dephasing part and $\hat{U}_{ij}^{(\phi=\pi/2)}$ in \hat{U}_{ij}^{Tot} yields within Zurek's QD-model

$$|\Psi_{SE, L=n}^{out(R)}\rangle = \hat{U}_{ij}^{Tot(R)}(\alpha_1, \alpha_2, \gamma) (|\Psi_S^{in}\rangle \otimes |0_n\rangle) = (-i)^n (a |0\rangle |0_n\rangle + b |1\rangle |1_n\rangle), \quad (270)$$

i.e. QD appears, regardless of how one exchanges the dissipative and dephasing operators among each other. This is expected, since $\alpha_1 = \alpha_2 = \pi/2$ corresponds to the symmetric dissipative operator studied in section 9 and [32].

Finally, even if we choose non-zero γ -values with $\gamma \neq \pi$, we would conclude that dephasing does not influence the dynamics of $\hat{\rho}_{SE}^{in}$ in Zurek's qubit model: for instance, after setting $\alpha_1 = \alpha_2 = \gamma = \pi/2$ we see that (260), applied to $\hat{\rho}_{SE}^{in}$ in (12) in accord with Zurek's qubit model of QD, yields

$$|\Psi_{SE, L=n}^{out}\rangle = \frac{(1-i)^n}{2^{n/2}} (a |0\rangle |0_n\rangle - b |0\rangle |1_n\rangle), \quad (271)$$

with $\hat{\rho}_S^{\text{out}} = |0\rangle\langle 0|$ and $H(S) = H(S_{\text{class}}) = 0$ (no QD). On the other hand, exchanging the order of the dissipative-dephasing part and $\hat{U}_{ij}^{(\phi=\pi/2)}$ in $\hat{U}_{ij}^{\text{Tot}}$ yields within Zurek's QD-model

$$\left| \Psi_{SE=L=n}^{\text{out(R)}} \right\rangle = \hat{U}_{ij}^{\text{Tot(R)}} (\alpha_1 = \alpha_2 = \gamma = \pi/2) (|\Psi_S^{\text{in}}\rangle \otimes |0_n\rangle) = \frac{(1-i)^n}{2^{n/2}} (a|0\rangle|0_n\rangle + b|1\rangle|1_n\rangle), \quad (272)$$

i.e. QD appears. Apparently, since dephasing only alters the global phase of $\hat{\rho}_{SE}^{\text{out}}$, it does not influence the dynamics of open systems in the course of Zurek's qubit model.

10.2 Numerical reconstruction of the dissipative-dephased attractor space

We concentrate again on the following cases, this time however within the framework of the random unitary evolution model:

I) RUO QD-model, case $\alpha_1 \neq \alpha_2 > 0$, $\gamma = 0$ (asymmetric dissipation): We set, without loss of generality, $\alpha_1 = 2\pi/3 \neq \alpha_2 = \pi/3$: for this parameter choice (260) has eigenvalues $\lambda_{1/2} = \pm 1$ and $\lambda_{3/4} = 0.43 \pm i \cdot 0.9$ and we see that (260), applied to $\hat{\rho}_{SE}^{\text{in}}$ in (12) in accord with (166)-(168), leads $\forall (\alpha_1 \neq \alpha_2 > 0)$ to the PIP in Fig. 38 below (with $n = 8$, $k = 1$ and for different N -values).

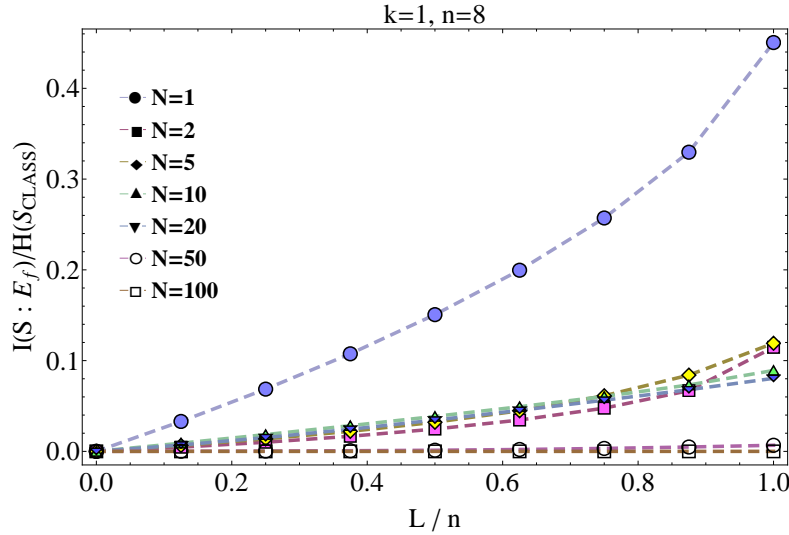


Figure 38: PIP of MI w.r.t. $0 < f = L/n \leq 1$ and different N -values for a $k = 1$ qubit pure $\hat{\rho}_S^{\text{in}}$, $\hat{\rho}_E^{\text{in}} = |0_{n=8}\rangle\langle 0_{n=8}|$ and $\hat{\rho}_{SE}^{\text{in}} = \hat{\rho}_S^{\text{in}} \otimes \hat{\rho}_E^{\text{in}}$ from (12), with $|a|^2 = |b|^2 = 2^{-1} \forall i \in \{0, 1\}$ and $H(S_{\text{class}}) = 1$, evolving iteratively by (166)-(167) and (258)-(264) (where $\alpha_1 = 2\pi/3 \neq \alpha_2 = \pi/3$, $\gamma = 0$).

The same PIP emerges $\forall (\alpha_1 \neq \alpha_2 > 0)$ in the limit $N \gg 1$ if one starts the random unitary evolution with $\hat{\rho}_{SE}^{\text{in}}$ from (12), whose $\hat{\rho}_S^{\text{in}}$ represents a pure, $k > 1$ qubit input-system S : we again see that $I(S : E_L) = 0 \forall (0 \leq L \leq n)$. When looking at the corresponding output state

$$\hat{\rho}_{SE}^{\text{out}} = 2^{-(k+n)} \cdot \hat{I}_{k+n} \quad (273)$$

from Fig. 38 for $n \gg k \geq 1$, we are tempted to conclude, by means of (266), that the attractor space capable of reproducing (273) should be associated with the eigenvalue $\{\lambda = 1\}$ of \hat{U}_e^{Tot} ($\alpha_1 = 2\pi/3 = 2\alpha_2$, $\gamma = 0$) from (260) and display the structure

$$\hat{\chi}_{\lambda=1, i=1} = 2^{-(k+n)/2} \cdot \hat{I}_{k+n}, \quad (274)$$

i.e. $d_{n \gg k}^{\lambda=1} = 1$ (dimensionality one). This would imply that asymmetric dissipation yields completely mixed S-E-output states (274) with

$$H(S, E_L) = H(S) + H(E_L) = H(S_{\text{class}}) + L = k + L \forall (0 \leq L \leq n), \quad (275)$$

implying indeed $I(S : E_L) = 0 \forall (0 \leq L \leq n)$, as suggested by Fig. 38. We will confirm (274) analytically in subsection 10.3, however, before doing that we want to mention another interesting issue: starting the random unitary evolution of $\hat{\rho}_{SE}^{\text{in}}$ from Fig. 38 with one of the two dissipative parameters set to zero, for instance with $\alpha_1 = 2\pi/3 \neq \alpha_2 = 0 = \gamma$, we would obtain a PIP in Fig. 39 below, which is similar to the PIP in Fig. 38.

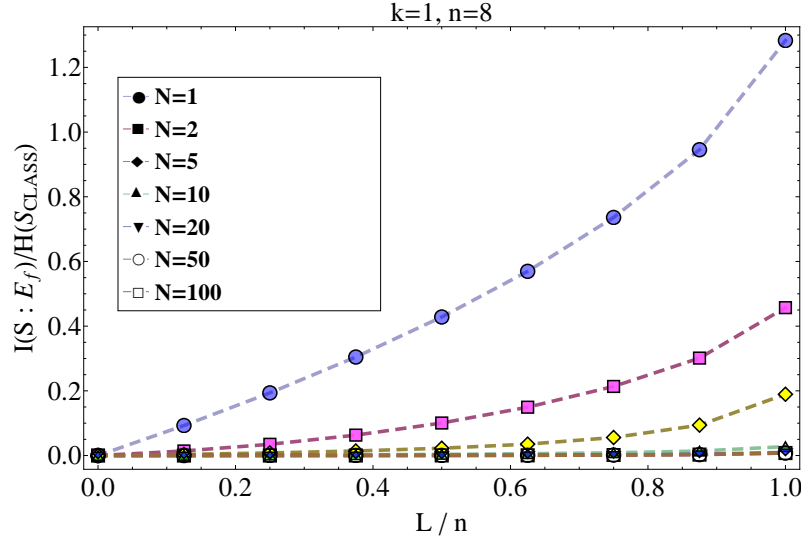


Figure 39: PIP of MI w.r.t. $0 < f = L/n \leq 1$ and different N -values for a $k = 1$ qubit pure $\hat{\rho}_S^{\text{in}}, \hat{\rho}_E^{\text{in}} = |0_{n=8}\rangle \langle 0_{n=8}|$ and $\hat{\rho}_{SE}^{\text{in}} = \hat{\rho}_S^{\text{in}} \otimes \hat{\rho}_E^{\text{in}}$ from (12), with $|a|^2 = |b|^2 = 2^{-1} \forall i \in \{0, 1\}$ and $H(S_{\text{class}}) = 1$, evolving iteratively by (166)-(167) and (258)-(264) (where $\alpha_1 = 2\pi/3 \neq \alpha_2 = 0 = \gamma$).

Certainly, there are differences between Fig. 38 and Fig. 39, especially when it comes to small N -values (i.e. $N = 1, 2, 5$): since $\alpha_1 = 2\pi/3 \neq \alpha_2 = 0 = \gamma$ means that \hat{U}_e^{Tot} contains less dissipative contributions than in the case $\alpha_1 = 2\pi/3 \neq \alpha_2 = \pi/3$, it is to be expected that the PIP in Fig. 39 allows us to store a higher amount of $H(S_{\text{class}})$ into E for $L = n$ and small N -values than the PIP in Fig. 38. Nevertheless, in the asymptotic limit $N \gg 1$, and this is the most significant conclusion, both PIPs in Fig. 38 and Fig. 39 tend to zero $\forall 0 \leq L \leq n$. This means that for $N \gg 1$ already the fact that at least one of the dissipative parameters does not vanish suffices to obtain completely mixed S-E-output states such as (273) and the corresponding $\{\lambda = 1\}$ attractor subspace (274) (which we assume to be the only eigenvalue subspace $\mathcal{A}_{\lambda=1}$ of non-zero dimension contributing to the entire attractor space \mathcal{A} in (171) above). On the other hand, we also may point out that Fig. 38 and Fig. 39 indicate the negative impact which asymmetric dissipation has on QD, since asymmetric values of α_1 and α_2 diminish in general the dimensionality of the $\{\lambda = 1\}$ attractor subspace (245) emerging from a symmetric ($\alpha_1 = \alpha_2 = \alpha$) dissipative random unitary evolution discussed in section 8 above, which in turn enables us to store a higher amount of $H(S_{\text{class}})$ in the limit $N \gg 1$ (namely $0.3 \cdot H(S_{\text{class}})$ according to the \bullet -dotted curve in Fig. 34) if we symmetrize the dissipative contributions in \hat{U}_e^{Tot} of (260), instead of setting $\alpha_1 \neq \alpha_2$ (which leads to $\lim_{N \gg 1} I(S : E_{L=n}) = 0$, as indicated by Fig. 38 and Fig. 39).

All above conclusions for this parameter choice in the limit $N \gg 1$ remain unchanged if we exchange the order of $\hat{U}_{ij}^{(\phi=\pi/2)}$ and $\hat{U}_{ij}^{(\alpha_1=2\pi/3=2\alpha_2, \gamma=0)}$ in (260), as was the case for the completely symmetric ($\alpha_1 = \alpha_2 = \alpha$) dissipative random unitary evolution discussed in section 8 above (s. Fig. 36).

II) RUO QD-model, case $\alpha_1 = \alpha_2 = 0, \gamma \neq 0$ (pure dephasing): We set, without loss of generality, $\alpha_1 = \alpha_2 = 0 \neq \gamma = \pi$: for this parameter choice (260) has eigenvalues $\lambda_{1/2} = \pm 1$ and $\lambda_{3/4} = \pm i$ and we see that (260), applied to $\hat{\rho}_{SE}^{\text{in}}$ in (12) in accord with (166)-(168), leads $\forall \gamma > 0$ to the PIP in Fig. 15 (with $n = 9, k = 1$ and for different N -values). In other words, the attractor space structure of the maximal attractor space associated with pure decoherence (s. (380)-(381) in Appendix H.2.2) remains unchanged if we add dephasing to the random unitary evolution of section 8. Indeed, when looking at the eigenspectrum of \hat{U}_e^{Tot} for this specific parameter choice, we may anticipate that eigenvalues $\lambda_{1/2} = \pm 1$ are precisely associated with the corresponding attractor subspaces (380)-(381) from Appendix H.2.2 (pure decoherence), whereas the attractor subspaces associated with eigenvalues $\lambda_{3/4} = \pm i$ of \hat{U}_e^{Tot} ($\alpha_1 = \alpha_2 = 0 \neq \gamma = \pi$) may be assumed to be zero-dimensional $\forall \gamma > 0$ and thus not contribute to the entire attractor space \mathcal{A} from (171) above. This is reasonable, since $\hat{U}_e^{(\gamma)}$ in \hat{U}_e^{Tot} of (260) would only iteratively change the phase in certain addends of the corresponding output state $\hat{\rho}_{SE}^{\text{out}}$, which should, however, not influence the asymptotic $N \gg 1$ evolution behavior of $\hat{\rho}_{SE}^{\text{in}}$ and its attractor space. We will confirm these assumptions analytically in the forthcoming subsection 10.3.

Also, all above conclusions for this parameter choice in the limit $N \gg 1$ remain unchanged if we exchange the order of $\hat{U}_{ij}^{(\phi=\pi/2)}$ and $\hat{U}_{ij}^{(\alpha_1=\alpha_2=0, \gamma \neq 0)}$ in (260).

III) RUO QD-model, case $\alpha_1 = \alpha_2 = \pi/2, \gamma = \pi$ (maximal dissipation and dephasing): Taking the above results

into account we may expect that the presence of dephasing should not affect the results of the random unitary evolution w.r.t. the symmetric dissipation obtained in [32]. Indeed, if we set, without loss of generality, $\alpha_1 = \alpha_2 = \pi/2 = \gamma/2$, then for this parameter choice (260) has eigenvalues $\lambda_{1/2} = \pm i$ and $\lambda_{3/4} = -\exp[\pm i \cdot \pi/6]$ and we see that (260), applied to $\hat{\rho}_{SE}^{\text{in}}$ in (12) in accord with (166)-(168), leads $\forall(\alpha, \gamma > 0)$ to the PIP in Fig. 40 below (with $n = 8$, $k = 1$ and for different N -values).

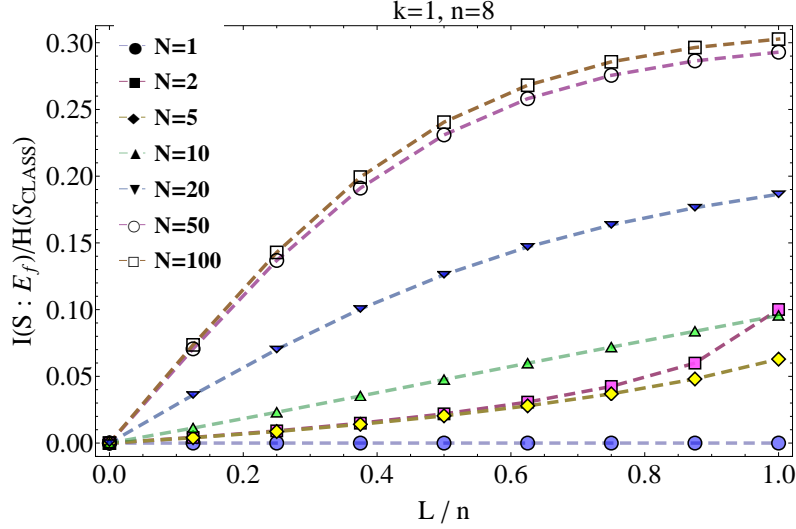


Figure 40: PIP of MI w.r.t. $0 < f = L/n \leq 1$ and different N -values for a $k = 1$ qubit pure $\hat{\rho}_S^{\text{in}}, \hat{\rho}_E^{\text{in}} = |0_{n=8}\rangle \langle 0_{n=8}|$ and $\hat{\rho}_{SE}^{\text{in}} = \hat{\rho}_S^{\text{in}} \otimes \hat{\rho}_E^{\text{in}}$ from (12), with $|a|^2 = |b|^2 = 2^{-1} \forall i \in \{0, 1\}$ and $H(S_{\text{class}}) = 1$, evolving iteratively by (166)-(167) and (258)-(264) (where $\alpha_1 = \alpha_2 = \pi/2 = \gamma/2$).

The PIP in Fig. 40 coincides in the limit $N \gg 1$ exactly with the \bullet -dotted curve of the PIP in Fig. 34 obtained with respect to the dissipative attractor space in section 8 above. Apparently, the dephasing part in $\hat{U}_e^{\text{Tot}} (\alpha_1 = \alpha_2 = \pi/2 = \gamma/2)$ of (260) does not change the asymptotic (long time) behavior of the MI. By looking at the corresponding output state $\hat{\rho}_{SE}^{\text{out}}$ emerging from Fig. 40 in the limit $N \gg 1$ of the random unitary evolution, we see that it is exactly the same as (245) from section 8 (s. also [32]). Also, all above conclusions for this parameter choice in the limit $N \gg 1$ remain unchanged if we exchange the order of $\hat{U}_{ij}^{(\phi=\pi/2)}$ and $\hat{U}_{ij}^{(\alpha_1=\alpha_2 \neq 0, \gamma \neq 0)}$ in (260) $\forall \alpha, \gamma > 0$.

This leads us to the conclusion that dephasing does not influence the (dis-)appearance of QD. On the contrary, QD appears to depend in $\hat{U}_e^{\text{Tot}} (\alpha_1 = \alpha_2 = \pi/2 = \gamma/2)$ of (260) only on the interplay between the dissipative and the pure decoherence part: in other words, in the random unitary model QD appears only if in \hat{U}_e^{Tot} of (260) we have $\alpha_1 = \alpha_2 = 0 \leq \gamma$, otherwise the MI-'plateau' remains suppressed as soon as $\alpha_1 \neq 0, \alpha_2 \neq 0$ or $(\alpha_1, \alpha_2) \neq 0$, regardless of the order, in which the CNOT, dissipative and the dephasing part in \hat{U}_e^{Tot} of (260) are applied to a given input state $\hat{\rho}_{SE}^{\text{in}}$. In the framework of Zurek's qubit model we, however, have to be cautious: it is certainly true that $\hat{U}_e^{\text{Tot}} (\alpha_1 = \alpha_2 = 0 \leq \gamma)$ would always lead to QD, regardless of the order, in which the CNOT and the dephasing part in \hat{U}_e^{Tot} of (260) are applied to a given input state $\hat{\rho}_{SE}^{\text{in}}$; on the other hand, in Zurek's qubit model the order in which the CNOT and the dissipative part in \hat{U}_e^{Tot} of (260) are applied to a given input state $\hat{\rho}_{SE}^{\text{in}}$ does matter for $\alpha_1 = \alpha_2 = \alpha$, which is why $\hat{U}_e^{\text{Tot}} (\alpha_1, \alpha_2, \gamma)$ and $\hat{U}_e^{\text{Tot(R)}} (\alpha_1, \alpha_2, \gamma) = \hat{U}_{ij}^{(\alpha_1, \alpha_2, \gamma)} \hat{U}_{ij}^{(\phi=\pi/2)}$ for (at least one) non vanishing dissipative parameter (i.e. $\alpha_1 \neq 0$ or $\alpha_2 \neq 0$ or $(\alpha_1, \alpha_2) \neq 0$) would not lead to QD, whereas $\hat{U}_e^{\text{Tot(R)}} (\alpha_1 = \alpha_2 = \alpha, \gamma)$ from (263) would allow us to see the MI-'plateau'.

We will confirm the above conclusions regarding the random unitary iterative dynamics analytically in the forthcoming subsection 10.3.

10.3 Analytic reconstruction of the dissipative-dephased attractor space

Applying the QR-decomposition method from Appendix G to (265) we obtain the following attractor spaces:

I) RUO QD-model, case $\alpha_1 \neq \alpha_2 > 0, \gamma = 0$ (asymmetric dissipation): After solving the eigenvalue equation (265) for $\lambda = 1$ and $n \geq k \geq 1$ by means of the QR-decomposition method, we obtain $\forall(\alpha_1 \neq \alpha_2) > 0$ the pre-configuration matrix

$$\hat{X}_{\lambda=1} = \boxtimes \cdot \hat{I}_{k+n} \quad (276)$$

(with $\boxtimes = \text{const}$), whereas for eigenvalues $\lambda \neq 1$ of \hat{U}_e^{Tot} from (260) the eigenvalue equation (265) and the QR-decomposition method yield vanishing attractor subspaces, i.e. $d_{n \geq k}^{\lambda \neq 1} = 0$. From (276) we see that the corresponding attractor subspace is one dimensional, $d_{n \geq k}^{\lambda=1} = 1$, with the single attractor state being

$$\hat{X}_{\lambda=1, i=1} = 2^{-(k+n)/2} \cdot \hat{f}_{k+n}. \quad (277)$$

Indeed, by means of (277) and (266) we are able to exactly reproduce the output state (273), which confirms our assumption (274) about the $\{\lambda = 1\}$ -attractor space structure from subsection 10.2, derived w.r.t. the parameter choice $\alpha_1 = 2\pi/3 = 2\alpha_2 \neq \gamma = 0$.

II) RUO QD-model, case $\alpha_1 = \alpha_2 = 0, \gamma \neq 0$ (pure dephasing): Without any loss of generality we again concentrate on \hat{U}_e^{Tot} with $\alpha_1 = \alpha_2 = 0 \neq \gamma = \pi$ and its eigenvalues $\lambda_{1/2} = \pm 1$ and $\lambda_{3/4} = \pm i$. After solving the eigenvalue equation (265) for $\lambda = \pm 1$ and $n \geq k \geq 1$ by means of the QR-decomposition method, we obtain $\forall \gamma \geq 0$ the dimensionally maximal attractor subspaces (380)-(381) from Appendix H.2.2 (pure decoherence), whereas the QR-decomposition enables us to conclude that (265) for $\lambda = \pm i$ and $n \geq k \geq 1$ yields zero-dimensional attractor subspaces, i.e. $d_{n \geq k}^{\lambda=\pm i} = 0$. This is clear if we recall that the eigenvalue equation (265) establishes relations (constraints) between (in general complex-valued) entries of the pre-configuration matrix of the type

$$a + ib = c + id, \quad (278)$$

with $a, b, c, d \in \mathbb{R}$. For instance, for $\lambda = \pm 1$ (265) would require that $a = c$ and $b = d$ should hold. W.r.t. $\lambda = \pm i$ (278) would acquire an additional phase factor when compared with the case $\lambda = \pm 1$, leading to the general constraint

$$a + ib = (\pm i)(a + ib), \quad (279)$$

as a modified version of (278) weighted by an additional phase factor i . Unfortunately, (279) has only one solution, namely the trivial one: $a = -a \Rightarrow a = 0 = b \forall \gamma \geq 0$ and for all entries of the pre-configuration matrix. This leads to the trivial solution

$$\hat{X}_{\lambda=\pm i} = \hat{0}_{2^{k+n} \times 2^{k+n}} \quad (280)$$

of (265) w.r.t. $\lambda = \pm i$ and $\forall \gamma \geq 0$, indicating that the dimensionality of $\{\lambda = \pm i\}$ -attractor subspaces is indeed zero. In other words, the dissipative part of \hat{U}_e^{Tot} from (260) does not contribute to the entire attractor space \mathcal{A} . This confirms conclusions of subsection 10.2.

III) RUO QD-model, case $\alpha_1 = \alpha_2 = \pi/2, \gamma = \pi$ (maximal dissipation and dephasing): For $\alpha_1 = \alpha_2 = \pi/2 = \gamma/2$ (260) has eigenvalues $\lambda_{1/2} = \pm i$ and $\lambda_{3/4} = -\exp[\pm i \cdot \pi/6]$ and we see that w.r.t. $\lambda_{1/2} = \pm i$ the eigenvalue equation (265) yields zero-dimensional attractor subspaces (as expected, since the dissipative part of \hat{U}_e^{Tot} from (260) does not contribute to the entire attractor space \mathcal{A}). On the other hand, the QRdecomposition reveals that the only attractor subspace of non-zero dimension for the above parameter choice with symmetric dissipation ($\alpha_1 = \alpha_2 = \alpha > 0$) is the $\{\lambda = 1\}$ -attractor subspace (251), despite of $\gamma > 0$ [32].

All these facts indicate that even w.r.t. \hat{U}_e^{Tot} ($\alpha_1 = \alpha_2 = \pi/2 = \gamma/2$) from (260) only contributions from the $\{\lambda = 1\}$ -attractor subspace (251) would persist in (264) in the limit $N \gg 1$, which would in turn explain the fact that the PIP in Fig. 40 exactly coincides with the \bullet -dotted curve of the PIP in Fig. 34 in the limit $N \gg 1$. Thus, we may conclude that within the random unitary model dephasing does not influence the (dis-)appearance of QD¹⁷, whereas symmetric and asymmetric dissipation, the latter in an even more drastic manner, suppress the MI-'plateau' in the asymptotic evolution limit $N \gg 1$, regardless of the order in which pure decoherence (CNOT), dissipation and dephasing within \hat{U}_e^{Tot} of (260) are applied to a given input state $\hat{\rho}_{SE}^{\text{in}}$ in accord with the iteration procedure (264).

In a similar fashion \hat{U}_e^{Tot} ($\alpha_1 \neq \alpha_2, \gamma \geq 0$) from (260) would lead in (266) only to the one-dimensional $\{\lambda = 1\}$ -attractor subspace (277) $\forall \gamma \geq 0$.

10.4 Summary and outlook

Results obtained in this section lead us to the following conclusions: the order of application of $\hat{U}_{ij}^{(\phi=\pi/2)}$ and $\hat{U}_{ij}^{(\alpha_1, \alpha_2, \gamma)}$ in (260) is relevant for the appearance of QD in Zurek's qubit model if $\alpha_1 = \alpha_2 = \alpha$. Otherwise, for $\alpha_1 \neq \alpha_2 > 0$ QD does not appear in Zurek's qubit model, regardless of the order in which one applies $\hat{U}_{ij}^{(\phi=\pi/2)}$ and $\hat{U}_{ij}^{(\alpha_1, \alpha_2, \gamma)}$ in (260). Only for $(\alpha_1 = \alpha_2 = 0, \gamma > 0)$ QD appears within Zurek's qubit model regardless of how one interchanges $\hat{U}_{ij}^{(\phi=\pi/2)}$ and $\hat{U}_{ij}^{(\gamma)}$ in (260) among each other.

¹⁷In other words, we may say that in the limit $N \gg 1$ of the random unitary model dephasing is, if present, being »averaged out« in the course of subsequent iterations.

We see that $\forall (\alpha_1 \neq \alpha_2) > 0, \gamma = 0$ (asymmetric dissipation) the $\{\lambda = 1\}$ attractor space is one dimensional ($d_{n \gg k}^{\lambda=1} = 1$), with the only attractor state

$$\hat{X}_{\lambda=1, i=1} = 2^{-(k+n)/2} \cdot \hat{I}_{k+n},$$

leading, for instance after random unitarily evolving Zurek's input state configuration $\hat{\rho}_{SE}^{\text{in}} = \hat{\rho}_S^{\text{in}} \otimes \hat{\rho}_E^{\text{in}}$ (with a $k \geq 1$ qubit pure $\hat{\rho}_S^{\text{in}}$ and $\hat{\rho}_E^{\text{in}} = |0_n\rangle \langle 0_n|$), to a completely mixed output state

$$\hat{\rho}_{SE}^{\text{out}} = 2^{-(k+n)} \cdot \hat{I}_{k+n},$$

with $I(S : E_L) = 0 \forall (0 \leq L \leq n)$. The same attractor space structure appears also if we set only one of the dissipative parameters to zero, i.e. $\alpha_1 = 0 \neq \alpha_2$ or $\alpha_2 = 0 \neq \alpha_1$ lead to the same attractor state $\hat{X}_{\lambda=1, i=1}$, whereas the dimensionality of attractor subspaces associated with the remaining three eigenvalues of $\hat{U}_e^{\text{Tot}}(\alpha_1, \alpha_2, \gamma = 0)$ is zero ($d_{n \gg k}^{\lambda \neq 1} = 0$) $\forall (\alpha_1, \alpha_2)$ as long as $\alpha_1 = \alpha_2 = 0$ does not hold.

In the random unitary evolution model $\hat{U}_{ij}^{(\gamma)}$ does not contribute to the structure of the attractor spaces emerging from the iterative application of pure decoherence $\hat{U}_{ij}^{(\phi=\pi/2)}$ or of the dissipative operation from (238). In other words, the attractor space obtained from (260) for $\alpha_1 = \alpha_2 = 0 \neq \gamma$ is always zero-dimensional for all corresponding eigenvalues of $\hat{U}_e^{\text{Tot}}(\alpha_1 = \alpha_2 = 0 \neq \gamma)$. This means that the (dis-)appearance of QD in the limit $N \gg 1$ of the random unitary model depends only on the interplay between the dissipative and the CNOT-part of \hat{U}_e^{Tot} in (260). The order of application of $\hat{U}_{ij}^{(\phi=\pi/2)}$ and $\hat{U}_{ij}^{(\alpha_1, \alpha_2, \gamma)}$ in (260) is irrelevant for the (dis-)appearance of QD in the limit $N \gg 1$ of the random unitary model. QD appears only for $\alpha_1 = \alpha_2 = 0 \leq \gamma$.

Since Quantum Darwinism appears for $N, n \gg k \geq 1$ only if

$$\begin{aligned} H(S) &\approx H(S_{\text{class}}) \wedge H(E_L) \geq H(S, E_L) \\ &\Leftrightarrow I(S : E_L) / H(S_{\text{class}}) \geq 1 \end{aligned}$$

holds $\forall k \leq L \leq n$, regardless of the order in which the n E-qubits are being successively traced out from the output state $\hat{\rho}_{SE}^{\text{out}}$ [5, 30] (s. also (155) above), we see that for all $\{(\alpha_1, \alpha_2, \gamma) \in \mathbb{R}\} \setminus \{\alpha_1 = \alpha_2 = 0\}$ (i.e. for $\hat{U}_e^{\text{Tot}} \neq \hat{U}_e^{(\phi=\pi/2)} \hat{U}_e^{(\gamma)}$) there is no $\hat{\rho}_{SE}^{\text{in}}$ within the dissipative-dephased random unitary model that leads to Quantum Darwinism. In Zurek's qubit-model, however, the (dis-)appearance of Quantum Darwinism depends on the order of application of $\hat{U}_{ij}^{(\phi=\pi/2)}$ and $\hat{U}_{ij}(\alpha_1 = \alpha_2 = \alpha, \gamma)$ in (260) $\forall \gamma \geq 0$.

11 Conclusions and outlook

The discussion of Quantum Darwinism (QD) from previous sections has shown that in the course of Zurek's qubit model the QD-condition (155) remains valid only if one starts the CNOT-evolution with a product input state $\hat{\rho}_{SE}^{\text{in}} = \hat{\rho}_S^{\text{in}} \otimes \hat{\rho}_E^{\text{in}}$, where $\hat{\rho}_S^{\text{in}}$ stands for the k -qubit pure input state of open system S and $\hat{\rho}_E^{\text{in}} = |y\rangle \langle y|$ represents a one-rank pure, n -qubit environmental registry state with $y \in \{0, \dots, 2^n - 1\}$, or with $\hat{\rho}_{SE}^{\text{in}}$ given by the entangled input state from Eq. (158), however only for $k = 1$ S-qubit. If one introduces dissipation into the model, then the order in which one applies the CNOT-operator and the dissipative operator (symmetric dissipation) from (237) in section 9 to a given input S-E-state $\hat{\rho}_{SE}^{\text{in}}$ is essential for the (dis-)appearance of QD. Namely, if symmetric dissipation acts upon $\hat{\rho}_{SE}^{\text{in}}$ before the CNOT-operator, QD definitely disappears in Zurek's evolution model. Certainly, in case of asymmetric dissipation QD disappears in Zurek's model, regardless of the order in which one applies the CNOT and the dissipative operation. On the other hand, the dephasing operator from (258) in section 10 does not influence the (dis-)appearance of QD in Zurek's qubit model, neither when coupled with pure decoherence, nor when added to the CNOT-evolution affected by dissipation: the (dis-)appearance of QD remains determined significantly by the interplay between the CNOT-operator and the dissipative operator even when dephasing is present. Thus, in the framework of Zurek's qubit model of QD dephasing does not significantly influence the dynamics of quantum systems.

In the random unitary model the situation is different: QD appears only in case of pure decoherence (CNOT-evolution) and only if one starts the CNOT-evolution with $\hat{\rho}_{SE}^{\text{in}} = \hat{\rho}_S^{\text{in}} \otimes \hat{\rho}_E^{\text{in}}$, where $\hat{\rho}_S^{\text{in}}$ stands for the $k = 1$ -qubit pure input state of open system S and $\hat{\rho}_E^{\text{in}} = |y\rangle \langle y|$ represents a one-rank pure, n -qubit E-registry state with $y \in \{0, \dots, 2^n - 1\}$, or with $\hat{\rho}_{SE}^{\text{in}}$ given by the entangled input state from Eq. (158), again with $k = 1$ S-qubit (completely controlled environments). Thus, w.r.t. pure decoherence, random unitary evolution seems to single out the $k = 1$ qubit pure input state of system S as the only input state which allows us to store system's Shannon-information into a qubit environment E efficiently by utilizing the process of effective decoherence (qudit-cell conjecture). As soon as one introduces dissipation into random unitary dynamics, QD disappears, regardless of the order in which one applies the CNOT-operator and the dissipative operator.

Finally, after introducing dephasing into the random unitary dynamics we see that within random unitary evolution model dephasing does not alter or influence the (dis-)appearance of Quantum Darwinism: i.e. the random unitary evolution governed by the unitary transformation enclosing pure decoherence (CNOT transformation), dissipation and dephasing is solely determined by the interplay between pure decoherence and dissipation, whereas the dephasing part of the random unitary evolution does not contribute to the corresponding attractor space of the asymptotic random unitary iteration.

Outlook

As a future possible research-project, it is interesting to test the qudit-cell conjecture in the course of the random unitary model by applying an appropriate qudit (2^k -level system) generalization of the one parameter transformation $\hat{U}_{ij}^{(\Phi)}$ from (9)-(10) and the generalized qudit-version of the CNOT-transformation from (11) [27, 28] to non-interacting environmental qudit-cells. Certainly, we can address all issues regarding pure decoherence, dissipation and dephasing within Zurek's and the random unitary model of QD (with mutually non-interacting or interacting E-constituents), which have been discussed (or mentioned) so far, from the point of view of the qudit-version of (11) and thus try to confirm the reasonable qudit-cell conjecture from section 8 when it comes to the appearance of QD.

However, even more interesting and involving appears a question whether QD emerges if one assumes that the two-qubit Kraus-operators appearing in (168) are non-unitary. In other words, one could ask what happens with the evolution of a certain physical input state subject to the unital quantum operation channel

$$\mathcal{P}_m(\bullet) \equiv \sum_{i=1}^m \sum_{e \in M} p_e \mathcal{K}_e^{(i)}(\bullet) \mathcal{K}_e^{(i)\dagger} \quad (281)$$

of an ID with a k -qubit S , an n -qubit E and interaction-edges $e \in M$, if the corresponding m Kraus-operators $\mathcal{K}_e^{(i)}$ w.r.t. a given edge e are non-unitary, with $\sum_i \underbrace{\mathcal{K}_e^{(i)\dagger} \mathcal{K}_e^{(i)}}_{\neq 1} = \sum_i \underbrace{\mathcal{K}_e^{(i)} \mathcal{K}_e^{(i)\dagger}}_{\neq 1} = 1$.

This would allow us to start the iteration (281) with non-unitary $\mathcal{K}_e^{(i)}$ and an input state $\hat{\rho}_{SE}^{\text{in}} = \hat{\rho}_S^{\text{in}} \otimes \hat{\rho}_E^{\text{in}}$, where $\hat{\rho}_S^{\text{in}}$ represents a $k = 1$ qubit pure system S and $\hat{\rho}_E^{\text{in}}$ stands, for example, for the ground state E with $\hat{\rho}_E^{\text{in}} = |0_n\rangle\langle 0_n|$ comprising n mutually non-interacting qubits. Then we could investigate for instance what happens with the output state $\hat{\rho}_{SE}^{\text{out}}$ after $N \gg 1$ iterations of (281). Is there a fixed point output state w.r.t. the Hilbert-Schmidt norm, i.e. $\lim_{N \gg 1} \|\hat{\rho}_{SE}^{\text{out}}(N) - \hat{\rho}_{SE}^{\text{out}}(N-1)\|_{\text{HS}} = 0$? Does the attractor space exist at all, at least within a certain finite interval of N -iterations? What happens with MI and QD w.r.t. f ? Finally, does a finite iteration number $1 \leq N = N_{\text{min}} < \infty$ exist, w.r.t. a fixed δ -value, for which $\hat{\rho}_{SE}^{\text{out}}(N = N_{\text{min}}) = \hat{\rho}_{SE}^{\text{out}}(N = 0) = \hat{\rho}_S^{\text{in}} \otimes \hat{\rho}_E^{\text{in}}$? However, these questions are beyond the scope of this book and serve only as an illustration of many possibilities for extending the random unitary operations model to non-unitary Kraus-operators and investigating their influence on efficient storage and transfer of Shannon-information about an open system S into its environment E .

Part III

Appendices

A On basis dependence of MI w.r.t. basis changes in Eq. (13)

In this Appendix we discuss basis dependence of MI w.r.t. basis changes in Eq. (13).

We can transform a certain QD-conformal density matrix structure of (13) to the other QD-conformal density matrix structure formulated w.r.t. another S-pointer basis $\{|\pi'_i\rangle\} \neq \{|\pi_i\rangle\} \equiv \{|0\rangle, |1\rangle\}$ (s. (13)) by directly deducing the dependence of the S-states $|\varphi'_i\rangle \in \{|\pi'_i\rangle\}$ on $|\varphi_i\rangle \in \{|\pi_i\rangle\}$ in (13) from $\hat{U}_{\text{int}}^{\text{SE}}$ in (7), where usually

$$\hat{U}_S = \bigotimes_{s=1}^k \hat{u}_s, \quad (282)$$

with a unitary one-qubit transformation \hat{u}_s acting on each S-qubit $|\chi\rangle \in \{|0\rangle, |1\rangle\}$ of (13) to yield $(\alpha_s, \beta_s \in \mathbb{C} \setminus \{0\})$, with $\alpha_s^* \beta_s \stackrel{!}{=} \alpha_s \beta_s^* \Leftrightarrow \alpha_s = c_s \cdot \beta_s$, $c_s \in \mathbb{R}$ and $c_s^2 = |\alpha_s|^2 \cdot |\beta_s|^{-2} \leq 1$, ergo $-1 \leq c_s = \pm |\alpha_s| \cdot |\beta_s|^{-1} \leq 1$

$$\hat{u}_s |\chi\rangle = |\chi'\rangle = (\alpha_s \delta_{\chi,0} + \beta_s \delta_{\chi,1}) |0\rangle + (\beta_s \delta_{\chi,0} - \alpha_s \delta_{\chi,1}) |1\rangle, \quad |\alpha_s|^2 + |\beta_s|^2 \stackrel{!}{=} 1. \quad (283)$$

(282) and (283) enable us to decompose each $|\varphi'_i\rangle = \hat{U}_S |\varphi_i\rangle \in \{|\pi'_i\rangle\}$ w.r.t. $|\varphi_i\rangle \in \{|\pi_i\rangle\}$, $i \in \{1, \dots, 2^k\}$ and vice versa: inserting $|\varphi_i\rangle = \hat{U}_S^\dagger |\varphi'_i\rangle$ into (13) will lead to the QD-conformal $\hat{\rho}_{\text{SE}}^{\text{out}}$ w.r.t. another $\{|\pi'_i\rangle\}$. In general, we need not organize \hat{U}_S in accord with (282)-(283) and may apply to $\hat{\rho}_{\text{SE}_{L=n}}^{\text{out}}$, given w.r.t. $\{|\pi_i\rangle\}$,

$$\hat{U}_{\text{int}}^{\text{SE}} = \hat{U}_S \otimes \hat{U}_E, \quad (284)$$

without changing the value of $I(S : E_L) / H(S_{\text{class}})$ by simply assuming a general unitary (not necessarily tensor product) form of \hat{U}_S , whereas \hat{U}_E would nevertheless have to be

$$\hat{U}_E = \bigotimes_{e=1}^n \hat{u}_e \quad (285)$$

with \hat{u}_e as in (283) if $I(S : E_L) / H(S_{\text{class}})$ is to remain unchanged after transforming $\hat{\rho}_{\text{SE}_{L=n}}^{\text{out}}$ and tracing out parts of E. Thus, after transforming for instance $\hat{\rho}_{\text{SE}_{L=n}}^{\text{out}}$ in (12) for $k=1$ and $L=n=2$ by (284)-(285), we see that

$$|\hat{\rho}_{S'E'_{L=n=2}}^{\text{out}}\rangle = \hat{U}_{\text{int}}^{\text{SE}} |\hat{\rho}_{\text{SE}_{L=n=2}}^{\text{out}}\rangle = a |0'_{S'(1)}\rangle \otimes |0'_{E'(1)}\rangle \otimes |0'_{E'(2)}\rangle + b |1'_{S'(1)}\rangle \otimes |1'_{E'(1)}\rangle \otimes |1'_{E'(2)}\rangle \quad (286)$$

(with $\hat{u}_K |\chi_K\rangle = |\chi'_{K'}\rangle$ and $\alpha_{K'} = c_{K'} \cdot \beta_{K'}$, $-1 \leq (c_{K'} = \pm |\alpha_{K'}| \cdot |\beta_{K'}|^{-1} \in \mathbb{R}) \leq 1$ as in (283), $K' \in \{S'(s), E'(e)\}$, $K \in \{S(s), E(e)\}$ $s \in \{1, \dots, k\}$, $e \in \{1, \dots, n\}$ and $|\chi'\rangle \in \{|0'\rangle, |1'\rangle\}$) leads to $I(S : E_{L=n=2}) = I(S' : E'_{L=n=2})$, with $H(S) = H(S') = H(S_{\text{class}}) \forall (k=1 \leq L \leq n=2)$.

(286) indicates that only applying $\hat{U}_{\text{int}}^{\text{SE}}$ from (284), with an arbitrary unitary \hat{U}_S and \hat{U}_E organized explicitly as in (285), to $\hat{\rho}_{\text{SE}_{L=n}}^{\text{out}}$ ensures unitary-invariance of $I(S : E_{L \leq n})$ w.r.t. $\hat{U}_{\text{int}}^{\text{SE}}$ [15, 16],

$$I(S : E_{L \leq n}) / H(S_{\text{class}}) = I(S' : E'_{L \leq n}) / H(S_{\text{class}}) \forall (0 \leq L \leq n), \quad (287)$$

since in this case we may argue that the eigenvalue spectra of $\hat{\rho}_{\text{SE}_{L \leq n}}^{\text{out}} = \text{Tr}_{E_{n-L}} [\hat{\rho}_{\text{SE}_{L=n}}^{\text{out}}]$ and its reduced density matrices

do not change after performing $\text{Tr}_{E_{n-L}} \left[\left(\hat{U}_{\text{int}}^{\text{SE}} \right) \left(\hat{\rho}_{\text{SE}_{L=n}}^{\text{out}} \right) \left(\hat{U}_{\text{int}}^{\text{SE}} \right)^\dagger \right] := \hat{\rho}_{S'E'_{L \leq n}}^{\text{out}}$ w.r.t. the basis of E, resulting in $H(S) = H(S')$, $H(E_L) = H(E'_L)$ and $H(S, E_L) = H(S', E'_L) \forall (k \leq L \leq n)$ [15, 16]. (286) contains three real-valued parameters $c_{K'}$ associated with the one S-qubit and each of the two E-qubits, transformed by (282)-(285). After tracing out the second E-qubit in (286) w.r.t. $\{|\pi_i\rangle\}$, i.e. for $L=1 < n=2$, we see that (287) holds $\forall [-1 \leq (c_{S'(1)}, c_{E'(1)}) \leq 1]$. Also after setting in (286) $n \gg k=1$ and tracing out $1 < L=m < n-1$ E-qubits (287) holds if we inductively increase $m \rightarrow m+1$ (with $m < L=m+1 \leq n-1$), leading to the PIP of $I(S' : E'_{L \leq n}) / H(S_{\text{class}})$ as in Fig. 1 \forall fixed $(c_{S'(1)}, c_{E'(1)}, \dots, c_{E'(m)})$ and variable $-1 \leq c_{E'(m+1)} \leq 1$.

A change of basis from $\{|\pi_i\rangle\}$ to $\{|\pi'_i\rangle\} \neq \{|\pi_i\rangle\}$ by $\hat{U}_{\text{int}}^{\text{SE}}$ in (284), with an E-part \hat{U}_E from (285), does not alter the value of $I(S : E_{L \leq n}) / H(S_{\text{class}}) \forall (0 < L \leq n \gg k)$. If a given $\hat{\rho}_{\text{SE}_{L \leq n}}^{\text{out}}$ w.r.t. $\{|\pi_i\rangle\}$ leads to QD, then $\hat{\rho}_{S'E'_{L \leq n}}^{\text{out}}$, emerging after unitarily transforming $\hat{\rho}_{\text{SE}_{L=n}}^{\text{out}}$ by (282)-(285), also validates (15) $\forall (k \leq L \leq n)$.

B Matrix realignment method for partial traces of $(\mathbb{C}^M \otimes \mathbb{C}^N)$ -density matrices

In this Appendix we summarize the matrix realignment method for partial traces used extensively in part I of this book.

According to [22] one can perform partial traces of density matrices for $\mathbb{C}^M \otimes \mathbb{C}^N$ composite quantum systems (where $M, N \in \mathbb{N}$) in a following manner: Assume that we start with a $M \times N$ density matrix $\hat{\rho}_{AB}$ of two physical systems A and B. Then one can perform partial traces $\hat{\rho}_B = \text{Tr}_A(\hat{\rho}_{AB})$ and $\hat{\rho}_A = \text{Tr}_B(\hat{\rho}_{AB})$ w.r.t. each of these two subsystems of $\hat{\rho}_{AB}$ by 1) writing $\hat{\rho}_{AB}$ as an $M \times M$ density matrix with $N \times N$ -block entries $A_{mm'}$ ($m, m' \in \{1, \dots, M\}$) acting on \mathbb{C}^N and 2) obtaining $\hat{\rho}_A$ and $\hat{\rho}_B$ by simply tracing out each $N \times N$ -block entry $A_{mm'}$ (»backward tracing«) or summing up all diagonal $N \times N$ -block entries $A_{mm'}\delta_{m,m'} = A_{mm}$ of $\hat{\rho}_{AB}$ (»forward tracing«), namely

$$\hat{\rho}_{AB} = \begin{pmatrix} A_{11} & \cdots & A_{1M} \\ \vdots & \ddots & \vdots \\ A_{M1} & \cdots & A_{MM} \end{pmatrix} \Rightarrow \hat{\rho}_A = \begin{pmatrix} \text{Tr}(A_{11}) & \cdots & \text{Tr}(A_{1M}) \\ \vdots & \ddots & \vdots \\ \text{Tr}(A_{M1}) & \cdots & \text{Tr}(A_{MM}) \end{pmatrix}, \hat{\rho}_B = \sum_{m=1}^M A_{mm}. \quad (288)$$

C QD-conformal matrix structures of $\hat{\rho}_{SE}^{\text{out}}$ for $(k = 1, n = 1)$

In this Appendix we identify basic complex-valued $(2^{k+L} \times 2^{k+L})$ -matrices $\hat{\rho}_{SE}^{\text{out}}(L)$ which adhere to (15).

Let us start with an S-E-output state $\hat{\rho}_{SE}^{\text{out}}(L)$ enclosing an open $k = 1$ qubit $\hat{\rho}_S^{\text{out}}$ and an $L = n = 1$ qubit $\hat{\rho}_E^{\text{out}}(L)$, $(a, e, h, j) \in \mathbb{R}_0^+$:

$$\hat{\rho}_{SE}^{\text{out}}(L = n = 1) = \begin{pmatrix} \begin{bmatrix} a & b \\ b^* & e \end{bmatrix} \\ \begin{bmatrix} c^* & f^* \\ d^* & g^* \end{bmatrix} \end{pmatrix} \begin{bmatrix} c & d \\ f & g \\ h & i \\ i^* & j \end{bmatrix} \Rightarrow \hat{\rho}_S^{\text{out}} \stackrel{!}{=} \begin{pmatrix} A & 0 \\ 0 & B \end{pmatrix}, \hat{\rho}_E^{\text{out}}(L = n = 1) \stackrel{!}{=} \begin{pmatrix} C & 0 \\ 0 & D \end{pmatrix}, \quad (289)$$

where $\hat{\rho}_S^{\text{out}}$ is, due to (15), to be regarded as effectively decohered (quasi-classical), and $H(E_{L=n=1}) = H(\hat{\rho}_E^{\text{out}}(L = n = 1))$ has to be maximized if we are to obtain $H(\hat{\rho}_E^{\text{out}}) \geq H(\hat{\rho}_{SE}^{\text{out}})$. Since each S-subspace of $\hat{\rho}_{SE}^{\text{out}}$ in (289) contains $2^L \times 2^L = 4$ matrix entries referring to the $\{\pi_i\}$ basis of E, we may extract the following conditions on the $\hat{\rho}_{SE}^{\text{out}}$ -entries by applying matrix realignment methods of *backward* and *forward partial traces* outlined in [22] (s. also appendix B) yielding

$$\begin{aligned} \hat{\rho}_E^{\text{out}}(L = n = 1) &= \begin{pmatrix} C & 0 \\ 0 & D \end{pmatrix} := \begin{pmatrix} a & b \\ b^* & e \end{pmatrix} + \begin{pmatrix} h & i \\ i^* & j \end{pmatrix} \text{ (forward tracing)} \\ \hat{\rho}_S^{\text{out}} &= \begin{pmatrix} A & 0 \\ 0 & B \end{pmatrix} := \begin{pmatrix} a+e & c+g \\ c^*+g^* & h+j \end{pmatrix} \text{ (backward tracing),} \end{aligned} \quad (290)$$

with $A := a + e$, $B := h + j$, as well as $b + i := 0$ (or $b + i \approx 0$) and $c + g := 0$ (or $c + g \approx 0$) (with $A + B \stackrel{!}{=} 1$, $C + D \stackrel{!}{=} 1$ and $a + e + h + j \stackrel{!}{=} 1$). Furthermore, $\hat{\rho}_E^{\text{out}}$ in (290) indeed maximizes $H(E_{L=n=1})$, as can be inferred from

$$\hat{\rho}_E^{\text{out}} = \begin{pmatrix} C & \tilde{E} \\ \tilde{E}^* & D \end{pmatrix}, C + D := 1, C \neq 0 \quad (291)$$

which leads (with $D = 1 - C < 1$ and, without loss of generality, $D \leq C$) to the eigenvalues (with $CD - |\tilde{E}|^2 := \det(\hat{\rho}_E^{\text{out}})$)

$$\det(\hat{\rho}_E^{\text{out}} - \lambda \hat{I}_1) \stackrel{!}{=} 0 \Rightarrow \lambda^2 - \lambda + \det(\hat{\rho}_E^{\text{out}}) \Rightarrow \lambda_{1/2} = 1/2 \pm \sqrt{1/4 - \det(\hat{\rho}_E^{\text{out}})} = 1/2 \pm \sqrt{(C - 1/2)^2 + |\tilde{E}|^2}, \quad (292)$$

which can be extremized w.r.t. $|\tilde{E}|^2 = \varepsilon \ll 1 \in \mathbb{R}^+$ by performing a Taylor-expansion to order $\mathcal{O}(\varepsilon^2)$ to yield

$$\lambda_1 \approx \lambda_1^* = C + \varepsilon/2 = C + \varepsilon', \lambda_2 \approx \lambda_2^* = 1 - C - \varepsilon/2 = D - \varepsilon/2 = D - \varepsilon'. \quad (293)$$

Finally, by utilizing formulas [12]

$$\log_2(1+x) = (\ln 2)^{-1} x + \mathcal{O}(\varepsilon^2), \log_2(1-x) = -(\ln 2)^{-1} x + \mathcal{O}(\varepsilon^2) \quad (294)$$

it is possible to verify that $-\lambda_1^* \log_2 \lambda_1^* - \lambda_2^* \log_2 \lambda_2^* < -C \log_2 C - D \log_2 D := H_E^{\varepsilon=0}$ ($0 \geq \tilde{a} := (\varepsilon/2) \log_2(D/C) > -\infty$),

$$-\lambda_1^* \log_2 \lambda_1^* - \lambda_2^* \log_2 \lambda_2^* \approx H_E^{\varepsilon=0} + \tilde{a} = H_E^{\varepsilon=0} - |\tilde{a}| < H_E^{\varepsilon=0}, \quad (295)$$

and since $H_E^{\varepsilon=0}|_{C=D=1/2} = H_E^{\max} = 1$ maximizes $H(E_{L=n=1})$ in (290), we may conclude that only $|\tilde{a}| = 0 \Rightarrow |\tilde{E}|^2 = 0$ implies $H(E_{L=n=1}) = H_E^{\varepsilon=0}$. In (292) we also see that $|\tilde{E}| = \sqrt{CD} = \sqrt{C(1-C)}$ leads to $H(E_{L=n=1}) = 0$, since in this case the eigenvalue spectrum $\lambda_{1/2} = 1/2 \pm 1/2 \Rightarrow \lambda_1 = 1, \lambda_2 = 0$ corresponds to the one of a pure state.

In the following we start with the characteristic polynomial $\det(\hat{\rho}_{SE}^{\text{out}} - \lambda \hat{I}_2) \stackrel{!}{=} 0$ of $\hat{\rho}_{SE}^{\text{out}}$ in (289) and apply the constraints $b + i = 0$ and $c + g = 0$ from (290) to obtain

$$\begin{aligned} &|b|^4 + |c|^4 + [abf - ach - cej + bfj + (-2bf + c)\lambda - 2c\lambda^2]c^* + dfc^{*2} + db^{*2}f^* + (a - \lambda)(j - \lambda) \left[(e - \lambda)(h - \lambda) - |f|^2 \right] \\ &\quad + d^* [b^2f - bc(e + h - 2\lambda) + d(e - \lambda)(-h + \lambda) + (c^2 + df)f^*] \\ &\quad + b^* [b(-ae - hj + \lambda - 2\lambda^2) - (2bc + d(e + h - 2\lambda))c^* + c(a + j - 2\lambda)f^*]. \end{aligned} \quad (296)$$

When looking at (296) we notice the following QD-compliant structures of $\hat{\rho}_{SE}^{\text{out}}$ in (289):

I). Inserting the configuration

$$(e, h) \neq 0 \wedge (f \neq 0 \vee f = 0) \quad (297)$$

into (289), we easily derive the eigenvalue spectrum of $\hat{\rho}_{SE}^{\text{out}}$ (with $h = C$ and $e = D$, as in (289)-(290))

$$\lambda_{1/2} = 0, \lambda_{3/4} = \frac{1}{2} \pm \sqrt{\frac{1}{4} + |f|^2 - he} = \frac{1}{2} \pm \sqrt{\frac{1}{4} + |f|^2 - CD} \Rightarrow \lambda_3 = \begin{cases} C & \text{if } f = 0 \\ 1 & \text{if } |f| = \sqrt{CD} \end{cases}, \lambda_4 = \begin{cases} D & \text{if } f = 0 \\ 0 & \text{if } |f| = \sqrt{CD}. \end{cases} \quad (298)$$

$|f|^2$ in (298) behaves equivalently to $|\tilde{E}|^2$ from (292), indicating that by changing its values within the range $1/4 \geq 1/4 + |f|^2 - CD \geq 0$ (with for example $C = D = 1/2$) we will always validate the QD-condition (15), since within this range of $|f|^2$ -values $H(S) = H(S_{\text{class}}) = -e \log_2 e - h \log_2 h = -A \log_2 A - B \log_2 B$ (with $h = C = A$ and $e = D = B$, as in (289)-(290) above) attains $H(S_{\text{class}})$ (i.e. S is effectively decohered), whereas $H(S, E)$ ranges between $H(S, E) = H(E) = H^{\max}(E) = H(S_{\text{class}}) = 1$ for $f = 0$ and $H(S, E) = 0 < H(E) = H^{\max}(E) = H(S_{\text{class}}) = 1$ for $|f| = \sqrt{CD} = \sqrt{C(1-C)}$. Thus, by increasing $|f|^2$ from 0 to $CD = 1/4$ we also gradually increase the purity of (297).

II). Inserting the configuration

$$(a, j) \neq 0 \wedge (d \neq 0 \vee d = 0) \quad (299)$$

into (289), we are led to the same eigenvalue spectrum if we apply the replacements $e \leftrightarrow a, h \leftrightarrow j$ and $f \leftrightarrow d$. Thus, the configuration (299) of $\hat{\rho}_{SE}^{\text{out}}$ matrix entries is also QD-compliant.

III). Inserting the configuration

$$(a, e, h, j) \neq 0 \wedge b = -i \neq 0 \quad (300)$$

into (289), we obtain the following characteristic polynomial from (296)

$$(a - \lambda)(e - \lambda)(h - \lambda)(j - \lambda) - |b|^2[(a - \lambda)(e - \lambda) + (h - \lambda)(j - \lambda)] + |b|^4 \stackrel{!}{=} 0. \quad (301)$$

Since in (301) $a + h := C$ and $e + j := D$, as indicated by (289)-(290) above, there are three possibilities for fixing the diagonal entries a, e, h and j :

1) We could choose $a = e = h = j := a_C \in \mathbb{R}^+$, which due to (301) necessitates us to insist on $|b| := a_C \in \mathbb{R}^+$, in accord with (15). This shows that only $a_C := 1/4$ suffices to obtain $a + e + h + j \stackrel{!}{=} 1$ and thus leads to the eigenvalues $\{\lambda_{1/2} = 0, \lambda_{3/4} = 1/2\}$ of (300). In this case $a = e = h = j = |b| := a_C \in \mathbb{R}^+$ corresponds to

$$\hat{\rho}_{SE}^{\text{out}}(L = n = 1) = |a_S|^2 |0_k\rangle \langle 0_k| \otimes |s_1^I\rangle \langle s_1^I| + |b_S|^2 |1_k\rangle \langle 1_k| \otimes |s_2^I\rangle \langle s_2^I|, \quad (302)$$

$\hat{\rho}_E^{\text{out}}(L = n = 1) = |a_S|^2 |s_1^I\rangle \langle s_1^I| + |b_S|^2 |s_2^I\rangle \langle s_2^I|$ and $\hat{\rho}_S^{\text{out}} = |a_S|^2 |0_k\rangle \langle 0_k| + |b_S|^2 |1_k\rangle \langle 1_k|$, with S -probability distribution $\{|a_S|^2 = |b_S|^2 = 1/2\}$ and E -states $|s_1^I\rangle = 2^{-L/2}(|0\rangle + |1\rangle)^{\otimes L}$, $|s_2^I\rangle = 2^{-L/2}(|0\rangle - |1\rangle)^{\otimes L}$, $\langle s_1^I | s_2^I \rangle = 0$, which are also invariant under (11)¹⁸. The eigenvalues in (302), $\{\lambda^{SE} | \lambda_{1/2}^{SE} = 0, \lambda_{3/4}^{SE} = 1/2\}$, $\{\lambda^E | \lambda_{1/2}^E = 1/2\}$ and $\{\lambda^S | \lambda_{1/2}^S = 1/2\}$, reveal that, due to $H(S, E_{L=n=1}) = H(E_{L=n=1}) = H(S) = H(S_{\text{class}}) = 1$, (302) validates (15); **2)** Alternatively, (302) suggests that we also may set $|a_S|^2 \neq |b_S|^2 > 0$ (corresponding to $|b|^2 = a \cdot e = h \cdot j \Rightarrow (e = h, a = j)$ or $(a = e, h = j)$, s. (304)-(310)), yielding eigenvalues

$$\lambda_{1/2}^{SE} = (|a_S|^2 \pm |a_S|^2)/2, \lambda_{3/4}^{SE} = (|b_S|^2 \pm |b_S|^2)/2; \lambda_{1/2}^E = 1/2 \pm (|a_S|^2 - |b_S|^2)/2 = 1/2 \pm (|a_S|^2 - 1/2). \quad (303)$$

¹⁸We may use in (302) $\hat{\rho}_{SE}^{\text{out}} = |a_S|^2 |0_k\rangle \langle 0_k| \otimes |s_2^I\rangle \langle s_2^I| + |b_S|^2 |1_k\rangle \langle 1_k| \otimes |s_1^I\rangle \langle s_1^I|$ with »interchanged« $\{|s_1^I\rangle, |s_2^I\rangle\}$ and identical eigenvalues.

But, in this case we deal with S characterized by $H(S) = H(S_{\text{class}}) < 1$ and obtain $H(S, E_{L=n=1}) = H(E_{L=n=1})$, validating (15). Therefore, only the equal S -probability distribution $\{|a_S|^2 = |b_S|^2 = 1/2\}$ leads to QD, enabling us to store $H(S_{\text{class}}) = 1$ into E , whereas $|a_S|^2 \neq |b_S|^2 > 0$ leads to QD with lower storage efficiency $H(S_{\text{class}}) < 1$. To explain (303) we look at what happens if we violate the partial tracing condition $b = -i$ in (290), as in

$$(a, e, h, j) \neq 0 \wedge (b \neq -i) \neq 0, \quad (304)$$

which modifies (300)-(302) as in (303) and yields, only by setting (with $2a + 2h \stackrel{!}{=} 1$) $a = e = b \neq h$ and $h = j = -i$, eigenvalues $\{\lambda_{1/2} = h \pm h, \lambda_{3/4} = a \pm a\}$ (for $\hat{\rho}_{SE}^{\text{out}}$) and $\{\lambda_{1/2} = 1/2 \pm \sqrt{1/4 - 4ah} = 1/2 \pm 2(h - 1/4)\}$ (for $\hat{\rho}_E^{\text{out}}$) that validate (15); **3)** Changing in (302) the weightings within $|s_1^L\rangle$ and $|s_2^L\rangle$ as $|s_{c_1}^L\rangle = (c_1|0\rangle + c_2|1\rangle)^{\otimes L}$ and $|s_{c_2}^L\rangle = (c_1|0\rangle - c_2|1\rangle)^{\otimes L}$, where $\langle s_{c_1}^L | s_{c_2}^L \rangle = 0$, $c_1^2 + c_2^2 \stackrel{!}{=} 1$ and $c_1 = \cos(\phi/2) \neq c_2 = \sin(\phi/2)$ ($0 \leq \phi \leq \pi$) demonstrates that QD appears only if

$$c_1^2 = c_2^2 = 1/2, \quad (305)$$

that maximizes $H(E_{L=n=1})$. Since (9)-(11) implies that $\{|0\rangle, |1\rangle\}$ will be the preferred (pointer) S -basis, we will maximize the storage capacity of E only if we use the CNOT-invariant states $\{|s_1^L\rangle, |s_2^L\rangle\}$ in (302) with (305), otherwise $c_1^2 \neq c_2^2$ will prevent us from seeing the QD-'plateau'.

IV). Since we know from (302) that solely the requirements $\{|a_S|^2 = |b_S|^2 = 1/2\}$ and (305) lead in (302) to the appearance of the most $H(S_{\text{class}})$ -storage efficient QD, we may insert the configuration

$$(a, e, h, j, b) \neq 0 \wedge (c = -g, f, d) \neq 0 \quad (306)$$

into (289) (with $a = e = h = j = b = (a_C \in \mathbb{R}^+) = 1/4$) and obtain the following characteristic polynomial from (296)

$$[a_C(2c + d - f - 2\lambda) - (d - \lambda)(f + \lambda) - c][a_C(2c + d - f + 2\lambda) + -(d + \lambda)(f - \lambda) + c] \stackrel{!}{=} 0. \quad (307)$$

Now, (307) indicates that there is only one way to fix the entries c, f and d such that QD appears: either $c = f = d = 0$ (s. also (304)-(310)), which leads us back to (302), or one chooses $f = c = a_C := 1/4$, in which case one inevitably has $d = -a_C := -1/4$. Thus, the configuration

$$\{a = e = h = j = b = f = c = a_C := 1/4 \wedge d = -a_C := -1/4\} \quad (308)$$

(or its equivalent version with $f \leftrightarrow d$) generates the pure state

$$\hat{\rho}_{SE}^{\text{out}}(L = n = 1) = 2^{-1} \{|\psi\rangle \langle \psi|\} \Rightarrow \lambda^3(\lambda - 4a_C) = \lambda^3(\lambda - 1) \stackrel{!}{=} 0 \quad (309)$$

(with $|\psi\rangle := (|x\rangle \otimes |s_1^L\rangle + |y\rangle \otimes |s_2^L\rangle)(1 - \delta_{x,y})$, $x, y \in \{0_k, 1_k\}$ and $\{|s_1^L\rangle, |s_2^L\rangle\}$ as in (302)). On the other hand, since $\{|s_1^L\rangle, |s_2^L\rangle\}$ from (302) are mutually orthogonal, $\hat{\rho}_{SE}^{\text{out}}$ and $\hat{\rho}_E^{\text{out}}$ will be effectively decohered, s. (302), implying $H(S, E) = 0$, $H(S) = H(E) = H(S_{\text{class}}) = 1 \Rightarrow I(S : E)/H(S_{\text{class}}) = 1 + 1 - 0 = 2$ (»quantum peak«).

Alluding to (304), we generalize (309) as w.r.t. the $(|a_S|^2 \neq |b_S|^2 > 0)$ -generalization (303) of (300)-(302) by

$$\hat{\rho}_{SE}^{\text{out}}(L = n = 1) = \{|\tilde{\psi}\rangle \langle \tilde{\psi}|\} \quad (310)$$

(with $|\tilde{\psi}\rangle := (a_S|x\rangle \otimes |s_1^L\rangle + b_S|y\rangle \otimes |s_2^L\rangle)(1 - \delta_{x,y})$, $a_S \neq (b_S \neq 0)$, $x, y \in \{0_k, 1_k\}$ and $\{|s_1^L\rangle, |s_2^L\rangle\}$ as in (302)), which corresponds to the configuration $(a, e, h, j) \neq 0 \wedge (c \neq -g) \neq 0 \wedge (b \neq -i) \neq 0$ of (289), would also validate (15).

V). Inserting the configuration

$$(a, e, h, j) \neq 0 \wedge (c = -g) \neq 0 \quad (311)$$

into (289), we obtain from (296) the following characteristic polynomials of $\hat{\rho}_{SE}^{\text{out}}$, $\hat{\rho}_E^{\text{out}}$ and $\hat{\rho}_S^{\text{out}}$

$$\hat{\rho}_{SE}^{\text{out}} : \left[(a - \lambda)(h - \lambda) - |c|^2 \right] \left[(e - \lambda)(j - \lambda) - |c|^2 \right] \stackrel{!}{=} 0 \Rightarrow \lambda_{1/2} = (a + h)/2 \pm \sqrt{D_1}, \lambda_{3/4} = (e + j)/2 \pm \sqrt{D_2} \quad (312)$$

$$D_1 := (a + h)^2/4 + |c|^2 - a \cdot h; \quad D_2 = D_1 (a \leftrightarrow e, h \leftrightarrow j); \quad \hat{\rho}_E^{\text{out}} : \{a + h, e + j\}; \quad \hat{\rho}_S^{\text{out}} : \{a + e, h + j\}.$$

(312) shows that $H(S) = H(S_{\text{class}}) = -(a + e) \log_2(a + e) - (h + j) \log_2(h + j)$, whereas $H(E) = -(a + h) \log_2(a + h) - (e + j) \log_2(e + j)$. Thus, $H(E)$ in (312) could never exceed $H(S, E)$ were there no outer-diagonal terms c and $-c$ in $\hat{\rho}_{SE}^{\text{out}}$, since the diagonal entries a and h and e and j , respectively, »merge« (are added) in $\hat{\rho}_E^{\text{out}}$, leading automatically to a decrement of $H(E)$.

The characteristic polynomial of $\hat{\rho}_{SE}^{\text{out}}$ in (312) suggests that $H(S, E_{L=n=1}) = H(E_{L=n=1})$ if

$$|c|^2 = a \cdot h = e \cdot j. \quad (313)$$

Additionally, the two entries c in (312) have to (at least approximately) cancell each other when tracing out $\hat{\rho}_E^{\text{out}}$ from $\hat{\rho}_{SE}^{\text{out}}$ in (312) (s. appendix B), otherwise $H(S)$ would decrease, annullating the decoherence of S , i.e. (311) validates (15) only if we apply to it (313). Indeed, for

$$(a, e, h, j) \neq 0 \wedge (c \neq -g) \neq 0 \quad (314)$$

we have to demand $|c|^2 = a \cdot h$ and $|g|^2 = e \cdot j$ to obtain $H(S, E) = H(E)$. However, since we assume in general $c \neq -g$, one would obtain a not effectively decohered $\hat{\rho}_{SE}^{\text{out}}$, meaning $H(S) < H(S_{\text{class}})$ (no QD). Only if $c + g \approx 0$, (314) would approximately correspond to the QD-conformal (312).

VI. Inserting the configuration

$$(a, e, h, j) \neq 0 \wedge (d, f) \neq 0 \quad (315)$$

into (289), we obtain the characteristic polynomials of $\hat{\rho}_{SE}^{\text{out}}$, $\hat{\rho}_E^{\text{out}}$ and $\hat{\rho}_S^{\text{out}}$ from (296)

$$\begin{aligned} \hat{\rho}_{SE}^{\text{out}} : \left[(a - \lambda)(j - \lambda) - |d|^2 \right] \left[(e - \lambda)(h - \lambda) - |f|^2 \right] \stackrel{!}{=} 0 &\Rightarrow \lambda_{1/2} = (a + j)/2 \pm \sqrt{D_1}, \lambda_{3/4} = (e + h)/2 \pm \sqrt{D_2} \\ D_1 := (a + j)^2/4 + |d|^2 - a \cdot j; D_2 = D_1 (a \leftrightarrow e, j \leftrightarrow h); \hat{\rho}_E^{\text{out}} : \{a + h, e + j\}; \hat{\rho}_S^{\text{out}} : \{a + e, h + j\}, \end{aligned} \quad (316)$$

which validate (15) only if we demand

$$\left. \begin{aligned} |d|^2 &= a \cdot j \\ |f|^2 &= e \cdot h \end{aligned} \right\} \Rightarrow \lambda_{1/2} = (a + j)/2 \pm (a + j)/2, \lambda_{3/4} = (e + h)/2 \pm (e + h)/2 \Rightarrow h \stackrel{!}{=} j, \quad (317)$$

for $\hat{\rho}_{SE}^{\text{out}}$ in (316)

without being forced to explicitly assume that $d + f \stackrel{!}{=} 0$, as in (312). On the contrary, since $d \in \mathbb{C} \setminus \{0\}$ and $f \in \mathbb{C} \setminus \{0\}$ occupy in (316) matrix entries of $\hat{\rho}_{SE}^{\text{out}}$ along the secondary diagonal, they do not contribute to the structure of outer-diagonal matrix entries in $\hat{\rho}_S^{\text{out}}$ that would influence the decoherence process of S . Therefore, in (316) we may choose

$$d = \pm f \text{ or } d \neq f. \quad (318)$$

In other words, as long as (317) remains valid, (315) and (318) will lead to QD. Finally, we also notice: **1)** the characteristic polynomials in (316) coincide with those in (312), since the structure of a characteristic polynomial remains the same if one aligns diagonal entries from outer-diagonal S -subspaces of $\hat{\rho}_{SE}^{\text{out}}$ (such as c and $-c$ in (312)) along its secondary diagonal (as done with d and f in (316)) [23, 24]; **2)** as in (312) and (316), c and $-c$, as well as d and f , »connect« diagonal entries of $\hat{\rho}_{SE}^{\text{out}}$ and thus lead to the decrement of $H(S, E)$ ¹⁹. Indeed, varying $\lambda_{1/2}$ and $\lambda_{3/4}$ in (312) and (316) within $(a + h)^2/4 \geq D_1 \geq 0$ and $(e + j)^2/4 \geq D_2 \geq 0$ shows that only (313) and (317)-(318) validate (15); **3)** Setting one or more diagonal entries in (312) and (316) to zero, the entries $(c, -c)$ or (d, f) , which connect the vanishing diagonal entries with other (non-vanishing) diagonal entries, also have to disappear, to avoid non-physical $\hat{\rho}_{SE}^{\text{out}}$. Setting for example $e = 0$ and $f \neq 0$, $\lambda_{1/2}$ and $\lambda_{3/4}$ in (316) and (317) yield QD-constraints

$$j^2/4 \stackrel{!}{=} D_1 = j^2/4 + |f|^2 \Rightarrow |f|^2 \stackrel{!}{=} 0 (?!); \wedge (a + j)^2/4 \stackrel{!}{=} (a + j)^2/4 + |d|^2 - a \cdot j \Rightarrow |d|^2 - a \cdot j \stackrel{!}{=} 0 \quad (319)$$

that always lead to a contradiction and non-physical $\hat{\rho}_{SE}^{\text{out}}$ w.r.t. $|f|^2$. Only by adopting conditions (313) and (317)-(319) one would validate (15). Now we consider $\hat{\rho}_{SE}^{\text{out}}$ in (289) with $(a, e, h, j) \neq 0$ which do not necessarily lead to QD:

VII. We can interpret the configuration

$$(a, e, h, j) \neq 0 \wedge (b = -i, c = -g) \neq 0 \quad (320)$$

as an extension of (300)-(303), supplemented by additional $c \neq 0$. Accordingly, we may ask (without any loss of generality) whether it is possible to find an appropriate »extension« of (300)-(303) different from the one displayed in (306)-(309) that would validate (15). Inserting (320) with $(a = e = h = j = b = a_C := 1/4) \wedge c \neq 0$ into (289), yields the characteristic $\hat{\rho}_{SE}^{\text{out}}$ -polynomial $(|c|^2 - \lambda^2) (|c|^2 - (\lambda - 2a_C)^2) \stackrel{!}{=} 0$, with a non-physical eigenvalue $\lambda_1 = -|c|$.

¹⁹»Connect« means that c occupies the $\hat{\rho}_{SE}^{\text{out}}$ -entry in (312) given as an intersection of the row containing a and the column containing h , whereas $-c$ marks the intersection of the row containing e and the column containing j , i.e. c and d in (316) »connect« a and j and e and h , respectively.

VIII). Similarly, we may view the configuration

$$(a, e, h, j) \neq 0 \wedge (c = -g, f, d) \neq 0 \quad (321)$$

as (306)-(309) without the outer-diagonal b-entries. Thus, without loss of generality, inserting (321) with $a = e = |A|^2/2 \neq 0$, $h = j = |B|^2/2$ and $c = d = f$ into (289) yields from (296) the characteristic polynomial

$$(\lambda^2 - \lambda/2 + |A|^2|B|^2/4 - 2|c|^2)^2 \stackrel{!}{=} 0 \Rightarrow \lambda_{1/2} = 1/4 \pm \sqrt{1/16 + 2|c|^2 - |A|^2|B|^2/4} \text{ (each 2 times)}, \quad (322)$$

whose eigenvalues collide with those in (312) and (316) (according to which $|c|^2 \stackrel{!}{=} |A|^2|B|^2/4$, leading in (322) always to potentially negative eigenvalues). Only if one would set $|c|^2 \stackrel{!}{=} |A|^2|B|^2/8$ in (322) in order to ensure the real valence of eigenvalues, one obtains $H(S, E) = H(E) = -2 \cdot (1/2) \log_2(1/2) = 1 \forall |A|^2 \neq 0$. Otherwise, insisting on $c \neq (d = f)$ reproduces solely (312) or (316) as the only reasonable QD-compliant physical $\hat{\rho}_{SE}^{\text{out}}$.

IX). Inserting the configuration

$$(a, e, h, j) \neq 0 \wedge (c = -g, d) \neq 0 \quad (323)$$

into (289), we obtain the characteristic polynomial of $\hat{\rho}_{SE}^{\text{out}}$ from (296)

$$[(a - \lambda)(h - \lambda) - |c|^2] [(e - \lambda)(j - \lambda) - |c|^2] - |d|^2(e - \lambda)(h - \lambda) \stackrel{!}{=} 0, \quad (324)$$

which supplements (312) with additional terms (monomials) associated with d. Taking (312)-(313) and (316)-(317) into account, we insert QD-compliant identities

$$|d|^2 = a \cdot j, h \stackrel{!}{=} j, |c|^2 = a \cdot h = e \cdot j \Rightarrow |d|^2 = |c|^2 = a \cdot j \Rightarrow a = e \quad (325)$$

into (324) and obtain the characteristic polynomial

$$(a - \lambda)(j - \lambda) [(a - \lambda)(j - \lambda) - 3|c|^2] + |c|^4 \stackrel{!}{=} 0 \quad (326)$$

which yields positive eigenvalues only for $|c|^2 = 0$. If $|c|^2 \neq 0$ in (326) would lead in general to complex-valued eigenvalues. Therefore, (323) represents a non-physical $\hat{\rho}_{SE}^{\text{out}}$. Due to symmetry arguments [23, 24] the same holds for

$$(a, e, h, j) \neq 0 \wedge (c = -g, f) \neq 0, \quad (327)$$

whose characteristic polynomial emerges from (326) after replacing $d \leftrightarrow f$.

For four non-vanishing diagonal entries of $\hat{\rho}_{SE}^{\text{out}}$ from (289) only (312) and (316) adhere to (15) for $L = n = k = 1$.

Now we consider $\hat{\rho}_{SE}^{\text{out}}$ in (289) with $(a, h, j) \neq 0$, violating the partial tracing conditions $b = -i$ and $c = -g$ in (290):

X). (304)-(314) show that QD-compliant $\hat{\rho}_{SE}^{\text{out}}$ can be obtained by imposing certain conditions on non-zero outer-diagonal entries. The reason why we need to deal with $\hat{\rho}_{SE}^{\text{out}}$ containing three non-zero diagonal entries follows from

$$(a, e, h, j) \neq 0 \wedge c \neq (-g = 0). \quad (328)$$

Inserting (328) into (289), we obtain $\hat{\rho}_{SE}^{\text{out}}$ -eigenvalues $\left\{ \lambda_1 = e, \lambda_2 = j; \lambda_{3/4} = (a + h)/2 \pm \sqrt{(a + h)^2/4 + |c|^2 - a \cdot h} \right\}$ that ensure $H(S, E) = H(E)$ only if $|c|^2 = a \cdot h$ and $(e = 0 \text{ or } j = 0)$, whereas $|c|^2 \approx 0$ yields $H(S) \approx H(S_{\text{class}})$, as in (15). On the other hand, choosing

$$(a, e, h, j) \neq 0 \wedge (c, f) \neq (-g = 0) \quad (329)$$

in (289) would also violate (15), since the diagonal entry j would remain completely »unconnected«, leading for example for $a = e = h = j := a_C = 1/4$ and $|c|^2 = |f|^2 = a_C^2 \ll 1$ to non-physical $\hat{\rho}_{SE}^{\text{out}}$ with eigenvalues $\left\{ \lambda_{1/2} = a, \lambda_{3/4} = a \pm \sqrt{2}a \right\}$. Setting, without loss of generality, $|c|^2 = |f|^2 = a_C^2/2 \ll 1$ yields real $\hat{\rho}_{SE}^{\text{out}}$ -eigenvalues $\left\{ \lambda_{1/2} = a, \lambda_{3/4} = a \pm a \right\}$, but we always obtain $H(S, E) > H(E)$ w.r.t. the $\hat{\rho}_{SE}^{\text{out}}$ -eigenvalues $\left\{ \lambda_{1/2} = 2a \right\}$. Fortunately, by fixing $a = e, h \neq 0, j = 0$ (or $a = e = h, j = 0$ as a special case) one could in principle validate (15), however only with $|c|^2 = |f|^2 = e \cdot h/2 = a \cdot h/2$ (colliding with constraints in (312) and (316)). Thus, we can extract the following $\hat{\rho}_{SE}^{\text{out}}$ with $(a, h, j) \neq 0$ that could validate (15):

XI). The configuration

$$(a, h, j) \neq 0 \wedge c \neq (-g = 0) \quad (330)$$

emerges from (328) after setting $e = 0$. Accordingly, the non-zero eigenvalues of $\hat{\rho}_{SE}^{\text{out}}$ are the same as in (328), whereas $\hat{\rho}_E^{\text{out}} = \text{diag}[a + h, j]$. Therefore, $H(E) = H(S, E)$ and $H(S) \approx H(S_{\text{class}})$, approximately validating (15) only if the following relations hold (s. also (311)-(312))

$$|c|^2 = a \cdot h, |c|^2 \approx 0. \quad (331)$$

XII). The configuration

$$(a, h, j) \neq 0 \wedge d \neq 0 \quad (332)$$

may be viewed as (299) extended by a non-vanishing diagonal entry h , or as (315)-(317) with $e = f = 0$. Therefore, $\hat{\rho}_S^{\text{out}} = \text{diag}[a, h + j]$ remains effectively decohered and the eigenvalues

$$\lambda_1^{SE} = h$$

$$\lambda_{2/3}^{SE} = (a + j) / 2 \pm \sqrt{(a + j)^2 / 4 + |d|^2 - a \cdot j}$$

of $\hat{\rho}_{SE}^{\text{out}}$ equal the eigenvalues of $\hat{\rho}_E^{\text{out}} = \text{diag}[a + h, j]$ only if we demand, as in (315)-(317),

$$|d|^2 = a \cdot j, h = j. \quad (333)$$

XIII). The configuration

$$(a, h, j) \neq 0 \wedge (c, d) \neq 0 \wedge (c \neq -g = 0) \quad (334)$$

displays the following ($k = 1, n = 1$)-structure of $\hat{\rho}_{SE}^{\text{out}}, \hat{\rho}_E^{\text{out}}$ and $\hat{\rho}_S^{\text{out}}$ (with $\mathbf{A}_0 = \text{diag}[a, 0], \mathbf{A}_1 = \text{diag}[h, j]$)

$$\hat{\rho}_{SE}^{\text{out}} = \begin{pmatrix} \mathbf{A}_0 & B_0 \\ B_0^\dagger & \mathbf{A}_1 \end{pmatrix}, B_0 = \begin{bmatrix} c & d \\ 0 & 0 \end{bmatrix}, \hat{\rho}_E^{\text{out}} = \text{diag}[a + h, j], \hat{\rho}_S^{\text{out}} = \begin{pmatrix} a & c \\ c^* & h + j \end{pmatrix}, \quad (335)$$

with $a + h + j \stackrel{!}{=} 1$. The characteristic polynomial of $\hat{\rho}_{SE}^{\text{out}}$ in (335), as a combination of (311) and (315), is

$$|c|^2 \lambda (j - \lambda) + |d|^2 \lambda (h - \lambda) - \lambda (a - \lambda) (h - \lambda) (j - \lambda) \stackrel{!}{=} 0, \quad (336)$$

which can lead to equal eigenvalues of $\hat{\rho}_{SE}^{\text{out}}$ and $\hat{\rho}_E^{\text{out}}$ only if $c = d$ and $j = h = \tilde{h}/2$, with

$$\lambda (\tilde{h}/2 - \lambda) [(\lambda - \lambda_1) (\lambda - \lambda_2)] \stackrel{!}{=} 0 \Rightarrow \lambda_{1/2} = (a + \tilde{h}/2) / 2 \pm \sqrt{(a + \tilde{h}/2)^2 / 4 + 2|c|^2 - a\tilde{h}/2}, \quad (337)$$

that adheres to (15) only if we demand that c should obey (313) and behave as

$$|c|^2 \stackrel{!}{=} 4^{-1} a \tilde{h} \approx 0. \quad (338)$$

There is no way to extend (334)-(337) in a QD-compliant manner: introducing $e \neq 0$ into (337) yields $H(S, E) > H(E)$, since e and j in $\hat{\rho}_{SE}^{\text{out}}$ would overlap when building $\hat{\rho}_E^{\text{out}}$ in (335). Introducing beside $e \neq 0$ also f into (334) as in

$$(a, e, h, j) \neq 0 \wedge (c, d, f) \neq 0 \wedge (c \neq -g = 0) \quad (339)$$

and simultaneously insisting on $c = d$, (338) and $j = h = \tilde{h}/2$, leads to the characteristic polynomial

$$(a - \lambda) (\tilde{h}/2 - \lambda) \left[(e - \lambda) (\tilde{h}/2 - \lambda) - |f|^2 \right] - |c|^2 \left[2(e - \lambda) (\tilde{h}/2 - \lambda) - |f|^2 \right], \quad (340)$$

yielding complex-valued eigenvalues. From (340) we even see that $|c|^2 \stackrel{!}{=} |f|^2 \neq 0$ always leads to contradictions $2(e - \lambda) (\tilde{h}/2 - \lambda) \stackrel{!}{=} |c|^2 \stackrel{!}{=} (e - \lambda) (\tilde{h}/2 - \lambda) \Rightarrow z_1 \stackrel{!}{=} |c|^2 \stackrel{!}{=} z_2, z_1 \neq z_2 \in \mathbb{R}^+$. Extending (334)-(337) by

$$(a, e, h, j) \neq 0 \wedge (c, d) \neq 0 \wedge (c \neq -g \neq 0) \quad (341)$$

leads to the characteristic polynomial from (340) by replacing $f \leftrightarrow g$, indicating that (341) is a non-physical $\hat{\rho}_{SE}^{\text{out}}$.

XIV). The configuration

$$(a, h, j) \neq 0 \wedge (c, i) \neq 0 \wedge (c \neq -g = 0) \wedge (-i \neq b = 0) \quad (342)$$

emerges from (328) by setting $e = 0$ and supplements (330) with non-vanishing outer-diagonal entries i , leading to $\hat{\rho}_{SE}^{\text{out}}$ as in (335) with

$$\mathbf{A}_1 = \begin{bmatrix} h & -i \\ -i^* & j \end{bmatrix}, \mathbf{B}_0 = \begin{bmatrix} c & 0 \\ 0 & 0 \end{bmatrix}, \hat{\rho}_E^{\text{out}} = \begin{pmatrix} a+h & -i \\ -i^* & j \end{pmatrix}, \hat{\rho}_S^{\text{out}} = \begin{pmatrix} a & c \\ c^* & h+j \end{pmatrix}, \quad (343)$$

with $a+h+j \stackrel{!}{=} 1$. We have to set $b = 0$ in (343) (compared with (289) above), since the diagonal value e , which should be »connected« with a , is missing. The characteristic polynomial of $\hat{\rho}_{SE}^{\text{out}}$ in (343), $(-\lambda)(j-\lambda)[(a-\lambda)(h-\lambda)-|c|^2] + \lambda|i|^2(a-\lambda) \stackrel{!}{=} 0$, in general leads to complex eigenvalues, since we cannot reduce it to a structure proportional to the polynomial of degree 2. To obtain physical $\hat{\rho}_{SE}^{\text{out}}$ we set in (343) $a \stackrel{!}{=} j$, yielding non-zero eigenvalues (with $j := (1-h)/2$ and $0 < j < 1$) $\left\{ \lambda_1 = j, \lambda_{2/3} = (j+h)/2 \pm \sqrt{(j+h)^2/4 + |c|^2 + |i|^2 - j \cdot h} \right\}$ (of $\hat{\rho}_{SE}^{\text{out}}$) and (for $\hat{\rho}_E^{\text{out}}$) $\left\{ \lambda_{1/2} = 1/2 \pm \sqrt{1/4 + |i|^2 - j(j+h)} \right\}$, with $H(S) \approx H(S_{\text{class}})$ and $H(S, E) = H(E)$ given by (as in (312)-(313)²⁰)

$$|c|^2 = j \cdot h \approx 0 \quad (344)$$

that enforces $i = 0$. Choosing $|c|^2 + |i|^2 = j \cdot h$ implies $|i|^2 \approx j \cdot h$ (since (344) still has to hold due to $H(S) \approx H(S_{\text{class}})$) and yields $H(E) < H(S, E)$ due to $i \neq 0$ in (343) (s. also (291)). Also, the $\hat{\rho}_E^{\text{out}}$ -eigenvalues $\lambda_{1/2}$ of (343), show that within $0 \leq |i|^2 \leq j(j+h)$ $H(E)$ decreases from²¹ $H(E) = -(j+h)\log_2(j+h) - j\log_2 j$ at $i = 0$ to $H(E) = 0$ at $|i|^2 = j(j+h) \forall (0 < j < 1)$. QD appears in (342) only if $|i|^2 \approx 0$, i.e. (342) violates (15).

XV). The configuration

$$(a, h, j) \neq 0 \wedge (d, i) \neq 0 \wedge (-i \neq b = 0) \quad (345)$$

supplements (332) with non-vanishing outer-diagonal entries i , leading to $\hat{\rho}_{SE}^{\text{out}}$ as in (343) with

$$\mathbf{B}_0 = \begin{bmatrix} 0 & d \\ 0 & 0 \end{bmatrix}, \hat{\rho}_E^{\text{out}} = \begin{pmatrix} a+h & -i \\ -i^* & j \end{pmatrix}, \hat{\rho}_S^{\text{out}} = \text{diag}[a, h+j], \quad (346)$$

with $a+h+j \stackrel{!}{=} 1$ and $h \stackrel{!}{=} j$ due to (316)-(317). The non-zero eigenvalues (with $j := (1-a)/2$ and $0 < j < 1$) $\left\{ \lambda_1 = j, \lambda_{2/3} = (a+j)/2 \pm \sqrt{(a+j)^2/4 + |d|^2 + |i|^2 - a \cdot j} \right\}$ (of $\hat{\rho}_{SE}^{\text{out}}$) and $\left\{ \lambda_{1/2} = 1/2 \pm \sqrt{1/4 + |i|^2 - j(a+j)} \right\}$ (of $\hat{\rho}_E^{\text{out}}$) in (346) show that only the condition (as in (316)-(317)²²)

$$|d|^2 = a \cdot j \approx 0 \quad (347)$$

enforces $i = 0$, leading to $H(S, E) = H(E)$, whereas $H(S) \approx H(S_{\text{class}})$ is already guaranteed by (346): thus (345) does not validate (15) as long as $i \neq 0$, since then $H(S, E) > H(E)$.

XVI). Inserting into (289) the configuration

$$(a, h, j) \neq 0 \wedge (c, d, i) \neq 0 \wedge (c \neq -g = 0) \wedge (-i \neq b = 0), \quad (348)$$

$\hat{\rho}_E^{\text{out}}$ is as in (343) and (346), and (336) is modified as $|c|^2 \lambda(j-\lambda) + |d|^2 \lambda(h-\lambda) - \lambda(a-\lambda)(h-\lambda)(j-\lambda) + \lambda(a-\lambda)|i|^2 + 2\lambda \text{Re}\{c \cdot d \cdot i\} \stackrel{!}{=} 0$, showing that only (338), with $\hat{\rho}_S^{\text{out}}$ given by (335) and (343), and $|i|^2 \approx 0$, $\text{Re}\{i\} \ll 1$ validate (15).

²⁰Since $c \neq -g$, we have, contrary to (313), $|c|^2 \neq |g|^2 = e \cdot j = 0$ and $e = 0$ thus does not need to be »connected« with $j \neq 0$ via g in (343).

²¹Ergo ($h = a = j = 1/3$) would be one possible probability distribution for $\hat{\rho}_{SE}^{\text{out}}$ in (342) above, whereas alternative probability distributions could also be ($a = j = 1/4 \wedge h = 1/2$) or, ($a + j = 1/2 \wedge h = 1/2$). In (337) only ($h = j = 1/4 \wedge a = 1/2 \neq j$) is allowed due to $d \neq 0$.

²²However, now we have, contrary to (317), $|f|^2 = e \cdot j = 0$, since $e = 0$ and therefore does not need to be »connected« with $j \neq 0$ via f .

D List of exemplary input and output states in Zurek's model of Quantum Darwinism

In the present appendix we list all exemplary environmental input states in $\hat{\rho}_{SE}^{\text{in}} = \hat{\rho}_S^{\text{in}} \otimes \hat{\rho}_E^{\text{in}}$ and their output states $\hat{\rho}_{SE_L}^{\text{out}}$ discussed in the course of Zurek's qubit model of Quantum Darwinism in section 7, Fig. 5.

$\hat{\rho}_E^{\text{in}}$	$\hat{\rho}_{SE_L}^{\text{out}}$ / entropies
1) $\frac{1}{2}(0_n\rangle\langle 0_n + 0_{n-1}1\rangle\langle 0_{n-1}1)$ $H(S) = H(S_{\text{class}}) \forall L$ • – dotted curve	$ a ^2 0\rangle\langle 0 \otimes \hat{\rho}_E^{\text{in}}$ $+ \frac{1}{2} b ^2 1\rangle\langle 1 \otimes (1_n\rangle\langle 1_n + 1_{n-1}0\rangle\langle 1_{n-1}0)$ $+ \frac{1}{2}ab^* 0\rangle\langle 1 \otimes (0_n\rangle\langle 1_n + 0_{n-1}1\rangle\langle 1_{n-1}0)$ $+ \frac{1}{2}a^*b 1\rangle\langle 0 \otimes (1_n\rangle\langle 0_n + 1_{n-1}0\rangle\langle 0_{n-1}1)$ $\left\{ \begin{array}{l} H_{SE} = H(S_{\text{class}}) + \delta_{L,n} \\ H_E = (1 - \delta_{L,n}) H(S_{\text{class}}) \\ + \delta_{L,n} (1 \leq L \leq n) \end{array} \right.$
2) $\frac{1}{2}(0_n\rangle\langle 0_n + 10_{n-1}\rangle\langle 10_{n-1})$ $H(S) = H(S_{\text{class}}) \forall L$ ■ – dotted curve	as in 1), with $ 0_{n-1}1\rangle \leftrightarrow 10_{n-1}\rangle$ $ 1_{n-1}0\rangle \leftrightarrow 01_{n-1}\rangle$ $\left\{ \begin{array}{l} H_{SE} = (1 - \delta_{L,n}) H(S_{\text{class}}) + 1 (1 \leq L \leq n) \\ H_E = 1 \text{ for } L = 1 \\ H_E = (1 - \delta_{L,n}) H(S_{\text{class}}) + H_{SE} (2 \leq L \leq n) \end{array} \right.$
3) $\frac{1}{2}(0_n\rangle\langle 0_n + 1_n\rangle\langle 1_n)$ $H(S) = H(S_{\text{class}}) \forall L$ ◆ – dotted curve	$(a ^2 0\rangle\langle 0 + b ^2 1\rangle\langle 1) \otimes \hat{\rho}_E^{\text{in}}$ $+ \frac{1}{2}(ab^* 0\rangle\langle 1 + a^*b 1\rangle\langle 0)$ $\otimes (0_n\rangle\langle 1_n + 1_n\rangle\langle 0_n)$ $\left\{ \begin{array}{l} (1 \leq L \leq n) : H_E = 1 \\ H_{SE} = (1 - \delta_{L,n}) H(S_{\text{class}}) + 1 \end{array} \right.$
4) $2^{-n}\hat{1}_n = (2^{-1}\hat{1}_1)^{\otimes n}$ $\{ x\rangle, y\rangle\} \in \{0, \dots, 2^n - 1\}$ $H(S) = H(S_{\text{class}}) \forall L$ ◆ – dotted curve	$(a ^2 0\rangle\langle 0 + b ^2 1\rangle\langle 1) \otimes \hat{\rho}_E^{\text{in}}$ $+ 2^{-n}ab^* 0\rangle\langle 1 \otimes \sum_{\substack{x \neq y=0 \\ 2^n-1}}^{2^n-1} x\rangle\langle y $ $+ 2^{-n}a^*b 1\rangle\langle 0 \otimes \sum_{\substack{x \neq y=0 \\ 2^n-1}}^{2^n-1} y\rangle\langle x $ $\left\{ \begin{array}{l} (1 \leq L \leq n) : H_E = L \\ H_{SE} = (1 - \delta_{L,n}) H(S_{\text{class}}) + L \end{array} \right.$
5) $\frac{1}{2}(0_n\rangle\langle 0_n + 1_{n-1}0\rangle\langle 1_{n-1}0)$ $H(S) = H(S_{\text{class}}) \forall L$ ▲ – dotted curve	as in 1), with $ 0_{n-1}1\rangle \leftrightarrow 1_{n-1}0\rangle$ $\left\{ \begin{array}{l} (1 \leq L \leq n) : H_E = 1 + \delta_{L,n} H(S_{\text{class}}) \\ H_{SE} = 1 + (1 - \delta_{L,n}) H(S_{\text{class}}) \end{array} \right.$
6) $ \Psi_E^{\text{in}}\rangle = \frac{1}{\sqrt{2}}(0_n\rangle + 1_n\rangle)$ ▼ – dotted curve	$\hat{\rho}_S^{\text{in}} \otimes \hat{\rho}_E^{\text{in}} \left\{ \begin{array}{l} H(S) = 0 < \forall L > 0 \\ H_E = H_{SE} = 1 - \delta_{L,n} (1 \leq L \leq n) \end{array} \right.$

Table 8: $\hat{\rho}_{SE_L}^{\text{out}}$ from Zurek's CNOT-evolution of $\hat{\rho}_{SE}^{\text{in}} = \hat{\rho}_S^{\text{in}} \otimes \hat{\rho}_E^{\text{in}}$ for different $\hat{\rho}_E^{\text{in}}$, s. Fig. 5.

E Quantum Darwinism and eigenstates of Eq. (9)-(10)

In this appendix we explain why the generalized $k > 1$ qubit version of (158) does not lead to Quantum Darwinism.

The ϕ -parameter family $\hat{u}_i^{(\phi)}$ of transformations in (9)-(10) has eigenstates $|s_{c_1}\rangle = (c_1|0\rangle + c_2|1\rangle)$ (eigenvalue $\lambda = 1$) and $|s_{c_2}\rangle = (c_2|0\rangle - c_1|1\rangle)$ (eigenvalue $\lambda = -1$), with $\langle s_{c_1}|s_{c_2}\rangle = 0$ and $c_1^2 + c_2^2 \stackrel{!}{=} 1$ ($c_1, c_2 > 0$) [11, 29, 30]. This allows us to parametrize c_1 and c_2 as $\left\{ c_1 = \cos\left(\frac{\phi}{2}\right), c_2 = \sin\left(\frac{\phi}{2}\right) \right\}$ and thus fix ϕ within the range $(0 \leq \phi \leq \pi)$. By means of this ϕ -parametrization we may generalize (158) according to

$$\begin{aligned} |\Psi_{SE}^{\text{out}}(L=n)\rangle &= a|0\rangle \otimes |s_{c_1}^L\rangle + b|1\rangle \otimes |s_{c_2}^L\rangle \\ \hat{\rho}_{SE}^{\text{out}}(L=n) &= |a|^2 |s_{c_1}^L\rangle\langle s_{c_1}^L| + |b|^2 |s_{c_2}^L\rangle\langle s_{c_2}^L|, \end{aligned} \quad (349)$$

with $|s_{c_1}^L\rangle = |s_{c_1}\rangle^{\otimes L}$, $|s_{c_2}^L\rangle = |s_{c_2}\rangle^{\otimes L}$, $\langle s_{c_1}^L|s_{c_2}^L\rangle = 0$. For $L = n$ one would always obtain $H(S) = H(S_{\text{class}})$ and $H(S, E_{L=n}) = 0 < H(E_{L=n})$, since (349) is a pure state, whereas the spectrum of $\hat{\rho}_{SE}^{\text{out}}(L=n)$ would, for simplicity for $L = n = 1$, contain the non-vanishing eigenvalues $\left\{ \lambda_{1/2}^{E(L=n=1)} = \frac{1}{2} \pm \sqrt{\frac{1}{4} - 4c_1^2c_2^2|a|^2|b|^2} \right\}$. Tracing out E-qubits in (349) forces $\hat{\rho}_{SE_L}^{\text{out}}$ to acquire the form

$$\hat{\rho}_{SE}^{\text{out}}(L < n) = |a|^2|0\rangle\langle 0| \otimes |s_{c_1}^L\rangle\langle s_{c_1}^L| + |b|^2|1\rangle\langle 1| \otimes |s_{c_2}^L\rangle\langle s_{c_2}^L|, \quad (350)$$

for which one in general has $H(S, E_{L < n}) > 0$. Again, without loss of generality, let us set in (350) $L = n = 1$: w.r.t. (350) $\hat{\rho}_{SE}^{\text{out}}(L = n = 1)$ remains the same as in (349), whereas $\hat{\rho}_{SE}^{\text{out}}(L = n = 1)$ from (350) leads $\forall \phi$ to non-zero eigenvalues $\{\lambda_1^{SE(L=n=1)} = |a|^2, \lambda_2^{SE(L=n=1)} = |b|^2\}$. Since $(c_1, c_2) > 0$ are parametrized by complementary transcendent functions of the ϕ -parameter, the only way to satisfy the MI-plateau condition between $H(S, E_L)$ and $H(E_L)$ is to demand $H(S, E_{L=n=1}) = H(E_{L=n=1})$, which can be achieved only if we choose

$$c_1^2 = c_2^2 = 1/2, \quad (351)$$

which leads to E-eigenstates $\{|s_1\rangle, |s_2\rangle\}$ of the CNOT-transformation $\hat{u}_j^{(\phi=\pi/2)}$ from (158). Otherwise, $\forall (c_1 \neq c_2)$ one has $H(S, E_{L=n=1}) > H(E_{L=n=1})$. Thus, (351) shows that w.r.t. the S-pointer basis given by the standard computational basis $\{|\pi_i\rangle\} \equiv \{|0\rangle, |1\rangle\}$ solely the CNOT-transformation allows Quantum Darwinism to appear.

However, what happens if we generalize (158) to $k > 1$ qubit system S ? Since there are only two eigenstates $\{|s_1\rangle, |s_2\rangle\}$ of $\hat{u}_j^{(\phi=\pi/2)}$ in (9)-(10), the easiest way to generalize (350)-(351) to $k > 1$ S-qubits is according to

$$\hat{\rho}_{SE}^{\text{out}}(L) = \left(\sum_{i=0}^{2^{k-1}-1} |a_i|^2 |i\rangle \langle i| \right) \otimes |s_1^L\rangle \langle s_1^L| + \left(\sum_{j=2^{k-1}}^{2^k-1} |a_j|^2 |j\rangle \langle j| \right) \otimes |s_2^L\rangle \langle s_2^L|, \quad (352)$$

w.r.t. an arbitrary S-probability distribution $1 > |a_i|^2 > 0, i \in \{0, \dots, 2^k - 1\}$. However, the eigenvalues of (352),

$$\begin{aligned} \hat{\rho}_{SE}^{\text{out}}(L) : \left\{ \lambda_i^{SE} = |a_i|^2 \right\}_{i=0}^{2^{k-1}-1} &\Rightarrow (1 - \delta_{k,1}) \cdot H(E_f) \leq H(S, E_f) = H(S_{\text{class}}^{k \geq 1}) \forall L \\ \hat{\rho}_{SE}^{\text{out}}(L) : \lambda_1^E &= \sum_{i=0}^{2^{k-1}-1} |a_i|^2, \lambda_2^E = \sum_{j=2^{k-1}}^{2^k-1} |a_j|^2 \Rightarrow H(E_f) = -\sum_{i=1}^2 \lambda_i^E \cdot \log_2 \lambda_i^E \leq 1 \forall L, \end{aligned} \quad (353)$$

indicate that QD appears for (352) if and only if $k = 1$, yielding $I(S : E_f) / H(S_{\text{class}}^{k \geq 1}) = H(E_f) / H(S_{\text{class}}^{k \geq 1}) = 1$. Accordingly, generalizing (349) with (351) as

$$\begin{aligned} |\Psi_{SE}^{\text{out}}(L)\rangle &= \sum_{i=0}^{2^{k-1}-1} a_i |i\rangle |s_1^L\rangle + \sum_{j=2^{k-1}}^{2^k-1} a_j |j\rangle |s_2^L\rangle, \quad \sum_{i=0}^{2^{k-1}-1} |a_i|^2 \stackrel{!}{=} 1 \\ \hat{\rho}_{SE}^{\text{out}}(L) &= |\Psi_{SE}^{\text{out}}(L)\rangle \langle \Psi_{SE}^{\text{out}}(L)|, \end{aligned} \quad (354)$$

where $H(E_f) = -\sum_{i=1}^2 \lambda_i^E \log_2 \lambda_i^E \leq 1 \forall L$ from (353), $H(S) = H(S_{\text{class}})$ and $H(S, E_f)$ behaves in a two-fold way: **1)** if $L = n \geq 1$, (354) is pure $H(S, E_f) = 0 < H(E_f)$, yielding $I(S : E_f) = 2H(S_{\text{class}})$ (»quantum peak«); **2)** For $1 \leq L < n$ (354) contains 2^{k-1} »diagonal S-subspaces«, half of which are organized according to $|s_1^L\rangle \langle s_1^L|$, whereas the remaining 2^{k-1} »diagonal S-subspaces« of (354) are ordered according to $|s_2^L\rangle \langle s_2^L|$. This implies $I(S : E_f) = H(S_{\text{class}})$, since $H(S, E_f) = H(E_f) = H(S_{\text{class}}^{k=1}) \forall (1 \leq L < n)$, as in (353). In (354) Quantum Darwinism does not appear for $k > 1$

and $1 \leq L \leq n$, since $\hat{\rho}_{SE}^{\text{out}}$ of (354) has for $k \geq 1$ only two eigenvalues $\lambda_1^S = \sum_{i=0}^{2^{k-1}-1} |a_i|^2$ and $\lambda_2^S = \sum_{j=2^{k-1}}^{2^k-1} |a_j|^2$ (with $\lambda_1^S + \lambda_2^S \stackrel{!}{=} 1$), corresponding to eigenvalues of $k = 1$ system S . Thus: if we organize $\hat{\rho}_{SE}^{\text{out}}(L)$ according to (354), we could maximally store $1 \geq H(S_{\text{class}}) = -\lambda_1^S \log_2 \lambda_1^S - \lambda_2^S \log_2 \lambda_2^S > 0$ of a $k = 1$ system S , even if one should insist on $k > 1$ (the PIP for $k = 1$ in (354) is given by Fig. 1), i.e. in (354) Quantum Darwinism appears only for $k = 1$.

F Gram-Schmidt orthonormalization

In this Appendix we summarize the Gram-Schmidt orthonormalization.

Given a finite set of linear independent operators $M = \{\hat{x}_1, \dots, \hat{x}_m\}$ with $m \in \mathbb{N}$. Then one can construct from it m orthonormalized basis vectors of an m -dimensional operator space $M_r = \{\hat{x}_{1r}, \dots, \hat{x}_{mr}\}$ by performing the following iterative Gram-Schmidt algorithm (s. [23], [37]):

Step 1: Chose one of the operators in M , say \hat{x}_1 , and set

$$\hat{x}_{1r} := \frac{\hat{x}_1}{\|\hat{x}_1\|_{HS}}, \quad (355)$$

where $\|\hat{x}_1\|_{\text{HS}}$ denotes the Hilbert-Schmidt norm (HS-norm) defined for an arbitrary bounded operator \hat{A} w.r.t. its vector basis $\{e_i\}$ as

$$\|\hat{A}\|_{\text{HS}} = \left(\sum_{i,j} |\langle e_i | \hat{A} | e_j \rangle|^2 \right)^{1/2} = \left(\text{Tr} \left[\hat{A} (\hat{A})^\dagger \right] \right)^{1/2}. \quad (356)$$

Step 2: Compute the remaining orthonormalized $m - 1$ basis operators \hat{x}_{ir} (mit $i = \{2, \dots, m\}$) by iteratively applying

$$\hat{x}_{ir} := \frac{\hat{x}_i - \sum_{n=1}^{i-1} \langle \hat{x}_{nr}, \hat{x}_i \rangle \hat{x}_{nr}}{\left\| \hat{x}_i - \sum_{n=1}^{i-1} \langle \hat{x}_{nr}, \hat{x}_i \rangle \hat{x}_{nr} \right\|_{\text{HS}}}, \quad (357)$$

with $\langle \hat{x}_{nr}, \hat{x}_i \rangle = \text{Tr} [\hat{x}_{nr} (\hat{x}_i)^\dagger]$ being a usual Hilbert-Schmidt scalar product of two bounded operators. After the last $(m - 1)$ -th iterative application of (357) we obtain the m -dimensional completely orthonormalized system $\{\hat{x}_{1r}, \dots, \hat{x}_{mr}\}$ of \hat{x}_i -operators.

G QR-decomposition

In this Appendix we summarize the QR-decomposition method.

We can solve a linear system of equations (with a given $(n \times 1)$ -column vector \mathbf{y})

$$A\mathbf{x} = \mathbf{y} \quad (358)$$

for a non-singular $(n \times n)$ -matrix A w.r.t. the $(n \times 1)$ -column vector \mathbf{x} by

1. decomposing A according to

$$A = QR \quad (359)$$

into an orthogonal (self-adjoint) diagonal $(n \times n)$ -matrix Q and a non-singular, upper-right triangular $(n \times n)$ -matrix R (with diagonal entries $r_{ii} \neq 0 \forall i$)

2. solving successively linear systems of equations

$$Q\mathbf{z} = \mathbf{y} \Rightarrow R\mathbf{x} = \mathbf{z} \Rightarrow \mathbf{x}, \quad (360)$$

which determine the $(n \times 1)$ -column vector \mathbf{z} and from it \mathbf{x} (w.r.t. numerical methods that can be implemented in this context s. for instance [23]). (169) contains $g := |M| \cdot 2^{2(k+n)}$ equations for $2^{2(k+n)}$ unknown $\hat{X}_{\lambda,i}$ -matrix entries w.r.t. the fixed λ -eigenvalue. We first reformulate (169) as a linear system of equations

$$A\mathbf{x} = \mathbf{0}, \quad (361)$$

with a $(g \times g)$ -matrix A and a $(1 \times g)$ -column vector \mathbf{x} containing the first $2^{2(k+n)}$ unknown $\hat{X}_{\lambda,i}$ -matrix entries and the remaining $g^2 - 2^{2(k+n)}$ zero entries. Then we can apply the QR-decomposition to A in (361) in accord with (358)-(360) and determine from the rank r of the corresponding R -matrix the dimensionality

$$d_{n \geq k}^\lambda = 2^{2(k+n)} - r \quad (362)$$

of the attractor (sub-)space in (170) for a fixed λ -value, whereas the Q -matrix leads to all allowed $d_{n \geq k}^\lambda$ configurations of $\hat{X}_{\lambda,i}$ -matrix entries in (170).

H Analytic reconstruction of attractor spaces

In this Appendix we intend to sketch how one can reconstruct the minimal, maximal and intermediate attractor spaces by utilizing the QR-decomposition method from Appendix G.

H.1 Minimal attractor space

Now we turn our attention to environments E whose all n qubits are allowed to mutually interact with each other, as depicted by the ID in Fig. 9 and already studied in [11, 29, 30].

H.1.1 Dimensionality

From [11, 29, 30] we know that E enclosing mutually via $\hat{u}_i^{(\phi)}$ interacting n qubits (with $n \geq k \geq 1$) leads to the most constrained (strongly connected) ID with an attractor subspace associated with the eigenvalue $\lambda = 1$ of (169) of minimal dimension

$$d_n^{\lambda=1, \min} = 4^k + 3 \cdot 2^k + 1, \quad (363)$$

whereas the dimensionality of the $\lambda = -1$ attractor subspace satisfies

$$d_n^{\lambda=-1, \min} = \begin{cases} 1 & \text{if } n = k = 1 \\ 0, & \text{otherwise.} \end{cases} \quad (364)$$

Since Quantum Darwinism involves environments E with $n \gg 1$ qubits, we may conclude that within the minimal attractor space only the $\lambda = 1$ subspace contributes to the evolution of $\hat{\rho}_{SE}^{\text{in}}$.

H.1.2 State structure

From [11, 29, 30] we know that (363) corresponds to the following structure of the linear independent (however not yet orthonormalized) $\hat{X}_{\lambda=1, i}$ -states

$$\begin{aligned} & |x\rangle \langle x| \otimes \hat{I}_n, |0_k\rangle \langle x| \otimes |0_n\rangle \langle s_{c_1}^n|, |x\rangle \langle 0_k| \otimes |s_{c_1}^n\rangle \langle 0_n| \\ & |x\rangle \langle y| \otimes |s_{c_1}^n\rangle \langle s_{c_1}^n|, |0_k\rangle \langle 0_k| \otimes |0_n\rangle \langle 0_n|, \end{aligned} \quad (365)$$

whereas (364) corresponds for $k = n = 1$ to the only non-zero orthonormalized $\hat{X}_{\lambda=-1, i}$ -state

$$\hat{X}_{\lambda=-1, i=1}^{n=k=1} = \frac{1}{\sqrt{6}} (|01\rangle \langle 11| - |10\rangle \langle 11| - |11\rangle \langle 01| + |11\rangle \langle 10| - |01\rangle \langle 10| + |10\rangle \langle 01|), \quad (366)$$

with $(x, y) \in \{0, \dots, 2^k - 1\}$, $\text{Tr}_E [\hat{I}_n] = 2^n$, $\hat{I}_n = \hat{I}_1^{\otimes n}$ and $\{|s_{c_1}^L\rangle, |s_{c_2}^L\rangle\}$ from (349)-(350). However, (366) does not contribute to the evolution of $\hat{\rho}_{SE}^{\text{in}}$ from the point of view of Quantum Darwinism, which necessitates us to start with $\hat{\rho}_{SE}^{\text{in}}$ enclosing environments E with $n \gg k \geq 1$ qubits.

We conclude this subsection by demonstrating how to deduce (365)-(366). To accomplish this task we start from the ϕ -transformation (166) and (169), i.e.

$$\hat{U}_e^{(\phi)} \hat{X}_{\lambda, i} \hat{U}_e^{(\phi)\dagger} = \lambda \hat{X}_{\lambda, i}, \quad \forall e \in M, \quad (367)$$

with $n = k = 1$, $M \equiv \{(1, 2)\}$ from Fig. 9, containing an edge between a single S-qubit 1 (control) and an E-qubit 2 (target), as well as a matrix representation $\hat{X}_{\lambda, i} = \sum_{k, l} X_{kl}^i (\lambda, i) |k\rangle_{SE} \langle l|$ ($X_{kl}^i \in \mathbb{R}$) in the standard computational S-E-basis

$k, l \in \{0, \dots, 2^{k+n} - 1\}$.

a) For $\phi = \pi/2$ (CNOT) and $\lambda = 1$ (367) leads to constraints (with $\bar{r}_E, r_E \in \{0, 1\}$)

$$\begin{aligned} \text{I)} & X_{0s\bar{r}_E}^{0s\bar{r}_E} (\lambda = 1, i) = X_{0s\bar{r}_E}^{0s\bar{r}_E} (\lambda = 1, i), \text{ II)} & X_{0s\bar{r}_E}^{1s0_E} (\lambda = 1, i) = X_{0s\bar{r}_E}^{1s1_E} (\lambda = 1, i) \\ \text{III)} & X_{1s0_E}^{0s\bar{r}_E} (\lambda = 1, i) = X_{1s1_E}^{0s\bar{r}_E} (\lambda = 1, i), \text{ IV)} & X_{1s0_E}^{1s0_E} (\lambda = 1, i) = X_{1s1_E}^{1s0_E} (\lambda = 1, i) \\ & & \text{V)} & X_{1s0_E}^{1s1_E} (\lambda = 1, i) = X_{1s1_E}^{1s1_E} (\lambda = 1, i), \end{aligned} \quad (368)$$

from which we conclude the following relations between $\hat{X}_{\lambda=1, i}$ -matrix entries

$$\begin{aligned} & 1) X_{0s0_E}^{1s0_E} (\lambda = 1, i) = X_{0s0_E}^{1s1_E} (\lambda = 1, i), 2) X_{0s0_E}^{0s0_E} (\lambda = 1, i) = X_{0s0_E}^{0s1_E} (\lambda = 1, i) \\ & 3) X_{0s0_E}^{0s1_E} (\lambda = 1, i) = X_{1s1_E}^{0s1_E} (\lambda = 1, i), 4) X_{0s1_E}^{1s0_E} (\lambda = 1, i) = X_{0s1_E}^{1s1_E} (\lambda = 1, i) \\ & 5) X_{1s1_E}^{1s0_E} (\lambda = 1, i) \text{ arbitrary}, 6) X_{1s0_E}^{1s0_E} (\lambda = 1, i) = X_{1s1_E}^{1s1_E} (\lambda = 1, i), 7) X_{1s0_E}^{1s1_E} (\lambda = 1, i) \text{ arbitrary} \\ & 8) - 11) X_{0s0_E}^{0s0_E} (\lambda = 1, i), X_{0s0_E}^{0s1_E} (\lambda = 1, i), X_{0s1_E}^{0s0_E} (\lambda = 1, i), X_{0s1_E}^{0s1_E} (\lambda = 1, i) \text{ arbitrary.} \end{aligned} \quad (369)$$

(369) leads to the general $\widehat{X}_{\lambda=1,i}$ -matrix structure (pre-configuration matrix, PM, with $a, b, c, d, e \in \mathbb{R}$, $\blacksquare \in \mathbb{R}$ arbitrary)

$$\hat{X}_{\lambda=1,i} = \left(\begin{array}{cc} \underbrace{\blacksquare}_{8)} & \underbrace{\blacksquare}_{10)} & \underbrace{a}_{2)} & a \\ \underbrace{\blacksquare}_{9)} & \underbrace{\blacksquare}_{11)} & \underbrace{b}_{3)} & b \\ \underbrace{d}_{1)} & \underbrace{c}_{4)} & \underbrace{e}_{6)} & \underbrace{\blacksquare}_{5)} \\ \underbrace{d}_{1)} & \underbrace{c}_{4)} & \underbrace{\blacksquare}_{7)} & e \end{array} \right), \quad (370)$$

from which we can mathematically construct many versions of $d_{n=1}^{\lambda=1, \min} = 11$ necessary $\widehat{X}_{\lambda=1, i}$ -states of the minimal attractor $\{\lambda = 1\}$ -subspace.

However, if we take physical symmetry aspects into account, we are able to establish physically justified structures of attractor states $\hat{X}_{\lambda=1,i}$ in (370) (with $i = 1, \dots, 11$). Since $\{|s_{c_1}^L\rangle, |s_{c_2}^L\rangle\}$ with (351) are the only symmetry states of the CNOT-transformation (166)-(167), (370) suggests that one has to choose for $\hat{X}_{\lambda=1,i}$ the states $|x\rangle\langle x| \otimes \hat{I}_{n=1}$ (the general fixed point state of an iterated random unitary evolution), $|0_{k=1}\rangle\langle 0_{k=1}| \otimes |0_{n=1}\rangle\langle 0_{n=1}|$ (the S-E-ground state) and $|x\rangle\langle y| \otimes |s_1^{n=1}\rangle\langle s_1^{n=1}|$ (involving a symmetry state $|s_1^n\rangle$ of the environment) from (365), with $\{|s_1^n\rangle, |s_2^n\rangle\}$ as in (158). Furthermore, (370) also indicates that the remaining four attractor states $\hat{X}_{\lambda=1,i}$ can be associated with structures $|0_{k=1}\rangle\langle x| \otimes |0_{n=1}\rangle\langle s_1^{n=1}|$ and $|x\rangle\langle 0_{k=1}| \otimes |s_1^{n=1}\rangle\langle 0_{n=1}|$ from (365), which correlate the S-pointer states with $|0_{n=1}\rangle$ and $|s_1^{n=1}\rangle$.

When extending (367) to $n = 2 > k = 1$ we obtain a strongly connected ID in Fig. 9 with one S-qubit (qubit 1), two E-qubits (qubit 2 and 3) and a set of CNOT-edges $M \equiv \{(1, 2), (1, 3), (2, 3), (3, 2)\}$ (with the second qubit within each edge being targeted) leading to the following constraints (with $\overline{m}_E, m_E, \overline{r}_S, r_S \in \{0, 1\}$)

[illegible]

All constraints from (371) taken together lead to, as in (368), the 11 state structures (pre-configuration matrices) of $\hat{X}_{\lambda=1, i}$ from (365) with $n = 2 > k = 1$ and $\{ |s_{c_1}^{n=2} \rangle, |s_{c_2}^{n=2} \rangle \} \equiv \{ |s_1^{n=2} \rangle, |s_2^{n=2} \rangle \}$ as in (158). Accordingly, similar constraints as those in (371), however for $n > 2 > k = 1$, or $n \geq k > 1$ would also confirm the validity of (365) for $k > 1$ and $\{ |s_{c_1}^n \rangle, |s_{c_2}^n \rangle \} \equiv \{ |s_1^n \rangle, |s_2^n \rangle \}$ as in (158). In this respect we may also numerically implement the QR-decomposition from section G in order to reconstruct the corresponding matrix structures $\hat{X}_{\lambda=1, i}$.

Finally, using the QR-decomposition (358)-(362) and constraints emerging from (367) for $\lambda = 1$, $\phi \neq \pi/2$ and $n \geq k \geq 1$ one would confirm (365) even for non-CNOT values of ϕ in (166)-(167) and $\left\{ \left| s_{c_1 \neq 1/2}^n \right\rangle, \left| s_{c_2 \neq 1/2}^n \right\rangle \right\}$.

b) For $\phi = \pi/2$ (CNOT) and $\lambda = -1$ (367) leads to constraints (with $\bar{r}_E, r_E \in \{0, 1\}$)

$$\begin{aligned}
\text{I)} & X_{0s\overline{r}E}^{0s\overline{r}E}(\lambda = -1, i) = -X_{0s\overline{r}E}^{0s\overline{r}E}(\lambda = -1, i) \\
\text{II)} & X_{0s\overline{r}E}^{1s\overline{r}E}(\lambda = -1, i) = -X_{0s\overline{r}E}^{1s\overline{r}E}(\lambda = -1, i) \\
\text{III)} & X_{0s\overline{r}E}^{0s\overline{r}E}(\lambda = -1, i) = -X_{0s\overline{r}E}^{0s\overline{r}E}(\lambda = -1, i) \\
\text{IV)} & X_{1s\overline{r}E}^{1s\overline{r}E}(\lambda = -1, i) = -X_{1s\overline{r}E}^{1s\overline{r}E}(\lambda = -1, i) \\
\text{V)} & X_{1s\overline{r}E}^{1s\overline{r}E}(\lambda = -1, i) = -X_{1s\overline{r}E}^{1s\overline{r}E}(\lambda = -1, i),
\end{aligned} \tag{372}$$

from which we conclude the following relations between $\hat{X}_{\lambda=-1,i}$ -matrix entries

$$\begin{aligned} & 1) X_{0s0E}^{1s0E}(\lambda = -1, i) = -X_{0s0E}^{1s1E}(\lambda = -1, i), \quad 2) X_{1s1E}^{0s0E}(\lambda = -1, i) = -X_{1s0E}^{0s0E}(\lambda = -1, i) \\ & 3) X_{1s0E}^{0s1E}(\lambda = -1, i) = -X_{1s1E}^{0s1E}(\lambda = -1, i), \quad 4) X_{1s1E}^{1s0E}(\lambda = -1, i) = -X_{1s0E}^{1s1E}(\lambda = -1, i) \\ & 5) X_{1s0E}^{1s0E}(\lambda = -1, i) \text{ arbitrary}, \quad 6) X_{0s1E}^{1s1E}(\lambda = -1, i) = -X_{0s0E}^{1s1E}(\lambda = -1, i), \quad 7) X_{1s0E}^{1s1E}(\lambda = -1, i) \text{ arbitrary} \\ & 8) X_{1s0E}^{0s1E}(\lambda = -1, i) = -X_{0s1E}^{1s1E}(\lambda = -1, i). \end{aligned} \quad (373)$$

(372) and (373) lead to the general $\hat{X}_{\lambda=-1,i}$ -matrix structure (PM with $a, b, c, d, e \in \mathbb{R}$, $\blacksquare \in \mathbb{R}$ arbitrary)

$$\hat{X}_{\lambda=-1,i} = \begin{pmatrix} \begin{array}{cc} 0 & 0 \\ 0 & 0 \end{array} & \begin{array}{c} \underbrace{d}_{2)} \\ \underbrace{e}_{3)} \end{array} & \begin{array}{c} -d \\ -e \end{array} \\ \begin{array}{cc} \underbrace{a}_{1)} & \underbrace{b}_{6)} \\ -a & -b \end{array} & \begin{array}{c} \underbrace{c}_{5)} \\ \underbrace{\blacksquare}_{4)+5)+7)} \end{array} & \begin{array}{c} \underbrace{\blacksquare}_{4)+5)+7)} \\ -c \end{array} \end{pmatrix}, \quad (374)$$

from which we can mathematically construct many versions of the $d_{n=1}^{\lambda=-1,\min} = 1$ necessary $\hat{X}_{\lambda=-1,i}$ -state of the minimal attractor $\{\lambda = -1\}$ -subspace.

Physically, we see from (374) that this time we cannot use $|0_{n=1}\rangle$ and $|s_1^{n=1}\rangle$ as building blocks for the necessary $\hat{X}_{\lambda=-1,i}$ -matrix structure, however, one of the simplest choices one could make is to set in (374) $c = -c = 0$, since (374) already implies that $\hat{X}_{\lambda=-1,i}$ is traceless. On the other hand, (374) also indicates that the outer diagonal S-subspaces $|0\rangle_S \langle 1|$ and $|1\rangle_S \langle 0|$ are not necessarily traceless, which means that we may set two of the four constant pairs $\{(a, -a), (b, -b), (d, -d), (e, -e)\}$ of matrix entries in (374) to zero. Since $|0_{k=1}\rangle \otimes |0_{n=1}\rangle$ does not contribute in (374), we fix $X_{1s0E}^{0s1E}(\lambda = -1, i) = -X_{0s1E}^{1s0E}(\lambda = -1, i)$ and $X_{1s1E}^{1s0E}(\lambda = -1, i) = -X_{0s1E}^{0s1E}(\lambda = -1, i)$, obtaining $b = e$ and $\blacksquare = e$, respectively (i.e. $a = -a = d = -d = 0$), which transforms (374) into (366). Indeed, the four pairs of matrix entries $\{(a, -a), (b, -b), (d, -d), (e, -e)\}$ correspond to the environmental CNOT-symmetry state $|s_2^{n=1}\rangle$ from (158), which we correlate with the S-pointer state $|1_{k=1}\rangle$ (since $|0_{k=1}\rangle \otimes |0_{n=1}\rangle$ does not appear in (374) above) and thus rewrite (366) as

$$\hat{X}_{\lambda=-1,i=1}^{n=k=1} = \frac{1}{\sqrt{3}} \left(2^{-1/2} |1\rangle_S \langle 1| \otimes |1\rangle_E \langle 0| - |0\rangle_E \langle 1| - [|0\rangle_S \langle 1| \otimes |1\rangle_E \langle s_2^{n=1}| + |1\rangle_S \langle 0| \otimes |s_2^{n=1}\rangle_E \langle 1|] \right). \quad (375)$$

When extending (367) to $n = 2 > k = 1$ we obtain a strongly connected ID in Fig. 9 with one S-qubit (qubit 1), two E-qubits (qubit 2 and 3) and a set of CNOT-edges $M = \{(1, 2), (1, 3), (2, 3), (3, 2)\}$ (with the second qubit within each edge being targeted) leading to the following constraints (with $\bar{m}_E, m_E, \bar{r}_S, r_S \in \{0, 1\}$)

$$\begin{aligned} & \text{I) } X_{0s\bar{r}_E\bar{m}_E}^{0s\bar{r}_E\bar{m}_E}(\lambda = -1, i) = -X_{0s\bar{r}_E\bar{m}_E}^{0s\bar{r}_E\bar{m}_E}(\lambda = -1, i) \\ & \text{II) } X_{1s0E}^{1s0E}(\lambda = -1, i) = -X_{1s1E}^{1s1E}(\lambda = -1, i) \\ & \text{III) } X_{1s1E}^{1s1E}(\lambda = -1, i) = -X_{1s0E}^{1s0E}(\lambda = -1, i) \\ & \text{IV) } X_{0s\bar{r}_E\bar{m}_E}^{1s0E}(\lambda = -1, i) = -X_{0s\bar{r}_E\bar{m}_E}^{1s1E}(\lambda = -1, i) \\ & \text{V) } X_{1s0E}^{0s\bar{r}_E\bar{m}_E}(\lambda = -1, i) = -X_{1s1E}^{0s\bar{r}_E\bar{m}_E}(\lambda = -1, i) \\ & \text{I) } X_{0s\bar{r}_E\bar{m}_E}^{0s\bar{r}_E\bar{m}_E}(\lambda = -1, i) = -X_{0s\bar{r}_E\bar{m}_E}^{0s\bar{r}_E\bar{m}_E}(\lambda = -1, i) \\ & \text{II) } X_{1s1E}^{1s1E}(\lambda = -1, i) = -X_{1s0E}^{1s0E}(\lambda = -1, i) \\ & \text{III) } X_{1s0E}^{1s0E}(\lambda = -1, i) = -X_{1s1E}^{1s1E}(\lambda = -1, i) \\ & \text{IV) } X_{0s\bar{r}_E\bar{m}_E}^{1s1E}(\lambda = -1, i) = -X_{0s\bar{r}_E\bar{m}_E}^{1s0E}(\lambda = -1, i) \\ & \text{V) } X_{1s1E}^{0s\bar{r}_E\bar{m}_E}(\lambda = -1, i) = -X_{1s0E}^{0s\bar{r}_E\bar{m}_E}(\lambda = -1, i) \\ & \text{I) } X_{r_S\bar{r}_E\bar{m}_E}^{r_S\bar{r}_E\bar{m}_E}(\lambda = -1, i) = -X_{r_S\bar{r}_E\bar{m}_E}^{r_S\bar{r}_E\bar{m}_E}(\lambda = -1, i) \\ & \text{II) } X_{r_S\bar{r}_E\bar{m}_E}^{r_S\bar{r}_E\bar{m}_E}(\lambda = -1, i) = -X_{r_S\bar{r}_E\bar{m}_E}^{r_S\bar{r}_E\bar{m}_E}(\lambda = -1, i) \\ & \text{III) } X_{r_S\bar{r}_E\bar{m}_E}^{r_S\bar{r}_E\bar{m}_E}(\lambda = -1, i) = -X_{r_S\bar{r}_E\bar{m}_E}^{r_S\bar{r}_E\bar{m}_E}(\lambda = -1, i) \\ & \text{IV) } X_{r_S\bar{r}_E\bar{m}_E}^{r_S\bar{r}_E\bar{m}_E}(\lambda = -1, i) = -X_{r_S\bar{r}_E\bar{m}_E}^{r_S\bar{r}_E\bar{m}_E}(\lambda = -1, i) \\ & \text{V) } X_{r_S\bar{r}_E\bar{m}_E}^{r_S\bar{r}_E\bar{m}_E}(\lambda = -1, i) = -X_{r_S\bar{r}_E\bar{m}_E}^{r_S\bar{r}_E\bar{m}_E}(\lambda = -1, i) \\ & \text{I) } X_{r_S\bar{r}_E\bar{m}_E}^{r_S\bar{r}_E\bar{m}_E}(\lambda = -1, i) = -X_{r_S\bar{r}_E\bar{m}_E}^{r_S\bar{r}_E\bar{m}_E}(\lambda = -1, i) \\ & \text{II) } X_{r_S\bar{r}_E\bar{m}_E}^{r_S\bar{r}_E\bar{m}_E}(\lambda = -1, i) = -X_{r_S\bar{r}_E\bar{m}_E}^{r_S\bar{r}_E\bar{m}_E}(\lambda = -1, i) \\ & \text{III) } X_{r_S\bar{r}_E\bar{m}_E}^{r_S\bar{r}_E\bar{m}_E}(\lambda = -1, i) = -X_{r_S\bar{r}_E\bar{m}_E}^{r_S\bar{r}_E\bar{m}_E}(\lambda = -1, i) \\ & \text{IV) } X_{r_S\bar{r}_E\bar{m}_E}^{r_S\bar{r}_E\bar{m}_E}(\lambda = -1, i) = -X_{r_S\bar{r}_E\bar{m}_E}^{r_S\bar{r}_E\bar{m}_E}(\lambda = -1, i) \\ & \text{V) } X_{r_S\bar{r}_E\bar{m}_E}^{r_S\bar{r}_E\bar{m}_E}(\lambda = -1, i) = -X_{r_S\bar{r}_E\bar{m}_E}^{r_S\bar{r}_E\bar{m}_E}(\lambda = -1, i) \end{aligned} \quad (376)$$

Already after combining constraints $\gg 1 \rightarrow 2\ll$, $\gg 1 \rightarrow 3\ll$ and $\gg 2 \rightarrow 3\ll$ or $\gg 1 \rightarrow 2\ll$, $\gg 1 \rightarrow 3\ll$ and $\gg 3 \rightarrow 2\ll$ from (376) one obtains $d_{n=2}^{\lambda=-1,\min} = 0$. Certainly, $d_{n=2}^{\lambda=-1,\min} = 0$ also appears if we take all constraints from (376) into account, (i.e. the only solution $\hat{X}_{\lambda=-1,i}$ to (367) and (376), with $\phi = \pi/2$ and $n = 2 > k = 1$, is a zero matrix.

Accordingly, similar constraints as those in (376), however for $n > 2 > k = 1$, or $n \geq k > 1$ would also confirm the validity of $d_{n>1}^{\lambda=-1, \min} = 0 \forall k \geq 1$. In this respect we may also numerically implement the QR-decomposition from section G in order to reconstruct the corresponding matrix structures (PM) $\hat{X}_{\lambda=-1, i}$.

Finally, using the QR-decomposition (358)-(362) and constraints emerging from (367) for $\lambda = -1$, $\phi \neq \pi/2$ and $n \geq k \geq 1$ one would confirm $d_{n>1}^{\lambda=-1, \min} = 0 \forall k \geq 1$ even for non-CNOT values of ϕ in (166)-(167).

H.2 Maximal attractor space

The maximal attractor space and its basis states $\hat{X}_{\lambda, i}$ of the random unitary evolution (166)-(168) w.r.t. a specific relevant eigenvalue λ follow as a solution to the eigenvalue equation (169) obtained by means of the QR-decomposition if we assume environment E to contain mutually non-interacting qubits. Since each directed edge of the ID in Fig. 9 corresponds to an additional linear equation (constraint) in (169), the minimal number of constraints (and thus the maximal attractor space dimension $d_{n \geq k}^{\lambda}$) one could allow within the random unitary evolution model is given by the so called Koenig-IDs [31], in which only the S-qubits interact with E-qubits. In the following we will first determine $d_{n \geq k}^{\lambda}$.

H.2.1 Dimensionality

By implementing the QR-decomposition (359)-(362) from Appendix G numerically one notices for $n \geq k$ that within the maximal attractor space there are only two subspaces with non-zero dimension d^{λ} associated with eigenvalues $\lambda = \pm 1$ of (169) [11, 29, 30].

n	$d_{k=1}^{\lambda=1}$	$d_{k=2}^{\lambda=1}$	$d_{k=3}^{\lambda=1}$	$d_{k=1}^{\lambda=-1}$	$d_{k=2}^{\lambda=-1}$	$d_{k=3}^{\lambda=-1}$
1	11	28	88	1	12	24
2	28	58	142	12	18	30
3	88	142	316	24	30	42
4	304	406	634	48	54	66
5	1120	1318	1738	96	102	114
6	4288	4390	5482	192	198	210
7	16768	17542	19114	384	390	402

Table 9: Numerical data for $d_{n \geq k}^{\lambda}$ from (362) in Appendix G w.r.t. $n \geq k \in \{1, 2, 3\} \forall \lambda \in \{1, -1\}$.

From the numerically available data in Tab. 9 one can easily deduce for $k = 1$ using the ansatz $d_{n \geq k=1}^{\lambda} = A \cdot 2^{Bn} + C \cdot 2^{Dn} + E$ that the five parameters $\{A, \dots, E\}$ have to be fixed as $\{A = 1, B = 2, C = 3, D = 1, E = \delta_{n,1}\}$ (for $\lambda = 1$) and $\{A = 0, C = 3, D = 1, E = -5 \cdot \delta_{n,1}\}$ (for $\lambda = -1$), yielding

$$d_{n \geq k=1}^{\lambda=1} = 2^n (3 + 2^n) + \delta_{n,1}, \quad d_{n \geq k=1}^{\lambda=-1} = 3 \cdot 2^n - 5 \cdot \delta_{n,1}. \quad (377)$$

Since for $k > 1$ $d_{n \geq k \geq 1}^{\lambda=1}$ has to reduce to (377), we use the ansatz $d_{n \geq k \geq 1}^{\lambda=1} = 4^n (2^{Ak} - 1) + 3 \cdot 2^n (2^{Bk} - 1) + (2^k - 1) C + \delta_{n,1} \delta_{k,1}$ and, for instance, the data $d_{n=k=2}^{\lambda=1}$, $d_{n=3>k=2}^{\lambda=1}$ and $d_{n=4>k=2}^{\lambda=1}$ from Tab. 9 to obtain $\{A = 1/2, B = 1, C = 2\}$. The same procedure for $d_{n=k=3}^{\lambda=1}$, $d_{n=4>k=3}^{\lambda=1}$ and $d_{n=5>k=3}^{\lambda=1}$ from Tab. 9 allows us to generalize the parameters $\{A, B, C\}$ to arbitrary $k > 1$ according to $\{A = k^{-1}, B = 1, C = 2^k - 2\}$, yielding

$$d_{n \geq k \geq 1}^{\lambda=1} = 4^n + 3 \cdot 2^n (2^k - 1) + (2^k - 1) (2^k - 2) + \delta_{n=k,1}. \quad (378)$$

Similarly, for $\lambda = -1$ we use the ansatz $d_{n \geq k \geq 1}^{\lambda=-1} = 3 \cdot 2^n (2^{Ak} - 1) + 3 \cdot 2^{kB} + C - 5 \cdot \delta_{n,1} \delta_{k,1}$ and, for instance, the data $d_{n=k=2}^{\lambda=-1}$, $d_{n=3>k=2}^{\lambda=-1}$, $d_{n=4>k=2}^{\lambda=-1}$, $d_{n=k=3}^{\lambda=-1}$, $d_{n=4>k=3}^{\lambda=-1}$ and $d_{n=5>k=3}^{\lambda=-1}$ from Tab. 9 to obtain for arbitrary $k > 1$ the parameter values $\{A = k^{-1}, B = 1, C = -6\}$, i.e.

$$d_{n \geq k \geq 1}^{\lambda=-1} = 3 \cdot 2^n + 3 \cdot 2^k - 6 - 5 \cdot \delta_{n=k,1}. \quad (379)$$

(378)-(379) reduce to (377) for $k = 1$ and can be easily proven by induction. Furthermore, one also sees from Tab. 9 that for $k > n$ one has $d_{n < k}^{\lambda} = d_{n \leftrightarrow k}^{\lambda} \forall \lambda$, i.e. $d_{n < k}^{\lambda}$ follows from $d_{n'=k \geq k'=n}^{\lambda}$ by interchanging k with n in (378)-(379).

H.2.2 State structure

Implementing the QR-decomposition (358)-(362) in Appendix G (s. [23]) for IDs with mutually non-interacting E-qubits and using the environmental $\hat{u}_j^{(\phi)}$ -symmetry states $\{|s_{c_1}^L\rangle, |s_{c_2}^L\rangle\}$ from (349)-(350) in Appendix E to classify the solutions (attractor states) $\hat{X}_{\lambda,i}$ of (169) one obtains $\forall (n \geq k \geq 1)$ the following two attractor subspaces associated with the two relevant eigenvalues $\lambda \in \{1, -1\}$:

$$\left. \begin{aligned} &|0_k\rangle\langle x| \otimes |y\rangle\langle s_{c_1}^n|, |x\rangle\langle 0_k| \otimes |s_{c_1}^n\rangle\langle y| \\ &|0_k\rangle\langle 0_k| \otimes |y\rangle\langle z| \\ &|x\rangle\langle x| \otimes \bigotimes_{i=1}^n A_{\gamma_i}, |x\rangle\langle w| \otimes |s_{c_1}^n\rangle\langle s_{c_1}^n| \end{aligned} \right\} \lambda = 1, \quad (380)$$

with $|\chi_k\rangle = |\chi\rangle^{\otimes k}$, $(\chi, \gamma_i) \in \{0, 1\}$, $(x, w) \in \{0, \dots, 2^k - 1\}$, $(y, z) \in \{0, \dots, 2^n - 1\}$, $(x \neq w) \neq 0_k$, $A_0 = |s_{c_1}\rangle\langle s_{c_1}|$, $A_1 = \hat{I} - |s_{c_1}\rangle\langle s_{c_1}|$ and

$$\left. \begin{aligned} &|0_k\rangle\langle 1_k| \otimes |y\rangle\langle s_{c_2}^n|, |1_k\rangle\langle 0_k| \otimes |s_{c_2}^n\rangle\langle y| \\ &|1_k\rangle\langle 1_k| \otimes \bigotimes_{i=1}^n B_{\gamma_i}, |x\rangle\langle x| \otimes |s_{c_2}^n\rangle\langle s_{c_2}^n| \\ &|x\rangle\langle 1_k| \otimes |s_{c_1}^n\rangle\langle s_{c_2}^n|, |1_k\rangle\langle x| \otimes |s_{c_2}^n\rangle\langle s_{c_1}^n| \end{aligned} \right\} \lambda = -1, \quad (381)$$

with $x \neq (0_k, 1_k)$, $B_0 = (\sqrt{2})^{-1}(|0\rangle\langle 1| - |1\rangle\langle 0|)$, $B_1 = (\sqrt{2})^{-1}[-\sin\phi|0\rangle\langle 0| + \sin\phi|1\rangle\langle 1| + \cos\phi|0\rangle\langle 1| + \cos\phi|1\rangle\langle 0|]$. (380)-(381) are in accord with (378)-(379) and contain orthonormalized attractor states $\hat{X}_{\lambda,i}$, with $\langle \hat{X}_{\lambda,i}, \hat{X}_{\lambda',i'} \rangle := \delta_{\lambda,\lambda'}\delta_{i,i'}$, as specified by the Hilbert-Schmidt scalar product $\langle \hat{X}_{\lambda,i}, \hat{X}_{\lambda',i'} \rangle := \text{Tr} \left[\hat{X}_{\lambda,i} \left(\hat{X}_{\lambda',i'} \right)^\dagger \right]$ (s. Appendix F).

The (dimensionally) maximal $\{\lambda = 1\}$ -attractor subspace (380) follows for $n = 2 > k = 1$ and $\phi = \pi/2$ from constraints $\gg 1 \rightarrow 2\ll$ and $\gg 1 \rightarrow 3\ll$ in (371). Accordingly, one can generalize (367) to the cases $\phi = \pi/2$ and $n \geq k \geq 1$ by numerically utilizing the QR-decomposition method from section G and thus confirm (380) also for non-CNOT parameter values $\phi \neq \pi/2$ in (166)-(167) and $\left\{ |s_{c_1 \neq 1/2}^n\rangle, |s_{c_2 \neq 1/2}^n\rangle \right\}$.

Similarly, (dimensionally) maximal $\{\lambda = -1\}$ -attractor subspace (381) follows for $n = 2 > k = 1$ and $\phi = \pi/2$ from constraints $\gg 1 \rightarrow 2\ll$ and $\gg 1 \rightarrow 3\ll$ in (376). Again, one can generalize (367) to the cases $\phi = \pi/2$ and $n \geq k \geq 1$ by numerically utilizing the QR-decomposition method from section G and thus confirm (380) also for non-CNOT parameter values $\phi \neq \pi/2$ in (166)-(167) and $\left\{ |s_{c_1 \neq 1/2}^n\rangle, |s_{c_2 \neq 1/2}^n\rangle \right\}$.

H.3 Intermediate attractor spaces

In the following subsection we describe the reduction of the maximal Koenig-digraph dimension from subsection H.2 when successively increasing the number of interaction arrows ($\hat{u}_j^{(\phi)}$ -bindings) between E-qubits from one upwards.

H.3.1 Dimensionality

By implementing the QR-decomposition algorithm from Appendix G one obtains for the $\lambda = 1$ attractor subspace numerical data in Tab. 10. Furthermore one notices (ignoring the irrelevant case $n = k = 1$) that (for $n \gg k \geq 1$) $d_n^{\lambda=-1} = 0$ as soon as one introduces already a single interaction arrow ($\hat{u}_j^{(\phi)}$ -binding) between two E-qubits of the Koenig-ID from subsection H.2, i.e. with $1 \leq h \leq 2(n-1)$ denoting a number of $\hat{u}_j^{(\phi)}$ -bindings between E-qubits in Fig. 9 one obtains $d_n^{\lambda=-1, h.\text{bind}} = 0 \forall h$.

Numerical results from Tab. 10 lead us also to the following conclusions: As soon as h is sufficiently high to ensure that the entire ID has a strongly connected structure (i.e. there is a closed path of interaction-arrows between all $n \geq k$ E-qubits [11, 29, 30]), we always obtain for the corresponding $d_n^{\lambda=1, h.\text{bind}}$ the value (363) of the minimal attractor subspace in subsection H.1.

n	$d_{k=1 2 3}^{0.\text{bind.}}$	$d_{k=1 2 3}^{1.\text{bind.}}$	$d_{k=1 2 3}^{2.\text{bind.}}$	$d_{k=1 2 3}^{3.\text{bind.}}$	$d_{k=1 2 3}^{4.\text{bind.}}$
2	28 58 —	19 43 —	11 29 —	— — —	— — —
3	88 142 316	58 100 229	32 62 146	20 44 101	11 29 89
4	304 406 634	196 274 475	104 158 332	62 104 233	32 62 146
5	1120 1318 1738	712 862 1186	368 470 698	212 290 491	104 158 332
6	4288 4390 5482	2704 2854 3610	1376 1579 1994	776 926 1250	368 470 698
7	16768 17542 19114	10528 10966 12298	5312 5414 6506	2960 3110 3866	1376 1574 1994
n	$d_{k=4 5 6}^{0.\text{bind.}}$	$d_{k=4 5 6}^{1.\text{bind.}}$	$d_{k=4 5 6}^{2.\text{bind.}}$	$d_{k=4 5 6}^{3.\text{bind.}}$	$d_{k=4 5 6}^{4.\text{bind.}}$
4	1186 — —	910 — —	650 — —	479 — —	410 — —
5	2674 4930 —	1930 3802 —	1250 2738 —	926 1946 —	650 1754 —
6	7186 10978 20098	4930 7954 15538	2930 5186 11234	1994 3866 8018	1250 2738 7250
7	22354 29218 44482	14770 20098 32290	8210 12002 21122	5186 8210 15794	2930 5186 11234
n	$d_{k=4 5 6}^{5.\text{bind.}}$	$d_{k=4 5 6}^{6.\text{bind.}}$	$d_{k=4 5 6}^{7.\text{bind.}}$	$d_{k=4 5 6}^{8.\text{bind.}}$	$d_{k=4 5 6}^{9.\text{bind.}}$
4	407 — —	305 — —	— — —	— — —	— — —
5	479 1742 —	410 1322 —	407 1319 —	305 1121 —	— — —
6	926 1946 7202	650 1754 5498	479 1742 5486	410 1322 5498	407 1319 4391
7	1994 3866 8018	1250 2738 7250	926 1946 7202	650 1754 5498	479 1742 5486
n	$d_{k=4 5 6}^{10.\text{bind.}}$	$\Rightarrow d_{n \geq k}^{4.\text{bind.}} = d_{n-1 \geq k}^{2.\text{bind.}}, \dots, d_{n \geq k}^{2(n-1).\text{bind.}} = d_{n-1 \geq k}^{(2n-4).\text{bind.}}$ for $n \geq 3$			
6	305 1121 4289				
7	410 1322 4394				

Table 10: Numerical data for $d_{n \geq k}^{\lambda=1}$ from (362) in Appendix G in case of $\hat{u}_j^{(\phi)}$ -bindings between E-qubits in ID of Fig. 9.

Tab. 10 also indicates that we can avoid the strong connectedness of an ID as long as the number h of interaction-arrows in environment E has not yet reached the value²³ $2(n-1)$; After introducing the first interaction-arrow into the Koenig-ID between two arbitrary E-qubits its $d_n^{\lambda=1, 1.\text{bind}}$ (for $n \geq k + 2 \cdot \delta_{k,1}$) is, according to Tab. 10, given by (using the indicator fuction $1_{\{\bullet\}}$)

$$d_n^{\lambda=1, 1.\text{bind}} = \frac{1}{2} \left(d_{n'}^{\lambda=1, 0.\text{bind}} \cdot 1_{\{n'=n-1 \geq k\}} + d_{n'=k \geq k'=n-1}^{\lambda=1, 0.\text{bind}} \cdot 1_{\{n-1 < k\}} + d_n^{\lambda=1, 0.\text{bind}} \right), \quad (382)$$

where $d_{n' \geq k'}^{\lambda=1, h.\text{bind}}$ denotes the attractor space dimension for a k' -qubit S and an n' -qubit environment E with h interaction arrows between E-qubits. Furthermore, one also obtains numerically $d_{n=2 > k=1}^{\lambda=1, 0.\text{bind}} = 28$ and $d_{n=2 > k=1}^{\lambda=1, 1.\text{bind}} = 19$. For environment E containing more than one $\hat{u}_j^{(\phi)}$ -binding (without being strongly connected) Tab. 10 suggests that, using the arguments displayed in subsection H.2.1, the following dimension formulas hold (where $n \geq k + 2 \cdot \delta_{k,1}$, $1 \leq l \leq \lfloor \frac{2n-3}{2} \rfloor$, $1 \leq r \leq \lceil \frac{2n-3}{2} \rceil$, $\lfloor x \rfloor = \max(c \in \mathbb{N}) | c \leq x$ and $\lceil x \rceil = \min(c \in \mathbb{N}) | c \geq x$)

$$\begin{aligned} d_n^{\lambda=1, (2l+1).\text{bind}} &= \left(d_{n-l}^{\lambda=1, \delta_{l,1}.\text{bind}} \cdot 1_{\{n-l \geq k\}} \cdot \delta_{l,1} + d_{n'=k \geq k'=n-l}^{\lambda=1, \delta_{l,1}.\text{bind}} \cdot 1_{\{n-l < k\}} + 2^{2(n-l-2)} \right) \\ d_n^{\lambda=1, (2r).\text{bind}} &= \left(d_{n-r}^{\lambda=1, 0.\text{bind}} \cdot 1_{\{n-r \geq k\}} \cdot \delta_{r,1} + d_{n'=k \geq k'=n-r}^{\lambda=1, 0.\text{bind}} \cdot 1_{\{n-r < k\}} + 2^{2(n-r-2)} \right), \end{aligned} \quad (383)$$

with

$$\left. \begin{aligned} d_{n \geq 3, k=1}^{\lambda=1, h.\text{bind}} &= d_{n-1 \geq k=1}^{\lambda=1, (h-2).\text{bind}} \\ d_{n > k > 1}^{\lambda=1, h.\text{bind}} &= d_{n-1 \geq k > 1}^{\lambda=1, (h-2).\text{bind}} \end{aligned} \right\} \forall 2(n-1) \geq h > 3,$$

whereas $d_{n=2 > k=1}^{\lambda=1, 2.\text{bind}} = 11$. By means of (382)-(383) we can obtain (for arbitrary values of $n \gg k \geq 1$) dimensions of intermediate ID-attractor spaces w.r.t. $\lambda = 1$, as long as their E-interaction structure may be regarded as not strongly connected within the ranges $1 \leq l < \lfloor \frac{2n-3}{2} \rfloor$, $1 \leq r < \lceil \frac{2n-3}{2} \rceil$: however, one has to bear in mind that for fixed values $n \geq 3 \cdot \delta_{k,1}$ and $n > k > 1$ we only need to determine from (382)-(383) $d_n^{\lambda=1, h.\text{bind}}$ -values for an n -qubit environment E containing $1 < h \leq 3$ interaction-arrows (i.e. for $l = r = 1$), whereas the remaining $2n - 5$ binding-values $4 \leq h \leq 2(n-1)$ of $d_n^{\lambda=1, h.\text{bind}}$ are equal to the last $2n - 5$ binding-values $4 \leq h \leq 2(n-1)$ of $d_{n-1 \geq k}^{\lambda=1, h.\text{bind}}$ for an $(n-1)$ -qubit environment E with h interaction arrows and a k -qubit system S . To be more precise: for $n \geq 3$ and $k = 1$ it

²³Certainly, we can strongly connect n E-qubits with less than $2(n-1)$ interaction-arrows, however $2(n-1)$ is the critical number of environmental qubit-interactions for which, as indicated in Tab. 10, we will definitely obtain a strongly connected ID with a minimal attractor space dimension (363).

suffices to determine $d_{n \geq 3, k=1}^{\lambda=1, h, \text{bind}}$ from (382)-(383) for $h \in \{1, 2, 3\}$, whereas for $2(n-1) \geq h > 3$ one has $d_{n \geq 3, k=1}^{\lambda=1, h, \text{bind}} = d_{n-1 \geq k=1}^{\lambda=1, (h-2), \text{bind}}$. Accordingly, for $n \geq k > 1$ one first determines $d_{n=k>1}^{\lambda=1, h, \text{bind}} \forall (1 \leq h \leq 2(n-1))$ by means of (382)-(383). Then, for $n > k > 1$ it suffices to determine $d_{n>k>1}^{\lambda=1, h, \text{bind}}$ from (382)-(383) for $h \in \{1, 2, 3\}$, whereas for $2(n-1) \geq h > 3$ one again has $d_{n>k>1}^{\lambda=1, h, \text{bind}} = d_{n-1 \geq k>1}^{\lambda=1, (h-2), \text{bind}}$, as indicated in Tab. 10.

H.3.2 State structure

Here we explicitly determine the attractor states $\hat{X}_{\lambda=1, i}$ emerging from (169) when successively increasing the number of $\hat{u}_j^{(\phi)}$ -bindings between E-qubits such that the corresponding IDs lead to the strongly connected interaction structure only after inserting into Fig. 9 the $2(n-1)$ -th interaction arrow. In order to deduce $\hat{X}_{\lambda=1, i}$ from the underlying IDs one can readily confirm, by using the QR-decomposition, as already done within subsection H.2, a set of useful rules (illustrated by Fig. 41) that will also be applied in subsection 8.4.

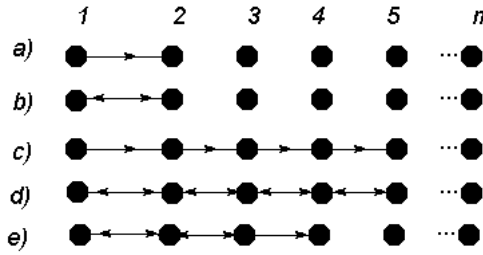


Figure 41: Typical interaction structures between $(n \gg k \geq 1)$ E-qubits of the ID in Fig. 9.

Primary and secondary E-registry states

Already after introducing into environment E a single $\hat{u}_j^{(\phi)}$ -binding (arrow) between two arbitrary qubits i and $j > i$ the $\lambda = -1$ attractor subspace from (381) vanishes, whereas the $\lambda = 1$ attractor subspace from (380) reduces to (365), however, with one important difference: as long as the interaction-structure of environment E does not correspond to a strongly connected digraph, (365) will contain, beside $|0_n\rangle$, more n -qubit E-registry states (but still less than (380), which is plausible). Then, Fig. 41 instructs us to subdivide the 2^n E-registry states into two subsets, the *primary* set $S_p \equiv \{|v\rangle\}$ and the *secondary* set $S_s \equiv \{|w\rangle\}$ (with lowest logical values²⁴ $v, w \in \{0, \dots, 2^n - 1\}$) according to the following rules:

a) of Fig. 41: S_p encloses $|v\rangle \equiv |q_1 \dots q_i \dots q_j \dots q_n\rangle$ that do not simultaneously contain the excited qubit combination $(q_i = 1 \wedge q_j = 1)$ at positions (i, j) (for example, in **a)** of Fig. 41 qubits $i = 1$ and $j = 2$ interact), and S_s encloses $|w\rangle \equiv |q_1 \dots q_i = 1 \dots q_j = 1 \dots q_n\rangle$ that do simultaneously contain the qubit combination $(q_i = 1 \wedge q_j = 1)$ at positions (i, j) ;

b) of Fig. 41: The binding pair between E-qubits q_i and q_j leads to $S_p \equiv \{|q_1 \dots q_i = 0 \dots q_j \dots q_n\rangle\}$ containing $|v\rangle$ in which the value of the i -th E-qubit is set to 0, whereas the j -th E-qubit belongs to the 2^{n-1} -dimensional subspace of E. Accordingly, $S_s \equiv \{|q_1 \dots q_i = 1 \dots q_j \dots q_n\rangle\}$ contains $|w\rangle$ in which the value of the i -th E-qubit is set to 1;

c) of Fig. 41: If there is an even number b of single $\hat{u}_j^{(\phi)}$ -bindings forming a “chain” between qubit q_i and q_j , $S_p \equiv \{|q_1 \dots q_i q_{i+1} = 0 \dots q_{i+b/2} = 0 q_{i+b/2+1} \dots q_{j-1} q_j \dots q_n\rangle\}$ contains $|v\rangle$ where the first $b/2$ qubits q_m (with $i < m < i + b/2 + 1 \leq j$) are set to 0, whereas S_s contains states $|w\rangle$ from $|q_1 \dots q_i q_{i+1} = 1 q_{i+2} = 0 \dots q_{i+b/2} = 0 q_{i+b/2+1} \dots\rangle$ to $|q_1 \dots q_i q_{i+1} = 1 \dots q_{i+b/2} = 1 q_{i+b/2+1} \dots\rangle$ in which precisely these first $b/2$ qubits q_m within the “chain” are successively set to 1;

d) of Fig. 41: If there are c $\hat{u}_j^{(\phi)}$ -binding pairs forming a “chain” between qubit q_i and q_j then the set of primary E-states $S_p \equiv \{|q_1 \dots q_{i-1} q_i = 0 \dots q_{i+c-1} = 0 q_{i+c} \dots q_j \dots q_n\rangle\}$ contains $|v\rangle$ where the first c qubits $q_{m'}$ (with $i \leq m' \leq i + c - 1 < j$) within the “chain” are set to 0, whereas the set of secondary E-states S_s contains states $|w\rangle$ from $|q_1 \dots q_{i-1} q_i = 1 q_{i+1} = 0 \dots q_{i+c-1} = 0 q_{i+c} \dots q_j \dots q_n\rangle$ to $|q_1 \dots q_{i-1} q_i = 1 \dots q_{i+c-1} = 1 q_{i+c} \dots q_j \dots q_n\rangle$ in which precisely these first c qubits $q_{m'}$ within the “chain” are successively set to 1;

²⁴The registry states $|v\rangle$ with logical values $v \in \{0, \dots, 2^n - 1\}$ of an $n \in \mathbb{N}$ qubit system are to be read in a chronological order, from left-to-right, i.e. $|v\rangle \equiv |q_1 \dots q_n\rangle = \sum_{i=1}^n q_i 2^{i-1}$, starting with qubit $q_1 \in \{0, 1\}$ and ending with qubit $q_n \in \{0, 1\}$.

e) of Fig. 41: If there is an odd number of $\hat{u}_j^{(\phi)}$ -bindings in E then one treats the even number of bindings between qubits with lowest position values i in accord with rules b)-d) and the remaining (odd) interaction arrow as in a).

This would lead in e) to $S_p \equiv \{|q_1 \dots q_{i-1} q_i = 0 \dots q_{i+c-1} = 0 \ q_{i+c} q_{i+c+1} \dots q_n\rangle\}$ containing $|v\rangle$ whose first c qubits $q_{m'}$ (with $i \leq m' \leq i+c-1 < n$) within the “chain” of c binding pairs are set to 0 and between qubits q_{i+c} and q_{i+c+1} interacting via the remaining arrow the simultaneously excited combination ($q_{i+c} = 1 \wedge q_{i+c+1} = 1$) is not allowed. Accordingly, the set of secondary E-states S_s would contain $|w\rangle$ from $|\dots q_{i-1} q_i = 1 \ q_{i+1} = 0 \dots q_{i+c-1} = 0 \ q_{i+c} \dots q_j \dots q_n\rangle$ to $|\dots q_{i-1} q_i = 1 \dots q_{i+c-1} = 1 \ q_{i+c} = 1 \ q_{i+c+1} = 1 \ q_{i+c+2} \dots q_n\rangle$ with the first c qubits $q_{m'}$ within the “chain” of binding pairs successively being set to 1 before considering those states $|w\rangle$ involving explicitly the least preferred qubit combination ($q_{i+c} = 1 \wedge q_{i+c+1} = 1$).

$d_{n \gg k}^{\lambda=1, h, \text{bind}}$, S_p , S_s and $\hat{X}_{\lambda=1, i}$ from Fig. 41

The intermediate attractor space for E, with mutually interacting qubits as in Fig. 41, also contains states $|x\rangle \langle x| \otimes \hat{I}_n$ ($2^k \times$) and $|x\rangle \langle y| \otimes |s_{c_1}^n\rangle \langle s_{c_1}^n|$ ($2^{2k} \times$, with $x, y \in \{0, \dots, 2^k - 1\}$), however, contrary to (365), we use beside $|0_n\rangle$ $m \leq |S_p| = 2^n - |S_s|$ primary registry states $|v\rangle$ of E within

$$\begin{aligned} & \mathbf{A}) |0_k\rangle \langle 0_k| \otimes |v\rangle \langle v|; \mathbf{B}) |0_k\rangle \langle 0_k| \otimes |v\rangle \langle v' \neq v| \\ & \mathbf{C}) |0_k\rangle \langle x' \neq 0_k| \otimes |v\rangle \langle s_{c_1}^n|, |x' \neq 0_k\rangle \langle 0_k| \otimes |s_{c_1}^n\rangle \langle v|; \mathbf{D}) |0_k\rangle \langle 0_k| \otimes |v\rangle \langle s_{c_1}^n|, |0_k\rangle \langle 0_k| \otimes |s_{c_1}^n\rangle \langle v| \end{aligned} \quad (384)$$

(with lowest logical values $v, v' \in \{0, \dots, 2^n - 1\}$) until $d_{n \gg k}^{\lambda=1, h, \text{bind}}$ (with $1 \leq h \leq 2(n-1)$) is reached. Since in (384) A) offers m states $\hat{X}_{\lambda=1, i}$, B) offers $m(m-1)$ states $\hat{X}_{\lambda=1, i}$, C) offers $2m(2^k - 1)$ states $\hat{X}_{\lambda=1, i}$ and D) offers $2m$ states $\hat{X}_{\lambda=1, i}$, we first determine a minimal number $m_{\min} \in \mathbb{N}$ of primary registry states $|v\rangle$ such that

$$r_{\min} = d_{n \gg k}^{\lambda=1, h, \text{bind}} - (m_{\min}^2 + 2^{k+1} m_{\min} + 2^k (2^k + 1)) \geq 0$$

is minimal. If $r_{\min} = 0$, then all $d_{n \gg k}^{\lambda=1, h, \text{bind}}$ attractor states in (384) with m_{\min} E-registry states $S_p^{m_{\min}} \equiv \{|v_1\rangle, \dots, |v_{m_{\min}}\rangle\} \subset S_p$ and their lowest logical values $v_i \in 2^n$ are determined in accord with the above ID-rules from Fig. 41. Otherwise, for $r_{\min} > 0$ we apply at the remaining primary registry states $S_p \setminus S_p^{m_{\min}} \equiv \{|\xi_{m_{\min}+1}\rangle, \dots, |\xi_{|S_p|}\rangle\} \subset S_p$ (with $\xi_i < \xi_{i+1} \forall i \in \{m_{\min} + 1, \dots, |S_p| - 1\}$) the following algorithm which fixes the priority with which attractor state structures in (384) are being filled with additional r_{\min} $|\xi_i\rangle$ -registry states with lowest logical values $\xi_i \in \{0, \dots, 2^n - 1\}$ (whose qubit structure is specified by the ID-rules of Fig. 41):

Start with $|v\rangle = |\xi_{p=m_{\min}+1}\rangle$. If there are highest (odd or even) non-zero values $\{r_{\text{even}}(p) \leq r_{\min}, r_{\text{odd}}(p) \leq r_{\min}\}$ such that

I) $r_{\min} = r_{\text{odd}}(p = m_{\min} + 1) = 1 \Rightarrow$ associate A) with $|v\rangle = |\xi_{p=m_{\min}+1}\rangle$.

II) $r_{\min} \geq 2 \Rightarrow$ associate $|v\rangle = |\xi_{p=m_{\min}+1}\rangle$ successively with structures A), C), D) and B) $\equiv \{|0_k\rangle \langle 0_k| \otimes |\xi_{m+1}\rangle \langle \xi_l|, |0_k\rangle \langle 0_k| \otimes |\xi_l\rangle \langle \xi_{m+1}\rangle\}$ ($l \in \{1, \dots, i\}$ with $i \in \{1, \dots, p-1\}$), such that the priority of filling structures in (384) with $|\xi_{p=m_{\min}+1}\rangle$ ranges in a descending order from 1) A) over 2) C) and 3) D) to 4) B). This leads to $r_{\text{even}}(p = m_{\min} + 1)$ or $r_{\text{odd}}(p = m_{\min} + 1)$.

- If $r_{\text{even}}(p = m_{\min} + 1) = r_{\min}$ or $r_{\text{odd}}(p = m_{\min} + 1) = r_{\min}$ we are done.

- If $r_{\text{even}}(p = m_{\min} + 1) < r_{\min}$ or $r_{\text{odd}}(p = m_{\min} + 1) < r_{\min}$, associate further $|v\rangle = |\xi_{p > m_{\min}+1}\rangle$ in a descending order with A), C), D) and B). This yields $r_{\text{even}}(p > m_{\min} + 1) < r_{\min}$ or $r_{\text{odd}}(p > m_{\min} + 1) < r_{\min}$. Repeat this procedure for primary states $|\xi_p\rangle \in \{|\xi_{m_{\min}+2}\rangle, \dots, |\xi_{|S_p|}\rangle\}$ until $\{r_{\text{even}}(p), r_{\text{odd}}(p)\}$ satisfy $\forall p$ the identity

$$\sum_{p=m_{\min}+1}^{g \leq |S_p|} [r_{\text{even}}(p) + r_{\text{odd}}(p)] = r_{\min} \text{ with } (m_{\min} + 1 \leq p \leq g \leq |S_p|). \text{ Remark: in C) } |v\rangle = |\xi_{p \geq m_{\min}+1}\rangle \text{ occupies subspaces } |x' \neq 0 \equiv 0_k\rangle \langle 0_k| \text{ and } |0_k\rangle \langle x' \neq 0 \equiv 0_k| \text{ of open system } S \text{ in a descending order, from } x' = 2^k - 1 \text{ to } x' = 1.$$

Thus, we always start with the lowest logical value $\xi_{p=m_{\min}+1}$ allowed by ID-rules in Fig. 41 and determine the highest non-zero values $\{r_{\text{even}}(p), r_{\text{odd}}(p)\} \forall p$ with $m_{\min} + 1 \leq p \leq g \leq |S_p|$ (such that the priority of filling structures in (384) with the registry state $|\xi_{p \geq m_{\min}+1}\rangle$ ranges in descending order from A) over C) and D) to B)), until, for a specific

$$p = g \leq |S_p|, \text{ one is led to } \sum_{p=m_{\min}+1}^{g \leq |S_p|} [r_{\text{even}}(p) + r_{\text{odd}}(p)] = r_{\min}.$$

If we cannot obtain r_{\min} even for $p = g = |S_p|$, we need to introduce into (384) secondary registry states of E from S_s in the following manner: among $|S_s|$ secondary E-registry states $\{|\chi_1\rangle, \dots, |\chi_{|S_s|}\rangle\} \in S_s$ we first determine a subset of $(t_{\min} \in \mathbb{N}_0) < |S_s|$ $|\chi_i\rangle$ with lowest logical values χ_i allowed by ID-rules of Fig. 41, such that

$$r_{\min}^{t_{\min}} = d_{n \gg k}^{\lambda=1, h, \text{bind}} - (|S_p|^2 + 2^{k+1} |S_p| + 2^k (2^k + 1) + t_{\min}^2 + 2^{k+1} t_{\min}) \geq 0$$

is minimal. This means: we first connect the t_{\min} registry states $|\chi_i\rangle$ among each other in accord with steps I-II) of the above algorithm. If this does not suffice to achieve $r_{\min}^{t_{\min}}$, we connect (in accord with step II) of the above algorithm) the t_{\min} registry states $|\chi_i\rangle$ with the lowest primary states $|\nu_i\rangle$ from $S_p^{m_{\min}} \subset S_p$ within the structure **B**) in (384). Finally, if we still need $|\chi_i\rangle \in S_s$ to achieve $r_{\min}^{t_{\min}}$, we use successively new lowest $|\chi_j\rangle$ with $j > t_{\min}$ to connect them first with other $\{|\chi_1\rangle, \dots, |\chi_{j-1}\rangle\}$ and then with the lowest primary states $|\nu_i\rangle \in S_p$ in accord with steps I-II) of the above algorithm. Eventually, by continuing this procedure we will reach $r_{\min}^{t_{\min}}$.

We end this subsection by discussing brief examples for the application of the above algorithm that will be relevant in subsection 8.4. The results of the forthcoming **Examples 1-5** can be also obtained by numerically implementing the QR-decomposition method from section G.

Example 1: $k = 1, n = 2$

1) One $\hat{u}_j^{(\phi)}$ -binding between qubits q_1 and q_2 as in **a**) of Fig. 41, $d_{n=2}^{\lambda=1, 1.\text{bind}} = 19$ (s. Tab. 10 and (382)-(383)): There are $|S_p| = 2^n - |S_s| = 2^n - 2^{n-2} = 3$ primary E-registry states $S_p \equiv \{|00\rangle, |10\rangle, |01\rangle\}$. Since distributing the first two S_p -registry states ($m_{\min} = 2$) over all structures **A**)-**D**) in (384) (and including structures $|\chi\rangle \langle \chi| \otimes \hat{I}_n (2\times)$ and $|\chi\rangle \langle y| \otimes |s_{c_1}^n\rangle \langle s_{c_1}^n| (4\times)$) one obtains $2^2 + 2 \cdot 2 + 2 \cdot 2 + 2 + 4 = 18 < 19$ ($r_{\min} = 1$), we do not have to introduce secondary E-registry states. Instead, it suffices to use the remaining primary E-registry state $|01\rangle$ in S_p in the form $|0_k\rangle \langle 0_k| \otimes |01\rangle \langle 01|$ to attain the desired dimension value $d_{n=2}^{\lambda=1, 1.\text{bind}} = 19$. These results follow also from the constraints $\gg 1 \rightarrow 2\ll, \gg 1 \rightarrow 3\ll$ and $\gg 2 \rightarrow 3\ll$ in (371) or by numerically implementing the QR-decomposition method from section G.

2) Two $\hat{u}_j^{(\phi)}$ -bindings as a binding-pair between qubits q_1 and q_2 , s. **b**) of Fig. 41, $d_{n=2}^{\lambda=1, 2.\text{bind}} = 11$ (s. Tab. 10 and (382)-(383)): we obtain a strongly connected ID and its minimal attractor space from (365).

Example 2: $k = 1, n = 3$

1) One $\hat{u}_j^{(\phi)}$ -binding between qubits q_1 and q_2 as in **a**) of Fig. 41, $d_{n=3}^{\lambda=1, 1.\text{bind}} = 58$ (s. Tab. 10 and (382)-(383)): There are $|S_p| = 2^n - |S_s| = 2^n - 2^{n-2} = 6$ primary E-registry states $S_p \equiv \{|000\rangle, |100\rangle, |010\rangle, |110\rangle, |001\rangle, |101\rangle\}$. Since distributing the first five lowest S_p -registry states ($m_{\min} = 5$) over all structures **A**)-**D**) in (384) (and including structures $|\chi\rangle \langle \chi| \otimes \hat{I}_n (2\times)$ and $|\chi\rangle \langle y| \otimes |s_{c_1}^n\rangle \langle s_{c_1}^n| (4\times)$) one obtains $5^2 + 2 \cdot 5 + 2 \cdot 5 + 2 + 4 = 51 < 58$ ($r_{\min} = 7$), we do not have to introduce secondary E-registry states. Instead, it suffices to use the remaining primary E-registry state $|\nu\rangle = |101\rangle$ from S_p in **A**), **C**) and **D**) of (384) (5 states) and in **B**) from (384) in the form $\{|0_k\rangle \langle 0_k| \otimes |101\rangle \langle 000|, |0_k\rangle \langle 0_k| \otimes |000\rangle \langle 101|\}$ to attain $d_{n=3}^{\lambda=1, 1.\text{bind}} = 58$.

2) Two $\hat{u}_j^{(\phi)}$ -bindings as a binding-pair between qubits q_1 and q_2 , s. **b**) of Fig. 41, $d_{n=3}^{\lambda=1, 2.\text{bind}} = 32$ (s. Tab. 10 and (382)-(383)): This time we have $|S_p| = 4$ related with $S_p \equiv \{|0q_2q_3\rangle\}$, from which only the first three lowest E-states $\{|000\rangle, |010\rangle, |001\rangle\}$ (i.e. $m_{\min} = 3$) enter into (384) and (together with $|\chi\rangle \langle \chi| \otimes \hat{I}_n (2\times)$ and $|\chi\rangle \langle y| \otimes |s_{c_1}^n\rangle \langle s_{c_1}^n| (4\times)$) yield $3^2 + 2 \cdot 3 + 2 \cdot 3 + 2 + 4 = 27$, alias $r_{\min} = 32 - 27 = 5$. We do not have to introduce secondary E-registry states. Instead, it suffices to use the remaining primary E-registry state $|\nu\rangle = |011\rangle$ from S_p in **A**), **C**) and **D**) of (384) (5 states) to attain $d_{n=3}^{\lambda=1, 2.\text{bind}} = 32$.

3) One $\hat{u}_j^{(\phi)}$ -binding-pair between qubits q_1 and q_2 and one $\hat{u}_j^{(\phi)}$ -binding between qubits q_2 and q_3 , s. **e**) of Fig. 41, $d_{n=3}^{\lambda=1, 3.\text{bind}} = 20$ (s. Tab. 10 and (382)-(383)): Now we have $m_{\min} = 2$ with a set of primary E-registry states $S_p \equiv \{|000\rangle, |010\rangle, |001\rangle\}$ from which only the first two lowest states enter into (384) and (together with $|\chi\rangle \langle \chi| \otimes \hat{I}_n (2\times)$ and $|\chi\rangle \langle y| \otimes |s_{c_1}^n\rangle \langle s_{c_1}^n| (4\times)$) yield $2^2 + 2 \cdot 2 + 2 \cdot 2 + 2 + 4 = 18$, alias $r_{\min} = 20 - 18 = 2$. The remaining two E-states are constructed from the third primary E-state $|001\rangle$ in S_p and the corresponding lowest secondary E-state $|100\rangle$ using the forms $\{|0_k\rangle \langle 0_k| \otimes |\nu_i\rangle \langle \nu_i|\}$ with $|\nu_i\rangle \in \{|001\rangle, |100\rangle\}$. The lowest secondary E-state has to be used, since inserting the third highest primary E-state into **C**) of (384) would lead to additional two states and thus overestimate the desired dimension value $d_{n=3}^{\lambda=1, 3.\text{bind}} = 20$.

4) Two $\hat{u}_j^{(\phi)}$ -binding-pairs between qubits q_1 and q_2 and q_2 and q_3 , s. **d**) of Fig. 41, $d_{n=3}^{\lambda=1, 4.\text{bind}} = 11$ (s. Tab. 10 and (382)-(383)): we obtain a strongly connected ID and its minimal attractor space from (365).

Example 3: $k = 1, n = 4$

1) One $\hat{u}_j^{(\phi)}$ -binding between qubits q_1 and q_2 as in **a**) of Fig. 41, $d_{n=4}^{\lambda=1, 1.\text{bind}} = 196$ (s. Tab. 10 and (382)-(383)): There are $|S_p| = 2^n - |S_s| = 2^n - 2^{n-2} = 12$ primary E-registry states $S_p \equiv \{|00q_3q_4\rangle, |10q_3q_4\rangle, |01q_3q_4\rangle\}$ and 2^2 secondary E-registry states $S_s \equiv \{|11q_3q_4\rangle\}$ (with $q_i \in \{0, 1\}$, $i \in \{3, 4, 5\}$). Distributing the first 11 lowest S_p -states ($m_{\min} = 11$) over all structures **A**)-**D**) in (384) (and including structures $|\chi\rangle \langle \chi| \otimes \hat{I}_n (2\times)$ and $|\chi\rangle \langle y| \otimes |s_{c_1}^n\rangle \langle s_{c_1}^n| (4\times)$) yields $11^2 + 2 \cdot 11 + 2 \cdot 11 + 2 + 4 = 171 < 196$ ($r_{\min} = 21$). The remaining attractor states are constructed from the

highest primary E-registry state $|v\rangle = |0111\rangle$ within **A**), **C**) and **D**) of (384) (5 states), as well as within **B**) of (384) with $\{|0_k\rangle\langle 0_k| \otimes |v\rangle\langle v| \mid v' \neq v\}$ and $|v'\rangle$ representing the eight lowest E-states in S_p .

2) Two $\hat{u}_j^{(\phi)}$ -bindings as a binding-pair between qubits q_1 and q_2 , s. **b**) of Fig. 41, $d_{n=4}^{\lambda=1,2,\text{bind}} = 104$ (s. Tab. 10 and (382)-(383)): This time we have $m_{\min} = |S_p| = 8$ related with $S_p \equiv \{|0q_2q_3q_4\rangle\}$ and all 8 lowest primary E-states that enter into (384) and (together with $|x\rangle\langle x| \otimes \hat{I}_n(2\times)$ and $|x\rangle\langle y| \otimes |s_{c_1}^n\rangle\langle s_{c_1}^n| (4\times)$) yield $8^2 + 2 \cdot 8 + 2 \cdot 8 + 2 + 4 = 102$, alias $r_{\min} = 104 - 102 = 2$. To construct the remaining two attractor states we need two lowest secondary E-states $S_s \equiv \{|1000\rangle, |1100\rangle\}$ within **A**) of (384) with $\{|0_k\rangle\langle 0_k| \otimes |v\rangle\langle v| \mid v \in S_s\}$ and $|v\rangle \in S_s$.

3) One $\hat{u}_j^{(\phi)}$ -binding-pair between qubits q_1 and q_2 and one $\hat{u}_j^{(\phi)}$ -binding between qubits q_2 and q_3 , s. **e**) of Fig. 41, $d_{n=4}^{\lambda=1,3,\text{bind}} = 62$ (s. Tab. 10 and (382)-(383)): Now we have $m_{\min} = 5 < |S_p| = 6$ with a set of primary E-registry states $S_p \equiv \{|000q_4\rangle, |010q_4\rangle, |001q_4\rangle\}$, from which only the lowest 5 E-states enter into (384) and (together with $|x\rangle\langle x| \otimes \hat{I}_n(2\times)$ and $|x\rangle\langle y| \otimes |s_{c_1}^n\rangle\langle s_{c_1}^n| (4\times)$) yield $5^2 + 2 \cdot 5 + 2 \cdot 5 + 2 + 4 = 51$, alias $r_{\min} = 62 - 51 = 11$. The remaining highest primary E-state in S_p , $|v\rangle = |0011\rangle$, is used within **A**), **C**) and **D**) of (384) (5 states), before we correlate it with the three lowest S_p -states of E, $|v'\rangle \in \{|0000\rangle, |0100\rangle, |0010\rangle\}$, within $\{|0_k\rangle\langle 0_k| \otimes |v\rangle\langle v| \mid v' \neq v\}$ of **B**) in (384) (6 attractor states).

4) Two $\hat{u}_j^{(\phi)}$ -binding-pairs between qubits q_1 and q_2 and q_2 and q_3 , s. **d**) of Fig. 41, $d_{n=4}^{\lambda=1,4,\text{bind}} = 32$ (s. Tab. 10 and (382)-(383)): Now we have $m_{\min} = 3 < |S_p| = 4$ with $S_p \equiv \{|00q_3q_4\rangle\}$, from which only the first three lowest E-states enter into (384) and (together with $|x\rangle\langle x| \otimes \hat{I}_n(2\times)$ and $|x\rangle\langle y| \otimes |s_{c_1}^n\rangle\langle s_{c_1}^n| (4\times)$) yield $3^2 + 2 \cdot 3 + 2 \cdot 3 + 2 + 4 = 27$, alias $r_{\min} = 32 - 27 = 5$. To construct the remaining 5 attractor states we simply insert the highest S_p -state $|0011\rangle$ into **A**), **C**) and **D**) of (384) (5 states). There is no need for the structure **B**) of (384). Apparently, this attractor space contains the attractor space from **Example 2** above with $d_{n=3}^{\lambda=1,2,\text{bind}} = 32$ as a subspace because of its specific ID-structure similar to the one discussed w.r.t. $d_{n=2}^{\lambda=1,2,\text{bind}} = 32$ of **Example 2**.

5) Two $\hat{u}_j^{(\phi)}$ -binding-pairs between qubits (q_1, q_2) and (q_2, q_3) and one $\hat{u}_j^{(\phi)}$ -binding between q_3 and q_4 , s. **e**) of Fig. 41, $d_{n=4}^{\lambda=1,5,\text{bind}} = 20$ (s. Tab. 10 and (382)-(383)): This time we have $m_{\min} = 2 < |S_p| = 3$ with $S_p \equiv \{|00q_3q_4\rangle\} \setminus \{|0011\rangle\}$, from which two lowest E-states enter into (384) and (together with $|x\rangle\langle x| \otimes \hat{I}_n(2\times)$ and $|x\rangle\langle y| \otimes |s_{c_1}^n\rangle\langle s_{c_1}^n| (4\times)$) yield $2^2 + 2 \cdot 2 + 2 \cdot 2 + 2 + 4 = 18$, alias $r_{\min} = 20 - 18 = 2$. The remaining two attractor-states are constructed by inserting the third highest S_p -state $|0001\rangle$ and the lowest secondary E-state $|1000\rangle$ into **A**) of (384) with $\{|0_k\rangle\langle 0_k| \otimes |v\rangle\langle v| \mid v \in \{|1000\rangle, |0001\rangle\}\}$ (two attractor states). Apparently, this attractor space contains the attractor space from **Example 2** above with $d_{n=3}^{\lambda=1,3,\text{bind}} = 20$ as a subspace because of its specific ID-structure similar to the one discussed w.r.t. $d_{n=3}^{\lambda=1,3,\text{bind}} = 20$ of **Example 2**.

6) Three $\hat{u}_j^{(\phi)}$ -binding-pairs between qubits (q_1, q_2) , (q_2, q_3) and (q_3, q_4) , s. **d**) of Fig. 41, $d_{n=4}^{\lambda=1,6,\text{bind}} = 11$ (s. Tab. 10 and (382)-(383)): we obtain a strongly connected ID and its minimal attractor space from (365).

Example 4: $k = 1, n = 5$

1) One $\hat{u}_j^{(\phi)}$ -binding between qubits q_1 and q_2 as in **a**) of Fig. 41, $d_{n=5}^{\lambda=1,1,\text{bind}} = 712$ (s. Tab. 10 and (382)-(383)): There are $|S_p| = 2^n - |S_s| = 2^n - 2^{n-2} = 24$ primary E-registry states $S_p \equiv \{|00q_3q_4q_5\rangle, |10q_3q_4q_5\rangle, |01q_3q_4q_5\rangle\}$ and 2^3 secondary E-registry states $S_s \equiv \{|11q_3q_4q_5\rangle\}$ (with $q_i \in \{0, 1\}$, $i \in \{3, 4, 5\}$). Since distributing all of the $m_{\min} = 24$ S_p -registry states over all structures **A**)-**D**) in (384) (and including structures $|x\rangle\langle x| \otimes \hat{I}_n(2\times)$ and $|x\rangle\langle y| \otimes |s_{c_1}^n\rangle\langle s_{c_1}^n| (4\times)$) one obtains $24^2 + 2 \cdot 24 + 2 \cdot 24 + 2 + 4 = 678 < 712$ ($r_{\min} = 34$), we have to introduce secondary E-registry states. Since $t_{\min} = 4$, we have, according to the above algorithm, a secondary attractor subspace of dimension $4^2 + 2 \cdot 4 + 2 \cdot 4 = 32$ ($r_{\min}^{t_{\min}} = 2$) associated with structures **A**)-**D**) in (384) and E-registry states $S_s^{t_{\min}} \equiv \{|11000\rangle, |11100\rangle, |11010\rangle, |11110\rangle\} \subset S_s$. The remaining 2 states of the attractor space correspond, according to the above algorithm, to the structures $\{|0_k\rangle\langle 0_k| \otimes |11000\rangle\langle 0_5|, |0_k\rangle\langle 0_k| \otimes |0_5\rangle\langle 11000|\}$ from **B**) in (384) that “connect” states $|0_5\rangle$ and $|11000\rangle$ with lowest logical values in S_p and $S_s^{t_{\min}}$, respectively.

2) Two $\hat{u}_j^{(\phi)}$ -bindings as a binding-pair between qubits q_1 and q_2 , s. **b**) of Fig. 41, $d_{n=5}^{\lambda=1,2,\text{bind}} = 368$ (s. Tab. 10 and (382)-(383)): This time we have $m_{\min} = |S_p| = 16$ related with $S_p \equiv \{|0q_2q_3q_4q_5\rangle\}$ that enter into (384) and (together with $|x\rangle\langle x| \otimes \hat{I}_n(2\times)$ and $|x\rangle\langle y| \otimes |s_{c_1}^n\rangle\langle s_{c_1}^n| (4\times)$) yield $16^2 + 2 \cdot 16 + 2 \cdot 16 + 2 + 4 = 326$, alias $r_{\min} = 368 - 312 = 42$. We again need secondary E-registry states from $S_s \equiv \{|1q_2q_3q_4q_5\rangle\}$, and since $t_{\min} = 4$, we need 4 of them with the lowest logical value, i.e. $S_s^{t_{\min}} \equiv \{|10000\rangle, |11000\rangle, |10100\rangle, |11100\rangle\} \subset S_s$. Associating the four secondary $S_s^{t_{\min}}$ -states with (384) we obtain a secondary attractor subspace with $4^2 + 2 \cdot 4 + 2 \cdot 4 = 32$ additional states (i.e. $r_{\min}^{t_{\min}} = 10$). The remaining 10 attractor states correspond to structures $\{|0_k\rangle\langle 0_k| \otimes |10000\rangle\langle v_i|, |0_k\rangle\langle 0_k| \otimes |v_i\rangle\langle 10000|\}$ from **B**) in (384) that “connect” the lowest state $|10000\rangle \in S_s^{t_{\min}}$ with the first five states $|v_i\rangle \in S_p$ ($i \in \{1, \dots, 5\}$) with lowest logical values v_i .

3) One $\hat{u}_j^{(\phi)}$ -binding-pair between qubits q_1 and q_2 and one $\hat{u}_j^{(\phi)}$ -binding between qubits q_2 and q_3 , s. **e**) of

Fig. 41, $d_{n=5}^{\lambda=1,3,\text{bind}} = 212$ (s. Tab. 10 and (382)-(383)): Now we have $m_{\min} = |S_p| = 12$ with a set of primary E-registry states $S_p \equiv \{|000q_4q_5\rangle, |010q_4q_5\rangle, |001q_4q_5\rangle\}$ that enter into (384) and (together with $|x\rangle \langle x| \otimes \hat{I}_n (2\times)$ and $|x\rangle \langle y| \otimes |s_{c_1}^n\rangle \langle s_{c_1}^n| (4\times)$) yield $12^2 + 2 \cdot 12 + 2 \cdot 12 + 2 + 4 = 198$, alias $r_{\min} = 212 - 198 = 14$. With $S_s \equiv \{|1q_2q_3q_4q_5\rangle\}$ and $t_{\min} = 2$ we distribute $S_s^{t_{\min}} \equiv \{|10000\rangle, |11000\rangle\} \subset S_s$ within (384), obtaining additional $2^2 + 2 \cdot 2 + 2 \cdot 2 = 12$ secondary E-registry states. Since $r_{\min}^{t_{\min}} = 2$ the remaining two attractor states correspond to structures $\{|0_k\rangle \langle 0_k| \otimes |10000\rangle \langle 0_n|, |0_k\rangle \langle 0_k| \otimes |0_n\rangle \langle 10000|\}$ from **B**) in (384) that “connect” the lowest state $|10000\rangle \in S_s^{t_{\min}}$ with $|0_n\rangle \in S_p$.

4) Two $\hat{u}_j^{(\phi)}$ -binding-pairs between qubits q_1 and q_2 and q_2 and q_3 , s. **d**) of Fig. 41, $d_{n=5}^{\lambda=1,4,\text{bind}} = 104$ (s. Tab. 10 and (382)-(383)): Now we have $m_{\min} = |S_p| = 8$ with $S_p \equiv \{|00q_3q_4q_5\rangle\}$ that enter into (384) and (together with $|x\rangle \langle x| \otimes \hat{I}_n (2\times)$ and $|x\rangle \langle y| \otimes |s_{c_1}^n\rangle \langle s_{c_1}^n| (4\times)$) yield $8^2 + 2 \cdot 8 + 2 \cdot 8 + 2 + 4 = 102$, alias $r_{\min} = 104 - 102 = 2$. According to the above algorithm $t_{\min} = 0$ and we have to use the two lowest secondary states $|v_i\rangle \in \{|10000\rangle, |01000\rangle\}$ from $S_s \equiv \{|10q_3q_4q_5\rangle, |01q_3q_4q_5\rangle, |11q_3q_4q_5\rangle\}$ and associate them with $\{|0_k\rangle \langle 0_k| \otimes |v_i\rangle \langle v_i|\}$ from **A**) in (384).

5) Two $\hat{u}_j^{(\phi)}$ -binding-pairs between qubits (q_1, q_2) and (q_2, q_3) and one $\hat{u}_j^{(\phi)}$ -binding between q_3 and q_4 , s. **e**) of Fig. 41, $d_{n=5}^{\lambda=1,5,\text{bind}} = 62$ (s. Tab. 10 and (382)-(383)): This time we have $m_{\min} = 5 < |S_p| = 6$ with E-states $S_p^{m_{\min}} \equiv S_p \setminus \{|00011\rangle\}$ (and $S_p \equiv \{|0000q_5\rangle, |0010q_5\rangle, |0001q_5\rangle\}$) that enter into (384) and (together with $|x\rangle \langle x| \otimes \hat{I}_n (2\times)$ and $|x\rangle \langle y| \otimes |s_{c_1}^n\rangle \langle s_{c_1}^n| (4\times)$) yield $5^2 + 2 \cdot 5 + 2 \cdot 5 + 2 + 4 = 51$, alias $r_{\min} = 62 - 51 = 11$. According to the above algorithm we have to use the sixth lowest E-registry state from S_p , $|00011\rangle$, first within structures **A**), **C**) and **D**) in (384) (which yields $1^2 + 2 \cdot 1 + 2 \cdot 1 = 5$ additional primary attractor states) and then recover the remaining 6 attractor states from **B**) in (384) by associating $|00011\rangle$ within $\{|0_k\rangle \langle 0_k| \otimes |00011\rangle \langle v_i|, |0_k\rangle \langle 0_k| \otimes |v_i\rangle \langle 00011|\}$ with $i \in \{1, 2, 3\}$ and the first 3 lowest E-registry states $|v_i\rangle$ from $S_p^{m_{\min}}$, namely $|00000\rangle, |00100\rangle$ and $|00010\rangle$.

6) Three $\hat{u}_j^{(\phi)}$ -binding-pairs between qubits (q_1, q_2) , (q_2, q_3) and (q_3, q_4) , s. **d**) of Fig. 41, $d_{n=5}^{\lambda=1,6,\text{bind}} = 32$ (s. Tab. 10 and (382)-(383)): Due to $m_{\min} = 3 < |S_p| = 4$, $S_p^{m_{\min}} \equiv S_p \setminus \{|00011\rangle\}$ (and $S_p \equiv \{|000q_4q_5\rangle\}$), 3 primary E-registry states enter into (384) and (together with $|x\rangle \langle x| \otimes \hat{I}_n (2\times)$ and $|x\rangle \langle y| \otimes |s_{c_1}^n\rangle \langle s_{c_1}^n| (4\times)$) yield $3^2 + 2 \cdot 3 + 2 \cdot 3 + 2 + 4 = 27$, alias $r_{\min} = 32 - 27 = 5$. These remaining 5 attractor states are obtained by associating the fourth lowest primary E-registry state $|v\rangle = |00011\rangle$ from S_p with structures **A**), **C**) and **D**) in (384), since then one obtains precisely $1^2 + 2 \cdot 1 + 2 \cdot 1 = 5$ additional attractor states.

7) Three $\hat{u}_j^{(\phi)}$ -binding-pairs between qubits (q_1, q_2) , (q_2, q_3) and (q_3, q_4) and a $\hat{u}_j^{(\phi)}$ -binding between q_5 and q_6 , s. **d**) and **e**) of Fig. 41, $d_{n=5}^{\lambda=1,7,\text{bind}} = 20$ (s. Tab. 10 and (382)-(383)): Since $m_{\min} = 2 < |S_p| = 3$, $S_p \equiv \{|000q_4q_5\rangle\} \setminus \{|00011\rangle\}$, 2 primary E-registry states $\{|00000\rangle, |00010\rangle\}$ enter into (384) and (together with $|x\rangle \langle x| \otimes \hat{I}_n (2\times)$ and $|x\rangle \langle y| \otimes |s_{c_1}^n\rangle \langle s_{c_1}^n| (4\times)$) yield $2^2 + 2 \cdot 2 + 2 \cdot 2 + 2 + 4 = 20$, alias $r_{\min} = 20 - 18 = 2$. The remaining two states are $\{|0_k\rangle \langle 0_k| \otimes |v_i\rangle \langle v_i|\}$ with $|v_i\rangle \in \{|00001\rangle, |10000\rangle\}$, where $|10000\rangle$ denotes the lowest secondary E-state.

8) Four $\hat{u}_j^{(\phi)}$ -binding-pairs between qubits (q_1, q_2) , (q_2, q_3) , (q_3, q_4) and (q_4, q_5) , s. **d**) of Fig. 41, $d_{n=5}^{\lambda=1,8,\text{bind}} = d_{n=5}^{\lambda=1,\text{min}} = 11$ (s. Tab. 10 and (382)-(383)): The ID is strongly connected with $2(n-1) = 8$ bindings, ergo its dimensionality is already minimal, corresponding to the minimal attractor space (365) with only one relevant primary E-registry state, namely $|0_n\rangle$. This example also shows that already after introducing a single interaction arrow between E-qubits in Fig. 9 the least preferred E-registry state $|1_n\rangle$ always remains secondary and does not contribute to $d_{n \gg k}^{\lambda=1}$ of intermediate (and minimal) attractor spaces, whereas $|0_n\rangle$ participates, being always a primary E-registry state, in all (maximal, minimal and intermediate) attractor spaces.

Example 5: $k = 2, n = 5$

1) One $\hat{u}_j^{(\phi)}$ -binding between qubits q_1 and q_2 as in **a**) of Fig. 41, $d_{n=5}^{\lambda=1,1,\text{bind}} = 862$ (s. Tab. 10 and (382)-(383)): There are $|S_p| = 2^n - |S_s| = 2^n - 2^{n-2} = 24$ primary E-registry states $S_p \equiv \{|00q_3q_4q_5\rangle, |10q_3q_4q_5\rangle, |01q_3q_4q_5\rangle\}$ and 2^3 secondary E-registry states $S_s \equiv \{|11q_3q_4q_5\rangle\}$ (with $q_i \in \{0, 1\}$, $i \in \{3, 4, 5\}$). Since distributing all of the $m_{\min} = 24$ S_p -registry states over all structures **A**)-**D**) in (384) (and including structures $|x\rangle \langle x| \otimes \hat{I}_n (2^{k-2}\times)$ and $|x\rangle \langle y| \otimes |s_{c_1}^n\rangle \langle s_{c_1}^n| (2^4\times)$) one obtains $24^2 + 6 \cdot 24 + 2 \cdot 24 + 4 + 16 = 788 < 862$ ($r_{\min} = 74$), we have to introduce secondary E-registry states. Since $t_{\min} = 5$, we have, according to the above algorithm, a secondary attractor subspace of dimension $5^2 + 6 \cdot 5 + 2 \cdot 5 = 65$ ($r_{\min}^{t_{\min}} = 9$) associated with structures **A**)-**D**) in (384) and E-registry states $S_s^{t_{\min}} \equiv \{|11000\rangle, |11100\rangle, |11010\rangle, |11110\rangle, |11001\rangle\} \subset S_s$. The remaining 9 states of the attractor space correspond, according to the above algorithm, to the structures $\{|0_k\rangle \langle 0_k| \otimes |11000\rangle \langle v|, |0_k\rangle \langle 0_k| \otimes |v\rangle \langle 11000|\}$ from **B**) in (384) that “connect” 4 primary E-states $|v\rangle$ and the secondary $|11000\rangle$, both with lowest logical values in S_p and $S_s^{t_{\min}}$, respectively (8 attractor states). The sixth lowest secondary E-state $|11101\rangle \notin S_s^{t_{\min}}$ from S_s appears within **A**) in (384), yielding $\{|0_k\rangle \langle 0_k| \otimes |11101\rangle \langle 11101|\}$ as the 862-th attractor state.

2) Two $\hat{u}_j^{(\phi)}$ -bindings as a binding-pair between qubits q_1 and q_2 , s. **b**) of Fig. 41, $d_{n=5}^{\lambda=1,2,\text{bind}} = 470$ (s. Tab. 10 and (382)-(383)):

This time we have $m_{\min} = |S_p| = 16$ related with $S_p \equiv \{|0q_2q_3q_4q_5\rangle\}$ that enter into (384) and (together with $|x\rangle\langle x| \otimes \hat{I}_n (4\times)$ and $|x\rangle\langle y| \otimes |s_{c_1}^n\rangle\langle s_{c_1}^n| (16\times)$) yield $16^2 + 6 \cdot 16 + 2 \cdot 16 + 4 + 16 = 404$, alias $r_{\min} = 470 - 404 = 64$. We again need secondary E-registry states from $S_s \equiv \{|1q_2q_3q_4q_5\rangle\}$, and since $t_{\min} = 4$, we need 4 of them with the lowest logical value, i.e. $S_s^{t_{\min}} \equiv \{|10000\rangle, |11000\rangle, |10100\rangle, |11100\rangle\} \subset S_s$. Associating the four secondary $S_s^{t_{\min}}$ -states with (384) we obtain a secondary attractor subspace with $4^2 + 6 \cdot 4 + 2 \cdot 4 = 48$ additional states (i.e. $r_{\min}^{t_{\min}} = 16$). The remaining 16 attractor states correspond to structures $\{|0_k\rangle\langle 0_k| \otimes |10000\rangle\langle v_i|, |0_k\rangle\langle 0_k| \otimes |v_i\rangle\langle 10000|\}$ from **B**) in (384) that “connect” the lowest state $|10000\rangle \in S_s^{t_{\min}}$ with the first eight states $|v_i\rangle \in S_p$ ($i \in \{1, \dots, 8\}$) with lowest logical values v_i .

3) One $\hat{u}_j^{(\phi)}$ -binding-pair between qubits q_1 and q_2 and one $\hat{u}_j^{(\phi)}$ -binding between qubits q_2 and q_3 , s. **e**) of Fig. 41, $d_{n=5}^{\lambda=1,3,\text{bind}} = 290$ (s. Tab. 10 and (382)-(383)): Now we have $m_{\min} = |S_p| = 12$ with a set of primary E-registry states $S_p \equiv \{|000q_4q_5\rangle, |010q_4q_5\rangle, |001q_4q_5\rangle\}$ that enter into (384) and (together with $|x\rangle\langle x| \otimes \hat{I}_n (4\times)$ and $|x\rangle\langle y| \otimes |s_{c_1}^n\rangle\langle s_{c_1}^n| (16\times)$) yield $12^2 + 6 \cdot 12 + 2 \cdot 12 + 4 + 16 = 260$, alias $r_{\min} = 290 - 260 = 30$. With $S_s \equiv \{|1q_2q_3q_4q_5\rangle\}$ and $t_{\min} = 2$ we distribute $S_s^{t_{\min}} \equiv \{|10000\rangle, |11000\rangle\} \subset S_s$ within (384), obtaining additional $2^2 + 6 \cdot 2 + 2 \cdot 2 = 20$ secondary E-registry states. Since $r_{\min}^{t_{\min}} = 10$ the remaining ten attractor states correspond to structures $\{|0_k\rangle\langle 0_k| \otimes |10000\rangle\langle v_i|, |0_k\rangle\langle 0_k| \otimes |v_i\rangle\langle 10000|\}$ from **B**) in (384) that “connect” the lowest secondary state $|10000\rangle \in S_s^{t_{\min}}$ with the first five lowest primary E-registry states $|v_i\rangle \in S_p$.

4) Two $\hat{u}_j^{(\phi)}$ -binding-pairs between qubits q_1 and q_2 and q_2 and q_3 , s. **d**) of Fig. 41, $d_{n=5}^{\lambda=1,4,\text{bind}} = 158$ (s. Tab. 10 and (382)-(383)): Now we have $m_{\min} = |S_p| = 8$ with $S_p \equiv \{|00q_3q_4q_5\rangle\}$ that enter into (384) and (together with $|x\rangle\langle x| \otimes \hat{I}_n (4\times)$ and $|x\rangle\langle y| \otimes |s_{c_1}^n\rangle\langle s_{c_1}^n| (16\times)$) yield $8^2 + 6 \cdot 8 + 2 \cdot 8 + 4 + 16 = 148$, alias $r_{\min} = 158 - 148 = 10$. According to the above algorithm $t_{\min} = 1$ and we have to use the two lowest secondary states $|v_i\rangle \in \{|10000\rangle, |01000\rangle\}$ from $S_s \equiv \{|10q_3q_4q_5\rangle, |01q_3q_4q_5\rangle, |11q_3q_4q_5\rangle\}$ and associate $|10000\rangle$ with **A**), **C**) and **D**) from (384) (9 attractor states), whereas $|01000\rangle$ remains associated with the 158-th attractor state $\{|0_k\rangle\langle 0_k| \otimes |01000\rangle\langle 01000|\}$ from **A**) in (384).

5) Two $\hat{u}_j^{(\phi)}$ -binding-pairs between qubits (q_1, q_2) and (q_2, q_3) and one $\hat{u}_j^{(\phi)}$ -binding between q_3 and q_4 , s. **e**) of Fig. 41, $d_{n=5}^{\lambda=1,5,\text{bind}} = 104$ (s. Tab. 10 and (382)-(383)): This time we have $m_{\min} = 6 = |S_p|$ with E-states $S_p \equiv \{|0000q_5\rangle, |0001q_5\rangle, |00001q_5\rangle\}$ that enter into (384) and (together with $|x\rangle\langle x| \otimes \hat{I}_n (4\times)$ and $|x\rangle\langle y| \otimes |s_{c_1}^n\rangle\langle s_{c_1}^n| (16\times)$) yield $6^2 + 6 \cdot 6 + 2 \cdot 6 + 4 + 16 = 104$, alias $r_{\min} = 104 - 104 = 0$. Therefore, we are finished.

6) Three $\hat{u}_j^{(\phi)}$ -binding-pairs between qubits (q_1, q_2) , (q_2, q_3) and (q_3, q_4) , s. **d**) of Fig. 41, $d_{n=5}^{\lambda=1,6,\text{bind}} = 62$ (s. Tab. 10 and (382)-(383)): Due to $m_{\min} = 3 < |S_p| = 4$, $S_p^{m_{\min}} \equiv S_p \setminus \{|00011\rangle\}$ (and $S_p \equiv \{|000q_4q_5\rangle\}$), 3 primary E-registry states enter into (384) and (together with $|x\rangle\langle x| \otimes \hat{I}_n (4\times)$ and $|x\rangle\langle y| \otimes |s_{c_1}^n\rangle\langle s_{c_1}^n| (16\times)$) yield $3^2 + 6 \cdot 3 + 2 \cdot 3 + 4 + 16 = 53$, alias $r_{\min} = 62 - 53 = 9$. These remaining 9 attractor states are obtained by associating the fourth lowest primary E-registry state $|v\rangle = |00011\rangle$ from S_p with structures **A**), **C**) and **D**) in (384), since then one obtains precisely $1^2 + 6 \cdot 1 + 2 \cdot 1 = 9$ additional attractor states.

7) Three $\hat{u}_j^{(\phi)}$ -binding-pairs between qubits (q_1, q_2) , (q_2, q_3) and (q_3, q_4) and a $\hat{u}_j^{(\phi)}$ -binding between q_5 and q_6 , s. **d**) and **e**) of Fig. 41, $d_{n=5}^{\lambda=1,7,\text{bind}} = 44$ (s. Tab. 10 and (382)-(383)): Since $m_{\min} = 2 < |S_p| = 3$, $S_p \equiv \{|000q_4q_5\rangle\} \setminus \{|00011\rangle\}$, 2 primary E-registry states $\{|00000\rangle, |00010\rangle\}$ enter into (384) and (together with $|x\rangle\langle x| \otimes \hat{I}_n (4\times)$ and $|x\rangle\langle y| \otimes |s_{c_1}^n\rangle\langle s_{c_1}^n| (16\times)$) yield $2^2 + 6 \cdot 2 + 2 \cdot 2 + 4 + 16 = 40$, alias $r_{\min} = 44 - 40 = 4$. The remaining four attractor states are the two attractor states $\{|0_k\rangle\langle 0_k| \otimes |v_i\rangle\langle v_i|\}$ associated with $|v_i\rangle \in \{|00001\rangle, |10000\rangle\}$, where $|10000\rangle$ denotes the lowest secondary E-state, and the 2 attractor states $\{|0_k\rangle\langle 3| \otimes |00001\rangle\langle s_{c_1}^n|, |3\rangle\langle 0_k| \otimes |s_{c_1}^n\rangle\langle 00001|\}$ from **C**) in (384).

8) Four $\hat{u}_j^{(\phi)}$ -binding-pairs between qubits (q_1, q_2) , (q_2, q_3) , (q_3, q_4) and (q_4, q_5) , s. **d**) of Fig. 41, $d_{n=5}^{\lambda=1,8,\text{bind}} = 29$ (s. Tab. 10 and (382)-(383)): The ID is strongly connected with $2(n-1) = 8$ bindings, ergo its dimensionality is already minimal, corresponding to the minimal attractor space (365).

I Gram-Schmidt-Orthonormalization (GSO) of the minimal $\{\lambda = 1\}$ attractor space in Eq. (365)

In this appendix we use the Gram-Schmidt-orthonormalization method (s. [23], [37]) of Appendix F in order to generate a complete orthonormal basis for the minimal $\{\lambda = 1\}$ -attractor space structure (365) in Appendix H. The efficiency and the computation cost of the GSO method depend crucially on an arbitrary choice of the \hat{x}_i -operators from a finite set of linear, independent operators $M = \{\hat{x}_1, \dots, \hat{x}_m\}$ (with $m \in \mathbb{N}$), from which we start to generate the desired chain of m orthonormalized basis vectors of an m -dimensional operator space $M_r = \{\hat{x}_{1r}, \dots, \hat{x}_{mr}\}$. In the following we demonstrate the most efficient way for choosing the starting \hat{x}_i -operator in order to generate an orthonormalized chain

out of the attractor states in (365) in a most efficient manner.

I.1 Case study: $k = 1$ qubit S , $n \geq 1$ qubit E

Let us start, without loss of generality, with a $k = 1$ open system S and CNOT-symmetry states $\{|s_1^{L=n}\rangle, |s_2^{L=n}\rangle\}$ (s. Appendix E) of an n -qubit E , where $\text{Tr}_E [\hat{I}_n] = 2^n$, $\langle s_1^{L=n} | s_1^{L=n} \rangle = \langle 0_n | 0_n \rangle = 1$, $\langle s_1^{L=n} | 0_n \rangle = \langle s_2^{L=n} | 0_n \rangle = 2^{-n/2}$ and $\langle 0_n | s_1^{L=n} \rangle = \langle 0_n | s_2^{L=n} \rangle = 2^{-n/2}$. In this case (365) contains 11 attractor states, which are grouped in classes w.r.t. the S -subspace with which the corresponding E -registry states are correlated, as depicted in Tab. 11.

S-subspace	\hat{x}_i -operators (attractor states)
$ 0\rangle\langle 0 $	$ 0\rangle\langle 0 \otimes \hat{I}_n, 0\rangle\langle 0 \otimes s_1^{L=n}\rangle\langle s_1^{L=n} , 0\rangle\langle 0 \otimes s_1^{L=n}\rangle\langle 0_n $ $ 0\rangle\langle 0 \otimes 0_n\rangle\langle s_1^{L=n} , 0\rangle\langle 0 \otimes 0_n\rangle\langle 0_n $
$ 0\rangle\langle 1 $	$ 0\rangle\langle 1 \otimes 0_n\rangle\langle s_1^{L=n} , 0\rangle\langle 1 \otimes s_1^{L=n}\rangle\langle s_1^{L=n} $
$ 1\rangle\langle 0 $	$ 1\rangle\langle 0 \otimes s_1^{L=n}\rangle\langle 0_n , 1\rangle\langle 0 \otimes s_1^{L=n}\rangle\langle s_1^{L=n} $
$ 1\rangle\langle 1 $	$ 1\rangle\langle 1 \otimes \hat{I}_n, 1\rangle\langle 1 \otimes s_1^{L=n}\rangle\langle s_1^{L=n} $

Table 11: \hat{x}_i -operators w.r.t. subspaces of an open $k = 1$ -qubit S , interacting with E via CNOT.

The GSO w.r.t. the $|0\rangle\langle 0|$ -subspace of S leads to the highest amount of computation cost. Nevertheless, depending on how one chooses the GSO-chain of \hat{x}_i -operators the amount of computation cost may vary considerably. The GSO-chain of the $|0\rangle\langle 0|$ -subspace in Tab. 11 starting with $\hat{x}_1 = |0\rangle\langle 0| \otimes \hat{I}_n$ and terminating with $\hat{x}_5 = |0\rangle\langle 0| \otimes |0_n\rangle\langle 0_n|$ minimizes indeed the computation cost, as we shall see now. Contrary to the $|0\rangle\langle 0|$ -subspace, the remaining S -subspaces from Tab. 11 contain only GSO-chains with two \hat{x}_i -operators, which is the reason why their computation cost remains minimal in the first place.

I.1.1 The $|0\rangle\langle 0|$ -subspace of S

Step 1: We start with $\hat{x}_1 = |0\rangle\langle 0| \otimes \hat{I}_n$ and set (with $\|\hat{x}_1\|_{\text{HS}} = 2^{-n/2}$)

$$\hat{x}_{1r} := \frac{|0\rangle\langle 0| \otimes \hat{I}_n}{2^{n/2}}. \quad (385)$$

Step 2: We perform four iteration steps of the GSO algorithm from Appendix F, in order to obtain all five orthonormalized basis \hat{x}_i -operators of the $|0\rangle\langle 0|$ -subspace of S .

Operator $\hat{x}_2 = |0\rangle\langle 0| \otimes |s_1^{L=n}\rangle\langle s_1^{L=n}|$

We have $\hat{x}_{2r} := \frac{\hat{x}_2 - \langle \hat{x}_{1r}, \hat{x}_2 \rangle \hat{x}_{1r}}{\|\hat{x}_2 - \langle \hat{x}_{1r}, \hat{x}_2 \rangle \hat{x}_{1r}\|_{\text{HS}}}$, with $\langle \hat{x}_{1r}, \hat{x}_2 \rangle = \text{Tr} \left[\left(\frac{|0\rangle\langle 0| \otimes \hat{I}_n}{2^{n/2}} \right) (|0\rangle\langle 0| \otimes |s_1^{L=n}\rangle\langle s_1^{L=n}|)^\dagger \right] = 2^{-n/2}$ and the HS-norm $\|\hat{x}_2 - \langle \hat{x}_{1r}, \hat{x}_2 \rangle \hat{x}_{1r}\|_{\text{HS}} = (1 - 2^{-n})^{1/2}$. This leads us to:

$$\hat{x}_{2r} := \frac{|0\rangle\langle 0| \otimes (|s_1^{L=n}\rangle\langle s_1^{L=n}| - 2^{-n} \hat{I}_n)}{(1 - 2^{-n})^{1/2}}. \quad (386)$$

Operator $\hat{x}_3 = |0\rangle\langle 0| \otimes |s_1^{L=n}\rangle\langle 0_n|$

From $\hat{x}_{3r} := \frac{\hat{x}_3 - \langle \hat{x}_{1r}, \hat{x}_3 \rangle \hat{x}_{1r} - \langle \hat{x}_{2r}, \hat{x}_3 \rangle \hat{x}_{2r}}{\|\hat{x}_3 - \langle \hat{x}_{1r}, \hat{x}_3 \rangle \hat{x}_{1r} - \langle \hat{x}_{2r}, \hat{x}_3 \rangle \hat{x}_{2r}\|_{\text{HS}}}$, with HS-scalar products

$$\begin{aligned} \langle \hat{x}_{1r}, \hat{x}_3 \rangle &= \text{Tr} \left[\left(\frac{|0\rangle\langle 0| \otimes \hat{I}_n}{2^{n/2}} \right) (|0\rangle\langle 0| \otimes |s_1^{L=n}\rangle\langle 0_n|)^\dagger \right] = 2^{-n} \\ \langle \hat{x}_{2r}, \hat{x}_3 \rangle &= \text{Tr} \left[\frac{|0\rangle\langle 0| \otimes (|s_1^{L=n}\rangle\langle s_1^{L=n}| - 2^{-n} \hat{I}_n)}{(1 - 2^{-n})^{1/2}} (|0\rangle\langle 0| \otimes |s_1^{L=n}\rangle\langle 0_n|)^\dagger \right] = 2^{-n/2} (1 - 2^{-n})^{1/2} \end{aligned}$$

and the HS-norm

$$\left\| \hat{x}_3 - \langle \hat{x}_{1r}, \hat{x}_3 \rangle \hat{x}_{1r} - \langle \hat{x}_{2r}, \hat{x}_3 \rangle \hat{x}_{2r} \right\|_{\text{HS}} = (1 - 2^{1-n} + 2^{-n})^{1/2} = (1 - 2^{-n})^{1/2},$$

one obtains:

$$\hat{x}_{3r} := \frac{|0\rangle \langle 0| \otimes (|s_1^{L=n}\rangle \langle 0_n| - 2^{-n/2} |s_1^{L=n}\rangle \langle s_1^{L=n}|)}{(1 - 2^{-n})^{1/2}}. \quad (387)$$

Operator $\hat{x}_4 = |0\rangle \langle 0| \otimes |0_n\rangle \langle s_1^{L=n}|$

From $\hat{x}_{4r} := \frac{\hat{x}_4 - \langle \hat{x}_{1r}, \hat{x}_4 \rangle \hat{x}_{1r} - \langle \hat{x}_{2r}, \hat{x}_4 \rangle \hat{x}_{2r} - \langle \hat{x}_{3r}, \hat{x}_4 \rangle \hat{x}_{3r}}{\left\| \hat{x}_4 - \langle \hat{x}_{1r}, \hat{x}_4 \rangle \hat{x}_{1r} - \langle \hat{x}_{2r}, \hat{x}_4 \rangle \hat{x}_{2r} - \langle \hat{x}_{3r}, \hat{x}_4 \rangle \hat{x}_{3r} \right\|_{\text{HS}}}$, with HS-scalar products

$$\begin{aligned} \langle \hat{x}_{1r}, \hat{x}_4 \rangle &= \text{Tr} \left[\left(\frac{|0\rangle \langle 0| \otimes \hat{I}_n}{2^{n/2}} \right) (|0\rangle \langle 0| \otimes |s_1^{L=n}\rangle \langle 0_n|) \right] = 2^{-n} \\ \langle \hat{x}_{2r}, \hat{x}_4 \rangle &= \text{Tr} \left[\frac{|0\rangle \langle 0| \otimes (|s_1^{L=n}\rangle \langle s_1^{L=n}| - 2^{-n} \hat{I}_n)}{(1 - 2^{-n})^{1/2}} (|0\rangle \langle 0| \otimes |s_1^{L=n}\rangle \langle 0_n|) \right] = 2^{-n/2} (1 - 2^{-n})^{1/2} \\ \langle \hat{x}_{3r}, \hat{x}_4 \rangle &= \text{Tr} \left[\frac{|0\rangle \langle 0| \otimes (|s_1^{L=n}\rangle \langle 0_n| - 2^{-n/2} |s_1^{L=n}\rangle \langle s_1^{L=n}|)}{(1 - 2^{-n})^{1/2}} (|0\rangle \langle 0| \otimes |s_1^{L=n}\rangle \langle 0_n|) \right] = 0 \end{aligned}$$

and the HS-norm

$$\left\| \hat{x}_4 - \langle \hat{x}_{1r}, \hat{x}_4 \rangle \hat{x}_{1r} - \langle \hat{x}_{2r}, \hat{x}_4 \rangle \hat{x}_{2r} - \langle \hat{x}_{3r}, \hat{x}_4 \rangle \hat{x}_{3r} \right\|_{\text{HS}} = (1 - 2^{-n})^{1/2},$$

one obtains:

$$\hat{x}_{4r} := \frac{|0\rangle \langle 0| \otimes (|0_n\rangle \langle s_1^{L=n}| - 2^{-n/2} |s_1^{L=n}\rangle \langle s_1^{L=n}|)}{(1 - 2^{-n})^{1/2}}. \quad (388)$$

Operator $\hat{x}_5 = |0\rangle \langle 0| \otimes |0_n\rangle \langle 0_n|$

From $\hat{x}_{5r} := \frac{\hat{x}_5 - \langle \hat{x}_{1r}, \hat{x}_5 \rangle \hat{x}_{1r} - \langle \hat{x}_{2r}, \hat{x}_5 \rangle \hat{x}_{2r} - \langle \hat{x}_{3r}, \hat{x}_5 \rangle \hat{x}_{3r} - \langle \hat{x}_{4r}, \hat{x}_5 \rangle \hat{x}_{4r}}{\left\| \hat{x}_5 - \langle \hat{x}_{1r}, \hat{x}_5 \rangle \hat{x}_{1r} - \langle \hat{x}_{2r}, \hat{x}_5 \rangle \hat{x}_{2r} - \langle \hat{x}_{3r}, \hat{x}_5 \rangle \hat{x}_{3r} - \langle \hat{x}_{4r}, \hat{x}_5 \rangle \hat{x}_{4r} \right\|_{\text{HS}}}$, with HS-scalar products

$$\begin{aligned} \langle \hat{x}_{1r}, \hat{x}_5 \rangle &= \text{Tr} \left[\left(\frac{|0\rangle \langle 0| \otimes \hat{I}_n}{2^{n/2}} \right) (|0\rangle \langle 0| \otimes |0_n\rangle \langle 0_n|) \right] = 2^{-n/2} \\ \langle \hat{x}_{2r}, \hat{x}_5 \rangle &= \text{Tr} \left[\frac{|0\rangle \langle 0| \otimes (|s_1^{L=n}\rangle \langle s_1^{L=n}| - 2^{-n} \hat{I}_n)}{(1 - 2^{-n})^{1/2}} (|0\rangle \langle 0| \otimes |0_n\rangle \langle 0_n|) \right] = 0 \\ \langle \hat{x}_{3r}, \hat{x}_5 \rangle &= \text{Tr} \left[\frac{|0\rangle \langle 0| \otimes (|s_1^{L=n}\rangle \langle 0_n| - 2^{-n/2} |s_1^{L=n}\rangle \langle s_1^{L=n}|)}{(1 - 2^{-n})^{1/2}} (|0\rangle \langle 0| \otimes |0_n\rangle \langle 0_n|) \right] = 2^{-n/2} (1 - 2^{-n})^{1/2} \\ \langle \hat{x}_{4r}, \hat{x}_5 \rangle &= \langle \hat{x}_{3r}, \hat{x}_5 \rangle = 2^{-n/2} (1 - 2^{-n})^{1/2} \end{aligned}$$

and the HS-norm

$$\left\| \hat{x}_5 - \langle \hat{x}_{1r}, \hat{x}_5 \rangle \hat{x}_{1r} - \langle \hat{x}_{2r}, \hat{x}_5 \rangle \hat{x}_{2r} - \langle \hat{x}_{3r}, \hat{x}_5 \rangle \hat{x}_{3r} - \langle \hat{x}_{4r}, \hat{x}_5 \rangle \hat{x}_{4r} \right\|_{\text{HS}} = (1 - 2^{-n})^{1/2} (1 - 2^{1-n})^{1/2},$$

one obtains:

$$\hat{x}_{5r} := \frac{|0\rangle \langle 0| \otimes (|0_n\rangle \langle 0_n| - 2^{-n} \hat{I}_n - 2^{-n/2} [|s_1^{L=n}\rangle \langle 0_n| + |0_n\rangle \langle s_1^{L=n}| - 2^{1-n/2} |s_1^{L=n}\rangle \langle s_1^{L=n}|])}{(1 - 2^{-n})^{1/2} (1 - 2^{1-n})^{1/2}}. \quad (389)$$

1.1.2 The $|1\rangle \langle 0|$ - and $|0\rangle \langle 1|$ -subspaces of S

We start in the $|1\rangle \langle 0|$ -subspace with $\hat{x}_6 = |1\rangle \langle 0| \otimes |s_1^{L=n}\rangle \langle 0_n|$ and set (with $\|\hat{x}_6\|_{\text{HS}} = 1$):

$$\hat{x}_{6r} := \hat{x}_6. \quad (390)$$

Operator $\hat{x}_7 = |1\rangle \langle 0| \otimes |s_1^{L=n}\rangle \langle s_1^{L=n}|$

$\hat{x}_{7r} := \frac{\hat{x}_7 - \langle \hat{x}_{6r}, \hat{x}_7 \rangle \hat{x}_{6r}}{\|\hat{x}_7 - \langle \hat{x}_{6r}, \hat{x}_7 \rangle \hat{x}_{6r}\|_{\text{HS}}}$, with $\langle \hat{x}_{6r}, \hat{x}_7 \rangle = \text{Tr}[(|1\rangle \langle 0| \otimes |s_1^{L=n}\rangle \langle 0_n|) (|1\rangle \langle 0| \otimes |s_1^{L=n}\rangle \langle s_1^{L=n}|)] = 2^{-n/2}$ and the HS-norm $\|\hat{x}_7 - \langle \hat{x}_{6r}, \hat{x}_7 \rangle \hat{x}_{6r}\|_{\text{HS}} = (1 - 2^{-n})^{1/2}$, yields:

$$\hat{x}_{7r} := \frac{|1\rangle \langle 0| \otimes (|s_1^{L=n}\rangle \langle s_1^{L=n}| - 2^{-n/2} |s_1^{L=n}\rangle \langle 0_n|)}{(1 - 2^{-n})^{1/2}}. \quad (391)$$

Analogous computation yields for the $|0\rangle \langle 1|$ -subspace (starting the GSO-algorithm with $\hat{x}_8 = |0\rangle \langle 1| \otimes |0_n\rangle \langle s_1^{L=n}|$ and terminating it with $\hat{x}_9 = |0\rangle \langle 1| \otimes |s_1^{L=n}\rangle \langle s_1^{L=n}|$) the orthonormalized basis operators:

$$\hat{x}_{8r} := \hat{x}_8$$

$$\hat{x}_{9r} := \frac{|0\rangle \langle 1| \otimes (|s_1^{L=n}\rangle \langle s_1^{L=n}| - 2^{-n/2} |0_n\rangle \langle s_1^{L=n}|)}{(1 - 2^{-n})^{1/2}}. \quad (392)$$

1.1.3 The $|1\rangle \langle 1|$ -subspace of S

We start with $\hat{x}_{10} = |1\rangle \langle 1| \otimes |s_1^{L=n}\rangle \langle s_1^{L=n}|$ and set (with $\|\hat{x}_{10}\|_{\text{HS}} = 1$):

$$\hat{x}_{10r} := \hat{x}_{10}. \quad (393)$$

Operator $\hat{x}_{11} = |1\rangle \langle 1| \otimes \hat{\mathbf{I}}_n$

$\hat{x}_{11r} := \frac{\hat{x}_{11} - \langle \hat{x}_{10r}, \hat{x}_{11} \rangle \hat{x}_{10r}}{\|\hat{x}_{11} - \langle \hat{x}_{10r}, \hat{x}_{11} \rangle \hat{x}_{10r}\|_{\text{HS}}}$, with $\langle \hat{x}_{10r}, \hat{x}_{11} \rangle = \text{Tr}[(|1\rangle \langle 1| \otimes |s_1^{L=n}\rangle \langle s_1^{L=n}|) (|1\rangle \langle 1| \otimes \hat{\mathbf{I}}_n)] = 1$ and the HS-norm $\|\hat{x}_{11} - \langle \hat{x}_{10r}, \hat{x}_{11} \rangle \hat{x}_{10r}\|_{\text{HS}} = (2^n - 1)^{1/2}$, yields:

$$\hat{x}_{11r} := \frac{|1\rangle \langle 1| \otimes (\hat{\mathbf{I}}_n - |s_1^{L=n}\rangle \langle s_1^{L=n}|)}{(2^n - 1)^{1/2}}. \quad (394)$$

Thus, for the minimal $\{\lambda = 1\}$ -attractor space (365) in Appendix H (with $\phi = \pi/2$ and $n \geq k = 1$) we obtain for all S-subspaces the complete set of GSO-operators \hat{x}_{ir} summarized in Tab. 12 below.

S-subspace	GSO-operators \hat{x}_{ir}	Remark
$ 0\rangle \langle 0 $	$\frac{ 0\rangle \langle 0 \otimes \hat{\mathbf{I}}_n}{2^{n/2}}$ $\frac{ 0\rangle \langle 0 \otimes (s_1^{L=n}\rangle \langle s_1^{L=n} - 2^{-n} \hat{\mathbf{I}}_n)}{(1 - 2^{-n})^{1/2}}$ $\frac{ 0\rangle \langle 0 \otimes (s_1^{L=n}\rangle \langle 0_n - 2^{-n/2} s_1^{L=n}\rangle \langle s_1^{L=n})}{(1 - 2^{-n})^{1/2}}$ $\frac{ 0\rangle \langle 0 \otimes (0_n\rangle \langle s_1^{L=n} - 2^{-n/2} s_1^{L=n}\rangle \langle s_1^{L=n})}{(1 - 2^{-n})^{1/2}}$ $\frac{ 0\rangle \langle 0 \otimes (0_n\rangle \langle 0_n - 2^{-n} \hat{\mathbf{I}}_n - 2^{-n/2} [s_1^{L=n}\rangle \langle 0_n + 0_n\rangle \langle s_1^{L=n} - 2^{1-n/2} s_1^{L=n}\rangle \langle s_1^{L=n}])}{(1 - 2^{-n})^{1/2} (1 - 2^{1-n})^{1/2}}$	
$ 0\rangle \langle 1 $	$\frac{ 0\rangle \langle 1 \otimes 0_n\rangle \langle s_1^{L=n} }{(1 - 2^{-n})^{1/2}}$ $\frac{ 0\rangle \langle 1 \otimes (s_1^{L=n}\rangle \langle s_1^{L=n} - 2^{-n/2} 0_n\rangle \langle s_1^{L=n})}{(1 - 2^{-n})^{1/2}} = \frac{ 0\rangle \langle 1 \otimes (\tilde{s}_1^{L=n}\rangle \langle s_1^{L=n})}{(1 - 2^{-n})^{1/2}}$	with $ \tilde{s}_1^{L=n}\rangle = s_1^{L=n}\rangle - 2^{-n/2} 0_n\rangle$
$ 1\rangle \langle 0 $	$\frac{ 1\rangle \langle 0 \otimes s_1^{L=n}\rangle \langle 0_n }{(1 - 2^{-n})^{1/2}}$ $\frac{ 1\rangle \langle 0 \otimes (s_1^{L=n}\rangle \langle s_1^{L=n} - 2^{-n/2} s_1^{L=n}\rangle \langle 0_n)}{(1 - 2^{-n})^{1/2}} = \frac{ 1\rangle \langle 0 \otimes (s_1^{L=n}\rangle \langle \tilde{s}_1^{L=n})}{(1 - 2^{-n})^{1/2}}$	with $ \tilde{s}_1^{L=n}\rangle = s_1^{L=n}\rangle - 2^{-n/2} 0_n\rangle$
$ 1\rangle \langle 1 $	$\frac{ 1\rangle \langle 1 \otimes s_1^{L=n}\rangle \langle s_1^{L=n} }{(2^n - 1)^{1/2}}$ $\frac{ 1\rangle \langle 1 \otimes (\hat{\mathbf{I}}_n - s_1^{L=n}\rangle \langle s_1^{L=n})}{(2^n - 1)^{1/2}}$	

Table 12: GSO-operators \hat{x}_{ir} in all subspaces of an open $k = 1$ qubit system S.

I.2 Generalization to open k-qubit S

In case of k-qubit-Systems with $k > 1$ the computational GSO-approach for $\phi = \pi/2$ outlined in the previous subsection remains the same. This also means that also the GSO-operators from 12 remain formally unchanged. However, one has to bear in mind that for open k-qubit systems S the pointer-state vectors $|x\rangle$ and $|y\rangle$ belong to the 2^k -dimensional standard computational basis. This is why the GSO-operators \hat{x}_{ir} from Tab. 12 generalized to k-qubit-Systems with $k > 1$ contain more S-subspaces, as indicated in Tab. 13 below.

S-subspace	GSO-operators \hat{x}_{ir}	Remark
$ 0_k\rangle\langle 0_k $	$\frac{ 0_k\rangle\langle 0_k \otimes \frac{\hat{I}_n}{2^{n/2}}}{ 0_k\rangle\langle 0_k \otimes (s_1^{L=n}\rangle\langle s_1^{L=n} - 2^{-n}\hat{I}_n)}$ $\frac{ 0_k\rangle\langle 0_k \otimes (s_1^{L=n}\rangle\langle 0_n - 2^{-n/2} s_1^{L=n}\rangle\langle s_1^{L=n})}$ $\frac{ 0_k\rangle\langle 0_k \otimes (0_n\rangle\langle s_1^{L=n} - 2^{-n/2} s_1^{L=n}\rangle\langle s_1^{L=n})}$ $\frac{ 0_k\rangle\langle 0_k \otimes (0_n\rangle\langle 0_n - 2^{-n}\hat{I}_n - 2^{-n/2}[s_1^{L=n}\rangle\langle 0_n + 0_n\rangle\langle s_1^{L=n} - 2^{1-n/2} s_1^{L=n}\rangle\langle s_1^{L=n}])}{(1-2^{-n})^{1/2}(1-2^{1-n})^{1/2}}$	with $ 0_k\rangle = 0\rangle^{\otimes k}$
$ 0_k\rangle\langle y $	$\frac{ 0_k\rangle\langle y \otimes 0_n\rangle\langle s_1^{L=n} }{ 0_k\rangle\langle y \otimes (s_1^{L=n}\rangle\langle s_1^{L=n} - 2^{-n/2} 0_n\rangle\langle \phi_n)} = \frac{ 0_k\rangle\langle y \otimes (s_1^{L=n}\rangle\langle s_1^{L=n})}$	with $ \tilde{s}_1^{L=n}\rangle = s_1^{L=n}\rangle - 2^{-n/2} 0_n\rangle$ $y \in \{1, \dots, 2^k - 1\}, y \neq 0$
$ y\rangle\langle 0_k $	$\frac{ y\rangle\langle 0_k \otimes s_1^{L=n}\rangle\langle 0_n }{ y\rangle\langle 0_k \otimes (s_1^{L=n}\rangle\langle s_1^{L=n} - 2^{-n/2} s_1^{L=n}\rangle\langle 0_n)} = \frac{ y\rangle\langle 0_k \otimes (\tilde{s}_1^{L=n}\rangle\langle s_1^{L=n})}$	with $ \tilde{s}_1^{L=n}\rangle = s_1^{L=n}\rangle - 2^{-n/2} 0_n\rangle$ $y \in \{1, \dots, 2^k - 1\}, y \neq 0$
$ y\rangle\langle y $	$\frac{ y\rangle\langle y \otimes s_1^{L=n}\rangle\langle s_1^{L=n} }{ y\rangle\langle y \otimes (\hat{I}_n - s_1^{L=n}\rangle\langle s_1^{L=n})}$	with $y \in \{1, \dots, 2^k - 1\}, y \neq 0$
$ y\rangle\langle x $	$ y\rangle\langle x \otimes s_1^{L=n}\rangle\langle s_1^{L=n} $	with $y, x \in y \in \{1, \dots, 2^k - 1\}$ $y \neq x$

Table 13: GSO-operators \hat{x}_{ir} in all subspaces of an open $k \geq 1$ qubit system S.

For $n \geq k \geq 1$ and $\phi \neq \pi/2$ the corresponding GSO-operators \hat{x}_{ir} emerge from Tab. 12 and Tab. 13 by substituting $|s_1^{L=n}\rangle \leftrightarrow |s_{c_1 \neq 2^{-1/2}}^{L=n}\rangle$. The GSO-algorithm is performed analogously as in subsection I.1.

J Output states $\hat{\rho}_{SE_L}^{\text{out}}$ of the random unitary evolution used in section 8

In this appendix we list the output states $\hat{\rho}_{SE_L}^{\text{out}}$ of the random unitary evolution used in section 8.

J.1 Output states $\hat{\rho}_{SE_L}^{\text{out}}$ of the random unitary evolution for the maximal attractor space

In this appendix we list the output states $\hat{\rho}_{SE_L}^{\text{out}}$ of the random unitary evolution used in section 8 of the main text when discussing Quantum Darwinism from the point of view of the maximal attractor space.

D) Input: $\hat{\rho}_{SE}^{\text{in}} = |\psi_S^{\text{in}}\rangle\langle \psi_S^{\text{in}}| \otimes \hat{\rho}_E^{\text{in}}, |\psi_S^{\text{in}}\rangle = \sum_{m=0}^{2^k-1} a_m |m\rangle, \hat{\rho}_E^{\text{in}} = |z^{L=n}\rangle\langle z^{L=n}|, \hat{u}_j^{(\phi=\pi/2)}$ -evolution

$$\begin{aligned}
\hat{\rho}_{SE}^{\text{out}} = & |\Psi'\rangle \langle \Psi'| + 2^{-n} \sum_{m=1}^{2^k-1} |a_m|^2 |m\rangle \langle m| \otimes \left(\hat{I}_n - |s_1^n\rangle \langle s_1^n| \right) \\
& + (-1)^N \cdot \left\{ 2^{-n/2} (-1)^M \left[a_0 a_{2^k-1}^* |0\rangle \langle 2^k-1| \otimes |z^n\rangle \langle s_2^n| + a_{2^k-1} a_0^* |2^k-1\rangle \langle 0| \otimes |s_2^n\rangle \langle z^n| \right] \right. \\
& + 2^{-n} \sum_{m=1}^{2^k-2} |a_m|^2 |m\rangle \langle m| \otimes |s_2^n\rangle \langle s_2^n| + (-1)^n \cdot 2^{-n/2} |a_{2^k-1}|^2 |2^k-1\rangle \langle 2^k-1| \otimes \bigotimes_{i=1}^n \hat{B}_1^{\pi/2} \\
& \left. + 2^{-n} \sum_{m=1}^{2^k-2} a_m a_{2^k-1}^* |m\rangle \langle 2^k-1| \otimes |s_1^n\rangle \langle s_2^n| + 2^{-n} \sum_{m=1}^{2^k-2} a_{2^k-1} a_m^* |2^k-1\rangle \langle m| \otimes |s_2^n\rangle \langle s_1^n| \right\}, \tag{395}
\end{aligned}$$

where $z^{L=n} \in \{0, \dots, 2^n-1\}$, $\{|s_1\rangle, |s_2\rangle\}$ as in (158), $\langle s_1|\xi\rangle = 2^{-1/2}$, $\langle s_2|\xi\rangle = (-1)^\xi 2^{-1/2}$ for $\xi \in \{0, 1\}$, $|\Psi'\rangle = a_0 |0\rangle \otimes |z^n\rangle + \sum_{m=1}^{2^k-1} a_m 2^{-n/2} |m\rangle \otimes |s_1^n\rangle$, $\hat{B}_1^{\pi/2} = (\sqrt{2})^{-1} [|1\rangle \langle 1| - |0\rangle \langle 0|]$, and M is the number of $|1\rangle$ -one qubit states in $|z^{L=n}\rangle$.

II) Input: $\hat{\rho}_{SE}^{\text{in}} = |\Psi_S^{\text{in}}\rangle \langle \Psi_S^{\text{in}}| \otimes \hat{\rho}_E^{\text{in}}, |\Psi_S^{\text{in}}\rangle = \sum_{m=0}^{2^k-1} a_m |m\rangle$, $\hat{\rho}_E^{\text{in}} = 2^{-1} (|0_n\rangle \langle 0_n| + |1_n\rangle \langle 1_n|)$, $\hat{u}_j^{(\phi=\pi/2)}$ -evolution

$$\begin{aligned}
\hat{\rho}_{SE}^{\text{out}} = & |a_0|^2 |0\rangle \langle 0| \otimes \hat{\rho}_E^{\text{in}} + |a_1|^2 |1\rangle \langle 1| \otimes 2^{-n} \hat{I}_n + \\
& 2^{-n/2-1} \cdot \left(a_0 a_1^* |0\rangle \langle 1| \otimes \left[|0_n\rangle \langle s_1^n| + |1_n\rangle \langle s_1^n| \right] + a_1 a_0^* |1\rangle \langle 0| \otimes \left[|s_1^n\rangle \langle 0_n| + |s_1^n\rangle \langle 1_n| \right] \right) \\
& + (-1)^N \left\{ 2^{-n/2-1} \left(a_0 a_1^* |0\rangle \langle 1| \otimes \left[|0_n\rangle \langle s_2^n| + (-1)^n |1_n\rangle \langle s_2^n| \right] + \right. \right. \\
& \left. \left. a_1 a_0^* |1\rangle \langle 0| \otimes \left[|s_2^n\rangle \langle 0_n| + (-1)^n |s_2^n\rangle \langle 1_n| \right] \right) + 2^{-1} |a_1|^2 |1\rangle \langle 1| \otimes 2^{-n/2} (1 + (-1)^n) \bigotimes_{i=1}^n \hat{B}_1^{\pi/2} \right\} \tag{396}
\end{aligned}$$

Remark: $\hat{\rho}_{SE=L=n}^{\text{out}}$ for $|\Psi_{E_{\text{pure}}}^{\text{in}}\rangle = 2^{-1/2} (|0_n\rangle + |1_n\rangle)$ emerges from $\hat{\rho}_{SE}^{\text{out}}$ in (396) by substituting $\hat{\rho}_E^{\text{in}} \leftrightarrow \left| \Psi_{E_{\text{pure}}}^{\text{in}} \right\rangle \left\langle \Psi_{E_{\text{pure}}}^{\text{in}} \right|$, $\hat{B}_1^{\pi/2} \leftrightarrow (\hat{B}_1^{\pi/2} + (-1)^n \hat{B}_0^{\pi/2})$ (with $\hat{B}_0^{\pi/2}$ as in (381)) and $\{|x\rangle \langle y| + \text{h.c.}\} \leftrightarrow \{2|x\rangle \langle y| \cdot \delta_{y,s_1^n} + (1 + (-1)^n)|x\rangle \langle y| \cdot \delta_{y,s_2^n} + \text{h.c.}\}$ (for $x \in \{0_n, 1_n\}$).

III) Input: $\hat{\rho}_{SE}^{\text{in}} = |\Psi_S^{\text{in}}\rangle \langle \Psi_S^{\text{in}}| \otimes \hat{\rho}_E^{\text{in}}, |\Psi_S^{\text{in}}\rangle = \sum_{m=0}^{2^k-1} a_m |m\rangle$, $\hat{\rho}_E^{\text{in}} = 2^{-n} \hat{I}_n$, $\hat{u}_j^{(\phi=\pi/2)}$ -evolution

$$\begin{aligned}
\hat{\rho}_{SE}^{\text{out}} (L=n) = & (|a_0|^2 |0\rangle \langle 0| + |a_1|^2 |1\rangle \langle 1|) \otimes 2^{-n} \hat{I}_n + \\
& (a_0 a_1^* |0\rangle \langle 1| + a_1 a_0^* |1\rangle \langle 0|) \otimes 2^{-n} (|s_1^{L=n}\rangle \langle s_1^{L=n}| + (-1)^N |s_2^{L=n}\rangle \langle s_2^{L=n}|) \tag{397}
\end{aligned}$$

IV) Input: $\hat{\rho}_{SE}^{\text{in}} = |\Psi_S^{\text{in}}\rangle \langle \Psi_S^{\text{in}}| \otimes \hat{\rho}_E^{\text{in}}, |\Psi_S^{\text{in}}\rangle = \sum_{m=0}^{2^k-1} a_m |m\rangle$, $\hat{\rho}_E^{\text{in}} = 2^{-1} (|0_n\rangle \langle 0_n| + |10_{n-1}\rangle \langle 10_{n-1}|)$, $\hat{u}_j^{(\phi=\pi/2)}$ -evolution

$\hat{\rho}_{SE}^{\text{out}} (L=n)$ emerges from (396) by applying the following substitutions:

$$\begin{aligned}
& |1_n\rangle \leftrightarrow |10_{n-1}\rangle \\
& (-1)^n (|1_n\rangle \langle s_2^{L=n}| + \text{h.c.}) \leftrightarrow (-1)^1 (|10_{n-1}\rangle \langle s_2^{L=n}| + \text{h.c.}) \\
& (1 + (-1)^n) \bigotimes_{i=1}^n \hat{B}_1^{\pi/2} \cdot \delta_{L,n} \leftrightarrow (-1)^{n-1} \bigotimes_{i=1}^n \hat{B}_1^{\pi/2} \cdot \delta_{L,n} \tag{398}
\end{aligned}$$

V) Input: $|\Psi_{SE}^{\text{in}}\rangle = a |0_{k=1}\rangle \otimes |s_1^{L=n}\rangle + b |1_{k=1}\rangle \otimes |s_2^{L=n}\rangle$, $\hat{u}_j^{(\phi=\pi/2)}$ -evolution

$$|\Psi_{SE=L=n}^{\text{out}}\rangle = a |0\rangle \otimes |s_1^n\rangle + (-1)^N b |1\rangle \otimes |s_2^n\rangle, \tag{399}$$

with non-zero eigenvalues of $\hat{\rho}_{SE}^{\text{out}}$ and $\hat{\rho}_E^{\text{out}}$: $\lambda_{1/2}^{SE} = \lambda_{1/2}^E \in \{|a|^2, |b|^2\} \forall (1 \leq L < n)$ and $\lambda_1^{SE} = 1 \neq \lambda_{1/2}^E \in \{|a|^2, |b|^2\}$ for $L=n$.

VI) Input: $\hat{\rho}_{SE}^{in} = |\Psi_S^{in}\rangle \langle \Psi_S^{in}| \otimes \hat{\rho}_E^{in}$, $|\Psi_S^{in}\rangle = \sum_{m=0}^{2^{k-1}-1} a_m |m\rangle$, $\hat{\rho}_E^{in} = |0_n\rangle \langle 0_n|$, $\hat{u}_j^{(\phi=\pi/3)}$ -evolution

$$\begin{aligned} \hat{\rho}_{SE}^{out} = & |\Psi'\rangle \langle \Psi'| + |\Psi''\rangle \langle \Psi''| + \\ & |a_1|^2 |1\rangle \langle 1| \otimes \sum_{\pi_1=1}^{n-1} \left\{ |s_{c_1}\rangle^{\otimes \pi_1} \langle s_{c_1}| (2^{-1}\sqrt{3})^{2\pi_1} \otimes \left(\hat{I} - |s_{c_1}\rangle \langle s_{c_1}| \right)^{\otimes (n-\pi_1)} (2^{-2})^{n-\pi_1} \right\} \\ & - |a_0|^2 |0\rangle \langle 0| \otimes |0_n\rangle \langle 0_n| + (-1)^N |a_1|^2 |1\rangle \langle 1| (-1)^n (2^{-1}\sqrt{3})^n 2^{-n/2} \bigotimes_{i=1}^n \hat{B}_1^{\pi/3}, \end{aligned} \quad (400)$$

where $|\Psi'\rangle = a_0 |0\rangle \otimes |0_n\rangle + a_1 (2^{-1}\sqrt{3})^n |1\rangle \otimes |s_{c_1}^n\rangle$, $|\Psi''\rangle = a_0 |0\rangle \otimes |0_n\rangle + (-1)^N a_1 2^{-n} |1\rangle \otimes |s_{c_2}^n\rangle$, $\{|s_{c_1}\rangle, |s_{c_2}\rangle\}$ (with $c_1 = \frac{\sqrt{3}}{2}$ and $c_2 = \frac{1}{2}$) as in (349)-(350), $\hat{B}_1^{\pi/3} = (\sqrt{8})^{-1} [\sqrt{3}|1\rangle \langle 1| - \sqrt{3}|0\rangle \langle 0| + |1\rangle \langle 0| + |0\rangle \langle 1|]$, $\langle s_{c_1} | \xi \rangle = c_1 \cdot \delta_{\xi,0} + c_2 \cdot \delta_{\xi,1}$, $\langle s_{c_2} | \xi \rangle = c_2 \cdot \delta_{\xi,0} - c_1 \cdot \delta_{\xi,1}$ for $\xi \in \{0, 1\}$.

Remark: for $1 > |a_0|^2 > 0$ the S-subspace $|1\rangle \langle 1|$ in (400) is dominated in the limit $n \gg k$ by the addend $\sim |s_{c_1}\rangle^n \langle s_{c_1}|$ which, according to E, always leads to $H(S, E_L) > H(E_L) \forall (1 \leq L \leq n)$. Then $\lim_{n \gg k} \hat{\rho}_{SE}^{out} = |a_0|^2 |0\rangle \langle 0| \otimes |0_n\rangle \langle 0_n| + |a_1|^2 |s_{c_1}\rangle^n \langle s_{c_1}|$ yields non-zero eigenvalues $\{\lambda_1^{SE} = |a_0|^2, \lambda_2^{SE} = |a_1|^2\}$ and $\lambda_{1/2}^E = 1/2 \pm \sqrt{1/4 - c_2^2 |a_0|^2 |a_1|^2}$ (for $\hat{\rho}_E^{out}$), with $H(S, E) > H(E) \forall (c_2 \neq 2^{-1/2}) > 0$, as argued by (349)-(351). Accordingly, tracing out E-qubits from $\lim_{n \gg k} \hat{\rho}_{SE}^{out}$ of (400) would, as demonstrated in Fig. 4 (■-dotted curve), only enforce $H(E_L) < H(S, E_L) \forall (1 \leq L < n)$, i.e. $I(S : E_L)$ would further decrease due to addends that were neglected when performing the limit $n \gg k$ in (400).

VII) Input: $\hat{\rho}_{SE}^{in} = |\Psi_S^{in}\rangle \langle \Psi_S^{in}| \otimes \hat{\rho}_E^{in}$, $|\Psi_S^{in}\rangle = 2^{-1/2} (|0\rangle + |2^{k-2} - 1\rangle)$ ($k = 2$ -qubit pure Bell-state), $\hat{\rho}_E^{in} = |0_n\rangle \langle 0_n|$, $\hat{u}_j^{(\phi=\pi/2)}$ -evolution

$$\begin{aligned} \hat{\rho}_{SE}^{out} = & \frac{1}{2} |0\rangle \langle 0| \otimes |0_n\rangle \langle 0_n| + 2^{-n/2-1} \cdot |0\rangle \langle 3| \otimes |0_n\rangle \langle s_1^n| + 2^{-n/2-1} \cdot |3\rangle \langle 0| \otimes |s_1^n\rangle \langle 0_n| + |3\rangle \langle 3| \otimes 2^{-n-1} \cdot \hat{I}_n \\ & + (-1)^N \left[2^{-n/2-1} \cdot |0\rangle \langle 3| \otimes |0_n\rangle \langle s_2^n| + 2^{-n/2-1} \cdot |3\rangle \langle 0| \otimes |s_2^n\rangle \langle 0_n| + (-1)^n 2^{-n/2-1} |3\rangle \langle 3| \bigotimes_{i=1}^n \hat{B}_1^{\pi/2} \cdot \delta_{L,n} \right] \end{aligned} \quad (401)$$

VIII) Input: $|\Psi_{SE}^{in}\rangle = 2^{-1/2} (|0_{k=1}0_n\rangle + |1_{k=1}1_n\rangle)$, $\hat{u}_j^{(\phi=\pi/2)}$ -evolution

$$\begin{aligned} \hat{\rho}_{SE}^{out} = & \frac{1}{2} \left\{ |0_{k=1}0_n\rangle \langle 0_{k=1}0_n| + 2^{-n/2} [|0_{k=1}0_n\rangle \langle 1_{k=1}s_1^n| + |1_{k=1}s_1^n\rangle \langle 0_{k=1}0_n|] + |1_k\rangle \langle 1_k| \otimes 2^{-n} \cdot \hat{I}_n \right. \\ & \left. (-1)^N \left[2^{-n/2} (-1)^n (|0_{k=1}0_n\rangle \langle 1_{k=1}s_2^n| + |1_{k=1}s_2^n\rangle \langle 0_{k=1}0_n|) + |1_k\rangle \langle 1_k| 2^{-n/2} \bigotimes_{i=1}^n \hat{B}_1^{\pi/2} \cdot \delta_{L,n} \right] \right\} \end{aligned} \quad (402)$$

IX) Input: $|\Psi_{SE}^{in}\rangle = 2^{-1/2} (|0_{k=1}\gamma_n\rangle + |1_{k=1}\mu_n\rangle)$, $\hat{u}_j^{(\phi=\pi/2)}$ -evolution

$$\begin{aligned} \hat{\rho}_{SE}^{out} = & |0\rangle \langle 0| \otimes |\gamma_n\rangle \langle \gamma_n| + 2^{-n-2} \left(1 + (-1)^{n+1} \right) |1\rangle \langle 1| \otimes |s_2^n\rangle \langle s_2^n| \\ & + (-1)^N \left[2^{-1-(n-1)/2} \left(1 + (-1)^{n+1} \right) \{ |0\rangle \langle 1| \otimes |\gamma_n\rangle \langle s_2^n| + |1\rangle \langle 0| \otimes |s_2^n\rangle \langle \gamma_n| \} \right. \\ & \left. 2^{-n/2-2} (1 + (-1)^n) |1\rangle \langle 1| \left\{ \bigotimes_{i=1}^n \hat{B}_1^{\pi/2} \cdot \delta_{L,n} + (-1)^{n+1} \bigotimes_{i=1}^n \hat{B}_0^{\pi/2} \cdot \delta_{L,n} \right\} \right], \end{aligned} \quad (403)$$

with $|\gamma_n\rangle = 2^{-1/2} (|0_n\rangle + |1_n\rangle)$ and $|\mu_n\rangle = 2^{-1/2} (|0_n\rangle - |1_n\rangle)$.

J.2 Output states $\hat{\rho}_{SE}^{out}$ of the random unitary evolution for the minimal attractor space

In this appendix we list the output states $\hat{\rho}_{SE}^{out}$ of the random unitary evolution used in section 8 of the main text when discussing Quantum Darwinism from the point of view of the minimal $\lambda = 1$ attractor subspace.

I) Input: $\hat{\rho}_{SE}^{\text{in}} = |\Psi_S^{\text{in}}\rangle \langle \Psi_S^{\text{in}}| \otimes \hat{\rho}_E^{\text{in}}, |\Psi_S^{\text{in}}\rangle = \sum_{m=0}^{2^k-1} a_m |m\rangle, \hat{\rho}_E^{\text{in}} = |0_n\rangle \langle 0_n|, \hat{u}_j^{(\phi=\pi/2)}$ -evolution

$$\hat{\rho}_{SE}^{\text{out}} = |\Psi'\rangle \langle \Psi'| + 2^{-n} \cdot \sum_{y=1}^{2^k-1} |a_y|^2 |y\rangle \langle y| \otimes \left(\hat{I}_n - |s_1^n\rangle \langle s_1^n| \right), \quad (404)$$

where $|\Psi'\rangle = a_0 |0\rangle \otimes |0_n\rangle + \sum_{y=1}^{2^k-1} a_y 2^{-n/2} |y\rangle \otimes |s_1^n\rangle$. $\hat{\rho}_{SE}^{\text{out}}$ contains those addends of (395) not proportional to $(-1)^N$.

II) Input: $\hat{\rho}_{SE}^{\text{in}} = |\Psi_S^{\text{in}}\rangle \langle \Psi_S^{\text{in}}| \otimes \hat{\rho}_E^{\text{in}}, |\Psi_S^{\text{in}}\rangle = \sum_{m=0}^{2^k-1} a_m |m\rangle, \hat{\rho}_E^{\text{in}} = |1_n\rangle \langle 1_n|, \hat{u}_j^{(\phi=\pi/2)}$ -evolution

$$\begin{aligned} \hat{\rho}_{SE}^{\text{out}} &= |a_0|^2 \cdot 2^{-n} (1 - 2^{-n})^{-1} |0\rangle \langle 0| \otimes \left(\hat{I}_n \cdot 2^{-n} - |0_n\rangle \langle 0_n| \right) + 2^{-n} \cdot \sum_{y=0}^{2^k-1} |a_y|^2 |y\rangle \langle y| \otimes \hat{I}_n \\ &\quad - 2^{-3n/2} \cdot (1 - 2^{-n})^{-1} \sum_{y=1}^{2^k-1} \left\{ a_0 a_y^* |0\rangle \langle y| \otimes |0_n\rangle \langle s_1^n| + a_y a_0^* |y\rangle \langle 0| \otimes |s_1^n\rangle \langle 0_n| \right\} \\ &\quad + 2^{-n} \cdot \sum_{(x \neq y)=1}^{2^k-1} \left\{ (1 - 2^{-n})^{-1} \cdot a_0 a_y^* |0\rangle \langle y| + (1 - 2^{-n})^{-1} \cdot a_y a_0^* |y\rangle \langle 0| + a_y a_x^* |y\rangle \langle x| \right\} \otimes |s_1^n\rangle \langle s_1^n| \end{aligned} \quad (405)$$

III) Input: $\hat{\rho}_{SE}^{\text{in}} = |\Psi_S^{\text{in}}\rangle \langle \Psi_S^{\text{in}}| \otimes \hat{\rho}_E^{\text{in}}, |\Psi_S^{\text{in}}\rangle = \sum_{m=0}^{2^{k-1}-1} a_m |m\rangle, \hat{\rho}_E^{\text{in}} = 2^{-1} (|0_n\rangle \langle 0_n| + |1_n\rangle \langle 1_n|), \hat{u}_j^{(\phi=\pi/2)}$ -evolution

$$\begin{aligned} \hat{\rho}_{SE}^{\text{out}} &= |a_0|^2 |0\rangle \langle 0| (1 - 2^{-n})^{-1} \otimes \left\{ \hat{I}_n \cdot 2^{-n-1} + |0_n\rangle \langle 0_n| (1 - 2^{1-n})^{-1} \left(\frac{1}{2} - 2^{1-n} + 2^{1-2n} \right) \right\} \\ &\quad + |a_1|^2 |1\rangle \langle 1| \otimes 2^{-n} \cdot \hat{I}_n + a_0 a_1^* 2^{-1} (1 - 2^{1-n})^{-1} |0\rangle \langle 1| \otimes \left\{ |0_n\rangle \langle s_1^n| \cdot 2^{-n/2} (1 - 2^{1-n}) + 2^{-n} |s_1^n\rangle \langle s_1^n| \right\} \\ &\quad + a_1 a_0^* 2^{-1} (1 - 2^{1-n})^{-1} |1\rangle \langle 0| \otimes \left\{ |s_1^n\rangle \langle 0_n| \cdot 2^{-n/2} (1 - 2^{1-n}) + 2^{-n} |s_1^n\rangle \langle s_1^n| \right\} \end{aligned} \quad (406)$$

Remark: $\hat{\rho}_{SE}^{\text{out}}$ for $\left| \Psi_{\text{E}_{\text{pure}}}^{\text{in}} \right\rangle = 2^{-1/2} (|0_n\rangle + |1_n\rangle)$ emerges from $\hat{\rho}_{SE}^{\text{out}}$ in (406) by **I)** multiplying the prefactors of $|x\rangle \langle y| \otimes |s_1^n\rangle \langle s_1^n|$ (with $x \neq y \in \{0, 1\}$), $|0\rangle \langle 1| \otimes |0_n\rangle \langle s_1^n|$ and $|1\rangle \langle 0| \otimes |s_1^n\rangle \langle 0_n|$ by 2, **II)** substituting in the prefactor of $|a_0|^2 |0\rangle \langle 0| \otimes |0_n\rangle \langle 0_n|$: $(1 - 2^{1-n})^{-1} \left(\frac{1}{2} - 2^{1-n} + 2^{1-2n} \right) \leftrightarrow \left(\frac{1}{2} - 2^{1-n} \right)$ and in the prefactor of $|a_1|^2 |1\rangle \langle 1| \otimes \hat{I}_n$: $2^{-n} \leftrightarrow (1 - 2^{1-n}) 2^{-n} (1 - 2^{-n})^{-1}$, and **III)** adding $(1 - 2^{-n})^{-1} \cdot \left\{ |a_0|^2 2^{-n/2-1} |0\rangle \langle 0| \otimes [|0_n\rangle \langle s_1^n| + |s_1^n\rangle \langle 0_n|] + 2^{-n} |a_1|^2 |1\rangle \langle 1| \otimes |s_1^n\rangle \langle s_1^n| \right\}$.

IV) Input: $\hat{\rho}_{SE}^{\text{in}} = |\Psi_S^{\text{in}}\rangle \langle \Psi_S^{\text{in}}| \otimes \hat{\rho}_E^{\text{in}}, |\Psi_S^{\text{in}}\rangle = \sum_{m=0}^{2^k-1} a_m |m\rangle, \hat{\rho}_E^{\text{in}} = 2^{-n} \hat{I}_n, \hat{u}_j^{(\phi=\pi/2)}$ -evolution

$$\hat{\rho}_{SE}^{\text{out}} = \sum_{x=0}^{2^k-1} |a_x|^2 |x\rangle \langle x| \otimes \hat{\rho}_E^{\text{in}} + 2^{-n} \cdot \sum_{(x \neq y)=0}^{2^k-1} a_x a_y^* |x\rangle \langle y| \otimes |s_1^n\rangle \langle s_1^n| \quad (407)$$

V) Input: $|\Psi_{SE}^{\text{in}}\rangle = a |0_{k=1}\rangle \otimes |s_1^I\rangle + b |1_{k=1}\rangle \otimes |s_2^I\rangle, \hat{u}_j^{(\phi=\pi/2)}$ -evolution

$$\hat{\rho}_{SE}^{\text{out}} = |a_0|^2 |0\rangle \langle 0| \otimes |s_1^n\rangle \langle s_1^n| + |a_1|^2 (2^n - 1)^{-1} |1\rangle \langle 1| \otimes \left(\hat{I}_n - |s_1^n\rangle \langle s_1^n| \right), \quad (408)$$

with eigenvalues $\forall (1 \leq L \leq n)$: **I)** $\lambda_1^{SE} = 1/2 ([1 - \delta_{L,0}] \text{times})$, $\lambda_2^{SE} = 1/2 (\delta_{L,0} \text{times})$, $\lambda_3^{SE} = 2^{n-L-1} (2^n - 1)^{-1} ([2^L - 1] \text{times})$, $\lambda_4^{SE} = (2^{n-L} - 1) \cdot 2^{-1} (2^n - 1)^{-1} (\delta_{L,0} \text{times})$ (for $\hat{\rho}_{SE}^{\text{out}}$); **II)** $\lambda_1^E = 2^{n-L-1} (2^n - 1)^{-1} ([2^L - 1] \cdot (1 - \delta_{L,0}) \text{times})$, $\lambda_2^E = (2^n - 1 - 2^{n-L-1}) \cdot (2^n - 1)^{-1} ([1 - \delta_{L,0}] \cdot [1 - \delta_{L,n}] \text{times})$, $\lambda_3^E = 1 (\delta_{L,0} \text{times})$, $\lambda_4^E = 1/2 (\delta_{L,n} \text{times})$ (for $\hat{\rho}_{SE}^{\text{out}}$); **III)** $\lambda_1^S = 1/2 (2 \text{times})$ (for $\hat{\rho}_S^{\text{out}}$).

VI) Input: $\hat{\rho}_{SE}^{in} = |\Psi_S^{in}\rangle \langle \Psi_S^{in}| \otimes \hat{\rho}_E^{in}$, $|\Psi_S^{in}\rangle = \sum_{m=0}^{2^k-1} a_m |m\rangle$, $\hat{\rho}_E^{in} = |0_n\rangle \langle 0_n|$, $\hat{u}_j^{(\phi=\pi/3)}$ -evolution

$$\begin{aligned} \hat{\rho}_{SE}^{out} = & |a_0|^2 |0\rangle \langle 0| \otimes \left\{ \left[\hat{I}_n 2^{-n} (1 - r^n) (1 - A_2) + A_1 |s_1^n\rangle \langle s_1^n| \right] (1 - 2^{-n})^{-1} \right. \\ & + A_2 |0_n\rangle \langle 0_n| + r^{n/2} \cdot (|s_1^n\rangle \langle 0_n| + |0_n\rangle \langle s_1^n|) (1 - A_2) + A_2 A_3 |s_1^n\rangle \langle s_1^n| \left. \right\} + \\ & r^{n/2} \{ a_0^* a_1 |1\rangle \langle 0| \otimes |s_1^n\rangle \langle 0_n| + a_1^* a_0 |0\rangle \langle 1| \otimes |0_n\rangle \langle s_1^n| \} \\ & + |a_1|^2 |1\rangle \langle 1| \otimes \left\{ r^n |s_1^n\rangle \langle s_1^n| + (1 - r^n) (2^n - 1)^{-1} (\hat{I}_n - |s_1^n\rangle \langle s_1^n|) \right\}, \end{aligned} \quad (409)$$

where $A_1 := 2^{1-n} r^n - r^n - 2^{-n}$, $A_2 := \left\{ \left[1 - 2^{1-n} + (2^{2-n} - 3) r^n \right] \cdot (1 - 2^{-n})^{-1} + 2r^{2n} \right\}^{-1} \cdot \left[\left(1 - 2^{1-n} + r^n (2^{2-n} - 2) \right) \cdot (1 - 2^{-n})^{-1} + r^n \cdot (r^n - 2) \right]$, $A_3 := r^n + 2^{-n} \cdot (1 - 2^{-n})^{-1}$ and $r = 3^n 2^{-2n} = (0.75)^n$ is the decoherence factor.

VII) Input: $\hat{\rho}_{SE}^{in} = |\Psi_S^{in}\rangle \langle \Psi_S^{in}| \otimes \hat{\rho}_E^{in}$, $|\Psi_S^{in}\rangle = \sum_{m=0}^{2^k-1} a_m |m\rangle$, $\hat{\rho}_E^{in} = 0.5 \cdot (|s_1^n\rangle \langle s_1^n| + |s_2^n\rangle \langle s_2^n|)$, $\hat{u}_j^{(\phi=\pi/2)}$ -evolution

$$\begin{aligned} \hat{\rho}_{SE}^{out} = & |a_0|^2 |0\rangle \langle 0| \otimes \hat{I}_n 2^{-n} \left[1 - \left(\frac{1}{2} - 2^{-n} \right) \cdot (1 - 2^{-n})^{-1} \right] + |0\rangle \langle 0| \otimes |s_1^n\rangle \langle s_1^n| |a_0|^2 \left(\frac{1}{2} - 2^{-n} \right) \cdot (1 - 2^{-n})^{-1} \\ & + \sum_{x=1}^{2^k-1} \{ |0\rangle \langle x| \otimes |s_1^n\rangle \langle s_1^n| \langle x| \hat{\rho}_S^{in} |0\rangle 2^{-1} + |x\rangle \langle 0| \otimes |s_1^n\rangle \langle s_1^n| \langle 0| \hat{\rho}_S^{in} |x\rangle 2^{-1} \} \\ & + \sum_{x=1}^{2^k-1} \{ |x\rangle \langle x| \otimes |s_1^n\rangle \langle s_1^n| \langle x| \hat{\rho}_S^{in} |x\rangle 2^{-1} \left(1 - (2^n - 1)^{-1} \right) + |x\rangle \langle x| \otimes \hat{I}_n \langle x| \hat{\rho}_S^{in} |x\rangle 2^{-1} (2^n - 1)^{-1} \} \\ & + 2^{-1} \cdot \sum_{x \neq y \neq 0}^{2^k-1} |s_1^n\rangle \langle s_1^n| \otimes \langle x| \hat{\rho}_S^{in} |y\rangle |y\rangle \langle x| \end{aligned} \quad (410)$$

VIII) Input: $\hat{\rho}_{SE}^{in} = |\Psi_S^{in}\rangle \langle \Psi_S^{in}| \otimes \hat{\rho}_E^{in}$, $|\Psi_S^{in}\rangle = 2^{-1/2} (|0\rangle + |2^{k=2}-1\rangle)$ ($k = 2$ -qubit pure Bell-state), $\hat{\rho}_E^{in} = |0_n\rangle \langle 0_n|$, $\hat{u}_j^{(\phi=\pi/2)}$ -evolution

$$\begin{aligned} \hat{\rho}_S^{out} = & \frac{1}{2} (|0\rangle \langle 0| + |3\rangle \langle 3| + 2^{-n} |0\rangle \langle 3| + 2^{-n} |3\rangle \langle 0|) \\ \hat{\rho}_E^{out} = & \frac{1}{2} (|0_n\rangle \langle 0_n| + 2^{-n} \cdot \hat{I}_n) \\ \hat{\rho}_{SE}^{out} = & \frac{1}{2} |0\rangle \langle 0| \otimes |0_n\rangle \langle 0_n| + 2^{-n-1} \cdot |0\rangle \langle 3| \otimes |0_n\rangle \langle s_1^n| + 2^{-n-1} \cdot |3\rangle \langle 0| \otimes |s_1^n\rangle \langle 0_n| + |3\rangle \langle 3| \otimes 2^{-n-1} \cdot \hat{I}_n \end{aligned} \quad (411)$$

IX) Input: $|\Psi_{SE}^{in}\rangle = 2^{-1/2} (|0_{k=1} 0_n\rangle + |1_{k=1} 1_n\rangle)$, $\hat{u}_j^{(\phi=\pi/2)}$ -evolution

$$\begin{aligned} \hat{\rho}_{SE}^{out} = & |0\rangle \langle 0| \otimes |0_n\rangle \langle 0_n| 2^{-1} + 2^{-n/2-1} \{ |0\rangle \langle 1| \otimes |0_n\rangle \langle s_1^n| + |1\rangle \langle 0| \otimes |s_1^n\rangle \langle 0_n| \} + 2^{-n-1} |1\rangle \langle 1| \otimes \hat{I}_n \\ \hat{\rho}_S^{out} = & 2^{-1} |0\rangle \langle 0| + 2^{-n-1} \{ |0\rangle \langle 1| + |1\rangle \langle 0| \} + 2^{-1} |1\rangle \langle 1| \\ \hat{\rho}_E^{out} = & |0_n\rangle \langle 0_n| 2^{-1} + 2^{-n-1} \hat{I}_n \end{aligned} \quad (412)$$

X) Input: $|\Psi_{SE}^{in}\rangle = 2^{-1/2} (|0_{k=1} \gamma_n\rangle + |1_{k=1} \mu_n\rangle)$, $\hat{u}_j^{(\phi=\pi/2)}$ -evolution

$$\begin{aligned} \hat{\rho}_{SE}^{out} = & |0\rangle \langle 0| \otimes 2^{-n-1} \hat{I}_n + |0\rangle \langle 0| \otimes 2^{-n-1} (1 - 2^{-n})^{-1} (|s_1^n\rangle \langle s_1^n| - 2^{-n} \hat{I}_n) + \\ & |0\rangle \langle 0| \otimes 2^{-1} (1 - 2^{-n})^{-1} 2^{-n/2} (1 - 2^{1-n}) (|s_1^n\rangle \langle 0_n| + |0_n\rangle \langle s_1^n| - 2^{1-n/2} |s_1^n\rangle \langle s_1^n|) \\ & |0\rangle \langle 0| \otimes 2^{-1} (1 - 2^{-n})^{-1} (1 - 2^{1-n})^{-1} \cdot A \cdot (|0_n\rangle \langle 0_n| - 2^{-n} \hat{I}_n - 2^{-n/2} [|s_1^n\rangle \langle 0_n| + |0_n\rangle \langle s_1^n| - 2^{1-n/2} |s_1^n\rangle \langle s_1^n|]) \\ & + 2^{-1} (2^n - 1)^{-1} |1\rangle \langle 1| \otimes (\hat{I}_n - |s_1^n\rangle \langle s_1^n|), \end{aligned} \quad (413)$$

with $A = 2^{-1} - 2^{-n} [1 + 2^{1/2} - 2^{2-n}]$, $|\gamma_n\rangle = 2^{-1/2} (|0_n\rangle + |1_n\rangle)$ and $|\mu_n\rangle = 2^{-1/2} (|0_n\rangle - |1_n\rangle)$.

J.3 Output state $\hat{\rho}_{SE}^{\text{out}}$ of the random unitary evolution for the intermediate attractor space

In this appendix we list the output state $\hat{\rho}_{SE}^{\text{out}}$ of the random unitary evolution used in section 8 of the main text when discussing Quantum Darwinism from the point of view of the intermediate $\lambda = 1$ attractor subspace with E containing $2n - 3$ bindings.

Input: $\hat{\rho}_{SE}^{\text{in}} = |\Psi_S^{\text{in}}\rangle \langle \Psi_S^{\text{in}}| \otimes \hat{\rho}_E^{\text{in}}, |\Psi_S^{\text{in}}\rangle = \sum_{m=0}^{2^{k=1}-1} a_m |m\rangle, \hat{\rho}_E^{\text{in}} = 2^{-1} (|0_n\rangle \langle 0_n| + |0_{n-2}10\rangle \langle 0_{n-2}10|), \hat{U}_j^{(\phi=\pi/2)}$ -evolution,
 $2n - 3$ bindings between E-qubits
 $\hat{\rho}_{SE}^{\text{out}}$ contains those addends of (396) not proportional to $(-1)^N$ after substituting

$$|0_{n-2}10\rangle \leftrightarrow |1_n\rangle. \quad (414)$$

K $\hat{U}_{ij}^{(\alpha_1, \alpha_2, \gamma)}$ from Eq. (258) for specific parameter values

Here we want to derive (258) and (259): (258) can be easily derived by noticing that [12, 23, 24]

$$\begin{aligned} \hat{U}_{ij}^{(\alpha_1, \alpha_2, \gamma)} &= \exp \left[\frac{i}{2} \hat{H}_\gamma^{\alpha_1, \alpha_2} \right] = \cos \left(\frac{\sqrt{(\hat{H}_\gamma^{\alpha_1, \alpha_2})^2}}{2} \right) + i \frac{\hat{H}_\gamma^{\alpha_1, \alpha_2}}{\sqrt{(\hat{H}_\gamma^{\alpha_1, \alpha_2})^2}} \sin \left(\frac{\sqrt{(\hat{H}_\gamma^{\alpha_1, \alpha_2})^2}}{2} \right) \\ &= S \cos \left(\frac{\sqrt{D_\gamma^{\alpha_1, \alpha_2}}}{2} \right) S^\dagger + i \frac{\hat{H}_\gamma^{\alpha_1, \alpha_2}}{S \sqrt{(D_\gamma^{\alpha_1, \alpha_2})^2} S^\dagger} S \sin \left(\frac{\sqrt{D_\gamma^{\alpha_1, \alpha_2}}}{2} \right) S^\dagger \\ &= \cos \left(\frac{\sqrt{D_\gamma^{\alpha_1, \alpha_2}}}{2} \right) \hat{I}_1^{(i)} \otimes \hat{I}_1^{(j)} + i \hat{H}_\gamma^{\alpha_1, \alpha_2} \sin \left(\frac{\sqrt{D_\gamma^{\alpha_1, \alpha_2}}}{2} \right) \left[\sqrt{D_\gamma^{\alpha_1, \alpha_2}} \right]^{-1}, \end{aligned} \quad (415)$$

where S represents an appropriate similarity matrix whose columns are the eigenvectors of $(\hat{H}_\gamma^{\alpha_1, \alpha_2})^2$ (similarity transformation) and

$$D_\gamma^{\alpha_1, \alpha_2} = \text{diag} [V_{00}, V_{10}, V_{01}, V_{11}]_{2^1 \times 2^1} = \sum_{\chi \in G} V_\chi |\chi\rangle \langle \chi|$$

denotes a diagonal eigenvalue matrix with $G \equiv \{(0_i, 0_j), (1_i, 0_j), (0_i, 1_j), (1_i, 1_j)\}$ eigenvalues V_χ specified in (258). Indeed, (415) corresponds to (258).

Now, using (258) we can easily obtain from

$$\begin{aligned} \hat{H}_\gamma^{\alpha_1, \alpha_2} &= \alpha_1 (|0\rangle_i \langle 1| + |1\rangle_i \langle 0|) \otimes (|0\rangle_j \langle 1| + |1\rangle_j \langle 0|) \\ &\quad - \alpha_2 (|0\rangle_i \langle 1| - |1\rangle_i \langle 0|) \otimes (|0\rangle_j \langle 1| - |1\rangle_j \langle 0|) \\ &\quad - \gamma (|0\rangle_i \langle 0| - |1\rangle_i \langle 1|) \otimes (|0\rangle_j \langle 0| - |1\rangle_j \langle 1|) \end{aligned}$$

the identities

$$\begin{aligned} \hat{H}_\gamma^{\alpha_1, \alpha_2} |00\rangle &= (\alpha_1 - \alpha_2) |11\rangle - \gamma |00\rangle \\ \hat{H}_\gamma^{\alpha_1, \alpha_2} |10\rangle &= (\alpha_1 + \alpha_2) |01\rangle + \gamma |10\rangle \\ \hat{H}_\gamma^{\alpha_1, \alpha_2} |01\rangle &= (\alpha_1 + \alpha_2) |10\rangle + \gamma |01\rangle \\ \hat{H}_\gamma^{\alpha_1, \alpha_2} |11\rangle &= (\alpha_1 - \alpha_2) |00\rangle - \gamma |11\rangle, \end{aligned} \quad (416)$$

which transform (258) into

$$\begin{aligned} \hat{U}_{ij}^{(\alpha_1, \alpha_2, \gamma)} &= (A_1 - i\gamma A_2) |00\rangle \langle 00| + i(\alpha_1 - \alpha_2) A_2 |11\rangle \langle 00| \\ &\quad + (A_3 + i\gamma A_4) |10\rangle \langle 10| + i(\alpha_1 + \alpha_2) A_4 |01\rangle \langle 10| \\ &\quad + (A_5 + i\gamma A_6) |01\rangle \langle 01| + i(\alpha_1 + \alpha_2) A_6 |10\rangle \langle 01| \\ &\quad + (A_7 - i\gamma A_8) |11\rangle \langle 11| + i(\alpha_1 - \alpha_2) A_8 |00\rangle \langle 11|, \end{aligned} \quad (417)$$

where $A_1 := \cos \left(\frac{\sqrt{V_{00}}}{2} \right), A_2 := \sin \left(\frac{\sqrt{V_{00}}}{2} \right) [\sqrt{V_{00}}]^{-1}, A_3 := \cos \left(\frac{\sqrt{V_{10}}}{2} \right), A_4 := \sin \left(\frac{\sqrt{V_{10}}}{2} \right) [\sqrt{V_{10}}]^{-1}, A_5 := \cos \left(\frac{\sqrt{V_{01}}}{2} \right),$
 $A_6 := \sin \left(\frac{\sqrt{V_{01}}}{2} \right) [\sqrt{V_{01}}]^{-1}, A_7 := \cos \left(\frac{\sqrt{V_{11}}}{2} \right)$ and

$A_8 := \sin\left(\frac{\sqrt{V_{11}}}{2}\right) [\sqrt{V_{11}}]^{-1}$. But (417) is precisely (259) if we identify $[1] \equiv (A_1 - i\gamma A_2)$, $[2] \equiv i(\alpha_1 - \alpha_2) A_8$, $[3] \equiv (A_3 + i\gamma A_4)$, $[4] \equiv i(\alpha_1 + \alpha_2) A_6$, $[5] \equiv i(\alpha_1 + \alpha_2) A_4$, $[6] \equiv (A_5 + i\gamma A_6)$, $[7] \equiv (\alpha_1 - \alpha_2) A_2$ and $[8] \equiv (A_7 - i\gamma A_8)$.

Finally, we also want to confirm that (258) leads for certain specialized values of α_1 , α_2 and γ to well known transformations: for instance, after setting in (258) $\alpha_1 = \alpha_2 = \alpha$ and $\gamma = 0$ we obtain $V_{00} = V_{11} = 0$ and $V_{10} = V_{01} = 4\alpha^2$ and thus

$$\hat{H}_Y^{\alpha_1, \alpha_2} = \hat{H}^\alpha = \alpha \left(\hat{\sigma}_x^{(i)} \otimes \hat{\sigma}_x^{(j)} + \hat{\sigma}_y^{(i)} \otimes \hat{\sigma}_y^{(j)} \right),$$

yielding

$$\begin{aligned} \hat{U}_{ij}^{(\alpha_1, \alpha_2, \gamma)} &= \hat{U}_{ij}^{(\alpha)} = \left[\hat{I}_1^{(i)} \otimes \hat{I}_1^{(j)} + i\hat{H}^\alpha \right] (|00\rangle \langle 00| + |11\rangle \langle 11|) \\ &+ \left[\cos(\alpha) \hat{I}_1^{(i)} \otimes \hat{I}_1^{(j)} + \frac{i \sin(\alpha)}{2\alpha} \hat{H}^\alpha \right] \left(\underbrace{|10\rangle \langle 10| + |01\rangle \langle 01|}_{:= 2^{-1}(\hat{I}_1^{(i)} \otimes \hat{I}_1^{(j)} - \hat{\sigma}_z^{(i)} \otimes \hat{\sigma}_z^{(j)})} \right) \\ &= \hat{I}_1^{(i)} \otimes \hat{I}_1^{(j)} + \left[\frac{\cos(\alpha) - 1}{2} \right] \left(\hat{I}_1^{(i)} \otimes \hat{I}_1^{(j)} - \hat{\sigma}_z^{(i)} \otimes \hat{\sigma}_z^{(j)} \right) \\ &+ i\hat{H}^\alpha (|00\rangle \langle 00| + |11\rangle \langle 11| + \frac{\sin(\alpha)}{2\alpha} [|10\rangle \langle 10| + |01\rangle \langle 01|]) \\ &= \hat{I}_1^{(i)} \otimes \hat{I}_1^{(j)} + \left[\frac{\cos(\alpha) - 1}{2} \right] \left(\hat{I}_1^{(i)} \otimes \hat{I}_1^{(j)} - \hat{\sigma}_z^{(i)} \otimes \hat{\sigma}_z^{(j)} \right) \\ &+ i\hat{H}^\alpha (|00\rangle \langle 00| + |11\rangle \langle 11| + \frac{\sin(\alpha)}{2\alpha} [\hat{I}_1^{(i)} \otimes \hat{I}_1^{(j)} - \hat{\sigma}_z^{(i)} \otimes \hat{\sigma}_z^{(j)}]). \end{aligned} \quad (418)$$

Now, since

$$\left. \begin{aligned} \hat{\sigma}_x &= (|0\rangle \langle 1| + |1\rangle \langle 0|) \\ \hat{\sigma}_y &= -i(|0\rangle \langle 1| - |1\rangle \langle 0|) \\ \hat{\sigma}_z &= (|0\rangle \langle 0| - |1\rangle \langle 1|) \end{aligned} \right\} \begin{aligned} \hat{\sigma}_k |0\rangle \langle 0| &= |1\rangle \langle 0| \cdot \delta_{k,x} + i|1\rangle \langle 0| \cdot \delta_{k,y} + |0\rangle \langle 0| \cdot \delta_{k,z} \\ \hat{\sigma}_k |1\rangle \langle 1| &= |0\rangle \langle 1| \cdot \delta_{k,x} - i|0\rangle \langle 1| \cdot \delta_{k,y} - |1\rangle \langle 1| \cdot \delta_{k,z} \end{aligned}$$

and

$$\begin{aligned} \hat{\sigma}_x \hat{\sigma}_z &= -i\hat{\sigma}_y \\ \hat{\sigma}_y \hat{\sigma}_z &= i\hat{\sigma}_x, \end{aligned}$$

we see that

$$\begin{aligned} \hat{H}^\alpha (|00\rangle \langle 00| + |11\rangle \langle 11|) &= 0 \\ \hat{H}^\alpha (\hat{I}_1^{(i)} \otimes \hat{I}_1^{(j)} - \hat{\sigma}_z^{(i)} \otimes \hat{\sigma}_z^{(j)}) &= \alpha [\hat{\sigma}_x^{(i)} \otimes \hat{\sigma}_x^{(j)} + \hat{\sigma}_y^{(i)} \otimes \hat{\sigma}_y^{(j)} - i^2 (\hat{\sigma}_y^{(i)} \otimes \hat{\sigma}_y^{(j)} + \hat{\sigma}_x^{(i)} \otimes \hat{\sigma}_x^{(j)})] \\ &= 2\alpha (\hat{\sigma}_x^{(i)} \otimes \hat{\sigma}_x^{(j)} + \hat{\sigma}_y^{(i)} \otimes \hat{\sigma}_y^{(j)}) = 2\hat{H}^\alpha, \end{aligned}$$

allowing us to write (418) as

$$\hat{U}_{ij}^{(\alpha_1, \alpha_2, \gamma)} = \hat{U}_{ij}^{(\alpha)} = \hat{I}_1^{(i)} \otimes \hat{I}_1^{(j)} + \left[\frac{\cos(\alpha) - 1}{2} \right] (\hat{I}_1^{(i)} \otimes \hat{I}_1^{(j)} - \hat{\sigma}_z^{(i)} \otimes \hat{\sigma}_z^{(j)}) + i \frac{\sin(\alpha)}{2} (\hat{\sigma}_x^{(i)} \otimes \hat{\sigma}_x^{(j)} + \hat{\sigma}_y^{(i)} \otimes \hat{\sigma}_y^{(j)}), \quad (419)$$

which is precisely the dissipative operator from (237). In other words, (258) behaves as expected for $\alpha_1 = \alpha_2 = \alpha \neq \gamma = 0$, yielding (259) with $V_{00} = V_{11} = 0$, $V_{10} = V_{01} = 4\alpha^2$ and non-zero entries $[1] = [8] \equiv 1$, $[3] = [6] \equiv \cos(\alpha)$ and $[4] = [5] \equiv i \sin(\alpha)$.

Accordingly, for $\alpha_1 = \alpha_2 = 0 \neq \gamma = \pi$ (maximal dephasing strength) (258) leads to (259) with $V_{00} = V_{11} = V_{10} = V_{01} = \pi^2$ and non-zero entries $[1] = [8] \equiv -i$ and $[3] = [6] \equiv i$, i.e. (258) behaves as it should also in case of pure, maximal dephasing. This case of maximal, pure dephasing is a special parameter-choice for γ in a generalized version

$$\begin{aligned} \hat{U}_{ij}^{(\alpha_1=\alpha_2=0, \gamma)} &= \exp \left[\frac{i}{2} \hat{H}_Y^{\alpha_1=\alpha_2=0} \right] = \exp \left[\frac{i}{2} \hat{H}_Y \right] \\ &= \exp \left[-\frac{i}{2} \hat{\sigma}_z^{(i)} \otimes \hat{\sigma}_z^{(j)} \right] = \cos\left(\frac{\gamma}{2}\right) \hat{I}_1^{(i)} \otimes \hat{I}_1^{(j)} + i \frac{\cos(\frac{\gamma}{2})}{\gamma} \hat{H}_Y \end{aligned}$$

of (258) and (415).

Certainly, inserting $\alpha_1 = \alpha_2 = \alpha = \gamma = 0$ into (258) we obtain (259) with $V_{00} = V_{11} = V_{10} = V_{01} = 0$ and non-zero entries $[1] = [3] = [6] = [8] \equiv 1$, indicating that (259) turns into an identity matrix, whereas $\hat{U}_{ij}^{\text{Tot}}(\alpha_1, \alpha_2, \gamma)$ from (260)-(261) turns into the CNOT-transformation (pure decoherence)

$$\hat{U}_{ij}^{\text{Tot}}(\alpha_1 = \alpha_2 = \gamma = 0) = \hat{U}_{ij}^{(\Phi=\pi/2)} \hat{U}_{ij}^{(\alpha_1=\alpha_2=\gamma=0)} = \hat{U}_{ij}^{(\Phi=\pi/2)} \hat{I}_1^{(i)} \otimes \hat{I}_1^{(j)} = \hat{U}_{ij}^{(\Phi=\pi/2)},$$

as expected.

Apparently, all these special values of parameters α_1 , α_2 and γ indicate that (260)-(261) represents an appropriate transformation structure which encloses the CNOT, dissipative and dephasing transformations. Also, by comparing the form of $\hat{U}_{ij}^{\text{Tot}}$ from (260) for $(\alpha_1 = \alpha_2 = 0, \gamma > 0)$ and $\left(\underbrace{\alpha_1}_{>0} - \underbrace{\alpha_2}_{>0} \right) \geq \gamma = 0$, we see that (415) and $\hat{U}_{ij}^{\text{Tot}}$ also may be expressed as (259) and (261), respectively, with

$$\begin{aligned} [1] &:= \cos\left(\frac{\sqrt{V_{00}}}{2}\right) - \frac{i\gamma}{\sqrt{V_{00}}} \sin\left(\frac{\sqrt{V_{00}}}{2}\right) \equiv \cos\left(\frac{\alpha_1 - \alpha_2}{2}\right) \exp\left[-\frac{i\gamma}{2}\right] & [2] &:= \frac{i(\alpha_1 - \alpha_2)}{\sqrt{V_{11}}} \sin\left(\frac{\sqrt{V_{11}}}{2}\right) \equiv i \sin\left(\frac{\alpha_1 - \alpha_2}{2}\right) \exp\left[-\frac{i\gamma}{2}\right] \\ [3] &:= \cos\left(\frac{\sqrt{V_{10}}}{2}\right) + \frac{i\gamma}{\sqrt{V_{10}}} \sin\left(\frac{\sqrt{V_{10}}}{2}\right) \equiv \cos\left(\frac{\alpha_1 + \alpha_2}{2}\right) \exp\left[\frac{i\gamma}{2}\right] & [4] &:= \frac{i(\alpha_1 + \alpha_2)}{\sqrt{V_{01}}} \sin\left(\frac{\sqrt{V_{01}}}{2}\right) \equiv i \sin\left(\frac{\alpha_1 + \alpha_2}{2}\right) \exp\left[\frac{i\gamma}{2}\right] \\ [5] &:= \frac{i(\alpha_1 + \alpha_2)}{\sqrt{V_{10}}} \sin\left(\frac{\sqrt{V_{10}}}{2}\right) \equiv i \sin\left(\frac{\alpha_1 + \alpha_2}{2}\right) \exp\left[\frac{i\gamma}{2}\right] & [6] &:= \cos\left(\frac{\sqrt{V_{01}}}{2}\right) + \frac{i\gamma}{\sqrt{V_{01}}} \sin\left(\frac{\sqrt{V_{01}}}{2}\right) \equiv \cos\left(\frac{\alpha_1 + \alpha_2}{2}\right) \exp\left[\frac{i\gamma}{2}\right] \\ [7] &:= \frac{i(\alpha_1 - \alpha_2)}{\sqrt{V_{00}}} \sin\left(\frac{\sqrt{V_{00}}}{2}\right) \equiv i \sin\left(\frac{\alpha_1 - \alpha_2}{2}\right) \exp\left[-\frac{i\gamma}{2}\right] & [8] &:= \cos\left(\frac{\sqrt{V_{11}}}{2}\right) - \frac{i\gamma}{\sqrt{V_{11}}} \sin\left(\frac{\sqrt{V_{11}}}{2}\right) \equiv \cos\left(\frac{\alpha_1 - \alpha_2}{2}\right) \exp\left[-\frac{i\gamma}{2}\right]. \end{aligned}$$

L S-E-output states for the asymmetric dissipation in Zurek's qubit model

In this appendix we derive generalized versions of output states from (267) discussed in the framework of Zurek's qubit model of Quantum Darwinism with respect to asymmetric dissipation.

For $(\alpha_1 \neq \alpha_2 > 0, \gamma = 0)$ we see that in (260) only terms

$$A = \cos\left(\frac{\alpha_1 - \alpha_2}{2}\right) |0\rangle_i \langle 0| \otimes |0\rangle_j \langle 0|, B = i \sin\left(\frac{\alpha_1 + \alpha_2}{2}\right) |0\rangle_i \langle 1| \otimes |1\rangle_j \langle 0|, C = i \sin\left(\frac{\alpha_1 - \alpha_2}{2}\right) |1\rangle_i \langle 0| \otimes |1\rangle_j \langle 0|$$

and

$$D = \cos\left(\frac{\alpha_1 + \alpha_2}{2}\right) |1\rangle_i \langle 1| \otimes |0\rangle_j \langle 0|$$

(which vanishes for $\alpha_1 = 2\pi/3$ and $\alpha_2 = \pi/3$ in (267)) for $i \in \{1\}$ and $j \in \{1, \dots, n\}$ contribute when acting upon $|\Psi_S^{\text{in}}\rangle \otimes |0_n\rangle$ from (12) within Zurek's QD-model. In order to anticipate those combinations of these four operators that act non-trivially upon $|\Psi_S^{\text{in}}\rangle \otimes |0_n\rangle$ in (267) we take into account only allowed changes of the S-qubit states $\{|0\rangle_i, |1\rangle_i\}$ due to $(A + B + C + D)^n$ for $L = n \geq 1$. For instance, for $L = n = 2$, the only allowed sequences of the four operators acting in a non-trivial way upon the S-states $|0\rangle_i$ and $|1\rangle_i$, respectively, are $\{A^2, CA, BC, DC\}$ and $\{AB, CB, BD, D^2\}$. These sequences generate the output state

$$\begin{aligned} |\Psi_{SE_L}^{\text{out}}\rangle &= a \left[\cos^2\left(\frac{\alpha_1 - \alpha_2}{2}\right) |0\rangle_i + i \cos\left(\frac{\alpha_1 - \alpha_2}{2}\right) \right. \\ &\quad \sin\left(\frac{\alpha_1 - \alpha_2}{2}\right) |1\rangle_i \left. \right] |0_2\rangle + b \left[i \cos\left(\frac{\alpha_1 - \alpha_2}{2}\right) \sin\left(\frac{\alpha_1 + \alpha_2}{2}\right) |0\rangle_i + \right. \\ &\quad i^2 \sin\left(\frac{\alpha_1 + \alpha_2}{2}\right) \sin\left(\frac{\alpha_1 - \alpha_2}{2}\right) |1\rangle_i \left. \right] |10\rangle + a \left[i^2 \sin\left(\frac{\alpha_1 + \alpha_2}{2}\right) \right. \\ &\quad \sin\left(\frac{\alpha_1 - \alpha_2}{2}\right) |0\rangle_i + i \sin\left(\frac{\alpha_1 - \alpha_2}{2}\right) \cos\left(\frac{\alpha_1 + \alpha_2}{2}\right) |1\rangle_i \left. \right] |01\rangle \\ &\quad + b \left[i \sin\left(\frac{\alpha_1 + \alpha_2}{2}\right) \cos\left(\frac{\alpha_1 + \alpha_2}{2}\right) |0\rangle_i + \cos^2\left(\frac{\alpha_1 + \alpha_2}{2}\right) |1\rangle_i \right] |11\rangle \end{aligned} \quad (420)$$

as a general version of (267), which induces $H(S) < H(S_{\text{class}}) \forall n \geq 1$, since w.r.t. $L = n > 2$ the allowed operator sequences lead to $|\Psi_{SE_L}^{\text{out}}\rangle$ from (267) equivalent to (420) for $\alpha_1 = 2\pi/3$ and $\alpha_2 = \pi/3$. Certainly, for $\alpha_1 = \alpha_2 = 0$ (420) coincides with (12). Accordingly, for the operators

$$A_R = A, B_R = i \sin\left(\frac{\alpha_1 - \alpha_2}{2}\right) |0\rangle_i \langle 1| \otimes |0\rangle_j \langle 0|, C_R = C, D_R = \cos\left(\frac{\alpha_1 - \alpha_2}{2}\right) |1\rangle_i \langle 1| \otimes |1\rangle_j \langle 0|$$

associated with (263) one can arrange allowed operator sequences in a similar way as done above, obtaining for $L = n = 2$ the output state

$$\begin{aligned} |\Psi_{SE_L}^{\text{out}(R)}\rangle &= \left[a \cos^2\left(\frac{\alpha_1 - \alpha_2}{2}\right) + ib \cos\left(\frac{\alpha_1 - \alpha_2}{2}\right) \right. \\ &\quad \sin\left(\frac{\alpha_1 - \alpha_2}{2}\right) \left. \right] |0\rangle_i |0_2\rangle + \left[ib \cos\left(\frac{\alpha_1 - \alpha_2}{2}\right) \sin\left(\frac{\alpha_1 - \alpha_2}{2}\right) + \right. \\ &\quad i^2 a \sin^2\left(\frac{\alpha_1 - \alpha_2}{2}\right) \left. \right] |0\rangle_i |10\rangle + \left[i^2 b \sin^2\left(\frac{\alpha_1 - \alpha_2}{2}\right) \right. \\ &\quad + ia \sin\left(\frac{\alpha_1 - \alpha_2}{2}\right) \cos\left(\frac{\alpha_1 - \alpha_2}{2}\right) \left. \right] |1\rangle_i |01\rangle \\ &\quad + \left[ia \sin\left(\frac{\alpha_1 - \alpha_2}{2}\right) \cos\left(\frac{\alpha_1 - \alpha_2}{2}\right) + b \cos^2\left(\frac{\alpha_1 - \alpha_2}{2}\right) \right] |1\rangle_i |11\rangle \end{aligned} \quad (421)$$

as a generalized version of (267), with $H(S) < H(S_{\text{class}}) \forall n \geq 1$. Again, for $\alpha_1 = \alpha_2 = 0$ (421) coincides with (12).

References, List of Figures, List of Tables and Index

References

- [1] H. Everett, Rev. Mod. Phys. **29**, 454–462 (1957); Albert, D., Loewer, B., Synthese **77**, 195-213 (1988).
- [2] Joos, E., Zeh, H. D., Kiefer, C., Giulini, D., Kupsch, J., Stamatescu, I.-O., »Decoherence and the Appearance of a Classical World in Quantum Theory« (Springer, 2003).
- [3] W. H. Zurek, Philos. Trans. R. Soc. London, Ser. A **356**, 1793–1821 (1998).
- [4] W. H. Zurek, arXiv: quant-ph/0707.2832v1 (2007); W. H. Zurek, Rev. Mod. Phys. **75**, 715-771 (2003).
- [5] W. H. Zurek, Nature Physics **5**, 181 - 188 (2009).
- [6] Schlosshauer, M., »Decoherence and the Quantum-to-Classical Transition« (Springer, 2007).
- [7] V. P. Belavkin, Foundations of Physics, **24**, No 5, 685714 (1994).
- [8] R. Blume-Kohout, W. H. Zurek, Found. Phys. **35**, 1857–1876 (2005); Zwolak, M., Riedel, C. J., Zurek, W. H., Phys. Rev. Lett. **112**, 140406 (2014).
- [9] Audretsch, J.: »Verschränkte Systeme« (WILEY-VCH, 2005).
- [10] W. H. Zurek, Phys. Rev. D **26**, 1862–1880 (1982); W. H. Zurek, Phys. Rev. Lett. **90**, No 12, 120404 (2003).
- [11] J. Novotný, G. Alber, I. Jex, Phys. Rev. Lett. **107**, 090501 (2011); Engel, K.-J., Nagel, R.: »One-Parameter Semigroups for Linear Evolution Equations« (Springer, New York, Heidelberg, Berlin, 2000).
- [12] Abramowitz, M., Stegun, I. A.: »Pocketbook of Mathematical Functions« (Harri-Deutsch, Frankfurt am Main, 1984); Bronstein, I. N., Semendjajew, K. A.: »Taschenbuch der Mathematik« (Harri-Deutsch, Frankfurt am Main, 2005); P. M. Morse, H. Feshbach: »Methods of Theoretical Physics«, part I-II (McGraw-Hill, New York, Toronto, London, Tokyo, 1953).
- [13] M. Berta, J. M. Renes, M. M. Wilde, IEEE **60**, 7987-8006 (2014).
- [14] F. G. S. L. Brandão, M. Piani, P. Horodecki, Nat. Com. **6**, 7908 (2015).
- [15] M. A. Nielsen, I. L. Chuang, »Quantum Computation and Quantum Information« (Cambridge University Press, 2010).
- [16] E. Desurvire, »Classical and Quantum Information Theory« (Cambridge University Press, 2010); Wilde, M. M.: »Quantum Information Theory« (Cambridge University Press, 2013).
- [17] C. E. Shannon, Bell Syst. Tech. J. **27** (1948), 379-423, 623-656.
- [18] H. J. Groenewald, Inter. Jour. of Theo. Physics **4**: 327 (1971);
- [19] A. Winter, Communications in Math. Physics **244**: 157 (2004).
- [20] D. S. Lemons, »A Student's Guide to Entropy« (Cambridge University Press, 2013).
- [21] Ch. H. Bennett, Inter. Jour. of Theo. Phys. **21**, 905-940 (1982); Ch. H. Bennett, arXiv: physics.class-ph/0210005v2 (2003).
- [22] W. Cheng, F. Xu, »Matrix Realignment Method for Calculating The Partial Transposes and The Partial Traces of Density Matrices« (Fourth International Conference on Natural Computation, 2008).
- [23] D. Serre, »Matrices - Theory and Applications« (Springer, 2010); Hornbeck, R. W.: »Numerical Methods« (Prentice-Hall, New Jersey, 1975); Press, W. H., Teukolsky, S. A., Vetterling, W. T., Flannery, B. P.: »Numerical Recipes in C« (Cambridge University Press, 1997); Logofatu, D.: »Algorithmen und Problemlösungen mit C++« (Vieweg, Wiesbaden, 2006); Breymann, U.: »C++ - Einführung und professionelle Programmierung« (Hanser, München-Wien, 2007).

- [24] R. Bhatia, »Matrix Analysis« (Springer, 1997); Ruiz-Tolosa, J.-R., Castillo E.: »From Vectors to Tensors« (Springer, Berlin-Heidelberg, 2005); Kowalsky, H.-J., Michler, G. O.: »Lineare Algebra« (De Gruyter, 12th Ed., Berlin-New York, 2003); Lovasz, L., Pelikan, J., Vesztergombi, K.: »Diskrete Mathematik« (Springer, Berlin-Heidelberg, 2005); Lau, D.: »Diskrete Mathematik«, vol. 1-2 (Springer, Berlin-Heidelberg, 2011).
- [25] J. v. Neumann, »Mathematische Grundlagen der Quantenmechanik« (Springer, 1996).
- [26] V. Scarani, M. Ziman, P. Stelmachovic, N. Gisin, V. Buzek, Phys. Rev. Lett. **88**, 097905 (2002).
- [27] G. Alber, A. Delgado, N. Gisin and I. Jex, J. Phys. A: Math. Theor. **34**, 8821 (2001).
- [28] L. Chen, Y. Bai, H. Lu, Journal of the Korean Physical Society, Vol. **58**, No. **3**, pp. 411-416 (2011).
- [29] J. Novotný, G. Alber, I. Jex: New Jour. Phys. **13**, 053052 (2011).
- [30] J. Novotný, G. Alber, I. Jex, J. Phys A **45**, 485301 (2012); »Asymptotic properties of quantum Markov chains«, arXiv: quant-ph/1208.0764v1 (2012).
- [31] R. A. Brualdi, D. Cvetkovic, »A Combinatorial Approach to Matrix Theory« (Taylor and Francis, 2010); Diestel, R.: »Graphentheorie« (Springer, Heidelberg, 2006); Brualdi, R. A., Ryser, H. J.: »Combinatorial Matrix Theory« (Cambridge University Press, 1991); Korte, B., Vygen, J.: »Kombinatorische Optimierung - Theorie und Algorithmen« (Springer, Berlin Heidelberg, 2012); Turau, V.: »Algorithmische Graphentheorie« (Oldenbourg, München, 2009); Even, S.: »Graph Algorithms« (Cambridge University Press, 2012); Tittmann, P.: »Graphentheorie« (Hanser, München, 2011); Krumke, S. O., Noltemeier, H.: »Graphentheoretische Konzepte und Algorithmen« (Springer-Vieweg, Wiesbaden, 2012); Reiss, K., Stroth, G.: »Endliche Strukturen« (Springer, Berlin-Heidelberg, 2011); Akiyama J., Kano, M.: »Factors and Factorizations of Graphs« (Springer, Berlin-Heidelberg, 2011); Cho, I.: »Algebras, Graphs and Their Applications« (Taylor & Francis, Boca Raton, 2014); J. Kepner, J. Gilbert, »Graph Algorithms in the Language of Linear Algebra« (SIAM, Philadelphia, 2011); Bapat, R. B.: »Graphs and Matrices« (Springer, London-Dordrecht-Heidelberg-New York, 1988); Balakrishnan, R., Ranganathan, K.: »A Textbook of Graph Theory« (Springer, New York, 2012).
- [32] M. Mendler, »Quantum Darwinism and Dissipation in open qubit systems«, BSc-Thesis, TU-Darmstadt (2014).
- [33] Braginsky, V. B. / Khalil, F. Ya.: »Quantum Measurement« (Cambridge University Press, 1995); Schwinger, J.: »Quantum Mechanics, A Symbolism of Measurements«, (Springer, Heidelberg 2003); Sen, R. N.: »Causality, Measurement Theory and the Differentiable Structure of Space-Time« (Cambridge University Press, 2010); Busch, P., Lathi, Pekka J., Mittelstaedt, P.: »The Quantum Theory of Measurement« (Springer, Berlin-Heidelberg, 1996); Breuer, H.-P., Petrucione, F.: »Relativistic Quantum Measurement« (Springer, Berlin-Heidelberg, 2000).
- [34] Bitbol, M., Kerszberg, P., Petitot, J.: »Constituting Objectivity: Transcendental Perspectives on Modern Physics« (Springer, 2010); Caponigro, M.: »Interpretations of Quantum Mechanics: a critical survey«, arXiv: physics.gen-ph/0811.3877v1 (2008); Omnes, R.: »Are There Unsolved Problems in the Interpretation of Quantum Mechanics?«, in »Open Systems and Measurements in Relativistic Quantum Theory«, ed by Heinz-Peter Breuer, Springer (1999); Mittelstaedt, P., International Journal of Theoretical Physics, Vol. **34**, No. **8**, (1995); d'Espagnat, B.: »Quantum Physics and Reality«, arXiv: quant-ph/1101.4545v3 (2011); Catren, G., Found Phys **38**, 470–487 (2008); Jaeger, G.: »Entanglement, Information and the Interpretation of Quantum Mechanics« (Springer, Berlin-Heidelberg, 2009).
- [35] Rivas, A., Huelga, S. F.: »Open Quantum Systems. An Introduction« (Springer, Berlin-Heidelberg, 2012), see also arXiv: quant-ph/1104.5242v2 (2012); Attal, S., Joye, A., Pillet, C.-A.: »Open Quantum Systems«, part I-III (Springer, Berlin-Heidelberg, 2006).
- [36] Whitney, R. S.: J.Phys. A: Math. Theory **41**, 175304 (2008).
- [37] Werner, D.: »Funktionalanalysis« (Springer, 2005); Courant, R., Hilbert, D.: »Methoden der mathematischen Physik« (Springer, Berlin-Heidelberg 1993); Schröder H.: »Funktionalanalysis« (Harri-Deutsch, Frankfurt am Main, 2000); Hirzebruch, F., Scharlau, W.: »Einführung in die Funktionalanalysis« (Spektrum, Heidelberg-Berlin, 1996).
- [38] Mahler, G., Weberruß, V. A.: »Quantum Networks - Dynamics of Open Nanostructures« (Springer, Berlin-Heidelberg, 1998).

List of Figures

- 1 Partial information plot (PIP) of mutual information (MI) and the redundancy $R_{\delta=0} = R$ of system's »classical« entropy $H(\hat{\rho}_S^{\text{out}}) \approx H(S_{\text{class}})$ stored in the n -qubit environment E w.r.t. the E -fraction parameter $0 < f = f_{\delta=0} = L/n \leq 1$ after the CNOT-evolution from (9)-(12) in accord with Zurek's qubit model: The initial S-E-state $\hat{\rho}_{SE}^{\text{in}} = \hat{\rho}_S^{\text{in}} \otimes \hat{\rho}_E^{\text{in}}$ involves a $k = 1$ qubit pure $\hat{\rho}_S^{\text{in}}$ (with $|\Psi_S^{\text{in}}\rangle = a|0\rangle + b|1\rangle$, $(a, b) \in \mathbb{C}$) and $\hat{\rho}_E^{\text{in}} = |0_n\rangle\langle 0_n|$ [4]. 28
- 2 Sketch of the protocol for state merging of a classically coherent state on systems $\hat{R}X_A X_B B$. P denotes the permutation of states in the orthonormal basis $\{|x\rangle\}$ of X_A , which splits X_A into two subsystems. The operation V is an isometry which performs the merging task by generating entanglement between X_A and X_B , as guaranteed by Uhlmann's theorem. Source: [13], courtesy of **J. Rennes**. 38
- 3 Venn-diagramms used w.r.t. (88). 57
- 4 PIP for (128), with $k = 1$, $0 < L \leq n = 9$, $f = L/n$, $\hat{\rho}_S^{\text{in}} = |\Psi_S^{\text{in}}\rangle\langle \Psi_S^{\text{in}}|$ (where $|\Psi_S^{\text{in}}\rangle = a|0\rangle + b|1\rangle$), $\hat{\rho}_E^{\text{in}} = |0_n\rangle\langle 0_n|$ and $\hat{\rho}_{SE}^{\text{in}} = \hat{\rho}_S^{\text{in}} \otimes \hat{\rho}_E^{\text{in}}$. After acting upon $\hat{\rho}_E^{\text{in}}$ by $\hat{u}_j^{(\phi=\pi/3)}$ from (9)-(10) in accord with Zurek's algorithm, no QD appears. 68
- 5 PIP for $\hat{\rho}_{SE}^{\text{out}}$ from $\hat{\rho}_{SE}^{\text{in}} = |\Psi_S^{\text{in}}\rangle\langle \Psi_S^{\text{in}}| \otimes \hat{\rho}_E^{\text{in}}$ (where $k = 1$, $n = 9$, $|\Psi_S^{\text{in}}\rangle = a|0\rangle + b|1\rangle$) and different $\hat{\rho}_E^{\text{in}}$ (s. also Tab. 8 in Appendix D) in Zurek's qubit model. 80
- 6 PIP for different $\hat{\rho}_{SE}^{\text{out}}$; for details s. main text. 81
- 7 PIP for $\hat{\rho}_{SE}^{\text{out}}$ from $\hat{\rho}_{SE}^{\text{in}} = |\Psi_S^{\text{in}}\rangle\langle \Psi_S^{\text{in}}| \otimes \hat{\rho}_E^{\text{in}}$ (where $k = 2$, $n' = 8 = 2 \cdot n$, $|\Psi_S^{\text{in}}\rangle = a|0\rangle + b|1\rangle$) and $\hat{\rho}_E^{\text{in}} = |0_n\rangle\langle 0_n|$ 82
- 8 Some directed graphs of interactions (interaction digraphs, IDs) between n environmental qubits. Arrows indicate the direction of interactions, pointing from a control qubit to the corresponding target qubit. . . . 84
- 9 Interaction digraph (ID) between system S and environment E with pure decoherence within the random unitary model [11]. 86
- 10 MI for an output state (174) of a $k = 1$ qubit S w.r.t. $f = L/n$ (with $0 \leq (L \in \mathbb{R}^+) \leq n$) of an $n = 9$ qubit E due to different decoherence factors r ($r = 0$, •-dotted curve; $r = 0.5$, ■-dotted curve; $r = 0.9$, ◆-dotted curve). 89
- 11 $I(S : E_{L=n})/H(S_{\text{class}})$ vs n after random iterative $\hat{u}_j^{(\phi=\pi/2)}$ -evolution of $\hat{\rho}_{SE}^{\text{in}} = |\Psi_S^{\text{in}}\rangle\langle \Psi_S^{\text{in}}| \otimes \hat{\rho}_E^{\text{in}}$ ($N \gg 1$), with a $k = 1$ qubit $|\Psi_S^{\text{in}}\rangle = \sum_{m=0}^1 a_m |m\rangle$ ($|a_m|^2 = 2^{-1} \forall m$) and different $\hat{\rho}_E^{\text{in}}$ (with $\geq 2(n-1)$ E-bindings). $I(S : E_{L=n})/H(S_{\text{class}})$ vs n for $\hat{\rho}_E^{\text{in}} = |0_n\rangle\langle 0_n|$ (blue, •-dotted curve, 0 E-bindings) is also displayed. 91
- 12 PIP for the random unitary CNOT-evolution of $\hat{\rho}_{SE}^{\text{in}} = \hat{\rho}_S^{\text{in}} \otimes \hat{\rho}_E^{\text{in}}$ ($N \gg 1$), with a pure $k = 1$ qubit system $\hat{\rho}_S^{\text{in}}$, $n = 9$ qubit $\hat{\rho}_E^{\text{in}} = \frac{1}{2}(|s_1^{L=n}\rangle\langle s_1^{L=n}| + |s_2^{L=n}\rangle\langle s_2^{L=n}|)$, $H(S) = 0.811 < H(S_{\text{class}})$ and a symmetric probability distribution $|a_0|^2 = |a_1|^2 = 1/2$ for each diagonal element of $\hat{\rho}_S^{\text{in}}$, $r = \frac{1}{2}$ 95
- 13 PIP for the random unitary CNOT-evolution of $\hat{\rho}_{SE}^{\text{in}} = \hat{\rho}_S^{\text{in}} \otimes \hat{\rho}_E^{\text{in}}$ ($N \gg 1$), with a pure $k = 2$ qubit Bell-system $|\Psi_S^{\text{in}}\rangle = 2^{-1/2}(|0\rangle + |2^{k=2}-1\rangle)$, $n = 9$ qubit $\hat{\rho}_E^{\text{in}} = |0_n\rangle\langle 0_n|$, $H(S) = 1 = H(S_{\text{class}}^{k=1})$ and a probability distribution $\{|a_0|^2 = |a_3|^2 = 1/2, |a_1|^2 = |a_2|^2 = 0\}$ for diagonal elements of $\hat{\rho}_S^{\text{in}}$, $r = 2^{-n}$. The same PIP occurs also for the random unitary CNOT-evolution of $|\Psi_{SE}^{\text{in}}\rangle = 2^{-1/2}(|0_{k=1}0_n\rangle + |1_{k=1}1_n\rangle)$, s. main text. 96
- 14 PIP for $\hat{\rho}_{SE}^{\text{out}}$ from $\hat{\rho}_{SE}^{\text{in}}$ in Fig. 1, ($a = b = 1/\sqrt{2}$) after acting upon $\hat{\rho}_E^{\text{in}}$ by $\hat{u}_j^{(\phi=\pi/3)}$ from (166)-(167) in Zurek's (•-dotted curve) and the random unitary (RUO) model (with $N \gg 1$, s. sections 4 and 7). 98
- 15 PIP of simulated, random unitarily CNOT-evolved MI vs $0 < f \leq 1$ for $\hat{\rho}_{SE}^{\text{in}} = \hat{\rho}_S^{\text{in}} \otimes \hat{\rho}_E^{\text{in}}$ in (12) and $\hat{\rho}_{SE}^{\text{out}}$ from (166)-(168) w.r.t. N (•, $N = 1$; ■, $N = 2$; ◆, $N = 5$; ▲, $N = 10$; ▼, $N = 10^3$; ○, $N = \infty$). For $N = \infty$ s. subsection 8.3.2. 100
- 16 PIP of simulated random unitary-MI vs f with $\phi = \pi/2$, for different N -values and an increasing number of CNOT-bindings between E-qubits. 101

17	PIP after random iterative $\hat{u}_j^{(\phi=\pi/2)}$ -evolution of $\hat{\rho}_{SE}^{in} = \Psi_S^{in}\rangle \langle \Psi_S^{in} \otimes 0_{n=9}\rangle \langle 0_{n=9} $ ($N \gg 1$), with a k qubit $ \Psi_S^{in}\rangle = \sum_{m=0}^{2^k-1} a_m m\rangle$ ($ a_m ^2 = 2^{-k} \forall m$), without ($k = 1$, ■-dotted curve; $k = 2$, ▲-dotted curve; $k = 3$, ▼-dotted curve) and with ≥ 1 interaction bindings ($k = 1$, ◆-dotted curve; $k = 2$, ○-dotted curve; $k = 3$, □-dotted curve) between E-qubits. The corresponding PIP of Zurek's model (●-dotted curve) is also displayed.	105
18	PIP after random iterative $\hat{u}_j^{(\phi=\pi/2)}$ -evolution of $\hat{\rho}_{SE}^{in} = \Psi_S^{in}\rangle \langle \Psi_S^{in} \otimes 0_n\rangle \langle 0_n $ ($N \gg 1$), with a $k = 2$ qubit $ \Psi_S^{in}\rangle = \sum_{m=0}^{2^k-1} a_m m\rangle$ ($ a_m ^2 = 2^{-k} \forall m$), without interaction bindings between E-qubits, plotted w.r.t. the number n of E-qubits.	105
19	PIP after random iterative $\hat{u}_j^{(\phi=\pi/2)}$ -evolution of $\hat{\mu}_{kSE}^{in} = 2^{-(k=1)} \{ 0\rangle \langle 0 \otimes 0_{L=n}\rangle \langle 0_{L=n} + 1\rangle \langle 1 \otimes 1_{L=n}\rangle \langle 1_{L=n} \}$ ($N \gg 1$), without interaction bindings between E-qubits, plotted w.r.t. the number n of E-qubits.	110
20	PIP after random iterative $\hat{u}_j^{(\phi=\pi/2)}$ -evolution of $\hat{\mu}_{kSE}^{in}$ in (224) ($N \gg 1$), without interaction bindings between E-qubits, plotted w.r.t. the number n of E-qubits.	111
21	PIP after random iterative $\hat{u}_j^{(\phi=\pi/2)}$ -evolution of $\hat{\rho}_{SE}^{in} = \Psi_S^{in}\rangle \langle \Psi_S^{in} \otimes \hat{\rho}_E^{in}$ ($N \gg 1$), with a pure $k = 1$ qubit $ \Psi_S^{in}\rangle = \sum_{m=0}^1 a_m m\rangle$ ($ a_m ^2 = 2^{-1} \forall m$), and $\hat{\rho}_E^{in} = 2^{-1} (0_n\rangle \langle 0_n + 1_n\rangle \langle 1_n)$ (0 E-bindings) w.r.t. n , s. main text.	112
22	PIP of $ I_{tot} - I_{part} / I_{tot}$ after random iterative $\hat{u}_j^{(\phi=\pi/2)}$ -evolution of $\hat{\rho}_{SE}^{in} = \Psi_S^{in}\rangle \langle \Psi_S^{in} \otimes \hat{\rho}_E^{in}$ ($N \gg 1$), with a pure $k = 1$ qubit $ \Psi_S^{in}\rangle = \sum_{m=0}^1 a_m m\rangle$ ($ a_m ^2 = 2^{-1} \forall m$), $n = 8$ and $\hat{\rho}_E^{in} = 2^{-1} (0_n\rangle \langle 0_n + 1_n\rangle \langle 1_n)$ (0 E-bindings) w.r.t. $f = L/n$, s. main text.	113
23	PIP after random iterative $\hat{u}_j^{(\phi=\pi/2)}$ -evolution of $\hat{\rho}_{SE}^{in} = \Psi_S^{in}\rangle \langle \Psi_S^{in} \otimes \hat{\rho}_E^{in}$ ($N \gg 1$), with a pure $k = 1$ qubit $ \Psi_S^{in}\rangle = \sum_{m=0}^1 a_m m\rangle$ ($ a_m ^2 = 2^{-1} \forall m$), $n = 8$ and different $\hat{\rho}_E^{in}$ (0 E-bindings), s. main text.	113
24	PIP after random iterative $\hat{u}_j^{(\phi=\pi/2)}$ -evolution of $\hat{\rho}_{SE}^{in} = \Psi_S^{in}\rangle \langle \Psi_S^{in} \otimes \hat{\rho}_E^{in}$ ($N \gg 1$), with a pure $k = 1$ qubit $ \Psi_S^{in}\rangle = \sum_{m=0}^1 a_m m\rangle$ ($ a_m ^2 = 2^{-1} \forall m$), and $\hat{\rho}_E^{in} = 2^{-n} \hat{I}_n$ (0 E-bindings) w.r.t. n , s. main text.	114
25	PIP after random iterative $\hat{u}_j^{(\phi=\pi/2)}$ -evolution of $\hat{\rho}_{SE}^{in} = \Psi_S^{in}\rangle \langle \Psi_S^{in} \otimes \hat{\rho}_E^{in}$ ($N \gg 1$), with a pure $k = 1$ qubit $ \Psi_S^{in}\rangle = \sum_{m=0}^1 a_m m\rangle$ ($ a_m ^2 = 2^{-1} \forall m$), and $\hat{\rho}_E^{in} = (\hat{I}_n - 1_n\rangle \langle 1_n) (2^n - 1)^{-1}$ (0 E-bindings) w.r.t. n , s. main text.	115
26	PIPs of (397) in Appendix J.1 after $N \gg 1$ iterations and w.r.t. $f = L/n$ ($n = 8$) (●-dotted curve for $\{\lambda = \pm 1\}$ attractor subspaces, ▲-dotted curve only for $\{\lambda = 1\}$ attractor subspace), (230) (■-dotted curve) and (407) in Appendix J.2 (◆-dotted curve), s. main text.	115
27	PIP of a random unitarily CNOT-evolved $\hat{\rho}_{SE}^{in} = \hat{\rho}_S^{in} \otimes \hat{\rho}_E^{in}$ ($N \gg 1$) with a $k = 1$ qubit pure $\hat{\rho}_S^{in}$ given by $ \Psi_S^{in}\rangle = \sum_{m=0}^1 a_m m\rangle$ and $\hat{\rho}_E^{in} = \frac{1}{2} (s_1^{L=n}\rangle \langle s_1^{L=n} + s_2^{L=n}\rangle \langle s_2^{L=n})$ w.r.t. n . The corresponding PIP w.r.t. $f = L/n$ and its curves for even and odd N -values are exactly the same.	116
28	PIPs w.r.t. n and $f = L/n$ of a random unitarily evolved $\hat{\rho}_{SE}^{in} = \hat{\rho}_S^{in} \otimes \hat{\rho}_E^{in}$ ($N \gg 1$), with a $k = 2$ -qubit pure Bell-state $ \Psi_S^{in}\rangle = 2^{-1/2} (0\rangle + 2^{k=2} - 1\rangle)$ and $\hat{\rho}_E^{in} = 0_n\rangle \langle 0_n $. $H(S) = H(S_{class}^{k=1}) < H(S_{class}^{k=2})$	118
29	PIPs w.r.t. n of a random unitarily evolved $ \Psi_{SE}^{in}\rangle = 2^{-1/2} (0_{k=1} 0_n\rangle + 1_{k=1} 1_n\rangle)$ ($N \gg 1$), $H(S) = H(S_{class}^{k=1}) = 1$. The corresponding PIP w.r.t. $f = L/n$ is given by the lower graph of Fig. 28 above.	118
30	PIPs w.r.t. n of a random unitarily CNOT-evolved $ \Psi_{SE}^{in}\rangle = 2^{-1/2} (0_{k=1} \gamma_n\rangle + 1_{k=1} \mu_n\rangle)$ ($N \gg 1$), $\lim_{n \gg 1} H(S) = 0 < H(S_{class}^{k=1}) = 1$	119
31	PIP after random iterative $\hat{u}_j^{(\phi=\pi/2)}$ -evolution of $\hat{\rho}_{SE}^{in} = \Psi_S^{in}\rangle \langle \Psi_S^{in} \otimes \hat{\rho}_E^{in}$ ($N \gg 1$), with a pure $k = 1$ qubit $ \Psi_S^{in}\rangle = \sum_{m=0}^1 a_m m\rangle$ ($ a_m ^2 = 2^{-1} \forall m$) and $\hat{\rho}_E^{in} = 0.5 \cdot (0_n\rangle \langle 0_n + 0_{n-2} 10\rangle \langle 0_{n-2} 10)$ ($2n - 3$ E-bindings) w.r.t. n , s. main text.	122
32	Interaction digraph (ID) between system S and environment E including dissipation within the random unitary evolution formalism [2].	124
33	PIP of MI vs f after the CNOT-evolution in accord with Zurek's and the random unitary model.	125
34	Random unitary evolution model: PIP of MI vs $0 < f \leq 1$ for $\alpha = \pi/2$, $\hat{\rho}_{SE}^{in} = \hat{\rho}_S^{in} \otimes \hat{\rho}_E^{in}$ ($N \gg 1$), with a $k = 1$ pure $\hat{\rho}_S^{in}$ and $\hat{\rho}_E^{in} = 0_n\rangle \langle 0_n $ (●-dotted curve), $\hat{\rho}_E^{in} = 0.5 \cdot (0_n\rangle \langle 0_n + 1_n\rangle \langle 1_n)$ (◆-dotted curve), $\hat{\rho}_E^{in} = 2^{-n} \cdot \hat{I}_n$ (■-dotted curve) [32].	126

35	Random unitary evolution model: maximal value $I(S : E_{L=n}) = I_{\max}(S : E)$ of MI and $H(S)$ from Fig. 34 (•-dotted curve, $N \gg 1$) vs $0 < \alpha \leq \pi/2$ for $L = n = 6$, [32].	127
36	PIP (for $\alpha = \pi/2$) of the MI-difference $[I(S : E_L) - I_R(S : E_L)]/H(S_{\text{class}})$ w.r.t. N and the random unitary evolution of $\hat{\rho}_{SE}^{\text{in}}$ from Fig. 33, leading (with (238)) to $I(S : E_L)$ and (with $\hat{U}_{ij}^{\text{Tot}}(\alpha) = \hat{U}_{ij}^{\text{Diss}}(\alpha) \hat{U}_{ij}^{(\phi=\pi/2)}$) to $I_R(S : E_L)$ [32].	127
37	Random unitary evolution model: MI $I(S : E_L)/H(S_{\text{class}})$ vs $0 < f \leq 1$ for $\alpha = \pi/2$ with respect to $\hat{\rho}_{SE}^{\text{in}}$ from Fig. 33 with $N = 100$ ($N \gg 1$), $k = 2, 3$, $p_i = 2^{-k} \forall i \in \{0, \dots, 2^k - 1\}$ and $H(S_{\text{class}}) = k$, evolving iteratively by (166)-(167) and (239)-(241) [32].	128
38	PIP of MI w.r.t. $0 < f = L/n \leq 1$ and different N -values for a $k = 1$ qubit pure $\hat{\rho}_S^{\text{in}}, \hat{\rho}_E^{\text{in}} = 0_{n=8}\rangle \langle 0_{n=8} $ and $\hat{\rho}_{SE}^{\text{in}} = \hat{\rho}_S^{\text{in}} \otimes \hat{\rho}_E^{\text{in}}$ from (12), with $ a ^2 = b ^2 = 2^{-1} \forall i \in \{0, 1\}$ and $H(S_{\text{class}}) = 1$, evolving iteratively by (166)-(167) and (258)-(264) (where $\alpha_1 = 2\pi/3 \neq \alpha_2 = \pi/3, \gamma = 0$).	135
39	PIP of MI w.r.t. $0 < f = L/n \leq 1$ and different N -values for a $k = 1$ qubit pure $\hat{\rho}_S^{\text{in}}, \hat{\rho}_E^{\text{in}} = 0_{n=8}\rangle \langle 0_{n=8} $ and $\hat{\rho}_{SE}^{\text{in}} = \hat{\rho}_S^{\text{in}} \otimes \hat{\rho}_E^{\text{in}}$ from (12), with $ a ^2 = b ^2 = 2^{-1} \forall i \in \{0, 1\}$ and $H(S_{\text{class}}) = 1$, evolving iteratively by (166)-(167) and (258)-(264) (where $\alpha_1 = 2\pi/3 \neq \alpha_2 = 0 = \gamma$).	136
40	PIP of MI w.r.t. $0 < f = L/n \leq 1$ and different N -values for a $k = 1$ qubit pure $\hat{\rho}_S^{\text{in}}, \hat{\rho}_E^{\text{in}} = 0_{n=8}\rangle \langle 0_{n=8} $ and $\hat{\rho}_{SE}^{\text{in}} = \hat{\rho}_S^{\text{in}} \otimes \hat{\rho}_E^{\text{in}}$ from (12), with $ a ^2 = b ^2 = 2^{-1} \forall i \in \{0, 1\}$ and $H(S_{\text{class}}) = 1$, evolving iteratively by (166)-(167) and (258)-(264) (where $\alpha_1 = \alpha_2 = \pi/2 = \gamma/2$).	137
41	Typical interaction structures between ($n \gg k \geq 1$) E-qubits of the ID in Fig. 9.	158

List of Tables

1	QD-compliant ($k = 1, n = 1$)-matrix structures of $\hat{\rho}_{SE}^{\text{out}}$ in (289)	49
2	QD-conformal $\hat{\rho}_{SE}^{\text{out}}$ -matrix structures for a k -qubit open S and its n -qubit E with ($k \geq 1, n \geq 1$).	72
3	Output states $\hat{\rho}_S^{\text{out}}, \hat{\rho}_E^{\text{out}}$ and $\hat{\rho}_{S,E}^{\text{out}}$ for input configuration $\hat{\rho}_{SE}^{\text{in}} = \hat{\rho}_S^{\text{in}} \otimes \hat{\rho}_E^{\text{in}}$ with $\hat{\rho}_E^{\text{in}} = s_1^{L=n}\rangle \langle s_1^{L=n} $	93
4	Output states $\hat{\rho}_S^{\text{out}}, \hat{\rho}_E^{\text{out}}$ and $\hat{\rho}_{S,E}^{\text{out}}$ for input configuration $\hat{\rho}_{SE}^{\text{in}} = \hat{\rho}_S^{\text{in}} \otimes \hat{\rho}_E^{\text{in}}$ with a one-qubit pure $\hat{\rho}_S^{\text{in}}$ and $\hat{\rho}_E = 2^{-n}(0\rangle - 1\rangle)^{\otimes n} (\langle 0 - \langle 1)^{\otimes n}$	94
5	Non-physical $\hat{\rho}_E^{\text{in}}$ -states	94
6	Convergence of (215) towards $H(E_L) = H(S, E_L) - H(S_{\text{class}})$ for increasing k -values.	109
7	$I(S : E_{L=n}) / H(S_{\text{class}})$ vs n for $\hat{\rho}_{SE}^{\text{out}}$ ($N \gg 1$) in Fig. 34 (•-dotted curve) [32].	130
8	$\hat{\rho}_{SE_L}^{\text{out}}$ from Zurek's CNOT-evolution of $\hat{\rho}_{SE}^{\text{in}} = \hat{\rho}_S^{\text{in}} \otimes \hat{\rho}_E^{\text{in}}$ for different $\hat{\rho}_E^{\text{in}}$, s. Fig. 5.	149
9	Numerical data for $d_{n \geq k}^{\lambda}$ from (362) in Appendix G w.r.t. $n \geq k \in \{1, 2, 3\} \forall \lambda \in \{1, -1\}$	155
10	Numerical data for $d_{n \geq k}^{\lambda=1}$ from (362) in Appendix G in case of $\hat{u}_j^{(\Phi)}$ -bindings between E -qubits in ID of Fig. 9.	157
11	\hat{x}_i -operators w.r.t. subspaces of an open $k = 1$ -qubit S , interacting with E via CNOT.	164
12	GSO-operators $\hat{x}_{i\tau}$ in all subspaces of an open $k = 1$ qubit system S	166
13	GSO-operators $\hat{x}_{i\tau}$ in all subspaces of an open $k \geq 1$ qubit system S	167

Index

- asymmetric dissipation, 133
- attractor (sub-)space dimension d^λ , 86
- Attractor »states« $\hat{X}_{\lambda,i}$, 86

- Bloch-vector decomposition, 98

- Classical channel capacity C , 33
- classical information, $H(S_{\text{class}})$, 26
- classically coherent states, 32
- CNOT-gate $\hat{\sigma}_x$, 28
- Coherent information I^{coh} , 35
- Copenhagen interpretation, 24
- cptp quantum measurement map, 40
- Criteria for QD, 55

- decoherence factor r , 30
- decoherence-induced transfer of $H(S_{\text{class}})$, 107
- density matrix $\hat{\rho}_X$ of (sub-)system X , 26
- Dephasing, 132
- dephasing rate γ , 132
- diamond norm $\|\cdot\|_\diamond$, 36
- direct sum \oplus , 86
- directed graph, digraph, 84
- Dissipation, 124
- dissipation strength α , 124

- effective decoherence, 28
- empty set \emptyset , 86
- entanglement cost e , 31
- entanglement monogamy, 37
- environment as a witness program, 15
- environmental fragments \mathcal{F}_i , 27
- exponentially suppressed dissipation, 132

- fraction parameter f , 27

- Gram-Schmidt orthonormalization, 150

- Hamming's bound, 41
- HSW Capacity Theorem, 34

- identity map, 86
- information gain g , 31
- interaction digraph (ID), 84

- kernel $\text{Ker}(\cdot)$, 86
- Koenig-ID, 101
- Kraus-operators K , 40

- Landauer's principle, 46

- many worlds interpretations, 13
- Maximal Attractor Space, 101
- Maxwell's demon, 45
- Minimal attractor space, 86

- non-demolition criterion, 27
- non-unitary Kraus-operators, 140

- Objectivity, 36
- optimal fraction-parameter f_{opt} , 47
- optimal redundancy R_{opt} , 47

- Partial Information Plot, 27
- ϕ -parameter transformation $\hat{u}_j^{(\phi)}$, 29
- pointer-states, 26
- POVM operators $\mathcal{M}(\cdot)$, 40
- pre-configuration matrix, PM, 153

- QD-'plateau' of mutual information, 28
- QD-condition, 30
- QR-decomposition, 151
- Quantum channel capacity χ , 34
- Quantum Darwinism, QD, 24
- Quantum error correction, 40
- Quantum Hamming's bound, 42
- Quantum Markov Chain, 86
- Quantum Measurement, 38
- quantum mutual information $I(S : E)$, 26
- quantum-to-classical transition, 13
- Qudit-cell conjecture, 106
- qudit-qudit CNOT, 140

- Random Unitary Evolution, 85
- real part $\Re(\cdot)$, 89
- redundancy R , 28
- relative state interpretation, 24

- Schumacher's quantum coding theorem, 42
- self-similarity of PIPs, 119
- Shannon's Coding Theorem, 33
- Shannon-entropy, s. $H(S_{\text{class}})$, 32
- Shannon-information hologram, 120
- Singleton-bound, 42
- Small N-limit, 99
- space of linear operators \mathcal{B} , 86
- Standard computational basis, 30
- State Merging Protocol, 38
- symmetric dissipation, 134

- transient random unitary iteration, 100

- Uhlmann's theorem, 39
- universal dynamical cptp-map, 103

- von Neumann entropy $H(X)$ of state $\hat{\rho}_X$, 26

- w.r.t. \equiv with respect to, 27

- Zurek's model of QD, 28